Stony Brook University

The official electronic file of this thesis or dissertation is maintained by the University Libraries on behalf of The Graduate School at Stony Brook University.

Evolution of the Peconic Estuary 'Oyster Terrain' Long Island, NY

A Dissertation Presented

by

Juliet West Kinney

to

The Graduate School

in Partial Fulfillment of the

Requirements

for the Degree of

Doctor of Philosophy

in

Marine & Atmospheric Science

(Marine Sciences)

Stony Brook University

May 2012

Stony Brook University
The Graduate School

Juliet West Kinney

We, the dissertation committee for the above candidate for the
Doctor of Philosophy degree, hereby recommend
acceptance of this dissertation.

Dr. Roger D. Flood, Dissertation Advisor
Professor, School of Marine and Atmospheric Sciences,
Stony Brook University

Dr. J. Kirk Cochran, Chair of Defense
Professor, School of Marine and Atmospheric Sciences,
Stony Brook University

Dr. Robert Cerrato
Associate Professor, School of Marine and Atmospheric Sciences
Stony Brook University

Dr. David Black
Assistant Professor, School of Marine and Atmospheric Sciences
Stony Brook University

Dr. Johan C. Varekamp
Harold T. Stearns Professor of Earth Sciences,
Earth and Environmental Sciences, Wesleyan University

This dissertation is accepted by the Graduate School

Charles Taber
Interim Dean of the Graduate School

ii

Abstract of the Dissertation
Evolution of the Peconic Estuary 'Oyster Terrain' Long Island, NY
by
Juliet West Kinney
Doctor of Philosophy
in
Marine & Atmospheric Science
(Marine Sciences)
Stony Brook University
2012

This study of the relict 'Oyster Terrain' in the Peconic Estuary of Long Island, NY using multibeam bathymetry, chirp sonar and sample analysis provides a history of estuarine evolution over thousands of years. More than 10,000 relict oyster reefs are exposed as mounds on the seabed within the Peconic Estuary, with more mounds imaged below the sediment surface. The tops of these relict oyster reefs are at water depths of ~6 m – 18 m and reef thicknesses of up to 6 m suggest active reef building over a few thousand years. At 28 psu, the present estuary is too saline for natural populations of the Eastern Oyster, *Crassostrea virginica,* to survive although transplanted oysters will grow. Morphological and shell data tell of a time when crowded oyster reefs once dominated the area; however, there has been a natural evolution in the Holocene to an environment where oysters are rare. Shells from relict oyster reefs provide the opportunity for a more detailed environmental reconstruction of this important transition through C-14 dating and geochemical proxies such as Sr-87/Sr-86 (salinity) and Ra-226 (submarine groundwater discharge). Reefs persisted in the Peconic Estuary despite rising salinities until ~1,350 years ago. Relict shells were compared to modern aquaculture shells grown in Peconic oyster farms. Submarine groundwater discharge seems to have dramatically decreased over time within the estuary according to concentrations of Ra-226 recorded in several sample shells. Sr isotope measurements indicate past variability in salinity was also captured in the relict shells. The era of abundant oyster reefs ended gradually suggesting that there was a gradual evolution to conditions that did not favor oyster survival. Surprisingly, the oyster reefs were growing in slightly deeper water than we anticipated before dying off. The youngest reefs were in only ~2.5 m of water 1,350 years ago; however, the oldest exposed reef tops we dated would have been active in ~10 m of water some 2,350 years ago. Our results suggest that oysters may have thrived in deeper waters more abundantly in the past than in modern stressed estuaries.

Dedication Page

To everyone who has helped along the way of writing the thesis. To those places along the sea that will always inspire. To all of those whose stories and presence in life have inspired me since I was small, and who have taught me much about the sea and the world through my experiences on the Island. To those who have influenced my path to this thesis who are no longer with us.

Frontispiece

Peconic Estuary on a calm day November, 2006

Table of Contents

Figure List

Appendix C

Table List

List of Abbreviations

GPS – Global Positioning System
ypb-Years before present
Ka-Thousand years
Ya- years ago
CHIRP - Compressed High Intensity Radar Pulse or Chirp – sub bottom profiling system that uses a swept frequency accoustic pulse, which is also known for its 'chirp' sound
MWP –water pulse
MLLW –Mean Low Low Water
UTM – Universal Transverse Mercator, map projection
ASCII-standard text file
SEG-Y- Society of Exploration Geophysicists standard seismic data file format
R/V – Research Vessel
SoMAS – School of Marine and Atmospheric Sciences
bsl -below sea level
Peconics-used here as abbreviation for the Peconic Estuary, including the Peconic Bays
NOAA-National Ocean and Atmospheric Administration
USGS-United States Geological Survey
USDA-United States Department of Agriculture
NAIP- National Agriculture Imagery Program
QTC-Quester Tangent^{TM} seabed classification program

Acknowledgments

CHAPTER 1: INTRODUCTION

TRANSGRESSIVE DEPOSITS:

     Transgressive deposits are often poorly preserved in the geological record because they tend to be destroyed on high energy continental shelves as sea level continues to rise. This is particularly true for nearshore or estuarine carbonate deposits such as oyster reefs that are generally unconsolidated and uncemented (Macintrye et al., 1978; Catteneo & Steel, 2003; Belknap & Kraft, 1981). For the last postglacial sea level rise there is a paucity of preserved intact transgressive carbonate deposits, including oyster reefs (Macintrye et al., 1978; Catteneo & Steel, 2003; Belknap & Kraft, 1981). Relict oyster shells have long been known to be ubiquitous across the U.S. East Coast continental shelf, and since 1965 they have been recognized as remnants of the post Wisconsian sea-level rise (Merrill et al., 1965). Oysters were commonly used in conjunction with salt marsh peat and terrestrial deposits as indicators of past sea levels due to their limitation to brackish salinities as in Milliman & Emery (1968) and Gutierrez et al. (2003). Indeed, most of the points and dates used in early post-glacial sea-level curves are oyster shell (Merrill et al., 1965; Fig. 1.1). However, the original position, depth and morphology of many shell deposits found drowned on the continental shelf are unknown because of the erosion and transport of the deposits on the present high-energy shelf (MacIntyre et al., 1978; Catteneo & Steel, 2003). High resolution studies of the structure of better preserved examples of such oyster shells deposited during the last transgression are needed to address questions about the environment in which these kinds of deposits form, the larger-scale patterns exhibited by the deposits, and the paleoceanographic record they contain.

     Oyster reefs are a type of bioherm. A bioherm is a mound that forms as a result of the buildup of debris from biological organisms, by trapping sediment with soft tissue or hard structures and/or by accreting biogenic material such as shells growing on top of

each other in a mounded structure or a coral reef (Riding, 2002; Bates & Jackson, 1984; Altermann, 2008). Bioherms may act to trap biogenic sediment particles such as fine shell hash or feces as well as sediment unassociated with the inhabitants of the mound. In the case of oyster reefs, oysters often trap organic and inorganic sediment between shells in the reef structure during the vertical growth of the reef. The term 'carbonate mud mounds' is often used to refer to bioherms, which contain sediment with a large percentage of mud and carbonate material (Middleton, 2003; Riding, 2002). Carbonate mud mounds, also known as carbonate reefs, are known to be common throughout the geological record, although they can be composed of different species at different times (Henriet et al., 2002; Middleton, 2003; Riding, 2002). The term carbonate mud mound is sometimes used in the literature to refer to more specific types of deposits, such as those found in deep water (Middleton, 2003), however here the term to refers to mounds in all water depths. Despite centuries of research, scientists rarely discovered examples of carbonate mud mounds in the Cenozoic geological record, although mud mounds were frequently found in the pre-Cenozoic record (Henriet et al., 2002). It was not until the 1990's when higher resolution mapping and subsequent sampling revealed similar sites in the deep sea (Henriet et al., 2002). Earlier examples of carbonate mud mound structures include brachiopod reefs in trangressive deposits in Carboniferous carbonate platform facies in Kazakstan (Cook et al., 2002), oyster deposits from the Pliocene and the Miocene reported by Pufahl et al. (2004) in Murray Basin, Australia and other carbonate mound deposits often associated with transgressions (Adams et al., 2005; Mel'nikov et al., 2005; Henriet et al., 2002; Huvaz, et al., 2007).

What appear to be intact examples of transgressive carbonate deposits preserved within the Peconic Estuary in eastern New York in the form of relict oyster reefs are referred to here as the 'Oyster Terrain' (Kinney & Flood, 2006; Flood & Kinney 2006; Kinney & Flood, 2007; Kinney & Flood, 2008; Kinney & Flood, 2009; Kinney & Flood, 2010; Kinney & Flood, 2011) (Fig. 1.2). The Oyster Terrain mound morphology observed in multibeam bathymetry may represent an example of a transgressive sequence of carbonate mounds or reefs that is poorly preserved in the geological record. Characterization of the distribution and evolution of intact transgressive

deposits such as oyster reefs are important to understanding the role of climate and sea level rise in coastal systems and the morphological changes that occur with the environmental evolution of coastal systems, as well as broader impacts aiding in interpreting modern and ancient deposits. The Peconic Estuary may provide a unique opportunity to examine such features and their evolution while gaining some new insight into climate variability and possibly large climate events.

Intact reef structures or bioherms are likely to preserve a depth /age relationship representing a chronological record of the environment of deposition, with minimal transport or other reworking. High resolution studies of the framework of the 'Oyster Terrain' will help distinguish the different deposits present in a spatially complex heterogeneous coastal environment. Identifying such features is a first step to studying deposits suitable for much needed, higher resolution paleoclimate reconstructions from temperate marine postglacial environments from the mid to early Holocene for which studies have been sparse (Saenger et al., 2006; Cronin et al., 2003; Varekamp et al., 2007; Donnelly et al., 2004; Van de Plassche, 2000). The high resolution study of such an extensive area of reefs as found in the Peconic Estuary may help understand past mound systems and transgressive sequences elsewhere in the geologic record.

PALEOCLIMATE AND PALEOENVIRONMENT- EVOLUTION OF COASTAL SYSTEMS:

It is important to understand how coastal systems responded to past changes such as sea level rise, changes in salinity, and estuarine environmental evolution because similar changes may be expected to take place in the future as a result of climate change, predicted sea level rise, and anthropogenic alteration. Anthropogenic alteration of coastal systems that may mimic past natural changes include a range of processes from direct physical alterations to the bathymetry (e.g. dredging, dumping, creation of hard structures), to increased sediment input rates, to altered river and freshwater discharge, as well as direct impacts on biological communities (including harvesting and introduction of new species) that may alter the physical and sediment dynamics of the

system. Other factors may include responses to other potential anthropogenic impacts such as changes in temperature, stratification, oxygen levels or nutrient levels. Examples of similar scale non-anthropogenic changes may be found recorded in the past. The past analogues of possible future change are especially important since large non-linear changes in coastal systems have been observed in places such as the Chesapeake Bay (Bratton et al., 2003) and Galveston Bays (Anderson, 2008). Chesapeake Bay and Galveston Bays are examples of systems where paleostudies show dramatic change in salinity, circulation and spatial extent after the system crossed a threshold. In the case of Galveston Bay, environmental changes including elevated salinity occurred when sea level rose above a critical elevation, and the bay went from a dominantly narrow deep bay to a predominantly wide shallow bay as former fluvial terraces flooded (Anderson, 2008). In Chesapeake Bay sea level elevation crossed a topographic threshold as it rose past the narrower cross-sectional area of the Susquehanna Cape Charles paleoriver valley, which changed the system from freshwater in the river channel to brackish in the same locations (Bratton et al., 2003).

The spatial gradient of relative sea level response coupled with the heterogeneity of most coastal environments makes it important to look at how specific places have responded to sea level rise in order to understand how these processes will affect other systems in the future. Many questions remain about how such coastal systems evolved with respect to past sea level rise. These include questions about morphology, climate, circulation, and ecological patterns in the coastal system. Examples of significant changes to these systems include those with non-linear responses to steady sea level rise because of the morphology of different systems (Bratton et al., 2003; Anderson, 2008). Significant changes in the evolution of coastal systems may have been caused by changes in climate such as shifts in precipitation or rapid rises in sea level. Well known examples of such events from the past 12,000 years include meltwater pulses 1B or 8.2 ka (Alley, 2003; Rohling & Palike, 2005; Bond et al., 1997; Bard, Hamelin, & Delanghe-Sabatier, 2010). Meltwater pulses are the release of glacial meltwater such as the 8.2 ka event, which can been seen as an abrupt jump in sea level in some records (Bratton et al., 2003) corresponding to the last meltwater pulse emptying the

4

North American glacial lake Ojibway into the North Atlantic via the Labrador Strait (Alley et al., 1997; Rohling & Pälike, 2005; Alley & Agustsdottir, 2005; Ellis et al., 2006). The 8.2 ka event slowed thermohaline circulation and deepwater formation on a smaller scale than the well-known Younger Dryas climate cooling over the course of 200 years or so (Alley et al., 1997; Rohling & Pälike, 2005; Alley & Agustsdottir, 2005; Ellis et al., 2006).

Paleoclimate studies with sufficiently high resolution are needed for temperate marine environments to understand the climatic evolution, as well as the sedimentary and morphological evolution in these complex coastal areas between the end of the last glacial maximum and the present. Studies with higher resolution records become increasingly sparse at earlier times in the Holocene. Studies of settings with preserved deposits and context are needed to construct higher resolution records in the early to mid-Holocene. Marine records in the form of transgressive deposits are often poorly preserved, especially those corresponding to the most recent post-glacial transgression of the past 10,000 years (MacIntyre et al., 1978; Catteneo & Steel, 2003; Belknap & Kraft, 1981). New opportunities may be found in a number of sites with high-resolution records that will help us reveal fluctuations in past climate.

Major questions exist about the role of spatial and temporal variability in large scale physical ocean-atmosphere patterns such as the Southern Oscillation (El Niño), Pacific Decadal Oscillation, North Atlantic Oscillation, meltwater pulses, and oceanic circulations with longer time scales. For example the position of the north wall of the Gulf Stream is correlated with the North Atlantic Oscillation (NAO) (Hameed & Piontkovski, 2004). However, using the position of the atmospheric highs and lows (e.g. Iceland Low/ Azores High) increases the strength of the correlation of these patterns (Hameed & Piontkovski, 2004). At longer time scales of centuries to millennia, it has been proposed that local climate changes have been affected by spatial changes in climate patterns such as the position of the north wall of the Gulf Stream off the Coast of Cape Hatteras (Sachs, 2006). Several relatively high resolution climate records for the last 1,000 to 7,000 years in the mid-latitude US have recently been published (Van de

Plassche, 2000; Donnelly et al., 2004; Cronin et al., 2003; Saenger et al., 2006; Varekamp, 2007), but yet more locations with even higher resolution will be needed to resolve major questions about spatial and temporal variability in our climate system.

A key to planning for the future and to understanding the potential impacts and risks of global climate change is an increased understanding of past variability from such records. However, in order to achieve this goal a much more detailed understanding of the geological evolution of coastal areas is needed. Through the combination of data sets of high resolution surface morphology, sediment layering, and sediment analysis one can examine the structural and climatic evolution of a system and its variability over time. In particular, packets of high resolution information on climate variability may be recorded in the annual growth bands of bivalve (i.e. oyster) shells. Oysters have clear annual growth breaks along the hinge, but it is more difficult to distinguish annual breaks within shells (Galstoff, 1964; Kirby, 1998; Kirby, 2000; Kraeutuer et al., 2007). This is in contrast to hard clams, which have visible growth lines at small increments (Schöne, 2008). Subannual scale variability within Eastern Oyster, *Crassostrea virginica,* growth bands have been reconstructed and geochemically matched with instrumental records (Surge et al., 2001; Surge et al., 2003).

EASTERN OYSTER:

The Eastern Oyster, *Crassostrea Virginica*, typically lives on soft and hard bottoms, in waters of reduced salinities and from the low-tide line to water 12 m deep (Meinkoth, 1981). However, oysters can tolerate a wide range of conditions (Stanley & Sellers, 1986; Galtsoff, 1964). Modern active oyster reefs are often associated with much shallower water of a few meters to intertidal depths, but oyster reefs have been found to live at depths of 40 m (Stanley & Sellers, 1986), which is deeper than the deepest mounds exposed in the Peconic Estuary. Significant changes in salinities and temperatures beyond the normal range to which an individual organism has acclimated reduces productivity, and affects the survival rates of offspring dramatically (Stanley & Sellers, 1986). Large changes in salinity are deadly to oysters (Galtsoff, 1964; Stanley

& Sellers, 1986). In many locations, freshets and flooding events will kill off oysters in the more brackish parts of an estuary (Stanley & Sellers, 1986). Mortality rates of oysters increase in deeper waters of stratified estuaries when conditions are hypoxic or anoxic (Lenihan & Peterson, 1998). Oysters can survive brief hypoxic episodes, but not indefinitely (Lenihan & Peterson, 1998).

At high salinity, diseases and predators of the Eastern Oyster flourish to the extent that modern natural oyster populations do not survive unless in protected shallow water settings (Stanley & Sellers, 1986). Oysters tend to flourish best in waters of 10 to 25 psu because there are fewer predators and diseases. The range of salinities at which oysters naturally survive is different than the physiological limit of salinity due to factors such as predation especially on young oysters (Stanley & Sellers, 1986; Galtsoff, 1964). Diseases such as Dermo and MSX for instance thrive at higher salinities (Ford, 1985; Ford & Haskins, 1988; Burreson et al. 1994; Powell et al., 2008; Bushek, 2010; Kreeger et al., 2010). Predators such as echinoderms and fish start to appear at salinities higher than 20 psu (Stanley & Sellers, 1986; Galtsoff, 1964). Another prominent predator that favors higher salinities is the oyster drill, *Urosalpinx cinerea*, which needs a minimum of 12 to 17 psu to survive depending on the temperature (Galtsoff, 1964). Those reefs that do survive at higher salinities exist in the very shallow water of the intertidal zone (Stanley & Sellers, 1986; Kreeger et al., 2010). Occasionally oysters are found in greater the 30 psu in intertidal areas, but physiological growth is affected at that salinity (Galtsoff, 1964). Freezing in winter is part of the climate of the Northeastern U. S. and Canada that inhibits oyster reef survival in shallow water and the intertidal zone (Kreeger et al., 2010). Any oysters that settle in such shallow water are routinely killed off every few years by cold, preventing the establishment of reefs (Kreeger et al., 2010).

Remnants of relict reefs in the region have long been documented. Ancient oyster shells found along the beaches of New Jersey and Long Island's South Shore have been eroded from old oyster reefs (Stoffer et al., 2005). Relict oyster shell deposits in the Peconic Estuary were noted prior to the introduction of historical aquaculture in those waters (Ingersoll, 1881). Ingersoll (1881) cited ancient reefs as evidence of past

environmental change because natural oysters would not survive in the Peconic Estuary because of the high salinity. Oysters fitting descriptions of those from this study were reported in previous studies of sediments in the Peconic Bays 30 to 40 years ago as non-living oysters in sediment grabs by Brennan (1973). Katuna (1974) also reported Oyster shells in a few places. These earlier studies lacked the context and detailed study of these shells, or comparisons with aquaculture maps, to distinguish the shells from active aquaculture and were unable to make suggestions about the origin of these ancient reefs.

INTACT REEF IMPLICATIONS:

There are many questions about the response of modern oyster reefs to global climate change and accelerated sea level rise, especially in the context of other anthropogenic stresses. For instance, numerous studies of estuaries using a variety of proxies have tried to reconstruct how salinity fluctuates due to the incursion of marine waters under sea level rise and climate change (Bratton et al, 2003; Cronin et al, 2005; Surge et al., 2003; Reinhardt et al., 1998; Thomas et al, 2006). A wide range of salinity proxies have been used in these studies including Re (Bratton et al, 2003), $\delta^{18}O$ with Mg/Ca ratios (Cronin et al., 2005), covariance of $\delta^{18}O$ and $\delta^{13}C$ (Surge et al., 2003) and $^{87}Sr/^{86}Sr$ (Reinhardt et al. 1998). Of the many proxies available, however, $^{87}Sr/^{86}Sr$ has no known vital effects. In many studies of salinity in estuaries, further questions arise as to whether fluctuations in proxy-inferred salinity were due to freshwater input or marine incursion caused by increased sea level. Were these related to changes in estuarine circulation dynamics and not just to a lateral shift in salinity caused by morphology, freshwater, or sea level changes? Were decreases in favorability of the oyster habitat a result of such factors as increased sedimentation, system changing events, gradual processes, salinity/climate variability, change in hydrology and temperature regimes, and/or biological ecosystem shifts? Many modern estuarine systems may gradually evolve over thousands of years with more rapid change occurring over a few hundred years or less due to the evolution of the estuarine morphology as mentioned in Bratton et al. (2003) and Anderson et al. (2008) or it may

be due to changes in hydrology and climate such as mentioned in Carbotte et al. (2004).

Characterization of the distribution and evolution of intact modern oyster reefs may have broader impacts through the interpretation of older, even ancient, and deeper deposits. For instance, many carbonate systems with reefs form oil reservoirs (Huvaz & Sarikaya, 2007; Cook et al, 2002; Mel'kinov et al., 2005; Jia et al., 2007). Spatial distribution of reefs has implications as to where one may find reservoirs of fluid including petroleum (Adams et al., 2005). Models are used to help predict variability within deposits and potential to find oil (Adams et al, 2005; Chen & Osadetz, 2006) and these models of spatial distribution of reefs would benefit from a comparative study of a large system of reefs such as the Peconic Estuary. A more detailed study of a carefully mapped system, covering a few thousand years may help to understand how the Peconic Estuary reef system evolved as well as responses in other systems both recent and ancient.

THE PECONIC ESTUARY:

The Peconic Estuary is located on the North Eastern Seaboard of North America on the eastern end of Long Island, New York (Fig. 1.3, 1.4). It opens onto the eastern end of Long Island Sound, Block Island Sound, and the open Atlantic Ocean, and is influence by the Gulf Stream offshore (Fig. 1.4, 1.5). Both the warm waters of the northward-flowing Gulf Stream, and the colder waters of the southward-flowing shelf current affect the region. The interaction of these waters appears to result in temperature and salinity fluctuations on interannual and longer time scales, and may be affected by temporal variability in ocean - atmosphere interactions such as the North Atlantic Oscillation (NAO) (Greene & Pershing, 2003; Visbeck et al., 2003; Hameed & Piontkovski, 2004; Drinkwater et al., 2003) and perhaps similar patterns operating on longer timescales such as in Sachs (2007).

The Peconic Estuary is located between the Wisconsian moraines that form the North Fork (Harbor Hills Moraine) and South Fork (Ronkonkoma Moraine) of Long Island (Veatch, 1903; Fuller, 1914; Olcott, 1999) (Fig. 1.4). Many spits and large islands are located within the Estuary. The moraines along with the large islands within the estuary, serve to protect seabed features from higher energy forces such as storm waves that dominate our present post-glacial continental shelf environment. Strong currents are found in some places in the estuary (Fig. 1.6). High-speed tidal currents through parts of the bay serve to keep relict features exposed by minimizing burial by fine sediments. The ebb and flood tides race through the constrictions between the bays at 1 m/s or more with a mean range of 0.76 m (Viera, 1990; Eisel, 1977; Hardy, 1976), readily seen as a 2 knot change in boat speed. These traits also serve to keep this estuary very well mixed, at close to 28 psu throughout the open bays (Viera & Wilson, 1990). The system covers an area of about 220 km^2 and has a basin length of approximately 20 km (DiLorenzo, 1986). Water depths of close to 30 m in places, protection from waves, and a relatively low sediment supply delivered to the estuary via the Peconic River have preserved relict morphologies relatively well, despite locally strong currents and anthropogenic activity. The average depth for Little Peconic and Noyack Bays is ~ 6.5 m based on NOAA bathymetry, which includes the wide shallow sandy banks that encircle the bays.

Shoreline erosion along the Peconic Estuary also contributes to the sediment input to the estuary. The coastline of the Peconic Estuary between Montauk and Orient Point, not including the islands within the bay is about 202 km (Eisel, 1977). The coasts are lined with mostly unconsolidated modern bluffed hills that range from close to 6 m high on the North Fork to 73 m on the South Fork (Eisel, 1977). The unbulkedheaded bluffs receded 0.31 to 0.4 m/yr between 1934-1961 and 1970 (Eisel, 1977). Rates of shoreline erosion of the sandy and gravelly beaches varied from negligible changes of 0.01 to 0.35 m/yr between 1838 and 1957 (Eisel, 1977). These high rates and the common high bluffs suggest that shoreline erosion may contribute a potentially significant volume of sediment to the beach, which then can be transported along or away from shore.

The Peconic Estuary has a relatively small watershed, compared to many estuaries on the mainland in North America, and is mostly composed of glacial material, which helps to constrain estimates of known hydrologic inputs and units. The major river to the estuary, the Peconic River, has a drainage basin composed mostly of glacial till with an area of approximately 180 km^2 (Xin, 1993). The total freshwater input to the Peconic Estuary from runoff, submarine groundwater discharge, and precipitation is estimated to be 3 –5 m^3/s (DiLorenzo, 1986). Two thirds of the freshwater input to the Peconic Estuary comes from the Forks and Islands via submarine discharge, and approximately two ninths flows through the Peconic River watershed from the main part of Long Island (Schubert, 1999). Freshwater inputs to the Peconic Estuary are concentrated near the head of the Peconic River Estuary and include the Peconic River as well as a sewage treatment outfall (Schubert, 1999; Breuer et al., 1999; Hardy, 1976).

Glacial aquifers and surface groundwater play an important role on Long Island estuaries, including the Peconic Estuary (Schubert, 1998; Dulaiova et al., 2006; Stieglitz et al., 2008). As in most places, submarine groundwater discharge on Long Island is believed to play an important role in estuarine processes (Moore, 1996; Moore, 1999; Beck et al., 2008; Collier et al., 2005; Dulaiova et al.; 2006; Stieglitz et al., 2008). Indeed, in Great South Bay – a shallow lagoon located along the south shore of Long Island – as much as 90% (36 – 94 m^3/s) of the bay's recirculated water – sea water in the sediment and water column that recirculates in the bay – may be from submarine groundwater discharge as opposed to recirculation between the bay and open ocean (Beck et al., 2008). Submarine groundwater discharge along channels or areas of stronger flow paths contributes substantially to the overall output (Beck et al., 2008). Studies of the Peconic Estuary have demonstrated substantial chemical and freshwater contributions of submarine groundwater discharge to the Estuary (Schubert, 1999; Dulaiova et al., 2006; Stieglitz et al., 2008). Approximately 78 to 84% of freshwater input to the Peconic Estuary including rainfall, runoff and sewage discharge is estimated to travel via submarine seepage (Shubert, 1999; Hardy, 1976).

Oysters cannot survive naturally and reproduce in modern conditions of 28 psu within the Peconic Estuary (Ingersoll, 1881). For more than a hundred years there has been a very well documented history of aquaculture through subaquatic leases within the Estuary (Davies et al., 2002; Davies et al., 2003). Oysters are bred and raised as seed oysters in tanks of more brackish water. Oysters transplanted to the Peconic Estuary that were not raised in facilities within it have been raised in Connecticut typically near the Mystic River since the onset of the practice in the late 1800's (Ingersoll, 1881; Davies et al, 2002; Rivera personal Communication 2009). Oysters do not tolerate sudden changes in temperature and salinity well. As mentioned earlier, oysters favor fresher waters than those of the main bodies of the Peconic Estuary. Today one may only find oysters naturally in the narrow restricted brackish creeks (Lightfoot, 1987).

Multibeam bathymetry and seismic profiles reveal mound features associated with relict oyster mounds covering an extensive area of the Peconic Estuary on Long Island, NY (Fig. 1.2). Exposed mounds are typically ~2 m high, but many are as high as 4 m, and are 10 to 50 m in diameter and are associated with high backscatter. Backscatter is the intensity of the return pulse from an echosounder, where softer materials such as mud tend to have lower backscatter than harder materials such as sand or shells that reflect more of the sound back. By examining the characteristics of features based on the multibeam backscatter and bathymetry data obtained as part of the ongoing benthic habitat mapping project (Flood et al., 2009), relatively high backscatter regions associated with the mound morphology are distinguished. Much of the data collected and used during this study was actually collected as part of that project (Fig. 1.2), including multibeam bathymetry and grab samples. Iron stained unarticulated oyster shells in grab samples characterize the tops of the mounds, but no living oysters. It is hypothesized that the mounds that are the object of this study are relict oyster reefs, which are referred to as the 'Oyster Terrain.' The unusually deep and widespread distribution suggests that oyster reefs in the Peconic Estuary were alive when sea level was much lower. Additionally, oysters require less saline water than the water of the Peconic Estuary to survive naturally today.

12

While it is relatively easy to distinguish oyster shells from modern aquaculture activities from the oyster shells of the ancient reefs, it is always possible that some of the oyster shells found in this study of the oyster terrain may have been left there as a result of aquaculture activities.   Aquaculture oysters could be on the bottom as a result of adding shell material as clutch to the bed since the Peconic Estuary has been used extensively for aquaculture (Davies et al., 2002; Davies et al., 2003). Seed shells or larger adult shells that were put out in the bay waters to grow out or that were transferred from more impacted estuarine systems to depurate in the Peconic Estuary before being suitable for market may have been left behind. The possible impact of these practices on the terrain will have to be addressed here.

These mounds are older features that may hold interesting paleoclimate records by preserving carbonate shells with annual growth bands during an earlier time of lower sea level during the mid to early Holocene when paleoclimate records for the region are sparse. The good preservation and easy accessibility of these features may create the opportunity to understand the stratigraphic framework and evolution of a post-glacial transgression on a large scale and at high resolution, including morphology analogous to reef deposits widespread in the geologic record. High resolution seismic and bathymetric mapping of the features should provide enough morphological context for higher resolution paleoclimate studies in this heterogeneous environment.

OUTLINE OF THESIS:

This study focuses on characterizing the 'Oyster Terrain' that has been found in the Peconic Estuary and determining the likely origin of this terrain. Characterizing the structural and climatic evolution of this terrain may allow us to understand a type of system that may have been widespread during our most recent post-glacial transgression, but has been poorly preserved on our present high-energy continental shelf. Multibeam and sedimentary data provide the initial description of these features, which is then augmented by seismic analysis. The hypothesis that these features were

last active during the mid to early Holocene will be tested through dating of shells from mounds topped by oyster shells. Geochemical proxies of sediments and oyster shells from grabs and gravity cores will aid in the characterization of the evolution of this terrain.

Chapter 2 describes the basic characteristics of the 'Oyster Terrain' believed to be exposed relict oyster reefs within the Peconic Estuary. The general setting, depth range, basic morphology, distribution, and basic sedimentary characteristics are described. The possible antiquity and scale of these relict deposits is also discussed.

Chapter 3 focuses on the morphology and spatial distribution of these features. For instance typical area size, depth, and density of mounds and different mound configurations are shown in more detail. Results are for features found in Little Peconic and Noyack Bays. The large scale and high resolution morphology may provide analogies to reef deposits widespread in the geologic record.

Chapter 4 focuses on the evolution of the Peconic Estuary, by focusing on mounds in Little Peconic Bay. A theory of the evolution of this terrain as relict oyster reefs is described and tested. Gravity cores were taken in Great Peconic Bay to test whether buried mounds had the same sediment characteristics as exposed mounds, oysters, and were indeed relict reefs. Part of the evolution of the terrain is the burial of reefs, which modern sedimentary processes and radionuclides traces can help us to understand. Oyster shells from this complex terrain were carefully chosen from the surface of mounds to date with ^{14}C. Selection and context of dated features are an important part of testing the hypothesis that the reefs are potentially thousands of years old. Characterization of this terrain includes distinguishing relict features from modern anthropogenic activities by comparing the setting of samples with examples of modern aquaculture.

Chapter 5 tries to bring together geochemical clues, especially ^{87}Sr/^{86}Sr and ^{226}Ra, to understand how this system evolved in terms of salinity and submarine groundwater

discharge. $\delta^{18}O$ and $\delta^{13}C$ were also measured. The same relict shells chosen for ^{14}C dating are used here to examine the evolution of the system over time. Modern aquaculture shells were used to compare both brackish and more saline present conditions with past conditions. Possible relationships with sea level rise and submarine groundwater discharge and salinity and implications for what this may have meant for the oyster reef community are discussed.

Chapter 6 presents the overall conclusions and implications of this investigation of the Peconic Oyster Terrain. The major findings of Chapters 2 to 5 are highlighted and there is a brief comparison to other large relict and living reefs give perspective to this system. Further implications are discussed.

Fig. 1.1: Sea level curve and oyster distribution from Merril et al. (1965) with Peconic peak mound depth (modified with permission of author M. Rubin and reprinted with permission from AAAS). The relict oyster, Crassostrea virginica, distribution across the continental shelf used by Merril et al. (1965) (left). The range of the peak of abundance of mound tops in the Peconic Estuary of ~10 m (Yellow) is plotted over both the sea level curve and histogram of oyster abundance with depth across the shelf from Merril et al. (1965) (right). The peak in the Peconic oyster reef depths corresponds to oyster deposits at the same depth that are ~8ka on the shelf. The plot also shows locations of shells that did not plot on the sea level curve, but were substantially deeper. Some of this is due to transport of shells, while others may have grown in deeper water.

▨ Depths of Peconic Estuary Mounds, correspond to time period & depth of relict oysters, Crassostrea virginica, found across the Atlantic Continental Shelf (used to create SL curves)
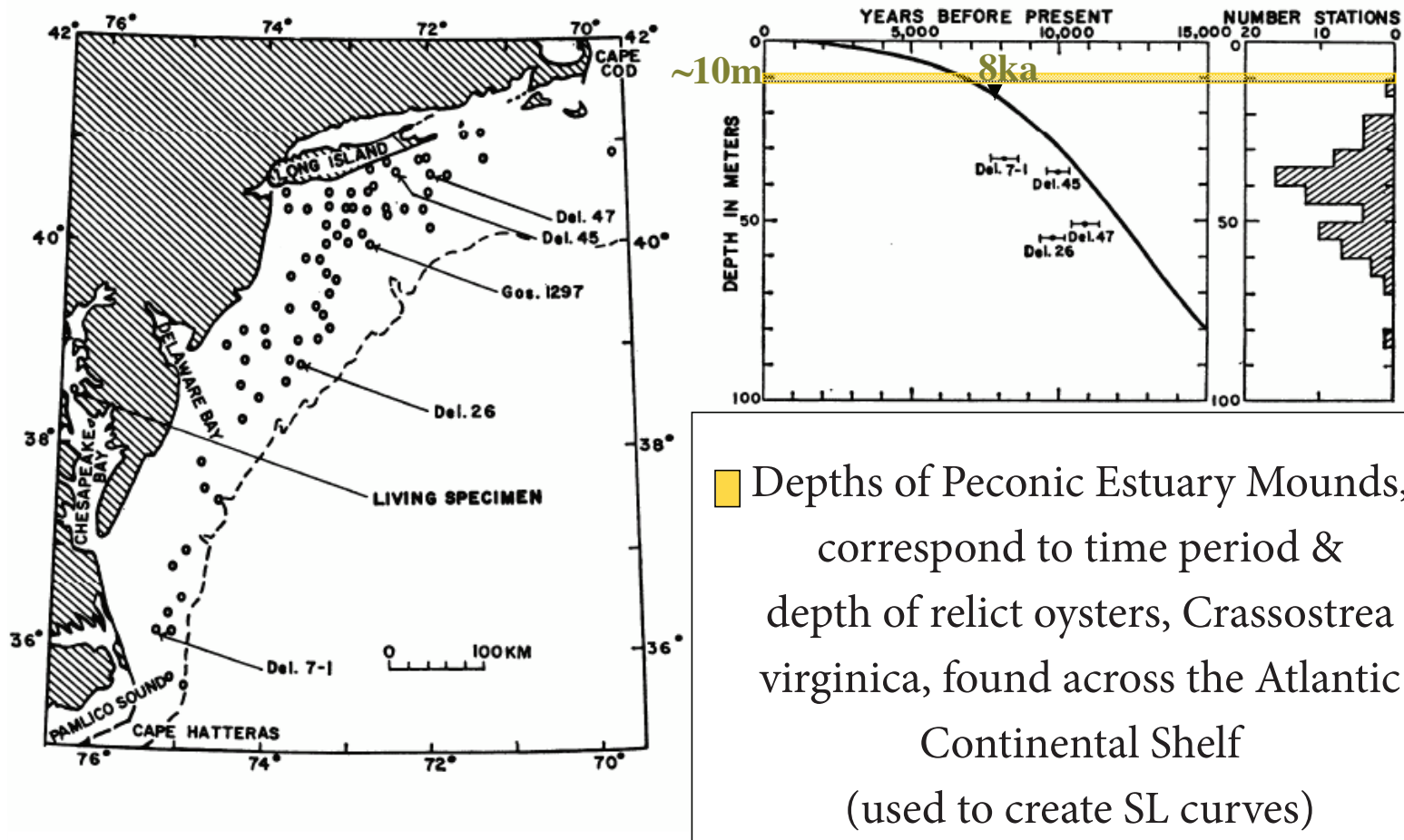
Fig. 1.2: The Peconic 'Oyster Terrain' revealed. View of the Peconic 'Oyster Terrain' as revealed by a multibeam bathymetry view of backscatter with shaded relief. Backscatter is color shaded with blues representing the lowest backscatter and yellows high backscatter. Oranges tones are the highest backscatter value and dark blues is the lowest backscatter value. Bathymetry overlays a basemap of digital orthophotos (i-cubed, 2009; USDA; NAIP; USGS).
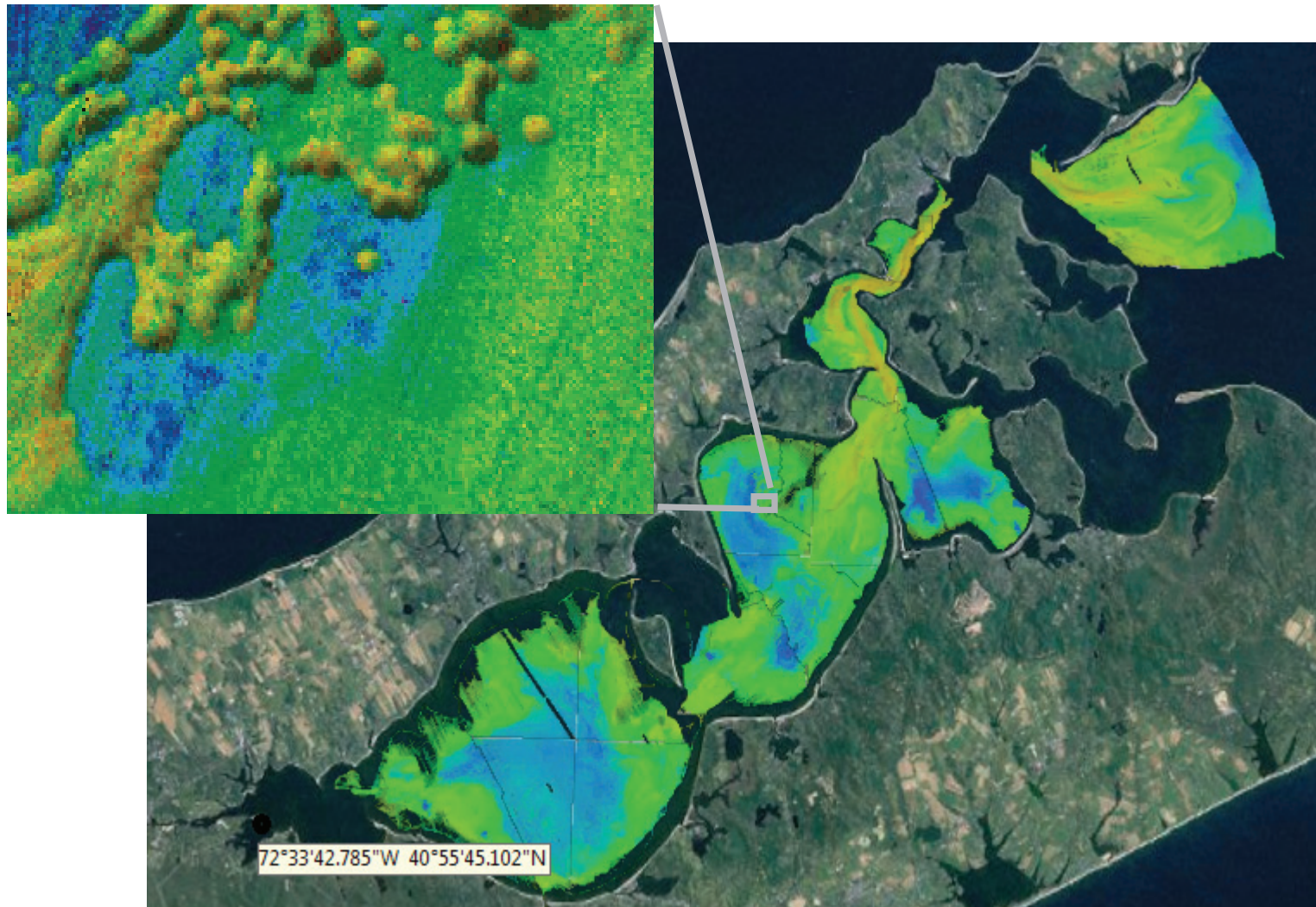
Fig. 1.3: Map showing the location of Long Island New York along the East Coast of the United States. SeaWifs image on the right (NASA, 2005, Satellite image courtesy of GeoEye, www.geoeye.com).

18
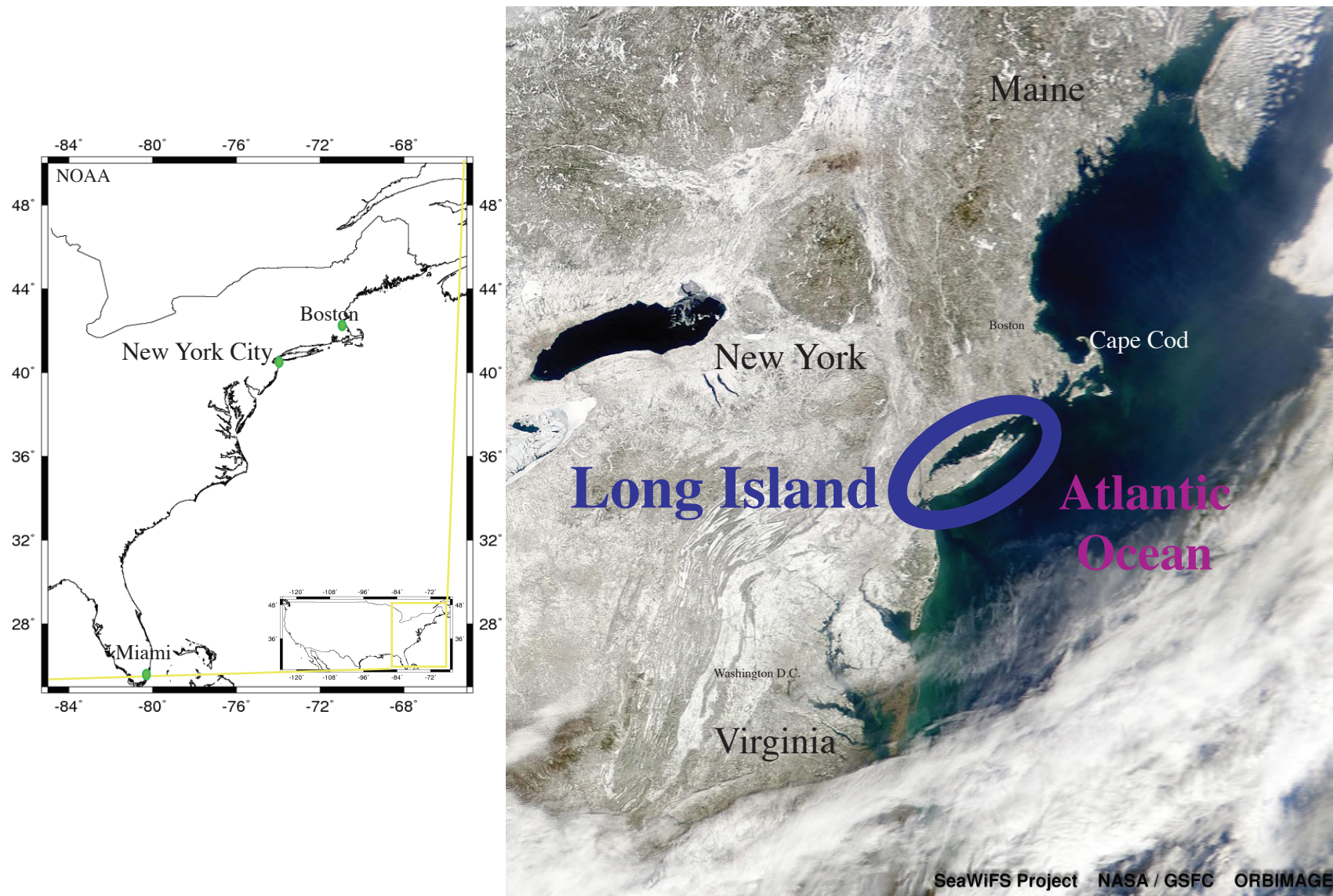
Fig. 1.4: Topography of Long Island (UGSS DEM/ NOAA bathymetry from NGCDC, Amante & Eakins, 2009). Hills along the North and South Shore, continuing along the North and South Forks, show the Harbor Hills and Ronkonkoma Morraine (Veatch, 1903; Fuller, 1914; Olcott 1999). Peconic Estuary is circled.
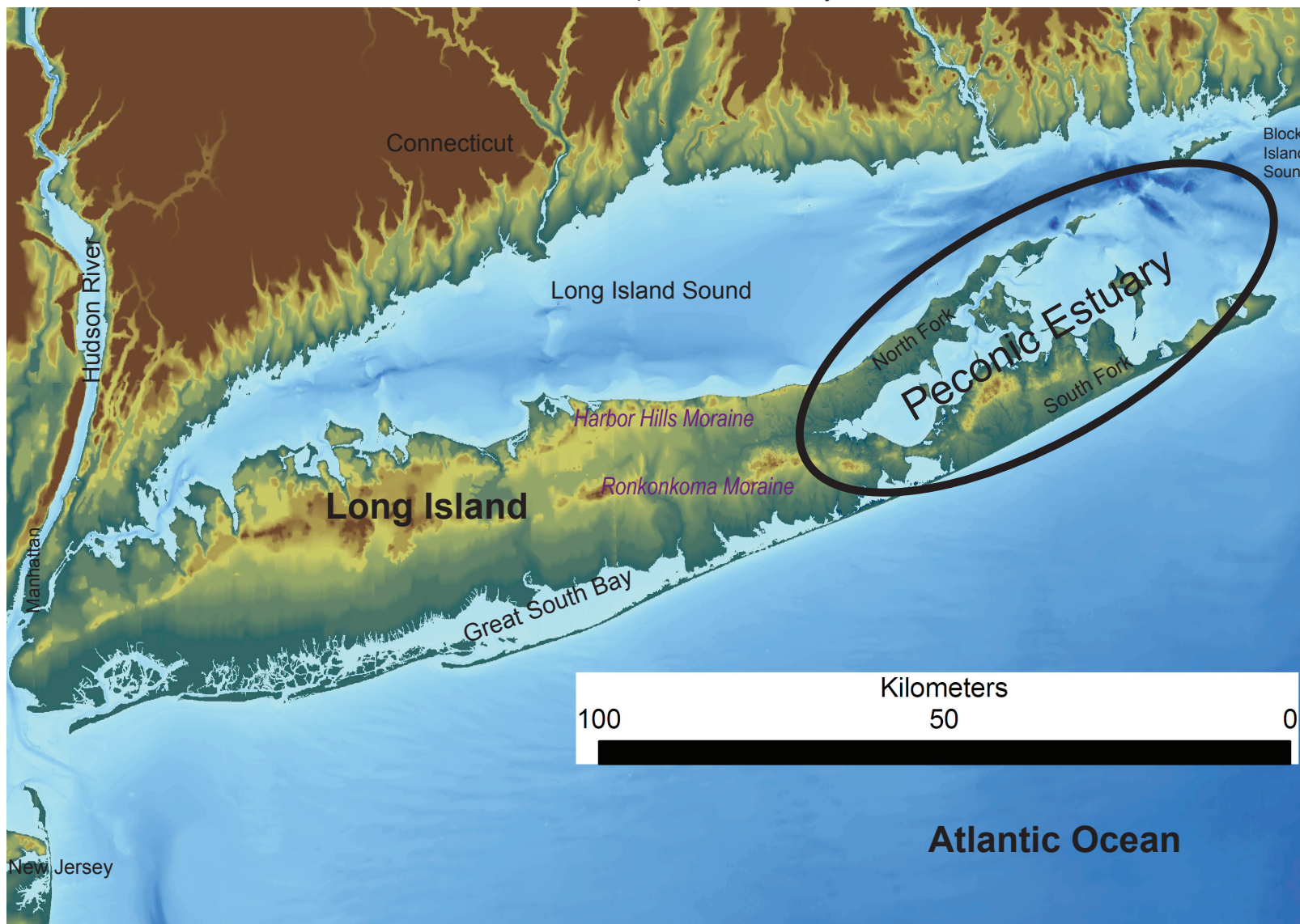
Fig. 1.5: SST view of Gulf Stream and shelf waters. Proximity of Long Island and the Peconic Estuary to the influence of both the Gulf stream (warm & saline) and the cold (& fresher) shelf waters from the North (from the Scotian Shelf). Water from the Labrador current makes its way south via Scotian Shelf and Gulf of Maine. (Satellite derived SST monthly composites from University of Maine). Febuary 2003 (right) and August 2004 (left) are shown. In the August image, an orange patch corresponding to Gulf Stream eddy water can be seen in the lower right hand corner. The cooler greens and light blues can be seen to the north, and in a patch around 70 W near Cape Cod and islands. The right, winter, image shows a warmer patch of water in the lower right hand corner that is influenced by the Gulf Stream. Note that the patch of warmer water in this winter image is much father away from shore than the warm patch shown in the summer image. These images (SST (AVHRR) images) are from Thomas, A., Satellite Oceanography Lab, School of Marine Science, University of Maine, wavy.umeoce.maine.edu).
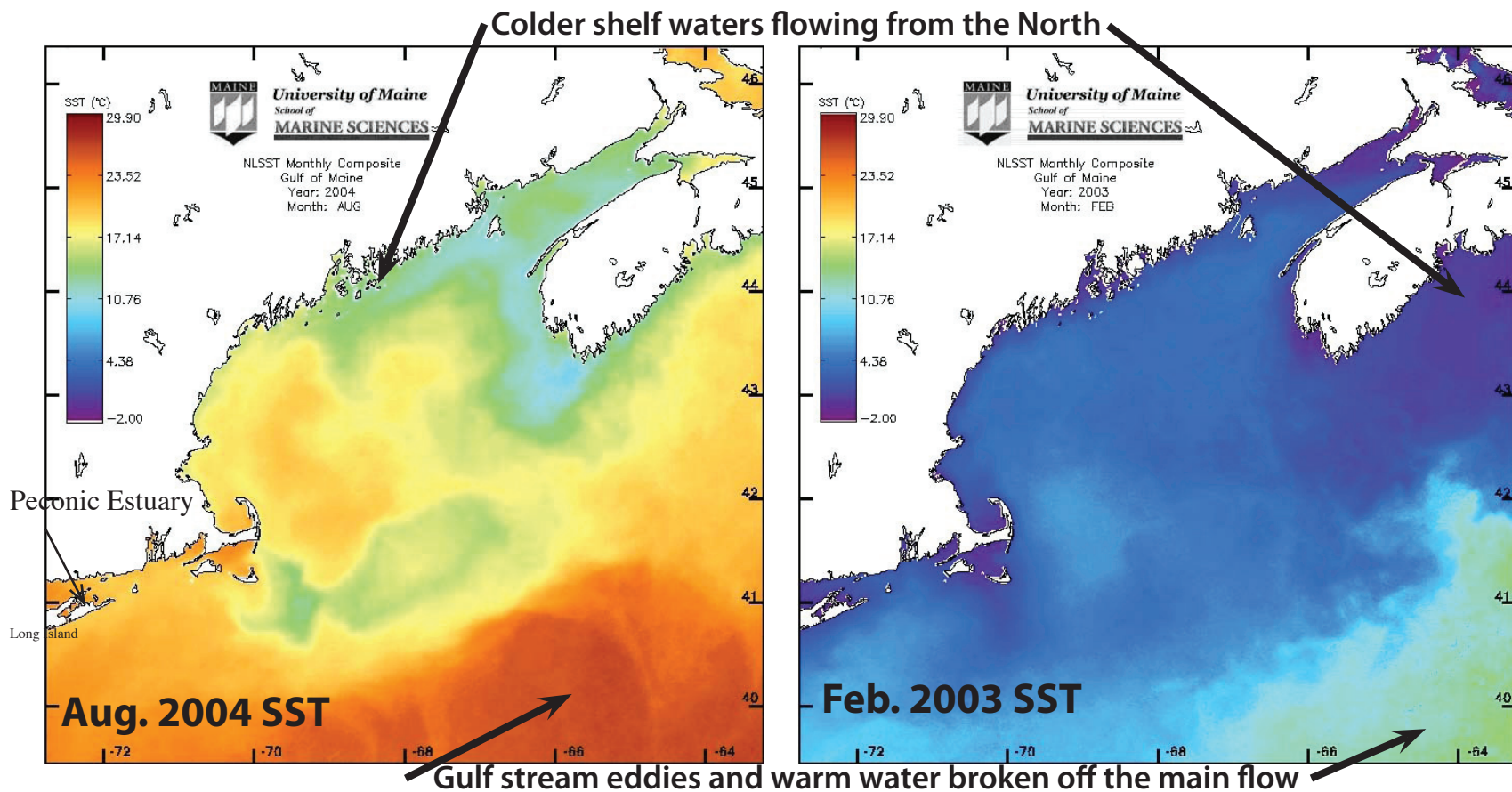
Fig. 1.5: Position of the Gulf Stream and Labrador and Scotian Shelf Currents compared to Long Island and the Peconic Estuary reprinted from Sachs (2007).
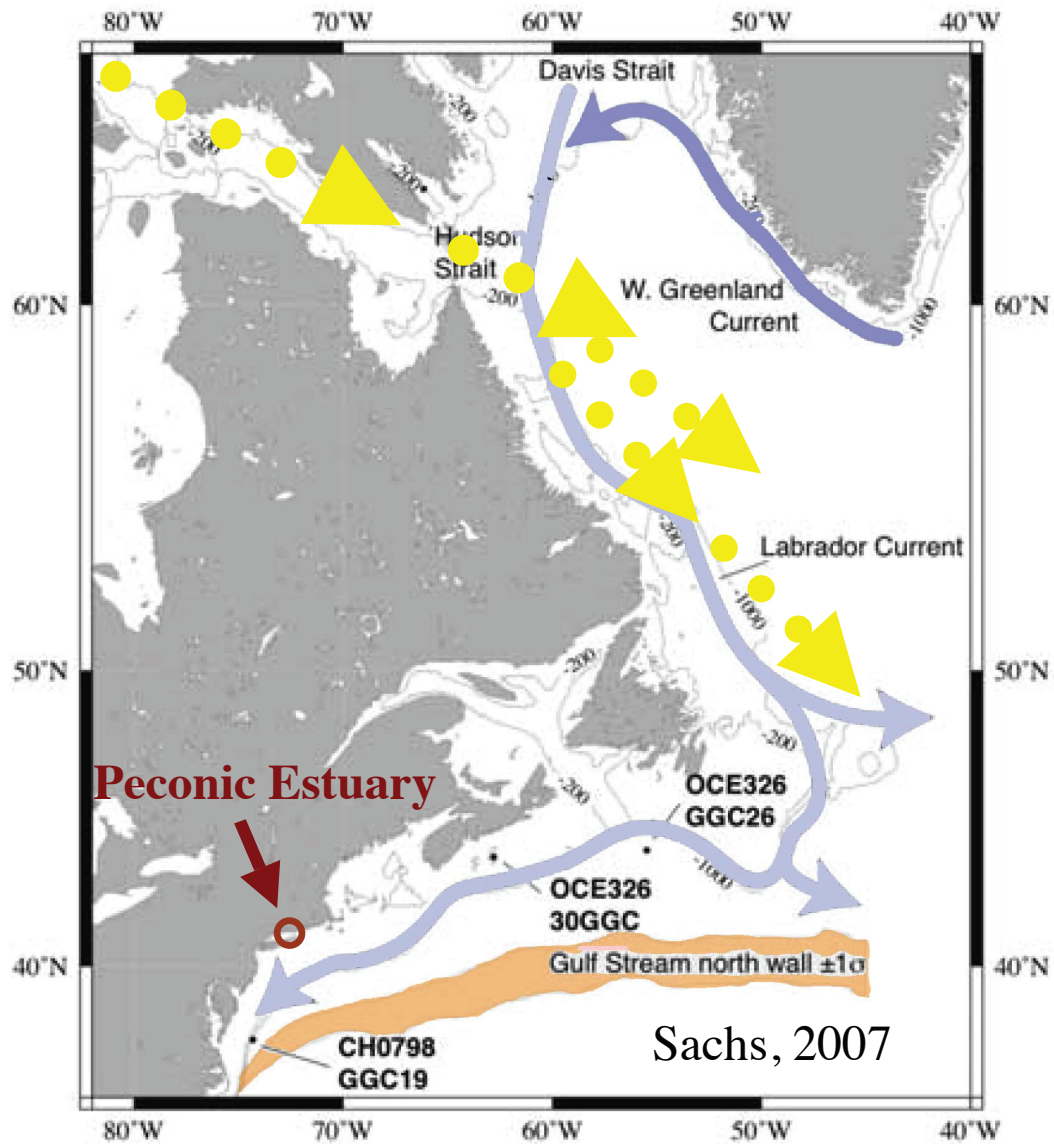
Fig. 1.6: Residual tidal flow (M2) from Gomez-Reyes (1989) over bathymetry map of the Peconic Estuary. Faster currents can be seen bewteen the narrow constrictions of the Estuary.
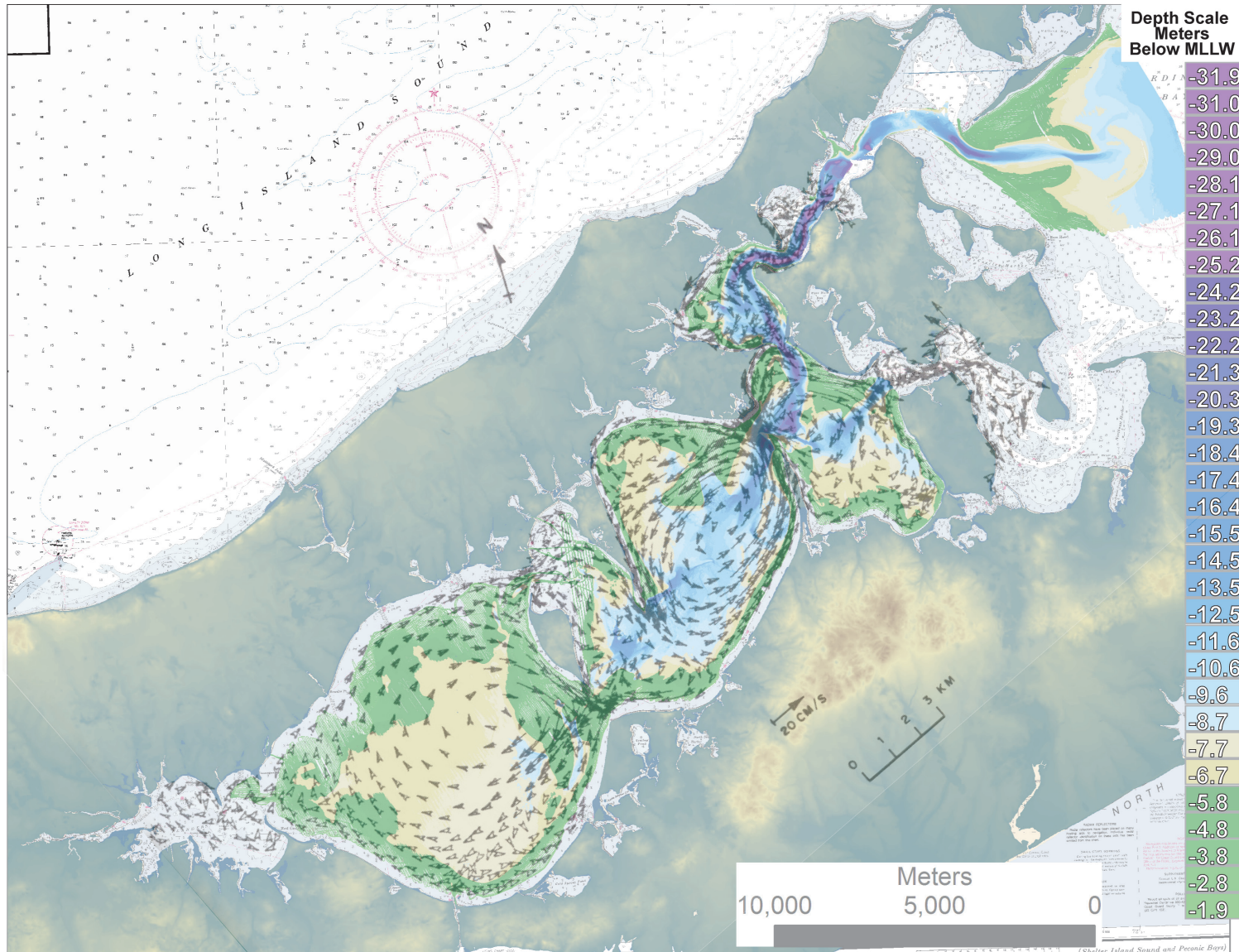
Fig. 1.7: Sub-bottom seismic profile showing buried mounds and exposed mounds.
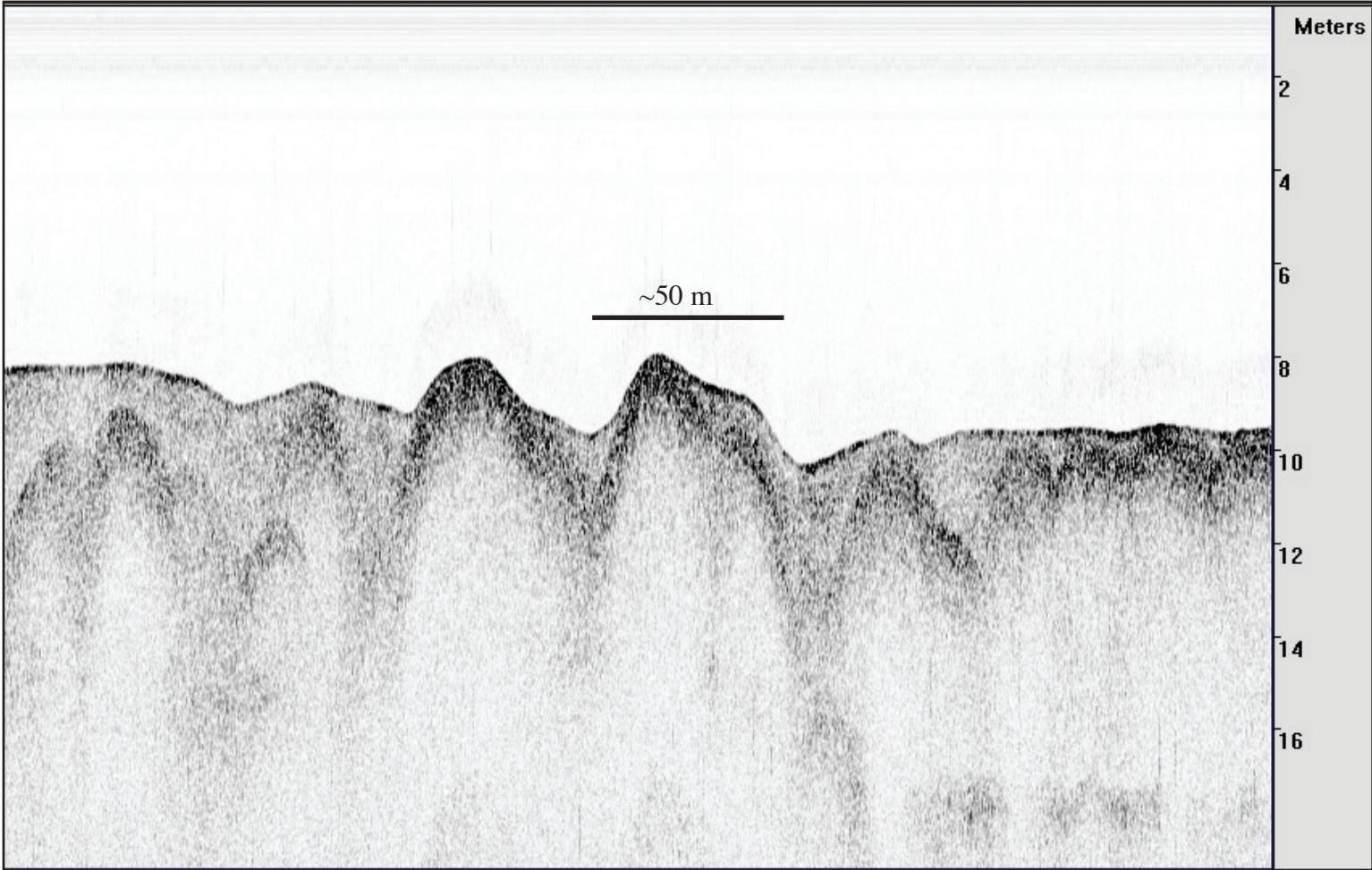
REFERENCES:

Adams, E. W., Grotzinger, J. P., Watters, W. A., Schroder, S., McCormick, D. S., Al-Siyabi, H. A., 2005, Digital characterization of thrombolite-stromatolite reef distribution in a carbonate ramp system (terminal Proterozoic, Nama Group, Namibia), AAPG Bulletin, v. 89, p. 1293-1318.

Alley, R. B., Meese, D. A., Shuman, C. A., Gow, A. J., Taylor, K. C., Grootes, P. M., White, J. W. C., Ram, M., Waddington, E. D., Mayewski, P. A., and Zielinski, G. A., 1993, Abrupt Increase in Greenland Snow Accumulation at the End of the Younger Dryas Event: Nature, v. 362, no. 6420, p. 527-529.

Alley, R. B., Mayewski, P. A., Sowers, T., Stuiver, M., Taylor, K. C., Clark, P. U., 1997, Holocene climatic instability: A prominent, widespread event 8200 yr ago, Geology, v. 25, n. 6, p. 483-486.

Alley, R. B., Ágústsdóttir, A. M., 2005, The 8k event: cause and consequences of a major Holocene abrupt climate change, Quaternary Science Reviews, v. 24, p. 1123–1149.

Altermann, W., 2008, Accretion, Trapping and Binding of Sediment in Archean Stromatolites—Morphological Expression of the Antiquity of Life, Space Science Reviews, v. 135, p. 55–79.

Amante, C., Eakins, B. W., 2009, ETOPO1 1 Arc-Minute Global Relief Model: Procedures, Data Sources and Analysis. NOAA Technical Memorandum NESDIS NGDC-24, March 2009, 19 p.

Anderson, J.B; Rodriguez, A. B; Milliken, K T; Taviani, M., 2008, The Holocene evolution of the Galveston estuary complex, Texas; evidence for rapid change in estuarine environments, Response of upper Gulf Coast estuaries to Holocene climate change and sea-level rise: Special Paper - Geological Society of America, v. 443, p. 89-104.

Bard, E., Hamelin, B., Delanghe-Sabatier, D., Deglacial Meltwater Pulse 1B and Younger Dryas Sea Levels Revisited with Boreholes at Tahiti, Science, v. 327, i. 5970, p. 1235-1237.

Bates, R. L., Jackson, J. A., eds.,1984, (AGI) Dictionary of Geological Terms, Anchor Books.

Beck, A. J., Rapaglia, J. P. Cochran, J. K., Bokuniewicz, H. B., Yang, S., 2008, Submarine groundwater discharge to Great South Bay, NY, estimated using Ra isotopes, v. 109, i. 3-4, p. 279-291.

Belknap, D. F., Kraft, J.C., 1981, Preservation Potential of Transgressive Coastal Lithosomes on the U.S. Atlantic Shelf, Marine Geology, v. 42, n. 1-4, p. 429-442.

Bond, G., Showers, W., Cheseby, M., Lotti, R., Almasi, P., deMenocal, P., Priore, P., Cullen, H., Hajdas, I., Bonani, G., 1997, A Pervasive Millennial-Scale Cycle in North Atlantic Holocene and Glacial Climates, Science, v. 278, n. 14, p. 1257-1266.

Bratton, J. F., S. M. Colman, E. R. Thieler, R. R. Seal, 2003, Birth of the modern Chesapeake Bay estuary between 7.4 and 8.2 ka and implications for global sea-level rise: Geo-Marine Letters, v. 22, p. 188-197.

Brennan, D. J., 1973, Sediment and water characteristics, Peconic Bays, Long Island, New York, Northeastern Section, 8th Annual Meeting, Abstracts with Programs - Geological Society of America, v. 5, n. 2, p. 141-142.

Breuer, E., Sañudo-Wilhelmy, S. A., Aller, R. C., 1999, Trace metals and dissolved organic carbon in an estuary with restricted river flow and a brown tide, Estuaries, v. 22, p. 603–615.

Carbotte, S. M., Bell, R. E., Ryan, W. B. F., McHugh, C., Slagle, A., Nitsche, F., Rubenston, J., 2004, Environmental change and oyster colonization within the Hudson River estuary linked to Holocene climate, Geo-Marine Letters, v. 24, p. 212–224.

Cattaneo, A., Steel, R. J., 2003, Transgressive deposits: a review of their variability, Earth Science Reviews, v. 62, p. 187-228.

Chen, Z. and K. Osadetz, 2006. Undiscovered petroleum accumulation mapping using model based stochastic simulation. Mathematical Geology, v. 38, p. 1-16.

Collier, K., Bokuniewicz, H., Coffey, R., 2005, Submarine Groundwater Discharge along Fire Island, NY, Long Island Geologists Conference 2005, Stony Brook, NY.

Cook, H. E., Zhemchuzhnikov, V. G., Zempolich, W. G., Zhaimina, V. Y., Buvtyshkin, B. M., Kotova, E. A, Golub, L. Y., Zorin, A. , Lehmann, P, Alexeiev, D. V., Giovannelli, A., Viggi, M., Fretwell, N., LaPointe, P., Carboy, J., 2002, Devonian and Carboniferous Carbonate platform facies in the Bolshoi Karatan, Southern Kazakhstan; outcrop analogs for coeval carbonate oil and gas fields in the North Caspian Basin, Western Kazakhstan, in Cook, H. E., W. G. Zempolich, SEPM (Society for Sedimentary Geology), ed., Special Publication-Society for Sedimentary Geology, Paleozoic carbonates of the Commonwealth of Independent States (CIS) : subsurface reservoirs and outcrop analogs, v.74: Tulsa, Oklahoma, SEPM, p. 81-122.

Cronin, T. M., R. Thunell, G. S. Dwyer, C. Saenger, M. E. Mann, C. Vann, R. R. Seal II, 2005, Multiproxy evidence of Holocene climate variability from estuarine sediments, eastern North America, Paleoceanography, 20, PA4006.

Cronin, T. M., Dwyer, G. S., Kamiya, T., Schwede, S., Willard, D. A., 2003, Medieval Warm Period, Little Ice Age and 20th century temperature variability from Chesapeake Bay, Global and Planetary Change, v. 36, n. 1-2, p. 7-29.

Davies, D. S., Isles, T. A., Daly, J., Fischer, L., Frisenda, T., Leogrande, V., Lind, C., Verbarg, R., Waide, D., Walsh, C., Kennedy, K., Sonnichsen, D., Burns, Hon. B. B., Cohen, E., Walter, P. E., Dawydiak, P. E., Fahey, C., Guldi, Hon. G., Kotula, Vice Chairman J., LaValle, Secretary Wells, P. , Lessard, Lt. D., McAllister, K., McMahon, J., Potter, Hon. J., Proios, G., Sawicki, J., Jr., Semlear, Hon. J., Siller, Hon. G., 2002, Policy Guidance for Suffolk County on Shellfish Cultivation in Peconic And Gardiners Bays, Report of the Suffolk County Aquaculture Committee, June 2002, Suffolk County Department of Planning, Hauppauge, New York June 2002, 90 p. http://www.co.suffolk.ny.us/planning.

Davies, D. S., Isles, T. A., Fischer, L., Verbarg, R., Di Cola, L. M., Lind, C., Daly, J., Frisenda, T., Leogrande, V., Walsh, C. E., 2003, Survey Plan for Shellfishing Cultivation Leasing for Gardiner's and Peconic Bays, April, 2003, Suffolk County Department of Planning, Suffolk County Department of Health Services, Suffolk County Department of Public Works, Suffolk County, NY.

DiLorenzo, J. L., 1986, The Overtide and Filtering Response of Inlet/Bay Systems [PhD Dissertation], MSRC, Stony Brook University.

Donnelly, J. P., Cleary, P., Newby, P., Ettinger, R., 2004, Coupling instrumental and geological records of sea-level change: Evidence from southern New England of an increase in the rate of sea-level rise in the late 19th century, Geophysical Research Letters, v. 31, p. L05203.

Drinkwater, K. F. Belgrano, A., Borja, A., Conversi, A., Edwards, M., Greene, C. H., Ottersen, G., Pershing, A. J., Walker, H., 2003, 'The Response of Marine Ecosystems to Climate Variability Associated With the North Atlantic Oscillation', The North Atlantic Oscillation: Climatic Significance and Environmental Impact: Geophysical Monograph 134, American Geophysical Union, Washington, DC, p. 211-34.

Dulaiova, H., Burnett, W. C., Chanton, J. P., Moore, W. S., Bokuniewicz, H. J., Charette, M. A., Sholkovitz, E., 2006, Assessment of groundwater discharges into West Neck Bay, New York, via natural tracers, Continental Shelf Research, v. 26, i. 16, p. 1971-1983.

Eisel, M. T., 1977, Shoreline survey; Great Peconic, Little Peconic, Gardiners, and Napeague bays, Special Report - Marine Sciences Research Center, State University of New York, n. 5, p. 37.

Ellison, C. R. W., Chapman, M. R., Hall, I. R., 2006, Surface and Deep Ocean Interactions During the Cold Climate Event 8200 Years Ago, Science, v. 312, p. 1929-1932.

Flood, R. D., Kinney, J., Weaver, M., 2006, Underwater Landscape Evolution in the Peconic Bays (Long Island, NY) as revealed by High-Resolution Multibeam Mapping, Eos Trans. AGU, vol. 87, no. 52, Fall Meet. Suppl., Abstract H33B-1506, Dec 2006.

Flood, R.D., Cerrato, R., Kinney, J., 2009, Benthic Mapping and Habitat Classification in the Peconic Estuary, Phase II, Final Report to the Long Island Chapter of the Nature Conservancy.

Flood, R. D., Kinney, J., 2009, New Insights on the Origin of the Peconic Bays from a New Detailed Bathymetric Map, Sixteenth Conference on the Geology of Long Island and Metropolitan New York, Long Island Geologists, March 2009 Meeting, Stony Brook, NY.

Fuller, M. L., 1914, The Geology of Long Island New York: United States Geological Survey Professional Paper 82.

Galtsoff, P. S., 1964, The American Oyster, Crassostrea Virgina Gemlin, Fish and Wildlife Service, Fishery Bulletin v. 64, p. 457.

Greene, C. H., A. J. Pershing, 2003, The flip-side of the North Atlantic Oscillation and modal shifts in slope-water circulation patterns: Limnology and Oceanography, v. 48, p. 319-322.

Gutierrez, B. T., Uchupi, E., Driscoll, N. W., Aubrey, D. G., 2003, Relative sea-level rise and the development of valley-fill and shallow-water sequences in Nantucket Sound, Massachusetts, Marine Geology, v. 193, p. 295-314.

Hameed, S., Piontkovski, S., 2004, The dominant influence of the Icelandic Low on the position of the Gulf Stream northwall, Geophysical Research Letters, v. 31, n. 9, p. L09303(1-4).

Hardy, C. D., New York Ocean Science Laboratory, 1976. A preliminary description of the Peconic Bay estuary. Stony Brook, N.Y., Marine Sciences Research Center State University of New York.

Huvaz, O., Sarikaya, H., Isik, T., 2007, Petroleum systems and hydrocarbon potential analysis of the northwestern Uralsk basin, NW Kazakhstan, by utilizing 3D basin modeling methods: Marine and Petroleum Geology, v. 24, p. 247-275.

Ingersoll, E., 1881, The Oyster-Industry, The History and Present Condition of the Fishery Industry, Report on the oyster-industry of the United States, U.S. Department of the Interior, Washington D.C., Government Printing Office, Prepared under the Direction of Prof. S.F. Baird, U. S. Commissioner of the Fish and Fisheries and by G. Brown Good, Assistant Direction U.S. National Museum and a staff of associates.

i-cubed, USDA, NAIP, USGS, 2009, Digital Orthophotographs produced through USGS,USDA, NAIP, distributed by the company i-cubed for automatic linkage to use in ArcGIS 10, last accessed 2012.

Jia, C. Z., B. L. Li, X. Y. Zhang, Li, C. X., 2007, Formation and evolution of the Chinese marine basins: Chinese Science Bulletin, v. 52, p. 1-11.

Katuna, M. P., 1974, The sedimentology of Great Peconic Bay and Flanders Bay, Long Island, New York [M.S. Thesis]: Flushing, NY, United States, Queens College (CUNY), 97 p.

Kinney, J., Flood, R. D., 2006, Multibeam Bathymetry Reveals a Variety of Sedimentary Features in the Peconics Potentially Significant to Management of the System, Long Island Sound Research and New England Estuarine Research Society Joint Conference, October 26-28, 2006, United States Coast Guard Academy, New London, CT. Paper in Long Island Sound Research Conference Proceedings 2006.

Kinney, J., Flood, R. D., 2007, Multibeam Sonar Reveals Mound Features Associated with Oyster Terrain in the Peconics Estuary, Fourteenth Conference on the Geology of Long Island and Metropolitan New York, Long Island Geologists, April 2007 Meeting, Stony Brook, NY.

Kinney, J., Flood, R. D., 2007, Possible Association of Oyster Terrain Mound Features in the Peconic Estuary on Long Island, NY with 8.2ka Meltwater Pulse? Eos Trans. AGU, v. 88, n. 52, Fall Meet. Suppl., Abstract H34B-07, December 2007, San Francisco, CA.

Kinney, J., Flood, R. D., 2008, Peconic Estuary "Oyster Terrain": Carbonate Mound Transgressive Sequence? Fifteenth Conference on the Geology of Long Island and Metropolitan New York, Long Island Geologists, April 2008 Meeting, Stony Brook, NY.

Kinney, J., Flood, R. D., 2009, Holocene Reefs and the Evolution of the Peconic 'Oyster Terrain', Sixteenth Conference on the Geology of Long Island and Metropolitan New York, Long Island Geologists, March 2009 Meeting, Stony Brook, NY.

Kinney, J., Flood, R. D., 2011, Investigation of the Peconic Estuary, Long Island, NY Reveals Clues to the Evolution of an Estuarine 'Oyster Terrain', ASLO meeting February 2011, San Juan, Peurto Rico.

Kirby, M.X., Soniat, T.M., Spero, H.J., 1998, Stable isotope sclerochronology of Pleistocene and Recent oyster shells (Crassostrea virginica): Palaios, v. 13, p. 560–569.

Kirby, M. X., 2000, Paleoecological Differences Between Tertiary and Quaternary Crassostrea Oysters, as Revealed by Stable Isotope Sclerochronology, Palaios, v. 15, p. 132–141.

Kraeuter, J. N, Ford, S., Cummings, M., 2007, Oyster Growth Analysis: A Comparison of Methods, Journal of Shellfish Research, v. 26, n. 2, p. 479-491.

Lightfoot, K. G., Kalin, R., Moore, J., Contributions: Cerrato, R. , Conover, M., Rippel-Erikson, S., 1987, Prehistoric Hunter-Gatherers of Shelter Island, New York: An Archaeological Study of the Mashomack Preserve. Contributions of the University of California Archaeological Research Facility No. 46. University of California, Berkeley, California.

MacIntyre, I.G., Pilkey, O. H., Stuckenrath, R., 1978, Relict Oysters on United-States Atlantic Continental-Shelf - Reconsideration of Their Usefulness in Understanding Late Quaternary Sea-Level History, Geological Society of America Bulletin, v. 89, i. 2, p. 277-282.

Mel'nikov, N. V., Sitnikov, V. S., Vasil'ev, V. I., Doronina, S. I., Kolotova, L. V., 2005, Bioherms of the Lower Cambrian Osa Horizon in the Talakan-Upper Chona zone of petroleum accumulation, Siberian platform: Russian Geology and Geophysics, v. 46, p. 834-841.

Merrill, A. S., Emery, K. O., Rubin, M., 1965, Ancient Oyster Shells on Atlantic Continental Shelf: Science, v. 147, p. 398-400, *DOI:10.1126/science.147.3656.398, http://www.sciencemag.org/content/147/3656/398.abstract?sid=49bc8db0-fc26-48c4-8ee4-6be0920c8965*.

Milliman J. D., Emery K.O., 1968, Sea Levels during the Past 35,000 Years, Science, v. 162, i. 3858, p. 1121-1123.

Moore W. S., 1996, Large groundwater inputs to coastal waters revealed by Ra-[226] enrichments. Nature, v. 380, n. 6757, p. 612-614.

Moore, W. S., 1999, The subterranean estuary: a reaction zone of groundwater and sea water, Marine Chemistry, v. 65, p. 111-125.

NASA, GeoEye, 2005, SeaWifs Satellite Imagery come from NASA and are distributed through GeoEye. Image originally a satellite image of the day from NASA, and NOAA Operational Significant Event Imagery, last accessed 2005, http://www.osei.noaa.gov, http://earthobservatory.nasa.gov, http://www.geoeye.com

NOAA & USGS 2009, ETOPO1 Global Relief Model, NOAA Bathymetry and USGS Topography at 1 arc minute scale available at National Geospatial Data Clearinghouse through www.ngdc.noaa.gov as custom grids (15 arc seconds for the east coast), last accessed 2010
http://www.ngdc.noaa.gov/mgg/gdas/gd_designagrid.html?dbase=grdet1.

Olcott, P. G., 1999, USGS OFR 1999-559: Ground Water Atlas of the United States

Connecticut, Maine, Massachusetts, New Hampshire, New York, Rhode Island, Vermont HA 730-M, Surficial and Northern Atlantic Coastal Plain aquifer systems, Long Island, http://capp.water.usgs.gov/gwa/ch_m/.

Reinhardt, E. G., Stanley, D. J., Patterson, R. T., 1998, Strontium isotopic-paleontological method as a high-resolution paleosalinity tool for lagoonal environments, Geology, v. 26, n. 11, p. 1003–1006.

Riding, R., 2002, Structure and composition of organic reefs and carbonate mud mounds: concepts and categories, Earth-Science Reviews, v. 58, n. 1, July 2002 , p. 163-231.

Rohling, E., Palike, H., 2005, Centennial-scale climate cooling with a sudden cold event around 8,200 years ago, Nature, v. 434, p. 975 –979.

Sachs, J. P., 2007, Cooling of Northwest Atlantic slope waters during the Holocene: Geophysical Research Letters, v. 34, p. L03609 (1-4).

Saenger, C., Cronin, T., Thunell, R., Vann, C., 2006, Modelling river discharge and precipitation from estuarine salinity in the northern Chesapeake Bay: application to Holocene paleoclimate, The Holocene, v. 16, p. 467-477.

Schöne, B. R., 2008, The curse of physiology—challenges and opportunities in the interpretation of geochemical data from mollusk shells, Geo-Marine Letters, v. 28, p. 269–285.

Schubert, C. E., 1998, Areas contributing ground water to the Peconic Estuary and ground-water budgets for the North and South Forks and Shelter Island, eastern Suffolk County, New York: U.S. Geological Survey Water-Resources Investigations Report 97-4136, 36 p., 1 pl.

Schubert, C. E., 1999, Ground-Water Flow Paths and Traveltime to Three Small Embayments within the Peconic Estuary, Eastern Suffolk County, New York, U.S. Geological Survey Water-Resources Investigations Report 98-4181, 43 p.

Stanley, J. G., M.A. Sellers, 1986, Species profiles : lifehistories and environmental requirements of coastal fishes and invertebrates (Mid-Atlantic)--American oyster. U. S. , *in* F. W. S. B. Rep., ed., U.S. Army Corps of Engineers, 25 p.

Stieglitz, T., Rapaglia, J., Bokuniewicz, H., 2008, Estimation of submarine groundwater discharge from bulk ground electrical conductivity measurements, Journal of Geophysical Research, v. 113, n. C8, p. 15.

Stoffer, P. W., Chamberlain, J. A., Jr., Scal, Roland, Messina, Paula, 2005, Late Quaternayr and early Holocene fossils from New York City beaches; implications for stability in coastal environments in western Long Island and New Jersey, Geological

Society of America, 2005 annual meeting, Oct 15-19, 2005, Abstracts with Programs – Geological Society of America, v. 37, n.7, p. 366.

Surge, D., K. C. Lohmann, D. L. Dettman, 2001, Controls on isotopic chemistry of the American oyster, Crassostrea virginica: implications for growth patterns: Palaeogeography Palaeoclimatology Palaeoecology, v. 172, p. 283-296.

Surge, D. M., Lohmann, K. C., Goodfriend, G. A., 2003, Reconstructing estuarine conditions: oyster shells as recorders of environmental change, Southwest Florida, Estuarine Coastal and Shelf Science, v. 57, n. 5-6, p. 737-756.

Thomas, A., School of Marine Science, University of Maine, SST imagery last accessed 2011, wavy.umeoce.maine.edu.

Thomas, E., Varekamp, J. C., Avener, E., 2006, Multiproxy records of Eutrophication in Long Island Sound Geological Society of America Abstracts with Programs, , 2006 Annual Meeting, Oct 22-25, 2006, Paper No. 130-10, v. 38, n. 7, p. 323.

Van de Plassche, O., 2000, North Atlantic Climate–Ocean Variations and Sea Level in Long Island Sound, Connecticut, Since 500 cal yr A.D., Quaternary Research, v. 53, p. 89–97.

Varekamp, J. C., 2006, The Historic Fur Trade and Climate Change, Eos, 87, n.52, p. 593, 596-597.

Veatch, O., Stephenson, L. W., 1911, "Geology of the Georgia Coastal Plain", Bulletin No. 26, Geological Survey of Georgia, Foote & Davies Co., p. 240-252, 466.

Visbeck, M., Chassignet, E. P., Curry, R. G., Delworth, T. L., Dickson, R. R., Krahmann, G., 2003, 'The Ocean's Response to North Atlantic Oscillation Variability' The North Atlantic Oscillation: Climatic Significance and Environmental Impact: Geophysical Monograph 134, American geophysical Union Washington, DC, p. 113-146.

Wilson, R. E.,Viera, M. E. C., 1989, Residiual Currents in the Peconic Bays Estuary, Estuarine Circulation, eds. Bruce J. Neilson, Albert Kuo, John Brubaker, Huama Press Inc., Cresent Manor, Clifton, NJ, p. 87-96.

Xin, G., 1993, Strontium Isotope Study of the Peconic River Watershed, Long Island, New York [M. S. Thesis], State University of New York, Stony Brook.

CHAPTER 2: CHARACTERIZING THE 'OYSTER TERRAIN'

INTRODUCTION:

An 'Oyster Terrain' associated with mound features thought to be relict oyster reefs that cover an extensive area of the Peconic Estuary on Long Island, NY has been revealed by multibeam bathymetry and seismic profiles (Fig. 2.1). This terrain consists of exposed mounds typically ~2 m high, but as tall as 4 m in exposed relief, 10 to 50 m in diameter and associated with high backscatter (Fig. 2.1). The surfaces of mounds are associated with stained and unarticulated oyster shells recovered in grab samples, but no living oysters (Fig. 2.1). By examining the characteristics of features based on the multibeam backscatter and bathymetry data obtained as part of an ongoing benthic habitat mapping project we can distinguish relatively high backscatter regions associated with the mound morphology (Fig. 2.1). We need to fully characterize this distinctive mound pattern, as well as the setting of this terrain in order to understand this terrain. Mounds topped by oyster shells suggest oyster reefs, but more characterization of these features is needed to support this theory. Seismic profiles throughout the bays are also needed to characterize the mounds both to resolve example patches of separate mounds and to show their distribution and evolution in the system in order to understand their origin. The presence of oyster aquaculture in the Peconic Estuary and other anthropogenic activities are also important to discuss in order to discern if the mounds are indeed relict oyster reefs. Here we map out and describe this terrain in order to compare the terrain characteristics with modern oyster reefs seen elsewhere. This Oyster Terrain may represent a more widespread morphology that may capture an early Holocene climate. Characterization of this terrain will help to see what potential there may be for climate records and for insight into other transgressive terrains.

METHODS: Multibeam

Multibeam bathymetry surveys were conducted as part of a Benthic Habitat Mapping project, in the Peconic Estuary, on Long Island, NY (Flood et al., 2003; Flood et al., 2009). Bathymetric and backscatter data was collected using an EM 3000D echosounder operating at 300 kHz. Thus far, this project has mapped most of the Peconic Estuary inside of (to the west) of Shelter Island, that is greater than ~2 m deep within navigable waters. This project included use of sidescan sonar operating at 100 kHz that allowed recording of backscatter data into water of ~2 m or less within navigable waters as the side-scan sonar swath occasionally reached to the shore in places. Multibeam swath coverage was 100% throughout much of the area, although less than 100% for waters shallower than 4.5 m as survey lines were spaced at a minimum 45 m apart in water 4.5 m or shallower. Most of the data focused on here was collected in surveys from summer 2006 to winter 2008 which consisted of Phases II and III of the benthic mapping project. The surveys in Phase II used a pole-mounted dual-head system and were conducted during the summer to fall/winter of 2006. The surveys in Phase III used a hull-mounted dual-head system and were conducted in fall 2007 and early winter 2008. All surveying was conducted on the 28-foot School of Marine and Atmospheric Sciences (SoMAS) research vessel the R/V Donald W. Pritchard.

Data from the surveys in Phase I of the Benthic Habitat Mapping Project conducted in 2001/2003 are also included in the base maps of the entire Peconic Estuary Benthic Habitat Mapping data set. Multibeam data from Phase I of the benthic mapping study adjacent to Robins Island was previously reported by Arlotta (2003), Flood et al. (2003), Maher (2006), and Cerrato & Maher (2007).

NOAA tidal data for the region is available along with predicted values based on historical deployments (NOAA, 2009a, b). Additionally, tide gauges were deployed in different parts of the estuary near survey areas to measure water level during the surveys. Some variations in tidal amplitude and the timing of the tides were expected

due to length and a number of constrictions in the estuary separating different bays as can be seen from the NOAA historical gauges. All depths were calculated with respect to mean low low water (MLLW) as defined at the NOAA tide gauge at South Jamesport. Meteorological variations between bays like wind-induced surge variations are not factored into our tidal offsets. Overlapping sections of map areas are checked for height offsets as part of our processing. This approach is used to assure that the correct offsets have been used. Offsets on the order of 0.25 m were applied in some bays between gauges.

Data processing was done using the OMG–UNB (Ocean Mapping Group, University of New Brunswick) SwathEd Program (Hughes Clarke, 1998; Ferrini, 2004; Beaudoin, 2002). The final bathymetric grid and backscatter tiff data files were created using the OMG programs. All multibeam data was gridded at 1 m resolution. ESRI ArcGIS[TM] and Fledermaus[TM] (IVSD3, 2009) have been used to display and interpret data. Shaded relief maps have been made using OMG SwathEd programs, as well as in ArcGIS [TM] with the "Hillshade" tool. Shaded relief was then superimposed over backscatter and bathymetry as a semitransparent layer in ArcGIS 9.3 [TM]. This was done to allow one to highlight the shapes of different features with respect to both the backscatter and depth. ArcScene[TM] in ESRI ArcGIS 9.3[TM], along with Fledermaus[TM] were used to depict 3D views of the datasets. Depth contour line files and layers were produced by ArcGIS[TM].   Basemaps include USGS 7.5 DEM topographic data (USGS 2008), and NOAA charts (NOAA, 2010). NOAA (2011) historical charts were available for comparison.

Mounds were identified in the first ~22 square kilometer area that was surveyed (summer 2006) in Eastern Little Peconic Bay by two independent approaches as the mounds were identified based on backscatter and shaded relief separately. A set of points was created in an ESRI shapefile with each point representing the top of a mound in a subset area of multibeam survey. A combined map superimposing backscatter on shaded relief was used to compare these features. The comparison of both techniques helped to distinguish mounds that were buried. Histograms of the

number of mounds per depth range were produced in Matlab^{TM} from the point (latitude, longitude, depth) information. This information was used to help define the depth ranges to highlight on the maps.

Sediment Sampling:

Grab samples were taken using a modified van Veen Grab Sampler to ground truth features based on backscatter and morphology, including the mounds described in this study. Sampling was conducted from the SoMAS vessels the R/V Pritchard and R/V Paumanok. Visual descriptions were made in the field. Further analysis and more detailed visual descriptions were made in the lab, including comments on the presence of oyster shells. More detailed descriptions of sediment analysis are found in Chapter 5.

Seismic Data:

Seismic lines ran parallel to the multibeam survey lines when possible to give regional coverage in a portion of the Peconic Estuary, and a smaller high resolution survey of an exposed patch of mounds and an adjacent muddy area was also conducted to give more detail in a small area. Seismic lines were collected using an Edgetech SB-424 portable sub-bottom profiler using full spectrum CHIRP swept frequencies that was loaned by Liviu Giosan at Woods Hole Oceanographic Institution (WHOI) (Fig. 2.2). Swept frequency pulse technology is referred to by the name CHIRP or Chirp or Compressed High Intensity Radar Pulse even though it is being used with acoustic rather than radar swept frequency radio pulses. The SB-424 Chirp operates in the 4 - 24 kHz range and is designed to have a vertical resolution of features down to 4 to 8 cm with typical penetration of sediments ranging from 2 to 40 m (Edgetech, 2009). This vertical feature resolution is close to the scale of the multibeam system, and gave sufficient resolution and depth penetration to capture the layers of interest. The sub-bottom profiler data was recorded in SEGY format. Edgetech Chirp Discoverer^{TM} program, SMT Kingdom Suite^{TM}, SeisSee^{TM}, and Fledermaus^{TM} (Edgetech, 2009; SMT,

2009; Pavlukhin, 2004; Pavlukhin, 2011; IVSD3, 2009) were used to manipulate and display the seismic profiles.

The sub-bottom profiler towfish was towed off of the side of vessel during surveying. The towfish was always towed off of the port side near the stern of the vessel during both the 2006 and 2008 surveys in the Peconic Estuary. In order to plot seismic data over multibeam data as accurately as possible we need to take into account the offset at which the sub-bottom profiler towfish was towed compared to the multibeam GPS navigation recorded (Fig. 2.2). The towfish moves quite a bit depending on boat speed, turning, wave conditions etc., so there is some uncertainty in its exact location or orientation. A sound velocity of 1500 m/s was used.

RESULTS:

Multibeam bathymetry of the Peconic Estuary ranges from ~2 m to ~32 m. Our survey area excluded the shallow perimeter of the bays shown in the NOAA chart, thus our survey area average is deeper than an average of the entire bay. The deepest areas in our survey, greater than 22 m, are adjacent to Shelter Island. The bases of these channels have faster flow morphologies such as larger sand waves. Little Peconic and Noyack Bays are deeper than some of the other bays in the Peconic Estuary. Little Peconic and Noyack Bays are deeper both in terms of average depth (approximately 7.5 m) within the survey area and maximum depth (~24 m). Its average depth is about 6.5 m when including the shallow perimeter based on NOAA charts. For instance the eastern half of Great Peconic Bay has an average depth of 5.7 m and a maximum depth of 13.9 m within our survey areas (Fig. 2.3). Little Peconic and Noyack Bays also seems to have higher current speeds than most of the Peconic Estuary based on exposed morphology and active features, in this case sand waves, (Fig. 2.3). This pattern of higher flow in Little Peconic and Noyack Bays has been verified by current measurements (Viera, 1990, Gomez-Reyes, 1989).

The generalized distribution pattern of sediment types, including the presence of shells, within the Peconic Estuary can be seen in the backscatter (Fig. 2.3). Muddy sediments have low backscatter values, with the very lowest (darkest) backscatter values always corresponding to the finest mud, i.e. with the least shell or other coarser material present. High backscatter areas represent coarser or harder materials, such as shells or coarse sand.

The most distinct features revealed in the high resolution multibeam bathymetry and backscatter surveys of the Peconic Estuary are the elevated mounds with high backscatter that compose the Oyster Terrain (Figs. 2.3, 2.4). These features are distinctive with diameters of 10 to 50 m typical for individual mounds. Exposed mounds were typically ~2 m high in relief, with some reaching close to 4 m (Figs. 2.3-2.5). The mounds can be seen to be considerably higher in backscatter than surrounding sediments (Figs. 2.1, 2.5). Large backscatter variability allows one to distinguish the high backscatter mound areas from surrounding sediment types even with the variation in the mixture of sediment and shells in grabs throughout the bay. The Oyster Terrain maintains a fairly distinctive pattern even with the range of backscatter values.

Most of the area of exposed Oyster Terrain is found in Little Peconic Bay and Noyack Bay (Fig. 2.4). An example of high backscatter associated with mounds can be seen depicted in Little Peconic Bay, which is a wide basin (Fig. 2.4). Not all the mounds are as circular or distinctive as others, but all maintain a rounded shape (Figs. 2.1, 2.5). Regardless of shape, even when they are more amorphous, the exposed mounds are consistently identifiable in the backscatter as higher backscatter areas. The shallowest mounds are consistently components of what resemble broader more massive bank structures where numerous individual mounds have merged into a few structures or one structure. In addition to banks, mounds that form linear patterns are another common pattern.

While there does seem to be some kind of more random distribution of mounds in certain areas, the multibeam bathymetry shows these features often line steep

channel walls, as well as seeming to outline channels that may have been deeper in the past and have now infilled. The channels have gradients sloping into the center of the bays and towards Shelter Island in the east. A dendritic pattern of mounds seem to outline channel systems in at least one area.

Mound Distribution:

Over 10,000 mounds are found within Little Peconic and Noyack Bay including isolated mounds, and any mound shape that composes a small conglomeration or a larger conglomeration such as a bank or chain (Fig. 2.6). One may notice that these mounds do not appear in the very shallow areas. The distribution of these mounds is from ~6 to 18 m. This pattern initially found within the 22 square kilometer subset of mounds, was found to have the same range and a similar peak in the 10,000 mound set (Fig. 2.7). Almost all of the mounds were found below 5.5 to 6 m depth, with only a few mounds found as shallow as 6 m. The peak abundance of mounds appears between 8-13 m. Analysis of shallow areas included the multibeam swath bathymetry, which had wide enough individual swaths even in the shallowest regions to check for mound morphology similar to that in the Oyster Terrain. We see little evidence of these kinds of mounds in the shallower deposits of the estuary either in the multibeam or in the more complete sidescan coverage of shallow areas.

A distribution of ~6 to 18 m in depth of exposed mound tops, suggests that these features may have been active when sea level was somewhat lower (Fig. 2.7). If we plot the peak abundance of mound as 8 to 12 m offset by 2 m of water as common water depth along a sea-level curve, we would estimate that the mounds would have been last active around 3,000 years ago (Fig. 2.7).

The area of exposed reef covers an extensive area, and close to 13 square kilometers of dense high backscatter Oyster Terrain are found within Little Peconic Bay (Fig. 2.8). This excludes areas with a few isolated mounds exposed, and areas with lower backscatter where oyster shells probably have a few centimeters of mud over

them. The dense mound areas, outlined in red, can be seen in contrast with the individual mound points shown as dots.   Areas outlined in red typically have a lot of mounds. However, the size of mounds included in the full mound data set varied widely from large mounds in banks to numerous small individual mounds of only about 10 m in diameter in Little Peconic Bay (Fig. 2.8).

When we look elsewhere in the Peconic Estuary, we begin to see evidence for even more mounds in depths greater than 6 m, and especially deeper than 8 m (Figs. 2.3, 2.6). For example we see mounds exposed in depths greater than 6 m in Southold Bay and Great Peconic Bay. Seismic profiles across other parts of the estuary reveal yet even more fields of mound structures in this depth range buried beneath the mud in places like Great Peconic Bay. Consistently, mound tops could be seen at depths of 8 to 14 m with a peak in the distribution at about 10 to 12 m. The seismic profiles suggest that thousands of mounds are buried within the estuary in addition to the 10,000 mounds exposed within Little Peconic and Noyack Bays. The only areas where we do not see much evidence for mounds is beneath the shallow sand banks along the perimeter of the bays. This suggests mounds cover about 100 square kilometer of estuary based on exposed mounds and similar patterns in locations where we have sub-bottom seismic profiles.

Oyster Shells:

In Phase I and Phase II 74 grab sites in Great Peconic, Little Peconic and Noyack Bays were chosen from the top of high backscatter mounds, which were associated with disarticulated oyster shells 100% of the time (Fig. 2.9). Some of these mound tops are composed mostly of shell with only a small percentage of mud or sand in grabs. The portion of shell to sand/mud volume (clastic mud) varies from a few shells in sediment to shell with some sediment, but the presence of large oyster shell pieces is consistent. Oyster shell hash composes a significant percentage (>50% by volume) of the coarse fraction of sediment in many of these sites, but the mud is primarily clastic and at least some of the sand is clastic too. The gravel and sand fraction is more likely

to include biogenic carbonate grains such as shell hash. If a layer of fresher sediment draped a site, sometimes shells were buried enough that they were not immediately obvious when the sediment sample was described on board ship.

These shells generally have thicknesses of greater than 1 or 2 cm and the thicknesses of some shells are greater than 2.5 cm. These shells are much thicker than aquaculture shells, which are typically less than 0.5 cm thick based on the samples we have examined (Fig. 2.10). There are some smaller thinner relict shells, but at least some portion of those shells tend to be greater than 1 cm thick. Many shells are stained a rusty red brown color, which did not seem to wash off, and some of the buried shells have a blackish stain. Sometimes this black oxidized to a rusty red-brown when exposed to the air once the mud was washed off. The shells recovered from the mounds are often in poor physical condition (Fig. 2.10). Many shells are very corroded and worn to pieces a few centimeters long and they are often characterized by pits and holes. Shells found in mud are typically visibly corroded, whereas shells in sand may look more worn by physical weathering. The tendency to have corroded shells in muds is probably related to higher pCO_2 (lower pH) in anoxic muddy sediments than in sandy sediments (Morse, 2005; Walter et al., 1993).

As noted above, many shells bear numerous small round bored holes ranging from less than 1 mm to 5 mm or so that are made by a sponge, *Cliona,* that lives on oyster shells (Fig. 2.10). Examples of similar holes are reported in the literature on oyster shells found in grabs from the shelf (Merrill et al., 1965), and they can be seen in their bottom photographs of these shells. Similar examples of bore holes made by the sponge *Cliona* are depicted in Galtsoff (1964). Oyster predators such as an oyster drill, e.g. *Urosalpinx cinerea*, (a type of gastropod) or a boring clam (Galtsoff, 1964) tend to leave individual holes, but the holes made by *Cliona* form a distinctive pattern of holes with variable sizes that may form a network. Mud worms and parasitic worms may also bore holes in oyster shells (Galtsoff, 1964). The boring sponges such as *Cliona* also help to breakdown shells after the organism has died (Galtsoff, 1964; Lescinsky et al., 2002; Lockwood & Work, 2006) and play a significant role in the dissolution of the shells

of the deceased organisms exposed on the bed (Galtsoff, 1964; Milliman, 1974). One shell (grab #13 in 2008 from Noyack Bay) even came up with bright yellow sponge growing on it. No other common predator marks were observed, although no whole articulated shells were recovered. Many predators leave there own marks such as the conch or whelks (e.g. *Busycon carica* and *Busycon canaliculatum*) which leave a characteristic straight line where the edge of the shell gets chipped off a live oyster (Galtsoff, 1964).

Seismic Data:

Mounds can clearly be seen in the sub-bottom seismic profiles with a typically strong reflective layer at the top of the mound, which presumably corresponds to the high-backscatter shell layer observed in the multibeam data. Often the penetration of the signal below the mound surface is very poor although we can see layers beneath and within mounds at times (Fig. 2.2). A layer of coarser material such as coarse sand or shell could cause the highly reflective surface and lack of penetration of the signal below the reflector. Indeed, the surface of the highly reflective mounds exposed at the bed in seismic profiles correlates to oyster shells in grabs. A layer thin layer of coarse material on top of a mound may not mean that sediments beneath the top have the same characteristics as the top of the mound. Gas pockets could also exist below the surface acting to block penetration. However, we know that gas alone is not causing the reflectors based on exposed mounds having the same profile character as buried mounds (Fig. 2.2). Layering within some mounds can be seen and layers below the mounds are occasionally seen (Fig. 2.2).

The seismic profiles show that many mounds are actually 2 to 6 m in height from top of mound to base of mound slope, with the greater height coming from the fact that the mounds are somewhat buried. The average vertical height is greater than 4 m in relief. Examination of the seismic profiles also suggests that these are indeed older features by revealing mounds buried under at least 3 m of sediment that fall within the exposed mound depth range of 6 m to at least 18 m. It may be possible to estimate the

length of time needed to form the mounds and the age when the mounds were last active by estimating growth rates for the mounds through radiocarbon dating. The likely ages of these mounds will be discussed in Chapter 4.

Features:

There is a lot of variability in the Oyster Terrain itself. Analysis of backscatter and shaded relief maps reveals transitions between different types of features including places where mounds in the more quiescent areas of the bay have been draped by mud (Figs. 2.3, 2.4). We can see that the areas with lower backscatter corresponding to mud in grabs from the area, mud which covers some of the mounds that are still visible in the shaded relief. Mounds visible in the shaded relief, but with only slightly higher backscatter than surrounding areas represent mounds that were buried by a thin sediment layers as we find only a few centimeters of mud over shells in grabs from those mounds. Seismic profiles also confirm that mounds with low backscatter often have a layer of sediment on top of them.

Aquaculture:

An important question for the Peconic Estuary is: are surficial sediments patterns of the Oyster Terrain due mostly to anthropogenic activity related to oyster aquaculture or to natural processes. Attempts were made to identify potential anthropogenic morphology and areas that might have had recent anthropogenic activities that could have deposited oyster shells on the bottom. Examples of potential anthropogenic morphology would be dredging for oyster harvesting, stirring up of the bottom with cages, and debris, or craters created by dumped debris or oyster shells. Morphologies of several areas of abandoned and active aquaculture operations matched aquaculture areas on NOAA nautical charts and maps of historical bottom lease areas available on the Suffolk County Planning website (Suffolk County Planning, 2011; County of Suffolk, 2001; County of Suffolk, 2002; County of Suffolk, 2003, Davies et al., 2003). Most aquaculture lease areas did not overlap with mound areas, and thus we do not expect

that grab sampling sites were in areas of large scale aquaculture activities. Morphologies associated with aquaculture did not occur inside of our mound areas and some heavily used aquaculture areas had to be avoided during the survey due to the cages, debris, and floats.

The thickness, amount of wear, rust colored stain, and number of holes in shells are all features which suggest that the Oyster Terrain oyster shells are very old. However, the presence of aquaculture in the area does make it necessary to ensure that the shells we analyzed in detail were not related to aquaculture. To this end we compared aquaculture shells (graciously supplied by Gregg Rivara Cornell Cooperative Extension) with the shells from grabs (Fig. 2.10). The shells in our grab samples from Little Peconic and Noyack Bays had a distinctively different appearance than the modern aquaculture shells. The relict oyster shells from the Oyster Terrain are far thicker than the intact, thin young oyster shells associated with modern Long Island aquaculture in Oyster Bay and the Peconic Estuary. The relict shells also had many more growth bands than modern aquaculture shells (Fig. 2.10). One can see the clear size difference, and even the growth breaks were consistent in the transferred shells. A large growth break associated with a change in direction of growth corresponds to when aquaculture shells were transferred. Other aspects of the morphology are different also. In particular, any of the shells found in the grabs had the narrow long shape of a shell that is typical of a crowded reef rather than an aquaculture shell.

While we avoided sampling in areas with anthropogenic activity in Little Peconic and Noyack Bays, we did sample in such areas in other parts of the study area during the Benthic Mapping Project. Katuna (1973) also sampled in areas denoted as aquaculture leases on NOAA charts. We notice that apparent aquaculture oysters were found in both data sets in Great Peconic Bay near Flanders Bay and in Pipes Cove. Oyster shells from these areas were shallower than the relict mounds and were typically much more recent looking having bright white shells, pearlescent luster and bright muscle scars on the interior side of the shell. Also these were isolated individual shells not associated with hash or with any of the other characteristics of the oyster terrain,

and the shells lacked the physical or chemical wear typical of the terrain shells. This more recent shell morphology more closely resembled the larger examples of aquaculture shells that had been transferred from Mystic to Southold Bay for bottom grow out provided by Gregg Rivara Cornell Cooperative Extension (see Chapter 4).

DISCUSSION:

It has long been known that oysters cannot survive naturally and reproduce in modern conditions of 28 psu within the Peconic Estuary (Ingersoll, 1881) as mentioned in Chapter 1. The presence of relict oyster reefs in the Peconic Estuary thus suggests that they correspond to a time of more favorable conditions. Conditions must have changed within the system to go from being favorable to unfavorable to oyster survival. There is very little change in salinity with storms or seasons. Increased salinity could have resulted from sea level rise without a corresponding increase in freshwater outflow, a regional change in ocean circulation patterns, or a change in regional precipitation patterns in the Northeast.

Many other factors can contribute to oyster mortality, many of which become much more effective at killing oysters when salinities increase. It is often the increase of these other stressors that actually kill oysters under high salinities, rather than high salinity by itself. For instance there are numerous common diseases and predators of oysters that favor higher salinities such as the oyster drill (a gastropod that bores a hole into the oyster to eat it). In some cases it may be that the oysters are merely more susceptible to a given pathogen or predator at higher salinities. Factors such as increased stratification as a result of changes in flow or increased salinity in an estuary could make oysters susceptible to lower oxygen levels, which would be a stress on their health (Lenihan & Peterson, 1998.) Increased salinity or changes in flow may affect other factors such as competition, changes in food substrate, the appearance of other species, or events similar to brown tide blooms that may be detrimental to a standing stock of oyster beds.

Aside from salinity changes, events such as extremely large storms or tsunamis that would act to bury reefs under a layer of sediment could also act to kill off a large oyster population (Milliman, 1974; Galtstoff, 1964). One would expect to see evidence in seismic profiles of a distinctive reflection horizon, and a similar horizon in cores if this was the case on a massive scale. While we see burial of mounds, the composition and distribution of sediment covering mounds is variable. Burial of mounds seems unrelated to a single event. For example migration of sand banks burying mounds may have occurred in the past, by sand overriding individual active mounds on the edges of the steep sandy bay, but this mechanism would not affect the terrain towards the middle of the bay that has mud overlying it.

Modern active oyster reefs are typically associated with shallower water of a few meters to intertidal depths (Stanley & Sellers, 1986; Kreeger et al., 2010; Meinkoth, 1981), but active reefs can be found at greater depths than the tops of deeper mounds we see exposed in the Peconic Estuary, around 18 m. However, only a few mounds are found at 6 m of depth, and none are found above 5.5 m within the Oyster Terrain. Deep mounds may have ceased to grow if they did not keep up with sea level rise and died from increased sedimentation and other stresses. Presumably oysters would have perished when conditions became unfavorable to oyster growth. This is hypothesized to have been in large part a result of increased salinity within the estuary.

The depth span of mounds suggests that the Oyster Terrain was last active thousands of years ago, when sea level was somewhat lower. Lack of oyster reefs in shallow waters less than 5.5 m below MLLW suggests that reefs must have died out when sea level lower was than today, as modern reefs tend to favor shallow water of a few meters. Examples of reefs that were active on Long Island in the 1800's in Great South Bay before being overharvested were in around 2 m of water (Ingersoll, 1881). A significant change in salinity is hypothesized as well, which would also suggest sea level was appreciably lower when the reefs were last active. The range of depths of mound tops and thickness of deposits also suggest that the terrain was active for thousands of years during the Holocene, a period of sea level rise (transgression).

Consistent presence of oyster shells on top of high backscatter mounds suggests that our mounds are relict oyster reefs. Initial sampling of the terrain did not include cores, which would seem necessary to verify that buried features are similar to exposed mounds and that the oysters are not a thin veneer of material on a preexisting feature. If shells are indeed a few thousands years old and have been continuously present at the surface, modification of the features surely has occurred either through addition of new shells of other species, accumulation of selective sediment (e.g. coarse material siliclastics or biogenic carbonate) or erosion and reworking to some extent. This raises the question as to what we can distinguish about this terrain with our sediment samples, which is a topic discussed in Chapter 4.

We examined the possibility of older anthropogenic deposits, i.e. oyster middens, early in the study and dismissed it as not being a likely origin of the mounds. Native American shell middens are common on Long Island and subject to archeological study. Such features are typically associated with charcoal, or other charred or cooked material, bones or other shells that were cooked, and other degraded resistant refuse. Such middens also typically started with cooking pits, had concave bases, and at least for examples from this area for the past few thousand years were about ~4 to 25 m diameter with a thickness of less than 1 m (Lightfoot et al., 1987). These features are smaller than the relict mound features found in the Peconic Estuary, which are up to 4 to 6 m in total relief and with many more than 50 m in diameter. Evidence of different sediment and structure of the interior would also be expected. Based on an examination of shells in the collection of the SBU Anthropology Department from middens on Shelter Island, near a smaller semi-enclosed bay, it appears that midden shells were twice the size of the largest shells in grabs of mounds.

Grabs and cores together may still exclude information about this terrain. The opening of grab and core devices is too small to successfully capture shells as large as those found in middens. This suggests that more large shells are present in the Peconic Oyster Terrain. Any structural integrity of the reefs, and post depositional

movement might be difficult to assess with standard grabs and cores. For instance if any shells are still cemented together in large clumps near the surface it is unlikely that any such shells would come up together intact in a grab. However, the number of successful grabs and shared characteristics of similar shell morphology including apparent age, thickness, size and condition suggest that large clumps of shells and shells too large to fit in a grab would not be the predominant characteristics of the terrain. Areas that would be most likely to have these larger samples though would probably correspond to the most difficult to sample sites with mostly oysters and very little matrix sediment (~80% large shells and ~90% shell and shell pieces > 2mm).

The Oyster Terrain mounds present in the Peconic Estuary may actually represent a more widespread morphology that may not be properly identified in other places if there is not adequate high-resolution survey data or if they are deeply buried. Understanding these kinds of transgressive environments may be valuable, for example, to interpreting deeper seismic records when searching for paleoclimate studies or even petroleum deposits deeper in the geologic record. It is possible that this type of environment may not have been identified in existing records, especially since profiles of these buried mound features could easily be interpreted as gas pockets or some other kind of feature (e.g. a kind of diapir, or mud-gas mounds; Duck & Herbert, 2006; Popescu et al., 2007; Liu, 2004) if based solely on a profile of buried features. The highly reflective surface and lack of penetration of the seismic signal below the reflector could be caused by a change in sediment properties. A layer of coarse material, for instance shells or coarse sand, could cause this reflection, and material such as shell or sand has much poorer signal penetration than mud. However, as one can see from profiles of exposed mounds, these particular features are not due to gas since the gas would be released at the surface where these features are exposed (Fig. 2.2). Our grab samples show us that we have shells rather than coarse sand that would explain this high reflection in the Peconic Estuary. A better characterization of these features would help to distinguish settings where these features might be present.

47

CONCLUSION:

An Oyster Terrain associated with mound features revealed by multibeam bathymetry and seismic profiles covers an extensive area of the Peconic Estuary on Long Island, NY, which may represent a more widespread morphology that may also capture an early Holocene climate record. We believe this to be a relict transgressive deposit composed of oyster reefs. The pattern in this terrain is distinctive enough compared to other features that it may prove useful in distinguishing other similar terrain and features elsewhere where the features are less numerous. This oyster reef terrain is distinguished by relatively high backscatter regions and a mound morphology associated with the oyster shell. Grabs have shown the mounds are topped with characteristic oyster shell sediment. Typically, the mounds are surrounded by modern muddy sediments (Figs. 2.1, 2.3-2.5). Individual mounds can be buried by mud or sand depending upon the modern setting. The high-resolution sub-bottom profiles demonstrated that the mounded terrain continues beneath the muddy sediments. This suggests that Oyster Terrain at one time covered most of the Estuary from Shelter Island to Great Peconic Bay. This statement is supported by observations of mounds in deeper parts of other bays.

The Oyster Terrain is comprised of thousands of mounds, with over 10,000 mounds exposed in the subsets of Eastern and Western Little Peconic Bay and Noyack Bays, with thousands more below the surface and exposed in other parts of the survey. The terrain covers on the order of tens of square kilometers, close to 100 square kilometers in the entire estuary, in a predictable pattern. This terrain and its individual feature components are substantial in size with typical thickness of 2 to 6 m, and diameters of 10 to 50 m for individual mounds, with even larger, massive banks covering 100's of square meters of area. While faster flow has kept large areas exposed, the consistent appearance of buried features is additional evidence of the antiquity of this terrain most likely to be a transgressive sequence including oyster reefs, and not due to recent or historical aquaculture practices. More of this effort to date the shells and the mounds is discussed in Chapter 4. The depth range of ~6 to 18 m

suggests that these mounds are older features and may hold interesting paleoclimate records by preserving carbonate shells with annual growth bands during a time of lower sea level during the mid to early Holocene when paleoclimate records for the region are sparse. Particularly the lack of any mounds above 5.5 m suggests that sea level was lower when the reefs were last active.

Fig. 2.1: Example of mounds (A) and grabs with oysters (B & C) from mounds. Part A shows mound morpohology associated with high backscatter typical of the Oyster Terrain. Relief is shaded and backscatter is shown in color: yellow and orange denote higher values and blue represents lower values. Part B and C grabs from mounds full of old stained oyster shells.
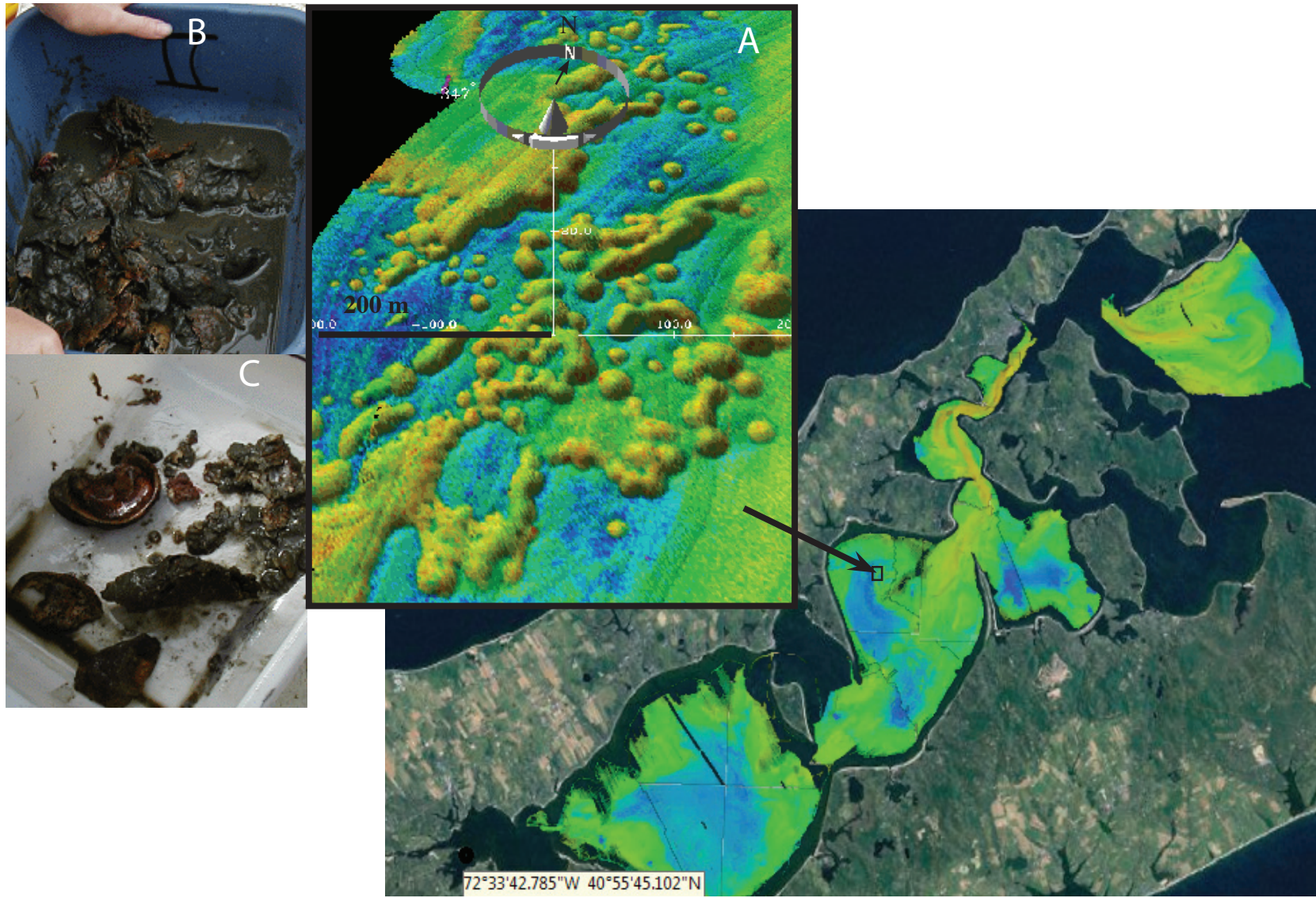
Fig. 2.2: Chirp sub-bottom seismic profiler and profiles.
Top Right: Diagram of Chirp Sub Bottom Seismic Profiler Tow Configuration.
Photographs of the Chirp SB-424 in the field.
Right middle: Lowering of towfish into Great Peconic Bay water.
Right bottom: Chirp starting to get towed. Examples of seismic profiles.
Left Bottom: Horizon below mounds visible in some places.
Left Middle: Exposed and buried mounds can be seen as well as subsurface layers.
Left Top: Example of mounds buried with at least 3 m of sediment.

Diagram of Research Vessel
and Seismic Profiling Towfish
During Survey
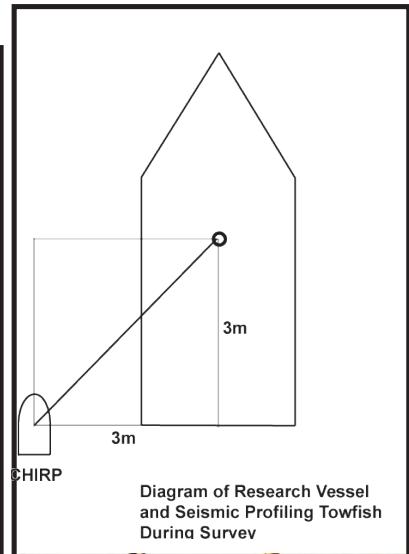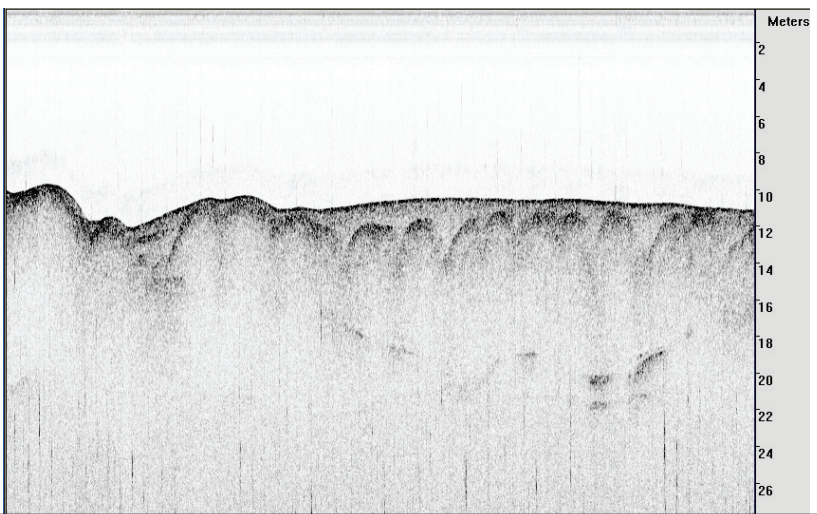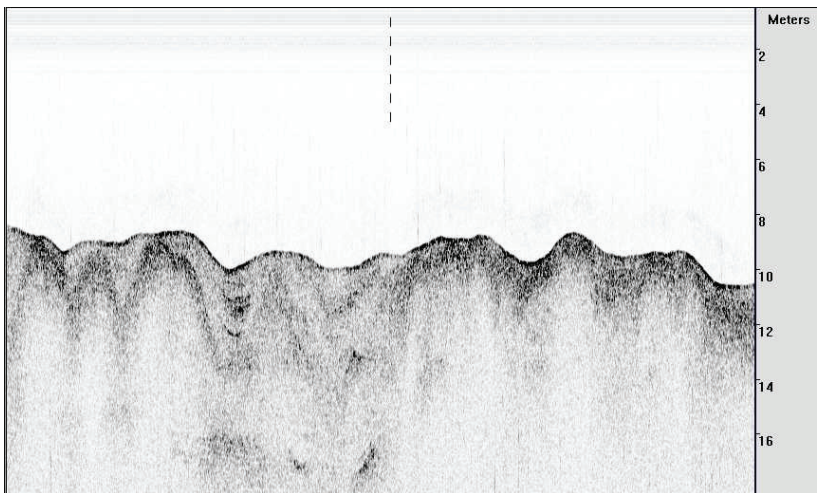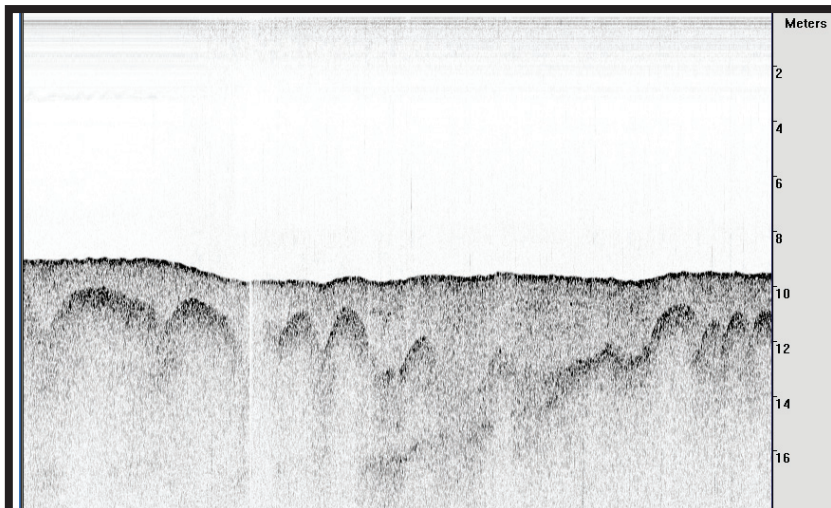
Fig. 2.3: Map of multibeam depth (color) and backscatter and sidescan sonar coverage (greyscale) for the Peconic Estuary Benthic Habitat Mapping Project extending from Great Peconic Bay to Orient Point. Backscatter ranges in greyscale from high values (light colors) to low (darker colors). Multibeam bathymetry with depth scale in meters below mean low low water (MLLW). Areas of higher backscatter correspond to coarser material, which tends to correspond to sand nearshore and or high energy/flow.

53
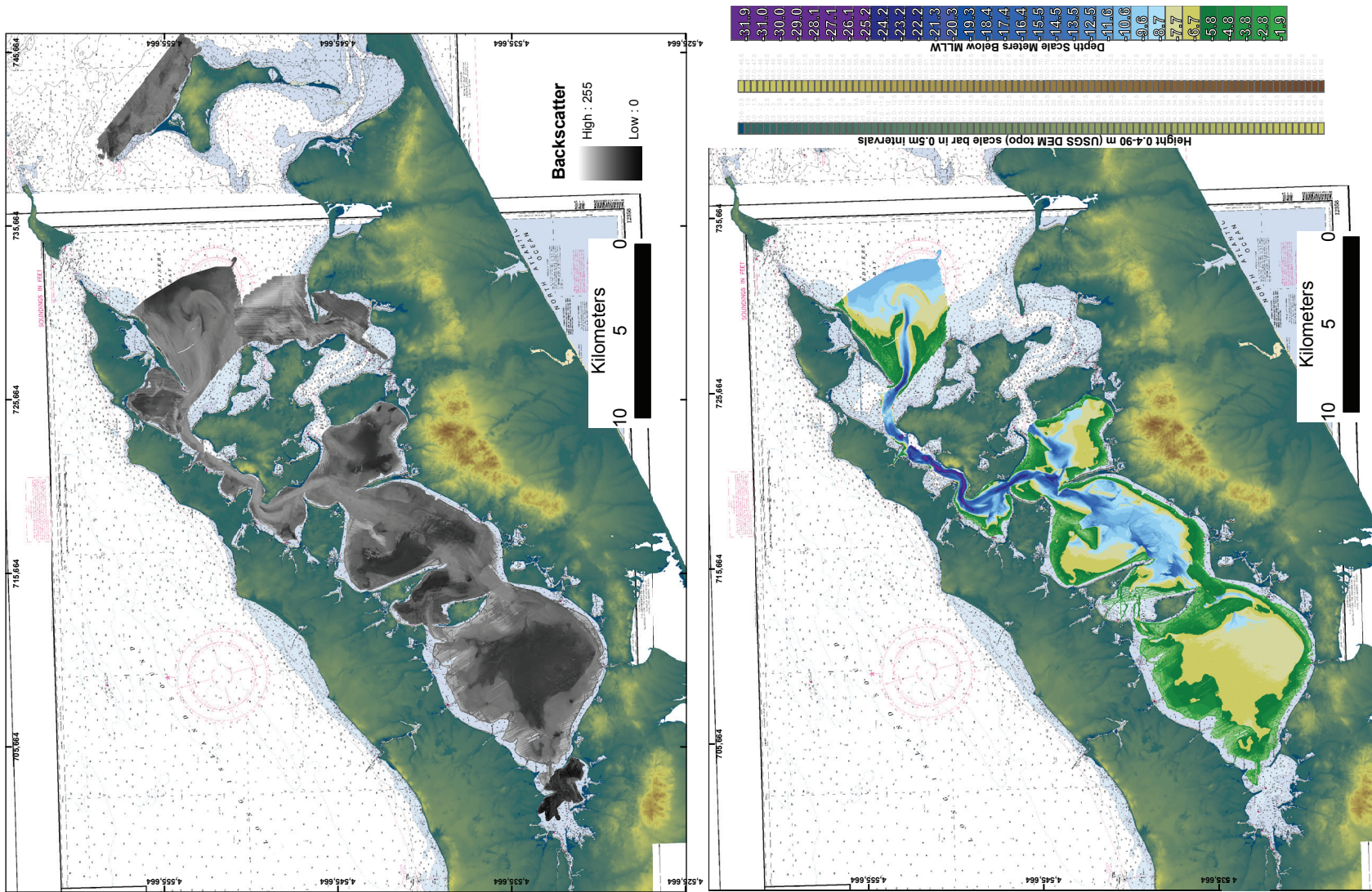
Fig. 2.4: Shaded relief bathymetry and backscatter maps of the focus area (Little Peconic & Noyack Bay). Red outlines focus area.
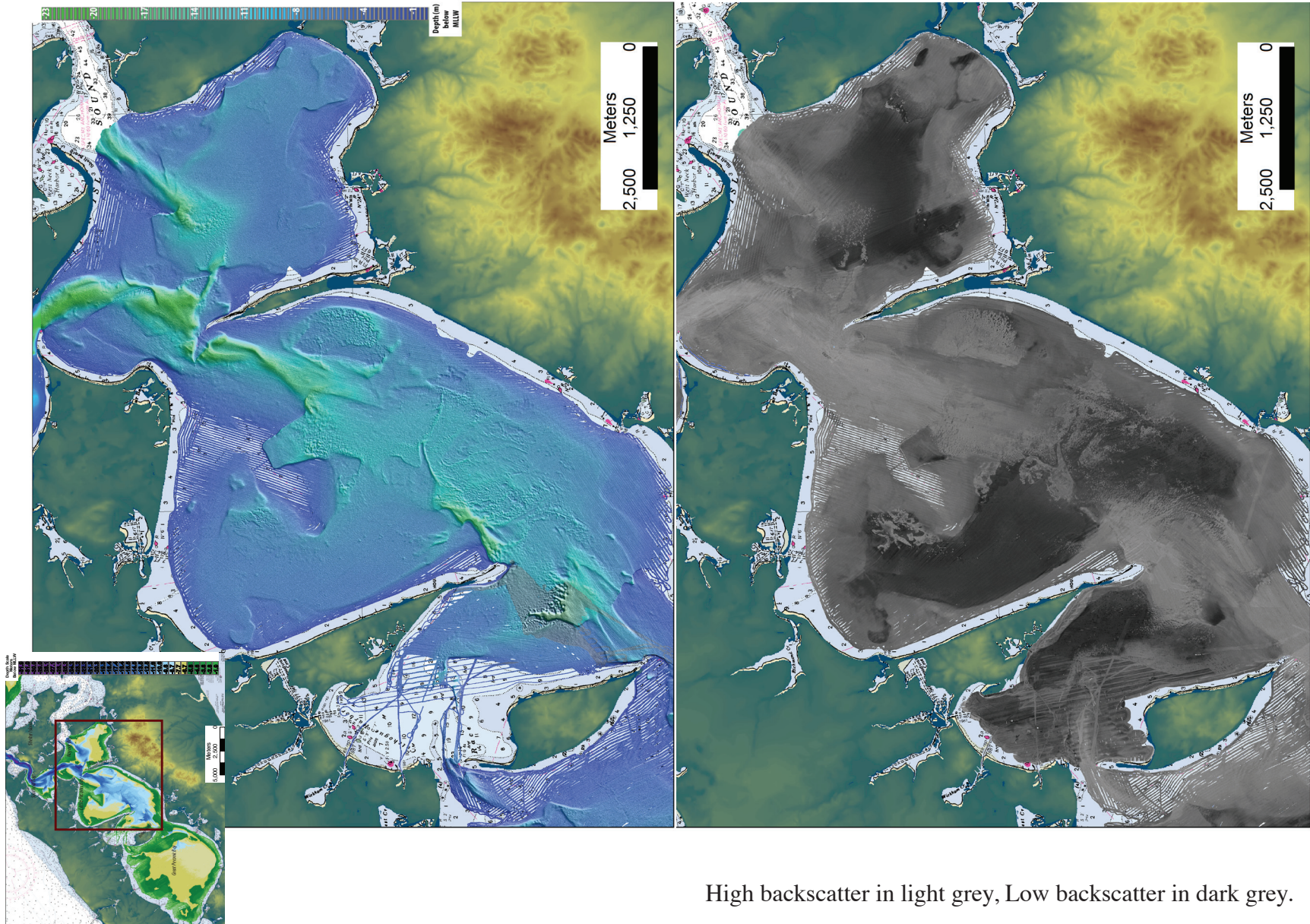
High backscatter in light grey, Low backscatter in dark grey.

Fig. 2.5: Example of configurations and scale of mounds in the multibeam bathymetry. Map of areas in bottom lefthand corner.
A: Bank SE of Jessup's Neck in Eastern Little Peconic Bay. Bank is ~ 1.5 km long. Near the eastern edge of this basin, but still several hundred meters from shore we find some of the shallowest mounds in this basin in within this massive bank. This particular plateau occurs about 7.7 m in depth. Close up of mounds inset. Mounds from 10- 50 m across can be seen. The vertical relief of some mounds of more 3-4 m can be seen in the color change from medium blues at the top of a mound to yellow greens at the base. Transition from individual isolated mounds to a dense bank can be seen in the inset. Greyscale image on the left shows backscatter in greyscale, high=lighter, low= darker. We also see some banks of mound, present at different depths in other areas. Other mound banks form plateaus of mounds at depths of about 6, 9.6 and 13 m (Fig. 2.3, 2.4).
B. Linear patterns or chains of mounds are shown in bathymetry with shaded relief and backscatter. Greyscale image on the left shows backscatter in greyscale, high=lighter, low= darker. This is a zoomed in view of the area shown in C.
C.   Bathymetry with shaded relief shows a 2 km long chain of mounds that is highlighted by a pink line.
D. Isolated Mounds near chain of mounds (Noyack)
E. Dense Field of Mounds. Individual mounds are more seperate than the banks, and the largest mounds are smaller in diameter.

E

D

C

2 km chain of mounds

A

B

Meters
500   250   0

Meters
100 50

Depth (m)
below
MLLW

Meters
500   250   0

Meters
100 50   0

Meters
100 50   0

Meters
2,000   1,000   0

Meters
2,500   1,250   0

Meters
100 50
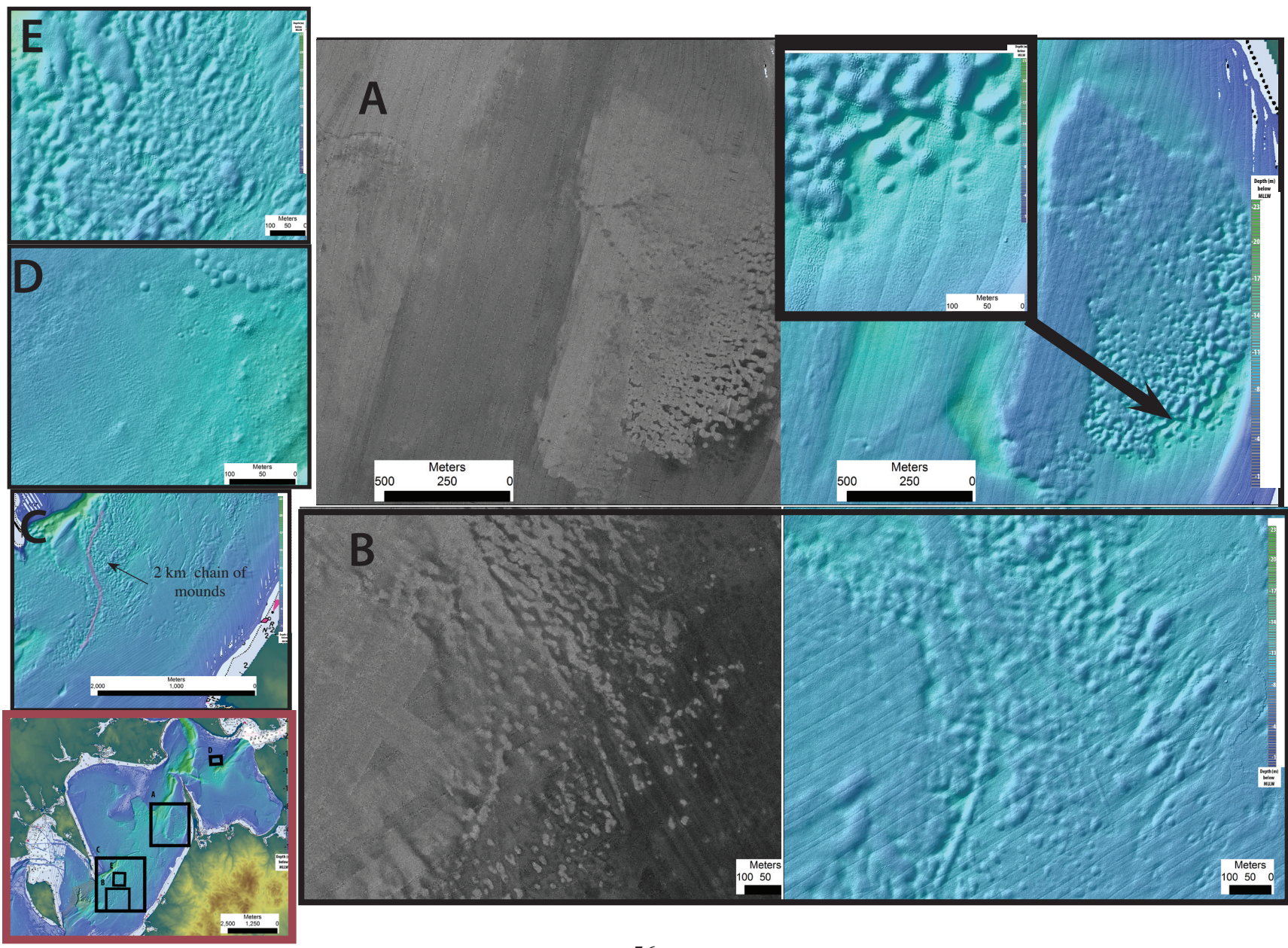
Depth (m)
below
MLLW

Fig. 2.6: Mounds in the focus area (each mound marked in blue) along with depth (left panel) and backscatter (right panel). Shown withd epth and with backscatter. Note the mounds occur in mostly blue (greater than 8 m) and some dark biege areas on the depth map, but none appear in the shallower green depths.
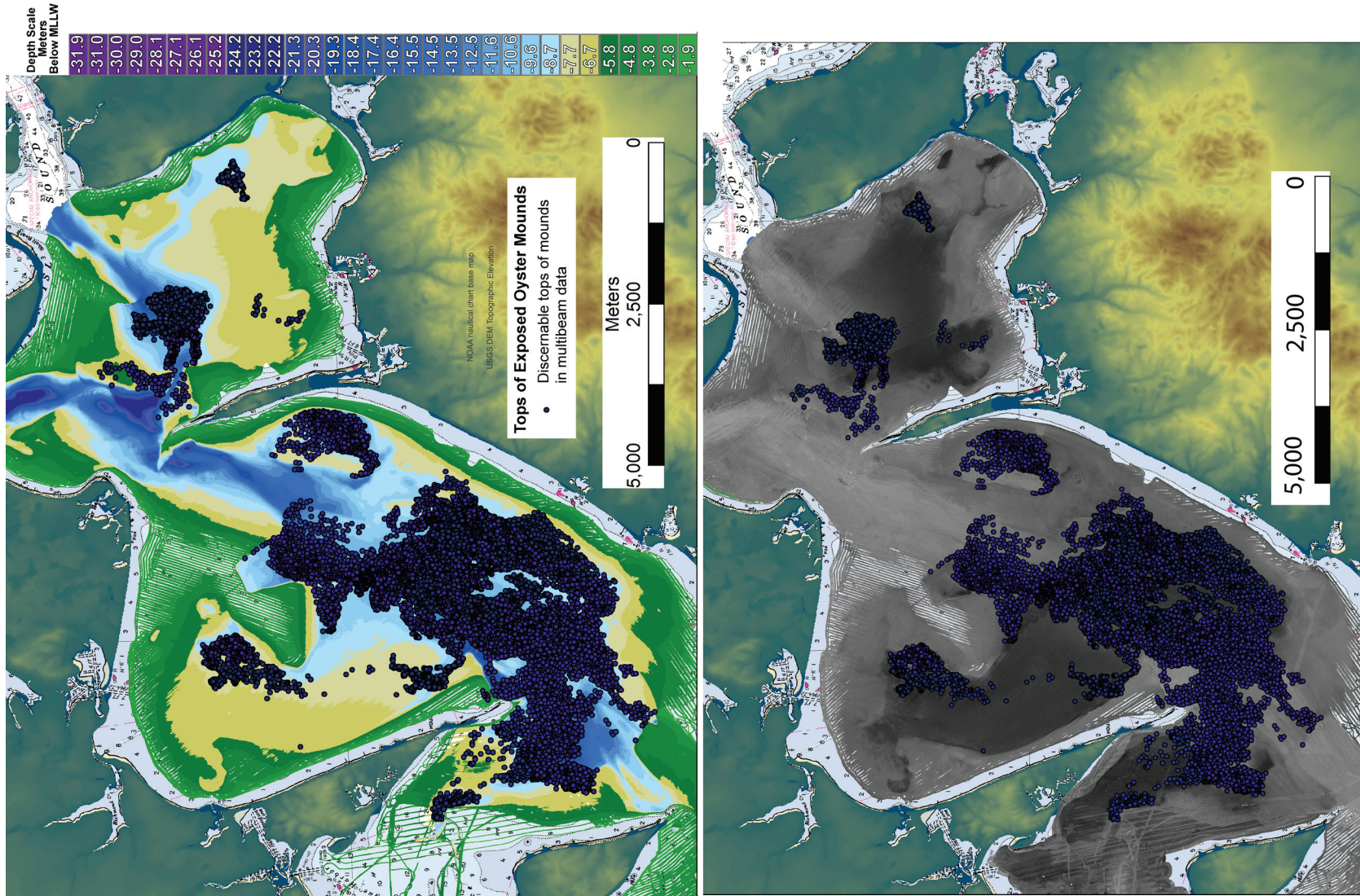
Fig. 2.7: Histogram of ~10,000 exposed mounds in Little Peconic and Noyack Bays. Inset graph of sea-level with mound depths.

Histogram of Depths of All Mounds

# of mounds

Depth (Meters)

Depth Below Present Mean Sea-Level (Meters)

Age (Calibrated Years Before Present)

Base Depth of Mounds

Extrapolation of Age based on SL curve
Depth range of mound tops
Mound tops + 2 m

Sea Level Curves for Nantucket, MA
Redfield and Rubin, 1962
Oldale and O'Hare, 1980
Gutierrez et al., 2003

Modified Sea Level Curve of Gutierrez et al., 2003

Fig. 2.8: The dense high backscatter exposed mound area with backscatter in Little Peconic and Noyack Bays is over 13 square kilometers. Top right inset map shows the same areas over the depth map. Bottom inset shows both mounds counted by points and the areas of dense mounds. Note that isolated mounds are not covered by the dense mound criteria nor are a large area of mounds in the southern portion of Little Peconic Bay. While these isolated mounds have slightly higher backscatter than surrounding sediments the difference was not large and these mounds seem to have a thin layer of mud on them.

Densely clustered high backscatter and mounded relief

• Discernable tops of mounds in multibeam data

Meters

5,000   2,500   0

Depth Scale
Meters
Below MLLW

Outline of 'Oyster Terrain'
Densely clustered exposed features

High Backscatter and mounded relief

1,250 625   0   1,250 Meters

Outline of 'Oyster Terrain'

Backscatter Base Map

Densely clustered exposed mound areas that have high backscatter and exposed mound relief

1,800   900   0   1,800 Meters

Fig. 2.9: Presence of oyster shells in grabs. 100% of grabs from mounds distinguishable by backscatter held oyster shells.

61
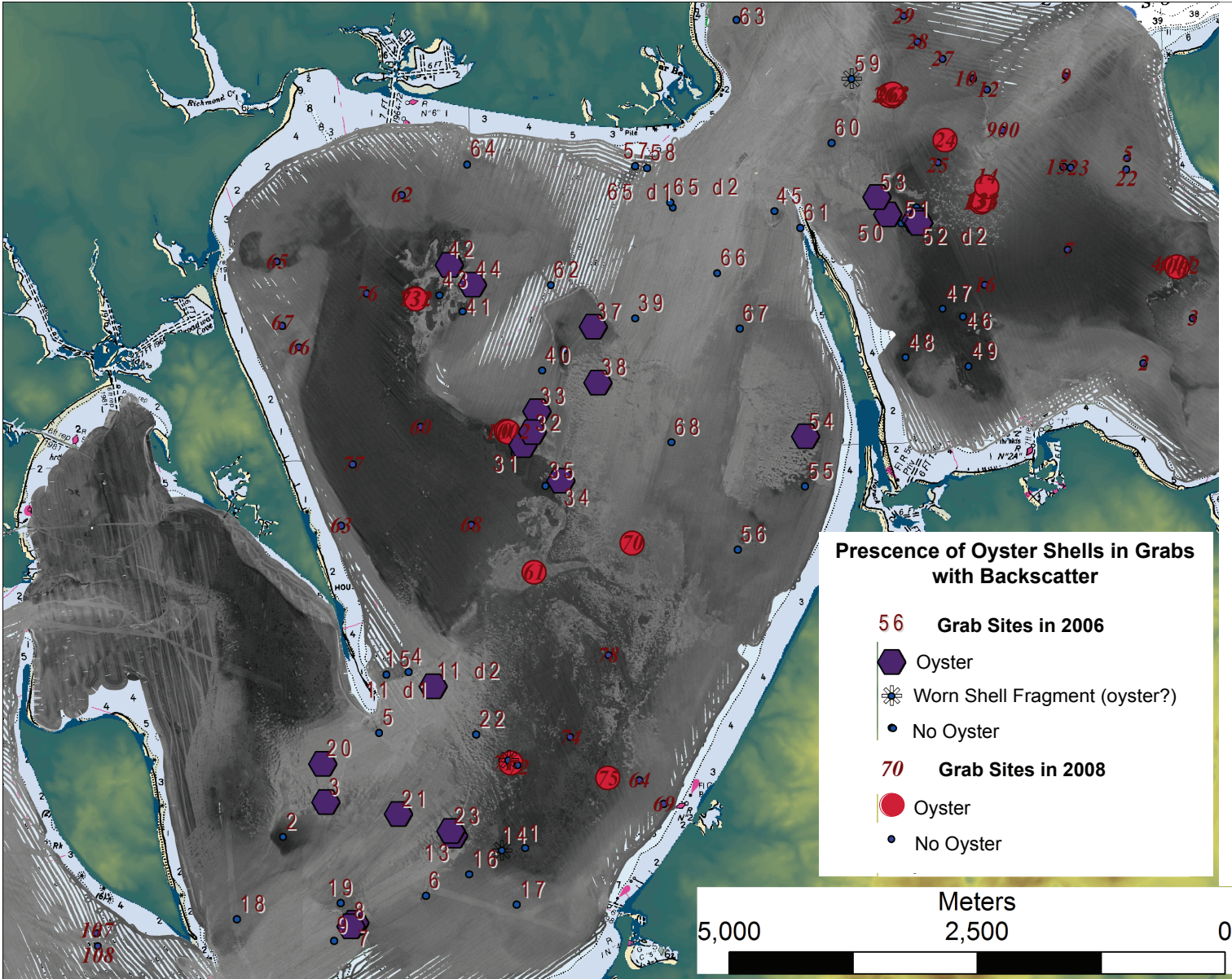
Fig. 2.10: Examples of shells in poor versus fairly good condition from Grab 61 -2008, (Little Peconic Bay). Shells are more than 2 cm thick. A second set of relict shells is shown on the left. Rinsed Peconic aquaculture shells are shown on the right. Note typical changes in direction of growth axis when shells transferred to new location/conditions (disturbed shell).
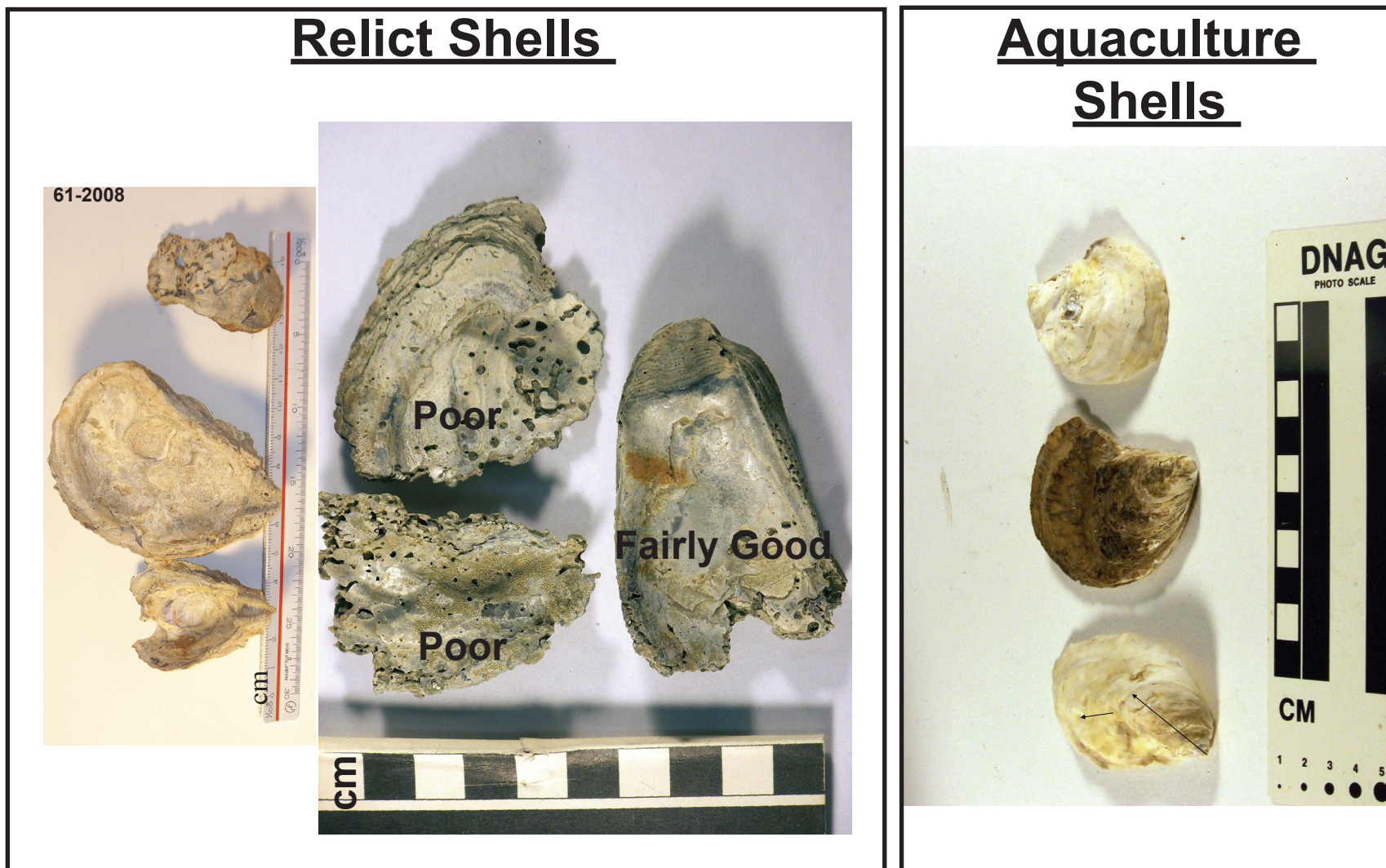
REFERENCES:

Arlotta, M., 2003, Benthic mapping as a tool for developing multidisciplinary maps of the Robin's Island area of the Peconic Estuary System of Long Island, New York [M.S. Thesis], Stony Brook University, Stony Brook, NY, 104 p.

Bonar, D. B., Coon, S. L., Walch, M., Weiner, R. M., Fitt, W., 1990, Control of Oyster Settlement and Metamorphosis by Endogenous and Exogenous Chemical Clues, Bulletin of Marine Science, v. 46, n. 2, p. 484-498.

Beaudoin, J., 2002, Hitchiker's Guide to Swathed …, Ocean Mappin Group, University of New Brunswick, last accessed 2010, www.omg.unb.ca/~jonnyb/processing/definitive-swathed/index.html.

Cerrato, R. M., Maher, N. P., 2007, Benthic mapping for habitat classification in the Peconic Estuary: phase I groundtruth studies, Special report Stony Brook University Marine Sciences Research Center, n. 134, 276 p.

County of Suffolk, N.Y., 2001, Coastal Underwater Land Ownership, last accessed 2010, http://www.co.suffolk.ny.us/departments/planning/pdfs/Map1_Aqua.pdf.

County of Suffolk, N. Y., 2002, Peconic/ Gardiners Bays Underwater Land Parcel Tax Status, Towns of Riverhead, Shelter Island, Southold, Southampton, & East Hampton, Suffolk County, New York, Map by Suffolk County Department of Planning, Thomas A. Isles Director.

County of Suffolk, N. Y., 2002, Peconic/ Gardiners Bays Underwater Land – Private Oyster Grants, Towns of Riverhead, Shelter Island, Southold, Southampton, & East Hampton, Suffolk County, New York, Map by Suffolk County Department of Planning, Thomas A. Isles Director.

County of Suffolk, N.Y., 2002, Real Property Taxmap parcel linework used with permission of Suffolk County Real Property Tax Service Agency (R.P.T.S.A.), copyright 2002.

County of Suffolk, N.Y., 2003, Peconic/ Gardener's Bays Underwater Land Private Oyster Grants (Map), http://www.co.suffolk.ny.us/departments/planning/pdfs/Map1_OysterGrantParcels_11x17.pdf

County of Suffolk, N. Y., 2003, National Ocean Survey Nautical Chart 12358 with Private Oyster Grant Parcel Overlay, Towns of Riverhead, Shelter Island, Southold, Southampton, & East Hampton, Suffolk County, New York, Map by Suffolk County Department of Planning, Thomas A. Isles Director.

County of Suffolk, N. Y., 2003, National Ocean Survey Nautical Chart 13209 with

Private Oyster Grant Parcel Overlay, Towns of Riverhead, Shelter Island, Southold, Southampton, & East Hampton, Suffolk County, New York, Map by Suffolk County Department of Planning, Thomas A. Isles Director.

Davies, D. S., Isles, T. A., Fischer, L., Verbarg, R., Di Cola, L. M., Lind, C., Daly, J., Frisenda, T., Leogrande, V., Walsh, C. E., 2003, Survey Plan for Shellfishing Cultivation Leasing for Gardiner's and Peconic Bays, April, 2003, Suffolk County Department of Planning, Suffolk County Department of Health Services, Suffolk County Department of Public Works, Suffolk County, NY.

Duck, R. W., Herbert, R. A., 2006, High-resolution shallow seismic identification of gas escape features in the sediments of Loch Tay, Scotland: tectonic and microbiological associations, Sedimentology, v. 53, p. 481–493.

Edgetech, 2009, Edgetech Sub-bottom profilers, accessed 2009, www.edgetech.com/edgetech.

Ferrini, V. L., 2004, Dynamics of nearshore sedimentary environments revealed through the analysis of multibeam sonar data [Ph.D. Dissertation], MSRC, Stony Brook University, Stony Brook, NY, 161 p.

Flood, R. D., Cerrato, R., Goodbred, S., Maher, N., Arlotta, M., Zaleski, L., 2003, Benthic Habitat Mapping in the Peconic Bays, Program for the Tenth Conference on Geology of Long Island and Metropolitan New York, April 12, 2003.

Flood, R. D., Cerrato, R., Kinney, J., 2009, Benthic Mapping and Habitat Classification in the Peconic Estuary, Phase II, Final Report to the Long Island Chapter of the Nature Conservancy.

Galtsoff, P. S., 1964, The American Oyster, Crassostrea Virgina Gemlin, Fish and Wildlife Service, Fishery Bulletin v. 64, p. 457.

Gomez-Reyes, Eugenio, 1989, Tidally Driven Lagrangian Residual Velocity in Shallow Bays [Ph.D. Dissertation], MSRC, State University of New York at Stony Brook, December 1989, 129 p.

Hughes-Clarke, J., 1998, SwathEd, Ocean Mapping Group, University of New Brunswick, last accessed 2010, www.omg.unb.ca/~jhc/SwathEd.html.

Ingersoll, E., 1881, The Oyster-Industry, The History and Present Condition of the Fishery Industry, Report on the oyster-industry of the United States, U.S. Department of the Interior, Washington D.C., Government Printing Office, Prepared under the Direction of Prof. S.F. Baird, U. S. Commissioner of the Fish and Fisheries and by G. Brown Good, Assistant Direction U.S. National Museum and a staff of associates.

IVSD3, 2009, Fledermaus Refence Manual, Interactive Visualization Systems, Inc.,

Fredericton, New Brunswick, Canada, accessed 2007, last accessed 2009, http://ivsd3.com/support/documentation, http://ivsd3.com/docs/Referenc_Manual.pdf .

Katuna, M. P., 1974, The sedimentology of Great Peconic Bay and Flanders Bay, Long Island, New York [M.S. Thesis], Queens College (CUNY), Flushing, NY, United States, 97 p.

Kreeger, D., J. Adkins, P. Cole, R. Najjar, D. Velinsky, P. Conolly, Kraeuter J., June 2010, Climate Change and the Delaware Estuary: Three Case Studies in Vulnerability Assessment and Adaptation Planning, Partnership for the Delaware Estuary, PDE Report n. 10-01, p. 1-117.

Lenihan, H. S., Peterson, C. H., 1998, How Habitat Degradation through Fishery Disturbance Enhances Impacts of Hypoxia on Oyster Reefs, Ecological Applications, v. 8, n. 1, p. 128-140.

Lescinsky, H., Edinger, E., Risk, M. J., 2002, Mollusc Shell Encrustation and Bioerosion Rates in a Modern Epeiric Sea: Taphonomy Experiments in the Java Sea, Indonesia, Palaios, v. 17, p. 171-191.

Lightfoot, K. G., Kalin R., Moore, J., Contributions: Cerrato, R., Conover, M., Rippel-Erikson, S., 1987, Prehistoric Hunter-Gatherers of Shelter Island, New York: An Archaeological Study of the Mashomack Preserve, Contributions of the University of California Archaeological Research Facility No. 46. University of California, Berkeley, California.

Liu, J. P., Milliman, J. D., Gao, S., Chen, P., 2004, Holocene development of the Yellow River's subaqueous delta, North Yellow Sea, Marine Geology, v. 209, p. 45-67.

Lockwood, R., Work, L. A., 2006, Quantifying Taphonomic Bias in Molluscan Death Assemblages from the Upper Chesapeake Bay: Patterns of Shell Damage, Palaios, v. 21, p. 442-450.

Maher, N. P., 2006, A new approach to benthic biotope identification and mapping [Ph.D. Dissertation], Stony Brook University, Stony Brook, NY, 181 p.

Meinkoth, N. A., 1981, The Audubon Society Field Guide to North American Seashore Creatures, Chanticlear Press, Inc., Alfred A. Knopf, New York, p. 547.

Merrill, A. S., Emery, K. O., Rubin, M., 1965, Ancient Oyster Shells on Atlantic Continental Shelf: Science, v. 147, p. 398-400.

Milliman, J. D., 1974, Marine Carbonates, Recent Sedimentary Carbonates: Part 1, Springer Verlag; New York.

Morse, J. W., 2005, Formation and Diagenesis of Carbonate Sediments, Sediments, Diagenesis, and Sedimentary Rocks, ed. Fred T. Mackenzie, Treatise on Geochemistry H. D. Holland & K. K. Turekian (Executive Editors) v. 7, Elsevier, The Netherlands (Oxford, UK), p. 67-82, p. 80.

NOAA, 2009a, Make a Tide Prediction, accessed, 2009, http://tidesandcurrents.noaa.gov/.

NOAA, 2009b, Historical Tide Data –Select Station, NOAA, National Ocean Services, Center for Operational and Predictive Services, accessed 2009, http://tidesandcurrents.noaa.gov/Station_retrieve.shtml?type==Historic+Tide+Data.

National Oceanographic and Atmospheric Adminitstration (NOAA), 2010, Raster Navigational Charts: NOAA RNCs, last accessed 2010, http://www.nauticalcharts.noaa.gov/mcd/Raster/index.htm.

NOAA, 2011, National Oceanographic and Atmospheric Administration (NOAA) National Ocean Service Historical Hydrographic Data, National Geophysical Data Center, Office of Coast Survey and National Geophysical Data Center, accessed 2011, (http://surveys.ngdc.noaa.gov/mgg/NOS/coast), 1933-1935 surveys, available through the Hydrographic Data Viewer for downloading data at http://maps.ngdc.noaa.gov/viewer/nos_hydro.

Pavlukhin, S. I., 2004, SeiSee 2.15 User's Manual, Yuhno -Sakhalinsk, DMNG Geophysical Company, www.dmng.ru/seisview/html/SeiSeeEng.html.

Pavlukhin, S. I., 2011, SeiSee (Rev 2.16.1) SEG-Y and CWP-SU (Seismic Un*x) fileviewer, DMNG Geophysical Company, updated July 5, 2011, www.dmng.ru/seisview.

Popescu, I., Lericolais, G., Panin, N., De Batist, M., Gillet, H., 2007, Seismic expression of gas and gas hydrates across the western Black Sea, Geo-Marine Letters, v. 27, p. 73–183.

SMT Kingdom Suite, 2009, SMT Kingdom Suite Tutorials, accessed 2009, http://seismicmicro.com.

Stanley, J. G., Sellers, M. A., 1986, Species profiles : lifehistories and environmental requirements of coastal fishes and invertebrates (Mid-Atlantic)--American oyster. U. S. , in F. W. S. B. Rep., ed., U.S. Army Corps of Engineers, 25 p.

Suffolk County Planning, 2011, Publications and Information, Suffolk County, Long Island, New York, Planning, last accessed 2011, http://www.co.suffolk.ny.us/departments/planning/Publications%20and%20Information.aspx.

USGS 7.5 DEM New York State (10 mx10 m pixels), 2008, NY State DEM courtesy USGS & NYDEC available via the Cornell University Geospatial Information Depository, North American Datum of 1927 UTM 18N, http://cugir.mannlib.cornell.edu/mapsheet.jsp?coverageId=23&id=all.

Vieira, M. E. C., 1990, Observations of currents, temperature, salinity, and sea level in the Peconic Bays, 1984 : a data report, Northeastern Environmental Data System (NEEDS), Special data report; #4, #90-9, 199 p.

Walter, L. M., Bischof, S. A., Patterson, W. P., Lyons, T. W., 1993, Dissolution and recrystallization in modern shelf carbonates: evidence from pore water and solid phase chemistry, Philisophical Transransactions of the Royal Society London A, v. 344, p. 27-36.

CHAPTER 3: QUANTITATIVE CHARACTERIZATION OF THE 'OYSTER TERRAIN'

Detailed descriptions of the distribution of extensive oyster reef deposits may be useful in understanding growth patterns of modern oyster reefs and fossil reefs of other species. Spatial patterns of oyster reefs for example may provide insight to management and restoration efforts of oyster reefs. Extensive reef distribution pattern data may help to predict distributions in smaller settings better. For instance high resolution morphology of many reefs may provide more examples of growth of reef structures in response to flow patterns and reef modification of flow. Increased understanding of fossil reef distributions is also important due to the ability of ancient reefs to trap fluids including hydrocarbons. Reef deposits of various species including oysters are ubiquitous in the fossil record, but there are few detailed descriptions of distribution and size of reefs forming extensive deposits. Accounts of individual modern reefs and extensive fossil reefs abound. Several studies show the presence of recent reefs in bays or estuaries using geophysical techniques. However, few modern oyster reef systems have the thickness or extent of many fossil reefs due in part to the dredging of modern oyster reefs for harvesting or navigation. Natural patterns of reefs are also not commonly found today due to anthropogenic alteration because of pollution, increased sediment discharge, or changes in flow. While a few detailed studies of fossil reefs exist, there are very few high resolution studies of large reef systems in modern settings. The high resolution mapping with multibeam bathymetry of over 10,000 exposed but apparently relict mounds in the Peconic Oyster Terrain enables compilation of densities, depth, and areal distributions of mounds or other reef components. The typical sizes of fields of mounds versus dense banks are quantified for the Peconic Estuary and compared to each other.

INTRODUCTION:

Holocene and late Pleistocene oyster deposits are ubiquitous along the U.S. Eastern Atlantic seaboard (Merrill et al., 1965; Milliman & Emery, 1968; Emery & Uchupi, 1972), but intact relict oyster reef morphologies like those unveiled in the Peconic Estuary Oyster Terrain are less common. Early to Mid-Holocene transgressive deposits, oyster reefs in particular, are typically reworked on the open high energy shelf (MacIntyre et al., 1978; Cattaneo & Steel, 2003). In some places, transgressive deposits have been buried under enough sediment to preserve features, but they are often buried to an extent that makes it difficult to access them for study. Many historically active reefs have been removed or their morphologies have been otherwise altered by dredging (e.g. harvesting, navigation, etc.) (DeAlteris, 1988; Lenihan & Peterson, 1998; Woods et al., 2005). Multibeam maps of approximately a hundred square kilometers of relict reef terrain in the Peconic Estuary should help improve understanding of other systems including those with less extensive reef morphology.

BACKGROUND: Modern and Relict Oyster Reef Morphology

There are many bioherms in the marine record, and there are many high backscatter features or mounds besides bioherms, but oyster reefs can be identified with a combination of backscatter and morphology. Detailed characterization of these mound features may be useful to distinguish similar reef features elsewhere and to predict reef locations. Bioherm deposits of *C. virginica*, the eastern oyster, are found along the eastern North American seaboard from the Gulf of Mexico to Prince Edward Island (Galstoff, 1964; Meinkoth, 1981). Widespread relict deposits of *C. virginica* across the continental shelf have also long been known (Merrill et al., 1965; Emery & Uchupi, 1972; Purnachandra Rao et al., 2003). Detailed descriptions of recent reef morphologies including those found in the Peconic Oyster Terrain may help us to understand ancient geological deposits of carbonate reefs and to model the future and

past structure and evolution of oyster reef systems.

High resolution morphology maps of relict oyster terrains are significant because, despite reefs being common, most relict and active reefs have long been altered and leveled by anthropogenic activity in places such as Chesapeake Bay (Ingersoll, 1881; DeAlteris, 1988; Lenihan & Peterson, 1998; Woods et al., 2005). Anthropogenic harvesting, particularly dredging, reduced heights of existing reefs by a meter or more in examples from Virginia (DeAlteris, 1988; McCormick-Ray, 2005) and North Carolina (Lenihan & Peterson, 1998). Less destructive practices also limit reef growth when harvested shells are not returned to reefs (Grave, 1903; DeAlteris, 1988; Lenihan & Peterson, 1998) because living oysters and recent oyster shell are preferred surfaces for oyster cultch-larvae settling services (Bonar et al., 1990; Bushek at al., 2004). Low relief oyster beds often characterize areas of cultivation and harvesting due to regular removal of shell. Southern Louisiana oyster cultivation for example, typically has low relief beds with a mud-shell matrix (Allen et al., 2005). Many questions about oyster growth have arisen as a result of the desire to understand this commercially and ecologically important natural resource. Increased understanding of the evolution of recently active reefs will benefit our understanding of the evolution of both living and ancient reef system development.

The geological record contains many examples of carbonate mound structures, many of which have similar morphologies to those found in relict structures of the Peconic Estuary. Reefs of various species have long been observed to have distinct morphologies associated with different settings such as near shore fringing reefs, patch reefs in the middle of a bay, and barrier reefs along lagoon edges (Davis, 1928; Kennedy & Woodroffe, 2002). Morphology often varies with flow patterns and distance from shore. For example oyster patch reefs form isolated compact irregular beds away from shore while a fringing oyster reef grows right along the shore and string oyster reefs can occur at right angles to shore and tidal currents (Hedgepth, 1953; Parker, 1960; McCormick-Ray, 2005). The relationship of flow and *C. virginica* reef morphology

is largely based on work on modern reefs along the Gulf Coast (Hedgepth, 1953; Parker, 1960).

Detailed study of these kinds of structures may reveal more about common morphologies and larger scale structural patterns that may be biological strategies for particular physical settings. We may learn, for example, what shapes and distributions are likely to be found in different settings if reefs grow on very large scales. Other studies have tried to look at oyster reef distributions associated with more stabilized features such as channel levees and tidal deltas that provided more support than nearby mobile bottoms (Weaver et al., 2008). Such distribution patterns have implications not only for modern ecology, but also for understanding fossil reefs. Such distribution patterns are significant because fossil reefs are known to trap fluids such as hydrocarbons in many places (Cook et al., 2002; Mel'nikov et al., 2005; Adams et al., 2005; Huvaz et al., 2007). Although massive reefs have been studied since the beginning of geological science (Lyell, 1838, 1864; Darwin, 1842; Desor & Cabot, 1849), high resolution studies of the distribution of morphology on the scale of the Peconic Oyster Terrain are still uncommon (Adams et al., 2005; Pufahl et al., 2004). Both the geophysical modelers trying to predict reef distributions in order to increase the chances of finding oil and the ecological modelers working to understand modern growth distributions in order to understand reef health could benefit from such large reef distribution data sets. The goal of this chapter is to identify characteristics of reef distributions in the Peconic Estuary Oyster Terrain, including examining the statistical distributions of subsets of different reef morphologies within the Oyster Terrain in greater detail.

METHODS:

Data:

Multibeam data was collected with an EM3000D echosounder, and more detailed descriptions of the surveys, including sidescan and sub-bottom seismic profiler (CHIRP)

data collected during the same surveys, can be found in Chapter 2. Multibeam data has been gridded at 1 m resolution. The region was mapped in between the summer of 2006 and the summer of 2008 as part of Phase II and Phase III of the Benthic Habitat Mapping Project. Also included in larger scale maps of the Peconic Estuary are Phase I Benthic Habitat Mapping Project multibeam and sidescan data collected in 2001 and 2003 (Flood et al., 2003; Arlotta, 2003) although those data are not a focus of our detailed analysis. NOAA bathymetric charts are used as basemaps (NOAA, 2010), along with USGS topographic maps for the region that have been published as DEMs (USGS, 2010). Seismic profiles were converted to images, rescaled to a vertical sound velocity of 1500 m/s, cropped as needed and brought into Fledermaus[TM] as vertical images for 3D viewing with the multibeam data sets.

Distribution of Features in Multibeam Data Sets:

Individual mounds were marked on the multibeam and side-scan sonar data sets by creating points, X and Y coordinates, in ArcGIS[TM] shapefiles. Additional data from GIS layers were then extracted for these coordinates and added to the point files, including most importantly Z values from bathymetry grids. Point data sets were then exported from ArcGIS[TM] into text files for further analysis of distributions in Matlab[TM]. This process was done for the first (2006) survey of the eastern portion of the Little Peconic Bay/Noyack Bay (Little Peconic Bay 2006-22 sq km subset) as reported in Kinney & Flood (2006). This process was next expanded to include the western portion of the 2006 survey in the western portion of Little Peconic Bay (Kinney & Flood, 2008). Survey areas provided convenient subsets to be analyzed, and the mound locations in newly surveyed portions of the bay were added as the processing of the multibeam data was completed (Little Peconic and Noyack Bays and the remainder of Little Peconic Bay were added in 2008). Additionally, multibeam data collected off of the northeast end of Robins Island in the first phase of the Peconic Bays Mapping project was incorporated into this study to get the full extent of mounds in the Bay. Mounds were initially identified separately on sun illuminated (i.e. shaded relief) and backscatter

images and the resulting maps were found to be quite similar. Subsequently the mound point files were created using both the shaded relief and backscatter data combined into one image as described in Chapter 2.

The distribution of the depths, sizes and spatial patterns of mounds in different basins were made in smaller subareas within the basins of Little Peconic and Noyack Bay; each subset contained between several hundred to a few thousand mounds. These subsets were chosen in order to investigate reef morphologies, depths, sizes and spatial patterns in more detail. The subsets named 0, 26, 71, 13 and 61 are from areas near grab sites, which were considered for ^{14}C dating. Areas 13, 24 and 71 had somewhat different mound patterns that we chose to examine in detail while areas 0, 26 and 61 had more typical mound patterns. As detailed in Chapter 4 sites 0b, 26C, 61, and 70 that is near 71 were dated to give temporal context to some of these distribution patterns.

Boxes of equal area were drawn to delineate the smaller subset areas (Fig. 3.1). All mound shapes, whether individual or part of a large mass, which were visible in the multibeam backscatter and sun illuminated bathymetry were outlined with polygons in a shape file in order to calculate their areas. The tops of mounds were selected from the points created for Little Peconic and Noyack Bays as described above. The areas of individual mounds are reported in square meters and equivalent diameters determined assuming a circular shape for each area are also reported.

The Box Areas, which were each 321,269 square meters in area, were chosen to represent different mound morphologies showing a greater variety of mound distributions which fall within the original range of ~18 to ~6 m (Fig. 3.1). These subsets were analyzed in Little Peconic Bay (Box Area 38, Box Area 0, Box Area 61, Box Area 71), and Noyack Bay (Box Area 26, Box Area 24, Box Area 13). Box Area 38 represents a moderately deep field of mounds. Box Area 0 represents a medium depth bank with distinctive mounds and steep slopes. Box Area 61 represents a fairly flat

bank at medium depth with a slope along its edge. Box Area 71 represents linear chains of mounds. Box Area 13 represents a deep field of mounds forming a mound shaped mass. Box Area 26 represents a shallow bank top with indistinct mounds. Box Area 24 represents individual mounds in a small field. The density of mounds was also calculated for the different box areas as number of mounds per box and as total percentage of area covered by mounds.

Distribution of Features in Seismic Profiles:

The depths of buried mounds observed on seismic profiles were determined to allow the comparison between the buried and surficial mounds. X, Y, Z points from mound bases and tops were determined using the geo-picking option with the views of seismic profiles in Fledermaus and exported as text files. This allowed for three-dimensional viewing of profiles while picking points on tracks that included many turns in a single file. This picking was initially done for the small survey from November 2006 that crossed Little Peconic and Noyack Bays and then expanded to the full seismic data set.

RESULTS:

Reef Formations

While individual mounds have relief, most of the vertical relief of a bank comes along the slopes at its edges. The bank formations tend to be relatively flat-topped with less than 2 m of vertical relief in individual mounds, although the top of the bank may slope. Large banks are often characterized by rounded or scalloped edges, shapes suggesting the merging of larger individual mounds into a massive bank. In the very large banks, it becomes difficult to discern smaller mounds and the composite features of the bank typically include large (>50 m across), irregular (non-symmetric) mound shapes (Fig. 3.2). In many banks one can distinguish smaller mounds close to the

scale of the individual mounds one sees elsewhere in the bay (10 to 50 m across) (Fig. 3.2). These smaller banks included mounds that have started to grow into and on top of each other. These patterns tend to have less vertical relief than other mound configurations. Banks may have slightly more vertical relief even though their top surface tend to be smoothed, with greater relief being due to mounds occurring at the edges of the bank (Fig. 3.2). Fairly dense fields of mounds, by contrast, tend to have mounds with more relief than bank tops or widely separated mounds.

One example of mound variability is in the area associated with the shallowest mound tops, near sample 26C, because mound shapes there are not as distinctive as in other subset areas and this bank looks much smoother than neighboring banks (Figs. 3.1, 3.2). The backscatter signal shows a clear distinction between the bank and non-bank areas, and there is clearly bank morphology, but it is difficult to discern any individual smaller mounds that might be building such a larger bank. In addition, the scalloped edges are not quite as pronounced as the neighboring banks.

Depth and Spatial Patterns

The distributions of mound tops in four of the large subsets of mounds do not vary very much with peaks around 10-12 m (Fig 3.3), but the smallest subset near Robins Island had a much shallower distribution with peaks around 7 m and 9 m (Fig 3.3). Peak mound depths in the large subsets are similar to the values for the full mound dataset, as can be seen in Fig. 3.3; note the peaks around 10-12 m and around 9 m are found in multiple subsets, while a smaller peak around 7 m is only in a few (Fig. 3.4). Many subsets have a narrower peak of mound depths around 11 to 12 m. The mean mound depth is around 10 m with most mounds falling between 6-14 m. Only the smaller subset near Robins Island with a mean close to 7.5 m is very different. The distributions within these large subsets of the basins are skewed differently, and the tails of the depth distributions of shallowest and deepest mounds vary somewhat (Fig.

3.3). Bimodal patterns seen in the histograms are sometimes reflected in the skewness and kurtosity of the distribution (Fig. 3.4). The ranges of the large subsets only vary a bit from the total range of all mounds such as in: Western Little Peconic Bay (18.1 to 6.4 m), Little Peconic and Noyack 2006 (18.4 to 6.0 m), (Central) Little Peconic Bay 2008 (Little Peconic exclude Noyack 2008) (16.5 to 5.9 m), and Little Peconic and Noyack Bays 2008 (17.5 to 5.3 m) with the smaller Robins Island (10.0 to 5.6 m) subset showing the only major difference.

Our small equal area box subsets show smaller ranges in depth. The different types of mound distribution patterns may result in different depth distribution patterns. For instance the top of a bank may have little change in depth of mound tops across it. Only a few mounds along the slopes or base of the bank may offer outliers to the depth distribution. The larger subset, survey region, represents a variety of mound configurations where we may see multiple peaks, a wider peak or a lot of outliers representing slopes or other features. For example Noyack Bay has a large number of mounds deeper than 12 m, but also a small number of the extremely shallow mounds as well. Most of the subset Box Areas have peaks in distribution around 10 to 12 m with the exception of Box Area 26, which is our shallowest area with its few mounds that cover an extensive area in 7 to 5.5 m of water (Fig. 3.3). These different morphologies are reflected in different ranges, skewness, and kurtosis. Box Area 0 (bank) have Box Area 71 (field) are fairly similar distributions in that they have no mounds above 8 m. Box Area 0 has a peak closer to 9 m with a large tail to greater than 12 m, but Box Area 71 is very symmetrically distributed with a peak around 10 m. Box Area 61 (field and bank edge) is skewed toward deeper mounds to 14 m, with a peak at 11 m, but none above 9 m. Box Area 38 (field) is similar to Box Area 61, but has a more symmetric and narrower distribution range with none above 10 m (Fig. 3.3). Box Area 24 (separated mounds) is even more skewed toward deeper mounds, with a peak around 11 m as is Box Area 61, but Box Area 24 has no mounds above 10 m. Box Area 13 (separated mounds) is fairly evenly distributed, with a peak around 11.5 m, and the rest of the mounds are between 9 and 13 m.

The Box Area xyz plots show variability within all of the survey area subsets and bays. We can see slopes formed by mound tops and plateaus with steep slopes along the side, and areas with minimal slope such as Box Area 71 (Fig. 3.5). The difference between one large slope and smaller undulations in a field of mounds can be seen. The xyz plots show the presence of relatively flat areas with minimal slope and others with lots of mounds along a slope. The areas of continuous steep or gentle slope are in contrast to areas with more variation in slope in Noyack and Little Peconic Bays. The combination of depth data and xyz plots reveal the presence of large banks, or channels, versus large areas of gentle slope that are part of the full mound dataset distribution pattern or the slope of the sea floor between mounds. The sample of mounds found in the Box subsets were from a variety of areas such as the edges of dense mound banks, or more scattered mound areas that are reflected in the different depth distributions. For instance, one may see a few mounds along a steep bank, but the majority within a narrow depth range that represents the top of bank. In contrast xyz plots of other areas show gentler slopes over a wide to narrow ranges of depth.

Distinctive differences in mound sizes can also be seen in the subset box areas. An increase in typical mound area can be seen in the Box Area subsets starting at Box Area 24 through Box Areas 13, 61, 71, 0, and 38 up to 26 (Figs. 3.6, 3.7). These differences can be seen in the histograms of mound area (Fig. 3.7), percentage of total mounds and percentage total area in a subset (Fig. 3.6). Small distinctive separated mounds were found in Box Areas 24 and 13 that were dominated by mounds that were the equivalent of less than 707 square meters (equivalent of 30 m diameter). The mounds in Box Area 13 are slightly larger than Box Area 24 and are in increasingly dense clusters. Box Area 61 occupies the edge of a mound bank plateau and the adjacent slope into a field of separate mounds that has a slightly larger mound size distribution than Box Areas 24 and 13. The mounds in Box Area 61 are predominantly less than 707 square meters in area, but some are in the 1,257 - 1,964 square meters (40-50 m equivalent diameter) range. A wider and more evenly distributed set of mounds sizes can be found in Box Areas 71, 0, and 38 with a peak between 707 - 1,964 square meters (30-50 m equivalent diameter). In contrast the distribution of mounds

found in Box Area 26 representing a shallow wide bank is distinctly different from the other mound subsets. Box Area 26 is composed of mostly very large mounds-greater than 2,827 square meters (60 m equivalent diameter).

The smallest mounds found in the massive bank in Box Area 26 have areas of 800-1,000 square meters, which were equivalent to the largest mounds in other subset Box Areas. A moderately sized mound of 2,600 square meters within the Box 26 subset is much larger than the largest mounds in most others subsets. Larger mound components or individual mounds within mound formations with more relief such as in Box Areas 71, 61, and 13 were less than 2,500 square meters each for the most part (less than 55 meters equivalent diameter). Some of the other more massive bank areas also have larger component areas with little relief, such as around grab site 0a in Box Area 0, but most of component mounds are less than 3,000 square meters each (60 m equivalent diameter). It should be noted that because these larger mounds are irregular in size and more elongated, they are actually longer than 60 m. In general larger mounds represent a larger percentage of area than the percentage of number of mounds, but maintain a similar pattern of dominant mound sizes (Fig. 3.6). An exception is that the 30-40 m bin equivalent mounds in Box Area 61, 13, and 24 represent a larger percentage of total area than just the percentage of mounds resulting in a slightly bigger change in the distribution patterns.

The density of mounds differed between the different box areas (Table 3.1). Mound areas that were the most separated had the lowest density of mound coverage (5 to 27.5 %) due to distance between mounds and smaller mound sizes; however these areas could have comparable or higher numbers of mounds per square meter (0.00113- 0.00031) than the dense bank areas did (0.0006 -0.00006). The dense banks had among the highest percentage of area covered by mounds (71.9-82.5%). The fields of mounds covered a significant percentage of area as well (54.6-72.4%), but had a wide range of mounds per square meter (0.00062-0.00136).

Seismic Profiles

Other patterns that we see within reef morphologies are revealed by seismic profiles. We see deeper mounds buried in seismic profiles than are exposed in the multibeam dataset. We also see patterns of modification of reefs exposed at the surface as we can differentiate layers draped over the edges of mounds. Sediment layers partially draping over mounds are more common near areas where mounds are buried. We have more than one example of mounds that have grown on top of other mounds as seen in Chapter 2. A set of mounds growing on top of another set of mounds suggests periods of contemporaneous mound re-initiation along a horizon, while other larger adjacent mounds seem to have grown continuously. Many of the widest mounds, those greater than 40 m in eq. diameter, tend to be taller than mounds of smaller area. We also see that many mounds are actually wider than they appear in the multibeam view because the base is wider that the peak and the sides are buried.

A review of seismic profiles showed no mounds shallower than those found in the exposed multibeam data. A small subset of buried mound top depths showed a similar distribution to those found in our exposed mound subsets, with the major difference being the appearance of more mounds toward the deeper end of the range. While we see evidence for mounds buried in seismic profiles, especially at the deeper end of the depth range, we find no relationship between multibeam backscatter values and depth of mound tops.

Mounds comprising the largest banks were slightly less obvious initially yet were still distinctive compared to high backscatter sand banks. For example the massive bank in Box Area 26 in Noyack Bay does not have many individual mounds that we can discern in the multibeam. The total relief of these features on top of the flat-topped bank may be close to 0.5 to 1.5 m, but since they cover a much wider area they are more difficult to distinguish. These features are rising up out of the steep channel and

both the slopes of these banks and the mounds have the characteristic high backscatter pattern. The edge of this bank meets with a large backscatter area that within a few hundred meters was characterized by well sorted sands (Fig. 3.8). Individual mounds in this bank may be several meters in relief in seismic profiles, but the exposed morphology shows little vertical relief between mounds. However, mounds with the greatest vertical relief are at least 10 m thick, are found along the channel edge, and are closer to the relief of larger mounds in profiles.

DISCUSSION:

A range of mound sizes from under 10 m to about 60 m in equivalent diameter are common throughout the estuary. Extremely large mounds seem to be concentrated in large banks of mounds. The smaller mounds dominated the number of mounds in the more separated fields of mounds compared to denser mound formations. Depth distributions reflect that mounds in nearly all areas have a common depth distribution. Sometimes this includes banks of mounds all within similar depths, but frequently it reflects large areas of dense fields of mounds at similar depths throughout the bay.

As mentioned in Parker (1960) there are many estuaries that have oysters reefs perpendicular to flow (Fig. 3.30, 3.31) or other patterns related to flow. Patterns of chains or smaller elongated masses of reef distributions are often associated with flow and salinity (Parker, 1960). In the Peconic Estuary we see some chains of mounds perpendicular to flow. Ladd et al. (1957) show further Gulf Coast examples of oyster reefs aligned perpendicular to flow in estuaries, as well as examples of reefs aligned parallel to flow. Oyster reefs have been suggested to have different morphology patterns in places where the circulation has lots of eddies rather than a straight flow (Ladd et al., 1957; Hedgepth, 1953). Such eddies in flow are likely to occur near geographic protrusions into bays, such as the peninsulas in the Peconic Estuary (Gomez-Reyes, 1989). We do indeed see banks of oysters near some of the peninsulas too, but the exposed mounds are often more on one the leeside of maximum

flow near Jessup's Neck and Nassau Point.

The rounded reef features topped by oysters we see in the multibeam and sidescan data match the patterns we see published in the detailed mapping studies of oyster reefs using multibeam backscatter data (Clapp & Flood, 2004) and sidescan (Allen et al., 2005; Carbotte et al., 2005; Slagle et al., 2006; Osterman et al., 2009; Twichell et al., 2007). However, we lack many examples of morphology of reefs living in deeper estuaries. It is difficult to tell if similarities are due to maturity (age span of individual reefs) or if they are related to growth in similar shallow water depths. The shallowest of our reefs that are flat and form massive banks resemble the large areal expanses of long lived reefs in intertidal waters/shallow waters that have reached their vertical limit. For example in Noyack Bay the mound banks by 26 C along the channel include very flat reef tops, ~5.5 m, that are the largest individual mounds discerned in the morphology data. Other banks in deeper water have large mounds greater than 60 m in eq. diameter, but none are as large as those of the shallowest bank.

As we noted previously, the bank by 26 C is the shallowest mound area at ~5.5 m, good evidence of sea level being 3 -5m lower when these reefs were last active. If we look at this bank in more detail, the shallowest part of this bank has the lowest backscatter. This shallower area is at ~ 5.0 m, but is not the center of a mound (Fig. 3.8). It is possible this side of the bank was covered with some sediment that adds height and lowers the backscatter values or was otherwise modified. We see that the next shallowest area is found in the banks next to Robins Island. The remaining subsets have their highest banks at around 6 m or deeper. Mounds shallower than 7 m are small percentages of the distribution elsewhere in the Bay.

Multiple sets of mounds grew on top of others possibly overlapping each other in some deeper areas, such as in channels. More than one flat-lying horizon can be seen between the mounds (Fig. 1.7), which appear to pass beneath the mounds suggesting that there was sediment deposition before the mounds became common, although it is

not possible to actually trace the flat-lying horizons continuously beneath the mounds. Sediment horizons can also be observed between mounds, which are likely formed by sediment deposited between mounds when the mounds were active (Fig. 2.2). This suggests that some flatter banks may have been relatively flat for a significant portion of their growth, but others may have had more relief than today when last active.

The wide variety of mound size, depth, and density can be seen among the different types of mound formations. Mound areas that were the most separated had the lowest density of mound coverage of mounds per square meter and the smallest typical mound diameter. Separated or more isolated mounds were found at a variety of depths. The dense banks had among the highest percentage of area covered by mounds and the largest mound diameter, but few mounds per square meter. Banks by definition tend to have shallower tops, but they were found at variety of depths and their bases could be among our deepest areas. The fields of mounds had the most variability in diameter and density in terms of number of mounds per square meter, but always covered a significant percentage of area. Fields of mounds created a variety of patterns of mound top distribution: relatively flat, gentle slopes, channel shapes, and some created mound like shapes or linear patterns. Density may be particularly useful for studies hoping to predict buried reef locations in the sedimentary record. For instance areas with lots of mounds per square meter may cover a lower percentage of area because the mounds may be smaller. There were some places where we did not see reefs so information on where reefs do not like to grow would also be useful. However, reefs seemed to be abundant throughout most of our study area within the 6 - 22 m depth range.

CONCLUSION:

Considering the ubiquity of the oyster, and oyster deposits, it seems likely that more oyster terrains are likely to be discovered from the mid to early Holocene, especially in areas that have not been studied in such high resolution. Increasing

numbers of studies of such past estuarine environments seems to be showing more evidence of buried oyster reefs with sub-bottom seismic profiling (Osterman et al., 2009; Twichell et al., 2007; Weaver et al., 2008).

While the number of mounds with the smallest diameters in the individual mound areas may be high, the total area covered by these mounds in each area may not be all that large. The midsize mound that was initially noticed as being typical is found also to be the dominant component of the mound terrain. Midsize mounds are the most numerous in abundance across the terrain as well as within many fields or banks of mounds. The largest mound sizes comprise significant portions of the sea floor in some types of mound morphologies (banks). The density of reefs may be useful to other studies of reefs as we see that certain types of reefs tend to be found in different densities e.g. mounds may be less numerous in larger reefs, but be closer together and cover a larger area.

Our statistics show that most of the terrain is covered by mounds 20-50 m in equivalent diameter. The largest mounds tend to compose banks rather than being isolated mounds. Small and midsize mounds are found within all mound patterns, from banks to chains to isolated reefs. The different patterns, reliefs, and shapes of individual mound formations may be useful to compare with other locations.

Table. 3.1: Density of mounds in box area subsets.

Box Area ID	Total Mound Area (m²)	Equal size Box Area (m²)	Density of Mound Area % (% of area covered)	Number of Mounds (greater than 5 m²)	Density of number of mounds per area (mounds per m²)
38	190,261	321,269	59.2	200	0.00062
71	232,511	321,269	72.4	366	0.00114
61	175,346	321,269	54.6	436	0.00136
26	230,862	321,269	71.9	20	0.00006
24	16,054	321,269	5.0	101	0.00031
13	88,330	321,269	27.5	364	0.00113
0	265,028	321,269	82.5	192	0.00060

Fig. 3.1: Box subset areas outlined in green. Boxes 13, 26C, and 24 are in Noyack Bay.   Boxes 61, 38, 71 are in Little Peconic Bay.

Boxes showing Subset Areas of Mounds Along with Presence of Oyster shell in Grabs

Grab Sites in 2008

Oyster

No Oyster

Grab Sites in 2006

Oyster

worn shell fragment (oyster?)

No Oyster

Meters
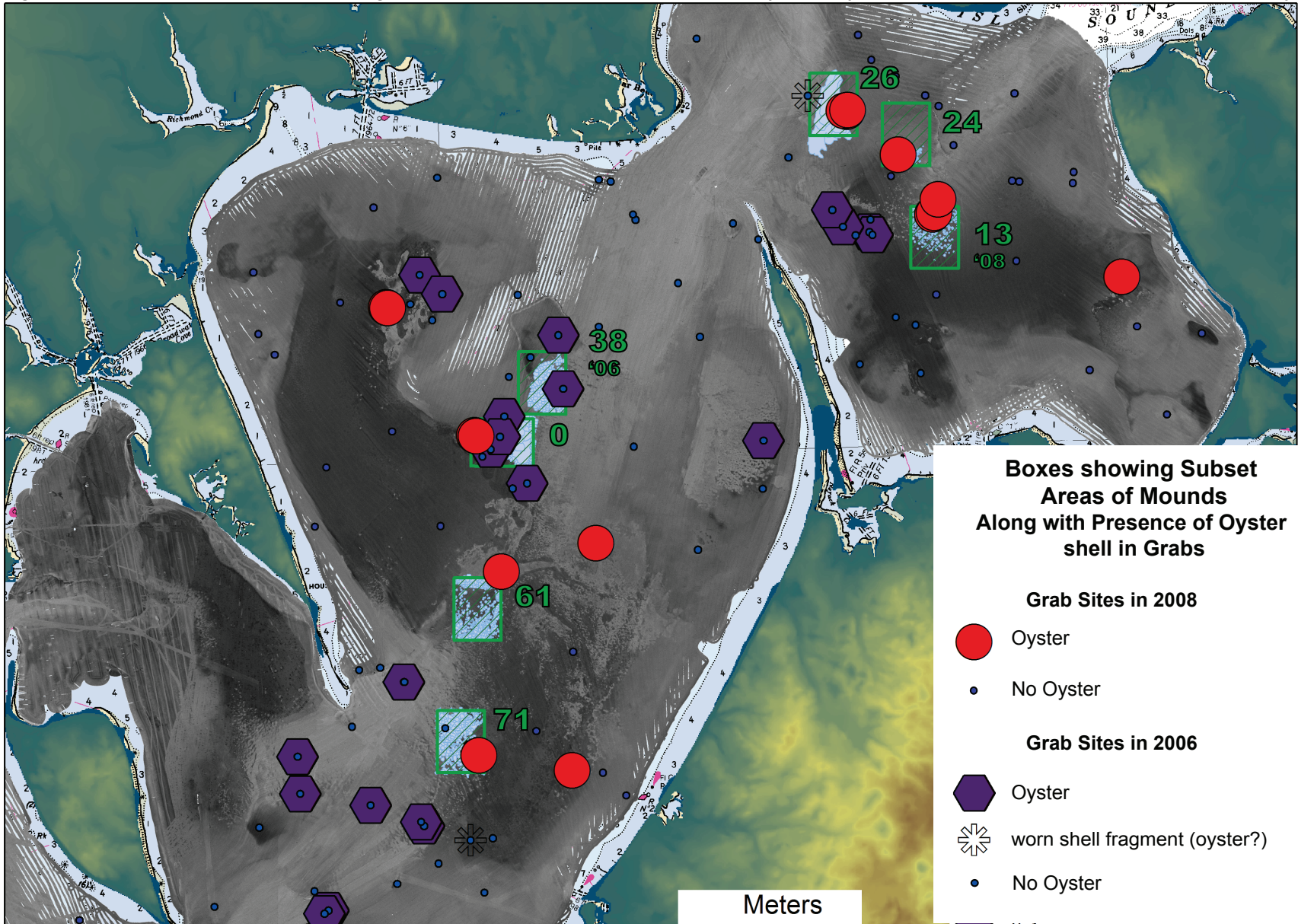
Fig. 3.2: Examples of some of the differences in subset morphology, difference in color of outlined mounds indicated differences in extent of vertical relief. Boxes 13 & 24 show mounds that are more separated. These mounds also have less variation in vertical relief. Boxes 26 & 0 show dense banks of mounds. The mounds that make up the banks also tend to have little vertical relief, but this changes along the edges where bases mounds may extend down the slope.

Box24

Box13

less relief

more relief

less relief

more relief

Shaded relief with bathymetry

Box26

less relief

more relief

Box 0

less relief

more relief
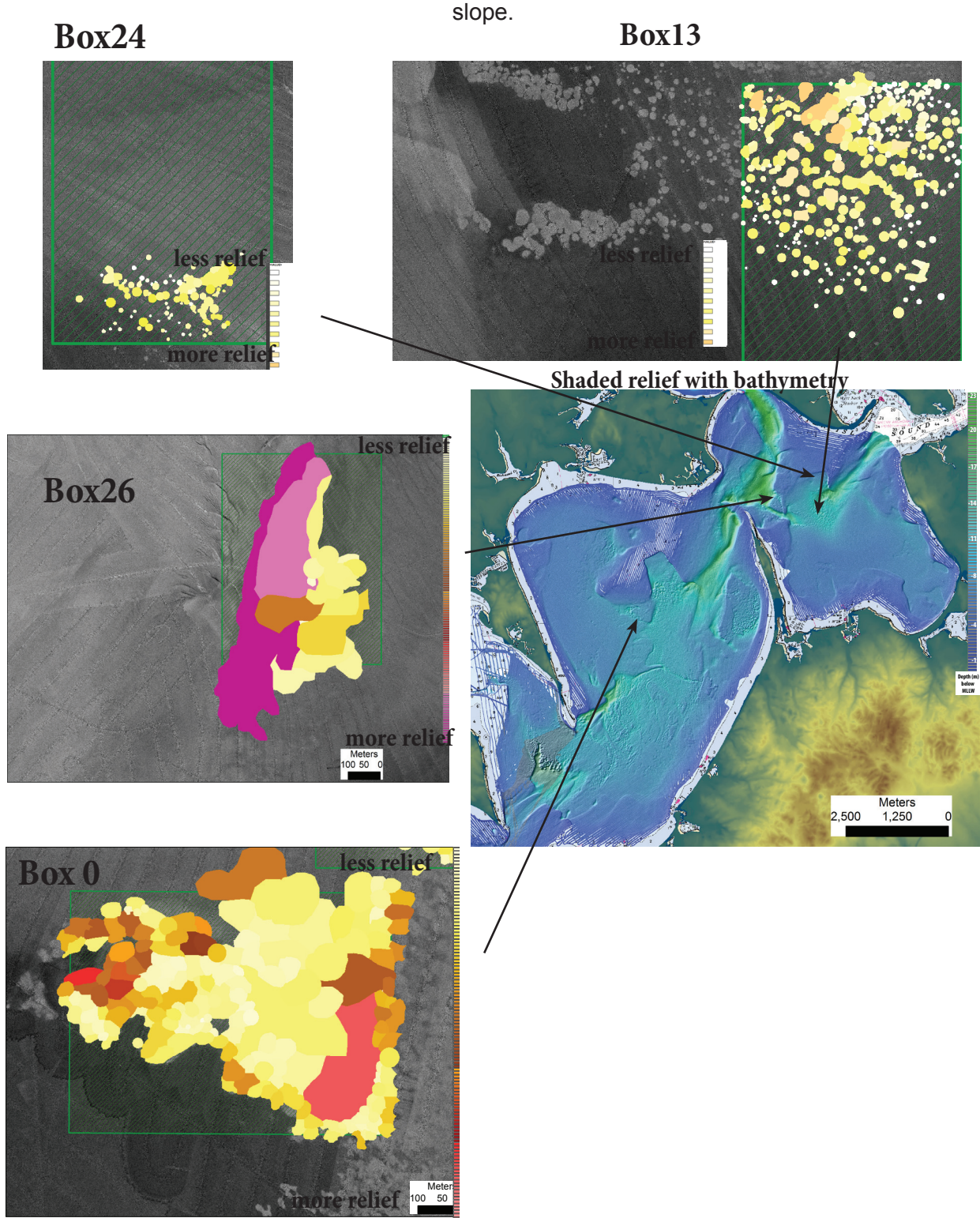
Fig. 3.3: Boxplots of depth distributions of mounds. Large subsets based on survey areas and equal area box subsets are shown. Maps showing the large subsets, survey areas, are shown below, only mound belonging to a given subset are plotted. Box plots: Red line in the box equals median. Boxes whose notches do not overlap indicated that the medians of the two groups differ at the 5% level. Upper and lower box lines represent upper and lower quartiles (25th and 75th percentiles). Whiskers extend to +/- 2.7 sigma. Outlier are plotted beyond the end of the whiskers.

Mound Distribution of Survey Area Based Subsets
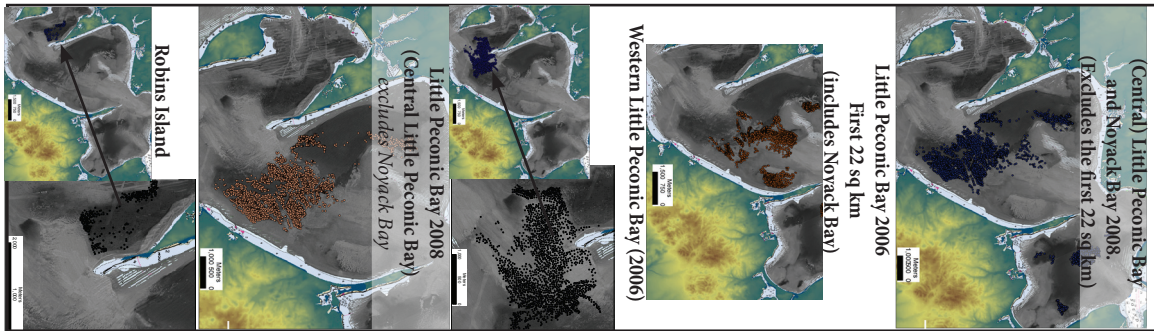
Boxplot of Depth Distribution of All Subset Areas
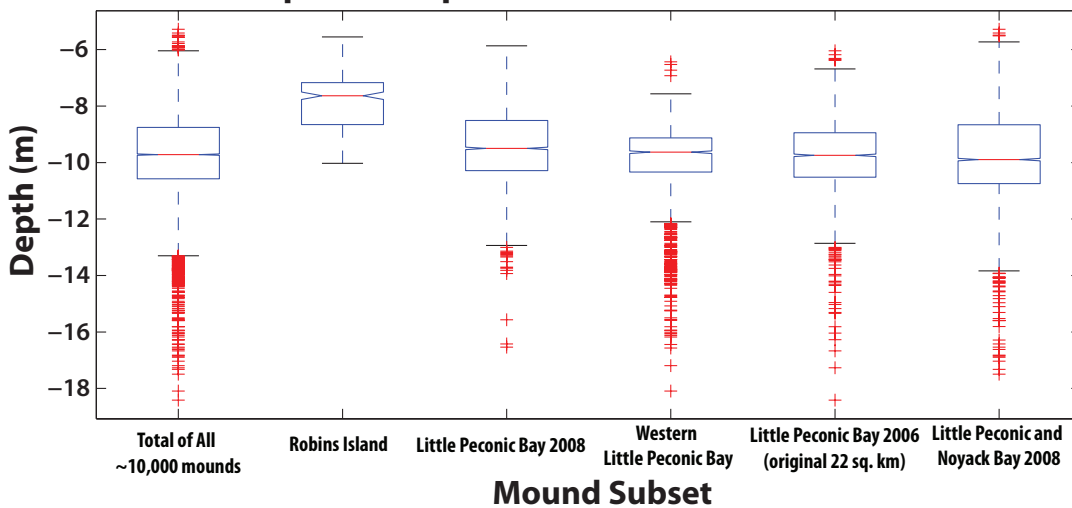
Boxplot of Depth Distribution in Equal Area Boxes
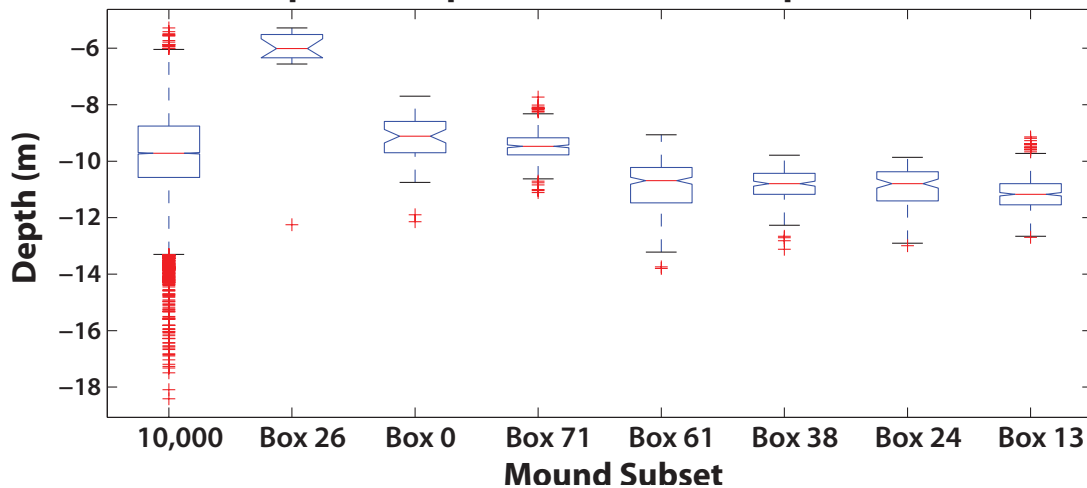
Fig. 3.4: 100 bin histograms of mound depth. Large subsets of mounds on the order of several hundred to thousands with the total combined data set (Total of All Mounds) shown for comparison.

Total of All ~10,000 mounds

Robbins Island

Little Peconic Bay 2008

Western Little Peconic Bay

Little Peconic Bay 2006 (original 22 sq. km)

Little Peconic and Noyack Bay 2008
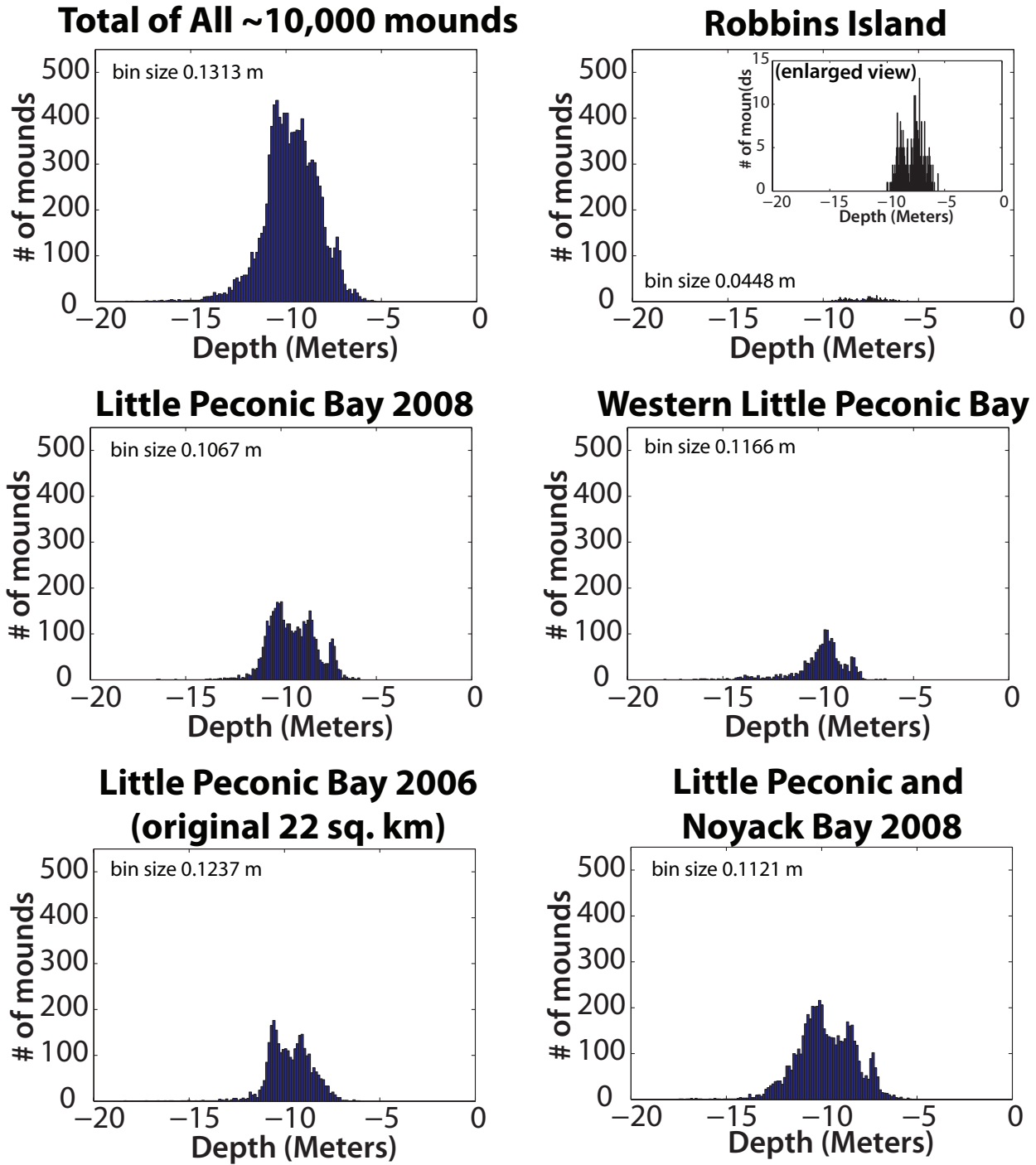
Fig. 3.5: XYZ plot: Angles are different for each subset to show the slopes and distribution in space better.
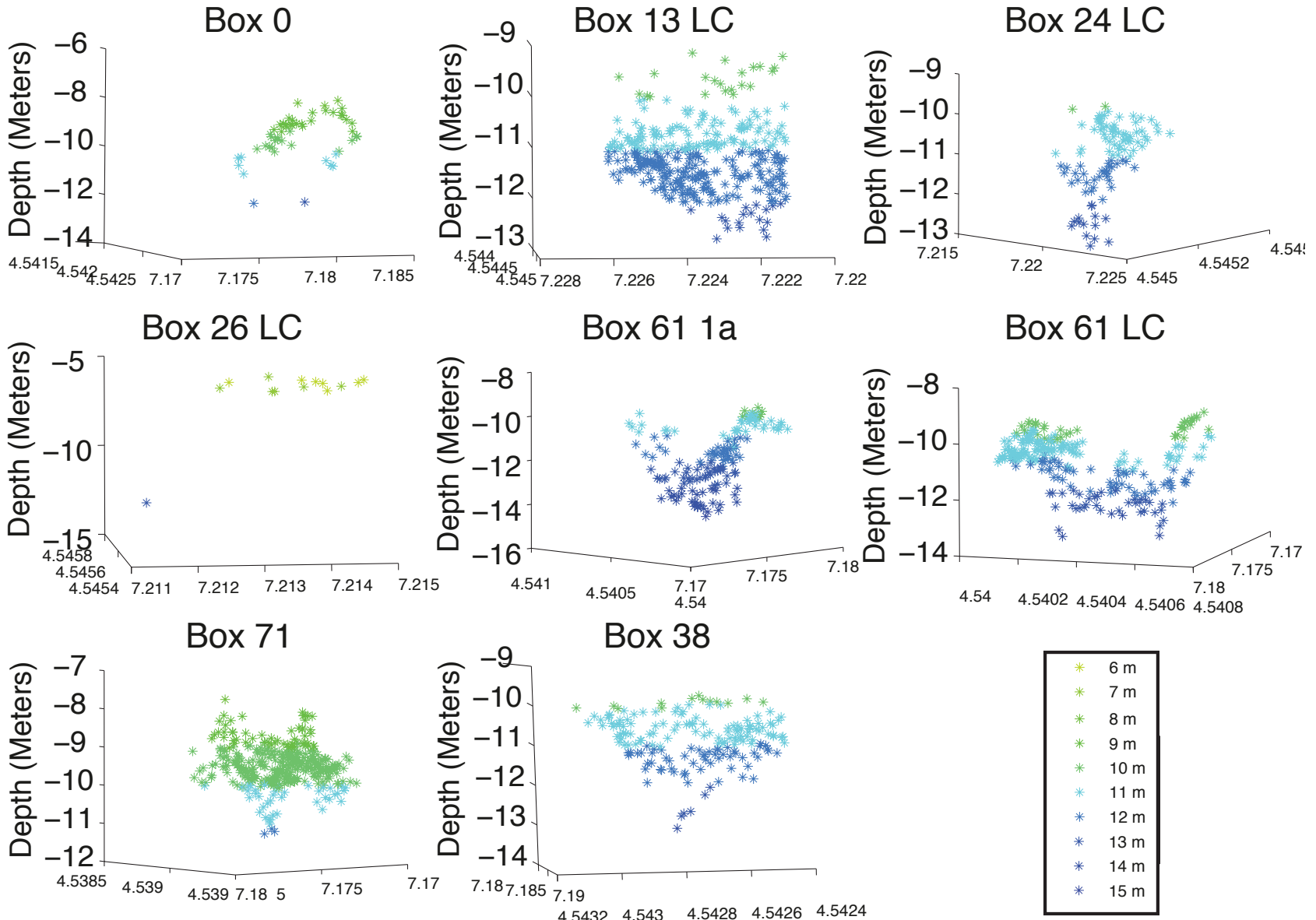
Fig. 3.6: Percentage of total area comprised by mounds of different sizes with box area subsets.

Mound Area: % of Total Number in a Subset Area

Mound Area: % of Mounds by Area out of Total Area of Mound in a Subset Area
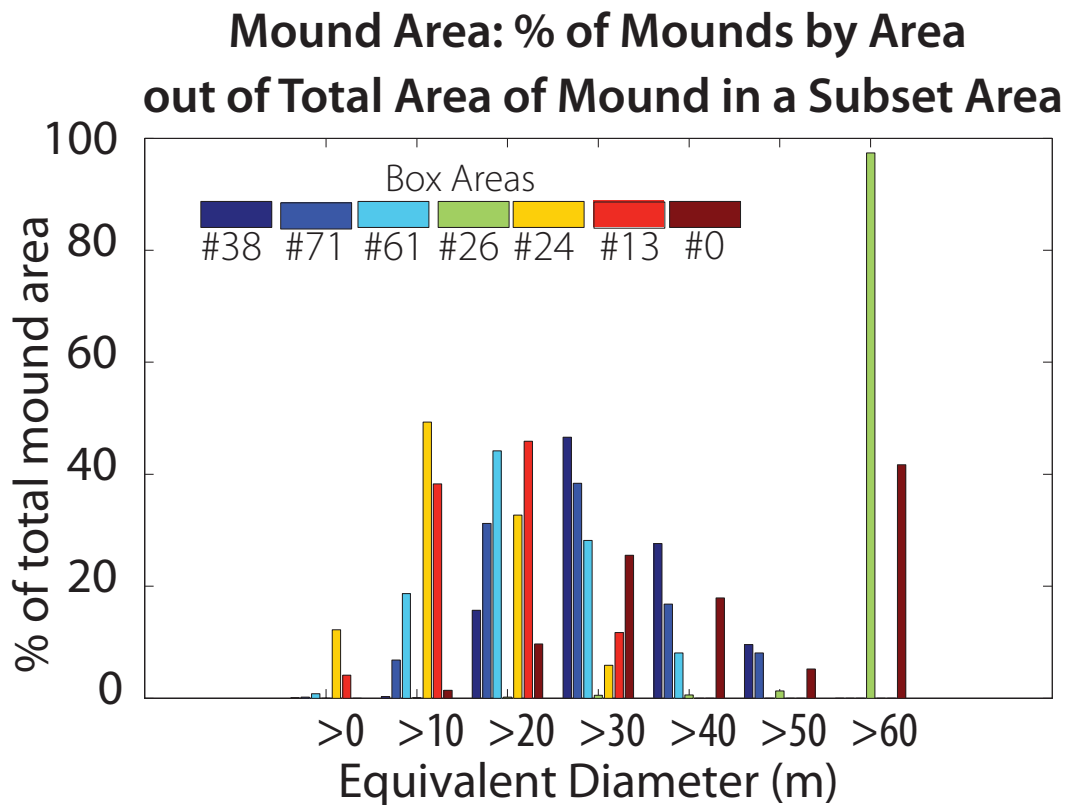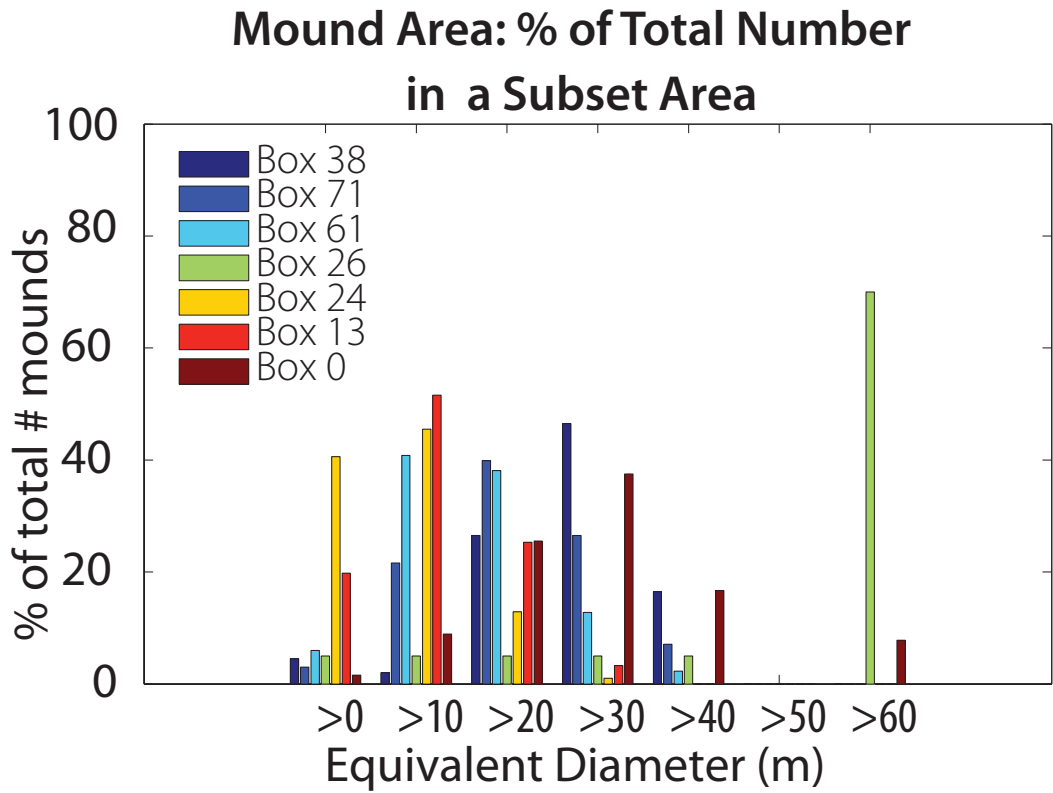
Fig. 3.7: Histograms of mound area for the different box areas.
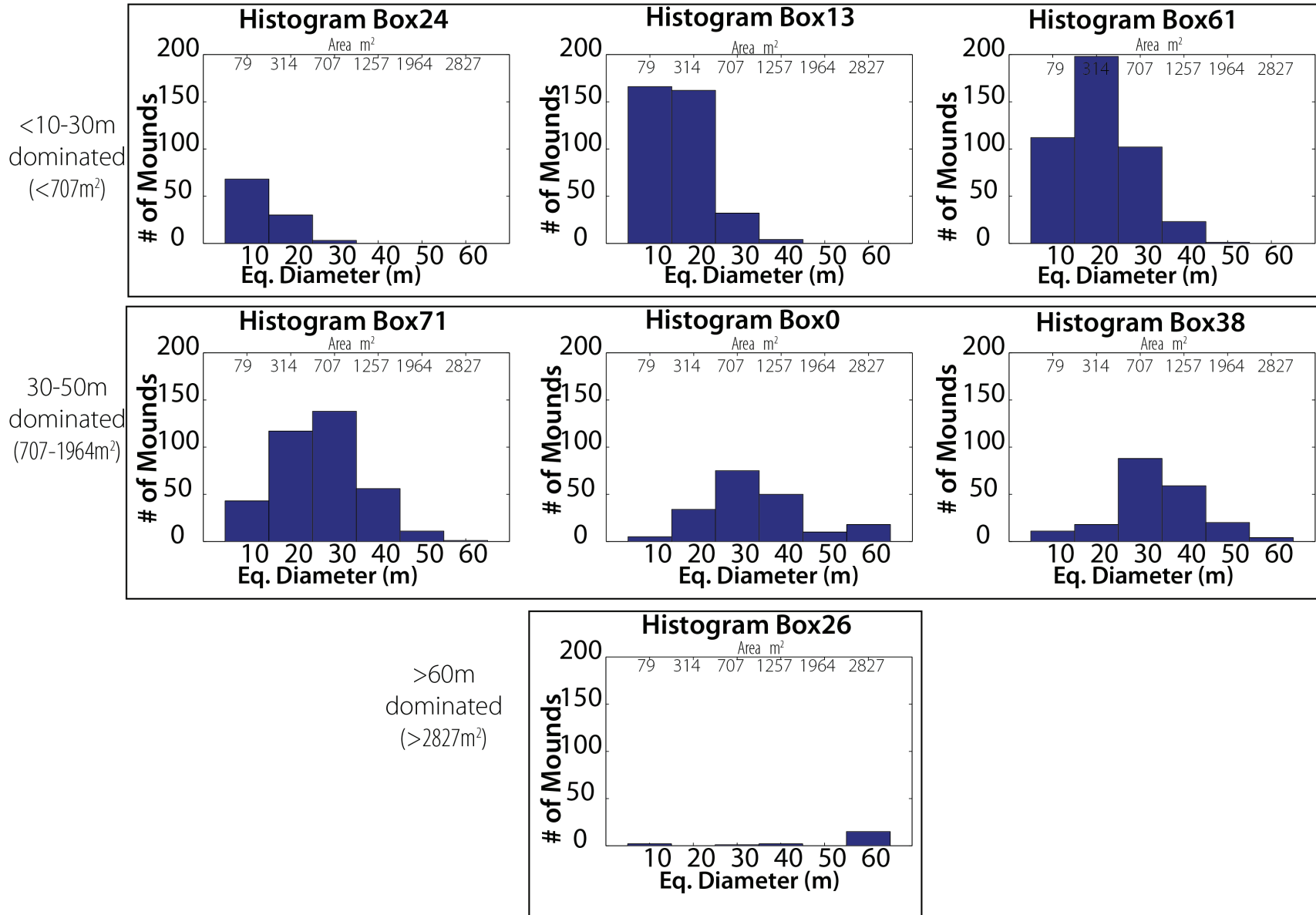
Fig. 3.8: Area and cross-sectional diagrams of typical mounts with the highest point shown. Most mounds are tallest near the center of the mound, and thus the approach of using the center of mounds to calculate heights of mound tops is employed. However, the shallowest area of one of the mounds within the bank at 26C has its shallowest part near the edge of the mound rather than near the center as shown in the area and cross section diagrams. These mounds were looked at more closely because this is the shallowest area with mounds and the mounds are large. The top center of the bank has less than 1 m of relief across it. So half a meter is considerable over the rest of the surface. The edges of the bank have the most relief. The shallowest area has a more typical lower backscatter as seen by the contours (A) and backscatter map (B), not higher backscatter as a would be expected of a more typical mound.
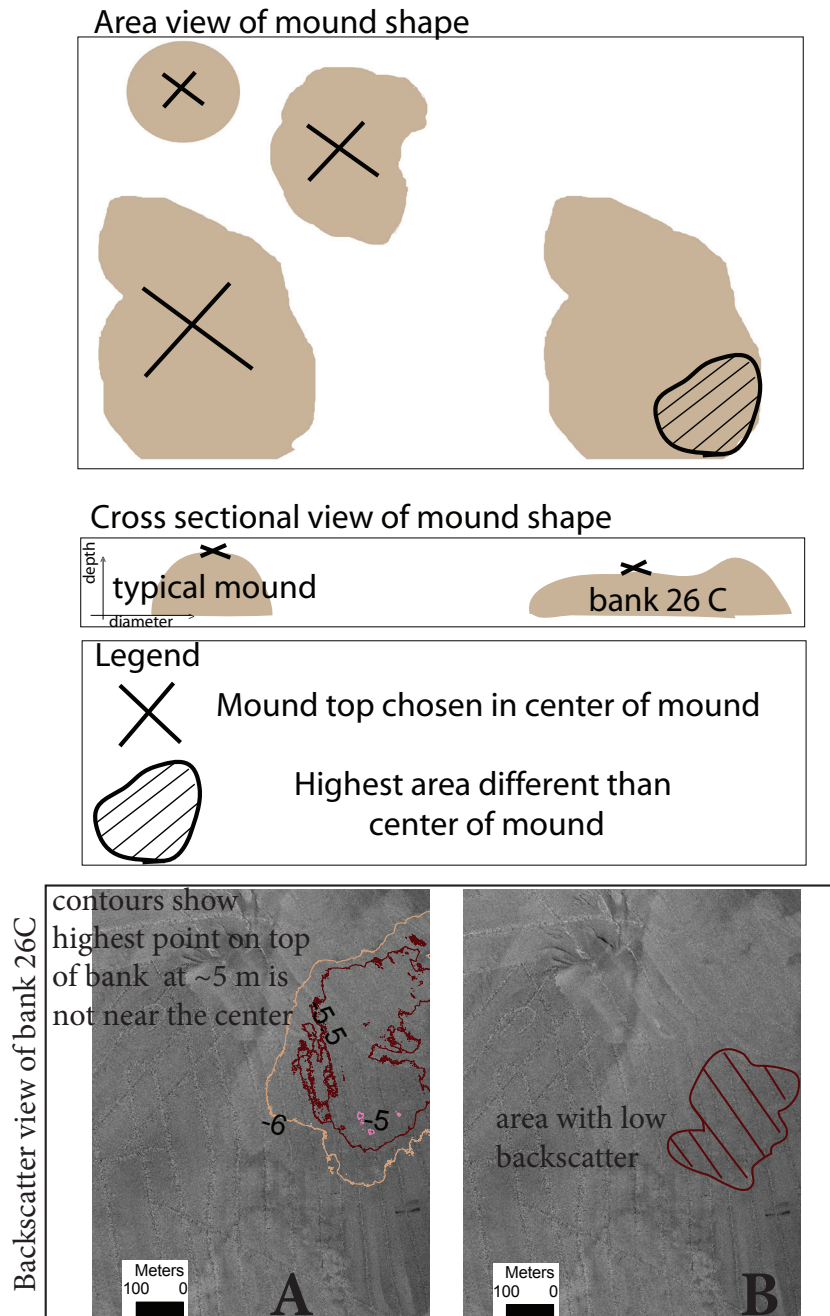
Area view of mound shape

Cross sectional view of mound shape

depth

typical mound

bank 26 C

diameter

Legend

☓ Mound top chosen in center of mound

Highest area different than center of mound

Backscatter view of bank 26C

contours show highest point on top of bank at ~5 m is not near the center

-5.5

-6   -5

A

area with low backscatter

B

Meters
100   0

Meters
100   0

92

REFERENCES:

Adams, E. W., Grotzinger, J. P., Watters, W. A., Schroder, S., McCormick, D. S., Al-Siyabi, H. A., 2005, Digital characterization of thrombolite-stromatolite reef distribution in a carbonate ramp system (terminal Proterozoic, Nama Group, Namibia), AAPG Bulletin, v. 89, p. 1293-1318.

Allen, Y. C., Wilson, C. A., Roberts, H. H., Supan, J., 2005, High Resolution Mapping and Classification of Oyster Habitats in Nearshore Louisiana Using Sidescan Sonar, Estuaries, v. 28, n. 3, p. 435-446.

Arlotta, Michelle, 2003, Benthic mapping as a tool for developing multidisciplinary maps of the Robin's Island area of the Peconic Estuary System of Long Island, New York [M.S. Thesis], Stony Brook University, Stony Brook, NY, 104 p.
Bonar, D. B., Coon, S. L., Walch, M., Weiner, R. M., Fitt, W., 1990, Control of Oyster Settlement and Metamorphosis by Endogenous and Exogenous Chemical Clues, Bulletin of Marine Science, v. 46, n. 2, p. 484-498.

Burnett, W. C., Tai, W.-C., 1992, Determination of Radium in Natural Waters by Liquid Scintillation, Analytical Chemistry, v. 64, p. 1691-1967.

Bushek, D. Richardson, D., Bobo, M. Y., Coen, L. D., 2004, Quarantine of oyster shell cultch reduces the abundance of Perkinsus marinus, Journal of Shellfish Research, v. 23, n. 2, p. 369-373.

Carbotte, S. M., Bell, R. E., Ryan, W. B. F., McHugh, C., Slagle, A., Nitsche, F., Rubenston, J., 2004, Environmental change and oyster colonization within the Hudson River estuary linked to Holocene climate, Geo-Marine Letters, v. 24, p. 212-224.

Cattaneo, A., Steel, R. J., 2003, Trangressive deposits: a review of their variability, Earth Science Reviews, v. 62, n. 3-4, p. 187-228.

Clapp, C. S., Flood, R. D., 2004, The Use of Side-scan Sonar for the Identification and Morphology of Sub-tidal Oyster Reefs in Great South Bay, Long Island Geologists, April 2004 Meeting Abstract.

Cook, H. E., Zhemchuzhnikov, V. G., Zempolich, W. G., Zhaimina, V. Y., Buvtyshkin, B. M., Kotova, E. A, Golub, L. Y., Zorin, A. , Lehmann, P, Alexeiev, D. V., Giovannelli, A., Viggi, M., Fretwell, N., LaPointe, P., Carboy, J., 2002, Devonian and Carboniferous Carbonate platform facies in the Bolshoi Karatan, Southern Kazakhstan; outcrop analogs for coeval carbonate oil and gas fields in the North Caspian Basin, Western Kazakhstan, in Cook, H. E., W. G. Zempolich, SEPM (Society for Sedimentary Geology), ed., Special Publication-Society for Sedimentary Geology, Paleozoic carbonates of the Commonwealth of Independent States (CIS): subsurface reservoirs and outcrop analogs, v.74: Tulsa, Oklahoma, SEPM, p. 81-122.

Darwin, C. R., 1842, The structure and distribution of coral reefs, Smith, Elder and Co., London, 214 p.

Davis, W.M., 1928, The coral reef problem, Special publication No. 9, Shaler Memorial Series, American Geographical Society, New York, 596 p.

DeAlteris, J. T., 1988, The Geomorphic Development of Wreck Shoal, a Subtidal Oyster Reef of the James River, Virginia, Estuaries, v. 11, p. 240-249.

Desor, E., Cabot, E. C., 1849, On the Tertiary and more recent deposits in the Island of Nantucket [Massachusetts], Quarterly Journal of the Geological Society of America, Geological Society of London, London, UK, p. 340 -344.

Emery, K. O., E. Uchupi, 1972, Western North Atlantic Ocean: Topography, Rocks, Structure, Water, Life and Sediments, Tulsa, OK, American Association of Petroleum Geologists, 532 p.

Flood, R. D., Cerrato, R., Goodbred, S., Maher, N., Arlotta, M., Zaleski, L., 2003, Benthic Habitat Mapping in the Peconic Bays, Program for the Tenth Conference on Geology of Long Island and Metropolitan New York, April 12, 2003.

Galtsoff, P. S., 1964, The American Oyster, Crassostrea Virgina Gemlin, Fish and Wildlife Service, Fishery Bulletin, v. 64, p. 457.

Gomez-Reyes, Eugenio, 1989, Tidally Driven Lagrangian Residual Velocity in Shallow Bays [Ph.D. Dissertation], MSRC, State University of New York at Stony Brook, December 1989, 129 p.

Grave, C., 1903, Investigations for the promotion of the oyster industry of North Carolina, U. S. Commission of Fish and Fisheries, George M. Bowers Commisioner, Extracted from the U. S. Fish Commission Report for 1903, p. 247-341.

Hedgpeth, J. W., 1953, An introduction to the zoogeography of the northwestern Gulf of Mexico with reference to the invertebrate fauna, Publications of the Institute of Marine Science, v. 3, p. 107-223.

Huvaz, O., Sarikaya, H., Isik, T., 2007, Petroleum systems and hydrocarbon potential analysis of the northwestern Uralsk basin, NW Kazakhstan, by utilizing 3D basin modeling methods: Marine and Petroleum Geology, v. 24, p. 247-275.

Ingersoll, E., 1881, The Oyster-Industry, The History and Present Condition of the Fishery Industry, Report on the oyster-industry of the United States, U.S. Department of the Interior, Washington D.C., Government Printing Office, Prepared under the Direction of Prof. S.F. Baird, U. S. Commissioner of the Fish and Fisheries and by G. Brown Good, Assistant Direction U.S. National Museum and a staff of associates.

Kennedy, D. M., Woodroffe, C. D., 2002, Fringing reef growth and morphology: a review, Earth-Science Reviews, v. 57, p. 255-277.

Kinney, J., Flood, R. D., 2006, Multibeam Bathymetry Reveals a Variety of Sedimentary Features in the Peconics Potentially Significant to Management of the System, Long Island Sound Research And New England Estuarine Research Society Joint Conference, October 26-28, 2006, United States Coast Guard Academy, New London, CT, Paper in Long Island Sound Research Conference Proceedings 2006.

Kinney, J., Flood, R. D., 2008, Peconic Estuary "Oyster Terrain": Carbonate Mound Transgressive Sequence? Fifteenth Conference on the Geology of Long Island and Metropolitan New York, Long Island Geologists, April 2008 Meeting, Stony Brook, NY.

Ladd, H. S., Hedgepeth, J. W., and Post, R., 1957, Environments and facies of existing bays on the central Texas coast, Chapter 22 of Ladd, H.S., ed., Paleoecology: Memoir - Geological Society of America, no. 0072-1069, 0072-1069, p. 599-639.

Lenihan, H. S., Peterson, C. H., 1998, How Habitat Degradation through Fishery Disturbance Enhances Impacts of Hypoxia on Oyster Reefs, Ecological Applications, v. 8, n. 1, p. 128-140.

Lyell, C., 1865, Elements of Geology or Ancient Changes of the Earth and its Inhabitants as Illustrated by Geological Monuments, London, 6th ed, First published 1838.

MacIntyre, I. G., Pilkey, O. H., Stuckenrath, R., 1978, Relict Oysters on United-States Atlantic Continental-Shelf - Reconsideration of Their Usefulness in Understanding Late Quaternary Sea-Level History, Geological Society of America Bulletin, v. 89, i. 2, p.277-282.

McCormick-Ray, J., 2005, Historical oyster reef connections to Chesapeake Bay- a framework for consideration, Estuarine, Coastal and Shelf Science, v. 64, p. 119-134.

Mel'nikov, N. V., Sitnikov, V. S., Vasil'ev, V. I., Doronina, S. I., Kolotova, L. V., 2005, Bioherms of the Lower Cambrian Osa Horizon in the Talakan-Upper Chona zone of petroleum accumulation, Siberian platform, Russian Geology and Geophysics, v. 46, p. 834-841.

Meinkoth, N. A., 1981, The Audubon Society Field Guide to North American Seashore Creatures, Chanticlear Press, Inc., Alfred A. Knopf, New York, p. 547.

Merrill, A. S., Emery, K. O., Rubin, M., 1965, Ancient Oyster Shells on Atlantic Continental Shelf, Science, v. 147, p. 398-400.

Milliman J. D., Emery K.O., 1968, Sea Levels during the Past 35,000 Years, Science, v. 162, i. 3858, p. 1121-1123.

National Oceanographic and Atmospheric Administration (NOAA), 2010, Raster Navigational Charts: NOAA RNCs, last accessed 2010, http://www.nauticalcharts.noaa.gov/mcd/Raster/index.htm.

Osterman, L. E., Twichell, D. C., and Poore, R. Z., 2009, Holocene evolution of Apalachicola Bay, Florida: Geo-Marine Letters, v. 29, no. 6, p. 395-404.

Parker, R. H., 1960, Ecology and distributional patterns of marine macro-invertebrates, northern Gulf of Mexico, *in* Shepard, F. P., ed., United States (USA).

Pufahl, P. K., James, N. P., Bone, Y., Lukasik, J. J., 2004, Pliocene sedimentation in a shallow, cool-water, estuarine gulf, Murray Basin, South Australia, Sedimentology, v. 51, p. 997-1027.

Purnachandra Rao, V., Rajagopalan, G., Vora, K. H., Almeida, F., 2003, Late Quaternary sea level and environmental changes from relic carbonate deposits of the western margin of India, Proceedings of the Indian Academy of Sciences, Journal of Earth System Science, v. 112, n. 1, p. 1-25.

Slagle, A. L., Ryan, W. B. F., Carbotte, S. M., Bell, R., Nitsche, F. O., Kenna, T., 2006, Late-stage estuary infilling controlled by limited accommodation space in the Hudson River, Marine Geology, v. 232, p. 181-202.

Twichell, D. C., Andrews, B. D., Edminston, H. L., and Stevenson, W. R., 2007, Geophysical Mapping of Oyster Habitats in a Shallow Estuary; Apalachicola Bay, Florida: U. S. Geological Survey Open File Report 2006-138.

USGS 7.5 DEM New York State (10 mx10 m pixels), 2010, NY State DEM courtesy USGS & NYDEC available via the Cornell University Geospatial Information Depository, North American Datum of 1927 UTM 18N, downloaded 2008, last accessed 2010, http://cugir.mannlib.cornell.edu/mapsheet.jsp?coverageId=23&id=all.

Weaver, E., Herbort, M., Dellapenna, T., and Simons, J., 2008, Geological Controls on the Distribution of Oyster Reefs and Substrates in Copano Bay, Texas, 2008 Joint Meeting of The Geological Society of America, Soil Science Society of America, American Society of Agronomy, Crop Science Society of America, Gulf Coast Association of Geological Societies with the Gulf Coast Section of SEPM, Geological Society of America Abstracts with Programs, v. 40, Geological Society of America, p. 15.

Woods, H., Hargis, W. J., Hershner, C. H., Mason, P., 2005, Disappearance of the natural emergent 3-dimensional oyster reef system of the James River, Virginia, 1871-1948, Journal of Shellfish Research, v. 24, i. 1, p 139-142.

CHAPTER 4: THE RELATIONSHIP BETWEEN AGE, SEDIMENT CHARACTERISTICS AND MOUND DEPTH

INTRODUCTION:

The 'Oyster Terrain' mound morphology exposed in the multibeam bathymetry of the Peconic Estuary is hypothesized to represent a relatively intact example of a transgressive sequence of carbonate mounds or reefs that is likely to be common throughout the geological record. In order to test this hypothesis on the origin and antiquity of this Oyster Terrain, sites were selected for dating based on a more detailed understanding of the sediments and shells and of the high resolution geophysical data presented in Chapters 2 and 3. Analysis of surface grab samples that were collected as ground truth for the high resolution backscatter and bathymetry data provided most of the information used for site selection. As in Chapter 3, this chapter initially focuses more detailed analysis on Little Peconic and Noyack Bays. A few short gravity cores from Great Peconic Bay also provided some additional information on these features and modern sedimentary processes. Morphological evidence has supported the hypothesis that the Oyster Terrain represents relict oyster reefs, but dates are needed in order to understand the evolution and significance of this terrain, radiocarbon dating of relict shells from grab samples helped us to determine the ages of these features. Analysis of buried mounds, including sedimentation rate estimates on overlying sediments, helped us to understand modern sedimentary processes.

The main hypothesis to be tested was that mound features are at least a few thousand years old, and grew in shallower, more brackish water than at present. Our initial interpretation of the antiquity and origin of this terrain was based on the depth distribution of the features, burial of features by at least 3 m of sediment in places, and age and quality of shells. A top priority was, therefore, to test the hypothesis that these features date from the early to mid Holocene and that relict oyster reefs of different

depths were last active at different times. One alternate hypothesis might be that reefs were active throughout the full water depth range at the same time and thus there was no systematic distribution of age of tops of mounds with depth. In such a large estuary it is possible that there are spatial and temporal patterns of ages. For example, mounds closer to the ocean might be older or reefs in different basins may have evolved separately, so dates were chosen from one basin within the estuary. In order to test the hypothesis, the author obtained AMS ^{14}C dating of the calcium carbonate in oyster shells collected from a subset of the tops of mounds representing a range of water depths. These shells also extend along the main axis (length) of this basin of the estuary and might also reveal a spatial pattern in ages. Additionally, by looking at inventories and profiles of ^{210}Pb (half-life of 22.3 years) as well as some of the shorter lived radionuclides such as ^{234}Th in sediment cores near mounds one can estimate mixing and sedimentation rates for recent times that may help to constrain the ages of these features. Cores were taken in Great Peconic Bay over buried mound features revealed by multibeam backscatter and morphology and by adjacent seismic lines. Cores help us understand whether mound features that are buried by low backscatter sediment are similar in all respects to the exposed mounds. Core samples will also help to distinguish the sedimentary characteristics of the mounds from those of more recent sediments.

In order to accurately date these features, and to test these hypotheses, the settings of the samples selected for age dating need to be carefully described. One particularly wants to be sure that no anthropogenic shell material is included in such analysis, which was ensured by comparing recovered shells with shells from present-day aquaculture operations.

METHODS:
^{14}C Sites & Dating

In order to test the main hypothesis of this study, AMS (Acceleratory Mass Spectrometry) ^{14}C dates of the calcium carbonate in oyster shells from mounds

representing a range of water depths were obtained. AMS ^{14}C dating analysis was conducted at PRIME (Perdue Rare Isotope Measurement Laboratory) at Purdue University. The AMS ^{14}C analysis was made possible by a seed grant program at PRIME that is funded by the National Science Foundation. Optimal sites and samples for ^{14}C dating were selected based on existing bathymetric data, seismic profiles and sediment samples. Five shells, one each from five different mounds, were dated. Both buried and exposed shell sites were selected, but shells were preferentially chosen for dating from sites draped in mud as indicated by mud overlying shells in the grab samples. The goal was to obtain at least one sample from a mound covered by at least a few centimeters of mud in order to reduce the likelihood of obtaining dates from shells that could be an artifact of recent anthropogenic activity such as aquaculture. Individual shells were selected from grab samples with these criteria in mind in order to reduce the risk of anthropogenic shell content, to obtain samples with better preservation, and to maximize shell usage for further geochemical analysis and study.

Five sites were chosen to represent different depths that fit into three categories: shallower than average, average, and deeper than average. Two sites from close to the same depth and three sites of different depths would help to understand the relative roles of depth and position in determining mound age. An effort was made to try to keep the samples within the same basin in order to reduce possible effects of lateral changes in the estuarine environment. However, while most of the samples were in the central part of Little Peconic Bay, one sample was in Noyack Bay (26 C) (Fig. 4.1). This is thought to be acceptable because the connection between Little Peconic and Noyack Bays near Jessup's neck is wide enough and deep enough that major changes would not be anticipated that would substantially alter the hydraulic interaction between the two bays over the past several thousand years. This assumption will need to be evaluated.

The sites chosen (Fig. 4.1) had the planned shallow, medium, and deep ranges within Little Peconic and Noyack Bays. Sites for grab samples were selected based on backscatter and bathymetric maps, which show the general distribution of mounds in

relation to surrounding sediment types including gravel, sand, and mud ratios and features (Fig. 4.1). Typically sites were chosen near the center of areas with similar backscatter and as close to the center of mounds as possible in order to avoid sampling deposits that might have been eroded from the top of a mound. The shells in individual samples of potential sites were evaluated for condition and quality of shell, which resulted in the final choices. Care was taken not to analyze pieces of oyster shell that had bryozoans, barnacles or other subsequent carbonate alteration attached to the surface. These sites also show a variety of mound terrain morphology discussed in Chapter 3. The final shells chosen were from sample sites 26C (2008), 0b (2008), 70 (2008), 61 (2008), and 38 (2006), where parenthesis indicate the year the sample was collected (Appendix B1). Site 26 C, water depth 5.5 m, is in a large shallow bank with the largest mounds in area. Site 61, water depth 9 m, comes from the middle top of a bank of intermediate depth. Another shell at similar depth, 9.6 m, was chosen at site 70. This shell was located within a very dense field of mounds, although individual mounds were more difficult to distinguish than in other areas described as banks. Deeper mound sites included site 38, water depth 11 m, which is in a field of distinct mounds and site 0b, depth of 13 m, which is the deepest site and is on a mound at the base of a slope of mounds (channel). This study was unable to date appropriate material from yet deeper mound sites because of biological alteration of recovered shells (living *Cliona*), proximity to anthropogenic activity, or a lack of samples from mounds in deeper water.

As noted in Chapter 1, the Peconic Estuary has a long history of aquaculture, and as a result there is a need to distinguish possible oyster shell added since the late 1880's from those there earlier. Oyster shells grown by aquaculture techniques tend to look different than specimens from uncultivated or unharvested populations, which should help us to identify modern aquaculture shells if they are present. Multibeam data as well as maps of historical bottom lease areas, available on the Suffolk County Planning website (Suffolk County Planning, N. Y., 2011; County of Suffolk, N. Y., 2002; County of Suffolk, N. Y., 2001), were used to identify areas of potential aquaculture activities when selecting sites for ^{14}C dating. Areas with disturbed bottom near a

historic aquaculture lease often could be seen in the multibeam data. Most aquaculture lease areas actually did not overlap with the mound areas, and thus most grab sampling sites were not affected by this consideration in the selection of shells to date. Relict shells looked very different from modern aquaculture shells based on thickness, number of growth bands, condition of shells and lack of distinctive growth breaks with changes in direction of growth seen in the transferred aquaculture shells (Fig. 4.2). Shells underwent μCT (micro computer tomography) prior to cutting. Images of shell interiors helped ensure that an intact portion of the shell was cut, i.e. the piece being cut would not be hollow. Images also show growth bands of shells, indicating they grew for many years.

The end portion of the shell farthest away from the hinge was cut off. The portion cut was at least 10 g in size. The samples to be dated were rinsed, brushed, and sonicated briefly until clean to try to remove as much sediment as possible, and the cleaned shell samples were sent to the PRIME AMS Lab. At least half of each shell piece sent to the PRIME lab was dissolved in acid there to ensure a clean specimen for dating (personal communication, PRIME lab, 2008). PRIME lab reported the results as ^{14}C ratios, counting errors and radiocarbon age. They also reported the δ^{13}C value.

Radiocarbon ages were converted to calendar years using both the Fairbanks 0107 curve (Fairbanks et al., 2005) and the Marine04 version of the Intercalib04 curve (Reimer et al., 2004; Stuiver et al., 1998; Hughen et al., 2004). Both the Fairbanks et al. (2005) curve and the InterCalib curves need a reservoir offset from the terrestrial curve to calculate marine values. The InterCal working group produced the Marine04 curve based on a standard ocean reservoir offset (Reimer et al., 2004; Hughen et al., 2004), while the Fairbanks et al. (2005) curve requires users to select a marine reservoir age from a published database loaded into Google Earth™ or Google Maps™ based on spatial proximity to the sampled environment (Butzin et al., 2005; Coa et al., 2007). In addition to reservoir offset and standard uncertainty within the curves, both of the standard curves include certain age rages with plateaus in the curve, such as between ~ about 2,700 calendar years before present (Cal BP) and 2,450 Cal BP (Reimer et al.,

2004), where there is greater age uncertainty within those intervals. Both the standard marine offset of 400 years and the offset of 228 years for shallow water carbonates around Long Island are used here for age estimates. The $\delta^{13}C$ values reported by PRIME were also examined and determined to have no unusual values or patterns that might indicate an anomalous carbon reservoir. The calendar age for years before present is set to 1950 A.D. as previously mentioned.

Core from Great Peconic Bay

The analysis of cores will help to constrain the age estimates of the buried mounds. First-order estimates of mixing and sedimentation rates in cores collected in a mound area can be made using radionuclides such as ^{210}Pb with a half-life of 22.3 years, which scavenge onto particles in the water column (Koide et al., 1972; Armentano & Woodwell, 1975; Henderson & Anderson, 2003; Swarzenski et al., 2003). Decay of ^{226}Ra via ^{222}Rn and other shorter lived daughters produces ^{210}Pb (Swarzenski et al., 2003). The supply of ^{210}Pb in the water column is delivered via rivers from weathered soil and rocks, lateral transport, fallout from atmospheric ^{222}Rn, and decay of ^{226}Ra in the water column (Swarzenski et al., 2003). In addition to ^{210}Pb, ^{234}Th also provides information on the delivery of particles to the sea floor and mixing, helping to characterize the sedimentary processes. ^{234}Th is a radiogenic radionuclide with a half-life of 24.1 days supplied to the ocean via decay of ^{238}U in the overlying water column, which is subsequently quickly scavenged onto particles (Cochran & Masqué, 2003). ^{234}Th inventory in bottom sediments in the open ocean should increase linearly with increasing water depth, which is important when there are large changes in depth (Cochran & Masqué, 2003). In an estuary, ^{234}Th input to the bottom sediments will tend to increase with increasing salinity since ^{238}U activity increases with salinity (Koide et al., 1972; Cochran & Masqué, 2003). As decay of parent radionuclides continues to occur in the sediment the amount of in situ decay in the sediment needs to be subtracted out so that one gets the excess or unsupported value (Attendorn & Bowen, 1997; Stokes & Walling, 2003). Excess ^{210}Pb was calculated by subtracting out the decay of parent radionuclides and excess ^{234}Th was calculated by subtracting out value

102

of ^{234}Th from the sample that was recounted after all of the original sample should have decayed. Thus one may be able to distinguish sedimentation transport and bioturbidation with the help of multiple tracers (Cochran & Masqué, 2003; Swarzenski et al., 2003). Bioturbidation in the sediments of the Peconic Estuary is significant so more than one process may need to be considered to help constrain the processes involved.

Cores were collected from the top of and adjacent to low backscatter mapped mounds in order to sample oysters buried by mounds and the sediment covering the mounds. Gravity cores were collected on a March 28, 2009 cruise for a WISE 187 undergraduate field trip on the R/V Shinnecock, captained by Don Getz, and assisted by Brian Gagliardi and crew, who were all from SoMAS–Southampton. This cruise was supported by SoMAS and provided the basis for an opportunity for a Women and Science and Engineering (WISE) session on Oceanography. The WISE students assisted in the cruise and subsequent core analysis, including heaving up cores using a hand pulley/winch system following a failure with the standard winch system. The gravity cores were taken using a free falling gravity corer with an extra 20 kg weight and a core catcher. The clear plastic gravity core tubes had a 6.6 cm inside diameter with a 0.3 cm thick liner that equals approximately 7.2 cm in total diameter. GPS coordinates were recorded at core sites, and the vessel was put at anchor while coring was in progress. A total of seven cores were taken from the area (Fig. 4.3).

Cores were refrigerated after being returned to the lab, and subsampling of cores #1, #3, and #4 was conducted two days after collection by the class. Cores were measured for length, photographed and described, and three separate subsamples were taken for each 2 cm interval by extruding sediment from the cores. Core #7, composed of very coarse material such as pebbles, was also extruded and described within two weeks of the cruise. Core #5 captured at least the top of the oyster layer and was also extruded and described later. Remaining cores were kept refrigerated for later analyses. For Core #4, subsamples for the first four two centimeter levels were combined into two samples, and those samples plus every other two centimeters till the bottom of the core were measured on a gamma detector for ^{210}Pb and ^{234}Th within a

month of collection due to the short half life of ^{234}Th radionuclides. Radionuclides of ^{210}Pb and ^{234}Th in cores were measured on 3 KeV gamma detectors. Inventories, and estimates of mixing and sedimentation rates based on ^{210}Pb in this core were determined following standard methods (Koide et al., 1972; Armentano & Woodwell, 1975; Feng et al., 1998; Cochran et al., 2000; Henderson & Anderson, 2003; Cochran & Masqué, 2003; Renfro, 2010).

Grain size in Grabs & Cores:

Grain size measurements were made on the sediment matrix of a sample. Shells or other items greater than 2 to 4 cm were excluded from analysis although the presence and type of shells in grab samples was recorded. Unless shells were a component of the gravel fraction they were not included in grain size percentages. This 'matrix sample' was a subsample that would fit into a spoon, or was spooned out around larger shells. Grain size of the matrix is reported as percent mud, sand and gravel, or as percent clay, silt, sand and gravel. The sand and mud components of grab samples were analyzed separately on a Sedigraph^{TM} 5100 and a settling column and results were combined to obtain grain size measurements at 0.5 phi intervals (Flood et al., 2009). Grain size for the sediment fraction smaller than 0 phi (1 mm) is reported here in 0.5 phi intervals. Percentages are reported as weight percent of the total matrix subsample. Selected subsamples in Core #4 were sieved to determine the mud, sand, and gravel percentages and composition-shells. Ternary plots were made using Triplot (Graham and Midgley, 2000).

RESULTS:
^{14}C Results:

Reported ^{14}C ratios and ratio uncertainty from PRIME in our relict shells ranged from 980.58 to 879.44 (+/-14 to 18) and δ^{13}C ranged from -0.3 to 1 ‰ (Table 4.1). The ^{14}C ratios equate to ages that range from 1820 radiocarbon years to 2695 radiocarbon years BP, which is not as old as originally predicted in this study (Table 4.1). No

unusual δ ^{13}C pattern was observed that would suggest a large reservoir offset. The difference between ages calculated using the Fairbanks 0107 calibration curve (Fairbanks et al., 2005; Butzin et al., 2005) with a 400 year reservoir offset (1345 to 2400 Calibrated Yr BP) and the Marine04 calibration curve (Reimer et al., 2004; Stuiver et al., 1998; Hughen et al., 2004) with a built in offset (1350 to 2350 Calibrated Yr BP) (Table 4.2) are too small to be of concern here. A similar range of 1517 to 2573 Calibrated Yr BP was determined using a 228 year reservoir (Butzin et al., 2005) (Table. 4.2). From here on calendar ages calibrated with the Hughen et al. (2004) Marine04 curve will be used unless otherwise noted (age range 1350 to 2350 Calibrated Yr BP) as it is more standard in the literature.

In order to estimate water depth when mounds were last active, the Gutierrez et al., 2003 sea-level elevation curve was used to determine sea-level elevation at time of each shell date. The sea-level depth when last active was then subtracted from the modern depth of the shell. The depth of the dated shells and their respective mound tops relative to mean sea level (MSL) with calibrated age have been plotted along with the sea level curve for Nantucket from Gutierrez et al. (2003) to show the approximate water depth that mounds grew in when last active. The shallowest mound, 26C, which is part of a very large bank, was dated to 1350 Cal ybp, giving a sea-level offset of ~3 m. This mound would have thus been last active in about 2.5 to 3 m of water (Fig. 4.4). The deepest and oldest mound that the author dated (0b) was dated to 2350 Cal ybp, with a sea-level offset of ~4 m; meaning it would have last been active in about 10 m of water (Fig. 4.4).

There is a linear trend with the tops of older mounds being found in progressively deeper water when last active (Table, 4.3, Fig. 4.4). Comparison of mound ages in Little Peconic Bay and Noyack Bay with latitude and longitude or along the length of the estuary axis from estuary mouth to head showed no relationship. No spatial relationship was found for δ^{13}C either. Neither did mean grain size, percentage clay nor other subdivisions of grain size seem to have a relationship to age in this set of dates (Table 4.4). No significant relationship between mound type and age of mounds was

105

noticed. The depth of mounds seemed to be the dominant control on mound age in this study's set of samples, however it is probably not the only control. Different reef morphologies were not well tied to age, but some morphologies tended to be younger or older. For instance, it was noticed that the bank reef at 26C seemed to be the flattest and appeared very mature. Its depth was the shallowest and its age was the youngest. Depth can be seen to be the dominant factor in age as one can see in the examples of the apparently mature bank (61) and an adjacent dense field of mounds (70) in approximately the same depth (the bank is 0.6 m shallower) that are about the same age (#61 is ~75 years older). The one morphology that was seen more in a certain age group was the individual mounds with the most distinctive relief as these were the deepest and oldest, 38 and 0b.

Sediment Characteristics of Mound Grabs:

The presence of shells in main grain size intervals and the grain size of grab samples shows that the difference between an exposed mound with a high backscatter top and the adjacent low backscatter areas is that the mound sediments have higher oyster shell content than the adjacent sediments. The high backscatter area has large oyster shell pieces and whole shell halves buried in mud and the gravel fraction of this sediment is 90-100% shell fragments and flakes. However, the sediment that these shells are in appears to have similar characteristics to the sediment between the mounds based on grain size measurements and visual appearance. For instance, mound grab sample 26-C (2008) is very sandy (~77%) as is the surrounding area, and the mound at grab 70 (2008) has a similar high sand content.

Not all mounds have the same level of intensity or difference in backscatter (DN scale of 0 to 250) compared to surrounding areas. In sandy areas shell rich mounds can average a DN of 170, while surrounding areas average a DN of 130. In contrast mounds in a muddy area might range from 130 to 170, while the surrounding areas DN average 60. Some of the mounds have lower backscatter values, one mound with a DN value of less than 100 was sampled, but the sampler did not recover any oyster shell

suggesting that the mound is buried by more recent sediment. There was at least one grab with an average DN of about 100 that had mud with shell buried at the base of the grab. A very distinct mound might return a backscatter value of 170 while a less distinct mound might average closer to 150 in the same area.

In our first round of sampling during 2006, our field descriptions noted the presence of obvious oyster shells associated with the most distinctive mounds, which had the highest backscatter values. Mounds with lower backscatter, which were less distinctive than neighboring mounds had a high matrix to oyster shell ratio (1 shell per 0.3 to 1 L of sediment). In particular, a grab sample from a low backscatter mound revealed that this mound was being buried or draped by a layer of ~10 centimeters of mud over the oyster shell layer. The amount of exposed shell material was in effect lower.

In general the 1 mm to 63 µm sand fraction of sediment samples was useful in characterizing mounds because it was distinctive. In all samples of our survey area, the presence of material coarser and finer than sand in a grab was mirrored in this 1 mm to 63 µm sand size distribution. For example, if there were gravel, pebble or cobble sized particles, then coarser sand grains were present, and the percentage of very fine sands increased with an increased percentage of mud. Mounds in particular mirrored the coarser shell present in the mound top, as well as the finer sediments in the 1 mm to 63 µm sand fraction. However, a subset of 20 samples of the 1 mm to 63 µm sand fraction of mound and non-mound sites were examined under the microscope, which confirmed that there were no broken shells, only siliclastic grains and foraminifera in this size fraction in Little Peconic Bay. The particles around 1 mm in size tended to be siliclastic grains, foraminifera tended to be slightly smaller, typically closer to 250 to 100 µm.

Another common characteristic of the mound sites with oyster shells was the presence of foraminifera in a brown mud within the matrix along with the abundant quartz sand grains. This description particularly matched the sites that were more than 80% shell. Spherical opaque whitish/cream colored grains were visible in the rinsed

(sieved) sand in this range, which upon magnification of a subset of samples were revealed to consistently be foraminifera. Sieved sand from sites such as 61 and 83 included the presence of foraminifera, which were especially abundant in samples 73b and 0a. Our initial sand descriptions reported 'rounded carbonate grains' for samples 71, 80, 0b, and 60 that were subsequently determined to be benthic foraminifera. Few foraminferas were found in other areas including areas around mounds, sand banks, sand waves, and flat muddy areas with 0 to 230 per g/matrix sediment versus more than 750 per g/matrix sediment on a mound with oysters (Table 4.5). Most non-mound areas had none to a few dozen per gram, with more shell rich sediments seeming to have slightly higher abundances.

Other sediment grain size characteristics shared between exposed mounds were not obvious. Mud content seemed to vary within the larger basin and is unrelated to the presence of mounds. Few large clastic grains were observed, such as the gravel or pebbles as seen near Great Hog Neck and in the channel near Shelter Island in the oyster rich grabs or surrounding areas. A subset of oyster mounds from our 2006 grabs reported the frequency of the presence of other shell types in mounds, primarily jingle and slipper shells (Fig. 4.6) and showed that oysters dominated reef sites. Most mounds only have oyster shells and no other species of mollusk shells present.

Mound sediments had a variety of matrix sediment to greater than 1 cm shell ratios. The proportion of shell material to sediment could be difficult to calculate accurately. Some grabs were almost all oyster shell (more than 90% shell), with just a small veneer of mud or sediment in the grab. The low sediment/ high shell content (less than 25% matrix) samples had very intact shells, and less fine shell hash. It is some of the more mixed samples (40-75% matrix), with high shell content and lots of shell hash that are different. There were examples of large oyster shell halves with minimal erosion buried in clumps of mud or sand. At other sites shell buried under a few cm had poorer preservation (i.e. more rounded, smaller pieces). High shell content and shell hash may act to buffer further degradation of shells in black anoxic mud as anoxic sediments may have higher CO_2 and thus lower pH. Shells at sites with both high and

low percentages of mud (5%-90%) had very thick shells, but the specimens buried in mud often appeared more eroded, worn, or dissolved.

There is mud in many grabs that seems to be burying the shells, and then there are other places where coarse sand from adjacent features is obviously burying the mounds. Examples of this can be seen in the sheet of sand near #70 (2008), in the sand banks near Robins Island and in the 'Rectangle' feature in Noyack Bay toward the channel on the south side of Shelter Island. Many of the exposed mounds are covered by a mix of more recent sediments and mound sediment. This suggests that there are patterns of sedimentation and transport in areas with exposed mounds. Indeed, when areas of repeated coverage of the same exposed reef areas were examined in Little Peconic Bay, a few examples of some movement of the mud veneer over reefs were noticed (Fig. 4.7). This is evidence of recent burial and short term variability in the surface sediments.

Results of Great Peconic Bay Cores:

Core #5 was collected from a mound in Great Peconic Bay. Unfortunately, the core was washed out on the sides, so the actual penetration is uncertain and the interpretation should be made with care. The effects of the washout could be seen in the sections that were loosely packed and missing much of their sediment matrix, while other sections remained as solidly packed shells in sediment. This makes us believe that the sections that were solidly packed should be representative of the sample deposit. The core contained oyster shells and sediment of a brown mud matrix with abundant quartz sand grains buried under almost 5 cm of muddy sediment (Fig. 4.8). A distinct contact layer was found between the top mud layer and the bottom shell rich layer. Sediment at the vertical transition 4 to 5 cm from the top of the core went from smooth textured mud (98% mud) to a coarser sediment matrix with foraminifera surrounding the oyster shells below. The coarser sediment with quartz sand and foraminifera with some mud matrix was very similar in appearance to the sediment of exposed mounds sampled by grab sampler in Little Peconic Bay, except that the oyster

shells in the Great Peconic Bay core were very black in color. The core cut through the oyster shells like a "cookie cutter" in the mound sediments, chopping off the edges of shells within multiple layers of stacked oyster shells. The mud/sand mix of this lower portion of the core included a coarser quartz rich sand with rounded carbonate (foraminifera) grains and oyster shells and oyster shell hash. This sediment matched the characteristics described here as common to mounds in surface grabs: coarser quartz sands, foraminifera, a brown mud, and shell hash. This oyster-rich sediment layer visibly resembled many of our other mound sites, especially those that were more exposed with more sandy sediment present at the surface that typically had a small percentage of light brown mud present.

The muddy surface of core #5 resembled adjacent longer gravity cores (#4 & #3) that were 20 to 30 cm and were retrieved from lower backscatter sediment near mounds. Those longer cores contained mostly mud – at least 98% mud, some very fine sand, and shell hash/small pieces of non oyster-shell (<1 mm). As with other grab sites from non-mound areas, few foraminifera were present after sieving (1 to 0 per 1 g).

Core Analysis: Radionuclides:

Very little accumulation of excess ^{210}Pb or excess ^{234}Th was seen at Core #4, no ^{210}Pb was found by 2 cm down in the 20 cm Core #4 and the ^{210}Pb total inventory (I_∞) was only 3.2 dpm/cm^2. ^{210}Pb persists to 12 cm depth in Core #1 and the ^{210}Pb I_∞ of Core #1 is 85.8 dpm/cm^2, which is much higher and suggests that there indeed is greater accumulation at this site. The profile for Core #1 (over 26 cm) shows no ^{210}Pb below 12 cm with a more mixed top 7 cm, but levels decreased by more than half within the 3 cm sample interval (10 cm) below the more homogenous surface. The total inventory for Core #1 is much higher than those found in Little and Great Peconic Bays by Cochran et al. (2000) (36.9 to 20.6 dpm/cm^2), but the penetration of detectable ^{210}Pb in the core is not very different (Fig. 4.9). Mixing processes or transport may cause an overestimation of sedimentation rates because particles may have been mixed to depth rather than buried via new deposition or surface layers may be more transient and not

result in large accumulation over hundreds of years. For example, in many of our grabs we found living fauna throughout the depth of the grab – clear evidence of some mixing which may confound estimates of sedimentation rate, at least those based on ^{210}Pb. This included tube mats of polychaetes that extended entirely through to at least 15 cm and below our grab, other burrowing organisms such as a large mantis shrimp a few cm in diameter to much smaller, but very active ~1 to 2 mm diameter worms.

The spatial patterns in inventories are similar to sedimentation patterns determined by comparing our survey depths with those collected in the 1930's by NOAA (0.0 to 0.4 cm/year not including sea level adjustments) (Fig. 4.9). Erosion in places of high flow can be seen between the NOAA data and today. Cochran et al. (2000) show that accumulation rates calculated based on ^{14}C (0.11 to 0.08 cm/yr) are smaller than ^{210}Pb accumulation rates (0.13 and 0.2 cm/yr) and thus ^{210}Pb may overestimate accumulation in the Peconic Estuary. Flat muddy areas overlying buried mounds should have higher sediment flux, including sites in Cochran et al. (2000), as more sediment has been observed covering mounds at those sites. These patterns make sense in terms of the changes in bathymetry.

Further evidence for the pattern of minimal sedimentation on top of mounds and higher rates at the base of exposed mound features is seen in our seismic profiles and the existence of exposed mounds at the same depths of many buried mounds. The structure of the mounds seems to reduce the amount of sediment that accumulates at the surface as the features become flatter over time. As the spaces between become filled in faster than the tops, the effect of the shape on flow should be reduced allowing the mounds to be buried faster. If tops of mounds are a source of sediment too, a similar pattern of reduced exposed mound relief would still lead to decreased flow and increased burial.

If one takes 0.08 cm/year to be a valid rate for an area where mounds are buried, then one would expect it to take 1,250 years for 1 m of sediment to accumulate. Modern accumulation rates may be higher than in the past, physical and biological

mixing and transport may alter the high values, and supply of particles is definitely higher in the flat muddy areas compared to other locations. However, this estimate seems reasonable based on ages of relict reefs. For example one can see mounds that are buried by 2 m of sediment at depths of mounds dated to close to 2,500 years ago, which is consistent with a sedimentation rate of 0.08 cm/yr.

DISCUSSION:

The radiocarbon ages tell us that the youngest mound dated was active until about 1,350 cal ybp (Marine04 curve), or about 1,500 years ago if the smaller reservoir correction is used. The oldest mound dated was active until ~2,350 cal ybp, or about 2,575 years ago with the smaller reservoir correction. This suggests that mounds of the same age as the surface features that was dated could have been buried by sediment for 1,350 to 2,575 years. Deeper mounds may have been buried while other active mounds continued to grow.

A maximum rate for reef growth can be made based on the assumption that all reefs grow at the same rate and that all reefs are in about the same water depth at the same time, i.e. the youngest reef was growing in the same water depth as the oldest reef when the oldest reef died. The fastest a reef could grow then would be the difference in age and height of the oldest and youngest (shallowest) reefs tops dated. Estimation of growth rate is made by finding the difference between the oldest and youngest dated shells (2,350 to 1,350=1,000), then dividing by the difference in the modern depth of these two shells (1,000yrs/7.5 m). Using this approach yields a rate of 133 years/ 1 m of reef height or 0.75 cm/ yr. If reefs grew at this rate, then the deepest mound bases would date back to at least 3,750 Calibrated ybp. Reefs probably grew more slowly than that – this is somewhat faster than estimates of 1 m per 200 years for a reef in the James River by DeAlteris (1988) (a submerged reef in an area of shallower reefs) and a lot faster than 1 m per few thousand years estimated for off the Suwannee River by Wright et al. (2005) (an emergent reef on the continental shelf) – but it is a first estimate of oyster reef growth in the Peconic Estuary.

An age range for when the oyster terrain may have been initiated was also estimated. The oldest age was based on a linear extrapolation of age and depth based on dated shell depths from this study (Fig. 4.4) and was consistent with the age range estimated by using mound depths and sea-level elevation from the curve for Nantucket published by Gutierrez et al. (2003). Deeper mounds would have been active since roughly 8,000 years ago if they were living in 2 m of water (Fig. 4.10). When the 2 to 6 m of relief of the mounds that now have tops at 12 to 18 m water depth is accounted for, one estimates that mound bases are in 14 to 24 m of water as is seen in the seismic data. When one uses the same approach, one finds that mound growth may have initiated 7,500 to 9,000 years ago. Thus the mounds may have started growing anywhere between 3,750 and more than 9,000 years ago.

A reason that the ages of the oysters were younger than expected based on their water depth is because no reefs were found in less than 5 m (MLLW) (5.45 m MLW) of water at present, even though there would have been areas within at least a meter or so of that depth that one would expect to be suitable when the last reefs were active. The youngest reef would have been active in ~4 m of water. While the author does not expect oyster reefs to be above MLLW in this climate, it was thought that reefs might be found slightly shallower, maybe 1 m. This suggests that the habitat in shallower depths at that time was not viable for reefs for some reason. One can think of many reasons why this study found no reefs at less than 5 m at present. Perhaps the sandy ledges at that depth were too active for new reefs to settle because of highly mobile sand beds with wave eroded sand from glacial hills. Winter ice dynamics might have also played a role. It is also possible that any such features were subsequently buried by the highly active sand banks rimming the estuary and were too deeply buried under the sand for the seismic profiler to penetrate. Evidence of a sand bank moving in the distinctive rectangle feature covering mound tops with 6 m of sediment was observed. This suggests that the previous coastline is buried and any mounds that may have initiated close to shore are likewise buried. Areas near shore also carry a high risk of burial by sand. Storms can destroy, create, or bury a reef just as they have historically

113

reconnected spits such as Cedar Point (Fig. 4.11) (Suffolk County, 2008). Erosion of the tops of these last active mounds is also possible. Increasing salinity may have also inhibited new reefs from forming, while only a few of the largest reefs continued to persist. Future analysis is necessary to understand this pattern.

The distinctive sediment found within the shell layer of Core #5, and in exposed mounds elsewhere, with its coarse quartz grains and foraminifera rich sediment, appears different from the overlying finer sediments. As foraminifera are widely used in paleoenvironmental studies, those in Peconic Estuary sediment may be useful to future research in the area. The change in sediment suggests either that a major change in sediment dynamics occurred or that inactive reefs were buried with finer sediments. In many estuaries, deeper reefs get quickly buried, and only those reefs that grow fast enough will survive. If an area is accumulating sediment, one would expect an inactive reef to get covered eventually if flow was insufficient to keep it exposed. The profile of Core #5 is consistent with the burial of mounds observed on seismic profiles. Buried mound shapes in profiles reflect the contrast of one type of sediment exposed at the surface, mud in this case, and the mound sediment. One can see a sediment type that seems to have dominated reefs, which is different than sediments burying relict reefs today. The presence of multiple layers of oyster shells within the base of Core #5 suggests that these reflective layers are not just a thin veneer of shells. The coarser fraction at the base of the core was especially similar to the very shell rich grabs, which suggests that they are closest to existing inactive reefs in sediment type. Multiple cores through reefs would be necessary to understand the composition and structure within reefs better.

CONCLUSION:

While the relict reefs are definitely relict, shells dated from mound tops were younger than anticipated. The youngest mound top was dated at 1,350 Cal ybp. The oldest surface dated to 2,350 Cal ybp. As only the tops of exposed mounds were

dated, the terrain is certainly older than this. The author estimates that the terrain would have initiated between 3,750 and 9,000 year ago.

Estimates of water depth at the time of oyster reef death were interesting because it is unusual to have such a high density of oyster reefs that lived in such deep water (Powell et al., 1992; Lenihan & Peterson, 1998; Allen et al., 2005; DeAlteris, 1988; Clapp & Flood, 2004; Powell et al., 2003; Osterman et al., 2009; Twichell et al., 2007). Many examples of a few reefs living in deeper water exist (Bratton et al., 2003; Smith et al., 2003), but it is common for older deeper reefs to start to get buried soon after they become inactive (Grave, 1903; Powell, 1993). Even the thickest of reefs cited in the literature tend to be buried and it is unlikely that their full thickness was ever simultaneously exposed (Bouma, 1976). Many estuaries have higher sedimentation rates in deeper areas that prevent survival. The presence of many oyster reefs in deeper water in the Peconic Estuary may suggest that low sediment supply and flow speeds throughout this estuary allowed reefs to persist living at greater depths and keep reefs exposed longer after their death.

The sediments in the shell layer of the core with its coarse quartz grains and foraminifera closely resembled the sediments found in exposed mounds elsewhere. The coarser fraction at the base of Core #5 was especially similar to the very shell rich ones, which confirms that Core #5 sampled to the top of a buried reef. This suggests that either some of the coarser material may be more representative of relict sediments near active mounds, or that processes such as sorting and deposition of only coarse material have occurred following reef death. The cores and grabs also seem to indicate a shared history of deposition of mud over mounds, and possibly other shared similarities in processes between burial and exposure. Staining and similar shell shapes including thickness and curvature as found in dense reef-like clusters are consistent throughout grab oyster shells.

The variation in exposure vs. burial is a complex pattern that suggests the reef morphology helps to keep mounds exposed. The Great Peconic Bay surface sediments

recovered seemed to show evidence of more recent erosion or redeposition upstream, to the west, from the high flow races by Robins Island between the 1930's and today. This area of and exposed mounds in Great Peconic Bay is in the path of high flow for this area modeled by Gomez-Reyes (1989) (Fig. 4.9), and this high current may be responsible for the exposure of these mounds. Current flow may change somewhat overtime, which may help to bury features in one area while exposing them in another area. Sedimentation rates should give an underestimate for the ages of buried features because burial of mound tops would not have happened until after reefs died and post colonial sedimentation rates have been found to be faster than in the past (Clarke & Patterson, 1985). Many more long cores representing mounds and adjacent areas using multiple radionuclide data sets in addition to ^{210}Pb will be needed to determine what kinds of sedimentation occurred and what sedimentation and mixing rates might be. Multiple samples of such a heterogeneous environment where ^{210}Pb showed virtually no accumulation to 0.35 cm/year are needed to understand the role of modern processes in altering the terrain characterized here. A first set of calculations based on Cochran et al. (2000) ^{14}C sedimentation rates seemed appropriate given reef ages. One can see that the processes that are going on are complicated and that the few core profiles now available are not enough to fully understand sedimentation patterns. The radioisotope tracers reflect the interaction of relief and sedimentation.

Deeper mound tops do seem to be older than shallow mound tops as hypothesized. However, reefs were growing in water deeper than originally hypothesized when they were last active and their tops are somewhat younger than anticipated. While oyster reefs can grow today in water deeper than a few meters, typically this is not the case in areas where oyster communities are stressed. Thus it is surprising that the relict reefs were active to such depths (3 to 10 m below MSL). The large number of reefs at such depths indicates that conditions were good for oysters. The estuary has most likely consistently had large tidal currents that would be good for oysters for thousands of years due to the geometry of the basin and the multiple deep constrictions in width of the bays. Sufficient flow is required to prevent mud and oyster feces from accumulating too quickly, while dense reefs require higher flow to provide

food (Galtsoff, 1964). Similar currents to today may have existed in the past that may have helped to keep oyster reefs from becoming too quickly buried. As the sediment in buried reefs is relatively sandy and quartz-rich, this suggests that current speed over mounds was faster than today in areas that are currently being buried. Significant alteration of sedimentation rates and inventories were observed that may be related to the alteration of boundary layer flow patterns due to the presence of mounded topography.

Many questions about the implications for other estuaries are raised by the continued persistence of reefs in this area for so long. The age of active mounds suggests that more estuaries may have had active reefs in water deeper than the 6 m of conventional wisdom. The depth and age of mounds now raises the question as to what the salinity was at the end of the age of active oyster reefs because the volume of water in the bay would not have been very different, but the smaller volume in the past implies slightly lower salinity then due to the relatively greater importance of freshwater input. However, relatively little is known about changes in groundwater input or precipitation that may have affected salinity in the estuary. Chapter 5 will address the question of paleosalinity from shell chemistry, which may help understand these changes. Interestingly, reefs from other non-lagoon estuaries seem to have been more abundant during times when the Peconic Oyster Terrain was alive, which will be discussed in Chapter 6.

Table 4.1: Radiocarbon and $\bar{\delta}^{13}$C results from PRIME Lab.

Shell ID	Ratio	δ^{13}C (‰)	Correction	Radiocarbon Age (yr)	Uncertainty in Ratio	Uncertainty in Radiocarbon Age
26C (2008)	980.6	0.9	0.974	1820	18	147
0b (2008)	879.4	1	0.974	2695	15	135
70 (2008)	937.5	-0.3	0.975	2171	14	119
61 (2008)	930.3	0.8	0.974	2241	17	150
38 (2006)	917.2	-0.1	0.975	2348	18	156

Table 4.2: Radiocarbon age to calendar years: Fairbanks et al. (2005) and IntCal04 - Marine04 curves. Calendar age in years before present (1950) and the standard deviation associated with that including the radiocarbon error using the Fairbanks0107 internet conversion tool. Radiocarbon data converted using the Marine04 Curve (Hughens et al. 2005). Converted values using both the Marine04 and the InterCal04 (Reimer et al., 2005) terrestrial values for comparison and additional error associated with estimating calendar age in that time period on top of the radiocarbon error for the closest point on curve to our radiocarbon ages. The value closest to our age is shown in parenthesis, however round to the nearest half decade for the values we actually used.

Shell	Radiocarbon Age		Calendar Age Fairbanks0107		Calendar age		Calendar Age Marine 04 (before rounding)	$\delta^{13}C$	Marine04 Nearest point Calendar BP	Intcal04 Nearest point Calendar BP
ID (Year)	Mean	1 std dev	Mean	1 std dev	400 yr reservoir	228 yr reservoir				
26C (2008)	1820	147	1745	172	1345	1517	1350 (1350)	0.9	1350 ± 26	1730 ± 16
70 (2008)	2171	119	2165	152	1765	1937	1775 (1774)	-0.3	1775 ± 27	2150 ± 14
61 (2008)	2241	150	2250	191	1850	2022	1850 (1850)	0.8	1850 ± 27	2220 ± 14
38 (2006)	2348	156	2384	206	1984	2156	1970 (1968)	-0.1	1970 ± 26	2350 ± 13
0b (2008)	2695	135	2801	146	2400	2573	2350 (2349)	1	2350 ± 26	2780 ± 13

Table 4.3: Water depth of mounds below mean sea level when last active. Values rounded. Water depth calculated using the Gutierrez et al. (2003) more generalize curve.

Shell ID (Year)	Water Depth of Active Reef Meters Below Mean Sea Level	Present Depth of Mound Meters Below Mean Sea Level
26C (2008)	4	6
70 (2008)	8	10
61 (2008)	7	10
38 (2006)	9	12
0b (2008)	10	14

Table 4.4: Relict shell ages, water depth and grain size of sites.

Shell ID (Year)	Cal BP (YR) (Hughens et al., 2005)	Radiocarbon Std dev	Plus Error Yr BP	Radiocarbon age (YR)	Water Depth in Meters (MLLW)	Mean Grain size (gravel free basis)	%Clay	%Fine	%Sand	%Gravel
26C (2008)	1350	147	26	1820	5.5	2.8	1.8	11.1	77.1	11.8
70 (2008)	1775	119	27	2171	9.6	4.8	15.3	37.3	59.5	3.2
61 (2008)	1850	150	27	2241	9.0	5.6	20.4	36.9	33.7	29.4
38 (2006)	1970	156	26	2348	11.0	3.0	5.7	40.0	47.0	40.0
0b (2008)	2350	135	26	2695	13.0	4.0	8.1	25.4	64.5	10.1

Table 4.5: Presence and abundance of foraminifera in mounds topped by oysters vs. non-mound sites.

ID (2008) Samples	Any Foraminifera?	Coiled Foraminifera?	Oysters?	Shells?	Shell hash in sand	Ratio coiled foraminifera per gram of matrix	Ratio coiled foraminifera per gram sand
26 c	y	y	y	y	y	1687	2790
20	y	y	n	y	y	44	63
42	y	y	y	y	y	809	1154
23	y	y	n	y	few	43	71
12	y	n	n	y	few	0	0
13c	y	y	y	y	y	1221	2269
13b	y	y	y	y	m	768	1346
45	y	y	n	y	y	227	286

Fig. 4.1: Location of five sites chosen for ^{14}C dating.

(5)

Grab Sample sites
with Oyster Shell chosen for
C14 dating

2,000 1,000   0   2,000 Meters
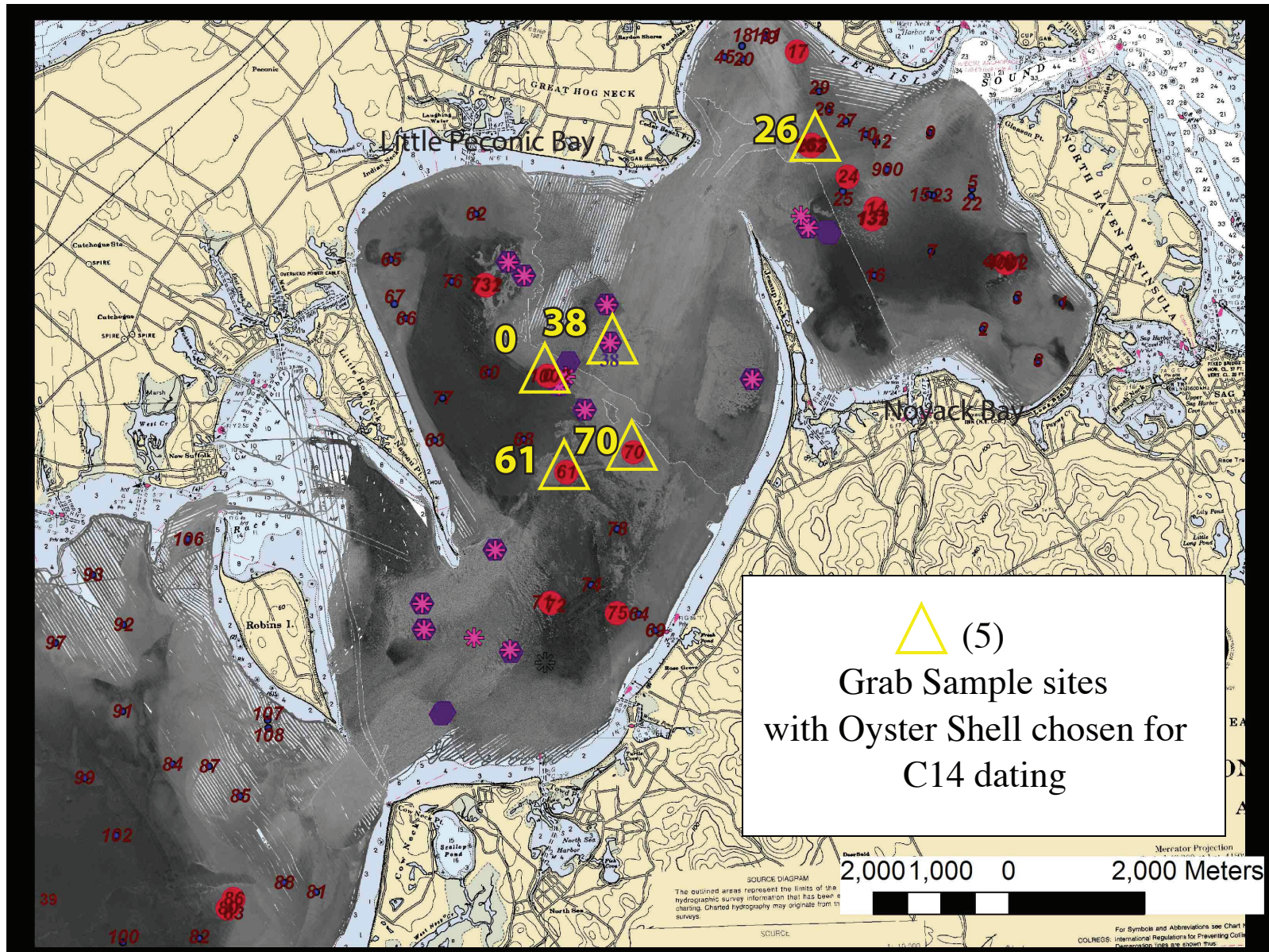
Fig. 4.2: Examples of relict and modern aquaculture oyster shells from the Peconic Estuary. Both samples have been washed and dried. Thickness and quality of shells in grab # 13 -2006 are very different than the very white small thin aquaculture shells. The non-chalky portion of the shells tends to look a little more grey or beige than the cleaned fresh aquaculture shells. Direction of growth has changed as noted by the dashed on the center shell.
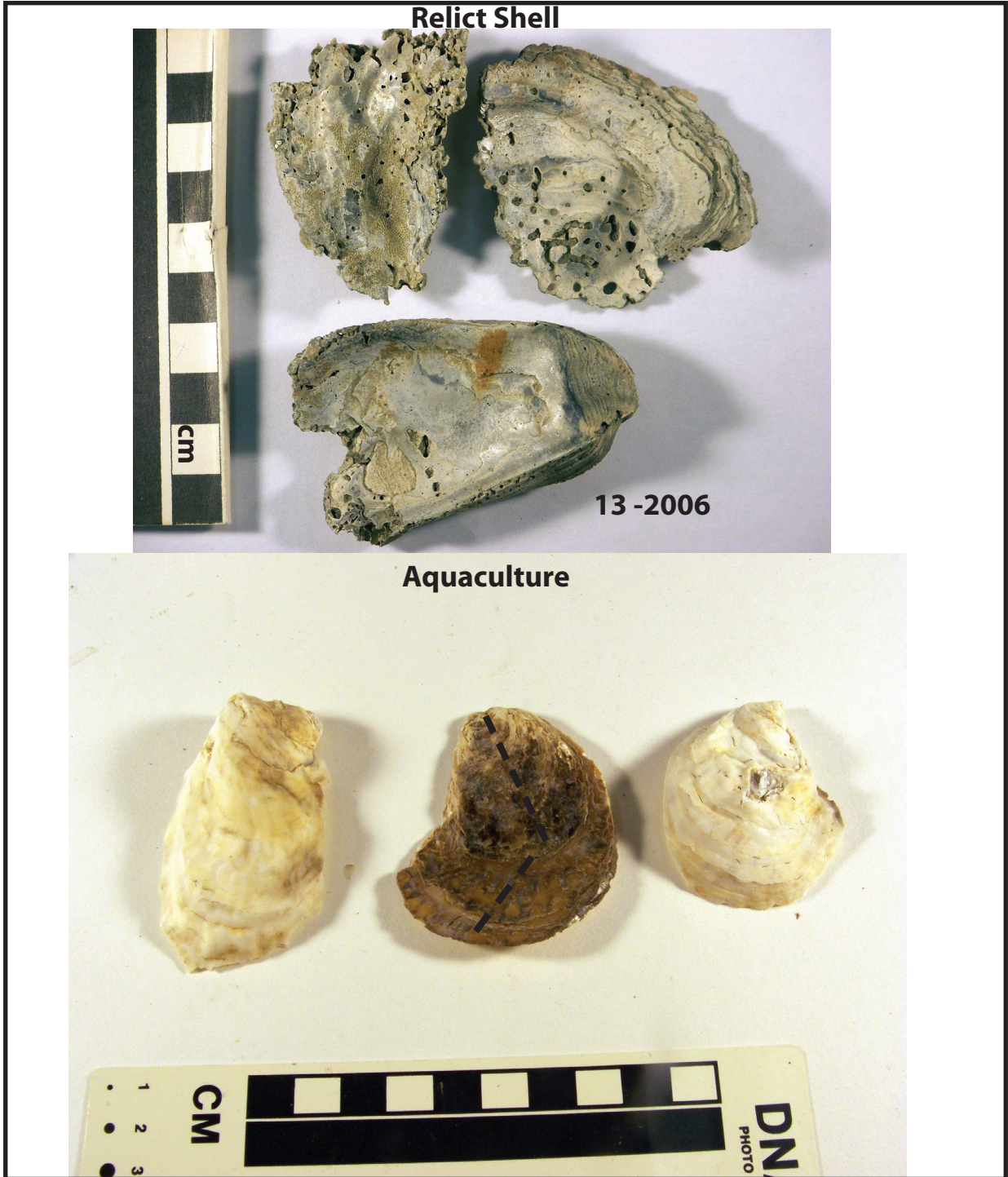
Fig. 4.3: Maps of backscatter & depth showing locations of cores 1-7. (Site 0 was a grab.) locations of cores 1-6 with backscatter, shaded relief (sun illuminated) relief, and shaded relief with depth (see color scale in previous figure). Sun illumination is from NW. UTM Top of page is North.

125
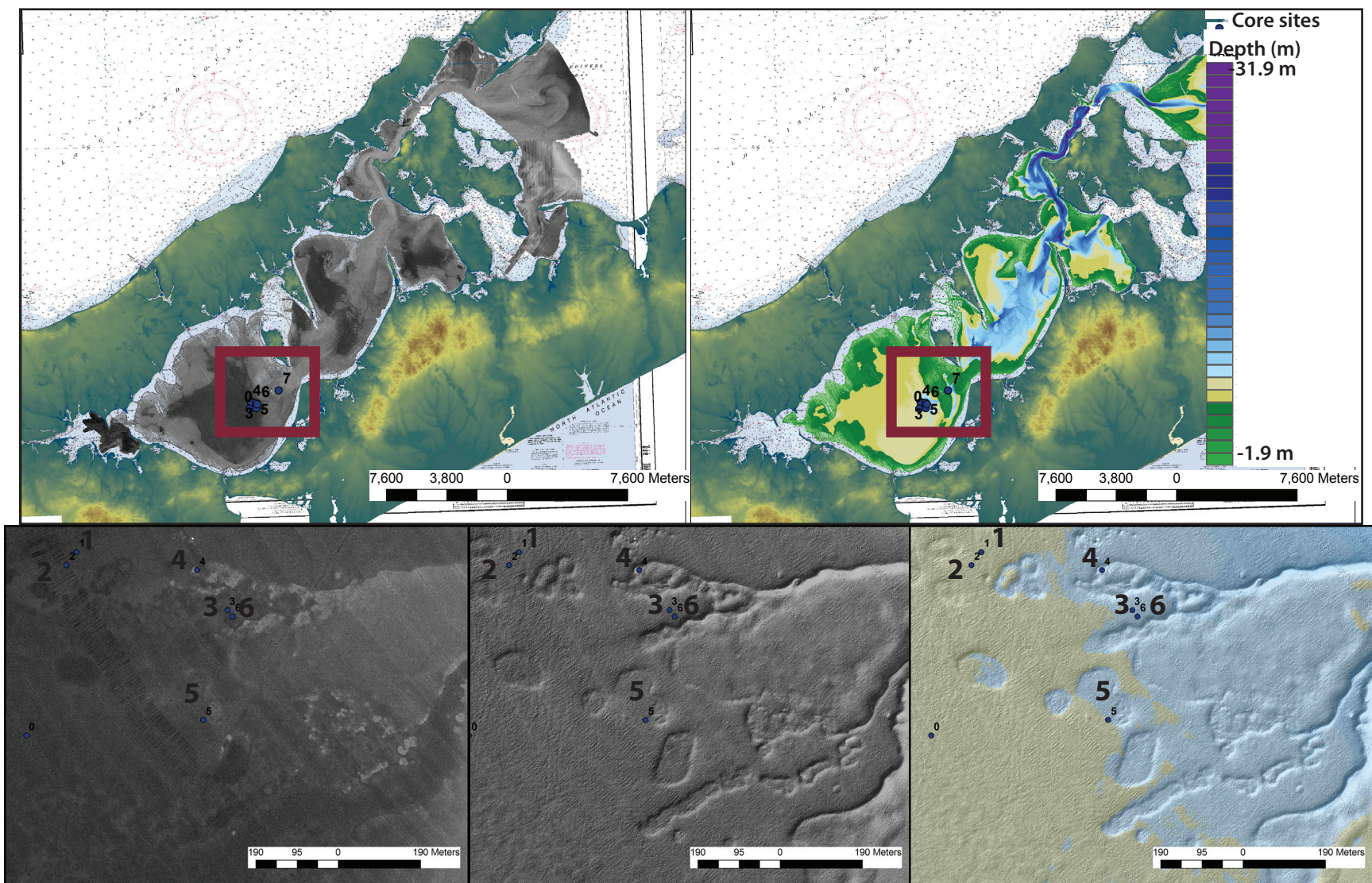
Fig. 4.4: Depths of mounds vs.age overplotted on the Gutierrez et al. (2003) sea level curve.

Sea Level Curves for Nantucket, MA

Redfield and Rubin, 1962
Oldale and O'Hare, 1980
Gutierrez et al., 2003

Age Yrs Before Present with Depth
(Depth in meters below present Mean SL)

Extrapolatin of Age based on age depth curve of dated shells

Extrapolation of Age based on SL curve

Base Depth of Mounds

Depth Below Present Mean Sea-Level (Meters)

Age (Calibrated Years Before Present)

Modified Sea Level Curve of Gutierrez et al., 2003

Fig. 4.5: Grain size of grabs in Central Little Peconic Bay 2008. Ternary plots of mud, sand, gravel in mound vs. non mound sites. Mound sites appear coarser in gravel as shell hash.
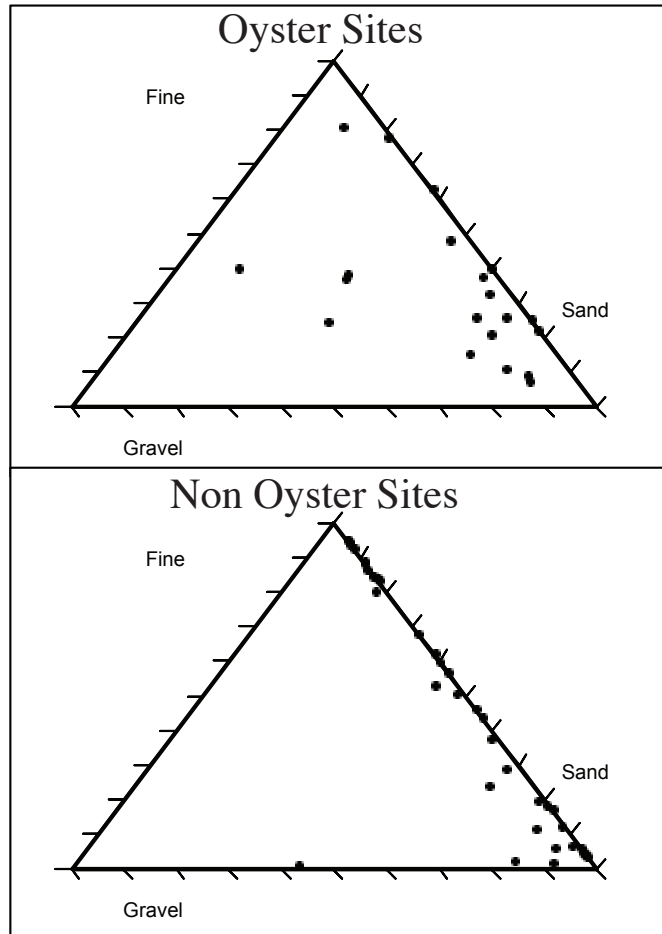
Fig. 4.6: Analysis of shell composition of a set of 10 grabs with oysters from the 2006 survey.   In our subsample nine out of ten sites with oysters were dominated by oyster shells. A total of six out of ten sites, 60%, contained only oyster shells, or six out of nine, 66.7%, of the sites that were dominated by oyster shells. The other types of shells that were found were Slipper Shells, Jingle Shells, and tiny white (~1 cm) clam shells. The one site that was not dominated by oysters had lots of slipper shells in particular present, as well as jingle shells. Weaver (2006).

2006 Grabs

Sample ID

% Oyster Shell

■	**3**
■	**13**
■	**31**
■	**34**
■	**38**
■	**42**
■	**44**
■	**52d1**
■	**52d2**
■	**54**
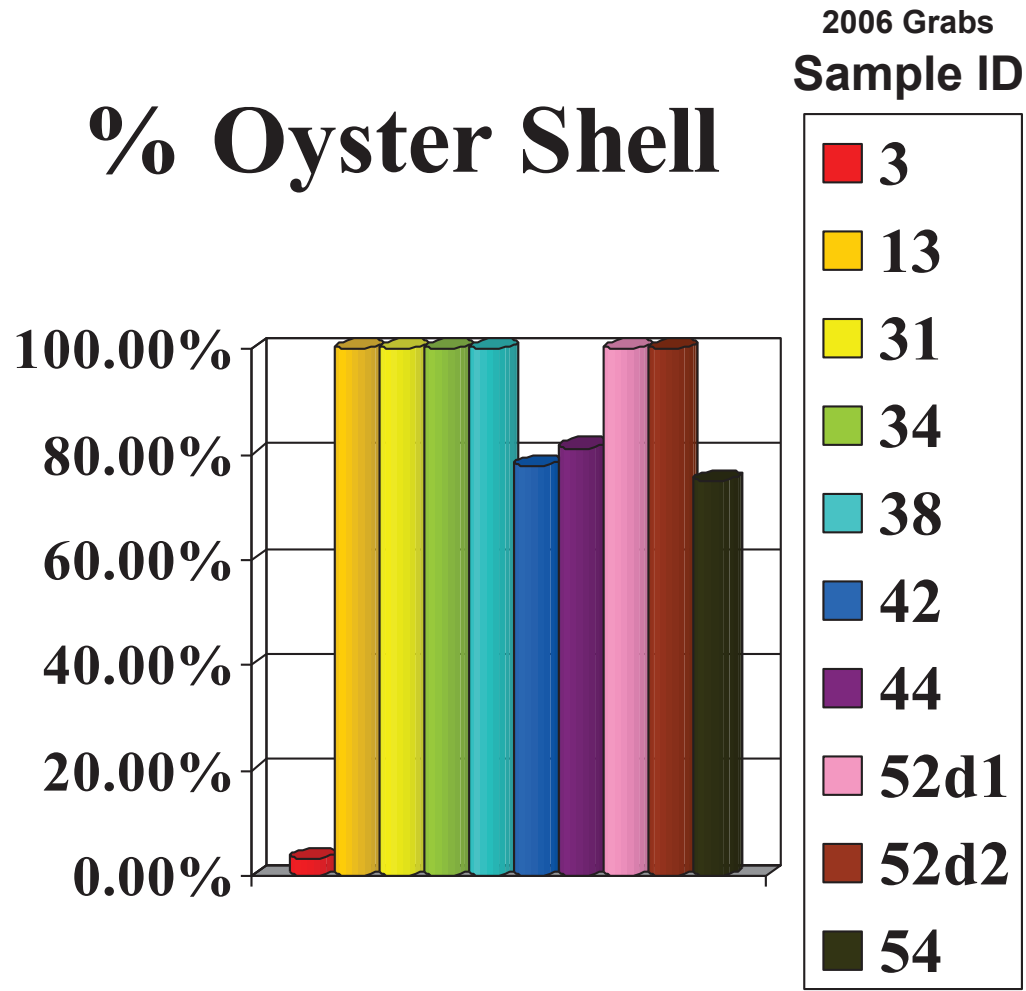
Fig. 4.7: Changes in the backscatter patterns of muddy sediments covering mounds between 2006 and 2008. Differences are visible in the area near Grab 0b-2008 (LH) as well as the area near Grab 70-2008 (RH) in Central Little Peconic Bay.
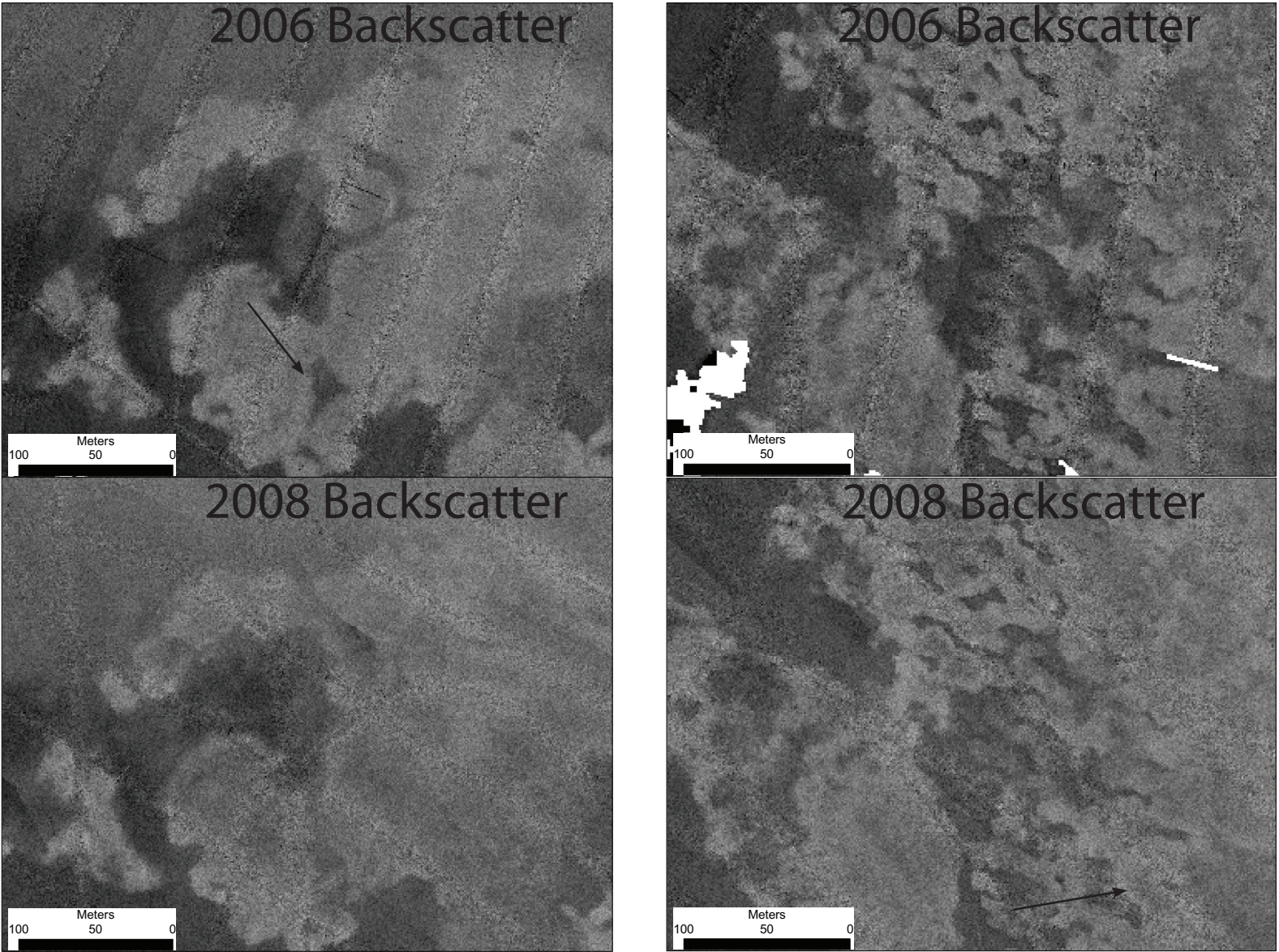
Fig. 4.8: Photograph and description of core #5 with oyster shells.
Starting at 0 cm as the core top to 4 to 4.5 cm is mud, fairly consolidated and cohesive. This mud has a visually apparent sand component with some bits of shell. The core started with 0-2 cm of smooth textured mud (i.e. little sand present and a high clay fraction), 2-3 cm of more smooth textured mud, in 3-4.5 cm the smooth mud starts to have coarse sand in it then bits of shell hash, then an abrupt contact of mud and shell over 0.5 due to the curvature of the shells in contact with the mud. Within the oyster shell layer (4.5 cm to 12 cm) the matrix of sediment in with shells is a mixture of sand and mud. The middle section has a little mud, but not as much as the bottom of the core. The bottom of the core has more shell hash and the matrix is fairly coarse (more sand) with mud. The sediment in the cores is a grey brown color. The sediment in the base of the core actually contains some very coarse sand and some small gravel bits as well, even though much of the sediment matrix that is not composed of shell is a medium to fine grained sand with mud. The middle section of the core seems to have more of the fine to medium sand with mud suggesting a decrease in sand size towards the end of the activity of this mound.

0 cm

mud

3 cm

mud with increasing amount of sand and shell pieces present

4.5 cm

mud /oyster shell contact

oyster layer with mixture of sand and brown mud matrix

12 cm

130
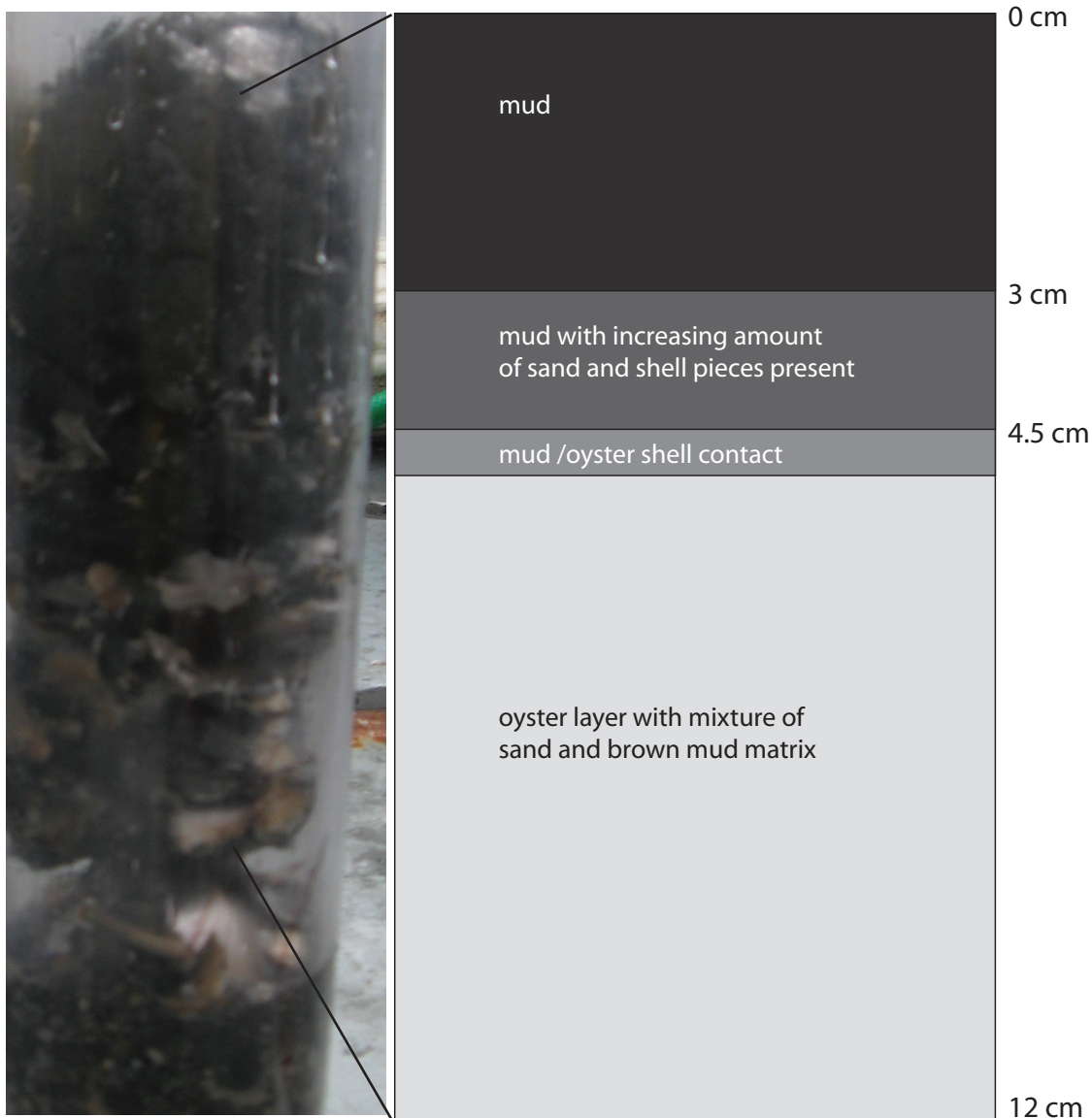
Fig. 4.9: Map of depth and M2 Currents from Gomez-Reyes (1989). Deeper areas of the bay tend to lined up with areas of higher flow as seen in the residual M_2 currents from Gomez-Reyes. Open flatter areas tend to be quieter and muddier. Estimated sedimentation rates using radioisotope chronology from this study and Cochran et al. (2000).

131
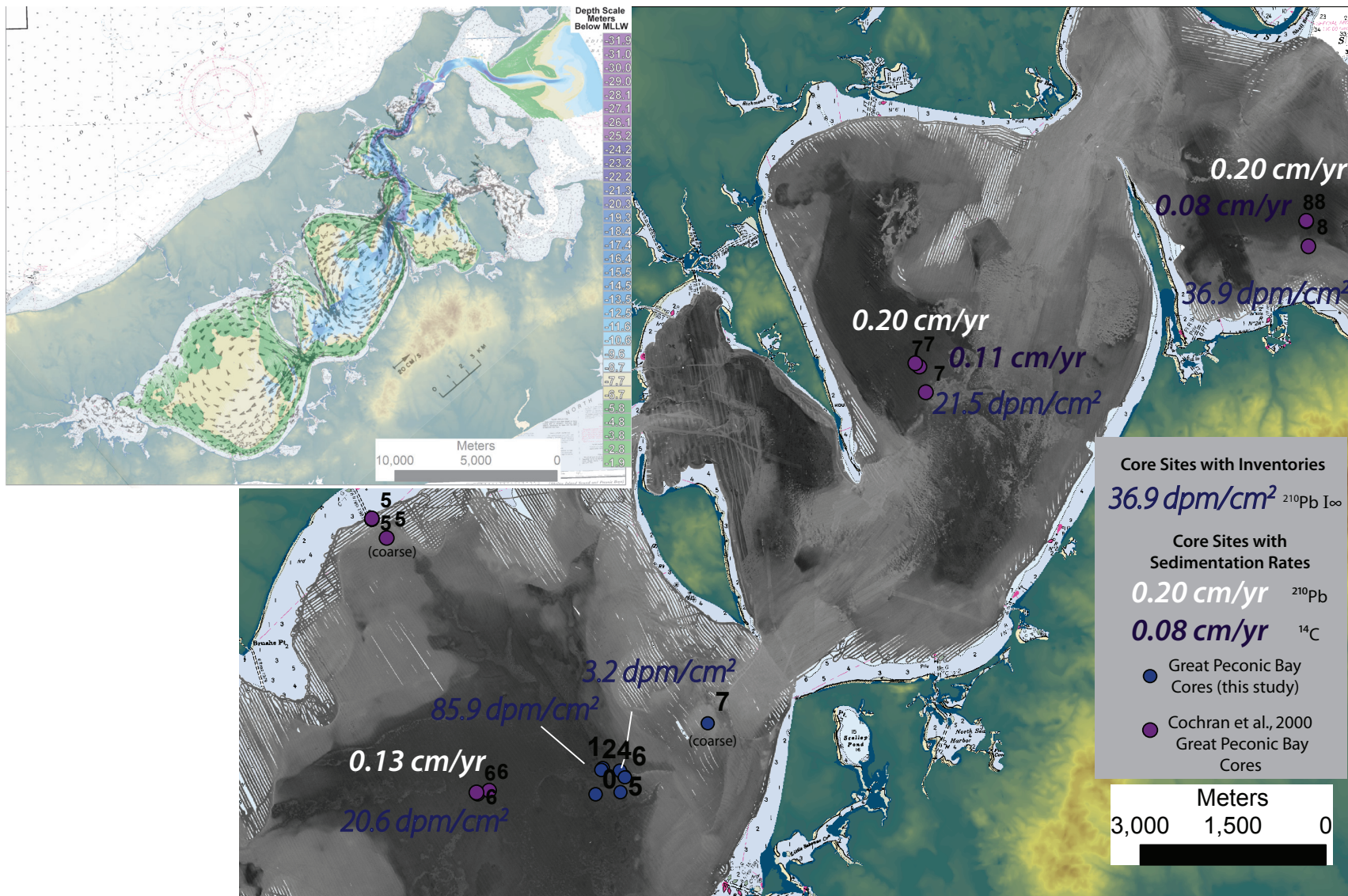
Fig. 4.10: Mound age extrapolated based on sea-level elevation from the Gutierrez et al. (2003) curve. Depth range of mounds within the Peconic Estuary is plotted over the sea level curve for nearby Nantucket by Gutierrez et al. (2003). Top yellow bar shows the range of sea level if tops of mounds were active in 2 m of water (mound depth plus 2 m). The bottom yellow-orange bar shows the range of depths of bases of mounds in seismic profiles and multibeam. ~20 m (22 m - 2 m water depth for an active reef) would mean that it is possible that something that started in 20 m could have started to grow more than 8,000 years ago.

132
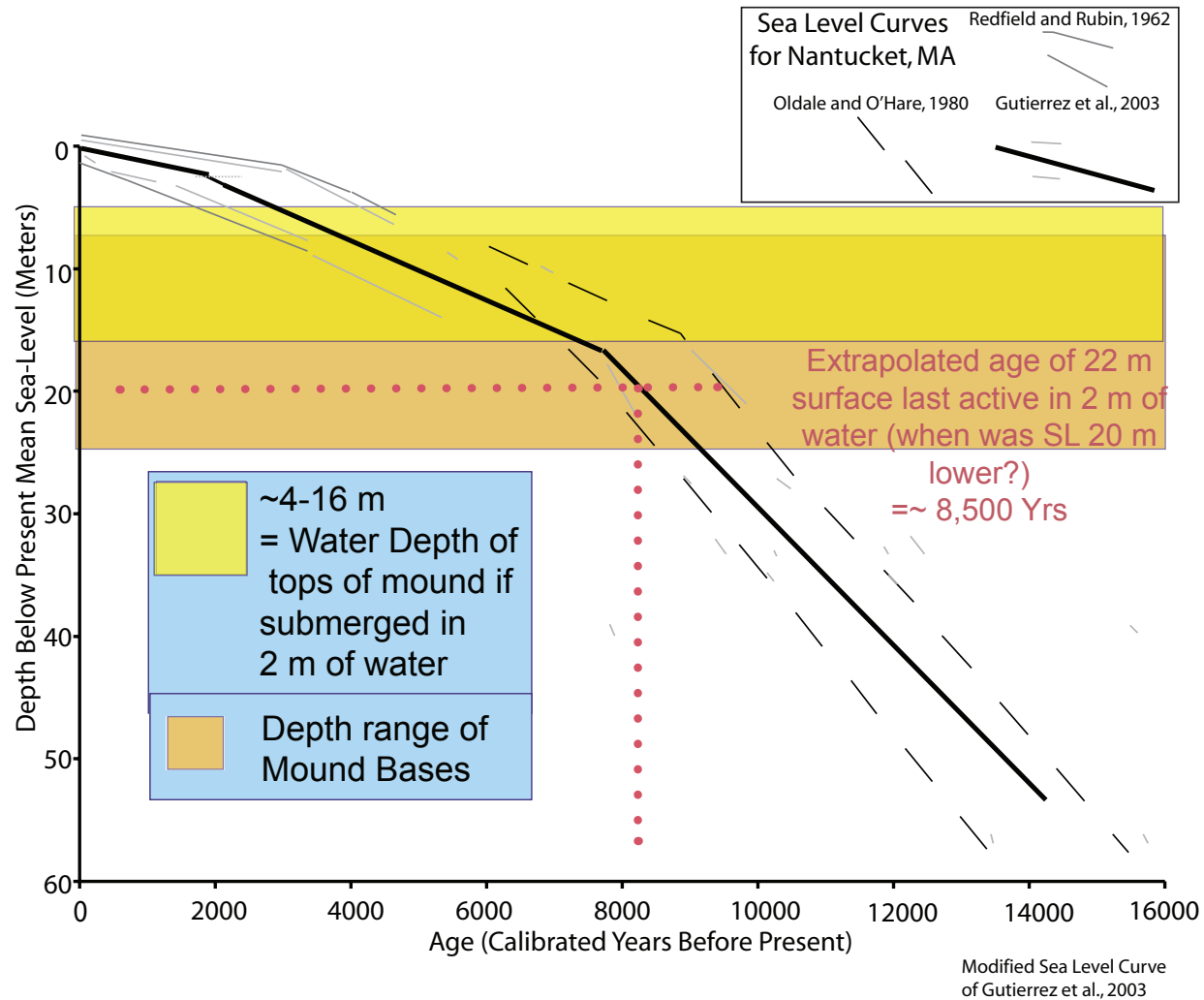
Fig. 4.11. : Locations within the Peconic Estuary including Cedar Point, East Hampton and the Peconic River dam. Cedar Beach Point is shown to avoid confusion.
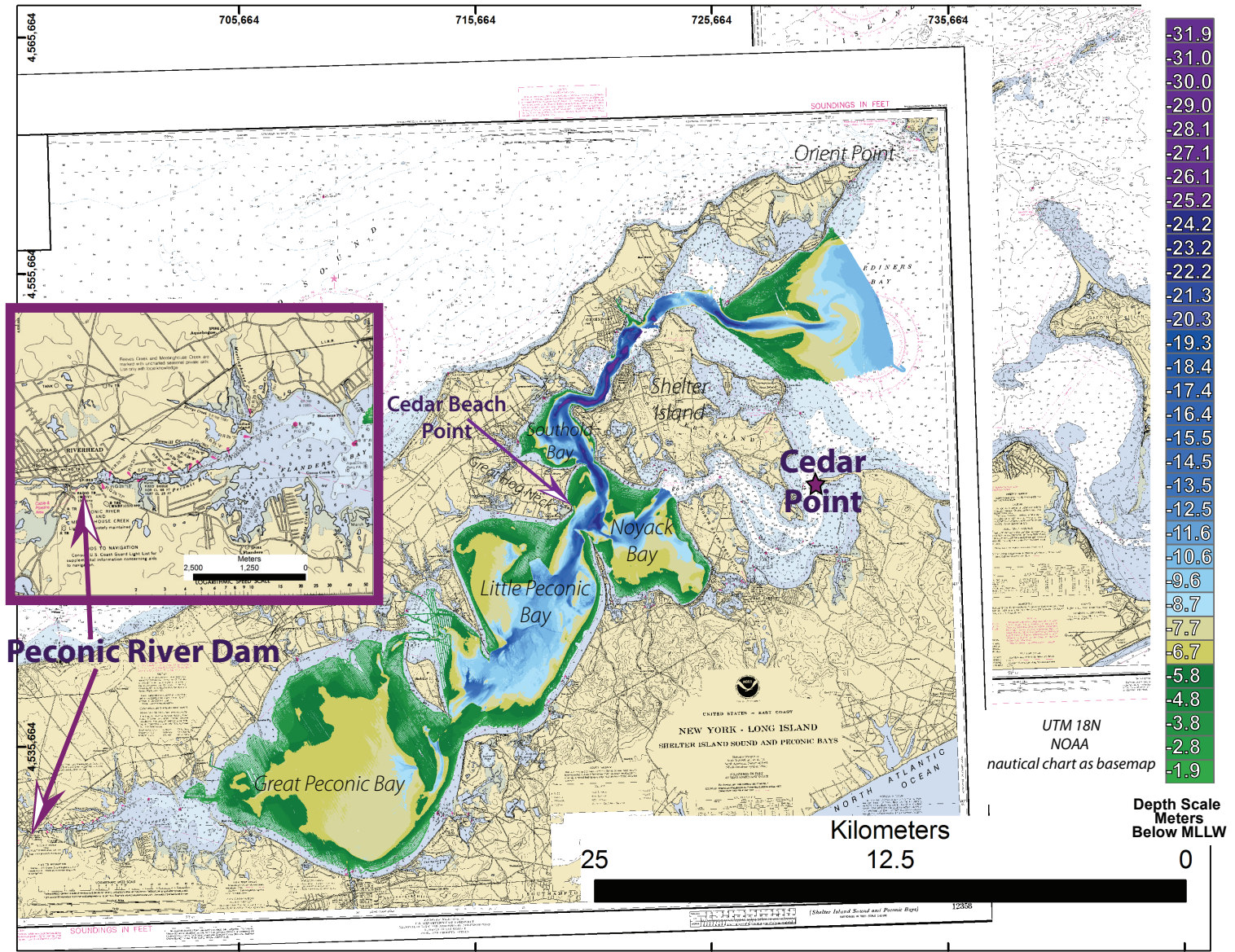
REFERENCES:

Allen, Y. C., Wilson, C. A., Roberts, H. H., Supan, J., 2005, High Resolution Mapping and Classification of Oyster Habitats in Nearshore Louisiana Using Sidescan Sonar, Estuaries, v. 28, n. 3, p. 435-446.

Armentano, T. V., Woodwell, G. M., 1975, Sedimentation Rates in a Long Island Marsh Determined by 210 Pb Dating, Limnology and Oceanography, v. 20, n. 3, p. 452-456.

Attendorn, H. G., Bowen, R., 1997, Radioactive and stable isotope geology, London, Chapman & Hall, p. 522.

Bouma, A. H., 1976, Subbottom characteristics of San Antonio Bay, *in* Bouma, A. H., ed., Shell Dredging and Its Influence in Gulf Coast Environments, Houston, TX, Gulf Publishing Co., p. 132-148.

Bratton, J. F., S. M. Colman, E. R. Thieler, R. R. Seal, 2003, Birth of the modern Chesapeake Bay estuary between 7.4 and 8.2 ka and implications for global sea-level rise: Geo-Marine Letters, v. 22, p. 188-197.

Butzin, M., Prange, M., Lohmann, G., 2005, Radiocarbon simulations for the glacial ocean: the effects of wind stress, Southern Ocean sea ice and Heinrich events. *Earth & Planetary Science Letters*, v. 235, p. 45-61.
Butzin, M., Prange, M., Lohmann, G., Fairbanks, R. G., Naik, N., 2005, Marine Radio Carbon Reservoir Age, http://radiocarbon.LDEO.columbia.edu/, accessed February 2011.

Cao, L., R.G. Fairbanks, M. Butzin and N. Naik, 2007, The marine radiocarbon reservoir age, Radiocarbon, in prep.

Clapp, C. S., Flood, R. D., 2004, The Use of Side-scan Sonar for the Identification and Morphology of Sub-tidal Oyster Reefs in Great South Bay, Long Island Geologists, April 2004 Meeting Abstract.

Clark, J. S., Patterson, W. A. III, 1985, The Development of a Tidal Marsh: Upland and Oceanic Influences, Ecological Monographs, v. 55., n. 2, p. 189-217.

Cochran, J. K., Hirschberg, D. J., Amiel, D., 2000, Particle mixing and sediment accumulation rates of Peconic Estuary sediments: A sediment accretion study in support of the Peconic Estuary Program, Final Report of Project #0014400498181563, Marine Sciences Research Center, State University of New York, Stony Brook, NY, 11794-5000.

Cochran, J. K., Masqué, P., 2003, Short-lived U/Th Series Radionuclides in the Ocean: Tracers for Scavenging Rates, Export Fluxes and Particle Dynamics, Reviews in

Mineralogy & Geochemistry Vol 52: Urananium-Series Geochemistry, ed. Bourdon B, Henderson, G. M., Lundstrom, C. C., Turner, S. P., p. 461-492.

County of Suffolk, N.Y., 2001, Coastal Underwater Land Ownership, accessed December 2011, http://www.co.suffolk.ny.us/departments/planning/pdfs/Map1_Aqua.pdf.

County of Suffolk, N.Y., 2002, Real Property Taxmap parcel linework used with permission of Suffolk County Real Property Tax Service Agency (R.P.T.S.A.).

DeAlteris, J. T., 1988, The Geomorphic Development of Wreck Shoal, a Subtidal Oyster Reef of the James River, Virginia: Estuaries, v. 11, p. 240-249.

Fairbanks, R. G., Mortlock, R. A., Chiu, T.-C., Cao, L., Kaplan, A., Guilderson, T.P., Fairbanks, T. W., Bloom, A.L., 2005, Marine Radiocarbon Calibration Curve Spanning 0 to 50,000 Years B.P. Based on Paired 230Th/234U/238U and 14C Dates on Pristine Corals, Quaternary Science Reviews, v. 24, p. 1781-1796.

Fairbanks, R. G., Mortlock, R.A., Chiu, T.-C., Cao, L., Kaplan, A., Guilderson, T. P., Fairbanks, T.W., Bloom, A. L., 2005, Radiocarbon age to calendar age conversion: 'Fairbanks0107' calibration curve, accessed February 2011, http://radiocarbon.ldeo.columbia.edu/research/radcarbcal.htm.

Feng, H., Kirk Cochran, J., Hirschberg, D. J., Wilson, R. E., 1998, Small-scale spatial variations of natural radionuclide and trace metal distributions in sediments from the Hudson River estuary: Estuaries, v. 21, p. 263-280.

Flood, R. D., Cerrato, R. and Kinney, J., 2009, Benthic Mapping and Habitat Classification in the Peconic Estuary, Phase II, Final Report to the Long Island Chapter of the Nature Conservancy.

Galtsoff, P. S., 1964, The American Oyster, Crassostrea Virgina Gemlin, Fish and Wildlife Service, Fishery Bulletin, v. 64, 457 p.

Gomez-Reyes, E., 1989, Tidally Driven Lagrangian Residual Velocity in Shallow Bays, Doctoral Dissertation, MSRC, State University of New York at Stony Brook, December 1989, p.129

Graham, D. J., Midgley, N. G., 2000, Graphical representation of particle shape using triangular diagrams: an Excel spreadsheet method. Earth Surface Processes and Landforms, v. 25, n. 13, p. 1473-1477.

Grave, C., 1903, Investigations for the promotion of the oyster industry of North Carolina, U. S. Commission of Fish and Fisheries, George M. Bowers Commisioner, Extracted from the U. S. Fish Commission Report for 1903, p. 247-341.

Gutierrez, B. T., Uchupi, E., Driscoll, N. W., Aubrey, D. G., 2003, Relative sea-level rise and the development of valley-fill and shallow-water sequences in Nantucket Sound, Massachusetts, Marine Geology, v. 193, p. 295-314.

Henderson, G. M. & Anderson, R. F., 2003, U-series Toolbox for Paleoceanography, Reviews in Mineralogy & Geochemistry Vol 52: Urananium-Series Geochemistry, ed. Bourdon B, Henderson, G. M., Lundstrom, C. C., Turner, S. P., p. 493-529.

Hughen, K. A., Baillie, M. G. L., Bard, E., Bayliss, A., Beck, J. W., Blackwell, P. G., Buck, C. E., Burr, G. S., Cutler, K. B., Damon, P. E., Edwards, R. L., Fairbanks, R. G., Friedrich, M., Guilderson, T. P., Herring, C., Kromer, B., McCormac, F. G., Manning, S. W., Ramsey, C. B., Reimer, P. J., Reimer, R. W., Remmele, S., Southon, J. R., Stuiver, M., Talamo, S., Taylor, F. W., van der Plicht, J., Weyhenmeyer, C. E., 2004, Marine04 Marine radiocarbon age calibration, 0-26 cal kyr BP, Radiocarbon, v. 46, n. 3, p. 1059-1086.

Koide, M., A. Soutar, E. D. Goldberg, 1972, Marine Geochronology with Pb-210, Earth and Planetary Science Letters, v. 14, p. 442-446.

Lenihan, H. S., Peterson, C. H., 1998, How Habitat Degradation through Fishery Disturbance Enhances Impacts of Hypoxia on Oyster Reefs: Ecological Applications, v. 8, no. 1, p.128-140.

NOAA, 2011, National Oceanographic and Atmospheric Administration (NOAA) National Ocean Service Historical Hydrographic Data, National Geophysical Data Center, Office of Coast Survey and National Geophysical Data Center, (http://surveys.ngdc.noaa.gov/mgg/NOS/coast), 1933 -1935 surveys, available through the Hydrographic Data Viewer for downloading data, accessed 2011, http://maps.ngdc.noaa.gov/viewer/nos_hydro.

Osterman, L. E., Twichell, D. C., Poore, R. Z., 2009, Holocene evolution of Apalachicola Bay, Florida: Geo-Marine Letters, v. 29, no. 6, p. 395-404.

Powell, E. N., Song, J., Ellis, M., 1992, The Status of Oyster Reefs in Galveston Bay, Texas, Galveston Bay oyster reefs map series: Houston, TX.

Powell, E. N., 1993, Status and trends analysis of oyster reef habitat in Galveston Bay, in Jensen, R. W., Kiesling, R. W., Shipley, F. S., eds.,The Second State of the Bay Symposium: Austin, TX, Galveston Bay National Estuary Program, p. 207-209.
PRIME lab, 2008, personal communication, regarding protocols for samples that arrive for radiocarbon dating at PRIME lab, Purdue University, Indiana, USA, e-mail correspondence.

Reimer, P. J., Baillie, M. G., Bard, E., Bayliss, A., Beck, J. W., Bertrand, C. J. H., Blackwell, P. G., Buck, Caitlin, E., Burr, G. S., Cutler, K. B., Damon, P. E., Edwards, R.

L., Fairbanks, R. G., Friedrich, M., Guilderson, T. P., Hogg, A. G., Hughen, K. A., Kromer, B., McCormac, G., Manning, S., Ramsey, C. B., Remier, R. W., Remmele, S., Southon, J. R., Stuiver, M., Talamo, S., Taylor, F. W., van der Plicht, J., Weyhenmeyer, C. E., 2004, INTCAL04 Terrestrial Radiocarbon Age Calibration, 0-26 CAL KYR BP, Radiocarbon, v. 46, n. 3, p. 1029-1058.

Renfro, A., 2010, Particle-Reactive Radionuclides (Thorium-234, Beryllium-7 and Lead-210) As Tracers of Sediment Dynamics in an Urban Coastal Lagoon (Jamaica Bay, NY) [Ph.D. Dissertation], Stony Brook, NY, Stony Brook University.

Smith, G. F., Roach, E. B., Bruce D. G., 2003, The location, composition, and origin of oyster bars in mesohaline Chesapeake Bay, Estuarine, Coastal and Shelf Science, v. 56, p. 391-409.

Stokes, S., Walling, D. E., 2003, Radiogenic and isotopic methods for the direct dating of fluvial sediments, United Kingdom (GBR), John Wiley & Sons, Chichester, United Kingdom (GBR), 233-267 p.

Stuiver, N., Reimer, P. J., Braziunas, T. F., 1998, High-Precision Radiocarbon Age for Terrestrial and Marine Samples, Radiocarbon, v. 40, n. 3, p. 1127-1151.

Suffolk County Planning, 2011, Publications and Information, Suffolk County, Long Island, New York, Planning, last accessed December 2011, http://www.co.suffolk.ny.us/departments/planning/Publications%20and%20Information.aspx.

Suffolk County, 2008, Cedar Point County Park, last accessed December 2011, http://www.suffolkcountyny.gov/Departments/Parks/Parks/CedarPointCountyPark.aspx. Swarzenski, P. W., Porcelli, D., Andersson, P. S., & Smoak, J. M., 2003, The Behavior of U- and Th- series Nuclides in the Estuarine Environment, Reviews in Mineralogy & Geochemistry Vol 52: Urananium-Series Geochemistry, ed. Bourdon B, Henderson, G. M., Lundstrom, C. C., Turner, S. P. p. 557-600.

Twichell, D. C., Andrews, B. D., Edminston, H. L., Stevenson, W. R., 2007, Geophysical Mapping of Oyster Habitats in a Shallow Estuary; Apalachicola Bay, Florida: U. S. Geological Survey Open File Report 2006-138.

Weaver, M., 2006, Research Experience for Undergraduates Studies of Coastal Oceanographic and Atmospheric Processes, Summer 2006, Report/Presentation - Mapping the Peconics: Multibeam Bathymetry and Backscatter Analysis, Marine Sciences Research Center, Stony Brook University.

Wright, E. E., A. C. Hine, S. L. Goodbred, S. D. Locker, 2005, The effect of sea-level and climate change on the development of a mixed siliciclastic-carbonate, deltaic coastline: Suwannee River, Florida, USA: Journal of Sedimentary Research, v. 75, p. 621-635.

CHAPTER 5: EVIDENCE OF PALEOENVIRONMENTAL CONDITIONS IN THE PECONIC ESTUARY FROM ANALYSIS OF ^{87}SR/^{86}SR, ^{226}RA, AND δ^{18}O

INTRODUCTION:

The 'Oyster Terrain' in the Peconic Estuary (Long Island, NY) captures a history of estuarine evolution over thousands of years. We see evidence of a natural evolution of the Peconic Estuary in the Holocene from abundant Oyster reefs a few thousand years ago to none after ~1350 ybp (years before present). As noted in Chapter 2, the modern Peconic Estuary, at 28 psu, is too saline for natural populations of the Eastern Oyster, *Crassostrea virginica* to survive in the Northeast (Stanley & Sellers, 1986). While the very presence of relict oyster shells tells us salinity should have been lower in the past in order to flourish, the youngest of the relict oyster shells that we can recover with a grab sampler may preserve a record of conditions near the end of the active 'Oyster Terrain', including the salinity and submarine groundwater discharge.

The study of shell growth layers and reconstruction of conditions in which they grow is called sclerochronology (Buddemeier et al., 1974; Arnold et al., 2007; Oschmann, 2009). Oyster shells provide the opportunity for a more detailed environmental reconstruction of conditions when the Oyster Terrain was active through ^{14}C age dating and geochemical proxies in the same shells, such as ^{87}Sr/^{86}Sr (salinity) and ^{226}Ra (submarine groundwater discharge – SGD). Data from shells may allow for examining the spatial and temporal variability of changes in this system on a variety of timescales. Our analysis of a set of shells taken from a number of mounds within the estuary are designed to get a sense of variability and the potential for further investigations of paleoclimate within the estuary. Tens of square kilometers, indeed close to 100 square kilometers, of Oyster Terrain, several meters thick, over a range of ~6 m to ~22 m below sea level provides the potential for a long record of estuarine evolution within the Holocene. Surface samples at various depths were used to get a

range of ages in order to reconstruct conditions. The combination of the geomorphology, age, shell character, sediment characteristics and shell geochemistry can tell us substantial information about the evolution of this system.

BACKGROUND:

At the present time freshwater enters the Peconic Estuary through rainfall, runoff, sewage discharge, and submarine seepage. Approximately 78 - 84% of this freshwater input is through submarine seepage (Shubert, 1999; Hardy, 1976). Freshwater inputs are concentrated near the head of the Peconic River Estuary where the Peconic River enters, while the remaining groundwater inputs are spread along the length of the entire estuary. Submarine groundwater discharge at the shore is likely to be freshwater from groundwater mixed with recycled or recirculated seawater, i.e., seawater that flows through the sediment and back into the water column. Surface groundwater and aquifers on land that could potentially release into the bay are fresh except for the mostly saline deep aquifers of the North Fork, which are at least 30 or 60 m below sea level (Schubert, 1999; Schubert et al., 2004). The freshwater table is also thin along the north and south forks of Long Island (Schubert et al., 2004).

The Peconic Estuary is a well mixed estuary, churned by strong tidal currents. The estuary inside of Gardiner's Bay has a mean tidal range of 0.76 m (Hardy, 1976; Eisel, 1977; DiLorenzo, 1986) and a tidal prism of 1.7×10^8 m^3, which is equivalent to approximately 15% of the volume of the bay at MLW (mean low water) exchanging with a tide (Wilson, 1996) or 11.6×10^8 m^3 (Hardy, 1976;Wilson, 1996). A significant percentage of this volume gets recirculated or flushed back in after flushing out (Wilson, 1996). The estuary is 220 square kilometers in area (DiLorenzo, 1986). Salinity is fairly consistent within +/-1 psu of 28 psu within the open large bays of the Estuary such as Great Peconic Bay, Little Peconic Bay, Noyack Bay, Gardiner's Bay, Southold Bay, and Pipes Cove. The maximum variation in salinity during the year along the length of the estuary from the interior of Flanders Bay to Shelter Island Sound is about 3 psu. It is not until one reaches narrowly confined harbors and bays where exchange with the

open bays is limited that there is more variation in salinity on short timescales due to increased runoff. Goose Creek, for example, sometimes experiences fluctuations of salinity as large as 28 to 27 psu within a few days of a large storm (Gregg Rivara, Cornell-Cooperative Extension, 2009, personal communication), and West Neck Bay can experience changes of +/- 2 psu (Dulaiova et al., 2006). Indeed the transition from freshwater to 19-24 psu in the estuarine portion of the Peconic River occurs over a relatively short distance of a few kilometers, confined to within the channel of the Peconic River (Hardy, 1976; Wilson, 1996; Breuer et al., 1999; Wang et al., 2009). Upon reaching Flanders Bay there is typically a transition from the 24 psu to 28 psu over a relatively short distance (less than 1 km) (Hardy, 1976; Wilson, 1996; Breuer et al., 1999). Most of the larger spatial changes of salinity with tides, storms and seasons occur inside of Flanders Bay and in the Peconic River (Hardy, 1976; Wilson, 1996). Salinity is sometimes slightly higher at the base of the deeper channels (but not more than 0.5 psu greater), but conditions tend to be better mixed in the shallower water of the larger bays (Hardy, 1976).

$^{87}Sr/^{86}Sr$ in Seawater:

$^{87}Sr/^{86}Sr$ can be used as an indicator of salinity based on the mixing between a freshwater source whose $^{87}Sr/^{86}Sr$ signature reflects the sediment and bedrock of its watershed and the standard ratio within the ocean (Brass & Turekian, 1974; Palmer & Edmond, 1989; Veizer, 1989; Bryant, 1995; Ingram & Sloan, 1992; Ingram & Depaola, 1993; Ingram & Weber, 1999; Kim et al., 2003). As reported in Xin (1993) for the Peconic River system, there is some Sr in very low concentrations in precipitation, 0.003 - 0.015 µmol/L, and the concentration of Sr in water increases by 0.197 µmol/L after it reaches the ground, most notably in throughfall, which is the initial leaching through organic debris and soils/sediment. Groundwater has higher concentrations of strontium compared to surface water because the process of leaching from organic debris and sediment with prolonged contact with sediment will tend to increase the concentration. Other variables such as changes in pH or oxygen levels may also affect the amount of Sr that dissolves in water. Sr is found in much higher concentrations in

140

saline waters and the open ocean. As the concentration of Sr increases, the effect of any single estuary to the world's oceans becomes diluted. Typically Sr mixes conservatively and there is an increase in concentration on the order of 10:1 to 100:1 from freshwater to open ocean, which results in a dilution of the freshwater Sr concentration (Cochran et al., 2003). The conservative mixing diagram for $^{87}Sr/^{86}Sr$ is hyperbolic with as salinity as seen in Great South Bay on Long Island (Kallenberg, 2005). The relationship can be made linear by plotting $^{87}Sr/^{86}Sr$ vs. 1/[Sr] (Cochran et al., 2003).

Some rivers have very distinctive Sr isotopic signatures because of unusual rocks within their watershed (Ingram & Lin, 2002). Studies in the literature suggest that fresh and brackish groundwater maintain fairly similar isotopic signature to surrounding surface waters if the lithology is the same (Swarzenski et al., 2000; Basu et al., 2001; Dowling et al., 2003). However, submarine ground water discharge tends to have a different isotopic signature than surficial water (Cochran et al., 2003) due to residence time and processes of the 'subterranean estuary' (Moore, 1999; Charrette & Sholkovitz, 2006; Povinec et al., 2008; Young et al., 2008; Cochran et al., 2003). Long Island's glacial sediments provide a fairly typical and homogenized ratio (Kallenberg, 2005; Xin, 1993) that is close to the estimated global average of 0.711 (Palmer & Edmond, 1989). In contrast, other estuaries with multiple rivers and varying bedrock throughout their drainage basins such as the Ganges-Brahmaputra can have much different isotopic ratios than the global average (Basu et al., 2001).

$^{87}Sr/^{86}Sr$ ratios in groundwater and surface waters are fairly similar within the same lithologic area, even though the strontium concentration in the groundwater is much higher (Basu et al., 2001). In estuaries, the input of submarine groundwater discharge may be seen as a non-conservative increase in Sr concentration ([Sr]) away from the river to ocean along a conservative mixing line of [Sr] vs. salinity (Cochran et al., 2003; Kallenberg, 2005). As with fresh groundwater, brackish groundwater usually follows a similar pattern of a higher concentration than surface water, however its concentration is slightly elevated as it undergoes the processes of the 'subterranean

estuary' (Moore, 1999; Charrette & Sholkovitz, 2006; Povinec et al., 2008; Young et al., 2008; Cochran et al., 2003). Within the subterranean estuary, [Sr] increases with salinity, though not as rapidly as radium concentration, which shares similar chemical properties as an alkaline metal (Charrette & Sholkovitz, 2006; Povinec et al, 2008; Dowling et al., 2003; Young et al., 2008; Cochran et al., 2003). Submarine groundwater is known to carry higher [Sr] than surrounding seawater (Charrette & Sholkovitz, 2006; Povinec et al, 2008; Dowling et al., 2003; Young et al., 2008; Cochran et al., 2003). However the Sr isotopic ratios in submarine groudwater discharge may have a different signal from incoming river water so that estuarine water in the same spot may show similar $^{87}Sr/^{86}Sr$ ratios, but different concentrations (Swarzenski et al., 2000).

In order to test the hypothesis that the Oyster Terrain was active in a lower salinity environment, and to determine whether any variation in salinity could be detected when the terrain was last active, measurements of the salinity proxy ($^{87}Sr/^{86}Sr$) in carbonate shell were made. Careful studies of many taxa and environments have shown no vital effects for strontium isotopes within typical (±2 x 10^{-5}, 2 Std. Dev) mass spectrometer resolution (Reinhardt et al., 1999), which makes comparison of values more straight forward that other proxies such as elemental ratios of Sr/Ca, which are known to have vital effects (Reinhardt et al., 1999). However, it should be noted that it is difficult to statistically distinguish higher salinities, especially above 24 psu (Ingram and Sloan, 1992).

Radium-226 (^{226}Ra) in Seawater:

Radium isotopes, particularly ^{226}Ra are useful for tracing submarine groundwater discharge (SGD) and for dating features in aquatic/marine environments, such as shells. Radium behaves chemically similarly to calcium, thus it is found dissolved in water and it is naturally incorporated in trace amounts into carbonates such as shells while they are alive. In theory, the ^{226}Ra incorporated into a shell while an animal is alive should remain unaltered except by decay. This renders ^{226}Ra a useful radioisotope for understanding marine systems, particularly estuarine areas because it

can be used as a tracer of submarine groundwater discharge in the marine environment (Dulaiova et al., 2006; Schlueter et al., 2004; Beck et al., 2008; Moore, 1997; Charrette et al., 2003). This is because large fluxes of ^{226}Ra come from submarine groundwater input into the marine system, but the concentration present in freshwater is much smaller (Moore, 1996a). ^{226}Ra is the radioactive daughter of ^{230}Th (t $_{1/2}$ ^{230}Th=75,380 years). As thorium is highly associated with particles and sediment, ^{226}Ra is largely present in water due to the recoil of the Ra atoms produced from the decay of ^{230}Th in the sediments (Swarzenski et al., 2003). In addition to its utility in understanding variations in submarine groundwater fluxes, ^{226}Ra has been used to date carbonates on the order of thousands of years as it has a half-life of approximately 1,620 years (Schmidt & Cochran, 2010; Staubwasser et al., 2004; Schuller et al., 2004; Broecker, 1963). As with most radionuclides, one usually has about five half-lives before it has decayed too much to be measured accurately. Thus ^{226}Ra is useful as an environmental indicator in sediment or any archive that is less than 8,000 years old (Henderson & Anderson, 2003), which is appropriate to address our hypothesized terrain age. Use of ^{226}Ra as a dating technique or as an indicator of changes in submarine groundwater discharge requires consideration of both processes. The principle difficulty in using ^{226}Ra as a chronometer is determining the initial activity in the material to be dated. If ages are independently determined, it may be possible to use ^{226}Ra as an indicator of submarine groundwater discharge because the initial activity can be calculated. This allows us to distinguish if significant changes in estuarine inputs of submarine groundwater discharge existed.

This study uses ^{226}Ra values in modern shell in an attempt to assess present-day variability of ^{226}Ra in the Peconic Estuary system, and as a potential initial value to date shells, assuming that the initial values of radium in the shell would have been the same in the past and that any difference in values would be due to decay. Radiocarbon dates on the same oyster shells allow us to determine the initial ^{226}Ra values acquired when the shell formed (A_0). Shells from a suite of additional sites were also chosen to expand the number of sites studied for ^{226}Ra. The possibility of post-depositional alteration also needs to be considered when dealing with older samples and avoided if possible. For

143

example, we eliminated material that had obvious signs of alteration, such as staining by Fe or Mn oxides. In summary the, calibration of the results with ^{14}C should not only tell us about any possible spatial variation in the system that might preclude ^{226}Ra results being used as a chronometer, but also describe significant changes that may have occurred in ^{226}Ra over time.

METHODS:

Sampling of shells for geochemical analysis:

Subsamples of the dated shells plus a few others were taken for geochemical proxy analysis. More than one subsample (across shell average, individual layer subsamples) of oyster shell was run for isotopic analysis to determine an average of the shell as well as a set of subsamples of individual layers of the shells. The types of shells examined included the relict oyster reef shells from the Peconic Estuary bottom and recent shells grown in aquaculture that were put out in cages to finish growing in the Peconic Estuary. The aquaculture shells grown in the Peconic Estuary were initially grown under controlled conditions of salinity of about 15 psu (10 -15 psu), obtained by mixing seawater with tap water, and at standard temperatures. Shell C1 (1st part) was grown at the Cornell Co-op Extension aquaculture facility in the Peconics, while S1 (1st part) was grown by Aeros with Southold Bay water. Both the Cornell Co-op and Aeros known conditions sample shells were then transferred to the cages on the seabed to continue growing in the Peconic Estuary (Fig. 5.1). An additional sample, denoted as the "Bulk Sample" comprised shells that were grown in both Mystic, CT and in the Peconic Estuary. This sample was multiple large whole aquaculture shells that were ground for analysis. The shells grew in Mystic, CT for at least a year before being transferred to the Peconic Estuary (Southold Bay) for at least an additional year.

It is important to consistently sample the shell in the same way. Typically, sclerochronological analysis is done by subsampling from many shells in the same structural location on each shell (Schöne, 2008; Schöne et al., 2003; Surge et al.,

2001). Consistency in the location of subsamples within the shell is extremely important because it allows for comparison with other studies and to distinguish any patterns of variability (Schöne et al., 2006; Schöne et al., 2008). The importance of subsampling from the same part of the shell is in large part due to the growth patterns within the shell; one wants to make sure that subsamples are encompassing similar growth spans in each record. Some shells also have differences in mineralogy and trace chemical composition in different parts of the shell. Oysters shells are predominantly composed of calcite, but the purple muscle scar of the shell contains aragonite and there is some aragonite in the ligostratum, the very thin prismatic layer that allows attachment of ligament on the surface of the hinge (Galtsoff, 1964; Surge et al., 2001; Carriker & Palmer, 1979). There is also slightly less aragonite in the bigger left valve of the *Crasstrostrea virginica* shell than in the right valve. This is important to know, and differentiate, because aragonite typically has a noticeably different isotopic signature (O and C, but not Sr isotopes) than calcite, and an offset correction formula is usually applied to shells composed of aragonite as in Grossman & Ku (1986), Jones et al. (2005) and Gillikin et al. (2005).

Shell subsampling was also designed to leave material for subsequent work on selected layers within these shells. A separate large portion of each dated shell, opposite the hinge area, was used for ^{226}Ra analysis and a set of small subsamples was used for ^{87}Sr/^{86}Sr analysis. High-resolution µCT (Micro Computed Tomography) showing the surface and internal structure of the dated relict shells were made at Stony Brook University-Health Sciences Center (USB-HSB), thanks to the School of Medicine pilot research award program. The µCT scan results of these shells, in conjunction with outward appearance, helped to guide cutting of the shells and selection of layers to subsample. The freshly cut shell layer was assessed to ensure a clean unaltered sample was taken (i.e. no discoloration). Dental drills were used to remove material for subsamples. Scraping/milling the edge of the shell face as reported by Schöne (2008) is the preferred approach over drilling a deep hole in order to target the sample layer without unintentionally sampling preferentially the center of a layer. Our drilling followed Schöne's approach of removing a surface area equally, rather than making deep holes

145

(Schöne, 2008). As carbonate shells are potential archives of more than one kind of chemical proxy, we wished to preserve some of our dated shells for potential future analysis. A few of the samples of modern shells were subsamples of multiple crushed homogenized entire shells. The subsamples were large enough to run both strontium and oxygen or other analysis on the same subsample. Most subsamples had some remaining powdered sample after ^{87}Sr/^{86}Sr analysis to allow for δ^{18}O and δ^{13}C analysis.

Similar protocols for preparing marine carbonate samples for δ^{18}O, δ^{13}C, and strontium isotopes can be found, and all approaches cite the importance of thoroughly cleaning sample specimens by washing and scrubbing. Thorough cleaning is important for Sr ratios of older samples where diagenesis may alter some species or parts of shell faster than others, or where other carbonate may have adhered to the exterior of the specimens (Reinhardt et al., 2000). Deionized water (DI) was used for all rinsing during grain size analysis and treatment of shells, or any other analysis of sediment samples involving water in the lab. Shells were rinsed from initial sediment samples with DI water in sieves.

For the aquaculture shells, the outer portion of the shell, representing growth in the bay, was cut off with a rock saw. It was rinsed with DI, and then sonicated and rinsed a few times. The shell piece was put into HCl (1-6 N for several minutes) to dissolve the outermost layer of shell, leaving a clean exterior. Then it was rinsed with DI and put into the sonicator and rinsed with DI again. This piece (a few cm long) was ground into a powder and homogenized. Four shells were needed to make one sample. A portion of this material was then used for analysis.

Aquaculture and relict shells were micro subsampled for ^{87}Sr/^{86}Sr analysis using a drill with a dental drill bit to remove surficial material along the freshly cut face of the shell. An average of shell layers was taken across layers within the hinge of the shell, after the shell was cut. These subsamples are referred to as the "Avg" sample of a given shell (e.g. Avg 0b, Avg 60, Avg 26C, Avg 73, Avg 38, S1 Avg, C1 Avg). Depending on the shell, this sample included a varying amount of chalky versus foliated

146

calcite. Multiple subsamples of a bulk aquaculture shell sample were used to test reproducibility. The "Bulk Sample" was also used for radium analysis and is described further below.

The first growth layer of the shell, the oldest part, was also subsampled in some shells (e.g. S1 1st part, C1 1st part). This was done in the same manner as that of the single layer of age growth used for some relict shells and aquaculture specimens. In the aquaculture shells this first layer represented a growth break corresponding to being moved from aquaculture tables to the very different conditions of the bay as reported in Ch 4. This first band was formed in less than a year and corresponds to growth in water at 15 psu. For the Goose Creek –Cornell Cooperative shell, C1, this represented a mixture of Peconic seawater from Great Hog Neck creek water behind facility and ground water from the tap (Gregg Rivara, 2010, personal communication). The Southold Bay shell, S1, was grown under similar conditions with Southold Bay water and tap water (Gregg Rivara, 2010, personal communication). Shells were grown in an average of 18˚C water that ranged from 10˚C to 24˚C (Gregg Rivara, 2010, personal communication). Summer temperatures in the shallow bays range from around 20-30˚C (East Hampton, 2006-2009).

In the aquaculture shells an additional subsample was made of a layer of that was younger than the first part of the shell, grown within the bay (e. g. S1 2nd part, C1 2nd part). Subsamples for $^{87}Sr/^{86}Sr$ analysis in relict shells of just a single layer of age growth were taken (e.g. 70L, 0bL, 61L, 38L). This type of subsample was taken from an area in the hinge that was freshly cut. This subsample was similar to the layers sampled in the aquaculture shells referred to as 2nd part because they were younger than the first, but may have been from any of the many layers after the first layer. For $^{87}Sr/^{86}Sr$ analysis, a subsample of a clean white chalky layer of calcite was also taken (e.g. 26C Chalky Layer, S1 Chalky Layer), typically taken from an area away from the hinge. These samples did not include the purple aragonite layer of the muscle scar or the foliated calcite.

147

Annual growth layers were distinguished in the hinge area and most annual layers were identified by a ridge separating growth bands. These were the annual increments in the ligamental area (Kirby & Miller, 2005), which were visible inside the bisected hinge of the shell. A cut parallel to the long axis of the shell and through the central gully in the hinge area where layers initiate growth in a *Crassostrea virginica*, known as the resilifer (Surge et al., 2001) exposed a fresh face of the growth layers of the shell. This replicated the approach used to subsample *Crassostrea virginica* for isotopic and elemental ratio analysis used by Kirby & Miller (2005), Kirby (2000), Kirby et al. (1998), Surge et al. (2001), Surge et al. (2003), and Surge & Lohmann (2008). Similar methodology for other bivalves is reported for subsampling for both $\delta^{18}O$ and $^{87}Sr/^{86}Sr$ in Dettman et al. (2004). Images of sampled shells are found in Appendix C.

Larger subsamples of shells (at least several grams) were required for ^{226}Ra analysis compared to the milligram subsamples needed for strontium and possible later oxygen isotope analysis. As noted above, modern aquaculture shells were used as comparisons to our relict shells for ^{226}Ra analysis. Modern shells included the Southold Bay sample, which was cut to exclude the material grown in lower salinity. Shells actually grown in the Peconic Estuary included the Goose Creek – Cornell Cooperative Shells and Southold Bay sample. Careful attention to using only the outer portion of shell (end opposite the hinge) representative of growth in the Peconic Bays was made in preparing these samples. Another modern shell sample (Bulk Sample) was the Mystic Seed – Southold bulk average sample, which could show a slightly different signal due to transplantation of shells from the Mystic River to Southold Bay.

Sampling for radium analysis involved more shell material, and thus required more steps to clean the material. Shells were put through a series of cleaning steps: initial rinsing with DI, sonification, second rinsing with DI, and HCl rinsing (1-7N) and finally a third rinsing with DI. An effort was made to remove any sediment from the surface including any that was lodged within holes in the shells, and the HCl was used to dissolve outer material that may have had sediment attached or may have absorbed elements from the sediment. These cleansing steps were repeated until all sediment

148

had been removed from the surface and most of the iron staining had been eliminated. Physical brushing combined with DI rinsing was also used through the cleaning process.

For some shells there were many tiny sponge holes and channels that were clogged with sediment that needed more direct removal before radium analysis. Many of the iron stained shells exhibited this staining radiating out from sponge holes as well, which made cleaning shell material slightly more challenging. In these cases more direct dissolution of shell near the target holes or stain marks was used (i.e. dropping acid (1- 8N) onto the holes themselves), rather than soaking the entire shell. Another approach that was used was to break the shell into smaller pieces and to subsequently remove any pieces needing further cleaning for separate treatment if the holes were particularly difficult to clean. These smaller dirty pieces were put through the original cleaning steps to try to remove the targeted clogged sediment, or stained shell material. The amount of sediment found in most of the shells was actually somewhat surprising considering how much physical cleaning of the shells was done prior to applying acid and/or breaking it up into pieces. The least amount of sediment that was contained in the shells was found in the shells that were the cleanest and lightest in color to begin with. This combination of techniques was effective at removing any sediment stuck in holes in the shells.

Sr isotope analysis:

Analytical methods for total Sr and $^{87}Sr/^{86}Sr$ followed the same basic procedures outlined in Kallenberg (2005) and Cochran et al. (2003) with some modification. After drilled samples were prepared, the material was transferred into vials. The biggest change was that we were able to use a pneumatic pump to run multiple samples at one time with a controlled flow when isolating the Sr in a column containing Sr-spec^{TM} Resin.

The purified Sr fractions were loaded onto single baked-out Tungsten (W) filaments for the first series of samples (Appendix C). Subsequent samples were loaded and run on baked-out single Rhenium (Re) filaments (Appendix C). These samples followed a similar procedure with about one-fifth of the prepared sample volume loaded onto a filament via pipette. Sr loader was also added in preparation of the filament prior to adding the Sr. A similar volume was used while loading the strontium isotope standards, SRM (standard reference material) 987.

For strontium isotope analyses multiple aliquots of the same subsample of shell were run a Finnigan MAT 262 Thermal Ionization Mass Spectrometer (TIMS), in the Geosciences Department at Stony Brook University (Kallenberg, 2005; and Cochran et al., 2003). More than one subsample of the same part of a shell was run through the Sr chemistry and then a few aliquots of the resultant Sr were analyzed on the TIMS for multiple sets of runs to give a sense of how reproducible the chemistry was.

The software associated with the MAT 262 automatically calculates a mean $^{87}Sr/^{86}Sr$ ratio for a set of runs. Extreme outlier values, defined using the standard deviation of all runs in a set, were flagged as bad by the processing software and are not included in the mean. This program does not always catch all possible bad values so one must manually look for extreme outliers. Any $^{87}Sr/^{86}Sr$ ratio outliers that had a difference of greater than 0.01 than the mean ratio were automatically rejected as errors. For a specific group of runs of the same type of sample (individual shell), outliers that were +/- 0.0015 or greater than the sample mean ratio were removed manually. A few cases of more stringent rejections of values are described later. The remaining values were then included in the mean of a particular sample (e.g. shell). The software computed a 2^{σ} standard deviation for single sets of runs, which we use when reporting a single sample with a single run set.

Weighted means and standard deviations for both Re and W filaments combined were calculated. Correction was made for any offset between the SRM 987 ratio on the filament and the accepted value. In order to properly take into account the number of

runs of each sample when calculating the mean and standard deviation, a weighted mean was used based on the length of runs per sample value. This is important since not all samples had sets of runs that were the same length. The weighted mean combines weighted values for each of the two different filaments in these calculations. For further explanation of this step please refer to Appendix C.

Radium- 226 Analysis:

Samples were cleaned and crushed for measurement using the steps described above. ^{226}Ra was measured using its daughter ^{222}Rn via radon emanation on a scintillation counter. The basic principles of the radon emanation technique are described in detail by Lucas (1957) and compared to other methods by Burnette & Tai (1992).

Measurement of ^{226}Ra by the decay of ^{222}Rn was used to calculate the dpm/g of ^{226}Ra in a sample. Counting efficiency for ^{222}Rn via this method, radon emanation, is much higher than that of gamma spectroscopy counting for the decay of ^{226}Ra. The short half-life of ^{222}Rn (3.82 d) makes it suitable for measuring of its parent ^{226}Ra. The increased efficiency and lower errors of the radon emanation technique seemed appropriate, given the very low levels of ^{226}Ra in modern oyster shells.

Cleaned oyster shells were crushed with mortar and pestle for ^{226}Ra analysis via ^{222}Rn emanation. Approximately 10 g of shell material was the target amount to be used. The actual amount of clean ground shell varied from about 4 g to 21 g, with 7 g to 12 g being the most common sample sizes.

Shell samples 70, 71, 73, 0b, 26C, 38, Mystic Seed – Southold Bulk Average sample (Bulk Sample), and Goose Creek – Cornell Cooperative Shells (C1) were dissolved in HCl.   A minimum of 1% HCl or pH greater than 0.1, solution of dissolved shells was made, with actual concentrations greater and approaching the goal of 1N HCl. This was solution of shell was then transferred to glass washing bottles. A total

volume of solution of 115 mL was used for all of the samples in gas washing bottles of the same volume/size, which is just slightly more than 1/3 of the volume of the container. All samples were measured after ^{222}Rn had obtained secular equilibrium with ^{226}Ra.

Oxygen isotopes:

Seven samples, C1 1st, C1 2nd, and 0b Chalky, 61 Chalky, 70 Chalky, 38 Chalky, 0b Chalky were sent to the University of California Santa Cruz Stable Isotope Lab for δ^{18}O and δ^{13}C analysis. Aliquots of the same powder samples analyzed for Sr isotopes were analyzed for δ^{18}O and δ^{13}C. In order to interpret the δ^{18}O ratios and constrain the percentage of salinity and temperature variability a range of possible values were tested. Craig (1965) calcite temperature conversion curve was used for δ^{18}O. Conversion assuming constant salinity was done, and then conversion taking into account known salinities of aquaculture shells that gave a sense of the variability due to temperature versus salinity. Freshwater measurements of δ^{18}O$_{water}$ on Long Island (δ^{18}O=-6.6 (max), δ^{18}O=-7.2 (avg)) by Copen and Kendall, 2000 along with regional Atlantic seawater variability of the from Labrador Sea water and Scotian Shelf Waters to Gulf Stream water values from Smith et al., 2001 were compared. Approximate δ^{18}O$_{water}$ values were then calculated using known aquaculture and Peconic Bays temperature (~18˚C, summer in the 20˚C's) (East Hampton, 2006-2009) and salinities (~15 psu and 28 psu) in order to create a linear curve where δ^{18}O=-6.1 at 0 psu and 35 psu.

RESULTS:
^{87}Sr/^{86}Sr:

Three categories of shells were analyzed for ^{87}Sr/^{86}Sr: relict shells (26C, 70, 61, 38, 0b), two aquaculture shells grown under known conditions of 15 psu (S1 1st part and C1 1st part) and those same shells grown under 28 psu (S1 2nd part, and C1 2nd part) (Table 5.1). The two aquaculture shells were first grown in an aquaculture facility at 15

psu (1st part) and then moved to the Peconic seawater of 28 psu (2nd part). Goose Creek (C1) and Southold Bay (S1) are the areas within the Peconic Estuary where these shells were transferred to 28 psu seawater. The Goose Creek shell, C1 came from Cornell Cooperative, while the Southold Bay shell, S1 came from Aeros company on Southold Bay (Table 5.1).

The 15 psu aquaculture shells $^{87}Sr/^{86}Sr$ ratios are distinctly higher than the 28 psu isotopic ratios (Fig. 5.2). The initial growth band of the aquaculture shell, C1 1st part, grown at 15 psu has a $^{87}Sr/^{86}Sr$ ratio of 0.709313 (+/- 0.000064). The $^{87}Sr/^{86}Sr$ ratios of the same aquaculture shell, C1 2nd part, grown in 28 psu seawater in Goose Creek had a ratio of 0.709200 (+/-0.000017) (Table 5.1). S1 2nd part, grown in 28 psu in Southold Bay had a $^{87}Sr/^{86}Sr$ ratio of 0.709219 (+/-0.000074), while $^{87}Sr/^{86}Sr$ for the first part of S1 was 0.709262 (+/-0.0000047) (Table 5.2). The relict shells when taken all together are close to the 28 psu isotopic ratios, with most slightly lower in value (Fig. 5.2). Isotopic ratios of $^{87}Sr/^{86}Sr$ measured in relict shells ranged from 0.709159 (+/-0.000014) to 0.709292 (+/- 0.000025) (Table 5.1). The $^{87}Sr/^{86}Sr$ ratios for the aquaculture shells grown at 15 psu shells (C1 1st part and S1 1st part) have no overlap in standard deviation with the relict shells (26C, 70, 61, 38, 0b) and the same aquaculture shells after transfer to 28 psu (C1 2nd part and S1 2nd part). While most of the relict shells are close in value with many having some overlap in standard deviation, there is no overlap in the standard deviation range of #70 that has the highest $^{87}Sr/^{86}Sr$ value and of #26C and #61 that have the lowest $^{87}Sr/^{86}Sr$ ratios (Fig. 5.3).

Multiple subsamples of each relict shell were run through chemistry and analyzed for Strontium isotopic ratios multiple times to ensure that the Sr chemistry and TIMS results were reproducible and to get an indication as to whether there was any significant internal variability within the shells. No overlap of standard deviations was found when comparing $^{87}Sr/^{86}Sr$ ratios within individual relict shells (Table 5.3). Measurement of chalky calcite layers seemed to show no statistical difference from other layers, particularly the non-chalky layers (Tables 5.2, 5.3). In particular, the $^{87}Sr/^{86}Sr$ ratios in non-chalky layers were not statistically different than chalky layers.

153

The sample representing the average of a shell, for example Avg 26C, overlapped the ratios given for any single layer from the same relict shell (Table 5.3).

The ^{14}C ages of the shells as reported in Chapter 4 were used to plot the relict shell ^{87}Sr/^{86}Sr ratios. With the exception of #70, the relict shells seem to follow a trend of decreasing ^{87}Sr/^{86}Sr ratios towards the present (Table 5.1, Fig. 5.3), although all the relict shells are fairly close together given the standard deviation ranges. The differences in isotopic ratios between shells of different ages suggest longer term changes rather than interannual to several years worth of variability in our shells due to lack of significant differences between layers.

^{226}Ra Results:

The ^{226}Ra measured in a shell is ^{226}Ra, uncorrected for age, which may be different from the amount that was originally in the shell when it was alive because of radioactive decay (Table 5.4). The ^{226}Ra activity, uncorrected for age, in relict shells ranges from 0.18 (+/-0.01) to 0.039 (+/-0.003) dpm/g. The ^{226}Ra values of the aquaculture shells, which have not decayed, were much lower, with the Southold Bay-Mystic seed bulk sample having 0.014 (+/-0.0006) dpm/g and the Goose Creek sample having 0.028 (+/-0.0009) dpm/g.

The amount of ^{226}Ra present in a relict shell when alive was calculated for shells of known ages. Relict shells 71 & 73 are not included in this list as they are of unknown age. The shells range from around one to two half-lives of ^{226}Ra in age, so the age-corrected ^{226}Ra values are 2-4x the measured values. The range of age corrected ^{226}Ra in dated relict shells is 0.10 to 0.50 dpm/g. The highest value of ^{226}Ra is in the oldest shell 0b and the youngest relict shell, 26C, has the lowest value (Fig. 5.4). ^{226}Ra levels have decreased over time this can be seen in the uncorrected for age and corrected for age data. We can also see that shells #71 and #73, which are undated, plot in the middle of the range of ^{226}Ra values (Table. 5.4).

$\delta^{18}O$ and $\delta^{13}C$ Results:

Relict shells fast growth bands had $\delta^{18}O$ values of 3.09 to -2.23 per mil (Table 5.5), which were closer to the 28 psu summer temperature dominated aquaculture sample, C1 2nd, (-3.14 per mil) than the sample grown in cooler water (~18°C) and about 15 psu, C1 1st, (3.89 per mil). The most negative $\delta^{18}O$ in our aquaculture sample was C1 1st. Relict shells $\delta^{13}C$ ranged from -1.0 to 0.5 per mil (Table 5.5). C1 1st $\delta^{13}C$ was -4.2 per mil. C1 2nd $\delta^{13}C$ was -3.9 per mil. The aquaculture shells had the most negative $\delta^{13}C$ values.

DISCUSSION:

[226]Ra implications for submarine groundwater discharge:

Lower values in the modern shells compared to relict shells means that [226]Ra cannot be used as a chronometer in relict shells because decay should have decreased the amount of [226]Ra. Instead, the lower values in modern shells must reflect environmental change in the system over time. Both $^{87}Sr/^{86}Sr$ and Ra can be used to estimate the importance of estuarine mixing and the presence submarine groundwater discharge into an estuary (Brass & Turekian, 1974; Palmer & Edmond, 1989; Ingram & Sloan, 1992; Kallenberg, 2005; Cochran et al., 2003; Lin et al., 2010; Beck et al., 2008; Dulaiova et al., 2006; Garcia-Orellana, 2010; Yang, 2007) [226]Ra has separately been used to demonstrate the presence of submarine groundwater discharge into estuaries on Long Island (Dulaiova et al., 2006; Beck et al., 2008). Studies in the Peconic Estuary suggest that freshwater via groundwater inputs may be much higher than in Great South Bay, and it has been estimated that ~78 - 84% of freshwater flow into the Peconic Estuary is as submarine groundwater (Hardy, 1976; Schubert, 1999).

Trends seen in the radium data through time in the relict shells suggest that the low values found in aquaculture shells may be part of a general decrease in submarine groundwater flux over time (Fig. 5.4). However, in order to understand this pattern we

155

must first look at modern local radium fluxes into the Peconic Estuary. Modern rates of ^{226}Ra flux in the Peconic Estuary have been published for West Neck Bay, a small bay on Shelter Island, NY by Dulaiova et al. (2006). Reported values of ^{226}Ra in the submarine groundwater discharge (wells, piezometers and seepage meters) is 6 – 37 dpm/100L and in the water column the ^{226}Ra concentration is 13-18 dpm/100L, with the highest values in the water column occurring at high tide and the lowest values at low tide (Dulaiova et al., 2006). Beck et al. (2007) report a similar range of 5-20 dpm/100L in Great South Bay, but report elevated levels of up to 300 dpm/100L in groundwater. ^{226}Ra in aquaculture shells should reflect activity levels in waters with 13-18 dpm/100 L.

It is possible that natural shells that grow on the bottom on other shells or sediment may have ^{226}Ra values that are different from aquaculture shells grown in cages. This could be the case if the ^{226}Ra diffuses quickly above the bed. As we can see from Dulaiova et al. (2006) water column values are better mixed, whereas ^{226}Ra near the bed has larger peaks and lows that might average slightly higher in a shell near the bed than a shell suspended in the water column. Our aquaculture shells were still influenced by direct contact with sediment as the aquaculture shells often had inclusions of sediment within the shells. Sediment that got caught inside the living oyster that was not expelled was covered by new shell secreted within the interior of the oyster.

Submarine groundwater discharge is predicted to have higher flow rates at low tide, and lower discharge rates at high tide because there is less pressure from overhead water at low tide allowing the water table to discharge faster into the sea above (Collier et al., 2005; Rapaglia, 2005; Dulaiova et al., 2006). In general, measurements over a tidal cycle show higher concentrations of radium in saline submarine groundwater discharge at high tide when the volume of submarine groundwater discharge is lower and lower concentrations of radium at low tide when the volume is larger but diluted by freshwater from the aquifer (Dulaiova et al., 2006). Flow rates may also be affected by current flow with faster currents modulating pressure above the seabed creating higher discharge rates (Burnett et al., 2003).

^{226}Ra variability may be caused by temporal variability at time scales from millennia to tidal cycles, but it may also be due to spatial heterogeneity in the system. We chose shells from within one basin in part to try to reduce spatial variability in salinity. In order to avoid differences that might have existed between basins in the past or between the head and mouth of the estuary we concentrated our samples within a single area. The estuary is well mixed, and this was likely also the case in the past so values away from the bed and shoreline should be homogenous. Studies on Long Island have shown higher rates of submarine groundwater discharge typically nearshore (less than 50 m offshore), increasing as it reaches the shoreface (Dulaiova et al., 2006; Collier et al., 2005). Our sites were all much farther than that from any paleoshore line when the mounds were actively growing. It is unlikely that our shells would capture such near-shore gradients, as the shells we tested grew in deeper water, a few meters rather than the 1.5 m of West Neck Bay, and much farther from shore than the zone where large changes in ^{226}Ra variability are found today.

Variability in sediment types and permeability may create pockets of higher flow, so underground conduits of faster flow might exist. For example, off Fire Island in Great South Bay in Long Island there were places that had higher rates of discharge (Collier et al., 2005). Later studies showed that spatial heterogeneity in buried peat layers caused differences in submarine groundwater in Great South Bay (Bratton et al., 2009). This just highlights the possibility that we might see similar spatial heterogeneity in the Peconic Estuary. However, there may have been a different spatial gradient in the past. We may be seeing examples of spatial heterogeneity between different sedimentary feature types and their antecedent morphologies such as paleochannels. As mentioned in previous chapters our mounds seem to outline paleochannels. Buried paleochannels filled with coarser sediments are often conduits of groundwater flow and submarine groundwater discharge with their higher porosity (Gaswirth et al. 2002; Gallardo & Marui, 2006; Rapaglia, 2005). Other factors such as mud content in surface grabs showed no relationship to ^{226}Ra (Table 5.7). Examination of ^{226}Ra in undated relict shells, #71, #73 and #13, suggests that there is at least some spread in active depths of

mounds and/or some spatial variability assuming that the [226]Ra had the same age – depth and activity relationship as our dated shells (Table 5.7).

The trends in [226]Ra that are seen might be explained by temporal changes in the system, or spatial heterogeneity in submarine groundwater discharge flux. However, the variability does not show any pattern of lateral change along the length of the large bays examined. A decrease in seafloor groundwater flux could be due to changes in precipitation, but it could also be caused by changes in hydraulic pressure from sea level rise (Fig. 5.5). A progression of the dominant aquifers feeding into the Peconic Estuary over time on the order of thousands of years might occur as the deep aquifers transitioned from fresh to brackish. For example the now saline aquifers under the North Fork (Schubert, 1999 and Schubert 1998) would have been fresh when sea level was lower. Variability in submarine groundwater discharge in bays like the Peconic Estuary on Long Island has been tied to spatial atmospheric patterns such as the NAO (Laroche et al., 1997). Long term shifts in such atmospheric variables associated with NAO like patterns in the Northeast might also influence the long term changes in submarine groundwater discharge.

[87]Sr/[86]Sr and Salinity:

The Peconic River watershed seems to have much lower ambient strontium concentrations than the watershed of the Connetquot River that flows into Great South Bay (Kallenberg, 2005), but as groundwater from the forks is higher in concentration we think that the Great South Bay curve is appropriate to use. Slight differences between Great South Bay's Connetquot River and the Peconic River watershed Sr ratios and concentrations may exist due to differences in the residence time, or amount of time the water has spent in the aquifer before reaching the river or shoreline, while it percolates through the ground as well as due to slight differences in bedrock and soil mineralogy or percentage mud content. Lithologic differences in the clay/sand units of aquifers through which water discharges from the South Fork exist (Schubert, 1999) and could result in small changes in Sr concentrations and ratios. Most of the Sr in groundwater in

158

a sandy hydrologic unit is released from the mud size fraction and from oxalate surfaces on grains so changes in mud fraction in sandy sediments may create quantifiable differences in [Sr] and $^{87}Sr/^{86}Sr$ (Dowling et al., 2003). Sr concentrations reported in groundwater of the public water supply for the entire North Fork (1.0- 0.5µmol/L) near our aquaculture sites (1.0 µmol/L) are higher than in the public water supply for areas contiguous to Great South Bay (averaging 0.3-0.5 µmol/L with less than 0.1 µmol/L for Fire Island) (SCWA. 2010) and higher than reported for the Peconic River by Xin (1993) (0.3 µmol/L).

It has been shown that the Peconic River is an example of how flow through a watershed affects Sr ratios and increases its concentrations (Xin, 1993); therefore, if residence times differ between Great South Bay and the Peconic Estuary, this might create a difference in concentration and ratios. The Peconic River watershed has a calculated residence time of 50 years (Xin, 1993) with 90% of the Sr input estimated to be from the combination of dry precipitation and soil weathering (Xin, 1993). The dominant freshwater values may have a slightly different isotopic ratio from the Peconic River due to longer residence times of some aquifers compared to the Peconic River watershed and thus may also contribute higher concentrations of [Sr] and changes in isotopic ratios entering the Peconic Estuary than values seen in Xin (1993). The deeper aquifers on Long Island have longer residence times than the shallower aquifers and additional differences may occur between subunits resulting in variability across the estuary (Schubert, 1999). For instance, based on well data and hydrologic models, Sag Harbor Cove is calculated to have 25 year old water discharge near shore and a 190 year old subsea discharge (Schubert, 1999). These differences may result in one Peconic Estuary freshwater input being 10 –50 times older than a nearby freshwater input (Schubert, 1999). However, as the values from the river converge as they get closer to the Estuary (Xin, 1993) and the ratios found in Great South Bay are not that different, a significant difference is unlikely. Similar processes could cause larger spatial differences in Ra.

Groundwater and submarine ground water discharge are important to estuarine systems (Moore, 1996; Moore, 1999; Charette et al., 2003) especially on Long Island (Hardy, 1976; Breuer et al., 1999; Montlucon & Sanudo-Wilhelmy, 2001; Burnett et al., 2003; Dulaiova et al., 2006; Beck et al., 2008; Bratton et al., 2009). Submarine ground water discharge has a higher $^{87}Sr/^{86}Sr$ than predicted from the conservative mixing curve for Great South Bay water (Kallenberg, 2005). This is in line with previous and subsequent studies that show as much as 20–30% of the freshwater input to the bay may come from submarine groundwater discharge (Bokuniewicz and Zeitlin, 1980; Beck et al., 2008). The values for Great South Bay at 25 psu while close, plot just a little bit off the predicted $^{87}Sr/^{86}Sr$ vs. 1/[Sr] mixing line because elevated [Sr] indicate an additional fluid input to the estuary: submarine ground water discharge (Kallenberg, 2005). This suggests that a river to ocean mixing curve for the Peconic Estuary may not agree precisely with observed values due to the missing groundwater component.

The $^{87}Sr/^{86}Sr$ data from the aquaculture and relict shells show distinguishable ratios (Table 5.1, Fig. 5.2). $^{87}Sr/^{86}Sr$ in the initial growth layer of shells S1 and C1 grown in aquaculture at 15 psu (S1 1st part and C1 1st part) has a much higher isotopic ratio than the portion of the same shells grown in 28 psu seawater of the Peconic Estuary (S1 2nd part and C1 2nd part) (Fig. 5.2). This suggests that we should be able distinguish ratios representing brackish conditions from marine conditions, as well as ratios representing today's 28 psu. While it is difficult to statistically distinguish isotopic ratios in relict shells, we observe that ratios generally decreased with time suggesting an increase in salinity over time when we exclude #70 (Fig. 5.2). The higher ratio in #70 suggests a period of decreased salinity during a longer term trend of increasing salinity (Fig. 5.2). #70 has no overlap in standard deviation with #26C suggesting that its ratio is indeed higher (Fig. 5.2).

Relict oyster shells (26C, 70, 61, 38, 0b) have strontium isotopic ratios lower than or close to the values of the aquaculture shells grown in 28 psu Peconic Estuary seawater (S1 2nd part and C1 2nd part) (Fig. 5.2). The $^{87}Sr/^{86}Sr$ ratios cover a range that might suggest relict shells grew in waters of similar salinities to today with

160

increasing salinities to slightly more saline water. Plots of the $^{87}Sr/^{86}Sr$ on the Great South Bay curve (Fig. 5.6) show another view of how this might represent slightly more saline values, given the scatter of values. Our data does not quite fall on the Great South Bay curve, but we can still see a similar relationship (Fig. 5.6). The range of our ratios within our sample runs is high compared to the change in salinity represented by our change in mean value. If we take our average to be reliable and assume that our mixing curves apply to earlier times then it is possible that the salinity was similar, and indeed closer to 30 psu at the end of the terrain. Sometimes slight diagenesis of calcite will result in a lowering of $^{87}Sr/^{86}Sr$ ratios (Reinhardt et al., 2000). However, similar values for the various forms of calcite layers suggest that significant post-depositional alteration is unlikely.

There are two first-order mechanisms for long-term changes in salinity in an estuary. The first, and most critical to this research, is the long term flux of seawater in the estuary caused by changes in sea level or basin depth. Increased sea-level or scouring of the basin would increase salinity and vice versa. The second mechanism is changes in freshwater fluxes by changes in precipitation and runoff or groundwater discharge. Increased rates of marine incursion or decreased freshwater inputs would lead to higher salinity and vice versa.

Salinity might decrease locally due to a change in the hydraulics of mixing driven by bathymetric constraints or climate. Changes in wind forcing, for example, could alter the flow of water into the estuary. An example of a potential change in bathymetric constraints would be if tidal passages were shallow enough to slow tidal mixing rates. At present, one sees very little difference in salinity within the Peconic Estuary until one approaches the Peconic River mouth. However a change in mixing might alter the salinity gradient across the estuary.

Increased sea level is probably a more likely cause of a temporary increase in submarine groundwater discharge as the water table re-equilibrates because the increased pressure of water overhead will push near shore freshwater in an aquifer

below the encroaching ocean upward eventually. There should be a significant period of time after sea level rise decelerates where submarine groundwater discharge is increased considering the rate of flow and residence times in these systems. The ages of the relict shells correspond to a time when the rate of relative sea level rise slowed (Fig. 5.5).

In addition to precipitation, changes in regional currents such as the Gulf Stream and northern coastal shelf waters may also affect salinity and Sr values. For instance, if the waters became fresher than average due to a larger influence of fresher and colder shelf waters from the north, a freshening of the Peconics could follow. Freshening of these input waters could also occur if Long Island Sound and Block Island Sound had higher river discharge than now. Discharge is known to increase in years when higher snow volumes melt associated with a positive NAO (Rock et al., 2001). If the region had more or less submarine groundwater discharge than today such as from an NAO like pattern, then that might also alter the end member ratio and concentration near the mouth of the Estuary.

The lower $^{87}Sr/^{86}Sr$ ratio (Fig. 5.3) and ^{226}Ra activity (Fig. 5.4) of the youngest relict oyster shell, 26C, may suggest that groundwater and/ or surface water input were less than present resulting in a period of decreasing freshwater when this shell was growing. An increase in the size of the effective estuarine basin volume over time as open ocean water pushes farther in with sea level rise would also increase salinity. The most likely cause for a prolonged decrease in salinity over several hundred to a thousand years would be sedimentation decreasing the volume of the bay faster than it is offset by sea-level rise.

If the oysters did indeed survive at relatively high salinities, an area that was dominated by dense oyster reefs may have behaved in a different way than in this region today. For instance, oysters are strong filter feeders and high numbers of oysters might reproduce high enough numbers to survive, but might also filter out some of the larvae of predators as well. Dense communities would also provide protective

162

reef habitats for young to settle on. It is possible there were some kind of natural barriers present that protected oysters from predators such as a bathymetric barrier to the east. It also possible that it was just a matter of time before predators, competitors such as *Crepidula fornicata*, and disease made it impossible to survive. Predation stress may have also come from Native American occupants of the area. After the last of the Peconic Bay reefs died, 1,200 years ago +/-100, Native Americans were shellfishing for oysters and clams on Shelter Island's near brackish bays such as Coecles Bay (Lightfoot et al., 1987). The sites in greater than 2 m of water and far from shore were not harvested by early European settlers until the 1800's in Great South Bay (Ingersoll, 1881) so if human populations were impacting oysters thousands of years ago these less accessible sites might not have been threatened by shellfishing.

$\delta\,^{18}$O and $\delta\,^{13}$C:

The $\delta\,^{18}$O of the aquaculture shell grown between 10 -15 psu (C1 1st) and at 28 psu (C1 2nd) show distinctive differences in values (Table 5.5). The portion of shell grown in about 15 psu (C1 1st) grew in an average of ~18°C (range of °C) water.   The portion of shell grown in 28 psu grew during the summer so it reflects higher temperatures (20-25°C (East Hampton, 2006-2009)). A mixing curve was calculated using these values in order to constrain the conditions of our relict shells. A 1 per mil change in salinity equals about 4°C, where $T\,°C = 16.5 - 4.3\,(\delta\,^{18}O_{Calcite} - \delta\,^{18}O_{Water}) + 14\,(\delta^{18}O_{Calcite} - \delta\,^{18}O_{Water})^2$ (Epstein et al., 1953; Craig, 1965), but for our salinity curve for around 28 psu a 1 per mil change would equal about 5.6 psu. As the δ^{18}O variation could not be due to just salinity, the larger variations in $\delta\,^{18}$O represent temperature variability in the relict shells (Table. 5.5, 5.6), which supports our ^{87}Sr/^{86}Sr interpretation. A temperature reconstruction using the ^{87}Sr/^{86}Sr salinity estimates gives a reasonable summer temperature range comparable to the 2000's in Peconics (Table. 5.5). The aquaculture shells had the most negative $\delta\,^{13}$C values, which may reflect oyster diet. No correlation with salinity or temperature is seen in $\delta\,^{13}$C values.

Layers of relict shell were taken from the chalky part of the shell to get an initial sense of variability between layers. These layers represent fast growth of the shell and in this area should be dominated by summer warm temperatures. Some of the variability between layers is probably due to differences in sampling as this initial set of $\delta^{18}O$ measurements was not designed to be a comprehensive comparison, but was trying to demonstrate if changes in salinity and temperature could be determined. However, despite any variability in sampling, the values are still consistently within a few degrees on each other. There are too few samples to see much of a trend or warrant correlation with other locations from this time period. In future studies, subsamples from along the hinge such as average layer subsampling would be needed for $\delta^{18}O$ analysis in order to create more direct comparison.

The general pattern of salinities is similar to today, if not slightly higher, and this makes sense in terms of the volume of sea level rise and decrease in volume due to sedimentation over the last 2,000 years or so.   A similar salinity pattern is supported by the $\delta^{18}O$ values. This means that the majority of the $\delta^{18}O$ variability must be due to temperature during this time period. The combination of $\delta^{18}O$ and [Sr] isotopes may be used to look for changes in water masses influencing the estuary over the many thousands of years during which the Peconic Oyster Terrain thrived.

CONCLUSION:

Salinity levels near the end of the oyster terrain were fairly close to today or somewhat more saline compared with the more brackish salinities of 15 psu of an aquaculture hatchery. Salinity values in relict oyster shells from ~2000 -1700 ybp correspond to salinities comparable to those observed today (~28 psu). Salinity was increasing over time towards the end of the Oyster Terrain, with sometimes periods of lower salinity (#70). This probably led to increased stress that killed off the oysters, and corresponds to the decrease in depths of active reefs.

While we can tell that the salinity was clearly fairly high and we believe that we see trends in our data, this range of salinities is where it becomes increasingly difficult to obtain precise enough $^{87}Sr/^{86}Sr$ values to reliably distinguish salinities above 24 psu (Ingram and Sloan, 1992). However, even at the higher salinity we do see significant variability between some shells such as 26C and 70. This suggests that a longer time series of variability in salinity may be reconstructed from these shells from interannual/decadal patterns to thousands of years. Large changes in salinity within the estuary, making it less than 20 psu, would require several meters of sea level change based on the volume of tidal exchange and freshwater inputs to the bay. Such a lower sea level might correspond to the initiation of the earliest reefs in the estuary. The uncertainty in salinity with $^{87}Sr/^{86}Sr$ suggests that higher precision instruments are needed to know more than that the salinity was relatively high for oysters.

Both Sr isotopes and ^{226}Ra are in agreement with other studies showing significant submarine groundwater discharge inputs into the Peconic Estuary. ^{226}Ra levels were elevated in relict shells compared to today. The deeper, older shells have much more ^{226}Ra than the modern aquaculture shells. This suggests that submarine groundwater discharge has decreased over time while the rate of sea level rise decreased.

Table 5.1: ^{87}Sr/^{86}Sr values: aquaculture & dated oyster shells from grabs, age, δ^{13}C, water depth.

	ID	^{87}Sr/^{86}Sr Average	^{14}C radiocarbon years	Age in years before present using Hughes Mar04	δ^{13}C	Water Depth of Sample Today (MLLW)	Location in Peconic Estuary
Dated Oyster Shells from Grabs	#26C-2008	0.709164 ±0.000014	1820	1350	0.9	5.5	Noyack Bay
	#70-2008	0.709206 ±0.000014	2171	1775	-0.3	9.6	Little Peconic Bay
	#61-2008	0.709167 ±0.000018	2241	1850	0.8	9	Little Peconic Bay
	#38-2006	0.709184 ±0.000016	2348	1968	-0.1	11	Little Peconic Bay
	#0b-2008	0.709189 ±0.000025	2695	2350	1	13	Little Peconic Bay
	#13-2006	-	-	-	-	8.5	Little Peconic Bay
	#73-2008	-	-	-	-	7.3	Little Peconic Bay
	#71-2008	-	-	-	-	8.6	Little Peconic Bay
Aquaculture Oyster Shells	C1 10 psu (C1 1st part)	0.709313 ±0.000064					Cornell Co-op seed
	C1 28 psu (C1 2nd part)	0.709200 ±0.000017					Goose Creek
	S1 10 psu (S1 1st part)	0.709262 ±0.0000047					Aeros seed
	S1 28 psu (S1 2nd part)	0.709219 ±0.000074					Southold Bay

Table 5.2: $^{87}Sr/^{86}Sr$ values: aquaculture oyster shells subsampled layers.

ID	$^{87}Sr/^{86}Sr$ Average	**small number of runs *one run instrument 2 σ stdev*
S1 Chalky	0.709211 ±0.0000056	
S1 Hinge	0.709237 ±0.000072	**
S1 Avg of these	0.709219 ±0.000059	
C1_Shell	0.709179 ±0.0000096	**
C1 Hinge	0.709200 ±0.000021	**
C1 Avg	0.709232 ±0.000076	*

C1 =Goose Creek-Cornell Cooperative Seed, S1=Southold Bay -Aeros Seed

Table 5.3: Example of variability of subsamples within relict shells

	Shell ID	$^{87}Sr/^{86}Sr$	Notes **machine 2 σ standard deviation
Relict Shells	26C Layer	0.709144±0.000071	** * single run
	26C Avg	0.709166±0.0000051	mostly non chalky
	26C L (chalky layer)	0.709203±0.0000032	chalky
	26C All	0.709164±0.000014	(all runs avg)
Relict Shell 26C	38 Avg	0.709182±0.000016	chalky & non chalky
	38L shell	0.709187±0.000016	chalky
	61 Avg	0.709175±0.000018	non chalky mostly
	61 L	0.709157±0.000019	chalky
	70 Avg	0.709209±0.000012	non chalky
	70 L	0.709192±0.000022	chalky
	0b Avg	0.709190±0.000025	chalky & non chalky

Table 5.4: ^{226}Ra in relict & aquaculture shells uncorrected for age and ^{14}C age decay corrected

	Oyster Shell	^{226}Ra dpm/g	^{226}Ra ^{14}C age decay corrected dpm/g (where possible based on radiocarbon ages Table 5.1) no decay correction needed for aquaculture shells
Relict	#70 (2008)	0.071±0.002	0.153±0.004
	#38 (2006)	0.067±0.002	0.158±0.005
	#71 (2008)	0.079±0.003	-
	#73 (2008)	0.060±0.002	-
	#13 (2006)	0.053±0.002	-
	0b (2008)	0.179±0.004	0.498 ±0.012
	26C (2008)	0.038±0.001	
Aquaculture	Mystic Seed -Peconic Bays Bulk Sample	0.013±0.001	0.013±0.001
	Goose Creek Shell	0.028±0.001	0.028±0.001

Table 5.5: $\delta^{18}O$ and $\delta^{13}C$ results and temperature conversion table.

Oyster Shell Samples ID (Grab Year)	Results		T (°C) with constant Salinity	Salinity (psu)	Approximate $\delta^{18}O_{water}$ scales		Temperature Conversion using Salinity from $^{87}Sr/^{86}Sr$	
	$\delta^{18}O_{calcite}$ (‰) VPDB	$\delta^{13}C_{calcite}$ (‰)	T (°C); VSMOW ($\delta18O_{water}$ (‰) =-1) Craig (1965) eq.	Known and Reconstructed Salinity using $^{87}Sr/^{86}Sr$	$\delta^{18}O_{water}$ (‰) VSMOW made to fit *known T & S* ($\delta18O$-=0 at 35psu)	$\delta^{18}O_{water}$ (‰) VSMOW LI River (highest measured values)	Made to fit T (°C); Craig (1965) eq. *known T & S ($\delta18O$-=0 at 35psu)*	LI River T (°C); Craig (1965) eq.
C1-1st	-3.89	-4.17	29.0	~15 (10-15)	-3.4	-3.8	17.9	16.2
C1-2nd	-3.14	-3.87	25.3	28	-1.2	-1.3	24.4	23.9
26C (2008)	-2.36	0.03	21.7	30	-0.87	-0.9	22.3	22.2
70 (2008)	-2.44	0.36	22.1	28	-1.2	-1.3	21.2	20.7
61 (2008)	-3.09	-0.47	25.1	29	-0.97	-1	25.2	25.1
38 (2006)	-2.96	0.20	24.5	29	-1.1	-1.2	24.0	23.5
0b (2008)	-2.23	0.53	21.1	28	-1.2	-1.3	20.2	19.8

Table 5.6 δ¹⁸O Temperature Conversion Table.

$\delta^{18}O_{calcite}$ (‰) VPDB	$\delta^{18}O_{water}$ (‰) VSMOW Assume Constant	T (°C); Epstein et al. (1953) eq.	T (°C); Craig (1965) eq.
	Example of how δ¹⁸O changes with constant Salinity	**T (°C) with constant Salinity & VSMOW**	
-4	-1	29.5	29.5
-3	-1	24.5	24.7
-2	-1	19.8	20.1
-1	-1	15.4	15.8
0	-1	11.2	11.8

Table 5.7: ^{226}Ra in relict shells along with grain size and depth.

ID (Year)	^{226}Ra measured	% err	Water Depth of Sample	Mean based on gravel free	%Clay	%Fine	%Sand	%Gravel
#70 (2008)	0.07	2.5	9.6	4.82	15.3	37.3	59.5	3.2
#38 (2006)	0.07	2.9	11	3.0	5.7	40.0	47.0	40.0
#71 (2008)	0.08	3.3	8.6	7.30	61.2	77.3	21.6	1.0
#73 (2008)	0.06	2.9	7.3	6.89	69.8	80.4	11.5	8.1
#13 (2006)	0.05	3.1	8.5	4.3	23.1	44.9	47.5	7.5
0b (2008)	0.18	2.5	13	3.98	8.1	25.4	64.5	10.1
26C (2008)	0.06	2.8	5.5	2.76	1.8	11.1	77.1	11.8
#61 (2008)			9	5.61	20.4	36.9	33.7	29.4

Fig. 5.1 : Map of water sources for aquaculture shells and locations grown in Peconic Estuary.

Aquaculture facility source of seawater

Areas where oysters were grown at 28 psu

Southold Bay

Southold Bay input (Aeros)

Goose Creek

Cornell Co-op Cedar Beach Creek input

Meters

2,500   1,250   0

Depth Scale
Meters
Below MLLW

-31.9
-31.0
-30.0
-29.0
-28.1
-27.1
-26.1
-25.2
-24.2
-23.2
-22.2
-21.3
-20.3
-19.3
-18.4
-17.4
-16.4
-15.5
-14.5
-13.5
-12.5
-11.6
-10.6
-9.6
-8.7
-7.7
-6.7
-5.8
-4.8
-3.8
-2.8
-1.9
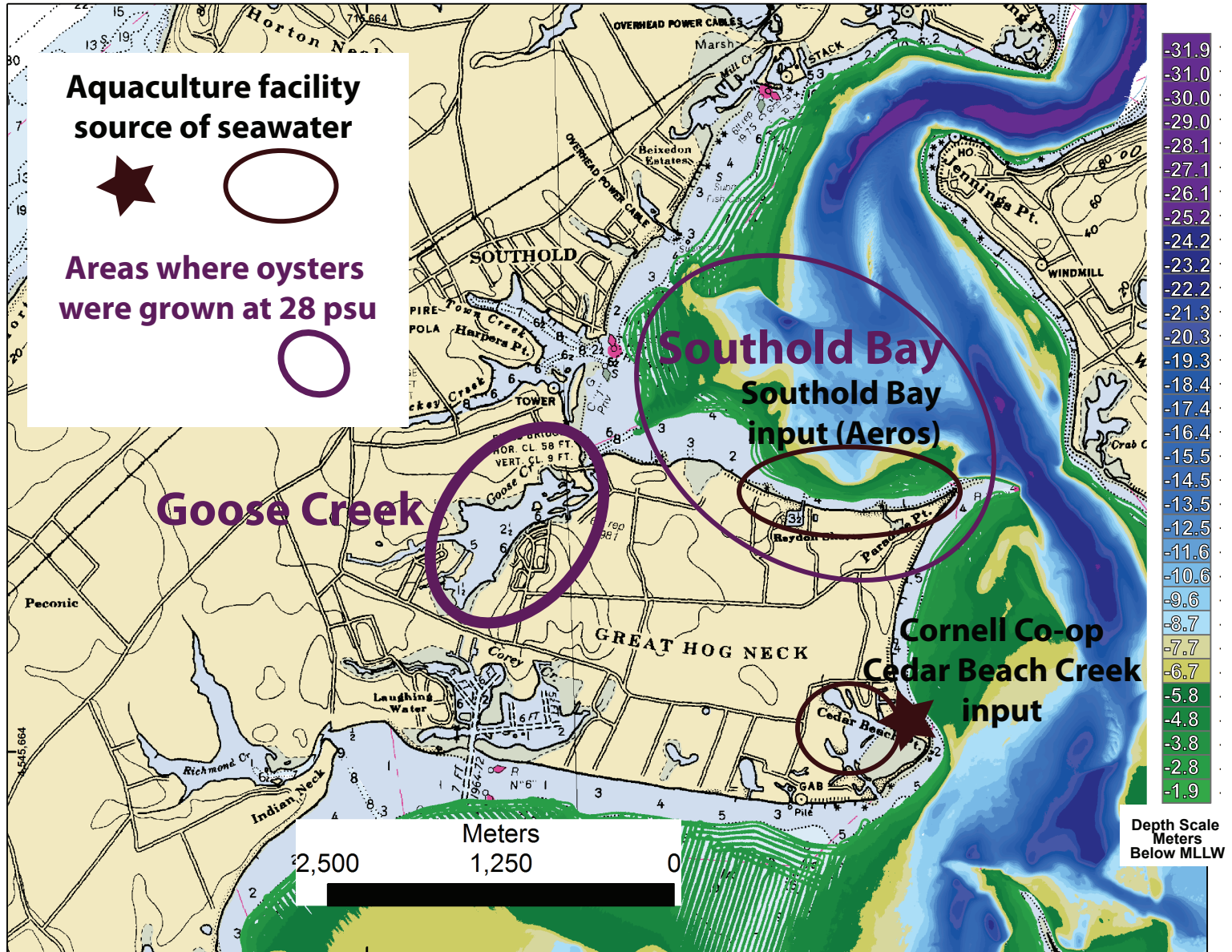
Fig. 5.2: ^{87}Sr/^{86}Sr in aquaculture shells and relict shells with error.

^{87}Sr/^{86}Sr in Oyster Shells

^{87}Sr/^{86}Sr with Age of Oyster Shells from Grabs
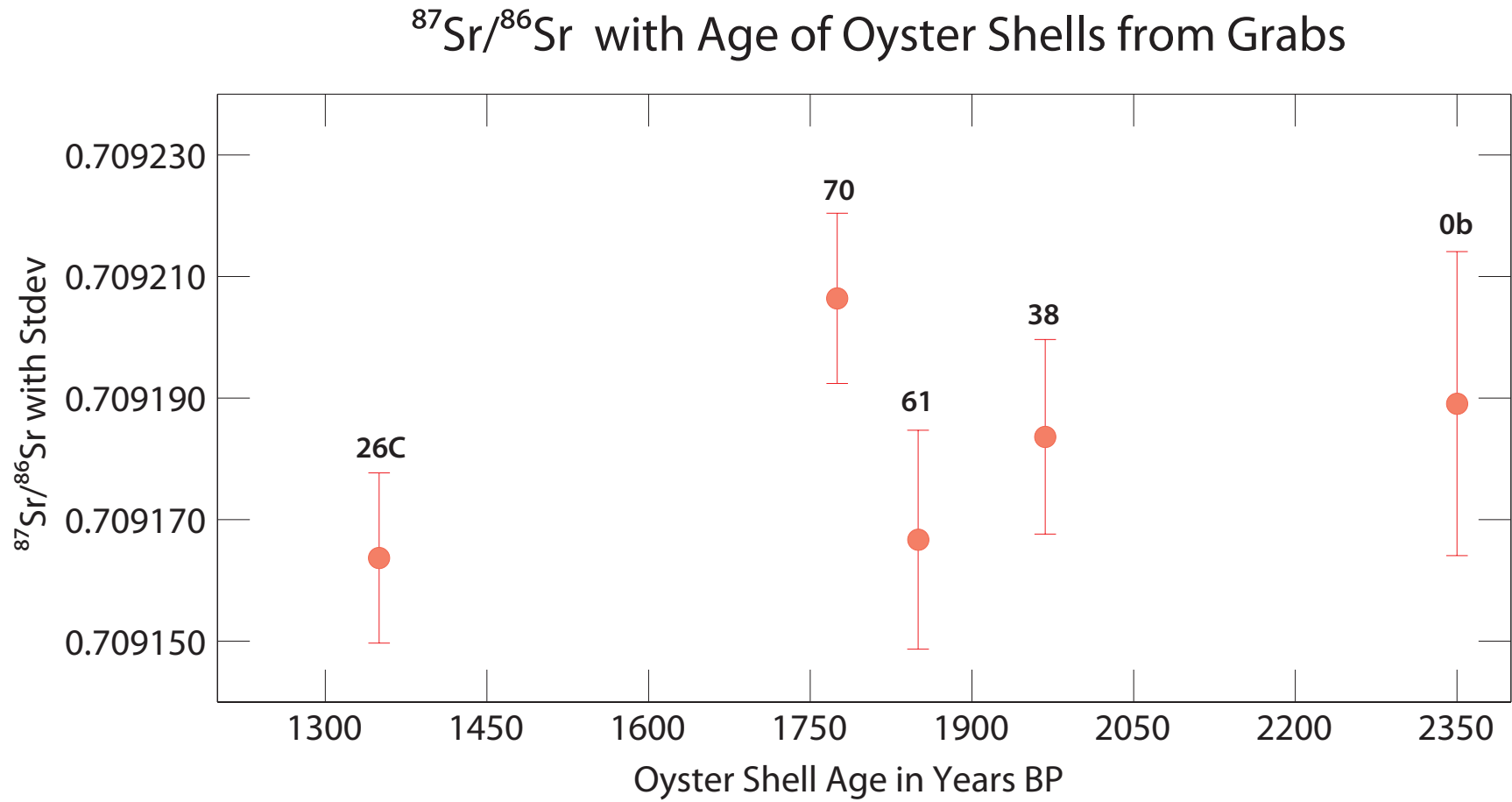
Fig. 5.4: ^{226}Ra (age corrected) with error in relict shells vs. age in calibrated years BP. Plot shows radiocarbon ages calibrated to years before 1950 AD.

^{226}Ra *(age corrected)* of Oyster Shells from Grabs
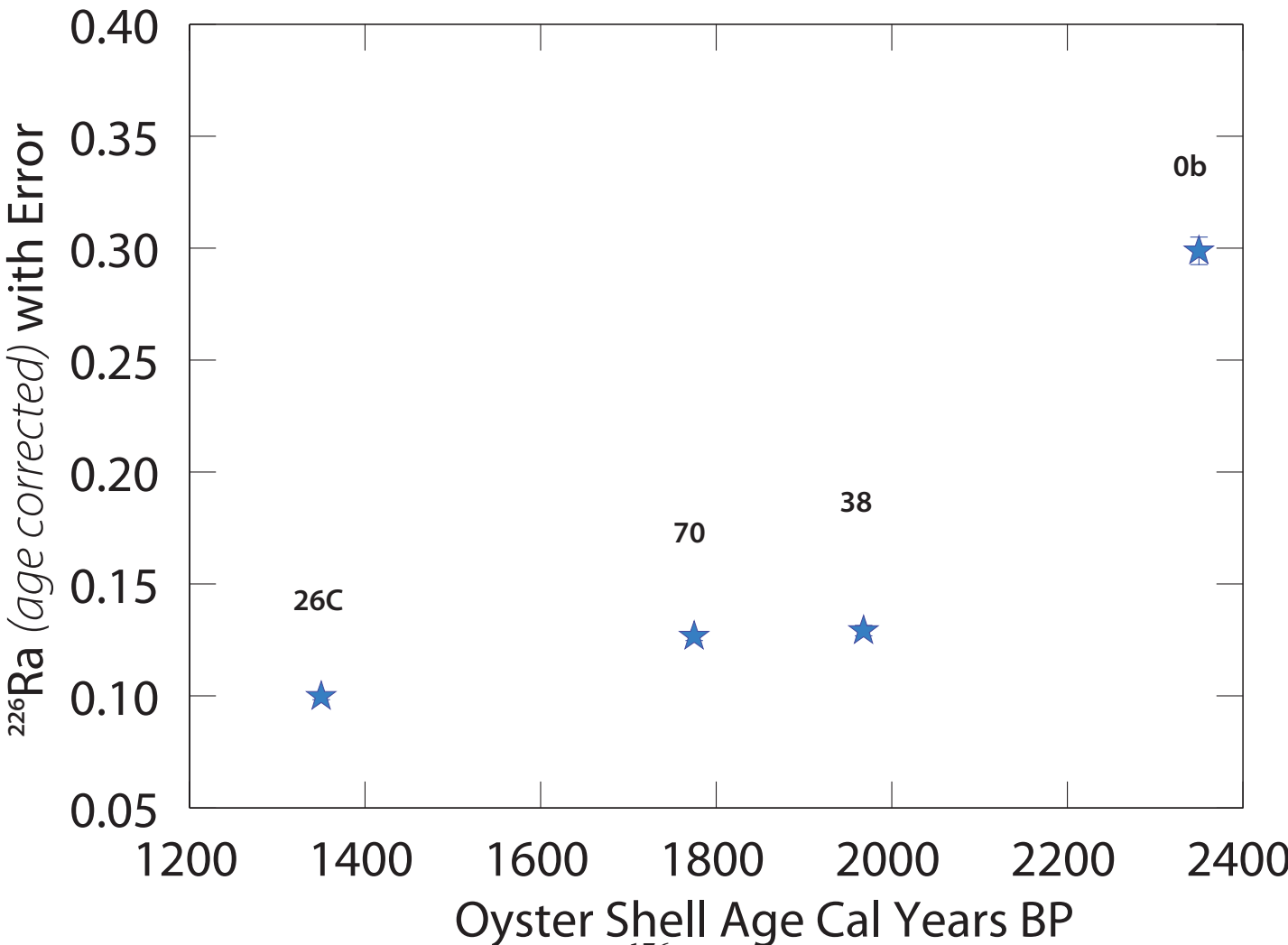
Fig. 5.5: Sea level curve for Nantucket from Gutierrez et al. (2008) with age of mound tops and ^{226}Ra values with age. Horizontal scale of Calibrated Age in Years the same. A change in slope of ^{226}Ra noted a little over 2000 years ago as the rate of sea level rise slows.

Sea Level and ^{226}Ra (age corrected) of Oyster Shells from Grabs

Mounds

— Extrapolatin of Age based on age depth curve of dated shells

— Extrapolation of Age based on SL curve

Gutierrez et al.,2003 SL curve

Depth Below Present Mean Sea Level (meters)

^{226}Ra dpm/g (age corrected) with Error

Age Cal Years BP
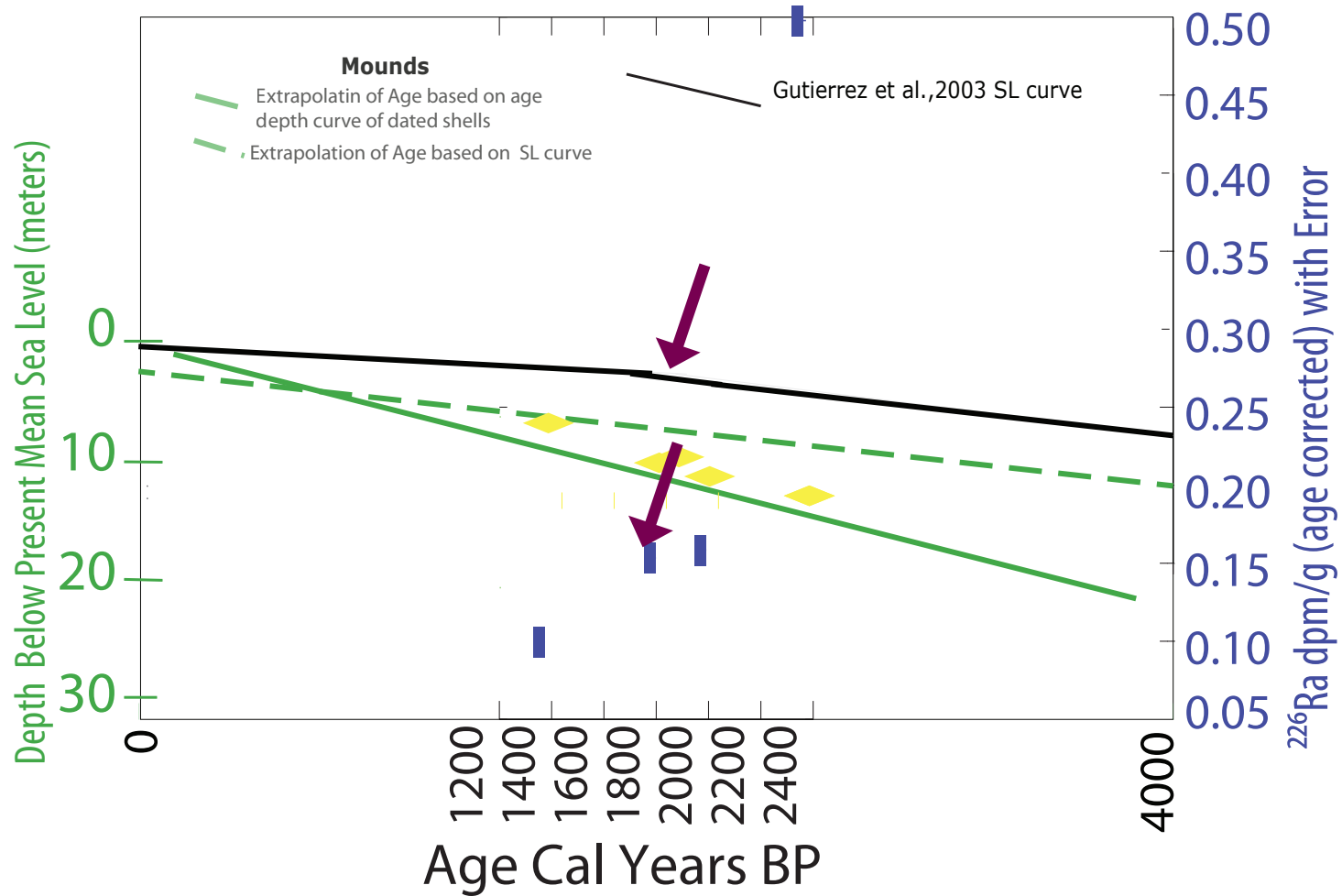
Fig. 5.6: $^{87}Sr/^{86}Sr$ in oyster shells compared to salinity. Inset shows predictive mixing lines based on $^{87}Sr/^{86}Sr$, [Sr] and salinity relationships. Great South Bay to Atlantic mixing line is shown in black from (Kallenberg, 2005 and Cochran, 2011 personal communication). Purple line is inferred relationship for the Peconic Estuary to Atlantic based aquaculture shells .

Mixing lines for Great South Bay with Peconic values

Inferred relationship for Peconic Estuary

Connetequout River to Atlantic

15 psu

Range of Relict Shells

Open ocean

Equivalent salinity (psu)

| 37.0 | 18.0 | 11.7 | 8.6 | 6.7 |

$^{87}Sr/^{86}Sr$

1/[Sr] μM^{-1}

Aq Shells w/ Err

Values from
Kallenberg, 2005
Great South Bay

87Sr/86Sr=0.00259(1/[Sr]+0.70913 7, [Sr]=2.64Salinity +2.39, where [Sr] is in μM, and Salinity is in psu (Kallenberg, 2005 and Cochran, 2011 personal communication). Rearrangement of the terms lets us solve for salinity using 87Sr/86Sr, where ((0.00259/(87Sr/86Sr-0.709137))+2.39)/2.64=Salinity.

REFERENCES:

Arnold, W. S., Jones, D. S., Quitmyer, I. R., Schöne, B. R., Surge, D. M., 2007, The 1st International Sclerochronology Conference held at St. Petersburg, FL, USA, July 2007, http://www.scleroconferences.de.

Basu, A. R., Jacobsen, S. B., Poreda, R. J., Dowling, C. B., Aggarwal, P. K., 2001, Large groundwater strontium flux to the oceans from the Bengal Basin and the marine strontium isotope record, Science, v. 293, p. 1470-1473.

Beck, A. J., Rapaglia, J. P., Cochran, J. K., Bokuniewicz, H. J., Yang, S., 2008, Submarine groundwater discharge to Great South Bay, NY, estimated using Ra isotopes, Marine Chemistry, v. 109, i. 3-4, p. 279-291.

Bokuniewicz, H. J., Zeitlin, M.J., 1980, Characteristics of groundwater seepage into Great South Bay, MSRC, Special Report, v. 35, SUNY, Stony Brook, NY, 30 p.

Brass, G. W., Turekian, K. K., 1974, Strontium distributions in GEOSECS oceanic profiles, Earth Planetary Science Letters, v. 23, p. 141-148.

Bratton, J. F., Crusius, J., Kroeger, K. D., Schubert, C., Coffey, R., Bokuniewicz, H., 2009, Submarine Groundwater Discharge to Great South Bay from Long Island and Fire Island, New York, Geological Society of America, 2009 Annual Meeting - October 2009, v. 41, n. 7, p. 396.

Breuer, E., Sañudo-Wilhelmy, S. A., Aller, R. C., 1999, Trace metals and dissolved organic carbon in an estuary with restricted river flow and a brown tide, Estuaries, v. 22, p. 603-615.

Broecker, W., 1963, A Preliminary Evaluation of Uranium Series Inequilibrium as a Tool for Absolute Age Measurement on Marine Carbonates, Lamont Geological Observatory Contribution 617, Journal of Geophysical Research, v. 68, n. 9, p. 2817-2834.

Bryant, J. D., Jones, D.. S., Meuller, P., A., 1995, Influence of Freshwater Flux on 87Sr/86Sr Chronostratigraphy in Marginal Marine Environments and Dating of Vertebrate and Invertebrate Faunas, Journal of Paleontology, v. 69, n. 1, p. 1-6.

Buddemeier, R. W., Maragos, J. E., Knutson, D. W., 1974, Radiographic studies of reef coral exoskeletons: rates and patterns of coral growth, Journal of Experimental and Marine Biology Ecology, v. 14, p. 179-200.

Burnett, W. C., Bokuniewicz, H., Huettel, M., Moore, W. S., Taniguchi, M., 2003, Groundwater and pore water inputs to the coastal zone, Biogeochemistry, v. 66, n. 1-2, p. 3-33.

Carriker, M. R., R. E. Palmer, 1979, A new mineralized layer in the hinge of the oyster, Science, v. 206, p. 691-693.

Charette, M. A., Splivallo, R., Herbold, C., Bollinger, M. S., Moore, W. S., 2003, Salt marsh submarine groundwater discharge as traced by radium isotopes, Marine Chemistry, v. 84, p. 113-121.

Charrette, M. A. & Sholkovitz, E. R., 2006, Trace Element Cycling in a subterranean Estuary; Part 2, Geochemistry of the pore water, Geochimica et Cosmochimica Acta, v. 70, n. 4, p. 811-826.

Cochran, J. K., Landman, N. H., Turekian, K. K., Michard, A., Schrag, D. P., 2003, Paleoceanography of the Late Cretaceous (Maastrichtian) Western Interior Seaway of North America: Evidence from Sr and O isotopes, Paleoceanography, Paleoclimatology, Paleoecology, v. 191, n. 1, p. 45-64.

Collier, K., Bokuniewicz, H., Coffey, R., 2005, Submarine Groundwater Discharge along Fire Island, NY, Long Island Geologists Conference 2005, Stony Brook, NY.

Craig, H., 1965, The measurement of oxygen isotope paleotemperatures, in Tongiorgi, E., ed.: Proceedings of the Spoleto Conference on Stable Isotopes in Oceanographic Studies and Paleotemperatures, Consiglio Nazionale delle Ricerche, Pisa, v. 3, p. 161–182.

Dettman, D. L., Flessa, K. W., Roopnarine, P. D., Schöne, B. R., Goodwin, D. H., 2004, The use of oxygen isotope variation in shells of estuarine mollusks as a quantitative record of seasonal and annual Colorado River discharge, Geochimica et Cosmochimica Acta, v. 68, n. 6, p. 1253-1263.

DiLorenzo, J. L., 1986, The Overtide and Filtering Response of Inlet/Bay Systems [Ph.D. Dissertation], MSRC, Stony Brook University.

Dowling, C. B., Poreda, R. J., Basu, A. R., 2003, The groundwater geochemistry of the Bengal Basin: Weathering, chemsorption, and the trace metal fluxes to the oceans, Geochimica et Cosmochimica Acta, v. 67, n. 12, p. 217-2136.

Dulaiova, H., Burnett, W. C., Chanton, J. P., Moore, W. S., Bokuniewicz, H. J., Charette, M. A., Sholkovitz, E., 2006, Assessment of groundwater discharges into West Neck Bay, New York, via natural tracers, Continental Shelf Research, v. 26, i. 16, p. 1971-1983.

East Hampton, 2006, Contributors: Aldred, J., Dunne, J., Gaites, J., Gould, O., Quevedo, F., Lester, R., Rice, J., Appendix 7-9 Water Temperatures, 2006 Annual Report of Operations, http://www.ehamptonny.gov/HtmlPages/Aquaculture/AquaAnnualReports.htm

East Hampton, 2007, Contributors: Aldred, J., Dunne, J., Gaites, J., Gould, J., Quevedo, F., Lester, R., Lester, D., Rice, J., Appendix Appendix 7- 2007 Water Temperatures, 2007 Annual Report of Operations, http://www.ehamptonny.gov/HtmlPages/Aquaculture/AquaAnnualReports.htm

East Hampton, 2008, Contributors: Aldred, J., Dunne, J., Gaites, J., Gould, J., Quevedo, F., Lester, R., Lester, D., Rice, J., McKenny, N., Perrone, J., Appendix 4-2008 Water Temperatures, 2008 Annual Report of Operations, http://www.ehamptonny.gov/HtmlPages/Aquaculture/AquaAnnualReports.htm

East Hampton, 2009, Contributors: Aldred, J., Dunne, J., Gaites, J., Gould, J., Quevedo, F., Lester, R., Lester, D., Rice, J., McKenny, N., Ruggerio, D., Appendix 4- 2009 Water Temperatures (Charts 7-9), 2009 Annual Report of Operations, http://www.ehamptonny.gov/HtmlPages/Aquaculture/AquaAnnualReports.htm

Eichrom Technologies, Inc. | A GCI Company, 2010, Sr-spec Resin © 2010, accessed: Jan 16, 2010, http://www.eichrom.com/products/info/sr_resin.cfm.

Eisel, M. T., 1977, Shoreline survey; Great Peconic, Little Peconic, Gardiners, and Napeague bays, Special Report - Marine Sciences Research Center, State University of New York, n. 5, 37 p.

Gallardo, A. H., Marui, A., 2006, Submarine groundwater discharge: an outlook of recent advances and current knowledge, Geo-Marine Letters, v. 26, p. 102-113.

Galtsoff, P. S., 1964, The American Oyster, Crassostrea Virgina Gemlin, Fish and Wildlife Service, Fishery Bulletin v. 64., 457 p.

Garcia-Orellana, J., Cochran, J. K., Bokuniewicz, H., Yang, S., Beck, A. J., 2010, Time-series sampling of 223Ra and 224Ra at the inlet to Great South Bay (New York): a strategy for characterizing the dominant terms in the Ra budget of the bay, Journal of Environmental Radioactivity, v. 101, p. 582-588.

Gaswirth, S. B., Ashley, G. B., Sheridan, R. E., 2002, Use of Seismic Stratigraphy to Identify Conduits for Saltwater Intrusion in the Vicinity of Raritan Bay, New Jersey, Environmental & Engineering Geoscience, v. 8, no. 3, p. 209-218.

Gillikin, D. P., Ridder, F. D., Ulens, H., Elskens, M., Keppens, E., Baeyensa, W., Dehairs, F., 2005, Assessing the reproducibility and reliability of estuarine bivalve shells (Saxidomus giganteus) for sea surface temperature reconstruction: Implications for paleoclimate studies, Palaeogeography, Palaeoclimatology, Palaeoecology, v. 228, p. 70-85.

Goldstein, S. ed., Isotope Geochemistry Lab Handbook, Version: August 4, 2003, Lamont-Doherty Earth Observatory of Columbia University, Reviewed by Sidney Hemming, First version coordinated by Conny Class, Contributions from: Merry Cai,

Anna Cipriani, Conny Class, Katie Donnelly, Marty Fleisher, Allison Franzese, Sarah Fonville, Steve Goldstein, Sidney Hemming, Dana Himmel, Alex LaGatta, Alex Piotrowski, Randye Rutberg, Kyla Simons, Gad Soffer, accessed 2009, https://beta.ldeo.columbia.edu/files/LDEO_Isolab_Handbook.pdf.

Grossman, E. L., Ku, T.-H., 1986, Oxygen and Carbon Isotope Fractionation in Biogenic Aragonite: Temperature Effects, Chemical Geology (Isotope Geoscience Section), v. 59., p. 59-74.

Hardy, C. D., 1976, A preliminary description of the Peconic Bay Estuary, Special Report 3, Marine Sciences Research Center, State University of New York, 76-4, 65 p.

Henderson, G. M. & Anderson, R. F., 2003, U-series Toolbox for Paleoceanography, Reviews in Mineralogy & Geochemistry Vol 52: Urananium-Series Geochemistry, ed. Bourdon B, Henderson, G. M., Lundstrom, C. C., Turner, S. P., p. 493-529.

Ingersoll, E., 1881, The Oyster-Industry, The History and Present Condition of the Fishery Industry, Report on the oyster-industry of the United States, U.S. Department of the Interior, Washington D.C., Government Printing Office, Prepared under the Direction of Prof. S.F. Baird, U. S. Commissioner of the Fish and Fisheries and by G. Brown Good, Assistant Direction U.S. National Museum and a staff of associates.

Ingram, B. L., Sloan, D., 1992, Strontium Isotopic Composition of Estuarine Sediments as Paleosalinity-Paleoclimate Indicator, Science, v. 255, i. 5040, p. 68 -72.

Ingram, B. L. and Depaolo, D. J., 1993, A 4300 year strontium isotope record of estuarine paleosalinity in San Francisco Bay, California, Earth and Planetary Science Letters, v. 119i. 1-2, p. 103 -119.

Ingram, B. L. and Weber, P., K., 1999, Salmon origin in California's Sacramento-San Joaquin river system as determined by otolith strontium isotopic composition, Geology, v. 27, p. 851-854.

Ingram, B. L., Lin, J.C., 2002, Geochemical tracers of sediment sources to San Francisco Bay, Geology, v. 30, n. 6, p. 575-578.

Jones, D.S., Quitmyer, I.R., Andrus, F. T., 2005, Oxygenisotopic evidence for greater seasonality in Holocene shells of Donax variabilis from Florida, Paleoceanography, Paleoclimatology, Paleoecology, v. 228, p. 96-108.

Kallenberg, K., 2005, 87Sr/86Sr as a Paleoceanographic Indicator in Ancient and Modern Marine Environments [M.S. Thesis], Stony Brook University.

Kim, Y., Lee, K.-S., Koh, D.-C., Lee, D.-H., Lee, S.-G., Park, W.-B., Koh, G.-W., Woo, N.-C., 2003, Hydrogeochemical and isotopic evidence of groundwater salinization in a

coastal aquifer: a case study in Jeju volcanic island, Korea, Journal of Hydrology, v. 270, p. 282-294.

Kirby, M. X., Soniat, T. M., Spero, H. J., 1998, Stable isotope sclerochronology of Pleistocene and Recent oyster shells (Crassostrea virginica), Palaios, v. 13, p. 560-569.

Kirby, M. X., 2000, Paleoecological Differences Between Tertiary and Quaternary Crassostrea Oysters, as Revealed by Stable Isotope Sclerochronology, Palaios, v. 15, p. 132 -141.

Kirby, M. X., Miller, H. M., 2005, Response of a benthic suspension feeder (Crassostrea virginica Gmelin) to three centuries of anthropogenic eutrophication in Chesapeake Bay, Estuarine, Coastal and Shelf Science, v. 62, p. 679-689.

Laroche, J., Nuzzi, R., Waters, R., Wyman, K., Falkowski, P. G., and Wallace, D. W. R., 1997, Brown Tide blooms in Long Island's coastal waters linked to interannual variability in groundwater flow, Global Change Biology, v. 3, no. 5, p. 397-410.

Lightfoot, K. G., R. Kalin and J. Moore, Contributions: Cerrato, R. , Conover, M., Rippel-Erikson, S., 1987, Prehistoric Hunter-Gatherers of Shelter Island, New York: An Archaeological Study of the Mashomack Preserve, Contributions of the University of California Archaeological Research Facility No. 46. University of California, Berkeley, California.

Lin, I.-T., Wang, C.-H., You, C.-F., Lin, S., Huang, K.-F., Chen, Y.-G., 2010, Deep submarine groundwater discharge indicated by tracers of oxygen, strontium isotopes and barium content in the Pingtung coastal zone, southern Taiwan, Marine Chemistry, v. 122, p. 51-58.

Montlucon, D., Sanudo-Wilhelmy, S. A., 2001, Influence of net groundwater discharge on metal and nutrient concentrations in a coastal environment: Flanders Bay Long Island, New York, Environmental Science and Technology, v. 35, p. 480-486.

Moore, W. S., 1996, Large groundwater inputs to coastal waters revealed by Ra-226 enrichments. Nature, v. 380, n. 6757, p. 612-614.

Moore, W. S., 1997, High fluxes of radium and barium from the mouth of the Ganges-Brahmaputra River during low river discharge suggest a large groundwater source, Earth and Planetary Science Letters, v. 150, n. 1-2, p. 141-150.

Moore, W. S., 1999, The subterranean estuary: a reaction zone of groundwater and sea water, Marine Chemistry, v. 65, p. 111-125.

Oschmann, W., 2009, 'Sclerochronology: editorial', International Journal of Earth Science (Geol Rundsch), v. 98, p. 1-2.

Palmer, M. R., Edmond, J. M., 1989, The strontium isotope budget of the modern ocean. Earth and Planetary Science Letters, v. 92, p. 11-26.

Povinec, P. P., de Oliveira, J., Braga, E. S., Comadnucci, J.-F., Gastaud, J., Groening, M., Levy-Palomo, I., Morgentstern, U., Top, Z., 2008, Isotopic trace element and nutrient characterization of coastal waters from Ubatuba inner shelf area, south-eastern Brazil. Estuarine, Coastal and Shelf Science, v. 76, p. 522-542.

Rapaglia, J., 2005, Submarine Groundwater Discharge into Venice Lagoon, Italy, Estuaries, v. 28, n., 5, p. 705-713.

Reinhardt, E. G., Blenkinsop, J., Patterson, R., T., 1999, Assessment of a Sr isotope vital effect (Sr-87/Sr 86) in marine taxa from Lee Stocking Island, Bahamas. Geo-Marine Letters, v. 18, i. 3, p. 241-146.

Reinhardt, E. G., Cavazza, W., Blekinsop, J., Patterson, R. T., 2000, Differential Diagenesis of sedimentary components and the implication for strontium isotope analysis of carbonate rocks, Chemical Geology, v. 164, p. 331-343.

Rivara, Gregg, Cornell-Cooperative Extension, 2009, Growth of Oysters produced by Cornell Co-op and Aeros in the Peconic Estuary, personal communication, in person, e-mail, and phone.

Rivara, Gregg, Cornell-Cooperative Extension, 2010, Growth Conditions Including Temeperature of Oysters in the Peconic Estuary, personal communication, e-mail.

Rock, B. N., Carter, L., Walker, H., Bradbury, J., Dingman, S. L., Federer, C. A., 2001, Chapter 6: Water Resources and Potential Climate Change Impacts, The New England Regional Assessment of The Potential Consequences of Climate Variability and Change, A Final Report, p. 63-83.

Schlueter, M., Sauter, E. J., Andersen, C. E., Dahlgaard, H., Dando, P. R., 2004, Spatial distribution and budget for submarine groundwater discharge in Eckernfoerde Bay (Western Baltic Sea), Limnology Oceanography, v. 49, p. 157-167.

Schmidt, S., and Cochran, J. K., 2010, Radium and radium-daughter nuclides in carbonates: a brief overview of strategies for determining chronologies, Journal of Environmental Radioactivity, v. 101, no. 7, p. 530-537.

Schöne, B. R., Flessa, K. W., Dettman, D. L., Goodwin, D. H., 2003, Upstream dams and downstream clams: growth rates of bivalve mollusks unveil impact of river management on estuarine ecosystems (Colorado River Delta, Mexico), Estuarine, Coastal and Shelf Science, v. 58, p. 715-726.

Schöne, B. R., 2008, The curse of physiology—challenges and opportunities in the interpretation of geochemical data from mollusk shells, Geo-Marine Letters, v. 28, p.

269–285.

Schöne, B. R., Rodland, D. L., Surge, D. M., Feibig, J., Gillikin, D. P., Baier, S. M., Goewert, A., 2006, Comment on: Stable carbon isotopes in fresh water mussel shells: Environmental record or marker for metabolic activity?" by J. Geist et al. (2005), Geochimica et Cosmochimica Acta, v. 70, n. 10, p. 2658-2661.

Schubert, C. E., 1998, Areas contributing ground water to the Peconic Estuary and ground-water budgets for the North and South Forks and Shelter Island, eastern Suffolk County, New York: U.S. Geological Survey Water-Resources Investigations Report 97-4136, 36 p., 1 pl.

Schubert, C. E., 1999, Ground-Water Flow Paths and Traveltime to Three Small Embayments within the Peconic Estuary, Eastern Suffolk County, New York, U.S. Geological Survey Water-Resources Investigations Report 98-4181, 43 p.

Schubert, C. E., Bova, R. G., Misut, P. E., 2004, Hyrdogeologic Framework of the North Fork and Surrounding Areas, Long Island, NY, U.S. Geological Survey Water-Resources Investigations Report 02-4284, 34 p.

Schuller, D., Kadko, D., Smith, C. R., 2004, Use of ^{210}Pb/ ^{226}Ra disequilibria in the dating of deep-sea whale falls, Earth and Planetary Science Letters, v. 218, n. 3-4, p. 277-289.

Stanley, J.G., Sellers, M.A., 1986, Species profiles : lifehistories and environmental requirements of coastal fishes and invertebrates (Mid-Atlantic)--American oyster. U. S. Fish Wildl. Serv. Biol. Rep. 82(11.65), U.S. Army Corps of Engineers, TR EL-82-4, p. 25.

Staubwasser M., Henderson, G. M, Berkman, P. A., Hall, B. L., 2004, Ba, Ra, Th, and U in marine mollusc shells and the potential of ^{226}Ra/Ba dating of Holocene marine carbonate shells, Geochimica et Cosmochimica Acta, v. 68, n.1, p.89-100.

Surge, D., K. C. Lohmann, D. L. Dettman, 2001, Controls on isotopic chemistry of the American oyster, Crassostrea virginica: implications for growth patterns: Palaeogeography Palaeoclimatology Palaeoecology, v. 172, p. 283-296.

Surge, D. M., Lohmann, K. C., Goodfriend, G. A., 2003, Reconstructing estuarine conditions: oyster shells as recorders of environmental change, Southwest Florida, Estuarine, Coastal and Shelf Science, v. 57, n.5-6, p. 737–756.

Surge, D., Lohmann, K. C., 2008, Evaluating Mg/Ca ratios as a temperature proxy in the estuarine oyster, Crassostrea virginica, Journal of Geophysical Research, v. 113, p. G02001 (1-9).

Swarzenski, P. W., Martin, J. B., Cable, J. E., Lindenberg, M. K., Boyton, B., Bowker, R., Signa, C. C., 2000, Quantifying Submarine Groundwater Discharge to Indian River Lagoon, Florida, USGS OFR 00-492.

Veizer, J., 1989, Strontium Isotopes in Seawater Through Time, Annual Review of Earth and Planetary Science, v. 17, p. 141-167.

Wilson, R. E., 1996, Aspects of tidal and subtidal flushing within the Peconic Bay Estuary, Proceedings of the Brown Tide summit Oct 20-21, 1995, ed. McElroy, A., NYSG SUNY, Stony Brook NYSG I W –95-001, p. 11.

Xin, G., 1993, Strontium Isotope Study of the Peconic River Watershed, Long Island, New York [M. S. Thesis], Geosciences Department, State University of New York, Stony Brook.

Yang, S., 2007, Quantification of the tidal exchange of radium as an indicator of submarine groundwater inputs to Great South Bay [M.S. Thesis], State University of New York, Stony Brook, 39 p.

Young, M. B., Gonneea, M. E., Fong, D. A., Moore, W. S., Herrera-Silveira, J., Payton, A., 2008, Characterizing sources of groundwater to a tropical coastal lagoon in a Karstic area using radium isotopes and water chemistry, Marine Chemistry, v. 109, p. 377-394.

CHAPTER 6: CONCLUSIONS

INTRODUCTION:

The characteristics of the Peconic Oyster Terrain and the environmental setting of the Peconic Estuary documented in Chapters 1 to 5 allow comparison of the terrain with other reefs. The main conclusions of Chapters 2 through 5 are first summarized and then the characteristics of this system are compared in more detail to others. Subsequently, how oyster reef morphologies relate to environmental factors are discussed. In particular, the age of the Oyster Terrain is compared with examples of other Crassostrea *virginica* reef systems in the Eastern United States, after which the morphologies are compared. Implications for more detailed climate records and mapping and discovery of other reefal deposits in the geologic record are discussed.

MAIN CHAPTER CONCLUSIONS:
Chapter 2:

Over 10,000 mounds comprising the 'Oyster Terrain' are discernible in multibeam bathymetry and backscatter within Little Peconic and Noyack Bay in the Peconic Estuary. This terrain consists of exposed mounds typically ~2 m high, but as tall as 4 m in exposed relief, 10 to 50 m in diameter and associated with high backscatter. The surfaces of mounds are covered with stained unarticulated oyster shells that were recovered in grab samples, but no living oysters. The Oyster Terrain covers more than 10,000 square km within the Peconic Estuary comprising both exposed and buried mounds as shown in the combination of multibeam and sub-bottom seismic profiler data. Mound centers and tops are submerged ~6 to 18+ m below MLLW as shown in the multibeam data, with none above 5.5 m below MLLW. The peak of exposed mound heights is around 11 to 12 m. While seismic coverage was limited outside of Little Peconic Bay, more mounds were found buried throughout the Estuary within this depth range. Exposed mounds covered most places within the Estuary inside of Shelter

187

Island and beyond (away from shore) the shallow sand ledges (less than 5 m) that form a perimeter around the bays, except for areas that have very coarse mobile sediment (e.g. sand waves) that are in the deeper channels of the bay. Bases of mounds were revealed in seismic profiles to have started even deeper, with the deepest mound bases at 18 to 24 m depth. Many mounds with seemingly little exposed relief were actually 4 m high beneath the surface.

Chapter 3:

The overall distribution of mounds within our focus area of Little Peconic and Noyack Bays reflects many different mound formations such as banks or fields of mounds, each with a unique distribution as seen within the smaller subset distributions. Seismic profiles reveal that our exposed mound depth distribution is skewed towards the shallower mounds and is missing many of the deeper mounds. The more detailed analysis of mound distribution was consistent with the depths shown in Chapter 2, except that the shallowest mound peak might be slightly higher (~5.0 m rather than the 5.5 m). The thickest exposed reef was at least 10 m in vertical relief with many more thick mounds revealed in sub-bottom profiles. Most individual mounds had an area equivalent to a circle with a diameter of 20 to 50 m, while mounds that were greater than 50 m in equivalent diameter tended to be found in banks. Additionally, certain types of reef formations tend to have different reef densities. For example, mounds on larger reefs may be less numerous, but these mounds tend to be larger and closer together and cover a larger area. Many of the most separated or non-overlapping mounds comprising a field of mounds were among the smallest mounds detected, roughly 10 to 20 m in equivalent diameter. Medium-sized mounds (20 to 40 m) tended to be dominant in the moderately dense mound clusters, which had a wide range of number of mounds per square meter. While a few areas of the highest flow near the constrictions in the bay had no reefs, almost the entire bay that is of sufficient depth – greater than 7 m – was covered by mounds. This quantification of reef characteristics may help to both understand modern reef growth better as well as identify other relict or fossil deposits.

Chapter 4:

The Oyster Terrain was dated as last active around 2,000 years ago. This confirmed the hypothesis that these were thousands of years old relict reefs. The shallowest and youngest mound dated was 1,350 Calibrated ybp and the deepest and oldest mound that dated was 2,400 Cal ybp. Two methods were used to estimate the age when the mounds were initiated. The age of initiation was estimated as 3,750 Cal ybp by assuming that all the mounds were initiated at the same time and as 7,500 to 9,000 Cal ybp by assuming that the mounds were initiated in 2 m of water. We suspect that mounds initiated toward the older end of this estimate.

The reefs of the Oyster Terrain grew in much deeper water than anticipated based on present-day ecology, as oysters were growing at depths of 4 to 10 m below MSL. While an age depth relationship with older mounds being deeper was seen, active mound depth was not directly correlated to sea level as might have been expected. The large depth range of active mounds suggests that reefs were active in deeper water than generally expected.

Heterogeneity in sedimentation patterns is visible in the large scale patterns of burial versus exposure of mounds. As one looks at the entire estuary, these patterns are visible over the scale of kilometers to less than 100 meters. These sedimentation patterns probably reflect the alteration of boundary layer flow patterns due to the presence of mounded topography. The higher relief mounds in the present bathymetry seem to have lower accumulation than areas between them and flatter ground as evidenced by variations in radioactive inventories and thickness of sediment covering mounds. Known accumulation rates for the estuary over deeply buried mounds are reasonable if those mounds are of the same age as mounds dated in this study at that depth.

Chapter 5:

Our geochemical analysis shows that the environment was changing toward the

end of Oyster Terrain activity between 1350 to 2350 Cal ybp, and that the relict shells lived in an environment very different from today. Comparison of $^{87}Sr/^{86}Sr$ in samples of aquaculture shells raised at 10 psu, samples from shells raised at 28 psu, and relict shells recovered from the mounds showed that the salinity when the oysters were growing on the mounds was close to the modern Peconic Estuary values of 28 psu. This relatively high salinity is also supported by $\delta^{18}O$ ratios in the oyster shells. Mean $^{87}Sr/^{86}Sr$ ratios of relict shells show an overall increase in salinity over time, with a brief freshening recorded around 1775 Cal ybp (175 AD). However, better precision in the $^{87}Sr/^{86}Sr$ measurements would have been needed to discern salinity trends in detail. In addition to high salinities close to or higher than today based on $^{87}Sr/^{86}Sr$, analysis of $\delta^{18}O$ in the chalky bands of the relict shells suggests summer temperature variability comparable to today. Additionally, results from the analysis of ^{226}Ra in oyster shells suggest that the rate of submarine groundwater discharge was decreasing as the rate of global and local sea-level rise decreased over this period (1350 to 2350 Cal ybp).

Our geochemical analysis shows that the environment was changing during this period, the relict shells lived in an environment that was very different than today and the environment was evolving during the late Holocene. The gradual evolution of estuarine conditions (i.e., deeper water and increased salinity) probably led to the increase in a number of stresses. As oysters only survived in increasingly shallower water as salinity increased it is likely that increased salinity contributed to the disappearance of oysters from the Peconic Estuary. Filtration and reproduction rates of a mature community may have been high enough to offset increased stresses associated with high salinity such as predation and disease for a period, but eventually they succumbed.

REEF COMPARISON:
Ages:

Oyster reefs and estuarine conditions initiated in most of the present-day deeper estuaries along the Eastern U.S. and Gulf of Mexico around 6 to 8.2 ka (Anderson et al., 2008; Bratton et al., 2003; Carbotte et al., 2004; Slagle et al., 2006). For example

oyster reefs in the Chesapeake (Bratton et al., 2003), Matagorda Bay, Sabine Lake, and Galveston Bay in the Gulf of Mexico were created as a result of sea-level rise and initial oyster deposits appeared within these estuaries around 8,000 years ago (Anderson et al., 2008). Based on mound depth, sea level would have been high enough to have the deeper mounds in the Peconic Oyster Terrain submerged at about 8,000 years bp. Thus it is possible the Oyster Terrain may date that far back as well.

Oyster reefs mark the incursion of marine waters in estuaries along the Eastern U.S. seaboard throughout the Holocene. Oysters have existed fairly continuously for thousands of years within many of the deepest estuaries in the Eastern U.S (Fig. 6.1). However, reefs have tended to migrate inland as sea-level rise pushes higher salinities further into tributaries. Continuous reef growth in one location for thousands of years is unusual in large part because most estuaries tend to have large lateral changes in salinity over time. For example in Chesapeake Bay, oyster reefs initiated in the paleo-river channel at the center of the bay, but are no longer found there (Bratton et al., 2003). Today, reefs are found in the shallow embayments along the edge of the main bay and in tributary estuaries (Bratton et al., 2003) such as the James River (DeAlteris, 1988).

Reefs were abundant in other deep estuaries during times when the Peconic Oyster Terrain was alive. For example, the Hudson River near the Tappan Zee Bridge between 6.1ka to ~5.6ka and 2.4ka to ~0.5ka (Carbotte et al., 2004; Slagle et al., 2006), the Chesapeake Estuary between ~8ka to present (Bratton et al., 2003), and Galveston Bay, TX between ~8ka to present all had abundant oyster reefs (Rodriguez et al., 2004; Anderson et al., 2008) (Fig. 6.1). Another oyster reef system located (~0.5 km to ~6 km) offshore of the Suwannee River in FL also overlaps with this time period (Wright et al., 2005) (Fig. 6.1). Examination of these systems allows one to see some of the differences between estuaries. Some estuaries, such as the Hudson River are long and variable in width, but largely narrow and are likely large lateral changes in salinity (DeAlteris, 1988; Carbotte et al., 2004; Bratton et al., 2003) compared to the Peconic Estuary. Many have much larger seasonal and interannual fluctuations in salinity (Carbotte et al., 2004; Bouma, 1976) than those seen in the Peconic Estuary. Few

estuaries have held continuous oyster populations within the same portion of the estuary (DeAlteris, 1988; Bratton et al., 2003; Slagle et al., 2006). For instance, even the reefs located offshore of the Suwannee River that initiated around~4,400 ybp ~6 km offshore die off and were replaced by reefs active today within ~0.5 to ~3 km of shore (Wright et al., 2005). Further offshore ~10 km out, an older (~5.5ka to 9ka) relict oyster reef system is covered by more recent sediments (Wright et al., 2005). Most of the Holocene is marked by formation of new reefs upstream, which is usually in conjunction with marine incursion pushing higher salinities farther upstream (DeAlteris, 1988; Bratton et al., 2003; Slagle et al., 2006). However, oysters sometimes regress back toward the ocean as estuaries infill, precipitation decreases, or other processes reduce the rate of marine water flux into the estuary (Bratton et al., 2003). Oyster reefs disappear at other times for unknown reasons (Slagle et al., 2006; Carbotte et al., 2004). An example of some of these movements in oyster reefs is found in the Chesapeake as oysters moved inland around 2 to 3 thousand years ago (ka), with a subsequent retreat toward the ocean before a gradual marine incursion with sea-level rise later causing the oysters to migrate inland again (Bratton et al., 2003) (Fig. 6.1). The continued marine incursion after the reef retreat 2 to 3 ka in many tributaries such as the James River caused the progressive movement of oyster reefs upstream over the last several hundred years within the Chesapeake (DeAlteris, 1988).

However, at least one example of suitable estuarine conditions persisting in one portion of an estuary for several thousand years exists (Bouma, 1976). A portion of San Antonio Bay, TX has consistently held reefs since ~9.5 ka. The bay has been consistently shallow throughout the time period while it has increased in salinity (Bouma, 1976). The area in which oysters grow has actually shrunk within San Antonio Bay, as the bay used to be much larger in the past. Barrier islands have migrated inland, however the typical migration of a bay inland with sea-level rise has been thwarted by sedimentation and the progradation of a delta of the main river into the bay (Bouma, 1976). The impact of the river on the characteristics of the central part of San Antonio Bay such as salinity (especially freshets), temperature and sedimentation actually increased with time, with the increase in sediment input from the rivers presumed to be a major factor in reef die off close to the river discharge (Bouma, 1976).

Closer to the Peconic Estuary, approximately 2,000 years ago, small, thin oyster reefs lived in the Hudson River during a period of increased salinity compared to today (Carbotte et al., 2004). The increase in Hudson river salinity corresponds well with our $^{87}Sr/^{86}Sr$ ratios, which indicate salinity increased during this time period until salinity was possibly slightly higher than today by the time the terrain stopped growing. Increased salinities compared to present in the Hudson and Peconic Estuaries suggests that some of the variables affecting salinity may have been common in the region. Salinities appear to have fluctuated over time in the Hudson, as reefs also appeared around 6,000 years ago in some of the same locations along with higher salinities than today (Carbotte et al., 2004; Pekar et al., 2004). This raises the question as to whether the numerous thick relict reefs of the Peconic Estuary represent the continuous presence oysters within the estuary that might record regional climate changes. Biological factors such as disease and predation may have played a role in the appearance and disappearance of reefs. Other physical attributes may also play a role, such as turbidity or frequency of storms or changes in snow melt leading to freshets that might alter the range of oysters in the Hudson River even if average salinity was tolerable.

Some of the salinity variability may have been due to climate patterns as we see evidence for variability at least on the centuries scale in addition to the longer term trend of increasing salinity, which is most likely due to sea-level rise. A period of regionally lower precipitation and runoff compared to today combined with sea-level rise may also have led to increased salinity in local estuaries. Infilling by sediment deposition as the rate of sea-level rise decreased during the past 1,350 years since the end of the Oyster Terrain may have decreased the volume of the Peconic Estuary resulting in a decrease in salinity. Variability in basin geometry would affect volume changes due to sea-level rise and thus salinity. Similar variability in sedimentation patterns would also affect changes in estuarine volume over this time period. A greater rate of infilling compared to sea-level rise as the rate of sea-level rise decreased may have occurred for a while in the Northeast.

A simple calculation for the Peconic Estuary based on present bathymetry alone suggests that there was a 39% increase in water volume from 2,350 ypb to 1,350 ypb (Fig 6.8). One can see that bay volume increases faster per unit of rise once the edges of the steep sand banks encircling the bay are breached. If one uses present bathymetry assuming no changes such as sedimentation, the area of the bay submerged in the last 1,350 years is less than that covered during last 1,000 years of active Oyster Terrain because of the decrease in the rate of sea-level rise. A simple calculation using sedimentation rates gives a better sense of the somewhat smaller volume increase over time caused by the difference in sea-level rise rate and sedimentation. The actual sedimentation pattern is much more complex than just assuming that any depth greater than 6 m has an average accumulation rate of 0.0008 m/yr believed typical from Chapter 4 because one has to consider coarser sediment such as sand eroded from shore and the movement of sand banks, reef growth rate during the active reef period, as well as marshes and other areas. Possible sedimentation rates for the Peconic Estuary for comparison include ~0.8 mm/yr (Cochran et al., 2000) in the bay centers, regional rates and higher rates within the estuary of ~1 mm/yr (Carbotte et al., 2004; Pekar et al., 2004; Rosen et al., 2003; Cochran et al., 2000), and a hypothetical higher rate of 2 to 2.5 mm/yr in the past based on regional rates (Carbotte et al., 2004; Pekar et al., 2004; Rosen et al., 2003) and Peconic beach erosion (Eisel, 1977), marshes (Redfield, 1967), and possible reef growth rates. Using the simple sea level curve (Gutierrez et al., 2003) a hypothetical sedimentation rate of ~2 to 1.5 mm/yr would have allowed bay volume to increase, but then resulted in a decrease in bay volume as sea-level rise fell. This sea level curve does not include fluctuations over a few hundred years including recent increases in sea-level rise rate for Long Island Sound (Varekamp et al., 1992; Varekamp et al., 1999; Nydick et al., 1995; Thomas & Varekamp, 2002; Larsen & Clarke, 2006) that may also play a role in some of the fluctuations in salinity. Thus a combination of precipitation, submarine groundwater discharge, sedimentation and sea-level rise may have led to different timescales of response in estuaries depending on the freshwater inputs and bathymetry to each estuary.

Morphology:

      Despite the widespread distribution and abundance of oysters, examples of *C. virginica* reefs of similar scale and shape to the mounds in the Peconic Estuary are not typical of existing active oyster reefs, however there are examples of historical *C. virginica* reefs approaching the scales of reefs in the Peconic Estuary. A striking example of a 20th Century live oyster reef is in Altamaha Sound, GA where an oyster reef almost 2 m high was reported to be exposed above the sea surface at low tide in 1925 (Galtsoff, 1964). Active oyster reefs typically are thin, have low relief (Rodriguez et al., 2004; Carbotte et al., 2004; Allen et al., 2005) and exist in intertidal depths to a meter or so (Ladd et al., 1957; Parker, 1960; Allen et al., 2005; Carbotte et al., 2004). The long lived reefs that grew in deeper waters may be thicker. For instance, the isolated James River reef was 1.5 to 3 m thick and in 1.5 m of water (DeAlteris, 1988). Even though there are examples of reefs at least 2 m thick (Galtsoff, 1964), most of the height of many active reefs has been lost due to oyster harvesting in the past (DeAlteris, 1988). However, in many estuaries even with sufficient depth, many of the oyster reefs are very thin (several cm) as in Galveston Bay (Rodriguez et al., 2004; Anderson et al., 2008), the Chesapeake (Bratton et al., 2003) and the Hudson River (Carbotte et al., 2004; Slagle et al., 2006).

      The extent and scale of the reef system in the Peconic Estuary are somewhat unusual as seen in the comparison of intact relict reef morphology from various long lived estuaries (Fig. 6.2) even though other estuaries are older. The unusal thickness of the reefs suggests that, while many estuaries are of similar or older ages, the conditions for oyster growth were optimal within the same portion of the estuary for longer in the Peconic Estuary than many other locations. Reef thickness and size is unusual, but even among thick reefs the scale is atypical. Large relict oyster banks are also found in the Hudson River, measure about 1 km in length with a maximum length of 3 km, are 0.6 to1 km wide, and cover 0.5 to 1.5 km^2 (Carbotte et al., 2004; Slagle et al., 2006) (Fig. 6.3). However, the Hudson River reefs lack the vertical relief of the reefs within the Peconic Estuary with most of the large reefs less than 0.5 m thick (Carbotte et al., 2004; Slagle et al., 2006) (Fig. 6.3). The thickest Hudson River reefs have exposed relief of

30 to 90 cm, with a buried thickness, as indicated on the seismic profile, of 3.75 m (Carbotte et al., 2004; Slagle et al., 2006). Some active and long lived oyster reefs a few meters thick can also be found offshore (within ~3 km), such as off of Florida where freshwater discharge maintains brackish seawater near the coast at the mouth of the Suwannee River (Wright et al., 2005) (Fig. 6.5). Farther offshore (more than 3 km) from the Suwannee, relict oyster reefs that form chains several kilometers long have also been described (Wright et al., 2005) (Fig. 6.5). These chains resemble some of the linear chains of mounds that are seen within Little Peconic Bay, and some reefs are of comparable width and thickness (3 m) to reefs in the Peconic Estuary (Fig. 6.6). The Suwannee oyster reefs that are close to sea level are active, but those that are below sea level have died off. The inactive mound tops suggest that they were last active when they were in the intertidal zone several hundred to more than 1,000 years ago (Wright et al., 2005). The area over which Suwannee oyster reefs are found is comparable to the Peconic Estuary. A number of other individual large, thick, long lived oyster reefs are characterized by seismic profiles and dated cores. These include a mid to early Holocene reef in the Damariscotta River, ME (Leach et al., 2006) and a late Holocene relict oyster reef that is 3 m thick in the James River Estuary, VA (DeAlteris, 1988).

One of the better known and studied estuaries with modern active oyster reefs is Apalachicola Bay, Florida (Osterman et al., 2009; Twichell et al., 2007). In Apalachicola Bay, the morphology of exposed reefs based on visual observation, sidescan, seismic profiles, and a 25 m bathymetric grid is very similar to our examples in the Peconic Estuary, especially those where mounds forming larger conglomerations are surrounded by large separate mounds as in the northwest part of Little Peconic Bay. Apalachicola Bay is somewhat similar to the Peconic Estuary, being a wide bay or basin, as opposed to having a more constrained deeper river channels and creeks typical of other estuaries. However, Apalachicola Bay has less than 2 m of water typically, which is much shallower than the Peconic Estuary. Many large Gulf Coast estuaries are similar in this regard, being large shallow lagoons, for example Mission Bay, TX (Parker, 1960; Ladd et al., 1957). Reef areal shapes are similar to the Oyster Terrain in Mission Bay, but the reefs lack the exposed relief of the Peconic Bay reefs

(Fig. 6.7). Great South Bay, NY is a similar shallow lagoon with around 2 m depth, and the relict reefs there also lack the height of the Peconic examples (Clapp & Flood, 2004).

One variable that may limit the number of places with thick reefs is that a location would have to maintain conditions suitable for oysters for a relatively long period of time in order to accumulate thick deposits like those seen in the Peconic Estuary. Oyster reefs of such thickness, based on the rates given in the examples of DeAlteris (1988) and Wright et al. (2005) require hundreds to thousands of years to grow in a stable enough environment to allow them to survive, and with enough water depth to not be limited by sea level. For example, the rate of growth of reefs off of the Suwannee in the Gulf is much slower (Wright et al., 2005) than in the James River in VA (DeAlteris, 1988) where sea-level rise is faster (Fig. 6.2). Even reefs seen in the Hudson River seem to have been faster growing (Carbotte et al., 2004; Slagle et al., 2006) than those off of the Suwannee. Such a relatively stable estuary for thick reef growth would be a large one that is not prone to events such as freshets or sediment discharges that might bury reefs. The only other reef system in the literature that comes close to both the thickness (~11 m) of individual reefs and extent of area of the Peconic Estuary is San Antonio Bay, TX (Bouma, 1976), which also has the longest growing reef communities in the same area of an estuary. The combination of modern and relict reefs in San Antonio Bay and adjacent bays such as Mission Bay is also the closest example we found of reef densities over a large area (Parker, 1960; Ladd et al., 1957; Bouma, 1976) as seen in the Peconic Estuary. A few places in the literature have banks or mounds of similar size in area, but not the total volume seen in the Peconic Estuary or San Antonio Bay.

While oysters are very good at surviving in estuaries under a wide range of conditions, they are frequently killed off by sudden changes in conditions such as salinity changes or increases in sedimentation rates. Additional biological factors such as disease, competition with other species, and predation may periodically wipe out active oyster communities. Places like the Chesapeake have well documented habitat loss, which can lead to the loss of oyster reefs (Ingersoll, 1881; DeAlteris, 1988;

197

Lenihan & Peterson, 1998; Woods et al., 2005). Matagorda Bay Texas for example lost 6,000 acres of oyster beds to silting of the Colorado River (Galtsoff, 1964; Milliman, 1974).

Locations with favorable conditions for oysters for thousands of years that allow large reef buildups and not just thin beds to develop such as the Suwannee seem more unusual. Amongst thick bedded deposits, water depth, continuously favorable salinity, lack of sudden burial, and rate of sea-level rise seem to be important limits on reef thickness. Water depth and rate of sea-level rise probably also affect reef growth rates.

Massive relict oyster beds have long been known on land and one can look to the geologic record to find relict oyster reef deposits with dimensions similar to those in the oyster terrain (6 m high and 50 m in diameter) although these are built by species other than C. *virginica*. Outcrops of Eocene oyster (Ostrea) deposits in Georgia are as thick as 9 m, but lack the internal structure of reefs (Veatch & Stepheson, 1911; Wiedmann, 1972). Pliocene deposits in Murray Basin, South Australia (*Ostrea angasi*) have oyster reef features that are a few meters high and tens of meters across and spread over a large estuary (Pufahl et al., 2004). Some Murray Basin reefs from the Pliocene and Miocene are 6 to 8 m in vertical relief and cover ~150 m, with thinner edges (Pufahl et al., 2004).

Many more examples of thick extensive reef deposits composed of various reef builders are found deeper in the geologic record, some of which preserve, intact, the morphology of individual reefs (Henriet et al., 2002; Cook et al., 2002; Adams et al., 2005; Huvaz, et al., 2007). Many fossil deposits not only hold intact morphology of individual reefs of comparable size, but the reef systems also cover extensive areas. For example, the terminal Proterozoic stramatolite-thrombolite carbonate mounds in Namibia, which include mounds of about 50 m in diameter (Adams et al., 2005) are on a similar scale to the features seen in the Peconic Estuary mounds. These carbonate mounds form a ~5 km long band within a much larger late Proterozoic carbonate unit (Nama Group, Kuibis Subgroup, Omykyk sequence 2) (Adams et al., 2005).

DISCUSSSION AND CONCLUSIONS:

Oyster reefs have long been known to be sensitive to disease, pollution, and sudden environmental shocks such as salinity changes (Ingersoll, 1881). Our limited knowledge of deposits along the continental shelf shows the cycling of dominant reef builders replacing each other over thousands of years (Milliman, 1974). While it has long known that multiple variables can kill a reef, specifying what caused changes in a particular estuary or long term cycles of dominant reef builders is often difficult. The apparent fact that the oyster reefs survived in the relatively high salinity of the Peconic Oyster Terrain, ~28 psu, suggests that perhaps sheer numbers helped oysters survive longer within the estuary at salinities that would have killed off oyster populations at the oyster densities found today. Diseases or sudden events may also play a role. Studies of the Hudson River salinity suggests that periods of no oyster reefs were not due to salinity that was too high or too low, even if the salinities were not as favorable as the optimum salinity (Carbotte et al., 2004).

Most of the modern reef deposits that have been identified thus far are not as thick or at a similar scale to the Peconic mound coverage with the exception of San Antonio Bay, TX. Exposed active and relict reefs show mounds, banks, or chains of mounds that resemble the features that one can see in the Peconic Bays, even if they are not always as distinctive or as large. Some of the better examples of similar reef characteristics are actually found in the fossil record.

Evidence of variations in salinity, and a decrease of submarine ground water discharge over the past 2,350 years in the Peconic Estuary suggest that further work is warranted to measure past variability in the system and to constrain the possible causes. Scenarios which might cause changes in salinity within the estuary include climate changes, sea level changes or changes in morphology affecting circulation. A number of kinds of climate changes might affect salinity in the estuary. For instance, local changes in precipitation may increase runoff and groundwater discharge into the estuary. In the case of the Peconic Estuary, precipitation changes might not have as large an influence as other similar sized estuaries with larger drainage basins. Regional

climate changes throughout the Northeast, especially in New England may also affect salinity. For instance, changes in precipitation and snow pack in New England have been shown to affect discharge of the major rivers into Long Island Sound (Rock et al., 2001). Other types of regional climate changes including shifts in ocean circulation such as a shift in shelf waters related to the NAO-like spatial patterns or climate related changes to water bodies to the north from increased runoff might also affect salinity of marine waters entering the estuary. Changes in stratification and mixing might also affect the salinity range.

Other kinds of climate variability may also affect sea level and to some extent salinity, such as large-scale changes in pressure and local and large-scale wind fields, by changing sea level and the extent to which ocean water is pushed into the estuary. Some of these variations might have a slightly more prolonged effect on submarine groundwater discharge before the system re-equilibrated. Climate variability affecting sea level may include more than just local storm-related sea level changes like storm surges. Longer term trends have long been noted. Atmospheric patterns such as the ENSO and NAO and decadal oceanic oscillations such as the Atlantic Multidecadal Oscillation have long been known to affect sea level (Clark & Patterson, 1985; Ryan & Noble, 2002; Ryan & Noble, 2006; Miller & Douglas, 2007; Kolker & Hameed, 2007), even if a specific atmospheric oscillation was not originally identified as causing the fluctuation such as for the period of higher relative sea level on Long Island of the 1920s (Clark & Patterson, 1985). Long term eustatic and relative sea-level rise would also affect salinity within an estuary by pushing the marine waters further inland assuming freshwater discharge is unchanged.

Changes in submarine groundwater discharge may affect salinity, but this would depend on the relationship between the salinity of that groundwater and the water above it with which it is mixing. The draining of a relatively fresh glacial aquifer via submarine groundwater discharge decreasing salinity near the bed may have been more important in the past, for instance. Again, local and regional changes in precipitation and pressure fields may lead to changes in submarine ground water discharge. Of these possible scenarios, the mechanism of slowing sea-level rise rates

causing lower submarine groundwater discharge rates seems most likely related to the longer term trend of decreasing submarine groundwater discharge. Shorter term variability of less than 1,000 years might primarily reflect climatic variations rather than sea-level rise.

Additional information about potential climate changes in the Long Island region during the period of the oyster terrain may come from paleovegetation studies. Initial evaluation of low-resolution pollen records from bogs on Long Island from Sirkin (1995) do not show any dramatic changes around 1,000 to 2,000 years ago in flora that might be indicative of a prolonged drought that could have ended the oyster terrain conditions. However, studies of Block Island bogs do show a continued succession of flora through that period (Sirkin, 1994), which may or may not relate to local microclimate changes.

A future more detailed analysis of the paleoenvironment of this system would allow a better understanding of the variations occurring within the system as was as enabling a better comparison to regional and global climate patterns. The role of different mechanisms on the evolution of the terrain could be investigated more.

In addition to helping us understand climate fluctuations better, analyzing Peconic Estuary system changes in more detail may help to understand the ecologically and economically important Eastern Oyster. Paleoenvironmental conditions such as submarine groundwater flow, salinity, sedimentation, sea-level rise rates, and temperature may be important to understanding the future of other modern stressed estuaries. For instance, continued presence of reefs in salinities too high for reefs to grow today suggests that stressed systems may be more vulnerable to collapse of oyster populations if oysters numbers are reduced suddenly by harvesting or other mechanisms. Future changes such anthropogenic changes resulting from alterations to land use or water usage that may affect freshwater inflow to a system or sediment influx, or expected natural changes such as continued sea-level rise may also be better planned for in other estuaries.

Many extensive reefs have been identified at lower resolution buried in the sedimentary rock record. An interest in the morphology of ancient reefs exists due in part to the role of reefs in trapping fluids such as hydrocarbons. Examples of descriptions of similar scale intact extensive deposits include Australian Pliocence deposits (Pufahl et al., 2004) and terminal Proterozoic stramatolite-thrombolite carbonate mounds from Namibia (Adams et al., 2005). High resolution studies may be low in number, but extensive reef deposits are found throughout the geologic record. Information about reef building may have implications beyond our modern ecology, including predicting and understanding hydrocarbon deposits. Most of the modern reef deposits that have been identified thus far are not as thick or at a similar scale to the Peconic mound coverage. The ubiquity of oyster deposits and increasing numbers of studies revealing buried reefs (Osterman et al., 2009; Twichell et al., 2007; Weaver et al., 2008) suggests that many large buried oyster terrains remain to be discovered.

Characterization of the Peconic Estuary has already provided unexpected results about the evolution of the Oyster Terrain that may have implications relevant to many other systems. The sheer size, location, and accessibility of the Peconic Oyster Terrain make it a suitable place for more detailed studies of the evolution of such an estuarine reef system. Reefs grew in deeper and much more saline water than was expected. More detailed analysis of the conditions over 10,000 exposed mounds, and many more below the surface may tell us even more about what made this system so productive for oysters. The shallowest bank also seems to be part of the thickest exposed composite reef structure with more than 10 m of high backscatter bank slope indicative of reef on one flank. Such exposed and buried thick mounds that start at the base of the paleochannels ($\geq$ 20 m) may be of particular interest for extensive coring within the system.

Appearance and Disappearance of Reefs in Holocene

Peconic Estuary NY

San Antonio Bay, TX ~9.4ka

Hudson River NY

Chesapeake 6-8.2ka
James River (within Chesapeake)

Galveston TX

Suwannee FL

0 1 2 3 4 5 6 7 8 9
Thousands of Years Ago

Studies of other Reefs

Legend:
— — — — reefs retreat seaward ✳
Many reefs of unkown size, or length of activity

■ ■ ■ ■ ■
Many reefs of various sizes in Peconic Estuary

⊢━━━⊣
Presumed continuous oysters across most of system, with some movement up and downstream

? · · ? Initial reefs start to grow

500 years

203

Fig. 6.2: Example of reef sizes with timescale of Holocene reefs.

Appearance and Disappearance of Reefs in Holocene

Peconic Estuary NY

San Antonio Bay, TX

~9.4ka

Hudson River NY

Chesapeake
James River
(within Chesapeake)

6-8.2ka

Galveston TX

3ka

4ka

Suwannee FL

Thousands of Years Ago

Studies of other Reefs

Reef Vertical Height

Individual Reef

4 m

8 m

500 years

reefs retreat seaward

Many reefs of unkown size, or length of activity

Many reefs of various sizes in Peconic Estuary

Presumed continuous oysters across most of system, with some movement up and downstream

? • • • ?
Initial reefs start to grow
(start age of individual reefs unknown)

204

Fig. 6.3: Hudson River Oyster Reefs from Slagle et al. (2006). Darker = higher backscatter. Note that the reefs are fairly wide and long in the map view. There are not many smaller patches of reefs in between the large masses with close to a 1 km length.
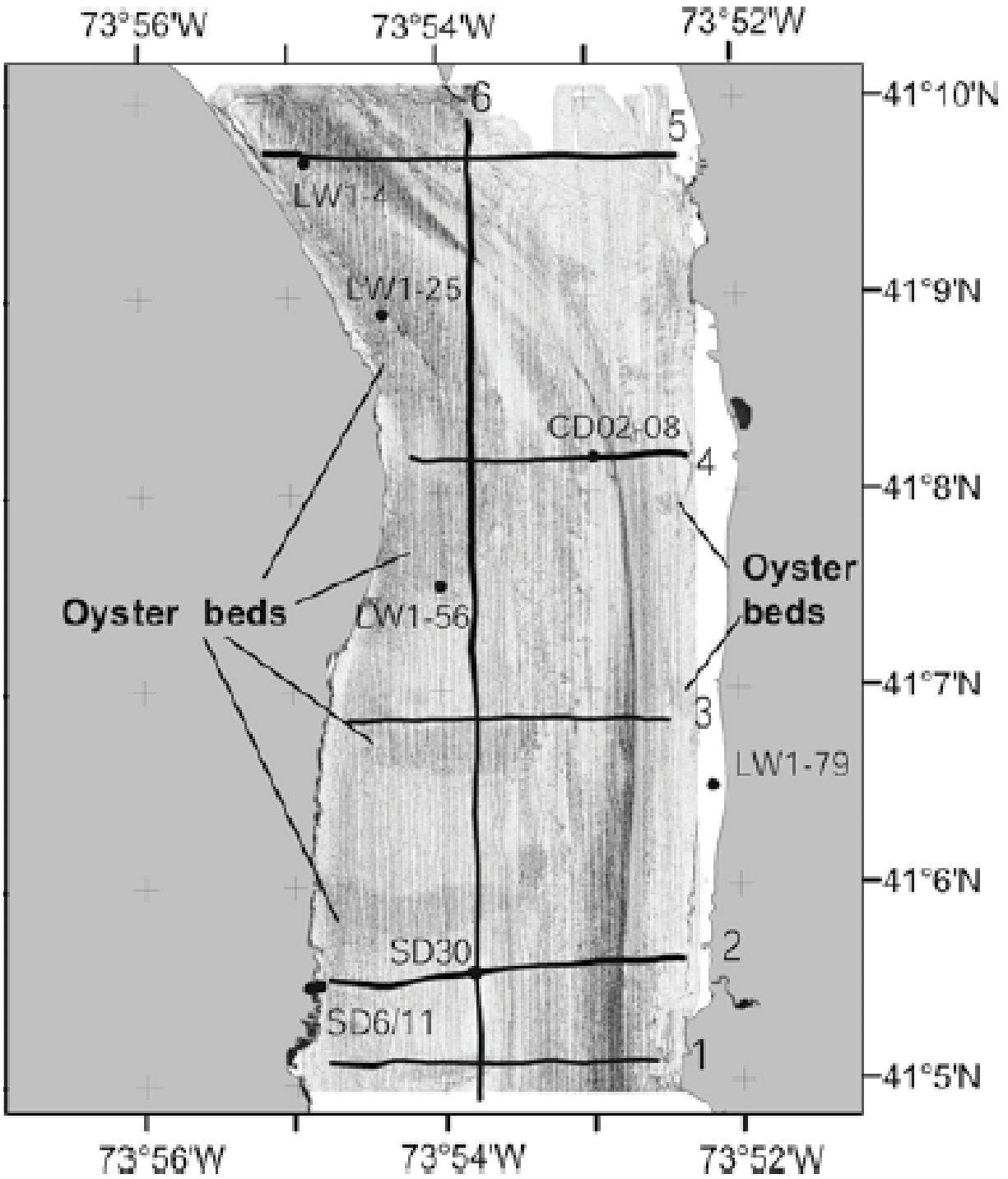
Fig. 6.4: Seismic profile of oyster reefs in the Hudson River from: Carbotte et al. (2004). Note the thickness of the reefs. Reefs may be up to 3.75 m, but thickness is difficult to determine due to seismic opacity caused by the reefs.
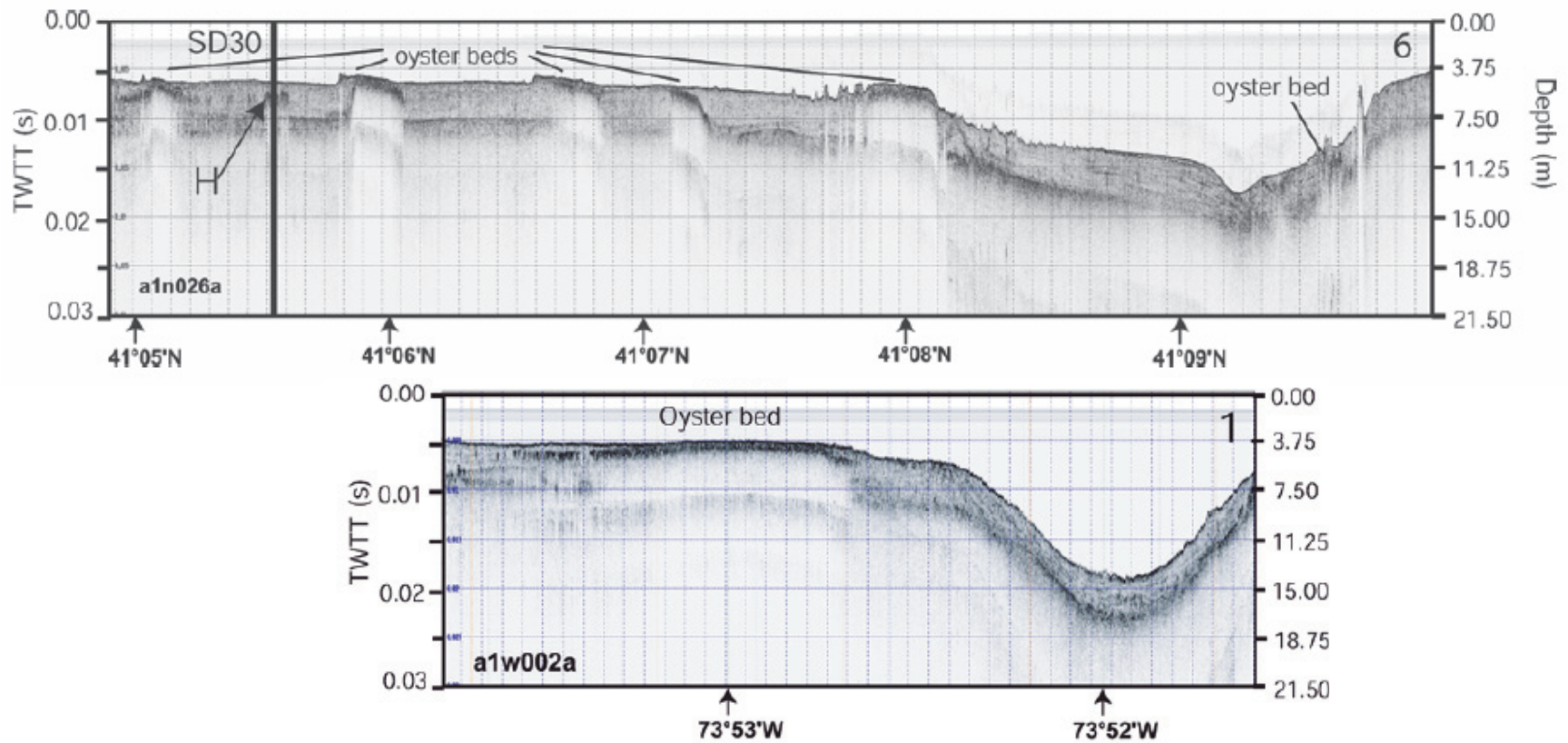
Fig. 6.5: Distribution of reefs near Suwannee River (Wright et al., 2005), two figures (1 & 2) superimposed with oyster reefs highlighted in yellow. (Satellite and bathymetery contour map with Wright et al. survey and core information overlayed.) Notice there are many large reefs similar to the Peconic Estuary, as well as similar formations such as chains of mounds Here mounds cover a wider open area, but are not as dense in coverage nor as thick.
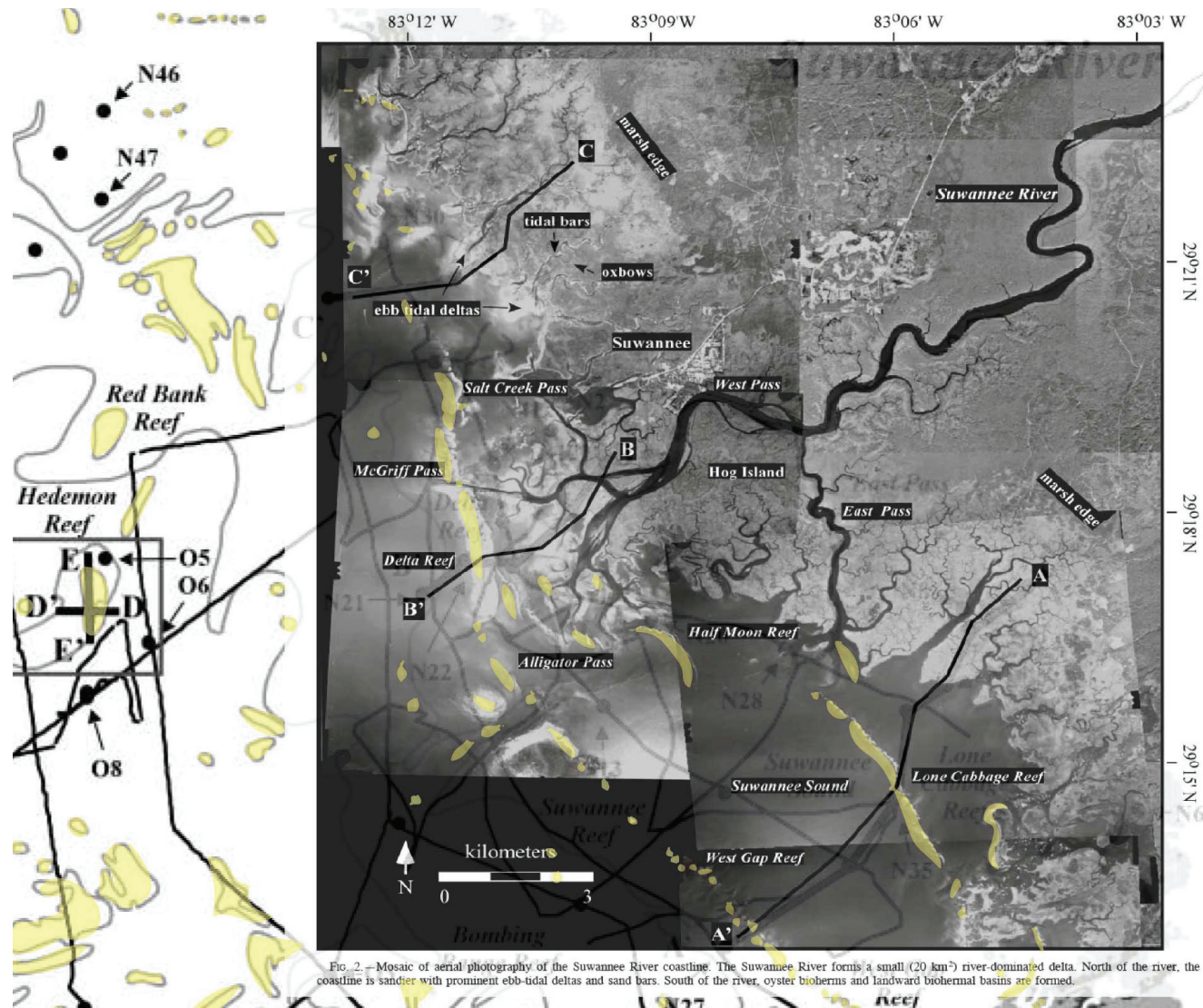
FIG. 2.—Mosaic of aerial photography of the Suwannee River coastline. The Suwannee River forms a small (20 km²) river-dominated delta. North of the river, the coastline is sandier with prominent ebb-tidal deltas and sand bars. South of the river, oyster bioherms and landward biohermal basins are formed.

207

Fig. 6.6: Vertical profile of oyster reefs off of the Suwannee River, FL by Wright et al. (2005). Oyster reefs are highlighted in yellow. Note many reefs are more than 3 m thick, while others are thin, less than 1 m, and cover a large area. These reefs are active in the intertidal zone. Note that submerged reefs are relict reefs.
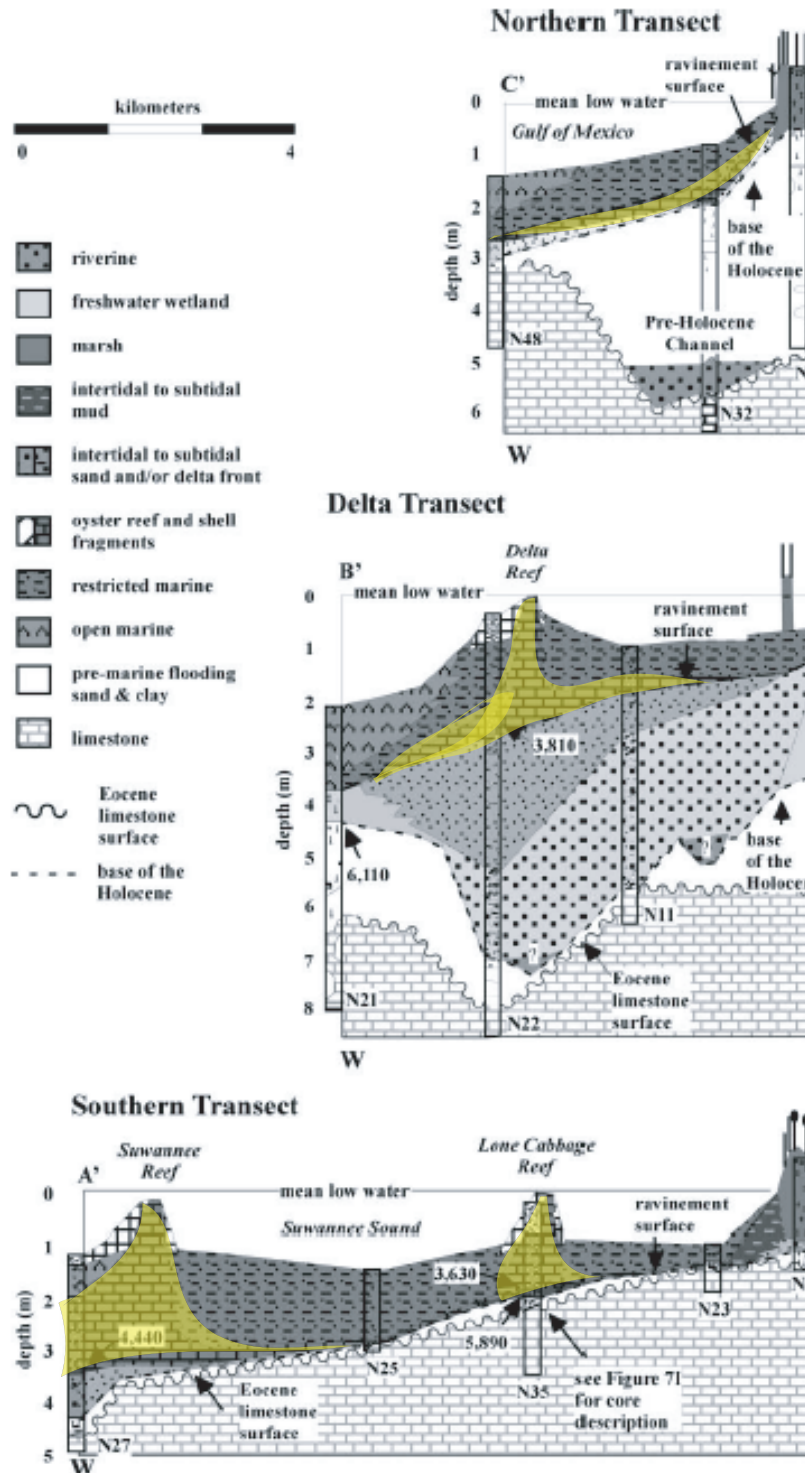
Fig. 6.7: Aerial image of Mission Bay, TX revealing circular oyster reef structures similar to the Peconics. Note: Individual round mounds isolated from others (A), linear chains of mounds (B), a field of round mounds (C), irregular but rounded mounds (D) (Texas 0.5 m Orthophotos via Texas Strategic Mapping Program, Texas Natural Resources Information System 2009/08/10. Photo taken 1/12/2009). Mission Bay is off of Copano Bay and Aransas Bay and adjacent to San Antonio Bay, TX.
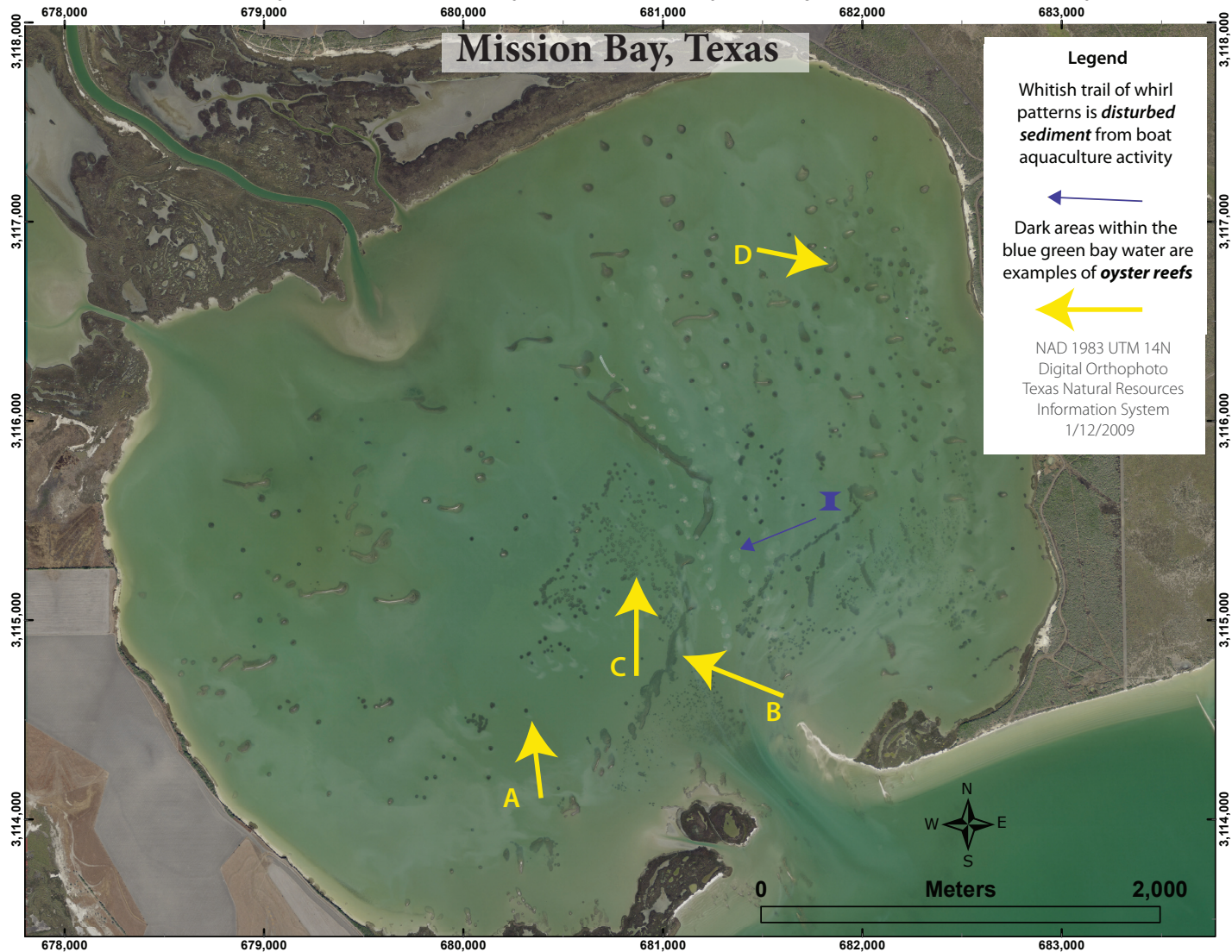
Figure 6.8: Volume change with sea-level rise and offset from sedimentation. Top: Sea level rise slowed as sea level has risen in the Holocene (Gutierrez et al., 2003) (top). Possible sedimentation rates for the Peconic Estuary for comparison, Peconic Estuary bay centers 0.8 mm/yr (Cochran et al., 2000), regional rates of 1mm/yr (Carbotte et al., 2004; Pekar et al., 2004; Rosen et al., 2003; Cochran et al., 2003), a hypothetical higher rate of 2 & 2.5 mm/yr based on higher regional rates (Carbotte et al., 2004; Pekar et al., 2004; Rosen et al., 2003), Peconic beach erosion (Eisel, 1977; Cochran et al., 2000), marshes (Redfield, 1967), and possible reef growth rates. Bottom: Change in volume and area with sea level rise.

Sea Level Rise Rate (Gutierrez et al., 2003) and Sedimentation Rates
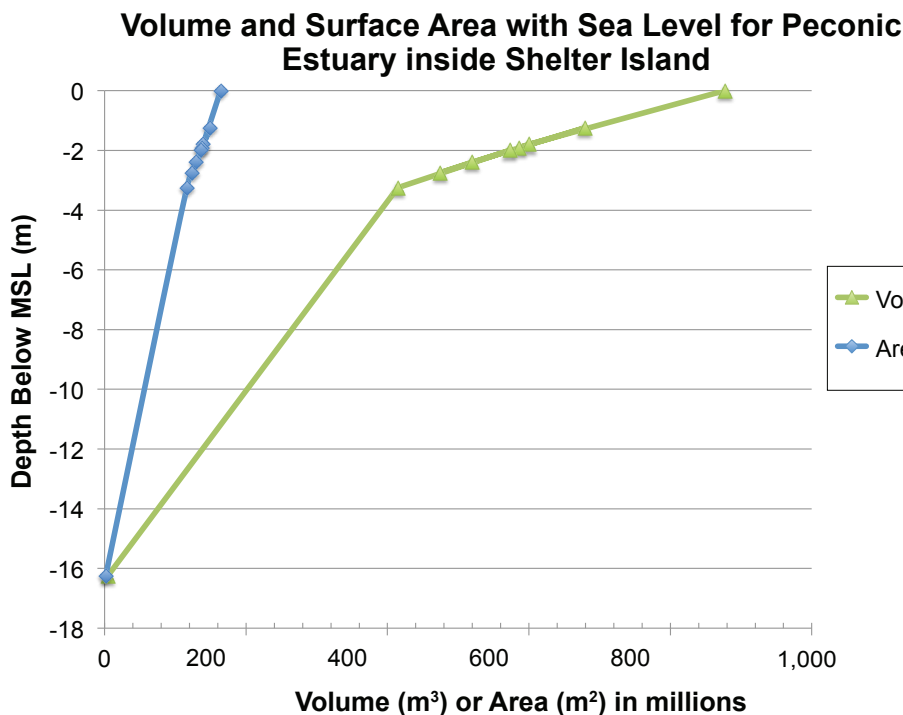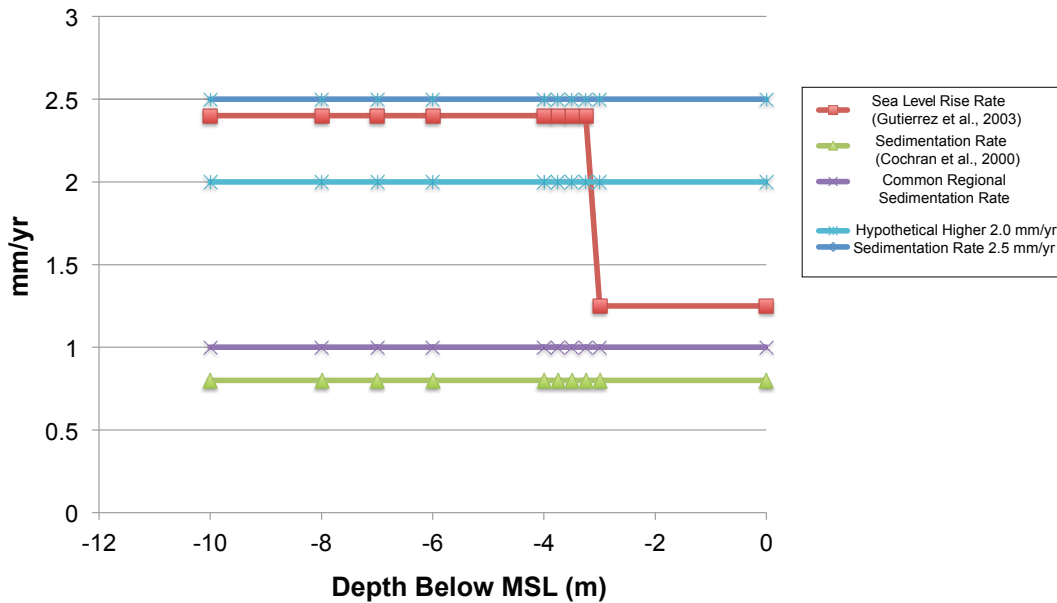
Volume and Surface Area with Sea Level for Peconic Estuary inside Shelter Island

REFERENCES:

Adams, E. W., Grotzinger, J. P., Watters, W. A., Schroder, S., McCormick, D. S., Al-Siyabi, H. A., 2005, Digital characterization of thrombolite-stromatolite reef distribution in a carbonate ramp system (terminal Proterozoic, Nama Group, Namibia), AAPG Bulletin, v. 89, p. 1293-1318.

Allen, Y. C., Wilson, C. A., Roberts, H. H., Supan, J., 2005, High Resolution Mapping and Classification of Oyster Habitats in Nearshore Louisiana Using Sidescan Sonar, Estuaries, v. 28, n. 3, p. 435-446.

Anderson, J. B., Rodriguez, A. B., Millikin, K. T., Taviani, M., 2008, The Holocene evolution of the Galveston estuary complex, Texas: Evidence for rapid change in estuarine environments, Response of upper Gulf Coast estuaries to Holocene climate change and sea-level rise, The Geological Society of America Special Paper 443, p. 89-104.

Bouma, A. H., 1976, Subbottom characteristics of San Antonio Bay, Bouma, A. H., ed. Shell Dredging and Its Influence in Gulf Coast Environments, Houston, TX: Gulf Publishing Co., p. 132-148.

Bratton, J. F., S. M. Colman, E. R. Thieler, R. R. Seal, 2003, Birth of the modern Chesapeake Bay estuary between 7.4 and 8.2 ka and implications for global sea-level rise, Geo-Marine Letters, v. 22, p. 188-197.

Carbotte, S. M., Bell, R. E., Ryan, W. B. F., McHugh, C., Slagle, A., Nitsche, F., Rubenston, J., 2004, Environmental change and oyster colonization within the Hudson River estuary linked to Holocene climate, Geo-Marine Letters, v. 24, p. 212–224.

Clapp, C. S., Flood, R. D., 2004, The Use of Side-scan Sonar for the Identification and Morphology of Sub-tidal Oyster Reefs in Great South Bay, Long Island Geologists, April 2004 Meeting Abstract.

Clark, J. S., Patterson, W. A. III, 1985, The Development of a Tidal Marsh: Upland and Oceanic Influences, Ecological Monographs, v. 55, n. 2, p. 289-217.

Cochran, J. K., Hirschberg, D. J., Amiel, D., 2000, Particle mixing and sediment accumulation rates of Peconic Estuary sediments: A sediment accretion study in support of the Peconic Estuary Program, Final Report of Project #0014400498181563, Marine Sciences Research Center, State University of New York, Stony Brook, NY, 11794-5000.

Cook, H. E., Zhemchuzhnikov, V. G., Zempolich, W. G., Zhaimina, V. Y., Buvtyshkin, B. M., Kotova, E. A, Golub, L. Y., Zorin, A. , Lehmann, P, Alexeiev, D. V., Giovannelli, A., Viggi, M., Fretwell, N., LaPointe, P., Carboy, J., 2002, Devonian and Carboniferous Carbonate platform facies in the Bolshoi Karatan, Southern Kazakhstan; outcrop

analogs for coeval carbonate oil and gas fields in the North Caspian Basin, Western Kazakhstan, in Cook, H. E., W. G. Zempolich, SEPM (Society for Sedimentary Geology), ed., Special Publication-Society for Sedimentary Geology, Paleozoic carbonates of the Commonwealth of Independent States (CIS): subsurface reservoirs and outcrop analogs, v.74: Tulsa, Oklahoma, SEPM, p. 81-122.

DeAlteris, J. T., 1988, The Geomorphic Development of Wreck Shoal, a Subtidal Oyster Reef of the James River, Virginia, Estuaries, v. 11, p. 240-249.

Eisel, M. T., 1977, Shoreline survey; Great Peconic, Little Peconic, Gardiners, and Napeague bays, Special Report - Marine Sciences Research Center, State University of New York, n. 5, p. 37.

Galtsoff, P. S., 1964, The American Oyster, Crassostrea Virgina Gemlin, Fish and Wildlife Service, Fishery Bulletin, v. 64, p. 457.

Henriet, J. P., Guidard, S., and the ODP "Proposal Team", 2002, Carbonate Mounds are Possible Example for Microbial Activity in Geological Processes, in G. Wefer, ed., Ocean margin systems, v. [1 v.], New York, Springer, p. 439-455.

Huvaz, O., Sarikaya, H., Isik, T., 2007, Petroleum systems and hydrocarbon potential analysis of the northwestern Uralsk basin, NW Kazakhstan, by utilizing 3D basin modeling methods, Marine and Petroleum Geology, v. 24, p. 247-275.

Ingersoll, E., 1881, The Oyster-Industry, The History and Present Condition of the Fishery Industry, Report on the oyster-industry of the United States, U.S. Department of the Interior, Washington D.C., Government Printing Office, Prepared under the Direction of Prof. S.F. Baird, U. S. Commissioner of the Fish and Fisheries and by G. Brown Good, Assistant Direction U.S. National Museum and a staff of associates.

Kolker, A. S, Hameed, S., 2007, Meteorologically driven trends in sea level rise, Geophysical Research Letters, v. 34, n. 23, p. L23616.

Ladd, H. S., Hedgepeth, J. W., Post, R., 1957, Environments and facies of existing bays on the central Texas coast, Chapter 22 of Ladd, H.S., ed., Paleoecology: Memoir - Geological Society of America, n. 0072-1069, 0072-1069, p. 599-639.

Larsen, C. E., Clark, I., 2006, A search for scale in sea-level studies, Journal of Coastal Research, v. 22, n. 4, p. 788–800.

Leach, P. A., Belknap, D. F., 2006, Geoarchaeological survey for submerged anthropogenic deposits in Damariscotta River, Maine, USA, Geological Society of America, Northeastern Section, 41st annual, Meeting, Abstracts with Programs - Geological Society of America, Mar 2006, v. 38, n. 2, p.6.

Lenihan, H. S., Peterson, C. H., 1998, How Habitat Degradation through Fishery Disturbance Enhances Impacts of Hypoxia on Oyster Reefs, Ecological Applications, v. 8, n. 1, p. 128-140.

Miller, L., Douglas, B. C., 2007, Gyre-scale atmospheric pressure variations and their relation to 19th and 20th century sea level rise, Geophysical Research Letters, v. 34, p. L16602.

Milliman, J. D., 1974, Marine Carbonates, Recent Sedimentary Carbonates: Part 1, Springer Verlag; New York.

Nydick, K. R., Bidwell, A. B., Thomas, E., Varekamp, J. C., 1995, A Sea-Level Rise Curve from Guilford, Connecticut, USA, Marine Geology, v. 124, n. 1-4, p. 137-159.

Osterman, L. E., Twichell, D. C., Poore, R. Z., 2009, Holocene evolution of Apalachicola Bay, Florida: Geo-Marine Letters, v. 29, n. 6, p. 395-404.

Parker, R. H., 1960, Ecology and distributional patterns of marine macro-invertebrates, northern Gulf of Mexico, *in* Shepard, F. P., ed., United States (USA).

Pekar, S. F., McHugh, C. M. G., Christie-Blick, N., Jones, M., Carbotte, S. M., Bell, R. E., Lynch-Stieglitz, J., 2004, Estuarine processes and their stratigraphic record: paleosalinity and sedimentation changes in the Hudson Estuary (North America), Marine Geology, v. 209, n. 1-4, p. 113-129.

Pufahl, P. K., James, N. P., Bone, Y., Lukasik, J. J., 2004, Pliocene sedimentation in a shallow, cool-water, estuarine gulf, Murray Basin, South Australia, Sedimentology, v. 51, p. 997-1027.

Redfield, A. C., 1967, Postglacial change in sea level in western North Atlantic Ocean, Science, v. 157, p. 687-692.

Rodriguez, A. B., Anderson, J. B., Siringan, F. P., Taviani, M., 2004, Holocene Evolution of the East Texas Coast and Inner Continental Shelf: Along-Strike Variability in Coastal Retreat Rates, Journal of Sedimentary Research, v. 74, n. 3, p. 405–421.

Rock, B. N., Carter, L., Walker, H., Bradbury, J., Dingman, S. L., Federer, C. A., 2001, Chapter 6: Water Resources and Potential Climate Change Impacts, The New England Regional Assessment of The Potential Consequences of Climate Variability and Change, A Final Report, p. 63-83.

Rosen, P. S., Brennikmeyer, B. M., Maybury, L. M., 1993, Holocene Evolution of Boston Inner Harbor, Massachusetts, Journal of Coastal Research, v. 9, n. 2, p. 363-377.

Ryan, H. F., Noble, M. A., 2002, Sea level response to ENSO along the central California coast: how the 1997–1998 event compares with the historic record, Progress in Oceanography, v. 54, i. 1-4, p. 149-169.

Ryan, H. F., Noble, M., A., 2006, Alongshore Wind Forcing of Coastal Sea Level as a Function of Frequency, Journal of Physical Oceanography, v. 36, p. 2173-2184.

Sirkin, L., 1994, Block Island Geology: History, Processes and Field Excursions, Coastal Geology Series by Les Sirkin, Book and Tackle Shop, Watch Hill, RI, USA.

Sirkin, L., 1995, Eastern Long Island Geology: History, Processes and Field Trips, Coastal Geology Series by Les Sirkin, Book and Tackle Shop, Watch Hill, RI, USA.

Slagle, A. L., Ryan, W. B. F., Carbotte, S. M., Bell, R., Nitsche, F. O., Kenna, T., 2006, Late-stage estuary infilling controlled by limited accommodation space in the Hudson River, Marine Geology, v. 232, p. 181-202.

Thomas, E., Varekamp, J. C., 2002, Sea Level Rise in Long Island Sound Over the Last Millennium, American Geophysical Union, Fall Meeting 2002, abstract #OS71D-0323.

Twichell, D. C., Andrews, B. D., Edminston, H. L., Stevenson, W. R., 2007, Geophysical Mapping of Oyster Habitats in a Shallow Estuary; Apalachicola Bay, Florida: U. S. Geological Survey Open File Report 2006-138.

Varekamp, J. C., Thomas, E., Vandeplassche, O., 1992, Relative Sea-Level Rise and Climate Change over the Last 1500 Years, Terra Nova, v. 4, n. 3, p. 293-304.

Varekamp, J. C., Thomas, E., Thompson, W. G., 1999, Sea level-climate correlation during the past 1400 yr: Comment, Geology, v. 27, n. 2, p. 189-190.

Veatch, O., Stephenson, L. W., 1911, Geology of the Georgia Coastal Plain, Bulletin No. 26, Geological Survey of Georgia, Foote & Davies Co., p.240-252, 466 p.

Weaver, E., Herbort, M., Dellapenna, T., Simons, J., 2008, Geological Controls on the Distribution of Oyster Reefs and Substrates in Copano Bay, Texas, 2008 Joint Meeting of The Geological Society of America, Soil Science Society of America, American Society of Agronomy, Crop Science Society of America, Gulf Coast Association of Geological Societies with the Gulf Coast Section of SEPM, Geological Society of America Abstracts with Programs, v. 40, Geological Society of America, p. 15.

Wiedemann, H. U., 1972, Shell Deposits and Shell Preservation in Quaternary and Tertiary Estuarine Deposits in Georgia, U. S. A., Sedimentary Geology, v. 7, p. 103-125.

Woods, H., Hargis, W. J., Hershner, C. H., Mason, P., 2005, Disappearance of the natural emergent 3-dimensional oyster reef system of the James River, Virginia, 1871-1948, Journal of Shellfish Research, v. 24, i. 1, p 139-142.

Wright, E. E., Hine, A. C., Goodbred, S. L., Locker, S. D., 2005, The effect of sea-level and climate change on the development of a mixed siliciclastic-carbonate, deltaic coastline: Suwannee River, Florida, USA, Journal of Sedimentary Research, v. 75, p. 621-635.

COMBINED REFERENCES:

Adams, E. W., Grotzinger, J. P., Watters, W. A., Schroder, S., McCormick, D. S., Al-Siyabi, H. A., 2005, Digital characterization of thrombolite-stromatolite reef distribution in a carbonate ramp system (terminal Proterozoic, Nama Group, Namibia), AAPG Bulletin, v. 89, p. 1293-1318.

Allen, Y. C., Wilson, C. A., Roberts, H. H., Supan, J., 2005, High Resolution Mapping and Classification of Oyster Habitats in Nearshore Louisiana Using Sidescan Sonar, Estuaries, v. 28, n. 3, p. 435-446.

Alley, R. B., Meese, D. A., Shuman, C. A., Gow, A. J., Taylor, K. C., Grootes, P. M., White, J. W. C., Ram, M., Waddington, E. D., Mayewski, P. A., and Zielinski, G. A., 1993, Abrupt Increase in Greenland Snow Accumulation at the End of the Younger Dryas Event: Nature, v. 362, no. 6420, p. 527-529.

Alley, R. B., Mayewski, P. A., Sowers, T., Stuiver, M., Taylor, K. C., Clark, P. U., 1997, Holocene climatic instability: A prominent, widespread event 8200 yr ago, Geology, v. 25, n. 6, p. 483-486.

Alley, R. B., Ágústsdóttir, A. M., 2005, The 8k event: cause and consequences of a major Holocene abrupt climate change, Quaternary Science Reviews, v. 24, p. 1123–1149.

Altermann, W., 2008, Accretion, Trapping and Binding of Sediment in Archean Stromatolites—Morphological Expression of the Antiquity of Life, Space Science Reviews, v. 135, p. 55–79.

Amante, C., Eakins, B. W., 2009, ETOPO1 1 Arc-Minute Global Relief Model: Procedures, Data Sources and Analysis. NOAA Technical Memorandum NESDIS NGDC-24, March 2009, 19 p.

Anderson, J. B., Rodriguez, A. B., Millikin, K. T., Taviani, M., 2008, The Holocene evolution of the Galveston estuary complex, Texas: Evidence for rapid change in estuarine environments, Response of upper Gulf Coast estuaries to Holocene climate change and sea-level rise, The Geological Society of America Special Paper 443, p. 89-104.

Arlotta, Michelle, 2003, Benthic mapping as a tool for developing multidisciplinary maps of the Robin's Island area of the Peconic Estuary System of Long Island, New York [M.S. Thesis], Stony Brook University, Stony Brook, NY, 104 p.

Bonar, D. B., Coon, S. L., Walch, M., Weiner, R. M., Fitt, W., 1990, Control of Oyster Settlement and Metamorphosis by Endogenous and Exogenous Chemical Clues,

Bulletin of Marine Science, v. 46, n. 2, p. 484-498.

Armentano, T. V., Woodwell, G. M., 1975, Sedimentation Rates in a Long Island Marsh Determined by 210 Pb Dating, Limnology and Oceanography, v. 20, n. 3, p. 452-456.

Arnold, W. S., Jones, D. S., Quitmyer, I. R., Schöne, B. R., Surge, D. M., 2007, The 1st International Sclerochronology Conference held at St. Petersburg, FL, USA, July 2007, http://www.scleroconferences.de.

Attendorn, H. G., Bowen, R., 1997, Radioactive and stable isotope geology, London, Chapman & Hall, p. 522.

Bard, E., Hamelin, B., Delanghe-Sabatier, D., Deglacial Meltwater Pulse 1B and Younger Dryas Sea Levels Revisited with Boreholes at Tahiti, Science, v. 327, i. 5970, p. 1235-1237.

Basu, A. R., Jacobsen, S. B., Poreda, R. J., Dowling, C. B., Aggarwal, P. K., 2001, Large groundwater strontium flux to the oceans from the Bengal Basin and the marine strontium isotope record, Science, v. 293, p. 1470-1473.

Bates, R. L., Jackson, J. A., eds.,1984, (AGI) Dictionary of Geological Terms, Anchor Books.

Beaudoin, J., 2002, Hitchiker's Guide to Swathed …, Ocean Mappin Group, University of New Brunswick, last accessed 2010, www.omg.unb.ca/~jonnyb/processing/definitive-swathed/index.html.

Beck, A. J., Rapaglia, J. P., Cochran, J. K., Bokuniewicz, H. J., Yang, S., 2008, Submarine groundwater discharge to Great South Bay, NY, estimated using Ra isotopes, Marine Chemistry, v. 109, i. 3-4, p. 279-291.

Belknap, D. F., Kraft, J.C., 1981, Preservation Potential of Transgressive Coastal Lithosomes on the U.S. Atlantic Shelf, Marine Geology, v. 42, n. 1-4, p. 429-442.

Bokuniewicz, H. J., Zeitlin, M.J., 1980, Characteristics of groundwater seepage into Great South Bay, MSRC, Special Report, v. 35, SUNY, Stony Brook, NY, 30 p.

Bonar, D. B., Coon, S. L., Walch, M., Weiner, R. M., Fitt, W., 1990, Control of Oyster Settlement and Metamorphosis by Endogenous and Exogenous Chemical Clues, Bulletin of Marine Science, v. 46, n. 2, p. 484-498.

Bond, G., Showers, W., Cheseby, M., Lotti, R., Almasi, P., deMenocal, P., Priore, P., Cullen, H., Hajdas, I., Bonani, G., 1997, A Pervasive Millennial-Scale Cycle in North Atlantic Holocene and Glacial Climates, Science, v. 278, n. 14, p. 1257-1266.

Bouma, A. H., 1976, Subbottom characteristics of San Antonio Bay, Bouma, A. H., ed. Shell Dredging and Its Influence in Gulf Coast Environments, Houston, TX: Gulf Publishing Co., p. 132-148.

Brass, G. W., Turekian, K. K., 1974, Strontium distributions in GEOSECS oceanic profiles, Earth Planetary Science Letters, v. 23, p. 141-148.

Bratton, J. F., S. M. Colman, E. R. Thieler, R. R. Seal, 2003, Birth of the modern Chesapeake Bay estuary between 7.4 and 8.2 ka and implications for global sea-level rise, Geo-Marine Letters, v. 22, p. 188-197.

Brennan, D. J., 1973, Sediment and water characteristics, Peconic Bays, Long Island, New York, Northeastern Section, 8th Annual Meeting, Abstracts with Programs - Geological Society of America, v. 5, n. 2, p. 141-142.

Breuer, E., Sañudo-Wilhelmy, S. A., Aller, R. C., 1999, Trace metals and dissolved organic carbon in an estuary with restricted river flow and a brown tide, Estuaries, v. 22, p. 603-615.

Broecker, W., 1963, A Preliminary Evaluation of Uranium Series Inequilibrium as a Tool for Absolute Age Measurement on Marine Carbonates, Lamont Geological Observatory Contribution 617, Journal of Geophysical Research, v. 68, n. 9, p. 2817-2834.

Bryant, J. D., Jones, D.. S., Meuller, P., A., 1995, Influence of Freshwater Flux on $87Sr/86Sr$ Chronostratigraphy in Marginal Marine Environments and Dating of Vertebrate and Invertebrate Faunas, Journal of Paleontology, v. 69, n. 1, p. 1-6.

Buddemeier, R. W., Maragos, J. E., Knutson, D. W., 1974, Radiographic studies of reef coral exoskeletons: rates and patterns of coral growth, Journal of Experimental and Marine Biology Ecology, v. 14, p. 179-200.

Burnett, W. C., Bokuniewicz, H., Huettel, M., Moore, W. S., Taniguchi, M., 2003, Groundwater and pore water inputs to the coastal zone, Biogeochemistry, v. 66, n. 1-2, p. 3-33.

Bushek, D. Richardson, D., Bobo, M. Y., Coen, L. D., 2004, Quarantine of oyster shell cultch reduces the abundance of Perkinsus marinus, Journal of Shellfish Research, v. 23, n. 2, p. 369-373.

Butzin, M., Prange, M., Lohmann, G., 2005, Radiocarbon simulations for the glacial ocean: the effects of wind stress, Southern Ocean sea ice and Heinrich events. *Earth & Planetary Science Letters*, v. 235, p. 45-61.

Butzin, M., Prange, M., Lohmann, G., Fairbanks, R. G., Naik, N., 2005, Marine Radio Carbon Reservoir Age, http://radiocarbon.LDEO.columbia.edu/, accessed February 2011.

Cao, L., R.G. Fairbanks, M. Butzin and N. Naik, 2007, The marine radiocarbon reservoir age, Radiocarbon, in prep.

Carbotte, S. M., Bell, R. E., Ryan, W. B. F., McHugh, C., Slagle, A., Nitsche, F., Rubenston, J., 2004, Environmental change and oyster colonization within the Hudson River estuary linked to Holocene climate, Geo-Marine Letters, v. 24, p. 212–224.

Carriker, M. R., R. E. Palmer, 1979, A new mineralized layer in the hinge of the oyster, Science, v. 206, p. 691-693.

Cattaneo, A., Steel, R. J., 2003, Trangressive deposits: a review of their variability, Earth Science Reviews, v. 62, n. 3-4, p. 187-228.

Cerrato, R. M., Maher, N. P., 2007, Benthic mapping for habitat classification in the Peconic Estuary: phase I groundtruth studies, Special report Stony Brook University Marine Sciences Research Center, n. 134, 276 p.

Charette, M. A., Splivallo, R., Herbold, C., Bollinger, M. S., Moore, W. S., 2003, Salt marsh submarine groundwater discharge as traced by radium isotopes, Marine Chemistry, v. 84, p. 113-121.

Charrette, M. A. & Sholkovitz, E. R., 2006, Trace Element Cycling in a subterranean Estuary; Part 2, Geochemistry of the pore water, Geochimica et Cosmochimica Acta, v. 70, n. 4, p. 811-826.

Chen, Z. and K. Osadetz, 2006. Undiscovered petroleum accumulation mapping using model based stochastic simulation. Mathematical Geology, v. 38, p. 1-16.

Clapp, C. S., Flood, R. D., 2004, The Use of Side-scan Sonar for the Identification and Morphology of Sub-tidal Oyster Reefs in Great South Bay, Long Island Geologists, April 2004 Meeting Abstract.

Clark, J. S., Patterson, W. A. III, 1985, The Development of a Tidal Marsh: Upland and Oceanic Influences, Ecological Monographs, v. 55, n. 2, p. 289-217.

Cochran, J. K., Hirschberg, D. J., Amiel, D., 2000, Particle mixing and sediment accumulation rates of Peconic Estuary sediments: A sediment accretion study in support of the Peconic Estuary Program, Final Report of Project #0014400498181563, Marine Sciences Research Center, State University of New York, Stony Brook, NY, 11794-5000.

Cochran, J. K., Landman, N. H., Turekian, K. K., Michard, A., Schrag, D. P., 2003, Paleoceanography of the Late Cretaceous (Maastrichtian) Western Interior Seaway of North America: Evidence from Sr and O isotopes, Paleoceanography, Paleoclimatology, Paleoecology, v. 191, n. 1, p. 45-64.

Cochran, J. K., Masqué, P., 2003, Short-lived U/Th Series Radionuclides in the Ocean: Tracers for Scavenging Rates, Export Fluxes and Particle Dynamics, Reviews in Mineralogy & Geochemistry Vol 52: Urananium-Series Geochemistry, ed. Bourdon B, Henderson, G. M., Lundstrom, C. C., Turner, S. P., p. 461-492.

Collier, K., Bokuniewicz, H., Coffey, R., 2005, Submarine Groundwater Discharge along Fire Island, NY, Long Island Geologists Conference 2005, Stony Brook, NY.

Cook, H. E., Zhemchuzhnikov, V. G., Zempolich, W. G., Zhaimina, V. Y., Buvtyshkin, B. M., Kotova, E. A, Golub, L. Y., Zorin, A. , Lehmann, P, Alexeiev, D. V., Giovannelli, A., Viggi, M., Fretwell, N., LaPointe, P., Carboy, J., 2002, Devonian and Carboniferous Carbonate platform facies in the Bolshoi Karatan, Southern Kazakhstan; outcrop analogs for coeval carbonate oil and gas fields in the North Caspian Basin, Western Kazakhstan, in Cook, H. E., W. G. Zempolich, SEPM (Society for Sedimentary Geology), ed., Special Publication-Society for Sedimentary Geology, Paleozoic carbonates of the Commonwealth of Independent States (CIS): subsurface reservoirs and outcrop analogs, v.74: Tulsa, Oklahoma, SEPM, p. 81-122.

County of Suffolk, N.Y., 2001, Coastal Underwater Land Ownership, accessed December 2011, http://www.co.suffolk.ny.us/departments/planning/pdfs/Map1_Aqua.pdf.

County of Suffolk, N. Y., 2002, Peconic/ Gardiners Bays Underwater Land Parcel Tax Status, Towns of Riverhead, Shelter Island, Southold, Southampton, & East Hampton, Suffolk County, New York, Map by Suffolk County Department of Planning, Thomas A. Isles Director.

County of Suffolk, N. Y., 2002, Peconic/ Gardiners Bays Underwater Land – Private Oyster Grants, Towns of Riverhead, Shelter Island, Southold, Southampton, & East Hampton, Suffolk County, New York, Map by Suffolk County Department of Planning, Thomas A. Isles Director.

County of Suffolk, N.Y., 2002, Real Property Taxmap parcel linework used with permission of Suffolk County Real Property Tax Service Agency (R.P.T.S.A.).

County of Suffolk, N.Y., 2003, Peconic/ Gardener's Bays Underwater Land Private Oyster Grants (Map), http://www.co.suffolk.ny.us/departments/planning/pdfs/Map1_OysterGrantParcels_11x17.pdf

County of Suffolk, N. Y., 2003, National Ocean Survey Nautical Chart 12358 with Private Oyster Grant Parcel Overlay, Towns of Riverhead, Shelter Island, Southold, Southampton, & East Hampton, Suffolk County, New York, Map by Suffolk County Department of Planning, Thomas A. Isles Director.

County of Suffolk, N. Y., 2003, National Ocean Survey Nautical Chart 13209 with Private Oyster Grant Parcel Overlay, Towns of Riverhead, Shelter Island, Southold, Southampton, & East Hampton, Suffolk County, New York, Map by Suffolk County Department of Planning, Thomas A. Isles Director.

Craig, H., 1965, The measurement of oxygen isotope paleotemperatures, *in* Tongiorgi, E., ed.: Proceedings of the Spoleto Conference on Stable Isotopes in Oceanographic Studies and Paleotemperatures, Consiglio Nazionale delle Ricerche, Pisa, v. 3, p. 161–182.

Cronin, T. M., R. Thunell, G. S. Dwyer, C. Saenger, M. E. Mann, C. Vann, R. R. Seal II, 2005, Multiproxy evidence of Holocene climate variability from estuarine sediments, eastern North America, Paleoceanography, 20, PA4006.

Cronin, T. M., Dwyer, G. S., Kamiya, T., Schwede, S., Willard, D. A., 2003, Medieval Warm Period, Little Ice Age and 20th century temperature variability from Chesapeake Bay, Global and Planetary Change, v. 36, n. 1-2, p. 7-29.

Darwin, C. R., 1842, The structure and distribution of coral reefs, Smith, Elder and Co., London, 214 p.

Davies, D. S., Isles, T. A., Daly, J., Fischer, L., Frisenda, T., Leogrande, V., Lind, C., Verbarg, R., Waide, D., Walsh, C., Kennedy, K., Sonnichsen, D., Burns, Hon. B. B., Cohen, E., Walter, P. E., Dawydiak, P. E., Fahey, C., Guldi, Hon. G., Kotula, Vice Chairman J., LaValle, Secretary Wells, P. , Lessard, Lt. D., McAllister, K., McMahon, J., Potter, Hon. J., Proios, G., Sawicki, J., Jr., Semlear, Hon. J., Siller, Hon. G., 2002, Policy Guidance for Suffolk County on Shellfish Cultivation in Peconic And Gardiners Bays, Report of the Suffolk County Aquaculture Committee, June 2002, Suffolk County Department of Planning, Hauppauge, New York June 2002, 90 p. http://www.co.suffolk.ny.us/planning.

Davies, D. S., Isles, T. A., Fischer, L., Verbarg, R., Di Cola, L. M., Lind, C., Daly, J., Frisenda, T., Leogrande, V., Walsh, C. E., 2003, Survey Plan for Shellfishing Cultivation Leasing for Gardiner's and Peconic Bays, April, 2003, Suffolk County Department of Planning, Suffolk County Department of Health Services, Suffolk County Department of Public Works, Suffolk County, NY.

Davis, W.M., 1928, The coral reef problem, Special publication No. 9, Shaler Memorial Series, American Geographical Society, New York, 596 p.

DeAlteris, J. T., 1988, The Geomorphic Development of Wreck Shoal, a Subtidal Oyster Reef of the James River, Virginia, Estuaries, v. 11, p. 240-249.

Desor, E., Cabot, E. C., 1849, On the Tertiary and more recent deposits in the Island of Nantucket [Massachusetts], Quarterly Journal of the Geological Society of America, Geological Society of London, London, UK, p. 340 -344.

Dettman, D. L., Flessa, K. W., Roopnarine, P. D., Schöne, B. R., Goodwin, D. H., 2004, The use of oxygen isotope variation in shells of estuarine mollusks as a quantitative record of seasonal and annual Colorado River discharge, Geochimica et Cosmochimica Acta, v. 68, n. 6, p. 1253-1263.

DiLorenzo, J. L., 1986, The Overtide and Filtering Response of Inlet/Bay Systems [Ph.D. Dissertation], MSRC, Stony Brook University.

Donnelly, J. P., Cleary, P., Newby, P., Ettinger, R., 2004, Coupling instrumental and geological records of sea-level change: Evidence from southern New England of an increase in the rate of sea-level rise in the late 19th century, Geophysical Research Letters, v. 31, p. L05203.

Dowling, C. B., Poreda, R. J., Basu, A. R., 2003, The groundwater geochemistry of the Bengal Basin: Weathering, chemsorption, and the trace metal fluxes to the oceans, Geochimica et Cosmochimica Acta, v. 67, n. 12, p. 217-2136.

Drinkwater, K. F. Belgrano, A., Borja, A., Conversi, A., Edwards, M., Greene, C. H., Ottersen, G., Pershing, A. J., Walker, H., 2003, 'The Response of Marine Ecosystems to Climate Variability Associated With the North Atlantic Oscillation', The North Atlantic Oscillation: Climatic Significance and Environmental Impact: Geophysical Monograph 134, American Geophysical Union, Washington, DC, p. 211-34.

Duck, R. W., Herbert, R. A., 2006, High-resolution shallow seismic identification of gas escape features in the sediments of Loch Tay, Scotland: tectonic and microbiological associations, Sedimentology, v. 53, p. 481–493.

Dulaiova, H., Burnett, W. C., Chanton, J. P., Moore, W. S., Bokuniewicz, H. J., Charette, M. A., Sholkovitz, E., 2006, Assessment of groundwater discharges into West Neck Bay, New York, via natural tracers, Continental Shelf Research, v. 26, i. 16, p. 1971-1983.

East Hampton, 2006, Contributors: Aldred, J., Dunne, J., Gaites, J., Gould, O., Quevedo, F., Lester, R., Rice, J., Appendix 7-9 Water Temperatures, 2006 Annual Report of Operations, http://www.ehamptonny.gov/HtmlPages/Aquaculture/AquaAnnualReports.htm

East Hampton, 2007, Contributors: Aldred, J., Dunne, J., Gaites, J., Gould, J., Quevedo, F., Lester, R., Lester, D., Rice, J., Appendix Appendix 7- 2007 Water Temperatures, 2007 Annual Report of Operations, http://www.ehamptonny.gov/HtmlPages/Aquaculture/AquaAnnualReports.htm

East Hampton, 2008, Contributors: Aldred, J., Dunne, J., Gaites, J., Gould, J., Quevedo, F., Lester, R., Lester, D., Rice, J., McKenny, N., Perrone, J., Appendix 4-2008 Water Temperatures, 2008 Annual Report of Operations, http://www.ehamptonny.gov/HtmlPages/Aquaculture/AquaAnnualReports.htm

East Hampton, 2009, Contributors: Aldred, J., Dunne, J., Gaites, J., Gould, J., Quevedo, F., Lester, R., Lester, D., Rice, J., McKenny, N., Ruggerio, D., Appendix 4- 2009 Water Temperatures (Charts 7-9), 2009 Annual Report of Operations, http://www.ehamptonny.gov/HtmlPages/Aquaculture/AquaAnnualReports.htm

Edgetech, 2009, Edgetech Sub-bottom profilers, accessed 2009, www.edgetech.com/edgetech.

Eichrom Technologies, Inc. | A GCI Company, 2010, Sr-spec Resin © 2010, accessed: Jan 16, 2010, http://www.eichrom.com/products/info/sr_resin.cfm.

Eisel, M. T., 1977, Shoreline survey; Great Peconic, Little Peconic, Gardiners, and Napeague bays, Special Report - Marine Sciences Research Center, State University of New York, n. 5, p. 37.

Ellison, C. R. W., Chapman, M. R., Hall, I. R., 2006, Surface and Deep Ocean Interactions During the Cold Climate Event 8200 Years Ago, Science, v. 312, p. 1929-1932.

Emery, K. O., E. Uchupi, 1972, Western North Atlantic Ocean: Topog- raphy, Rocks, Structure, Water, Life and Sediments, Tulsa, OK, American Association of Petroleum Geologists, 532 p.

Fairbanks, R. G., Mortlock, R. A., Chiu, T.-C., Cao, L., Kaplan, A., Guilderson, T.P., Fairbanks, T. W., Bloom, A.L., 2005, Marine Radiocarbon Calibration Curve Spanning 0 to 50,000 Years B.P. Based on Paired 230Th/234U/238U and 14C Dates on Pristine Corals, Quaternary Science Reviews, v. 24, p. 1781-1796.

Fairbanks, R. G., Mortlock, R.A., Chiu, T.-C., Cao, L., Kaplan, A., Guilderson, T. P., Fairbanks, T.W., Bloom, A. L., 2005, Radiocarbon age to calendar age conversion: 'Fairbanks0107' calibration curve, accessed February 2011, http://radiocarbon.ldeo.columbia.edu/research/radcarbcal.htm.

Feng, H., Kirk Cochran, J., Hirschberg, D. J., Wilson, R. E., 1998, Small-scale spatial variations of natural radionuclide and trace metal distributions in sediments from the Hudson River estuary: Estuaries, v. 21, p. 263-280.

Ferrini, V. L., 2004, Dynamics of nearshore sedimentary environments revealed through the analysis of multibeam sonar data [Ph.D. Dissertation], MSRC, Stony Brook University, Stony Brook, NY, 161 p.

Flood, R. D., Cerrato, R., Goodbred, S., Maher, N., Arlotta, M., Zaleski, L., 2003, Benthic Habitat Mapping in the Peconic Bays, Program for the Tenth Conference on Geology of Long Island and Metropolitan New York, April 12, 2003.

Flood, R. D., Kinney, J., Weaver, M., 2006, Underwater Landscape Evolution in the Peconic Bays (Long Island, NY) as revealed by High-Resolution Multibeam Mapping, Eos Trans. AGU, vol. 87, no. 52, Fall Meet. Suppl., Abstract H33B-1506, Dec 2006.

Flood, R. D., Cerrato, R. and Kinney, J., 2009, Benthic Mapping and Habitat Classification in the Peconic Estuary, Phase II, Final Report to the Long Island Chapter of the Nature Conservancy.

Flood, R. D., Kinney, J., 2009, New Insights on the Origin of the Peconic Bays from a New Detailed Bathymetric Map, Sixteenth Conference on the Geology of Long Island and Metropolitan New York, Long Island Geologists, March 2009 Meeting, Stony Brook, NY.

Fuller, M. L., 1914, The Geology of Long Island New York: United States Geological Survey Professional Paper 82.

Gallardo, A. H., Marui, A., 2006, Submarine groundwater discharge: an outlook of recent advances and current knowledge, Geo-Marine Letters, v. 26, p. 102-113.

Galtsoff, P. S., 1964, The American Oyster, Crassostrea Virgina Gemlin, Fish and Wildlife Service, Fishery Bulletin, v. 64, p. 457.

Garcia-Orellana, J., Cochran, J. K., Bokuniewicz, H., Yang, S., Beck, A. J., 2010, Time-series sampling of 223Ra and 224Ra at the inlet to Great South Bay (New York): a strategy for characterizing the dominant terms in the Ra budget of the bay, Journal of Environmental Radioactivity, v. 101, p. 582-588.

Gaswirth, S. B., Ashley, G. B., Sheridan, R. E., 2002, Use of Seismic Stratigraphy to Identify Conduits for Saltwater Intrusion in the Vicinity of Raritan Bay, New Jersey, Environmental & Engineering Geoscience, v. 8, no. 3, p. 209-218.

Gillikin, D. P., Ridder, F. D., Ulens, H., Elskens, M., Keppens, E., Baeyensa, W., Dehairs, F., 2005, Assessing the reproducibility and reliability of estuarine bivalve shells (Saxidomus giganteus) for sea surface temperature reconstruction: Implications for paleoclimate studies, Palaeogeography, Palaeoclimatology, Palaeoecology, v. 228, p. 70-85.

Gomez-Reyes, E., 1989, Tidally Driven Lagrangian Residual Velocity in Shallow Bays, [Ph.D. Dissertation], MSRC, State University of New York at Stony Brook, December 1989, p.129

Goldstein, S. ed., Isotope Geochemistry Lab Handbook, Version: August 4, 2003, Lamont-Doherty Earth Observatory of Columbia University, Reviewed by Sidney Hemming, First version coordinated by Conny Class, Contributions from: Merry Cai, Anna Cipriani, Conny Class, Katie Donnelly, Marty Fleisher, Allison Franzese, Sarah Fonville, Steve Goldstein, Sidney Hemming, Dana Himmel, Alex LaGatta, Alex Piotrowski, Randye Rutberg, Kyla Simons, Gad Soffer, accessed 2009, https://beta.ldeo.columbia.edu/files/LDEO_Isolab_Handbook.pdf.

Graham, D. J., Midgley, N. G., 2000, Graphical representation of particle shape using triangular diagrams: an Excel spreadsheet method. Earth Surface Processes and Landforms, v. 25, n. 13, p. 1473-1477.

Grave, C., 1903, Investigations for the promotion of the oyster industry of North Carolina, U. S. Commission of Fish and Fisheries, George M. Bowers Commisioner, Extracted from the U. S. Fish Commission Report for 1903, p. 247-341.

Greene, C. H., A. J. Pershing, 2003, The flip-side of the North Atlantic Oscillation and modal shifts in slope-water circulation patterns: Limnology and Oceanography, v. 48, p. 319-322.

Grossman, E. L., Ku, T.-H., 1986, Oxygen and Carbon Isotope Fractionation in Biogenic Aragonite: Temperature Effects, Chemical Geology (Isotope Geoscience Section), v. 59., p. 59-74.

Gutierrez, B. T., Uchupi, E., Driscoll, N. W., Aubrey, D. G., 2003, Relative sea-level rise and the development of valley-fill and shallow-water sequences in Nantucket Sound, Massachusetts, Marine Geology, v. 193, p. 295-314.

Hameed, S., Piontkovski, S., 2004, The dominant influence of the Icelandic Low on the position of the Gulf Stream northwall, Geophysical Research Letters, v. 31, n. 9, p. L09303(1-4).

Hardy, C. D., 1976, A preliminary description of the Peconic Bay Estuary, Special Report 3, Marine Sciences Research Center, State University of New York, 76-4, 65 p.

Hedgpeth, J. W., 1953, An introduction to the zoogeography of the northwestern Gulf of Mexico with reference to the invertebrate fauna, Publications of the Institute of Marine Science, v. 3, p. 107-223.

Henderson, G. M. & Anderson, R. F., 2003, U-series Toolbox for Paleoceanography, Reviews in Mineralogy & Geochemistry Vol 52: Urananium-Series Geochemistry, ed. Bourdon B, Henderson, G. M., Lundstrom, C. C., Turner, S. P., p. 493-529.

Henriet, J. P., Guidard, S., and the ODP "Proposal Team", 2002, Carbonate Mounds are Possible Example for Microbial Activity in Geological Processes, in G. Wefer, ed., Ocean margin systems, v. [1 v.], New York, Springer, p. 439-455.

Hughen, K. A., Baillie, M. G. L., Bard, E., Bayliss, A., Beck, J. W., Blackwell, P. G., Buck, C. E., Burr, G. S., Cutler, K. B., Damon, P. E., Edwards, R. L., Fairbanks, R. G., Friedrich, M., Guilderson, T. P., Herring, C., Kromer, B., McCormac, F. G., Manning, S. W., Ramsey, C. B., Reimer, P. J., Reimer, R. W., Remmele, S., Southon, J. R., Stuiver, M., Talamo, S., Taylor, F. W., van der Plicht, J., Weyhenmeyer, C. E., 2004, Marine04 Marine radiocarbon age calibration, 0-26 cal kyr BP, Radiocarbon, v. 46, n. 3, p. 1059-1086.

Hughes-Clarke, J., 1998, SwathEd, Ocean Mapping Group, University of New Brunswick, last accessed 2010, www.omg.unb.ca/~jhc/SwathEd.html.

Huvaz, O., Sarikaya, H., Isik, T., 2007, Petroleum systems and hydrocarbon potential analysis of the northwestern Uralsk basin, NW Kazakhstan, by utilizing 3D basin modeling methods, Marine and Petroleum Geology, v. 24, p. 247-275.

Ingersoll, E., 1881, The Oyster-Industry, The History and Present Condition of the Fishery Industry, Report on the oyster-industry of the United States, U.S. Department of the Interior, Washington D.C., Government Printing Office, Prepared under the Direction of Prof. S.F. Baird, U. S. Commissioner of the Fish and Fisheries and by G. Brown Good, Assistant Direction U.S. National Museum and a staff of associates.

Ingram, B. L., Sloan, D., 1992, Strontium Isotopic Composition of Estuarine Sediments as Paleosalinity-Paleoclimate Indicator, Science, v. 255, i. 5040, p. 68 -72.

Ingram, B. L. and Depaolo, D. J., 1993, A 4300 year strontium isotope record of estuarine paleosalinity in San Francisco Bay, California, Earth and Planetary Science Letters, v. 119i. 1-2, p. 103 -119.

Ingram, B. L. and Weber, P., K., 1999, Salmon origin in California's Sacramento-San Joaquin river system as determined by otolith strontium isotopic composition, Geology, v. 27, p. 851-854.

Ingram, B. L., Lin, J.C., 2002, Geochemical tracers of sediment sources to San Francisco Bay, Geology, v. 30, n. 6, p. 575-578.

IVSD3, 2009, Fledermaus Refence Manual, Interactive Visualization Systems, Inc., Fredericton, New Brunswick, Canada, accessed 2007, last accessed 2009, http://ivsd3.com/support/documentation, http://ivsd3.com/docs/Referenc_Manual.pdf .

i-cubed, USDA, NAIP, USGS, 2009, Digital Orthophotographs produced through USGS,USDA, NAIP, distributed by the company i-cubed for automatic linkage to use in ArcGIS 10, last accessed 2012.

Jia, C. Z., B. L. Li, X. Y. Zhang, Li, C. X., 2007, Formation and evolution of the Chinese marine basins: Chinese Science Bulletin, v. 52, p. 1-11.

Jones, D.S., Quitmyer, I.R., Andrus, F. T., 2005, Oxygenisotopic evidence for greater seasonality in Holocene shells of Donax variabilis from Florida, Paleoceanography, Paleoclimatology, Paleoecology, v. 228, p. 96-108.

Kallenberg, K., 2005, 87Sr/86Sr as a Paleoceanographic Indicator in Ancient and Modern Marine Environments [M.S. Thesis], Stony Brook University.

Katuna, M. P., 1974, The sedimentology of Great Peconic Bay and Flanders Bay, Long Island, New York [M.S. Thesis], Queens College (CUNY), Flushing, NY, United States, 97 p.

Kennedy, D. M., Woodroffe, C. D., 2002, Fringing reef growth and morphology: a review, Earth-Science Reviews, v. 57, p. 255-277.

Kim, Y., Lee, K.-S., Koh, D.-C., Lee, D.-H., Lee, S.-G., Park, W.-B., Koh, G.-W., Woo, N.-C., 2003, Hydrogeochemical and isotopic evidence of groundwater salinization in a coastal aquifer: a case study in Jeju volcanic island, Korea, Journal of Hydrology, v. 270, p. 282-294.

Kinney, J., Flood, R. D., 2006, Multibeam Bathymetry Reveals a Variety of Sedimentary Features in the Peconics Potentially Significant to Management of the System, Long Island Sound Research And New England Estuarine Research Society Joint Conference, October 26-28, 2006, United States Coast Guard Academy, New London, CT, Paper in Long Island Sound Research Conference Proceedings 2006.

Kinney, J., Flood, R. D., 2007, Multibeam Sonar Reveals Mound Features Associated with Oyster Terrain in the Peconics Estuary, Fourteenth Conference on the Geology of Long Island and Metropolitan New York, Long Island Geologists, April 2007 Meeting, Stony Brook, NY.

Kinney, J., Flood, R. D., 2007, Possible Association of Oyster Terrain Mound Features in the Peconic Estuary on Long Island, NY with 8.2ka Meltwater Pulse? Eos Trans. AGU, v. 88, n. 52, Fall Meet. Suppl., Abstract H34B-07, December 2007, San Francisco, CA.

Kinney, J., Flood, R. D., 2008, Peconic Estuary "Oyster Terrain": Carbonate Mound Transgressive Sequence? Fifteenth Conference on the Geology of Long Island and Metropolitan New York, Long Island Geologists, April 2008 Meeting, Stony Brook, NY.

Kinney, J., Flood, R. D., 2009, Holocene Reefs and the Evolution of the Peconic 'Oyster Terrain', Sixteenth Conference on the Geology of Long Island and Metropolitan New York, Long Island Geologists, March 2009 Meeting, Stony Brook, NY.

Kinney, J., Flood, R. D., 2011, Investigation of the Peconic Estuary, Long Island, NY Reveals Clues to the Evolution of an Estuarine 'Oyster Terrain', ASLO meeting February 2011, San Juan, Peurto Rico.

Kirby, M. X., Soniat, T. M., Spero, H. J., 1998, Stable isotope sclerochronology of Pleistocene and Recent oyster shells (Crassostrea virginica), Palaios, v. 13, p. 560-569.

Kirby, M. X., 2000, Paleoecological Differences Between Tertiary and Quaternary Crassostrea Oysters, as Revealed by Stable Isotope Sclerochronology, Palaios, v. 15, p. 132 -141.

Kirby, M. X., Miller, H. M., 2005, Response of a benthic suspension feeder (Crassostrea virginica Gmelin) to three centuries of anthropogenic eutrophication in Chesapeake Bay, Estuarine, Coastal and Shelf Science, v. 62, p. 679-689.

Koide, M., A. Soutar, E. D. Goldberg, 1972, Marine Geochronology with Pb-210, Earth and Planetary Science Letters, v. 14, p. 442-446.

Kolker, A. S, Hameed, S., 2007, Meteorologically driven trends in sea level rise, Geophysical Research Letters, v. 34, n. 23, p. L23616.

Kraeuter, J. N, Ford, S., Cummings, M., 2007, Oyster Growth Analysis: A Comparison of Methods, Journal of Shellfish Research, v. 26, n. 2, p. 479-491.

Kreeger, D., J. Adkins, P. Cole, R. Najjar, D. Velinsky, P. Conolly, Kraeuter J., June 2010, Climate Change and the Delaware Estuary: Three Case Studies in Vulnerability Assessment and Adaptation Planning, Partnership for the Delaware Estuary, PDE Report n. 10-01, p. 1-117.

Ladd, H. S., Hedgepeth, J. W., Post, R., 1957, Environments and facies of existing bays on the central Texas coast, Chapter 22 of Ladd, H.S., ed., Paleoecology: Memoir - Geological Society of America, n. 0072-1069, 0072-1069, p. 599-639.

Laroche, J., Nuzzi, R., Waters, R., Wyman, K., Falkowski, P. G., and Wallace, D. W. R., 1997, Brown Tide blooms in Long Island's coastal waters linked to interannual variability in groundwater flow, Global Change Biology, v. 3, no. 5, p. 397-410.

Larsen, C. E., Clark, I., 2006, A search for scale in sea-level studies, Journal of Coastal Research, v. 22, n. 4, p. 788–800.

Leach, P. A., Belknap, D. F., 2006, Geoarchaeological survey for submerged anthropogenic deposits in Damariscotta River, Maine, USA, Geological Society of America, Northeastern Section, 41st annual, Meeting, Abstracts with Programs - Geological Society of America, Mar 2006, v. 38, n. 2, p.6.

Lenihan, H. S., Peterson, C. H., 1998, How Habitat Degradation through Fishery Disturbance Enhances Impacts of Hypoxia on Oyster Reefs, Ecological Applications, v. 8, n. 1, p. 128-140.

Lescinsky, H., Edinger, E., Risk, M. J., 2002, Mollusc Shell Encrustation and Bioerosion Rates in a Modern Epeiric Sea: Taphonomy Experiments in the Java Sea, Indonesia, Palaios, v. 17, p. 171-191.

Lightfoot, K. G., R. Kalin and J. Moore, Contributions: Cerrato, R., Conover, M., Rippel-Erikson, S., 1987, Prehistoric Hunter-Gatherers of Shelter Island, New York: An Archaeological Study of the Mashomack Preserve, Contributions of the University of California Archaeological Research Facility No. 46. University of California, Berkeley, California.

Lin, I.-T., Wang, C.-H., You, C.-F., Lin, S., Huang, K.-F., Chen, Y.-G., 2010, Deep submarine groundwater discharge indicated by tracers of oxygen, strontium isotopes and barium content in the Pingtung coastal zone, southern Taiwan, Marine Chemistry, v. 122, p. 51-58.

Liu, J. P., Milliman, J. D., Gao, S., Chen, P., 2004, Holocene development of the Yellow River's subaqueous delta, North Yellow Sea, Marine Geology, v. 209, p. 45-67.

Lockwood, R., Work, L. A., 2006, Quantifying Taphonomic Bias in Molluscan Death Assemblages from the Upper Chesapeake Bay: Patterns of Shell Damage, Palaios, v. 21, p. 442-450.

Lyell, C., 1865, Elements of Geology or Ancient Changes of the Earth and its Inhabitants as Illustrated by Geological Monuments, London, 6th ed, First published 1838.

MacIntyre, I. G., Pilkey, O. H., Stuckenrath, R., 1978, Relict Oysters on United-States Atlantic Continental-Shelf - Reconsideration of Their Usefulness in Understanding Late Quaternary Sea-Level History, Geological Society of America Bulletin, v. 89, i. 2, p.277-282.

Maher, N. P., 2006, A new approach to benthic biotope identification and mapping [Ph.D. Dissertation], Stony Brook University, Stony Brook, NY, 181 p.

McCormick-Ray, J., 2005, Historical oyster reef connections to Chesapeake Bay- a framework for consideration, Estuarine, Coastal and Shelf Science, v. 64, p. 119-134.

Meinkoth, N. A., 1981, The Audubon Society Field Guide to North American Seashore Creatures, Chanticlear Press, Inc., Alfred A. Knopf, New York, p. 547.

Mel'nikov, N. V., Sitnikov, V. S., Vasil'ev, V. I., Doronina, S. I., Kolotova, L. V., 2005, Bioherms of the Lower Cambrian Osa Horizon in the Talakan-Upper Chona zone of

petroleum accumulation, Siberian platform, Russian Geology and Geophysics, v. 46, p. 834-841.

Merrill, A. S., Emery, K. O., Rubin, M., 1965, Ancient Oyster Shells on Atlantic Continental Shelf, Science, v. 147, p. 398-400, *DOI:10.1126/science.147.3656.398, http://www.sciencemag.org/content/147/3656/398.abstract?sid=49bc8db0-fc26-48c4-8ee4-6be0920c8965*.
Miller, L., Douglas, B. C., 2007, Gyre-scale atmospheric pressure variations and their relation to 19th and 20th century sea level rise, Geophysical Research Letters, v. 34, p. L16602.

Milliman J. D., Emery K.O., 1968, Sea Levels during the Past 35,000 Years, Science, v. 162, i. 3858, p. 1121-1123.

Milliman, J. D., 1974, Marine Carbonates, Recent Sedimentary Carbonates: Part 1, Springer Verlag; New York.

Montlucon, D., Sanudo-Wilhelmy, S. A., 2001, Influence of net groundwater discharge on metal and nutrient concentrations in a coastal environment: Flanders Bay Long Island, New York, Environmental Science and Technology, v. 35, p. 480-486.

Moore, W. S., 1996, Large groundwater inputs to coastal waters revealed by Ra-226 enrichments. Nature, v. 380, n. 6757, p. 612-614.

Moore, W. S., 1997, High fluxes of radium and barium from the mouth of the Ganges-Brahmaputra River during low river discharge suggest a large groundwater source, Earth and Planetary Science Letters, v. 150, n. 1-2, p. 141-150.

Moore, W. S., 1999, The subterranean estuary: a reaction zone of groundwater and sea water, Marine Chemistry, v. 65, p. 111-125.
National Oceanographic and Atmospheric Adminitstration (NOAA), 2010, Raster Navigational Charts: NOAA RNCs, last accessed 2010, http://www.nauticalcharts.noaa.gov/mcd/Raster/index.htm.

Morse, J. W., 2005, Formation and Diagenesis of Carbonate Sediments, Sediments, Diagenesis, and Sedimentary Rocks, ed. Fred T. Mackenzie, Treatise on Geochemistry H. D. Holland & K. K. Turekian (Executive Editors) v. 7, Elsevier, The Netherlands (Oxford, UK), p. 67-82, p. 80.

NASA, GeoEye, 2005, SeaWifs Satellite Imagery come from NASA and are distributed through GeoEye. Image originally a satellite image of the day from NASA, and NOAA Operational Significant Event Imagery, last accessed 2005, http://www.osei.noaa.gov, http://earthobservatory.nasa.gov, http://www.geoeye.com

NOAA & USGS 2009, ETOPO1 Global Relief Model, NOAA Bathymetry and USGS Topography at 1 arc minute scale available at National Geospatial Data Clearinghouse

through www.ngdc.noaa.gov as custom grids (15 arc seconds for the east coast), last accessed 2010
http://www.ngdc.noaa.gov/mgg/gdas/gd_designagrid.html?dbase=grdet1.

NOAA, 2009a, Make a Tide Prediction, accessed, 2009,
http://tidesandcurrents.noaa.gov/.

NOAA, 2009b, Historical Tide Data –Select Station, NOAA, National Ocean Services, Center for Operational and Predictive Services, accessed 2009,
http://tidesandcurrents.noaa.gov/Station_retrieve.shtml?type==Historic+Tide+Data.

National Oceanographic and Atmospheric Administration (NOAA), 2010, Raster Navigational Charts: NOAA RNCs, last accessed 2010,
http://www.nauticalcharts.noaa.gov/mcd/Raster/index.htm.

NOAA, 2011, National Oceanographic and Atmospheric Administration (NOAA) National Ocean Service Historical Hydrographic Data, National Geophysical Data Center, Office of Coast Survey and National Geophysical Data Center, (http://surveys.ngdc.noaa.gov/mgg/NOS/coast), 1933 -1935 surveys, available through the Hydrographic Data Viewer for downloading data, accessed 2011,
http://maps.ngdc.noaa.gov/viewer/nos_hydro.

Nydick, K. R., Bidwell, A. B., Thomas, E., Varekamp, J. C., 1995, A Sea-Level Rise Curve from Guilford, Connecticut, USA, Marine Geology, v. 124, n. 1-4, p. 137-159.

Olcott, P. G., 1999, USGS OFR 1999-559: Ground Water Atlas of the United States Connecticut, Maine, Massachusetts, New Hampshire, New York, Rhode Island, Vermont HA 730-M, Surficial and Northern Atlantic Coastal Plain aquifer systems, Long Island, http://capp.water.usgs.gov/gwa/ch_m/.

Oschmann, W., 2009, 'Sclerochronology: editorial', International Journal of Earth Science (Geol Rundsch), v. 98, p. 1-2.

Osterman, L. E., Twichell, D. C., Poore, R. Z., 2009, Holocene evolution of Apalachicola Bay, Florida: Geo-Marine Letters, v. 29, n. 6, p. 395-404.

Palmer, M. R., Edmond, J. M., 1989, The strontium isotope budget of the modern ocean. Earth and Planetary Science Letters, v. 92, p. 11-26.

Parker, R. H., 1960, Ecology and distributional patterns of marine macro-invertebrates, northern Gulf of Mexico, in Shepard, F. P., ed., United States (USA).

Pavlukhin, S. I., 2004, SeiSee 2.15 User's Manual, Yuhno -Sakhalinsk, DMNG Geophysical Company, www.dmng.ru/seisview/html/SeiSeeEng.html.

Pavlukhin, S. I., 2011, SeiSee (Rev 2.16.1) SEG-Y and CWP-SU (Seismic Un*x) fileviewer, DMNG Geophysical Company, updated July 5, 2011, www.dmng.ru/seisview.

Pekar, S. F., McHugh, C. M. G., Christie-Blick, N., Jones, M., Carbotte, S. M., Bell, R. E., Lynch-Stieglitz, J., 2004, Estuarine processes and their stratigraphic record: paleosalinity and sedimentation changes in the Hudson Estuary (North America), Marine Geology, v. 209, n. 1-4, p. 113-129.

Popescu, I., Lericolais, G., Panin, N., De Batist, M., Gillet, H., 2007, Seismic expression of gas and gas hydrates across the western Black Sea, Geo-Marine Letters, v. 27, p. 73–183.

Povinec, P. P., de Oliveira, J., Braga, E. S., Comadnucci, J.-F., Gastaud, J., Groening, M., Levy-Palomo, I., Morgentstern, U., Top, Z., 2008, Isotopic trace element and nutrient characterization of coastal waters from Ubatuba inner shelf area, south-eastern Brazil. Estuarine, Coastal and Shelf Science, v. 76, p. 522-542.

Powell, E. N., Song, J., Ellis, M., 1992, The Status of Oyster Reefs in Galveston Bay, Texas, Galveston Bay oyster reefs map series: Houston, TX.

Powell, E. N., 1993, Status and trends analysis of oyster reef habitat in Galveston Bay, *in* Jensen, R. W., Kiesling, R. W., Shipley, F. S., ed., The Second State of the Bay Symposium: Austin, TX, Galveston Bay National Estuary Program, p. 207-209. PRIME lab, 2008, personal communication, regarding protocols for samples that arrive for radiocarbon dating at PRIME lab, Purdue University, Indiana, USA, e-mail correspondence.

Pufahl, P. K., James, N. P., Bone, Y., Lukasik, J. J., 2004, Pliocene sedimentation in a shallow, cool-water, estuarine gulf, Murray Basin, South Australia, Sedimentology, v. 51, p. 997-1027.

Purnachandra Rao, V., Rajagopalan, G., Vora, K. H., Almeida, F., 2003, Late Quaternary sea level and environmental changes from relic carbonate deposits of the western margin of India, Proceedings of the Indian Academy of Sciences, Journal of Earth System Science, v. 112, n. 1, p. 1-25.

Rapaglia, J., 2005, Submarine Groundwater Discharge into Venice Lagoon, Italy, Estuaries, v. 28, n., 5, p. 705-713.

Redfield, A. C., 1967, Postglacial change in sea level in western North Atlantic Ocean, Science, v. 157, p. 687-692.

Reimer, P. J., Baillie, M. G., Bard, E., Bayliss, A., Beck, J. W., Bertrand, C. J. H., Blackwell, P. G., Buck, Caitlin, E., Burr, G. S., Cutler, K. B., Damon, P. E., Edwards, R. L., Fairbanks, R. G., Friedrich, M., Guilderson, T. P., Hogg, A. G., Hughen, K. A., Kromer, B., McCormac, G., Manning, S., Ramsey, C. B., Remier, R. W., Remmele, S.,

Southon, J. R., Stuiver, M., Talamo, S., Taylor, F. W., van der Plicht, J., Weyhenmeyer, C. E., 2004, INTCAL04 Terrestrial Radiocarbon Age Calibration, 0-26 CAL KYR BP, Radiocarbon, v. 46, n. 3, p. 1029-1058.

Reinhardt, E. G., Stanley, D. J., Patterson, R. T., 1998, Strontium isotopic-paleontological method as a high-resolution paleosalinity tool for lagoonal environments, Geology, v. 26, n. 11, p. 1003–1006.

Reinhardt, E. G., Blenkinsop, J., Patterson, R., T., 1999, Assessment of a Sr isotope vital effect (Sr-87/Sr 86) in marine taxa from Lee Stocking Island, Bahamas. Geo-Marine Letters, v. 18, i. 3, p. 241-146.

Reinhardt, E. G., Cavazza, W., Blekinsop, J., Patterson, R. T., 2000, Differential Diagenesis of sedimentary components and the implication for strontium isotope analy Rodriguez, A. B., Anderson, J. B., Siringan, F. P., Taviani, M., 2004, Holocene Evolution of the East Texas Coast and Inner Continental Shelf: Along-Strike Variability in Coastal Retreat Rates, Journal of Sedimentary Research, v. 74, n. 3, p. 405–421.

Renfro, A., 2010, Particle-Reactive Radionuclides (Thorium-234, Beryllium-7 and Lead-210) As Tracers of Sediment Dynamics in an Urban Coastal Lagoon (Jamaica Bay, NY) [Ph.D. Dissertation], Stony Brook, NY, Stony Brook University.

Riding, R., 2002, Structure and composition of organic reefs and carbonate mud mounds: concepts and categories, Earth-Science Reviews, v. 58, n. 1, July 2002 , p. 163-231.

Rivara, Gregg, Cornell-Cooperative Extension, 2009, Growth of Oysters produced by Cornell Co-op and Aeros in the Peconic Estuary, personal communication, in person, e-mail, and phone.

Rivara, Gregg, Cornell-Cooperative Extension, 2010, Growth Conditions Including Temeperature of Oysters in the Peconic Estuary, personal communication, e-mail.

Rock, B. N., Carter, L., Walker, H., Bradbury, J., Dingman, S. L., Federer, C. A., 2001, Chapter 6: Water Resources and Potential Climate Change Impacts, The New England Regional Assessment of The Potential Consequences of Climate Variability and Change, A Final Report, p. 63-83.

Rohling, E., Palike, H., 2005, Centennial-scale climate cooling with a sudden cold event around 8,200 years ago, Nature, v. 434, p. 975 –979.

Rosen, P. S., Brennikmeyer, B. M., Maybury, L. M., 1993, Holocene Evolution of Boston Inner Harbor, Massachusetts, Journal of Coastal Research, v. 9, n. 2, p. 363-377.

Ryan, H. F., Noble, M. A., 2002, Sea level response to ENSO along the central California coast: how the 1997–1998 event compares with the historic record, Progress in Oceanography, v. 54, i. 1-4, p. 149-169.

Ryan, H. F., Noble, M., A., 2006, Alongshore Wind Forcing of Coastal Sea Level as a Function of Frequency, Journal of Physical Oceanography, v. 36, p. 2173-2184.

Sachs, J. P., 2007, Cooling of Northwest Atlantic slope waters during the Holocene: Geophysical Research Letters, v. 34, p. L03609 (1-4).

Saenger, C., Cronin, T., Thunell, R., Vann, C., 2006, Modelling river discharge and precipitation from estuarine salinity in the northern Chesapeake Bay: application to Holocene paleoclimate, The Holocene, v. 16, p. 467-477.

Schlueter, M., Sauter, E. J., Andersen, C. E., Dahlgaard, H., Dando, P. R., 2004, Spatial distribution and budget for submarine groundwater discharge in Eckernfoerde Bay (Western Baltic Sea), Limnology Oceanography, v. 49, p. 157-167.

Schmidt, S., and Cochran, J. K., 2010, Radium and radium-daughter nuclides in carbonates: a brief overview of strategies for determining chronologies, Journal of Environmental Radioactivity, v. 101, no. 7, p. 530-537.

Schöne, B. R., Flessa, K. W., Dettman, D. L., Goodwin, D. H., 2003, Upstream dams and downstream clams: growth rates of bivalve mollusks unveil impact of river management on estuarine ecosystems (Colorado River Delta, Mexico), Estuarine, Coastal and Shelf Science, v. 58, p. 715-726.

Schöne, B. R., 2008, The curse of physiology—challenges and opportunities in the interpretation of geochemical data from mollusk shells, Geo-Marine Letters, v. 28, p. 269–285.

Schöne, B. R., Rodland, D. L., Surge, D. M., Feibig, J., Gillikin, D. P., Baier, S. M., Goewert, A., 2006, Comment on: Stable carbon isotopes in fresh water mussel shells: Environmental record or marker for metabolic activity?" by J. Geist et al. (2005), Geochimica et Cosmochimica Acta, v. 70, n. 10, p. 2658-2661.

Schubert, C. E., 1998, Areas contributing ground water to the Peconic Estuary and ground-water budgets for the North and South Forks and Shelter Island, eastern Suffolk County, New York: U.S. Geological Survey Water-Resources Investigations Report 97-4136, 36 p., 1 pl.

Schubert, C. E., 1999, Ground-Water Flow Paths and Traveltime to Three Small Embayments within the Peconic Estuary, Eastern Suffolk County, New York, U.S. Geological Survey Water-Resources Investigations Report 98-4181, 43 p.

Schubert, C. E., Bova, R. G., Misut, P. E., 2004, Hyrdogeologic Framework of the North Fork and Surrounding Areas, Long Island, NY, U.S. Geological Survey Water-Resources Investigations Report 02-4284, 34 p.

Schuller, D., Kadko, D., Smith, C. R., 2004, Use of ^{210}Pb/ ^{226}Ra disequilibria in the dating of deep-sea whale falls, Earth and Planetary Science Letters, v. 218, n. 3-4, p. 277-289.

Sirkin, L., 1994, Block Island Geology: History, Processes and Field Excursions, Coastal Geology Series by Les Sirkin, Book and Tackle Shop, Watch Hill, RI, USA.

Sirkin, L., 1995, Eastern Long Island Geology: History, Processes and Field Trips, Coastal Geology Series by Les Sirkin, Book and Tackle Shop, Watch Hill, RI, USA.

Slagle, A. L., Ryan, W. B. F., Carbotte, S. M., Bell, R., Nitsche, F. O., Kenna, T., 2006, Late-stage estuary infilling controlled by limited accommodation space in the Hudson River, Marine Geology, v. 232, p. 181-202.

Smith, G. F., Roach, E. B., Bruce D. G., 2003, The location, composition, and origin of oyster bars in mesohaline Chesapeake Bay, Estuarine, Coastal and Shelf Science, v. 56, p. 391-409.

SMT Kingdom Suite, 2009, SMT Kingdom Suite Tutorials, accessed 2009, http://seismicmicro.com.

Stanley, J.G., Sellers, M.A., 1986, Species profiles : lifehistories and environmental requirements of coastal fishes and invertebrates (Mid-Atlantic)--American oyster. U. S. Fish Wildl. Serv. Biol. Rep. 82(11.65), U.S. Army Corps of Engineers, TR EL-82-4, p. 25.

Staubwasser M., Henderson, G. M, Berkman, P. A., Hall, B. L., 2004, Ba, Ra, Th, and U in marine mollusc shells and the potential of ^{226}Ra/Ba dating of Holocene marine carbonate shells, Geochimica et Cosmochimica Acta, v. 68, n.1, p.89-100.

Stieglitz, T., Rapaglia, J., Bokuniewicz, H., 2008, Estimation of submarine groundwater discharge from bulk ground electrical conductivity measurements, Journal of Geophysical Research, v. 113, n. C8, p. 15.

Stoffer, P. W., Chamberlain, J. A., Jr., Scal, Roland, Messina, Paula, 2005, Late Quaternayr and early Holocene fossils from New York City beaches; implications for stability in coastal environments in western Long Island and New Jersey, Geological Society of America, 2005 annual meeting, Oct 15-19, 2005, Abstracts with Programs – Geological Society of America, v. 37, n.7, p. 366.

Stuiver, N., Reimer, P. J., Braziunas, T. F., 1998, High-Precision Radiocarbon Age for Terrestrial and Marine Samples, Radiocarbon, v. 40, n. 3, p. 1127-1151.

Suffolk County Planning, 2011, Publications and Information, Suffolk County, Long Island, New York, Planning, last accessed December 2011, http://www.co.suffolk.ny.us/departments/planning/Publications%20and%20Information.aspx.

Suffolk County, 2008, Cedar Point County Park, last accessed December 2011, http://www.suffolkcountyny.gov/Departments/Parks/Parks/CedarPointCountyPark.aspx,. Surge, D., K. C. Lohmann, D. L. Dettman, 2001, Controls on isotopic chemistry of the American oyster, Crassostrea virginica: implications for growth patterns: Palaeogeography Palaeoclimatology Palaeoecology, v. 172, p. 283-296.

Surge, D. M., Lohmann, K. C., Goodfriend, G. A., 2003, Reconstructing estuarine conditions: oyster shells as recorders of environmental change, Southwest Florida, Estuarine, Coastal and Shelf Science, v. 57, n.5-6, p. 737–756.

Surge, D., Lohmann, K. C., 2008, Evaluating Mg/Ca ratios as a temperature proxy in the estuarine oyster, Crassostrea virginica, Journal of Geophysical Research, v. 113, p. G02001 (1-9).

Swarzenski, P. W., Martin, J. B., Cable, J. E., Lindenberg, M. K., Boyton, B., Bowker, R., Signa, C. C., 2000, Quantifying Submarine Groundwater Discharge to Indian River Lagoon, Florida, USGS OFR 00-492.

Swarzenski, P. W., Porcelli, D., Andersson, P. S., & Smoak, J. M., 2003, The Behavior of U- and Th- series Nuclides in the Estuarine Environment, Reviews in Mineralogy & Geochemistry Vol 52: Urananium-Series Geochemistry, ed. Bourdon B, Henderson, G. M., Lundstrom, C. C., Turner, S. P. p. 557-600.

Thomas, A., School of Marine Science, University of Maine, SST imagery last accessed 2011, wavy.umeoce.maine.edu.

Thomas, E., Varekamp, J. C., 2002, Sea Level Rise in Long Island Sound Over the Last Millennium, American Geophysical Union, Fall Meeting 2002, abstract #OS71D-0323.

Thomas, E., Varekamp, J. C., Avener, E., 2006, Multiproxy records of Eutrophication in Long Island Sound Geological Society of America Abstracts with Programs, , 2006 Annual Meeting, Oct 22-25, 2006, Paper No. 130-10, v. 38, n. 7, p. 323.

Twichell, D. C., Andrews, B. D., Edminston, H. L., Stevenson, W. R., 2007, Geophysical Mapping of Oyster Habitats in a Shallow Estuary; Apalachicola Bay, Florida: U. S. Geological Survey Open File Report 2006-138.

USGS 7.5 DEM New York State (10 mx10 m pixels), 2010, NY State DEM courtesy USGS & NYDEC available via the Cornell University Geospatial Information Depository,

North American Datum of 1927 UTM 18N, downloaded 2008, last accessed 2010, http://cugir.mannlib.cornell.edu/mapsheet.jsp?coverageId=23&id=all.

Van de Plassche, O., 2000, North Atlantic Climate–Ocean Variations and Sea Level in Long Island Sound, Connecticut, Since 500 cal yr A.D., Quaternary Research, v. 53, p. 89–97.

Varekamp, J. C., Thomas, E., Vandeplassche, O., 1992, Relative Sea-Level Rise and Climate Change over the Last 1500 Years, Terra Nova, v. 4, n. 3, p. 293-304.

Varekamp, J. C., Thomas, E., Thompson, W. G., 1999, Sea level-climate correlation during the past 1400 yr: Comment, Geology, v. 27, n. 2, p. 189-190.

Varekamp, J. C., 2006, The Historic Fur Trade and Climate Change, Eos, 87, n.52, p. 593, 596-597.

Veatch, O., Stephenson, L. W., 1911, Geology of the Georgia Coastal Plain, Bulletin No. 26, Geological Survey of Georgia, Foote & Davies Co., p.240-252, 466 p.

Veizer, J., 1989, Strontium Isotopes in Seawater Through Time, Annual Review of Earth and Planetary Science, v. 17, p. 141-167.

Vieira, M. E. C., 1990, Observations of currents, temperature, salinity, and sea level in the Peconic Bays, 1984 : a data report, Northeastern Environmental Data System (NEEDS), Special data report; #4, #90-9, 199 p.

Visbeck, M., Chassignet, E. P., Curry, R. G., Delworth, T. L., Dickson, R. R., Krahmann, G., 2003, 'The Ocean's Response to North Atlantic Oscillation Variability' The North Atlantic Oscillation: Climatic Significance and Environmental Impact: Geophysical Monograph 134, American geophysical Union Washington, DC, p. 113-146.

Walter, L. M., Bischof, S. A., Patterson, W. P., Lyons, T. W., 1993, Dissolution and recrystallization in modern shelf carbonates: evidence from pore water and solid phase chemistry, Philisophical Transransactions of the Royal Society London A, v. 344, p. 27-36.

Weaver, Meghan , 2006, Research Experience for Undergraduates Studies of Coastal Oceanographic and Atmospheric Processes, Summer 2006, Report/Presentation - Mapping the Peconics: Multibeam Bathymetry and Backscatter Analysis, Marine Sciences Research Center, Stony Brook University.

Weaver, E., Herbort, M., Dellapenna, T., Simons, J., 2008, Geological Controls on the Distribution of Oyster Reefs and Substrates in Copano Bay, Texas, 2008 Joint Meeting of The Geological Society of America, Soil Science Society of America, American Society of Agronomy, Crop Science Society of America, Gulf Coast Association of Geological Societies with the Gulf Coast Section of SEPM, Geological Society of

America Abstracts with Programs, v. 40, Geological Society of America, p. 15.

Wiedemann, H. U., 1972, Shell Deposits and Shell Preservation in Quaternary and Tertiary Estuarine Deposits in Georgia, U. S. A., Sedimentary Geology, v. 7, p. 103-125.

Wilson, R. E.,Viera, M. E. C., 1989, Residiual Currents in the Peconic Bays Estuary, Estuarine Circulation, eds. Bruce J. Neilson, Albert Kuo, John Brubaker, Huama Press Inc., Cresent Manor, Clifton, NJ, p. 87-96.

Wilson, R. E., 1996, Aspects of tidal and subtidal flushing within the Peconic Bay Estuary, Proceedings of the Brown Tide summit Oct 20-21, 1995, ed. McElroy, A., NYSG SUNY, Stony Brook NYSG I W –95-001, p. 11.

Woods, H., Hargis, W. J., Hershner, C. H., Mason, P., 2005, Disappearance of the natural emergent 3-dimensional oyster reef system of the James River, Virginia, 1871-1948, Journal of Shellfish Research, v. 24, i. 1, p 139-142.

Wright, E. E., Hine, A. C., Goodbred, S. L., Locker, S. D., 2005, The effect of sea-level and climate change on the development of a mixed siliciclastic-carbonate, deltaic coastline: Suwannee River, Florida, USA, Journal of Sedimentary Research, v. 75, p. 621-635.

Xin, G., 1993, Strontium Isotope Study of the Peconic River Watershed, Long Island, New York [M. S. Thesis], Geosciences Department, State University of New York, Stony Brook.

Yang, S., 2007, Quantification of the tidal exchange of radium as an indicator of submarine groundwater inputs to Great South Bay [M.S. Thesis], State University of New York, Stony Brook, 39 p.

Young, M. B., Gonneea, M. E., Fong, D. A., Moore, W. S., Herrera-Silveira, J., Payton, A., 2008, Characterizing sources of groundwater to a tropical coastal lagoon in a Karstic area using radium isotopes and water chemistry, Marine Chemistry, v. 109, p. 377-394.

APPENDIX A: MAPS

Fig. A.1: Multibeam bathymetry map of the Peconic Estuary with USGS topography scale used in figures throughout thesis.
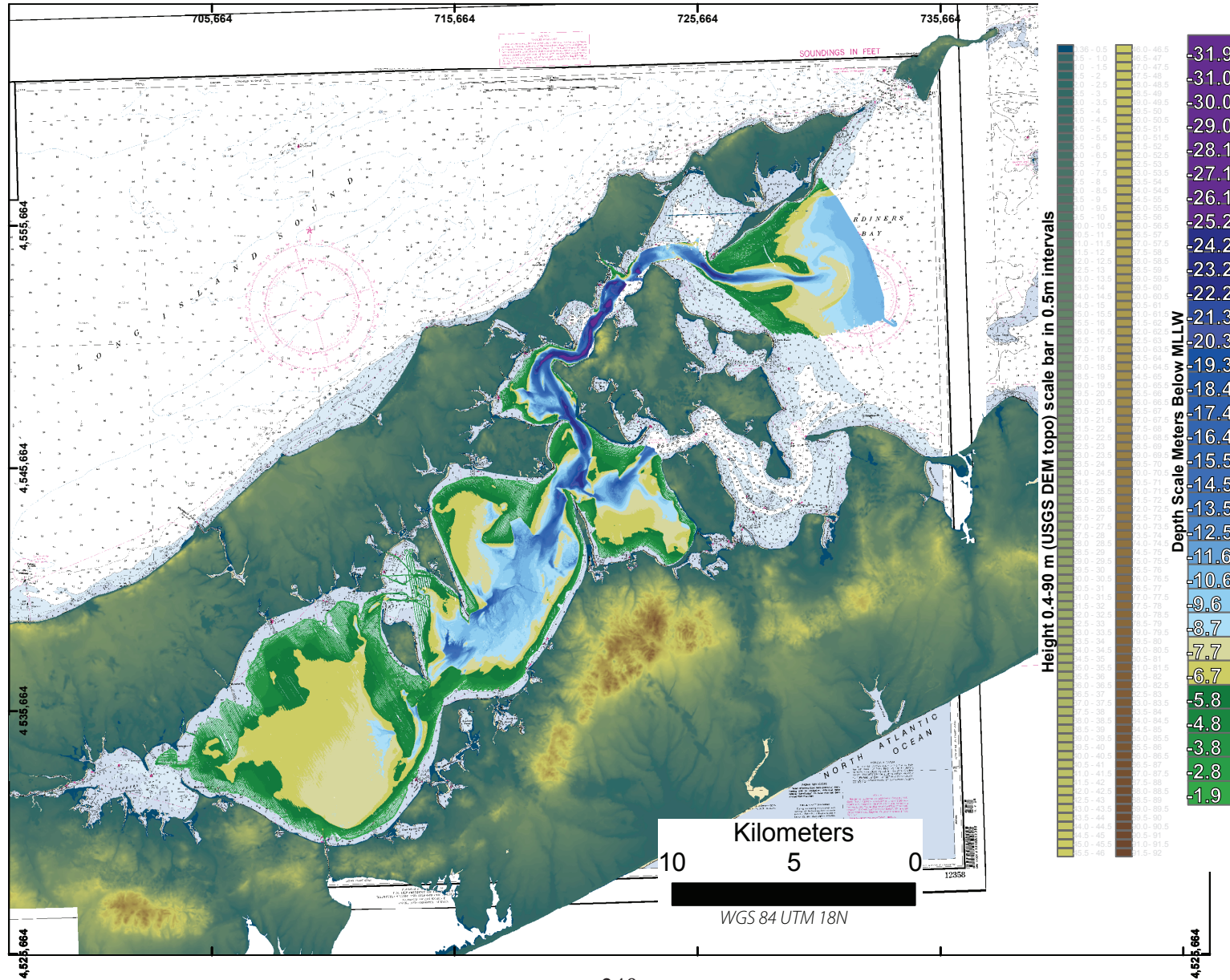
Fig. A.2: Multibeam backscatter map of the Peconic Estuary.
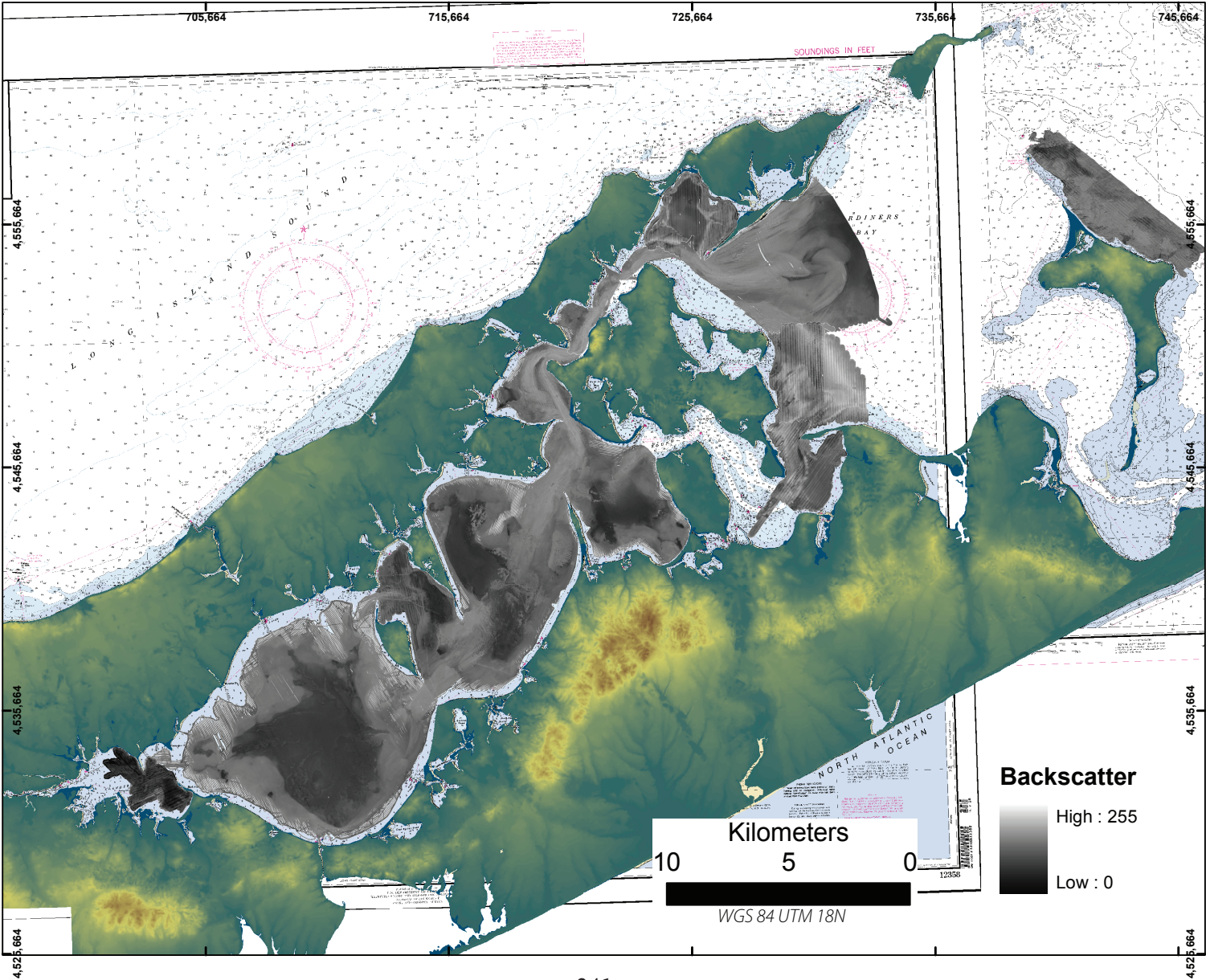
Fig. A.3: Miniature high resolution seismic survey tracks over buried mounds with sidescan data and NOAA nautical chart basemap. Tracklines of survey can be seen as white outlined by black. Purple box shows the area of the high resolution survey. Also shown are plots of grainsize distribution for the mud to sand fraction including grab #61.

242
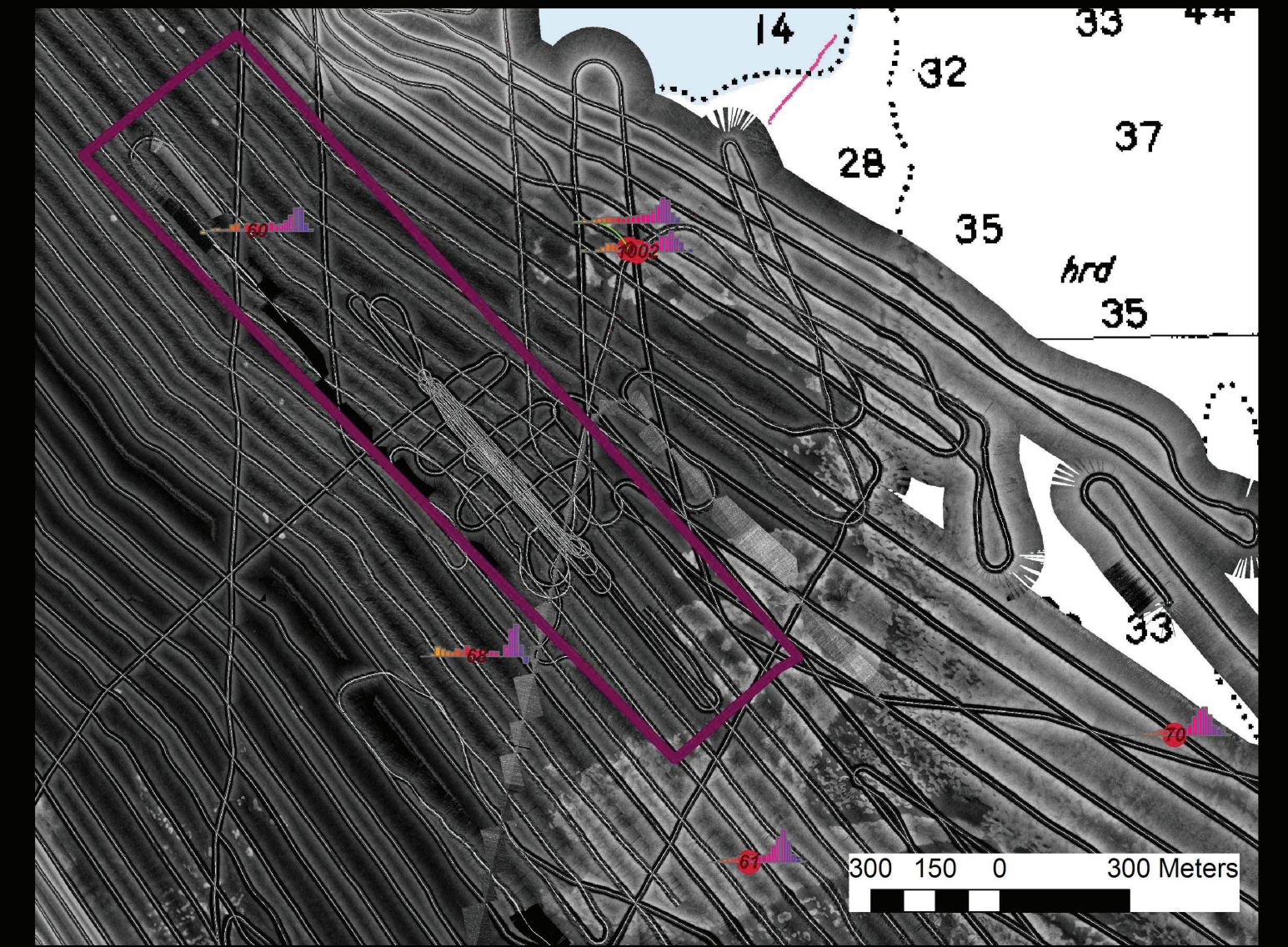
Fig. A.4: Map with δ ^{13}C values and ages of radiocarbon dated shells.
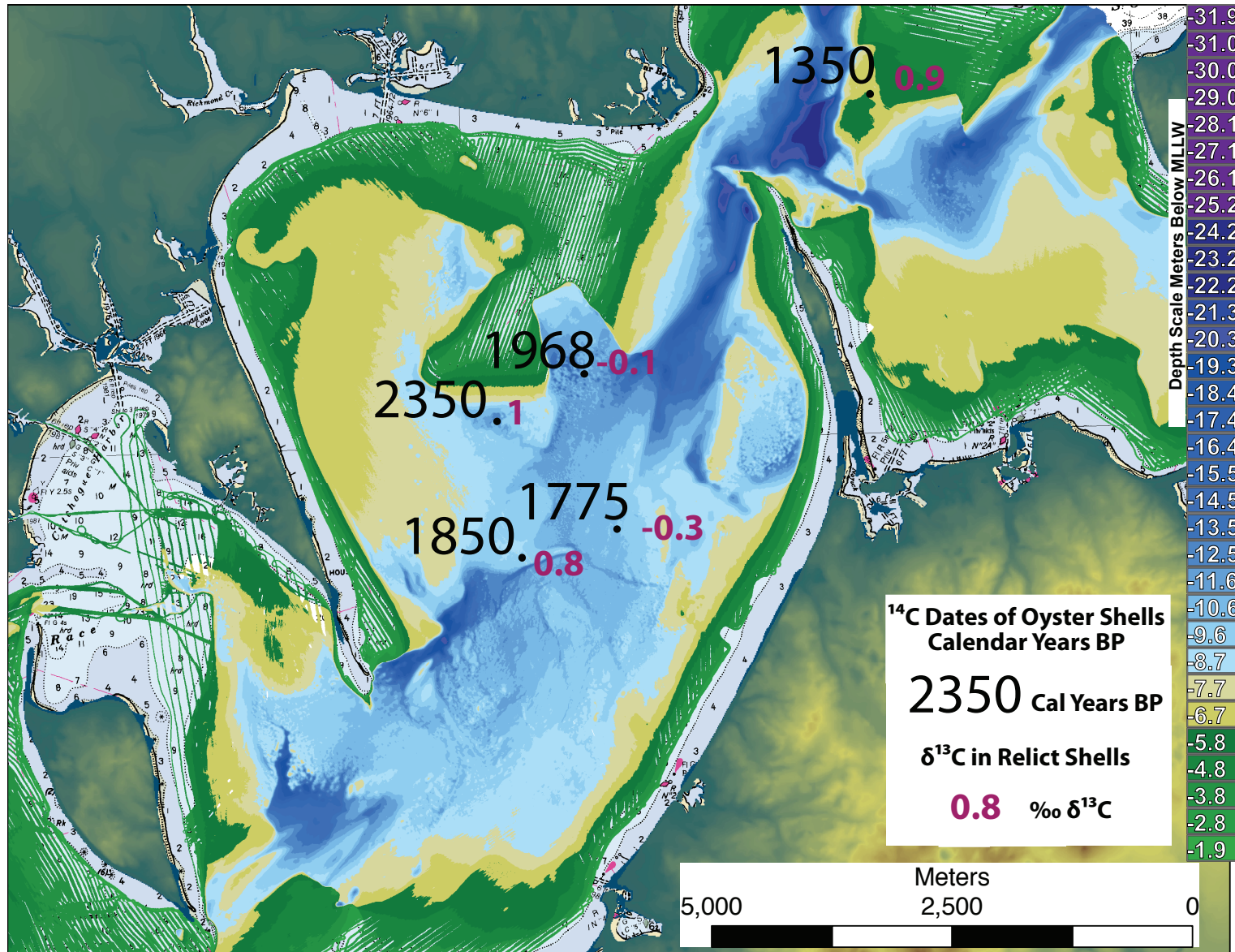
Fig. A.5: Little Peconic Bay 2008 1 mm to 63 μm sand fraction in grabs. Half-phi intervals.
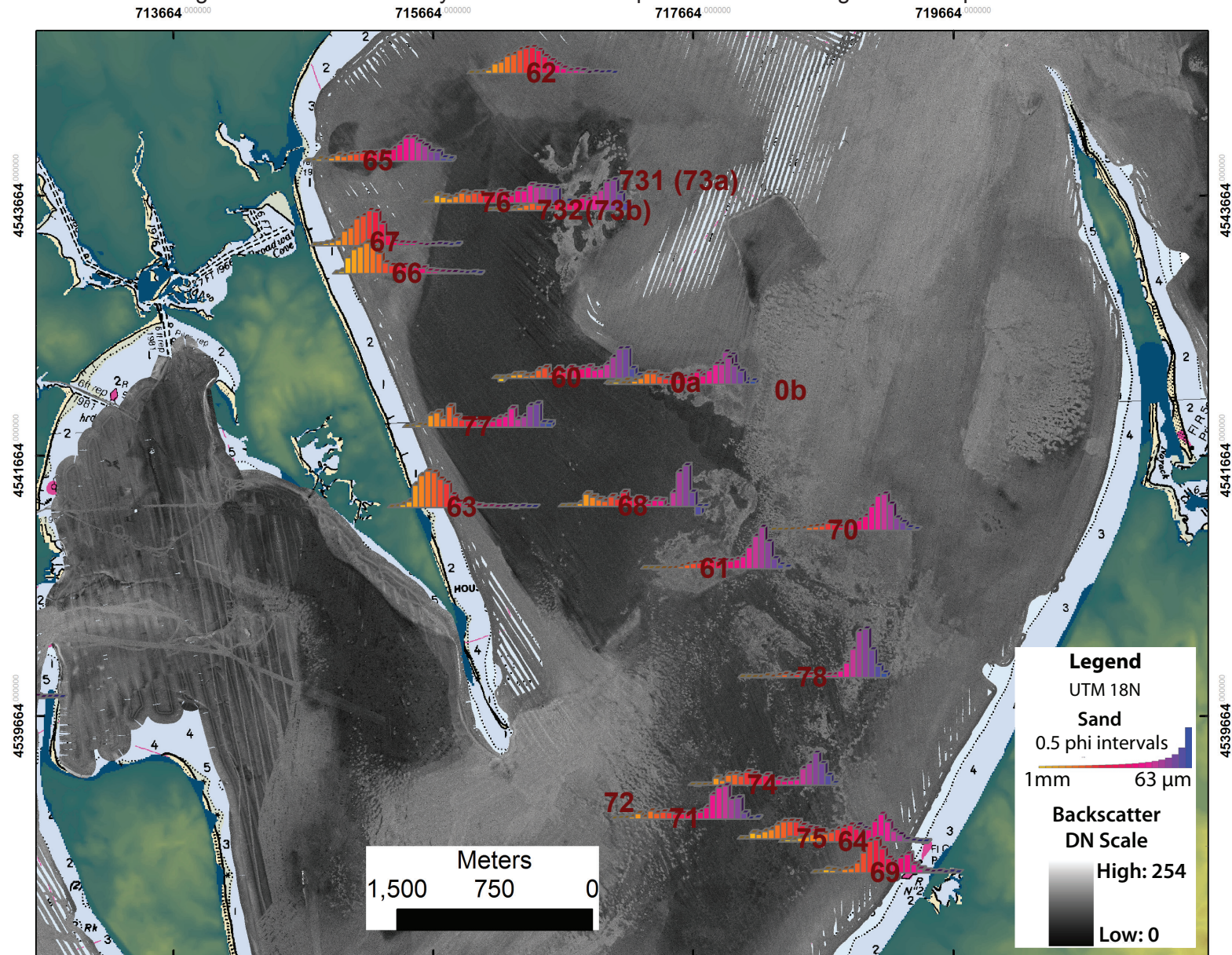
Fig. A.6: Great Peconic Bay 2008 1 mm to 63 µm sand fraction in grabs. Half-phi intervals.
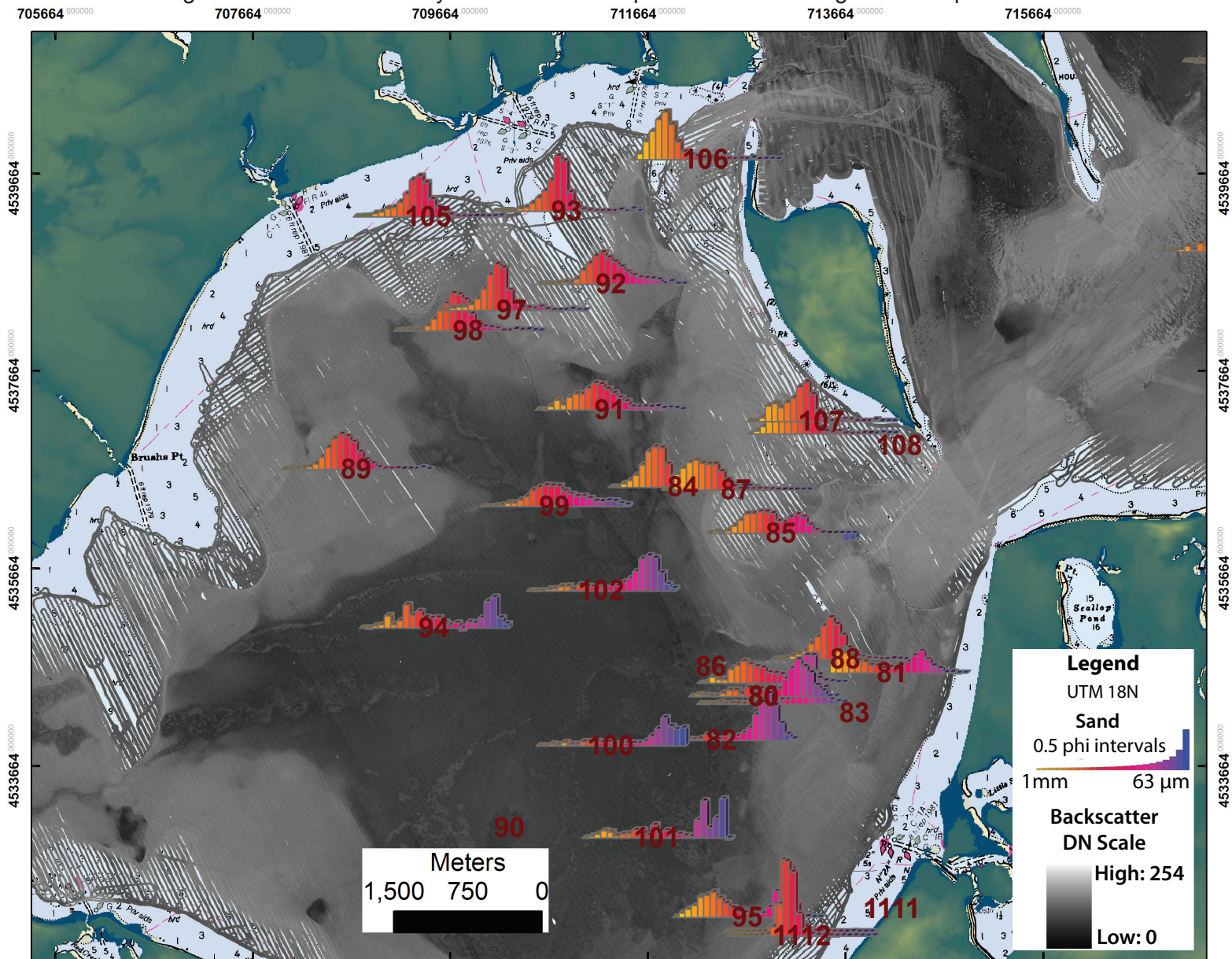
Fig. A.7: Noyack Bay 2008 1 mm to 63 μm sand fraction in grabs. Half-phi intervals.
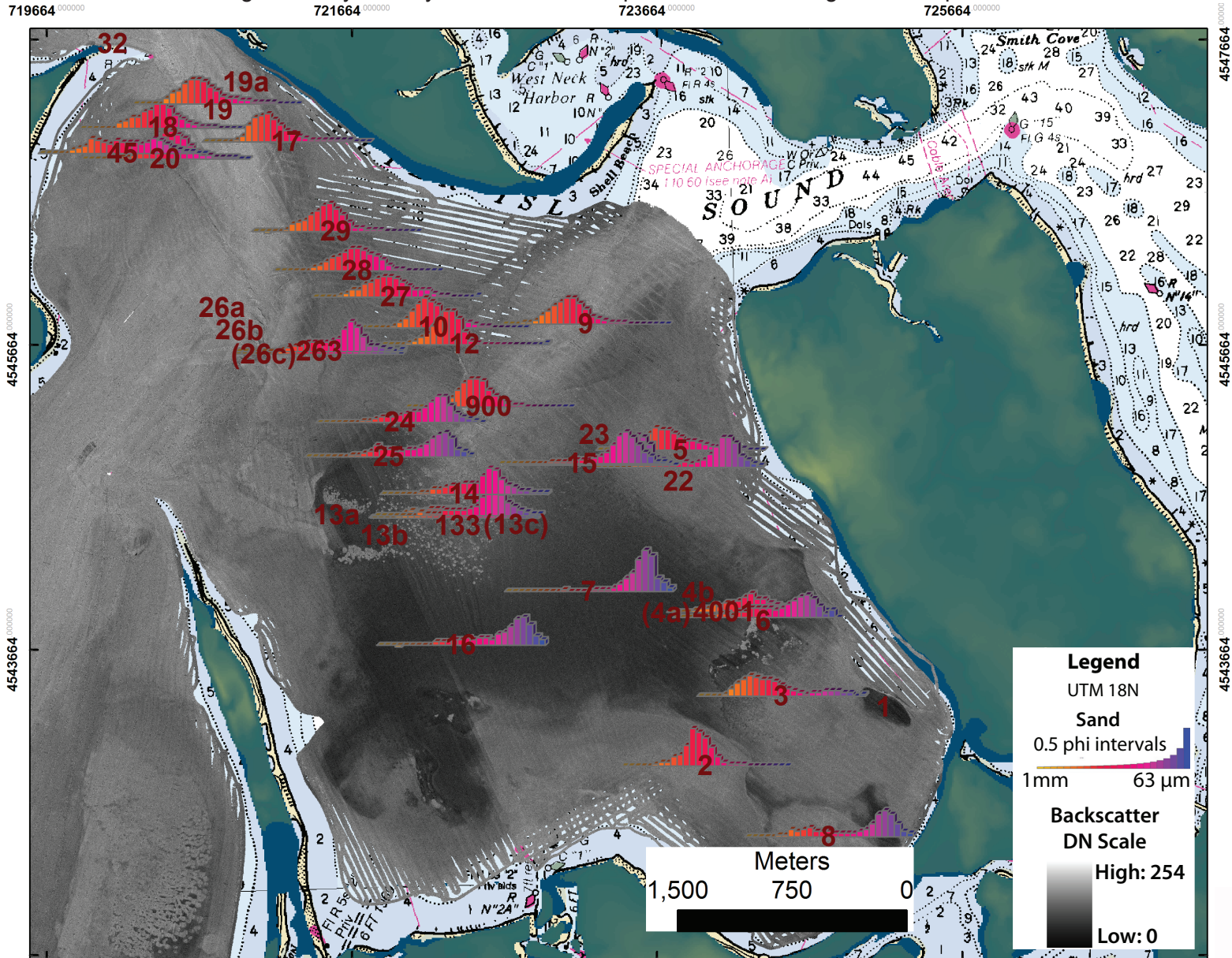
Fig. A.8: Grain size of grabs in Central Little Peconic Bay 2008. Bottom right is in Little Peconic Bay near grabs 0b & 0a (mound) & 60 (mud). Mound sites appear coarser in gravel as shell hash. Bar graphs show the 1mm-63μm sand fraction. Presence of oyster shells shown by red circles. A bimodal pattern can be seen at oyster mounds, with a large magenta-purple peak and a smaller second coarser peak (orange).

247
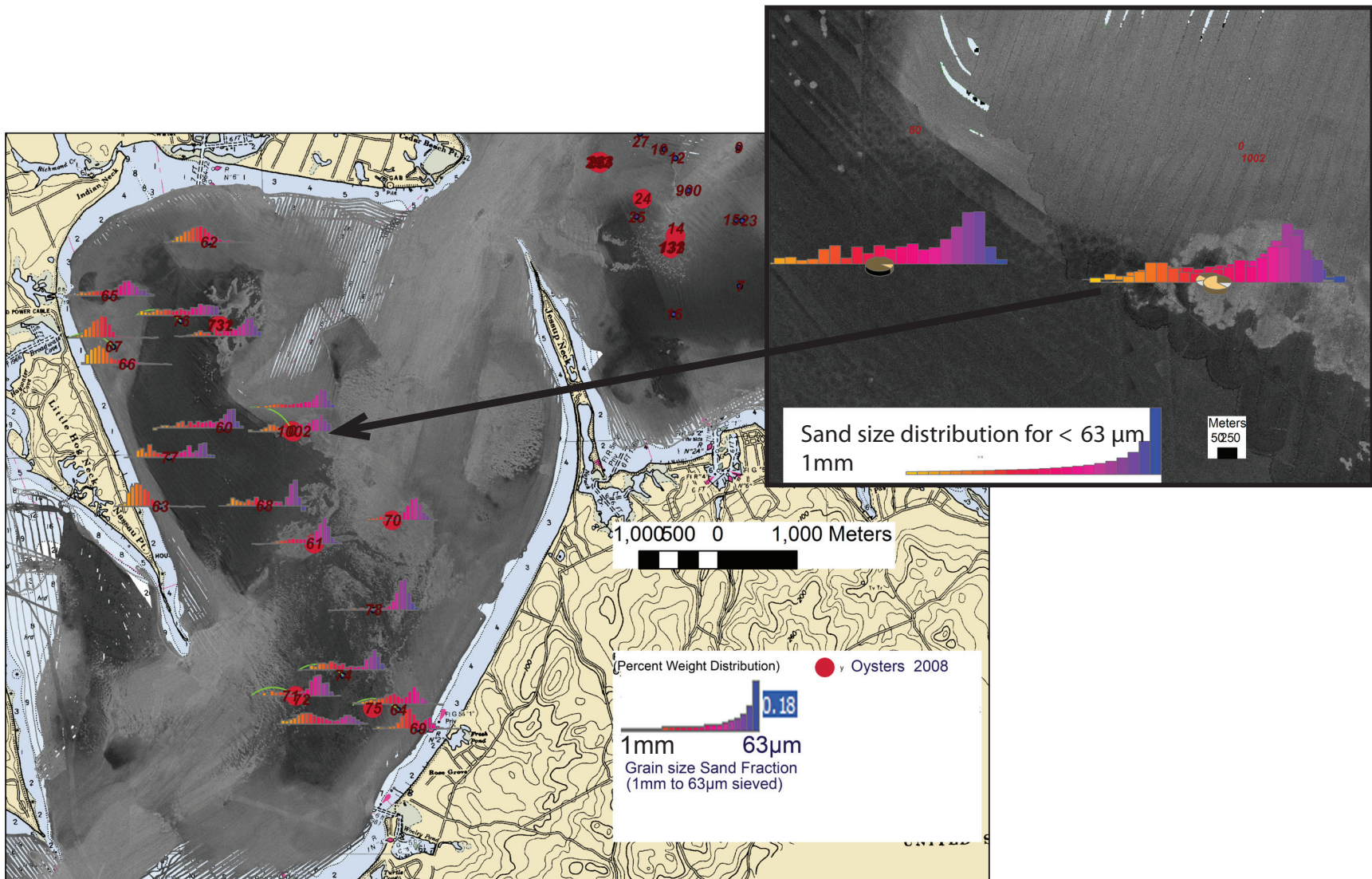
Fig. A.9: Percentage mud, sand and gravel in sediment matrix. Pie charts show percentages and oyster presence are marked on top of backscatter map.
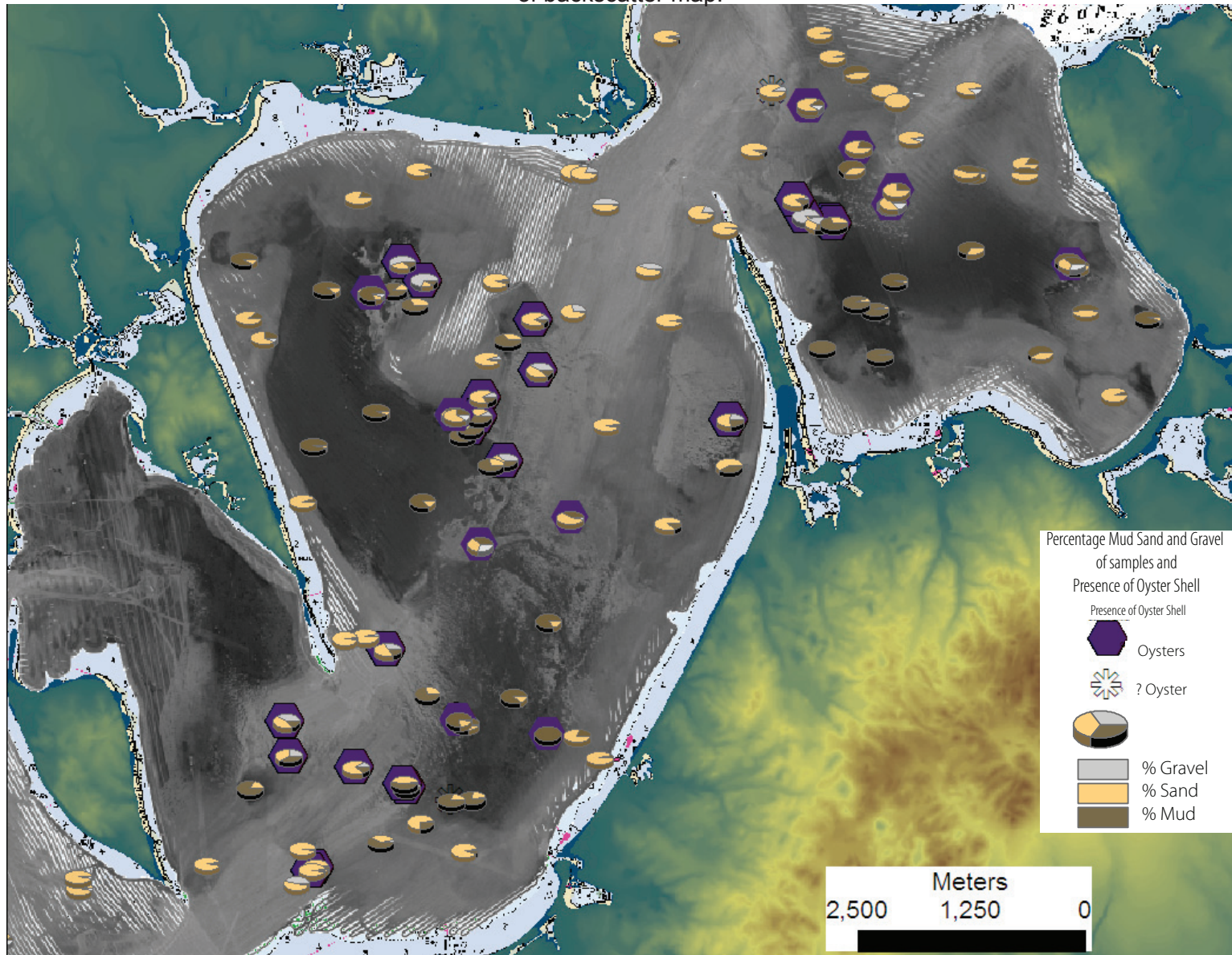
Fig. A.10: Map with backscatter and visual description of samples.

249
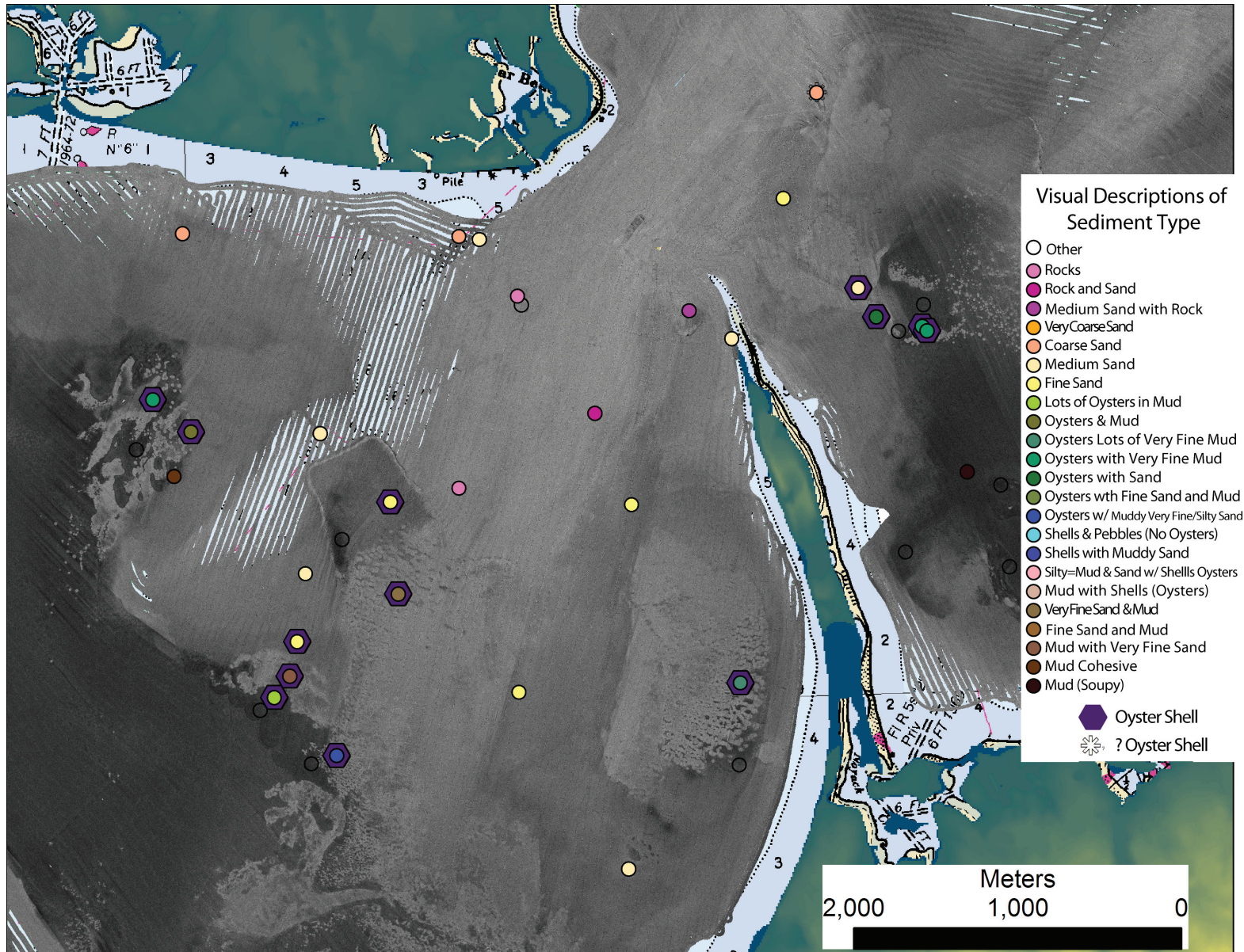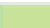
Fig. A.11 Map with backscatter characterized visually and by QTC program. Associated sediments are described.

Categorization By Backscatter Values
with Associated Sediments

- high basckatter/ coarse sediment
- med high backscatter/ medium coarse sediment
- moderate backcatter difference / mounds
- high and low backscatter/ mounds
- medium backscatter/ intermediate grain sizes
- lower backscatter/ medium sand and silts with mud
- low backscatter fine grained muds

1,000
Meters

250
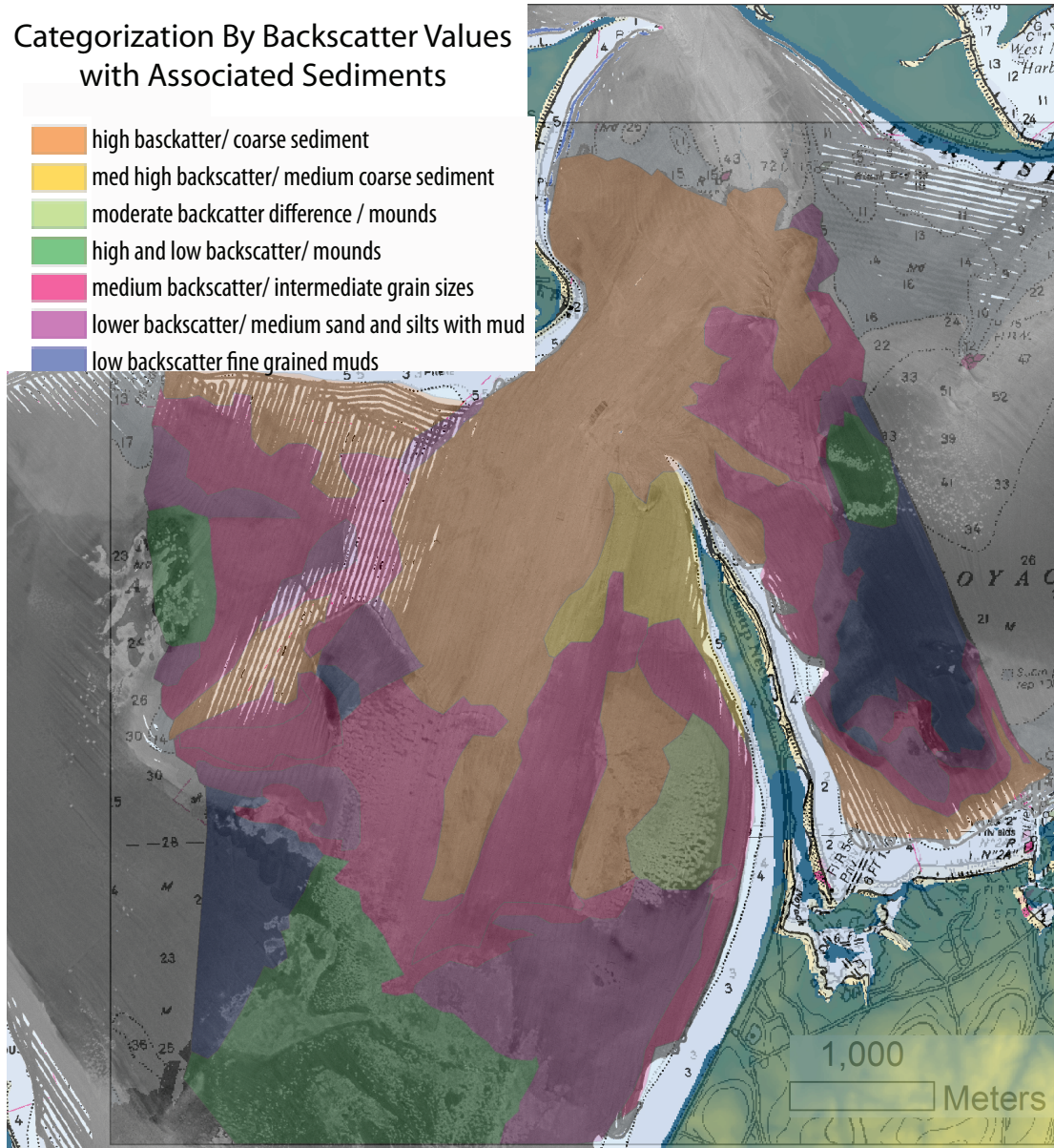
Fig. A.12: Profile of mounds lining channel near Jessup's Neck in Fledermaus. Second Horizon beneath mounds can be clearly seen. More buried mounds were found as well.
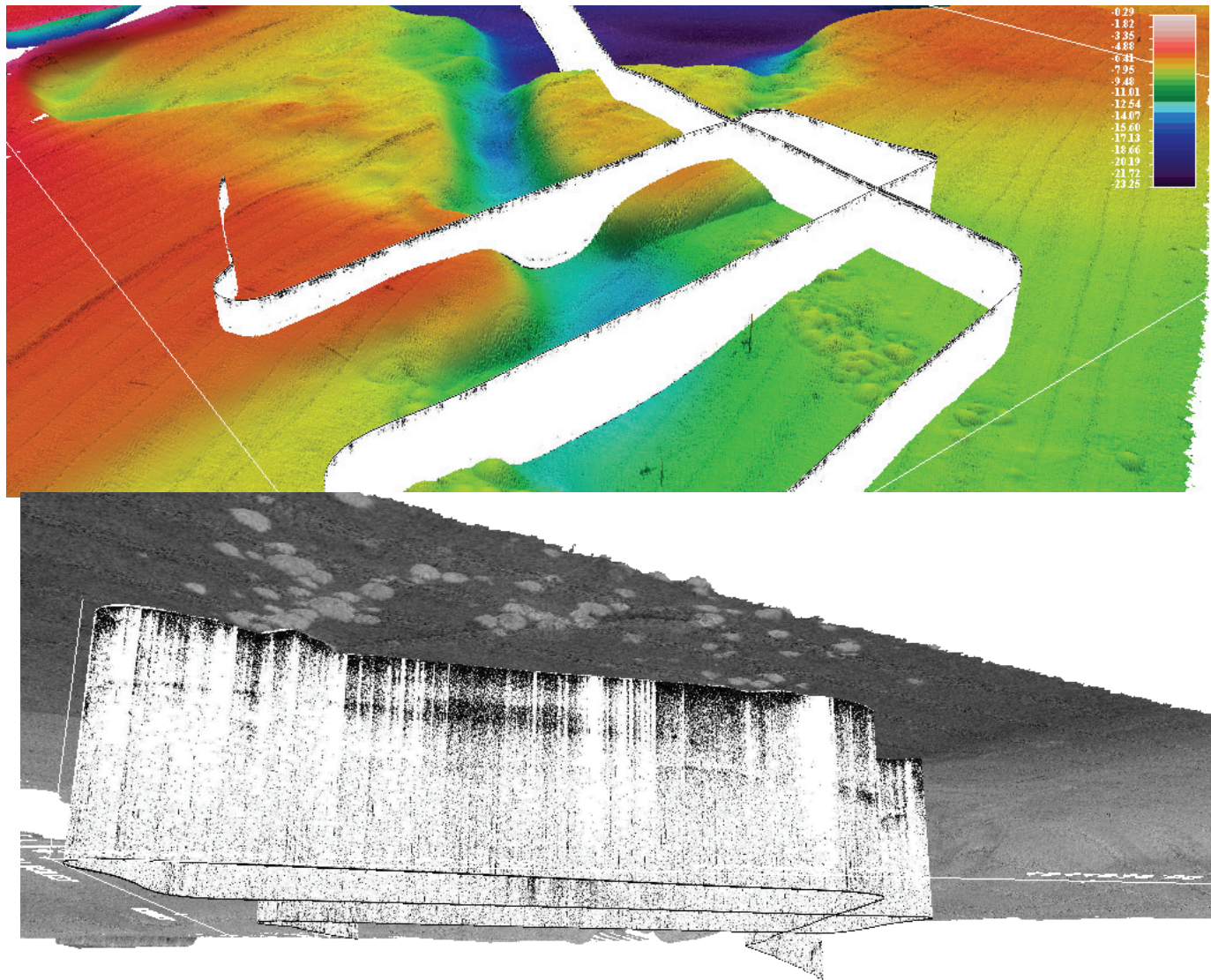
APPENDIX B: SHELLS AND GRAIN SIZE

Table B1.1: Peconic Estuary 2006 sample location and visual description. VF=very fine sand, VFM=very fine mud, FS= fine sand, MS=medium sand, Sh=shell, VS, SS=Silty Sand, frags=fragments. Sand classification in this table visually compared to standard scale card.

Survey Area	ID	Year	Code	Latitude	Longitude	Water Depth	Visual Description
Little Peconic Bay West	1	2006	70001	40.964	-72.412	7.8	Mud
Little Peconic Bay West	2	2006	70002	40.966	-72.441	13.33	Mud
Little Peconic Bay West	3	2006	70003	40.969	-72.436	11.18	Mud w/ VF sand
Little Peconic Bay West	4	2006	70004	40.979	-72.423	7.7	Coarse Sand
Little Peconic Bay West	5	2006	70005	40.975	-72.430	10.07	Very Coarse
Little Peconic Bay West	6	2006	70006	40.960	-72.425	9.95	Mud
Little Peconic Bay West	7	2006	70007	40.958	-72.433	7.91	Medium Sand
Little Peconic Bay West	8	2006	70008	40.958	-72.434	7.35	Oysters w/ FS &mud
Little Peconic Bay West	9	2006	70009	40.956	-72.436	4.23	Shells
Little Peconic Bay West	10	2006	70010	40.972	-72.414	9.81	Mud
Little Peconic Bay West	11d1	2006	70110	40.972	-72.423	9.29	Shell w/ muddy sand
Little Peconic Bay West	11d2	2006	70011	40.979	-72.423	7.79	Shell w/ muddy sand
Little Peconic Bay West	12	2006	70012	40.972	-72.413	9.86	Mud
Little Peconic Bay West	13	2006	70013	40.966	-72.421	8.06	Mud with Shells
Little Peconic Bay West	14	2006	70014	40.964	-72.415	7.74	Mud
Little Peconic Bay West	15	2006	70015	40.980	-72.428	2.7	Medium Sand
Little Peconic Bay West	16	2006	70016	40.962	-72.419	7.21	Fine sand & mud
Little Peconic Bay West	17	2006	70017	40.959	-72.414	5.98	Medium Sand
Little Peconic Bay West	18	2006	70018	40.959	-72.447	7.17	Medium Sand
Little Peconic Bay West	19	2006	70019	40.960	-72.435	8.92	Fine Sand
Little Peconic Bay West	20	2006	70020	40.972	-72.436	8.72	Silt=Mud&Sand w/Sh
Little Peconic Bay West	21	2006	70021	40.968	-72.428	9.58	Fine Sand
Little Peconic Bay West	22	2006	70022	40.975	-72.418	10.89	Mud
Little Peconic Bay West	23	2006	70023	40.966	-72.421	11.16	Mud w/ VF sand
Little Peconic Bay East	30	2006	70030	41.000	-72.412	9.26	Mud
Little Peconic Bay East	31	2006	70031	41.001	-72.411	9.74	Lots of Oysters in
Little Peconic Bay East	32	2006	70032	41.002	-72.410	8.61	Mud w/ VF sand
Little Peconic Bay East	33	2006	70033	41.004	-72.410	7.67	Fine Sand
Little Peconic Bay East	34	2006	70034	40.997	-72.407	10.81	Sh w/ muddy VS SS
Little Peconic Bay East	35	2006	70035	40.997	-72.409	10.3	Mud
Little Peconic Bay East	36	2006	70036	41.009	-72.406	11.26	Mud
Little Peconic Bay East	37	2006	70037	41.011	-72.402	19.37	Fine Sand
Little Peconic Bay East	38	2006	70038	41.006	-72.402	10.29	Very Fine Sand &mud
Little Peconic Bay East	39	2006	70039	41.012	-72.397	5.99	Rocks

Survey Area	ID	Year	Code	Latitude	Longitude	Water Depth	Visual Description
Little Peconic Bay East	40	2006	70040	41.008	-72.409	4.3	Medium Sand
Little Peconic Bay East	41	2006	70041	41.013	-72.418	8.02	Mud very cohesive
Little Peconic Bay East	42	2006	70042	41.017	-72.419	7.12	Oysters with VFM
Little Peconic Bay East	43	2006	70043	41.015	-72.421	7.4	Mud
Little Peconic Bay East	44	2006	70044	41.016	-72.417	10.08	Mud
Little Peconic Bay East	45	2006	70045	41.021	-72.380	11.11	(MS with Rock) Medium
Little Peconic Bay East	46	2006	70046	41.011	-72.358	6.13	Mud
Little Peconic Bay East	47	2006	70047	41.012	-72.361	6.28	Mud soupy
Little Peconic Bay East	48	2006	70048	41.008	-72.365	6.01	Mud
Little Peconic Bay East	49	2006	70049	41.007	-72.358	6.68	Mud
Little Peconic Bay East	50	2006	70050	41.021	-72.367	5.25	Oysters with sand
Little Peconic Bay East	51	2006	70051	41.020	-72.365	10.58	Mud
Little Peconic Bay East	52d1	2006	70520	41.020	-72.363	12.01	Oysters with VFM
Little Peconic Bay East	52d2	2006	70521	41.020	-72.363	10.06	Oysters with VFM
Little Peconic Bay East	52A	2006	70052	41.021	-72.363	11.49	Mud
Little Peconic Bay East	53	2006	70053	41.022	-72.368	15.31	Medium Sand
Little Peconic Bay East	54	2006	70054	41.001	-72.377	8.28	Oysters lots VFM
Little Peconic Bay East	55	2006	70055	40.996	-72.378	10.09	Mud
Little Peconic Bay East	56	2006	70056	40.991	-72.386	7.74	Medium Sand
Little Peconic Bay East	57	2006	70057	41.026	-72.397	2.24	Coarse Sand
Little Peconic Bay East	58	2006	70058	41.026	-72.395	2.45	Medium Sand
Little Peconic Bay East	59	2006	70059	41.033	-72.371	10.83	Coarse Sand
Little Peconic Bay East	60	2006	70060	41.027	-72.373	22.16	Fine Sand
Little Peconic Bay East	61	2006	70061	41.020	-72.377	2.07	Medium Sand
Little Peconic Bay East	62	2006	70062	41.015	-72.407	2.83	Medium Sand
Little Peconic Bay East	63	2006	70063	41.039	-72.384	4.76	Coarse Sand
Little Peconic Bay East	64	2006	70064	41.026	-72.417	4.29	Coarse Sand
Little Peconic Bay East	65d1	2006	70650	41.022	-72.393	5.64	Rocks
Little Peconic Bay East	65d2	2006	70065	41.022	-72.393	5.68	Rocks
Little Peconic Bay East	66	2006	70066	41.016	-72.387	10.98	Rock and Sand
Little Peconic Bay East	67	2006	70067	41.011	-72.385	21.27	Fine Sand
Little Peconic Bay East	68	2006	70068	41.001	-72.394	12.51	Fine Sand
Great Peconic Bay West	1	2006	100001	40.922	-72.533	5.01	Mud with sand and shell (lots) jingle and slipper shells
Great Peconic Bay West	2	2006	100002	40.935	-72.537	6.4	Mud
Great Peconic Bay West	3	2006	100003	40.924	-72.560	5.12	Mud and shells, jingle shells, razor clam and barnacles

Survey Area	ID	Year	Code	Latitude	Longitude	Water Depth	Visual Description
Great Peconic Bay West	4	2006	100004	40.922	-72.548	6.29	Soft mud
Great Peconic Bay West	5	2006	100005	40.914	-72.526	6.46	Mud
Great Peconic Bay West	6	2006	100006	40.905	-72.501	6.94	Mud some grit present
Great Peconic Bay West	7	2006	100007	40.924	-72.519	6.64	Soft mud
Great Peconic Bay West	8	2006	100008	40.933	-72.557	5.2	Sand with slipper shells
Great Peconic Bay West	9	2006	100009	40.930	-72.577	3.29	Shells with mud and sand (lots of slipper shells)
Great Peconic Bay West	10	2006	100010	40.930	-72.574	1.49	Sand
Great Peconic Bay West	11	2006	100011	40.929	-72.568	2.03	Medium-fine beige quartz sand with a few shell frags
Great Peconic Bay West	13	2006	100013	40.942	-72.535	5.73	Sand with some shell
Great Peconic Bay West	14	2006	100014	40.939	-72.531	6.56	Cohesive mud with fine sand visible in mud matrix, dark grey brown surface/ dark grey underneath
Great Peconic Bay West	15	2006	100015	40.938	-72.531	6.6	Mud
Great Peconic Bay West	16	2006	100016	40.932	-72.536	6.67	Soft mud
Great Peconic Bay West	17	2006	100017	40.932	-72.538	6.55	Soft mud
Great Peconic Bay West	18	2006	100018	40.931	-72.555	6.24	Mud
Great Peconic Bay West	19	2006	100019	40.931	-72.562	5.66	Mud
Great Peconic Bay West	20	2006	100020	40.914	-72.513	6.74	Mud
Great Peconic Bay West	21	2006	100021	40.914	-72.514	6.79	Mud
Great Peconic Bay West	22	2006	100022	40.915	-72.515	6.77	Mud
Great Peconic Bay West	23	2006	100023	40.918	-72.550	1.96	Very clean sand with 1 slipper shell
Great Peconic Bay West	24	2006	100024	40.922	-72.562	3.49	Mud with sand, pebbles and a lot of shells of many species
Great Peconic Bay West	25	2006	100025	40.927	-72.569	3.04	Sand
Great Peconic Bay West	26	2006	100026	40.946	-72.532	2.45	Sand, 1 snail and empty bleached snail shells
Great Peconic Bay West	27	2006	100027	40.909	-72.501	7.21	Mud
Great Peconic Bay West	28	2006	100028	40.904	-72.503	4.93	Sand with a little mud
Great Peconic Bay West	29	2006	100029	40.940	-72.549	1.63	Sand, mostly quartz
Great Peconic Bay West	30	2006	100030	40.938	-72.548	1.68	Sand
Great Peconic Bay West	31	2006	100031	40.927	-72.571	3.32	Quartz sand (beige) with a few shell frags

Survey Area	ID	Year	Code	Latitude	Longitude	Water Depth	Visual Description
Great Peconic Bay West	32	2006	100032	40.926	-72.572	3.26	Coarse sand (beige), mostly quartz
Great Peconic Bay West	34	2006	100034	40.925	-72.542	5.21	Sand with mud and shells, mostly shells (oyster shell)
Great Peconic Bay West	35	2006	100035	40.928	-72.559	4.94	Mud with sand and lots of shells
Great Peconic Bay West	36	2006	100036	40.946	-72.551	2.07	Sand beige-grey mostly quartz with a tiny bit of mud
Great Peconic Bay West	37	2006	100037	40.928	-72.580	2.13	Well sorted sand (tiny % mud)
Great Peconic Bay West	38	2006	100038	40.930	-72.532	6.57	Soft mud
Great Peconic Bay West	39	2006	100039	40.933	-72.505	6.6	Soft mud
Great Peconic Bay West	40	2006	100040	40.931	-72.522	6.43	Mud
Great Peconic Bay West	41	2006	100041	40.907	-72.511	5.31	Sand with some shells
Great Peconic Bay West	42	2006	100042	40.902	-72.510	2.43	Clean sand with practically no shells
Great Peconic Bay West	43	2006	100043	40.944	-72.558	1.76	Quartz sand with a few shell frags
Great Peconic Bay West	44	2006	100044	40.916	-72.541	2.48	Coarse sand with shell
Great Peconic Bay West	45	2006	100045	40.938	-72.560	3.78	Medium-coarse sand with slipper shells
Great Peconic Bay West	46	2006	100046	40.914	-72.533	3.78	Sand with mud and shell
Great Peconic Bay West	47	2006	100047	40.949	-72.545	1.83	Sand with mud and shell hash
Great Peconic Bay West	48	2006	100048	40.941	-72.541	5.53	Sand with shells (jingle and slipper shells)
Great Peconic Bay West	49	2006	100049	40.908	-72.518	5.39	Sand with mud and some shells
Great Peconic Bay West	50	2006	100050	40.927	-72.529	5.63	Sand with mud and lots of slipper shells
Great Peconic Bay West	51	2006	100051	40.921	-72.558	2.33	Coarse sand
Great Peconic Bay West	52	2006	100052	40.916	-72.520	6.37	Mud
Great Peconic Bay West	53	2006	100053	40.926	-72.573	2.45	Brown beige to grey mostly quartz sand with a few shells
Great Peconic Bay West	54	2006	100054	40.922	-72.554	5.08	Mud with sand and slipper and jingle shells
Great Peconic Bay West	55	2006	100055	40.938	-72.556	3.76	Sand

Survey Area	ID	Year	Code	Latitude	Longitude	Water Depth	Visual Description
Great Peconic Bay West	56	2006	100056	40.938	-72.552	2.57	Sand with some shell, looks very clean
Great Peconic Bay West	57	2006	100057	40.928	-72.546	7.49	Mud with lots of shells and some sand
Great Peconic Bay West	58 (0)	2006	100580	40.905	-72.521	2.85	Shells in jaw, sample washed out
Great Peconic Bay West	58 (1)	2006	100058	40.905	-72.521	2.87	Sand with lots of shells (slipper shells mostly), 1 scallop shell, 1 snail, seaweed?
Great Peconic Bay West	59	2006	100059	40.934	-72.543	6.49	Mud with sand
Great Peconic Bay West	60	2006	100060	40.936	-72.527	6.34	Mud
Great Peconic Bay West	61	2006	100061	40.920	-72.521	6.16	Mud with sand and a few shells
Orient Delta	60-OD	2006	110060	41.102	-72.241	6.97	Sand and some mud
Orient Delta	61-OD	2006	110061	41.106	-72.255	9.28	Soft mud
Orient Delta	62	2006	110062	41.112	-72.232	10.44	Soft mud
Orient Delta	64	2006	110064	41.094	-72.224	10.44	Mud with a small amount of grit and a few shells
Orient Delta	65	2006	110065	41.094	-72.228	10.34	Soft mud
Orient Delta	66	2006	110066	41.095	-72.227	10.22	Soft mud with large shell and a little grit
Orient Delta	67	2006	110067	41.089	-72.248	6.79	Mud with some shell present
Orient Delta	68	2006	110068	41.087	-72.248	7.95	Fine sand with mud (some shell hash)
Orient Delta	69	2006	110069	41.090	-72.250	6.49	Sand with mud
Orient Delta	70	2006	110070	41.100	-72.260	14.35	Soft mud with a small amount of grit
Orient Delta	73	2006	110073	41.102	-72.267	7.48	Sand some mud (includes shell and tube worm)
Orient Delta	74	2006	110074	41.115	-72.285	4.21	Coarse sand (clean)
Orient Delta	75	2006	110075	41.113	-72.286	3.41	Sand, shells and shell hash (with living slipper shells)
Orient Delta	76	2006	110076	41.117	-72.286	4.03	Soft mud with slipper shells (were alive)
Orient Delta	78	2006	110078	41.111	-72.284	5.01	Sand with mud, pebbles, rock (>4cm) and shells
Orient Delta	79	2006	110079	41.131	-72.249	6.59	Sand with some mud

Survey Area	ID	Year	Code	Latitude	Longitude	Water Depth	Visual Description
Orient Delta	80	2006	110080	41.132	-72.250	7.02	Soft mud with lots of slipper shells (living) in large clumps
Orient Delta	81 (2)	2006	110081	41.133	-72.249	5.61	Coarse sand with lots of pebbles and some shells (slipper, oyster and scallop)
Orient Delta	82	2006	110082	41.133	-72.249	5.79	Coarse sand some mud
Orient Delta	86	2006	110086	41.128	-72.250	9.73	Mud with some grit
Orient Delta	90	2006	110090	41.108	-72.238	8.99	Soft mud with small amount of grit
Orient Delta	92	2006	110092	41.109	-72.255	8.29	Soft mud with some fine sand
Orient Delta	93	2006	110093	41.123	-72.261	6.33	Sand with some mud and slipper shells (alive when collected)
Orient Delta	98	2006	110098	41.117	-72.286	3.03	Sand
Orient Delta	100	2006	110100	41.116	-72.289	3.08	Sand with lots of slipper shells (alive when collected)
Orient Delta	101	2006	110101	41.094	-72.282	4.75	Medium sand, well sorted
Orient Delta	104	2006	110104	41.089	-72.279	4.43	Shells with sand and mud (lots of slipper shells together)
Orient Delta	106	2006	110106	41.101	-72.291	16.16	Coarse sand and shell hash with some shells
Orient Delta	108	2006	110108	41.095	-72.292	4.59	Sand and large shells
Orient Delta	109	2006	110109	41.098	-72.293	6.61	Medium-coarse sand plus shell hash lots of small old slipper shells
Orient Delta	111	2006	110111	41.118	-72.252	9.36	Soft mud with a few shells and a little grit
Orient Delta	112	2006	110112	41.089	-72.229	10.18	Soft mud (tube worms) with a few shells a little grit
Orient Delta	116	2006	110116	41.104	-72.302	4.96	Sand, shell hash and pebbles with lots of shells (slipper, jingle)
Orient Delta	117 (0)	2006	111170	41.102	-72.302	22.39	A rock

Survey Area	ID	Year	Code	Latitude	Longitude	Water Depth	Visual Description
Orient Delta	1370A	2006	111371	41.085	-72.267	5.76	Slipper shells and rocks
Orient Delta	1370B	2006	111370	41.085	-72.267	5.78	Mud with sand and shells (slipper shells)
Pipes Cove	131	2006	110131	41.088	-72.369	8.51	Mud with some shells, little grit
Pipes Cove	132	2006	110132	41.089	-72.369	7.84	Sand with mud
Pipes Cove	134	2006	110134	41.091	-72.366	3.83	Sand
Pipes Cove	139	2006	110139	41.090	-72.376	3.83	Sand with mud
Pipes Cove	140	2006	110140	41.090	-72.375	4.73	Mud with fine sand and buried shells (~1cm, lots of slipper shells, scallop pieces), red worms present
Pipes Cove	141	2006	110141	41.088	-72.373	9.01	Mud with some sand and shell
Pipes Cove	142	2006	110142	41.088	-72.372	9.87	Mud with lots of sand and small shells
Pipes Cove	145	2006	110145	41.088	-72.375	6.86	Mud with sand and large shells (oyster)
Pipes Cove	146	2006	110146	41.087	-72.381	2.57	Soft mud with sand
Pipes Cove	148	2006	110148	41.087	-72.377	5.12	Mud with sand and lots of shells (slipper shells)
Pipes Cove	150	2006	110150	41.092	-72.373	1.77	Sand with mud
Pipes Cove	151	2006	110151	41.091	-72.367	9.49	Sand with mud, large shells, jingle shells scallops, and live worms
Pipes Cove	152	2006	110152	41.092	-72.369	3	Sand with a very small amounts of mud
Pipes Cove	153	2006	110153	41.086	-72.371	4.53	Sand with lots of mud and shell
Pipes Cove	154	2006	110154	41.090	-72.371	2.71	Sand with mud
Pipes Cove	155	2006	110155	41.086	-72.376	8.56	Mud with lots of shells
Pipes Cove	156	2006	110156	41.091	-72.372	1.92	Coarse sand with mud
Pipes Cove	157	2006	110157	41.090	-72.366	4.52	Sand with a tiny amount of mud
Pipes Cove	160	2006	110160	41.091	-72.377	4.08	Mud with large shells
Pipes Cove	164	2006	110164	41.089	-72.372	3.6	Sand with some mud

Survey Area	ID	Year	Code	Latitude	Longitude	Water Depth	Visual Description
Pipes Cove	168	2006	110168	41.089	-72.375	6.45	Sand with lots of mud, jingle shells, 1 rock 3cm
Pipes Cove	169	2006	110169	41.092	-72.370	1.7	Sand
Pipes Cove	174	2006	110174	41.086	-72.374	4.46	Sand with some mud at

Table B1.2: Peconic Estuary 2008 sample location and field visual description. Description based on field and lab notes.

Survey Area	ID	Planned ID	Code	Time Order	Time (GMT)	Latitude	Longitude	Water Depth (m)	Description
West Shelter Island	40	40	120040	1	06/19/2008 13:38	41.07125	-72.38865	-15.43	Sand. Medium dried 1 mm - 63 mm sediment is sand
West Shelter Island	43	43	120043	2	06/19/2008 13:48	41.06573	-72.39473	-14.74	Sand, lots of shells
West Shelter Island	33	33	120033	4	06/19/2008 13:52	41.06302	-72.39223	-15.48	Rocks, lots of mud, shell hash, pebbles. Large Shell (Anderrra ?), Tube worms, bryazoans attached to rocks.
West Shelter Island	39	39	120039	5	06/19/2008 14:02	41.06580	-72.38355	-8.37	Sand.
West Shelter Island	31	31	120031	6	06/19/2008 14:13	41.06322	-72.38985	-9.54	Sand.
West Shelter Island	36	36	120036	7	06/19/2008 14:21	41.05968	-72.37800	-8.43	Sand. Brown sand, tiny shrimps
West Shelter Island	42	42	120042	8	06/19/2008 14:28	41.05683	-72.37475	-6.77	Sand, oyster shells. Brown sand, fairly coarse
West Shelter Island	41	41	120041	9	06/19/2008 14:33	41.05647	-72.37558	-8.32	Sand. Brown and black sand, tubeworm casings
West Shelter Island	441	44 a	120441	10	06/19/2008 14:46	41.05870	-72.38933	-12.16	1st try - grab opened at surface -no sample
West Shelter Island	442	44 b	120442	11	06/19/2008 14:51	41.05828	-72.38900	-11.02	2nd try - grab opened at surface-no sample
West Shelter Island	44	44	120044	12	06/19/2008 14:53	41.05000	-72.38785	-3.15	Rocks and shells, plus sand.
West Shelter Island	341	34a	120341	13	06/19/2008 14:58	41.05858	-72.38112	-20.09	1st try - grab opened at surface-no sample
West Shelter Island	34	34	120034	14	06/19/2008 15:00	41.05870	-72.38053	-18.55	Rocks and shells, plus sand.
West Shelter Island	37	37	120037	16	06/19/2008 15:12	41.05220	-72.38368	-5.16	Rocks & slipper shells (living) plus sand. Two crabs, red seaweed.
West Shelter Island	38	38	120038	17	06/19/2008 15:19	41.05253	-72.39342	-10.13	Mud, oyster shells, and sand. Mud with sand -brownish mud to dark grey with frequent shell fragments visible. Sea stars, pebbles also present.

Survey Area	ID	Planned ID	Code	Time Order	Time (GMT)	Latitude	Longitude	Water Depth (m)	Description
West Shelter Island	49	49	120049	18	06/19/2008 15:27	41.05258	-72.39500	-8.43	Mud, oyster shells, and sand. Mud with sand -brownish mud to dark grey frequent shell fragments visible
West Shelter Island	35	35	120035	19	06/19/2008 15:33	41.05618	-72.39967	-5.33	Sand with shell fragments. Brown and black sand, a little greenish, broken shell fragments. Has two layers - one like soup and one more solid.
West Shelter Island	481	48a	120481	20	06/19/2008 15:36	41.05702	-72.40193	-6.25	1st attempt
West Shelter Island	48	48	120048	21	06/19/2008 15:38	41.05697	-72.40202	-6.24	Sand, mud, a couple of rocks. Brown and black sediment, very smooth mud component. Two layers-bottom is sandier
West Shelter Island	30	30	120030	22	06/19/2008 15:44	41.05813	-72.40285	-6.08	Mud. Green/grey/brown to dark grey mud, very wet & mushy, Can't feel grit through bag. Can see some larger particles.
West Shelter Island	47	47	120047	23	06/19/2008 15:49	41.05958	-72.40067	-7.96	Mud with shell, shell hash visible, and sand. Cohesive brown/grey mud to grey/ black, (slightly browner than other muds). Can feel grit, large shell pieces in bag Oyster?, sea stars, and burrows
West Shelter Island	21	21	120021	24	06/19/2008 15:53	41.06085	-72.40177	-8.26	Mud with sand, fine shell and rocks. Very mushy grey mud has visible large several cm size & heavy, rounded egg shape rock, another pebble, and shell fragments.
West Shelter Island	46	46	120046	25	06/19/2008 15:58	41.05965	-72.38810	-4.90	Mud with sand. Very cohesive sticky green/grey/ brown to dark grey/black mud. Can feel grit & see a few shells.
Noyack Bay	18	18	120018	26	06/19/2008 16:38	41.04513	-72.37738	-5.69	Sand with shell hash, shells and seaweed.
Noyack Bay	191	19a	120191	27	06/19/2008 16:44	41.04648	-72.37318	-23.58	Sand with shell hash. Jelly fish on grab.

Survey Area	ID	Planned ID	Code	Time Order	Time (GMT)	Latitude	Longitude	Water Depth (m)	Description
Noyack Bay	19	19	120019	28	06/19/2008 16:48	41.04610	-72.37308	-23.36	Pebbles and sand. Lots of large pebbles greater than 2cm (Rocks), lots of shell hash and coarse sand.
Noyack Bay	20	20	120020	29	06/19/2008 16:53	41.04332	-72.37730	-4.26	Black sand, and oyster shell, shell hash. Smelly.
Noyack Bay	45	45	120045	30	06/19/2008 16:58	41.04373	-72.38060	-6.69	Sand, shell hash, and pebbles
Noyack Bay	17	17	120017	31	06/19/2008 17:07	41.04413	-72.36782	-8.08	Brown sand and small oyster shells
Noyack Bay	29	29	120029	32	06/19/2008 17:14	41.03875	-72.36415	-3.71	Sand. Two layers of sand, dark layer on bottom.
Noyack Bay	28	28	120028	33	06/19/2008 17:19	41.03638	-72.36258	-4.41	Sand.
Noyack Bay	27	27	120027	34	06/19/2008 17:23	41.03477	-72.35963	-4.42	Sand. Two layers of sand, dark layer on bottom.
Noyack Bay	10	10	120010	35	06/19/2008 17:29	41.03288	-72.35602	-4.30	Sand. Hermit crab.
Noyack Bay	12	12	120012	36	06/19/2008 17:34	41.03185	-72.35440	-3.81	Sand with some small shells. Course sand.
Noyack Bay	9	9	120009	37	06/19/2008 17:41	41.03283	-72.34493	-10.73	Sand with lots of shells. Orange coloring
Noyack Bay	5	5	120005	38	06/19/2008 17:49	41.02523	-72.33785	-6.78	Coarse brown and black sand with mud. "Cohesive dry globs" present.
Noyack Bay	4001	4a	124001	39	06/19/2008 17:56	41.01555	-72.33273	-8.08	Mud. Black mud under surface brown mud layer. Green/grey/brown to dark grey mud, no grit. Very wet & mushy mud, kind of soupy - something small & hard (shell? In bag).
Noyack Bay	4002	4b	124002	41	06/19/2008 18:08	41.01523	-72.33228	-8.07	Mostly oyster shells.
Noyack Bay	3	3	120003	42	06/19/2008 18:13	41.01055	-72.33058	-7.47	Mud. Green/grey/brown to grey mud, very wet & mushy, can feel some grit through bag. One large lump of something hard (shell?). Can see larger particles/grit. Upon dissaggregation - can see small gravel stones & coarse sand grains.

Survey Area	ID	Planned ID	Code	Time Order	Time (GMT)	Latitude	Longitude	Water Depth (m)	Description
Noyack Bay	1	1	120001	43	06/19/2008 18:19	41.00970	-72.32260	-7.72	Mud. Almost black, green/grey/brown to dark grey mud, very wet & mushy (soupy). Can't feel grit through bag. Looks very smooth like mostly clay with no sand. Smelly.
Noyack Bay	8	8	120008	44	06/19/2008 18:30	41.00217	-72.32722	-5.71	Sand with mud. Almost black, Green-brown muddy sand, some tiny broken shells (small slipper shells) and small tubeworms.
Noyack Bay	2	2	120002	45	06/19/2008 18:37	41.00657	-72.33667	-4.85	Mud and sand. Dark, green/brown - a lot of water in the bag.
Noyack Bay	16	16	120016	46	06/19/2008 18:46	41.01412	-72.35540	-6.27	Mud. Dark, grey/brown/green tinge (slightly browner than 6) to dark grey mud. Smooth, very wet & mushy, can't feel grit through bag. Can see some larger particles (small clam shell/bivalve ~1cm was in subsample not visible until disaggregated in beaker)
Noyack Bay	7	7	120007	47	06/19/2008 18:55	41.01707	-72.34532	-6.82	Mud. Almost black, green/grey/brown to very very dark grey mud, very wet & mushy, can't feel grit through bag. Can see some larger particles, a few small shell fragments.

Survey Area	ID	Planned ID	Code	Time Order	Time (GMT)	Latitude	Longitude	Water Depth (m)	Description
Noyack Bay	23	23	120023	49	06/19/2008 19:11	41.02452	-72.34468	-8.15	Mud, shell hash, pebbles, sand. Green/grey/brown with lots of dark black/grey mud, mushy - quite a few shell pieces present looks pretty smooth.
Noyack Bay	15	15	120015	50	06/19/2008 19:16	41.02462	-72.34555	-8.02	Mud and sand, shell hash, pebbles and a shell. Leaves in sample. Looks like a cohesive mud with sands (brown - lots of dark black underneath), brown sand clearly visible (large shell (scallop) present sample bag), brown oak leaf in sample (something like a red or pin oak, pointed lobes), polychaetes.
Noyack Bay	900	900	120900	51	06/19/2008 19:23	41.02813	-72.35267	-11.87	Sand, shell hash, pebbles.
Noyack Bay	131	13a	120131	52	06/19/2008 19:30	41.02167	-72.35568	-12.09	Sandy mud, brown, includes an oyster shell. Two attached shell pieces, little broken shells. Mud dark.
Noyack Bay	132	13b	120132	53	06/19/2008 19:33	41.02163	-72.35557	-11.44	Mostly oyster shells. Yellow sponge.
Noyack Bay	133	13c	120133	54	06/19/2008 19:36	41.02177	-72.35535	-10.97	Oyster shells present, with green brown sandy mud.
Noyack Bay	14	14	120014	55	06/19/2008 19:39	41.02302	-72.35480	-11.28	Muddy sand, oyster shells. Brown mud/sand.
Noyack Bay	25	25	120025	56	06/19/2008 19:47	41.02537	-72.36057	-10.90	Mud. Brown/grey/greenish tinged to dark black/grey mud, very wet & mushy, can feel very fine grit through bag. Can see some fine sized shell particles. Tubeworms.
Noyack Bay	24	24	120024	57	06/19/2008 19:51	41.02737	-72.35962	-10.75	Lots of oyster shells, dark, green/brown sandy mud.
Noyack Bay	261	26a	120261	58	06/19/2008 19:58	41.03155	-72.36580	-5.49	Sand and shell hash mix with oyster shells. Brown sand, lots of water in the bag, some broken oyster shells with spongy orange material attached.
Noyack Bay	262	26b	120262	59	06/19/2008 20:01	41.03163	-72.36617	-5.53	Oyster shells.

Survey Area	ID	Planned ID	Code	Time Order	Time (GMT)	Latitude	Longitude	Water Depth (m)	Description
Noyack Bay	263	26c	120263	60	06/19/2008 20:03	41.03170	-72.36573	-5.67	Oyster shells, sand.
Little Peconic Bay	62	62	120062	61	06/20/2008 13:05	41.02388	-72.42495	-5.72	Sandy mud. Sandy greenish mud, tubeworm casings, small shells.
Little Peconic Bay	731	73a	120731	62	06/20/2008 13:17	41.01443	-72.42372	-7.26	Oyster shells and mud. Green mud.
Little Peconic Bay	732	73b	120732	63	06/20/2008 13:19	41.01437	-72.42360	-7.30	Oyster shells almost entirely and a tiny bit of mud. Shells stained orange.
Little Peconic Bay	76	76	120076	64	06/20/2008 13:25	41.01502	-72.42947	-6.51	Mud. Dark grey gooey mud. Black layer of mud beneath green mud, huge tubeworm casing.
Little Peconic Bay	65	65	120065	65	06/20/2008 13:32	41.01813	-72.44013	-6.03	Mud. Green mud, grey/ black mud and lots of tubeworm casings.
Little Peconic Bay	67	67	120067	66	06/20/2008 13:38	41.01230	-72.43973	-4.49	Mud and sand. Some shells. Grey, green sediment.
Little Peconic Bay	66	66	120066	67	06/20/2008 13:43	41.01030	-72.43780	-5.64	Coarse sandy mud with rocks. Almost Black.
Little Peconic Bay	77	77	120077	68	06/20/2008 13:51	40.99955	-72.43178	-6.28	Black/green -grey gooey mud. Sea stars.
Little Peconic Bay	63	63	120063	69	06/20/2008 13:56	40.99402	-72.43340	-4.25	Sand (coarse) with a little shell hash, shells, and very little mud. Grey/brown. Tubeworms.
Little Peconic Bay	60	60	120060	70	06/20/2008 14:18	41.00275	-72.42350	-7.70	Mud. Tubworms, including a fat worm tube in mud. Sea stars. Black, "very mushy" mud.
Little Peconic Bay	0	0a	120000	71	06/20/2008 14:24	41.00215	-72.41327	-11.31	Oyster shells, mud. Green mud.
Little Peconic Bay	1002	0b	121002	72	06/20/2008 14:29	41.00208	-72.41303	-12.91	Grey sandy mud w/ big oyster shells. Green/ black mud. 0b~ subsample brown sand mud- oyster shells (mushier mud on surface/ stiffer sandier with large shells below (more compact?) little bivalve clam shells present in mud). Shrimp? Light colored with big shell.
Little Peconic Bay	68	68	120068	73	06/20/2008 14:35	40.99373	-72.41778	-7.75	Mud. Brown/black, grey gooey mud with sea stars.

Survey Area	ID	Planned ID	Code	Time Order	Time (GMT)	Latitude	Longitude	Water Depth (m)	Description
Little Peconic Bay	61	61	120061	74	06/20/2008 14:41	40.98927	-72.41043	-9.00	Oyster Shells in sand with Mud on top. More mud than 73. "Gushy" mud in top layer.
Little Peconic Bay	70	70	120070	75	06/20/2008 14:48	40.99165	-72.39858	-9.79	Oyster shells, mud with sand. Broken oyster shells and other shells. Smooth brown mud.
Little Peconic Bay	78	78	120078	76	06/20/2008 14:56	40.98153	-72.40183	-9.61	Mud. Gooey green/black, grey mud with thin layer of brown mud above. Lots of sea stars.
Little Peconic Bay	74	74	120074	77	06/20/2008 15:03	40.97418	-72.40668	-9.06	Mud. Black, grey gooey "goopy" mud with thin layer of brown mud above.
Little Peconic Bay	75	75	120075	79	06/20/2008 15:08	40.97037	-72.40235	-8.73	Oyster shells with mud & fine sand (top only). Brown mud. Large shells-oyster shell pieces.
Little Peconic Bay	64	64	120064	80	06/20/2008 15:15	40.97008	-72.39857	-7.02	Sand with mud and broken shells. Thin layer of brown sediment on top of black sediment.
Little Peconic Bay	69	69	120069	81	06/20/2008 15:20	40.96787	-72.39572	-3.99	Sand with some shells and a little bit of mud. Fine sand.
Little Peconic Bay	72	72	120072	82	06/20/2008 15:29	40.97157	-72.41303	-10.01	Mud. Gooey grey mud. Lots of sea stars and tube worms.
Little Peconic Bay	71	71	120071	83	06/20/2008 15:33	40.97202	-72.41388	-8.42	Mud with sand and oyster shells. Mushy mud on top of muddy sand with lots of oyster shells. Can feel grit.
Great Peconic Bay	108	108	120108	84	06/20/2008 16:22	40.95648	-72.46400	-2.94	Coarse sand with shell pieces. Sandy brown with shells with reduced, black area.
Great Peconic Bay	107	107	120107	85	06/20/2008 16:25	40.95762	-72.46407	-2.99	Sand with shell pieces. Coarse sand. Lots of shells, tube worms, sandy, grey/brown
Great Peconic Bay	106	106	120106	86	06/20/2008 16:37	40.98182	-72.47710	-6.56	Sand with shell pieces. Coarse brown sand with patches of black and shells and worms
Great Peconic Bay	93	93	120093	87	06/20/2008 16:46	40.97745	-72.49397	-2.78	Sand. Clean sand with live snails.

Survey Area	ID	Planned ID	Code	Time Order	Time (GMT)	Latitude	Longitude	Water Depth (m)	Description
Great Peconic Bay	98	98	120098	89	06/20/2008 17:01	40.96680	-72.50623	-5.35	Sand with shells, a little bit of mud, pebble. Fine sand, shrimp.
Great Peconic Bay	97	97	120097	90	06/20/2008 17:06	40.96855	-72.50088	-3.61	Sand, and shells. Medium to fine sand, Slipper shells - 5 cm high, dark brown fairly course (medium) sand, shells.
Great Peconic Bay	92	92	120092	91	06/20/2008 17:14	40.97070	-72.48887	-5.46	Sand with mud and shells. Slipper shells stacked 7 cm high, seaweed clot on the way down, hydra/sponge coral
Great Peconic Bay	91	91	120091	92	06/20/2008 17:21	40.95923	-72.48945	-6.42	Sandy mud. Brown sand
Great Peconic Bay	89	89	120089	93	06/20/2008 17:33	40.95447	-72.52017	-4.87	Sand and mud with lots of shells, shell hash. Live slipper shells. Sponge. Old jingle shells. Brown sediment.
Great Peconic Bay	99	99	120099	94	06/20/2008 17:42	40.95057	-72.49643	-6.53	Mud. Gooey dark, brown mud. Sea stars and tubeworms.
Great Peconic Bay	102	102	120102	95	06/20/2008 17:48	40.94277	-72.49110	-6.60	Mud. Gooey dark grey, brown mud. Worms and sea stars.
Great Peconic Bay	84	84	120084	96	06/20/2008 17:54	40.95200	-72.48095	-5.82	Sand with mud, lots of shells. Brown sediment, "leaded" shells- small clam shells.
Great Peconic Bay	87	87	120087	97	06/20/2008 17:58	40.95160	-72.47455	-3.36	Sand with lots of shells. Gravel sized coarse sand. Red algae. Lots of good sized living slipper shells.
Great Peconic Bay	85	85	120085	98	06/20/2008 18:02	40.94753	-72.46930	-4.37	Sand with lots of shell. Fairly coarse sand.
Great Peconic Bay	88	88	120088	99	06/20/2008 18:09	40.93588	-72.46200	-3.83	Sand and shell pieces, with little shells. Brown sand with light grey underneath with shells.
Great Peconic Bay	81	81	120081	100	06/20/2008 18:13	40.93450	-72.45643	-8.04	Sandy mud. Dark grey.
Great Peconic Bay	83	83	120083	101	06/20/2008 18:20	40.93202	-72.47105	-8.55	Mud and a little sand with shells. Black, grey sediment

Survey Area	ID	Planned ID	Code	Time Order	Time (GMT)	Latitude	Longitude	Water Depth (m)	Description
Great Peconic Bay	86	86	120086	102	06/20/2008 18:24	40.93390	-72.47097	-8.23	Mud with stiffer sand and oyster layer below. One oyster shell, "spongy, orange animal in mud" (dead sponge).
Great Peconic Bay	80	80	120080	103	06/20/2008 18:28	40.93272	-72.47202	-8.68	Oyster shells, mud and sand, shell hash. Black, brown, green, mud.
Great Peconic Bay	82	82	120082	104	06/20/2008 18:34	40.92882	-72.47718	-7.58	Mud. Black gooey mud.
Great Peconic Bay	100	100	120100	105	06/20/2008 18:40	40.92860	-72.49050	-7.02	Mud. Black gooey mud with some shells and sea stars.
Great Peconic Bay	101	101	120101	106	06/20/2008 18:47	40.92008	-72.48530	-7.18	Mud. Black gooey mud with lots of tubeworms.
Great Peconic Bay	95	95	120095	107	06/20/2008 18:56	40.91262	-72.47470	-6.76	Mud and sand. Black. Shrimp, sea stars, and worms.
Great Peconic Bay	1111	111a	121111	108	06/20/2008 19:00	40.91115	-72.46857	-1.64	Sand. Well-sorted sand.
Great Peconic Bay	1112	111b	121112	109	06/20/2008 19:06	40.91078	-72.46825	-1.54	Sand. Well-sorted sand, with critters (worms).
Great Peconic Bay	90	90	120090	110	06/20/2008 19:17	40.92138	-72.50293	-6.75	Mud. Black gooey mud. Sea stars.
Great Peconic Bay	94	94	120094	111	06/20/2008 19:34	40.93982	-72.51132	-6.30	Mud. Black, dark grey gooey mud. Lots of tubeworms.

Table B1.3: Grain size and water content 2006. Percentage gravel, sand, mud and then clay and silt. Percentage Water Content and Loss on Ignition (LOI).

Survey Area	ID	Code	% Gravel	% Sand	% Mud (Silt+Clay)	%Silt	%Clay	% Water Content	% LOI
Little Peconic Bay West	1	70001	1.8	22.7	75.5	34.2	41.2	48.9	0.6
Little Peconic Bay West	2	70002	17.6	82.4	46.4	36.0	51.3	0.5	
Little Peconic Bay West	3	70003	24.6	34.5	40.9	23.7	17.2	39.8	
Little Peconic Bay West	4	70004	3.3	96.0	0.8	0.5	0.2	24.0	
Little Peconic Bay West	5	70005	100.0	50.4	49.6	22.0			
Little Peconic Bay West	6	70006	4.5	37.2	58.3	28.2	30.1	51.1	0.5
Little Peconic Bay West	7	70007	2.9	94.3	2.8	1.3	1.5	21.1	
Little Peconic Bay West	8	70008	6.6	91.1	2.3	1.4	0.9	15.8	
Little Peconic Bay West	9	70009	45.1	51.1	3.9	2.0	1.9	40.5	
Little Peconic Bay West	10	70010	4.8	34.6	60.6	31.0	29.5	44.7	0.4
Little Peconic Bay West	11d1	70110							
Little Peconic Bay West	11d2	70011	32.3	51.0	16.8	7.8	8.9	32.0	
Little Peconic Bay West	12	70012	11.2	88.8	46.4	42.5	54.4	0.6	
Little Peconic Bay West	13	70013	7.5	47.5	45.0	21.8	23.1	45.6	
Little Peconic Bay West	14	70014	0.9	20.7	78.5	34.5	44.0	57.3	0.6
Little Peconic Bay West	15	70015	1.0	97.8	1.1	0.7	0.5	23.9	
Little Peconic Bay West	16	70016	1.5	72.4	26.1	12.3	13.8	30.3	
Little Peconic Bay West	17	70017	1.8	90.7	7.5	4.3	3.2	25.0	
Little Peconic Bay West	18	70018	1.7	94.9	3.4	1.5	2.0	24.7	
Little Peconic Bay West	19	70019	0.8	95.4	3.8	1.8	2.0	21.9	
Little Peconic Bay West	20	70020	39.9	43.6	16.5	9.4	7.1	25.9	
Little Peconic Bay West	21	70021	12.1	73.3	14.6	7.7	7.0	24.4	
Little Peconic Bay West	22	70022	26.9	73.1	36.6	36.5	50.6	0.5	
Little Peconic Bay West	23	70023	1.6	47.6	50.9	26.3	24.6	43.5	
Little Peconic Bay East	30	70030	1.7	20.6	77.7	43.6	34.1	46.1	0.5
Little Peconic Bay East	31	70031	36.1	18.8	45.1	23.4	21.7	44.1	
Little Peconic Bay East	32	70032	9.6	36.0	54.4	27.6	26.8	45.3	
Little Peconic Bay East	33	70033	10.0	72.4	17.7	8.3	9.3	30.3	
Little Peconic Bay East	34	70034	39.0	23.0	38.0	21.1	16.9	38.0	
Little Peconic Bay East	35	70035	0.3	28.0	71.7	36.7	35.0	49.7	0.5
Little Peconic Bay East	36	70036	0.8	34.3	64.9	31.9	33.0	46.1	0.5
Little Peconic Bay East	37	70037	9.4	80.5	10.1	4.5	5.6	26.1	
Little Peconic Bay East	38	70038	40.0	47.0	12.9	7.3	5.7	28.0	
Little Peconic Bay East	39d1	70039	26.8	72.0	1.2	0.8	0.4	22.9	
Little Peconic Bay East	40	70040	6.8	88.6	4.7	2.0	2.7	21.8	
Little Peconic Bay East	41	70041	0.8	32.4	66.8	36.5	30.3	49.1	
Little Peconic Bay East	42	70042	55.1	30.5	14.4	8.8	5.6	30.0	
Little Peconic Bay East	43	70043	12.0	88.0	43.3	44.7	53.5	0.5	
Little Peconic Bay East	44	70044	70.3	18.7	11.0	6.8	4.2	26.6	0.3

Survey Area	ID	Code	% Gravel	% Sand	% Mud (Silt+Clay)	%Silt	%Clay	Water Content	% LOI
Little Peconic Bay East	45	70045	18.1	80.4	1.5	0.5	1.0	17.8	
Little Peconic Bay East	46	70046	4.7	95.3	46.2	49.1	60.1	0.6	
Little Peconic Bay East	47	70047	7.4	92.7	49.1	43.5	56.5	0.5	
Little Peconic Bay East	48	70048	0.1	99.9	51.0	48.8	53.8	0.5	
Little Peconic Bay East	49	70049	2.7	97.3	51.1	46.2	54.3	0.6	
Little Peconic Bay East	50	70050	83.3	11.4	5.3	3.2	2.1	18.1	
Little Peconic Bay East	51	70051	41.3	27.7	31.0	18.8	12.2	37.7	0.4
Little Peconic Bay East	52d1	70520	44.0	13.0	43.0	49.9			
Little Peconic Bay East	52d2	70521	57.1	18.4	24.5				
Little Peconic Bay East	52A	70052	1.0	31.4	67.6	33.6	34.0	45.4	0.4
Little Peconic Bay East	53	70053	5.3	82.1	12.5	7.2	5.3	20.8	
Little Peconic Bay East	54	70054	23.6	53.6	22.9	13.6	9.3	32.0	
Little Peconic Bay East	55	70055	1.0	57.4	41.6	22.6	19.0	34.5	0.4
Little Peconic Bay East	56	70056	1.2	85.9	12.9	5.8	7.1	20.8	
Little Peconic Bay East	57	70057	4.2	95.3	0.5	0.3	0.2	23.4	
Little Peconic Bay East	58	70058	18.5	80.5	1.0	0.5	0.5	25.4	
Little Peconic Bay East	59	70059	9.7	89.8	0.5	0.1	0.4	25.4	
Little Peconic Bay East	60	70060	0.8	91.4	7.8	3.0	4.8	22.2	
Little Peconic Bay East	61	70061	1.1	96.4	2.5	1.3	1.2	26.3	
Little Peconic Bay East	62	70062	1.4	93.0	5.7	1.6	4.0	24.7	
Little Peconic Bay East	63	70063	4.2	88.9	6.9	2.6	4.3	19.2	
Little Peconic Bay East	64	70064	1.5	91.3	7.2	3.4	3.8	17.8	
Little Peconic Bay East	65d1	70650	2.9	93.9	3.2				
Little Peconic Bay East	65d2	70065	50.1	47.4	2.5	1.1	1.4	28.0	
Little Peconic Bay East	66	70066	42.1	56.0	1.9	0.9	1.0	13.1	
Little Peconic Bay East	67	70067	1.7	95.0	3.4	1.7	1.6	20.9	
Little Peconic Bay East	68	70068	1.2	94.0	4.8	2.7	2.1	21.1	
Great Peconic Bay West	1	100001	16.1	71.9	12.0	5.6	6.3	20.9	0.8
Great Peconic Bay West	2	100002	0.2	26.5	73.3	36.4	36.9	45.5	1.6
Great Peconic Bay West	3	100003	13.5	53.2	33.3	12.0	21.3	36.6	1.7
Great Peconic Bay West	4	100004	0.0	5.7	94.4	42.3	52.1	59.6	2.2
Great Peconic Bay West	5	100005	0.0	9.0	91.0	35.2	55.8	57.3	2.6
Great Peconic Bay West	6	100006	0.0	60.7	39.3	21.4	17.9	33.4	1.4
Great Peconic Bay West	7	100007	0.0	18.6	81.4	41.6	39.8	47.1	1.9
Great Peconic Bay West	8	100008	8.4	83.5	8.1	3.6	4.5	19.1	0.6
Great Peconic Bay West	9	100009	44.0	40.6	15.4	7.9	7.5	30.5	1.5
Great Peconic Bay West	10	100010	2.6	96.5	0.9	0.5	0.3	16.6	0.3
Great Peconic Bay West	11	100011	0.1	99.2	0.7	0.5	0.2	22.5	
Great Peconic Bay West	13	100013	4.1	85.1	10.8	5.7	5.1	20.9	0.5
Great Peconic Bay West	14-T	100014	0.7	4.5	94.8	57.9	36.9		

Survey Area	ID	Code	% Gravel	% Sand	% Mud (Silt+Clay)	%Silt	%Clay	Water Content	% LOI
Great Peconic Bay West	15	100015	1.0	25.5	73.5	35.1	38.4	48.5	1.9
Great Peconic Bay West	16	100016	0.0	12.2	87.8	40.5	47.3	52.8	1.9
Great Peconic Bay West	17	100017	0.3	8.7	91.0	46.9	44.1	54.4	1.9
Great Peconic Bay West	18	100018	1.4	49.2	49.4	21.8	27.6	35.1	0.8
Great Peconic Bay West	19	100019	5.6	8.9	85.5	38.6	46.8	50.3	2.0
Great Peconic Bay West	20	100020	0.0	9.1	90.9	40.9	50.0	49.4	2.0
Great Peconic Bay West	21	100021	4.7	28.5	66.9	29.0	37.8	47.8	2.1
Great Peconic Bay West	22	100022	0.6	8.0	91.4	34.4	57.1	48.4	2.2
Great Peconic Bay West	23	100023	0.1	98.9	1.0	0.7	0.3	20.0	0.2
Great Peconic Bay West	24	100024	24.8	67.1	8.1	3.3	4.8	20.5	0.6
Great Peconic Bay West	25	100025	14.8	85.2	0.0	0.0	0.0	20.0	0.4
Great Peconic Bay West	26-B	100026	3.4	95.8	0.8	0.4	0.4		
Great Peconic Bay West	27	100027	0.0	7.5	92.5	45.9	46.6	51.3	2.2
Great Peconic Bay West	28	100028	8.6	86.4	5.0	1.9	3.1	16.7	0.6
Great Peconic Bay West	29	100029	0.5	98.7	0.8	0.4	0.5	19.9	
Great Peconic Bay West	30	100030	0.3	99.7	0.0	0.0	0.0	20.5	0.2
Great Peconic Bay West	31	100031	1.3	98.2	0.5	0.3	0.2	15.3	
Great Peconic Bay West	32	100032	1.2	98.4	0.4	0.3	0.0	20.0	
Great Peconic Bay West	34	100034	42.9	54.2	3.0	1.7	1.2	18.3	1.6
Great Peconic Bay West	35	100035	9.6	83.7	6.7	1.9	4.8	19.5	0.5
Great Peconic Bay West	36	100036	0.5	99.0	0.5	0.4	0.1	19.9	
Great Peconic Bay West	37-S	100037	2.4	97.1	0.5	0.4	0.1	19.0	0.2
Great Peconic Bay West	38	100038	0.0	0.2	99.9	43.2	56.7	47.2	2.0
Great Peconic Bay West	39	100039	14.1	5.7	80.2	42.5	37.6	51.3	1.2
Great Peconic Bay West	40	100040	0.0	7.1	92.9	45.3	47.6	47.8	2.8
Great Peconic Bay West	41	100041	2.2	91.4	6.3	2.6	3.7	19.5	0.4
Great Peconic Bay West	42	100042	0.9	98.5	0.6	0.4	0.2	21.9	0.3
Great Peconic Bay West	43	100043	1.1	98.9	0.0	0.0	0.0	20.4	0.2
Great Peconic Bay West	44	100044	0.7	98.9	0.4	0.4	0.0	18.2	0.1
Great Peconic Bay West	45	100045	14.6	81.5	3.9	1.8	2.1	18.8	0.4
Great Peconic Bay West	46	100046	6.7	90.2	3.2	1.0	2.2	18.3	0.4
Great Peconic Bay West	47	100047	3.1	95.8	1.1	0.5	0.6	20.8	0.3
Great Peconic Bay West	48	100048	9.5	81.2	9.3	3.6	5.7	20.9	0.5
Great Peconic Bay West	49	100049	0.2	92.7	7.1	2.8	4.3	18.4	0.5
Great Peconic Bay West	50	100050	16.9	78.5	4.6	1.9	2.7	20.2	0.5
Great Peconic Bay West	51	100051	2.0	97.1	0.9	0.4	0.5	18.2	0.2
Great Peconic Bay West	52	100052	2.0	62.2	35.8	23.8	12.1	31.2	1.2
Great Peconic Bay West	53	100053	1.7	97.6	0.7	0.4	0.2	18.7	
Great Peconic Bay West	54	100054	1.9	13.8	84.4	0.0	0.0	20.3	0.7
Great Peconic Bay West	54r2	100054	8.9	79.3	11.8	4.3	7.5		

Survey Area	ID	Code	% Gravel	% Sand	% Mud (Silt+Clay)	%Silt	%Clay	Water Content	% LOI
Great Peconic Bay West	55	100055	8.2	89.1	2.8	1.2	1.6	21.4	0.8
Great Peconic Bay West	56	100056	3.5	95.8	0.8	0.6	0.2	20.8	0.3
Great Peconic Bay West	57	100057	25.8	54.7	19.5	8.4	11.1	21.1	0.2
Great Peconic Bay West	58(0)	100580	26.6	1.1					
Great Peconic Bay West	58(1)	100058	12.5	86.0	1.5	1.1	0.5	24.7	0.4
Great Peconic Bay West	59	100059	0.0	56.7	43.3	21.7	21.6	31.6	1.5
Great Peconic Bay West	60	100060	0.0	6.6	93.4	44.3	49.1	53.4	1.3
Great Peconic Bay West	61	100061	0.2	76.0	23.8	10.5	13.3	24.7	0.8
Orient Delta	60-OD	110060	3.1	91.1	5.9	3.8	2.1	18.9	0.5
Orient Delta	61-OD	110061	0.0	29.7	70.3	42.2	28.0	43.2	2.0
Orient Delta	62	110062	0.0	15.3	84.7	50.5	34.2	47.5	2.0
Orient Delta	64	110064	0.9	23.3	75.8	50.4	25.4	43.4	1.7
Orient Delta	65	110065	0.0	47.7	52.3	30.6	21.7	32.9	1.2
Orient Delta	66	110066	1.1	27.8	71.1	45.3	25.8	43.1	1.7
Orient Delta	67	110067	7.4	65.7	26.9	16.4	10.5	22.9	1.0
Orient Delta	68	110068	9.1	72.7	18.3	9.3	8.9	22.1	0.4
Orient Delta	69	110069	7.2	82.0	10.9	4.8	6.0	17.8	0.4
Orient Delta	70	110070	0.0	28.3	71.8	40.6	31.2	54.0	1.7
Orient Delta	73	110073	11.4	84.0	4.6	2.5	2.1	19.1	0.4
Orient Delta	74	110074	10.1	88.6	1.3	0.7	0.7	18.0	0.3
Orient Delta	75	110075	15.2	82.2	2.6	0.3	2.3	20.6	0.5
Orient Delta	76	110076	53.5	16.4	30.2	11.9	18.3	38.5	1.5
Orient Delta	78	110078	22.7	66.4	11.0	5.0	5.9	21.0	0.7
Orient Delta	79	110079	4.7	87.5	7.8	3.8	4.0	17.6	0.3
Orient Delta	80	110080	30.3	23.6	46.1	18.4	27.6	37.1	1.5
Orient Delta	81(drop2)	110081	16.2	83.3	0.5	0.2	0.3	13.7	0.1
Orient Delta	82	110082	8.6	84.4	7.0	2.7	4.3	16.5	0.2
Orient Delta	86	110086	3.1	54.4	42.5	25.7	16.9	29.1	1.2
Orient Delta	90	110090	0.0	38.7	61.3	34.1	27.2	37.6	1.7
Orient Delta	92	110092	0.0	62.9	37.1	20.8	16.3	28.7	0.9
Orient Delta	93	110093	13.3	78.0	8.7	4.0	4.7	20.1	0.5
Orient Delta	98	110098	9.8	89.3	1.0	0.6	0.3	16.4	0.2
Orient Delta	100	110100	7.8	88.8	3.4	2.0	1.5	18.7	0.4
Orient Delta	101	110101	0.9	97.4	1.7	0.9	0.7	19.3	0.2
Orient Delta	104	110104	13.2	67.4	19.4	7.8	11.6	24.1	1.2
Orient Delta	106	110106	38.7	57.8	3.4	1.5	2.0	13.4	0.5
Orient Delta	108	110108	2.2	96.3	1.5	0.7	0.8	21.7	0.5
Orient Delta	109	110109	12.9	81.7	5.5	2.0	3.5	17.8	0.3
Orient Delta	111	110111	1.6	23.9	74.6	50.3	24.2	42.7	1.6
Orient Delta	112	110112	0.0	28.3	71.7	44.1	27.6	41.6	1.9

Survey Area	ID	Code	% Gravel	% Sand	% Mud (Silt+Clay)	%Silt	%Clay	Water Content	% LOI
Orient Delta	116	110116	28.8	70.7	0.5	0.2	0.2	12.5	0.4
Orient Delta	117(0)	111170							
Orient Delta	117(1)	110117	37.8	61.4	0.9	0.4	0.5	17.0	0.4
Orient Delta	118	110118	0.3	58.5	41.2	22.4	18.8	31.1	0.7
Orient Delta	119	110119	1.5	89.3	9.2	4.8	4.5	19.6	0.5
Orient Delta	120	110120	33.6	64.0	2.3	1.0	1.3	14.2	0.3
Orient Delta	121	110121	3.4	86.0	10.7	4.4	6.2	25.4	0.9
Orient Delta	122	110122	0.0	18.4	81.6	56.5	25.1	49.4	2.0
Orient Delta	123	110123	46.3	47.9	5.9	2.6	3.3	27.7	0.5
Orient Delta	124	110124	0.0	23.5	76.5	49.8	26.7	44.8	2.0
Orient Delta	125	110125	10.3	25.7	64.0	38.5	25.5	38.1	1.0
Orient Delta	126	110126	0.0	16.2	83.8	51.7	32.1	42.8	1.0
Orient Delta	127	110127	13.8	85.0	1.1	0.9	0.3	17.8	0.4
Orient Delta	128	110128	8.4	18.8	72.8	45.9	26.9	42.6	1.8
Orient Delta	129	110129	15.4	77.9	6.7	3.0	3.7	20.1	0.6
Orient Delta	130	110130	2.5	45.8	51.7	32.1	19.6	32.4	0.9
Orient Delta	1300	111300	6.8	81.0	12.2	7.9	4.3	17.6	0.3
Orient Delta	1310	111310	8.9	90.0	1.2	0.6	0.6	16.5	0.2
Orient Delta	1320	111320	2.9	91.4	5.7	3.6	2.1	16.8	0.4
Orient Delta	1340	111340	4.0	46.5	49.5	30.6	18.9	35.3	1.4
Orient Delta	1350	111350	0.3	55.2	44.6	25.8	18.8	31.0	1.2
Orient Delta	1360	111360	29.8	64.3	5.9	3.0	2.9	18.8	0.4
Orient Delta	1370A	111371	99.5	0.0	0.4	0.2	0.2		
Orient Delta	1370B	111370	13.4	75.7	10.9	0.0	10.9	29.1	1.2
Pipes Cove	131	110131	0.0	45.0	55.0	18.7	36.3		
Pipes Cove	132	110132	0.4	90.5	9.1	4.6	4.5	19.7	0.7
Pipes Cove	134	110134	4.5	94.0	1.5	0.1	1.3	18.0	0.3
Pipes Cove	139	110139	3.0	69.7	27.4	15.5	11.9	27.4	1.2
Pipes Cove	140	110140	4.5	78.4	17.1	7.3	9.7	21.0	0.7
Pipes Cove	141	110141	4.0	68.3	27.7	0.0	27.7	31.9	2.0
Pipes Cove	142	110142	16.1	55.3	28.7	15.1	13.6	30.1	1.9
Pipes Cove	145	110145	15.5	52.5	32.0	16.2	15.9	28.6	1.6
Pipes Cove	146	110146	1.2	44.8	54.0	36.2	17.8	32.7	1.8
Pipes Cove	148	110148	13.3	56.5	30.2	14.1	16.1	26.7	1.0
Pipes Cove	150	110150	1.8	91.7	6.5	3.3	3.3	17.4	0.5
Pipes Cove	151	110151	4.2	78.6	17.2	9.0	8.2	24.6	1.3
Pipes Cove	152	110152	0.6	96.5	3.0	1.5	1.4	17.9	0.3
Pipes Cove	153	110153	15.7	77.5	6.7	3.5	3.3	20.2	0.7
Pipes Cove	154	110154	0.4	91.7	8.0	3.0	5.0	22.9	0.1
Pipes Cove	155	110155	25.6	44.6	29.9	16.3	13.6	32.6	1.4

Survey Area	ID	Code	% Gravel	% Sand	% Mud (Silt+Clay)	%Silt	%Clay	Water Content	% LOI
Pipes Cove	156	110156	0.4	96.5	3.1	1.8	1.3	19.2	0.3
Pipes Cove	157	110157	0.4	95.8	3.8	2.1	1.7	17.6	0.5
Pipes Cove	160	110160	4.0	66.1	29.9	19.3	10.6	22.2	0.9
Pipes Cove	164	110164	0.3	92.1	7.7	4.3	3.4	18.1	0.5
Pipes Cove	168	110168	4.9	67.2	27.9	13.8	14.2	29.0	1.3
Pipes Cove	169	110169	4.0	93.7	2.2	1.2	1.0	16.2	0.3
Pipes Cove	174	110174	4.6	91.6	3.8	1.2	2.5	16.8	0.4
Pipes Cove	177	110177	0.3	88.0	11.7	5.8	6.0	21.3	0.8

Table B1.4: Grain size and water content 2008. Percentage gravel, sand, mud and then percentage breakdown of 1-2 mm (-1 to 0 phi) and less than 1 mm (0 phi) sand fractions, clay, and silt. Water Content as percentage of wet weight, and percentage water content (WC) for samples with greater than 20% mud. Percentage Loss on Ignition (LOI).

Survey Area	Planned ID	Code	% Gravel	% Sand	% Mud (Silt + Clay)	%Sand 1-2 mm	%Sand < 1 mm	%Silt	%Clay	Water Content (%wet weight)	WC > 20% Mud	% LOI
West Shelter Island	40	120040	0.05	97.50	2.45	0.25	97.25					
West Shelter Island	43	120043	7.26	85.72	7.02	38.55	47.17			25.32		1.06
West Shelter Island	33	120033	46.33	51.79	1.88			0.85	1.03	26.85		0.68
West Shelter Island	39	120039	12.12	87.88	0.00	7.44	80.44			27.97		0.55
West Shelter Island	31	120031	3.82	96.06	0.11	10.06	86.00			24.26		0.62
West Shelter Island	36	120036	0.00	95.70	4.30	3.35	92.35			29.79		0.65
West Shelter Island	42	120042	8.78	82.21	9.02	11.70	70.51			34.92		1.29
West Shelter Island	41	120041	0.00	91.90	8.10	1.13	90.77	4.14	3.96	30.08		1.27
West Shelter Island	44 a	120441										
West Shelter Island	44 b	120442										
West Shelter Island	44	120044	4.53	93.29	2.18	51.32	41.97			24.79		0.44
West Shelter Island	34a	120341										
West Shelter Island	34	120034	7.70	89.17	3.13	48.08	41.09					
West Shelter Island	32	120032	75.34	17.85	6.81			2.94	3.88	36.32		2.32
West Shelter Island	37	120037	89.72	9.42	0.86			0.34	0.52			
West Shelter Island	38	120038	0.00	37.44	62.56	0.00	37.44	33.55	29.01	37.54	37.54	1.95
West Shelter Island	49	120049	0.00	60.16	39.84	0.00	60.16	24.56	15.28	40.51	40.51	1.90
West Shelter Island	35	120035	0.00	89.08	10.92	11.02	78.06	4.59	6.33	27.19		0.88
West Shelter Island	48a	120481										
West Shelter Island	48	120048	0.00	84.84	15.16	12.23	72.61	9.54	5.62	37.35		2.02
West Shelter Island	30	120030	0.00	14.81	85.19	0.00	14.81	44.82	40.37	52.53	52.53	3.69
West Shelter Island	47	120047	0.00	0.00	100.00	0.00	0.00	59.61	40.39	39.41	39.41	2.72
West Shelter Island	21	120021	0.00	45.89	54.11	0.00	45.89	27.10	27.01	40.73	40.73	2.69
West Shelter Island	46	120046	0.00	39.26	60.74	0.00	39.26	41.83	18.91	39.99	39.99	2.38
Noyack Bay	18	120018	5.11	89.11	5.79	6.33	82.78			25.95		0.52
Noyack Bay	19a	120191										
Noyack Bay	19	120019	55.91	42.86	1.23	5.58	32.27			23.44		0.69
Noyack Bay	20	120020	5.74	82.92	11.33	11.48	71.44	4.52	6.81	38.08		1.58
Noyack Bay	45	120045	8.88	88.10	3.01	7.58	80.53	1.43	1.58	44.14		0.43
Noyack Bay	17	120017	9.09	83.90	7.02	10.24	73.66	3.06	3.96	31.61		0.83
Noyack Bay	29	120029	0.24	96.61	3.15	2.98	93.63	1.54	1.61	26.16		0.42
Noyack Bay	28	120028	0.33	95.75	3.93	0.00	95.75			25.94		0.41

Survey Area	Planned ID	Code	% Gravel	% Sand	% Mud (Silt + Clay)	%Sand 1-2 mm	%Sand < 1 mm	%Silt	%Clay	Water Content (%wet weight)	WC > 20% Mud	% LOI
Noyack Bay	27	120027	0.00	97.53	2.47	8.16	89.37			26.31		0.38
Noyack Bay	10	120010	0.44	99.56	0.00	2.45	97.11			24.20		0.49
Noyack Bay	12	120012	0.58	99.42	0.00	4.96	94.46			23.26		0.23
Noyack Bay	9	120009	14.42	83.22	2.36	8.94	74.28	1.25	1.11	36.76		0.60
Noyack Bay	5	120005	0.00	83.18	16.82	8.65	74.53	9.48	7.34	35.09		0.85
Noyack Bay	4a	124001	0.00	6.24	93.76	0.00	6.24	49.53	44.23	56.73	56.73	4.33
Noyack Bay	6	120006	0.00	16.62	83.38	0.00	16.62	50.58	32.80	54.56	54.56	3.06
Noyack Bay	4b	124002	28.25	33.69	38.06	16.93	16.76	22.83	15.23			
Noyack Bay	3	120003	1.58	48.29	50.14	0.00	48.29	24.99	25.15	39.76	39.76	2.14
Noyack Bay	1	120001	0.00	5.76	94.24	0.00	5.76	92.58	1.66	64.54	64.54	5.53
Noyack Bay	8	120008	0.00	94.25	5.75	9.14	85.11	2.88	2.87	23.56		0.45
Noyack Bay	2	120002	0.00	40.53	59.47	0.00	40.53	58.77	0.70	28.45	28.45	0.56
Noyack Bay	16	120016	0.00	5.48	94.52	0.34	5.14	47.61	46.91	56.23	56.23	4.13
Noyack Bay	7	120007	0.00	32.50	67.50	0.00	32.50	35.44	32.06	56.25	56.25	3.60
Noyack Bay	22	120022	0.00	54.02	45.98	0.00	54.02	31.08	14.90	47.37	47.37	3.70
Noyack Bay	23	120023	1.41	61.30	37.29	0.85	60.45	19.29	18.00	37.71	37.71	2.37
Noyack Bay	15	120015	0.00	56.38	43.62	0.89	55.49	24.52	19.10	42.07	42.07	2.72
Noyack Bay	900	120900	7.54	90.69	1.77	3.33	87.36	0.96	0.81	25.65		0.62
Noyack Bay	13a	120131	0.90	68.44	28.60	2.87	65.57	15.57	13.03	34.00		1.81
Noyack Bay	13b	120132	4.29	63.45	32.27	5.21	58.24	17.75	14.52			
Noyack Bay	13c	120133	16.80	68.35	14.85	12.38	55.97	6.63	8.22			
Noyack Bay	14	120014	0.00	75.10	24.90	9.84	65.26	11.32	13.58	31.56	31.56	1.72
Noyack Bay	25	120025	0.00	38.24	61.76	0.00	38.24	36.07	25.69	51.30	51.30	4.06
Noyack Bay	24	120024	0.29	77.72	21.99	3.92	73.80	7.44	14.55	34.63	34.63	1.86
Noyack Bay	26a	120261	9.57	69.59	20.84	1.70	67.89	8.36	12.48			
Noyack Bay	26b	120262										
Noyack Bay	26c	120263	11.81	77.13	11.07	15.78	61.35	4.36	6.71	29.77		0.95
Little Peconic Bay	62	120062	0.36	81.62	18.02	1.67	79.95	10.60	7.42	29.68		1.32
Little Peconic Bay	73a	120731	38.52	36.86	24.63	4.47	32.39	15.98	8.65			
Little Peconic Bay	73b	120732	8.12	11.52	80.37	1.40	10.11	52.17	28.20			
Little Peconic Bay	76	120076	0.00	11.49	88.51	0.67	10.81	47.53	40.98	52.92	52.92	3.80
Little Peconic Bay	65	120065	0.00	11.84	88.16	0.00	11.84	53.31	34.85	56.96	56.96	4.64
Little Peconic Bay	67	120067	0.68	87.33	11.99	1.55	85.78	7.04	4.95	36.01		1.52
Little Peconic Bay	66	120066	8.68	67.42	23.90	11.93	55.49	12.84	11.06	29.07	29.07	1.53
Little Peconic Bay	77	120077	0.00	4.95	95.05	0.00	4.95	49.09	45.96	57.78	57.78	4.81
Little Peconic Bay	63	120063	1.47	91.89	6.65	2.79	89.10	3.50	3.15	23.86		0.58
Little Peconic Bay	60	120060	0.00	7.57	92.43	0.00	7.57	46.28	46.16	58.82	58.82	5.15

Survey Area	Planned ID	Code	% Gravel	% Sand	% Mud (Silt + Clay)	%Sand 1-2 mm	%Sand < 1 mm	%Silt	%Clay	Water Content (%wet weight)	WC > 20% Mud	% LOI
Little Peconic Bay	62	120062	0.36	81.62	18.02	1.67	79.95	10.60	7.42	29.68		1.32
Little Peconic Bay	73a	120731	38.52	36.86	24.63	4.47	32.39	15.98	8.65			
Little Peconic Bay	73b	120732	8.12	11.52	80.37	1.40	10.11	52.17	28.20			
Little Peconic Bay	76	120076	0.00	11.49	88.51	0.67	10.81	47.53	40.98	52.92	52.92	3.80
Little Peconic Bay	65	120065	0.00	11.84	88.16	0.00	11.84	53.31	34.85	56.96	56.96	4.64
Little Peconic Bay	67	120067	0.68	87.33	11.99	1.55	85.78	7.04	4.95	36.01		1.52
Little Peconic Bay	66	120066	8.68	67.42	23.90	11.93	55.49	12.84	11.06	29.07	29.07	1.53
Little Peconic Bay	77	120077	0.00	4.95	95.05	0.00	4.95	49.09	45.96	57.78	57.78	4.81
Little Peconic Bay	63	120063	1.47	91.89	6.65	2.79	89.10	3.50	3.15	23.86		0.58
Little Peconic Bay	60	120060	0.00	7.57	92.43	0.00	7.57	46.28	46.16	58.82	58.82	5.15
Little Peconic Bay	0a	120000	47.92	12.02	40.06	0.65	11.38	24.26	15.80	60.42	60.42	4.62
Little Peconic Bay	0b	121002	10.13	64.50	25.37	5.32	59.18	14.66	10.71	47.66	47.66	2.48
Little Peconic Bay	68	120068	0.00	15.45	84.55	0.69	14.75	48.90	35.65	55.10	55.10	3.72
Little Peconic Bay	61	120061	29.44	33.66	36.90	2.57	31.09	21.83	15.07	52.57	52.57	2.92
Little Peconic Bay	70	120070	3.18	59.55	37.27	4.89	54.66	21.07	16.20	43.46	43.46	2.70
Little Peconic Bay	78	120078	0.00	17.23	82.77	0.47	16.76	47.18	35.59	56.16	56.16	4.18
Little Peconic Bay	74	120074	0.77	13.28	85.95	0.28	13.00	47.28	38.67	54.90	54.90	4.74
Little Peconic Bay	75	120075			100.00	0	0	59.02	40.98			
Little Peconic Bay	64	120064	1.45	79.41	19.15	1.83	77.58	11.02	8.12	30.69		0.93
Little Peconic Bay	69	120069	0.33	95.17	4.50	1.22	93.95	2.20	2.30	26.74		0.53
Little Peconic Bay	72	120072	2.09	18.14	79.77	0.37	17.77	42.57	37.20	55.87	55.87	3.66
Little Peconic Bay	71	120071	1.02	21.64	77.35	1.51	20.13	47.90	29.44	56.67	56.67	4.16
Great Peconic Bay	108	120108	3.30	95.58	1.12	8.74	86.84	0.56	0.56	23.45		0.29
Great Peconic Bay	107	120107	2.49	96.62	0.89	6.02	90.60	0.33	0.56	23.93		0.33
Great Peconic Bay	106	120106	2.58	95.28	2.13	14.93	80.35	0.55	1.58	20.89		0.33
Great Peconic Bay	93	120093	1.08	91.34	7.58	0.27	91.07	2.33	5.24	24.57		0.40
Great Peconic Bay	105	120105	0.28	98.89	0.84	0.85	98.04			24.63		0.38
Great Peconic Bay	98	120098	0.77	94.50	4.73	0.23	94.27	2.34	2.39	23.18		0.44
Great Peconic Bay	97	120097	3.11	92.97	3.92	0.88	92.10	1.55	2.37	28.15		0.84
Great Peconic Bay	92	120092	12.20	81.53	6.26	0.83	80.70	2.73	3.53	23.81		0.48
Great Peconic Bay	91	120091	0.89	63.29	35.82	0.22	63.07	25.01	10.80	36.65	36.65	1.84
Great Peconic Bay	89	120089	3.28	85.02	11.70	1.05	83.97	5.68	6.02	54.23		1.64
Great Peconic Bay	99	120099	0.00	16.83	83.17	0.00	16.83	34.50	48.67	55.51	55.51	4.83
Great Peconic Bay	102	120102	0.00	10.19	89.81	0.79	9.40	45.50	44.31	59.00	59.00	4.23
Great Peconic Bay	84	120084	0.66	89.98	9.36	1.76	88.22	5.11	4.25	24.26		0.56
Great Peconic Bay	87	120087	10.61	84.00	5.39	14.81	69.18	1.85	3.55	23.48		0.33
Great Peconic Bay	85	120085	9.63	83.63	6.74	6.52	77.11	2.27	4.48	65.39		0.79
Great Peconic Bay	88	120088	0.76	97.37	1.87	4.45	92.92	0.64	1.23	25.81		0.53

Survey Area	Planned ID	Code	% Gravel	% Sand	% Mud (Silt + Clay)	%Sand 1-2 mm	%Sand < 1 mm	%Silt	%Clay	Water Content (%wet weight)	WC > 20% Mud	% LOI
Great Peconic Bay	81	120081	11.51	85.79	2.71	8.16	77.63	1.16	1.54	20.14		0.35
Great Peconic Bay	83	120083	0.58	51.06	48.36	0.94	50.13	22.46	25.90	46.44	46.44	3.09
Great Peconic Bay	86	120086	4.20	70.09	25.71	3.98	66.11	13.85	11.86	38.25	38.25	2.25
Great Peconic Bay	80	120080	3.71	48.12	48.16	1.86	46.26	31.36	16.80	49.85	49.85	3.59
Great Peconic Bay	82	120082	0.46	16.87	82.67	0.00	16.87	37.79	44.89	56.59	56.59	4.88
Great Peconic Bay	100	120100	6.84	10.75	82.41	0.00	10.75	48.94	33.47	63.39	63.39	4.86
Great Peconic Bay	101	120101	0.00	10.67	89.33	0.00	10.67	48.62	40.71	58.76	58.76	4.20
Great Peconic Bay	95	120095	0.44	76.66	22.89	2.31	74.36	11.46	11.43	33.11	33.11	1.63
Great Peconic Bay	111a	121111	0.00	99.14	0.86	0.00	99.14			23.54		0.41
Great Peconic Bay	111b	121112	0.00	99.17	0.83	0.01	99.16			24.75		0.40
Great Peconic Bay	90	120090	0.00	0.00	100.00	0	0	54.99	45.01	52.94	52.94	3.86
Great Peconic Bay	94	120094	0.00	2.39	97.61	0.00	2.39	56.02	41.59	58.64	58.64	5.30

Table B1.5: Grain size in half-phi intervals 2006.

Survey Area	ID	Code	-1	-0.5	0	0.5	1	1.5	2	2.5	3	3.5	4	4.5	5	5.5	6	6.5	7	7.5	8	8.5	9	9.5	10	10.5	11	>11
Little Peconic Bay West	1	70001	0	0.22	0.92	1.93	2.25	2.66	2.17	2.35	2.73	3.02	4.57	2.56	3.44	4.49	5.00	5.04	4.95	5.29	4.98	4.82	4.18	3.84	3.57	3.46	3.75	17.81
Little Peconic Bay West	2	70002	0	0.00	0.01	0.07	0.24	0.61	0.54	1.18	2.47	5.34	4.81	5.17	4.43	5.97	7.18	7.44	6.53	6.12	5.49	4.27	3.97	3.20	3.33	3.28	3.04	15.33
Little Peconic Bay West	3	70003	0	0.19	0.30	1.69	4.17	7.22	7.37	3.73	4.29	7.10	4.89	1.67	3.87	5.24	5.25	5.22	4.94	4.27	4.30	4.08	3.44	3.50	3.36	3.46	3.76	2.69
Little Peconic Bay West	4	70004	0	0.22	2.47	14.01	51.29	25.18	2.09	0.84	0.90	0.79	0.69	0.55	0.08	0.09	0.09	0.07	0.05	0.05	0.08	0.05	0.08	0.06	0.09	0.09	0.06	0.05
Little Peconic Bay West	5	70005	0	0.00	0.00	0.00	0.00	0.00	0.00	0.00	0.00	0.00	0.93	3.52	5.56	8.54	8.60	7.84	5.59	6.03	4.86	4.91	4.69	4.47	5.99	5.23	4.33	18.91
Little Peconic Bay West	6	70006	0	0.00	0.00	0.14	1.22	2.62	2.75	2.92	8.99	12.75	5.88	2.54	2.72	3.86	4.48	4.41	4.00	4.10	4.06	3.73	3.44	3.21	2.85	3.03	3.09	13.17
Little Peconic Bay West	7	70007	0	0.00	0.00	0.72	5.68	11.34	30.19	31.99	8.66	1.31	4.87	0.81	0.12	0.21	0.29	0.26	0.23	0.22	0.26	0.30	0.28	0.26	0.30	0.31	0.34	1.10
Little Peconic Bay West	8	70008	0	0.27	1.76	5.84	14.29	19.62	15.94	17.99	16.24	2.57	0.38	0.11	0.19	0.31	0.38	0.34	0.27	0.27	0.28	0.21	0.18	0.22	0.25	0.25	0.27	1.56
Little Peconic Bay West	9	70009	0	0.76	1.74	5.84	13.17	25.39	24.96	6.55	2.45	1.45	3.33	2.94	0.36	0.57	0.72	0.70	0.60	0.67	0.69	0.72	0.75	0.68	0.70	0.65	0.59	3.00
Little Peconic Bay West	10	70010	0	0.04	0.18	0.54	1.38	2.55	3.68	4.52	8.08	10.03	5.09	3.20	3.62	4.62	5.02	4.86	4.14	3.96	3.62	3.13	3.07	2.82	2.63	2.58	2.51	14.15
Little Peconic Bay West	11 d1	70110																										
Little Peconic Bay West	11 d2	70011	0	0.00	0.78	3.11	6.36	10.87	10.37	11.72	10.34	14.57	7.08	1.03	1.66	1.90	1.71	1.61	1.33	1.18	1.30	1.12	1.05	1.03	1.00	0.94	1.05	6.91
Little Peconic Bay West	12	70012	0	0.01	0.06	0.03	0.19	0.27	0.37	0.29	0.86	3.69	5.47	3.70	4.87	6.58	7.35	7.34	6.08	5.41	5.56	4.67	3.93	4.27	4.73	4.17	3.59	16.52
Little Peconic Bay West	13	70013	0	0.25	1.42	2.53	4.84	5.52	3.06	4.09	7.28	12.40	7.29	1.90	2.29	3.13	3.52	3.69	3.33	3.23	3.00	2.71	2.79	2.37	2.24	2.26	2.22	12.62
Little Peconic Bay West	14	70014	0	0.14	0.25	0.51	1.15	2.11	2.19	1.52	2.25	5.20	4.57	3.50	3.41	4.40	5.11	5.14	4.85	4.65	4.54	4.23	3.77	3.71	3.72	3.73	3.74	21.61
Little Peconic Bay West	15	70015	0	0.51	1.25	8.50	31.73	43.76	9.83	1.98	0.00	0.00	0.00	0.02	0.10	0.13	0.12	0.11	0.12	0.12	0.10	0.09	0.12	0.13	0.13	0.15	0.13	0.82
Little Peconic Bay West	16	70016	0	1.42	4.23	10.84	16.26	18.33	12.23	4.77	1.38	1.13	1.15	1.33	1.56	1.78	1.85	1.87	1.78	1.70	1.64	1.46	1.30	1.21	1.16	1.20	1.22	7.21
Little Peconic Bay West	17	70017	0	0.46	1.17	3.38	10.33	27.79	26.36	10.33	4.88	1.93	2.64	1.27	0.68	0.73	0.70	0.63	0.57	0.44	0.55	0.40	0.41	0.52	0.42	0.44	0.47	2.52
Little Peconic Bay West	18	70018	0	0.22	0.52	1.42	4.20	16.10	37.35	23.42	8.18	3.92	1.17	0.20	0.26	0.29	0.26	0.23	0.22	0.20	0.15	0.20	0.17	0.15	0.13	0.13	0.13	0.77
Little Peconic Bay West	19	70019	0	0.01	0.13	0.99	3.91	8.59	22.32	36.08	17.18	3.77	1.58	0.69	0.06	0.22	0.34	0.29	0.27	0.32	0.31	0.27	0.30	0.33	0.35	0.29	0.29	1.12
Little Peconic Bay West	20	70020	0	0.55	2.03	2.59	6.32	10.77	9.83	7.27	10.28	7.98	3.29	2.97	2.92	2.80	2.52	2.54	2.29	2.05	2.06	1.92	1.80	1.63	1.72	1.55	1.59	8.74
Little Peconic Bay West	21	70021	0	0.00	0.41	1.22	3.67	6.11	6.22	21.63	23.25	10.64	6.50	1.44	0.86	1.12	1.32	1.33	1.23	1.20	1.24	1.15	1.08	1.04	1.01	0.93	0.86	4.51
Little Peconic Bay West	22	70022	0	0.01	0.05	0.20	0.35	0.58	0.31	1.06	6.37	11.29	4.71	4.30	3.73	5.03	5.69	5.65	5.17	4.59	3.67	3.45	3.35	3.14	3.14	3.12	3.12	17.94
Little Peconic Bay West	23	70023	0	0.12	1.18	1.21	2.19	2.81	4.44	4.89	8.64	13.79	6.49	4.03	2.87	3.62	3.70	3.63	3.56	3.45	3.26	2.87	2.57	2.30	2.16	2.18	2.12	11.92
Little Peconic Bay East	30	70030	0	0.01	0.03	0.10	0.30	0.42	0.78	1.52	2.13	5.69	9.16	6.08	6.30	6.70	6.31	5.87	5.17	4.35	4.11	3.31	2.92	3.26	2.78	2.70	2.84	17.18
Little Peconic Bay East	31	70031	0	0.01	0.24	1.53	5.66	5.98	2.55	2.39	2.95	4.09	4.30	3.67	4.92	5.64	5.57	5.05	4.39	3.99	3.66	3.27	2.93	2.58	2.45	2.63	2.88	16.68
Little Peconic Bay East	32	70032	0	0.01	0.07	0.31	0.55	1.28	2.10	2.38	4.45	10.80	11.30	5.84	4.19	4.48	4.32	4.14	3.75	3.70	3.11	3.02	2.81	2.49	2.84	2.70	2.88	16.48
Little Peconic Bay East	33	70033	0	0.30	1.06	5.41	21.26	28.19	9.89	5.37	4.45	3.60	0.16	0.70	1.18	1.45	1.36	1.37	1.25	1.27	1.19	0.90	0.83	0.90	0.89	1.03	0.93	5.06
Little Peconic Bay East	34	70034	0	0.00	0.06	0.08	0.29	1.43	2.13	2.78	6.26	13.01	9.04	5.52	5.05	5.19	5.39	4.58	3.75	3.61	2.89	2.68	2.55	2.33	2.21	2.01	2.26	14.91
Little Peconic Bay East	35	70035	0	0.01	0.09	0.12	0.35	0.45	0.59	1.15	2.79	11.92	10.52	4.46	5.52	5.09	5.26	4.96	4.65	3.83	3.25	3.28	3.07	2.94	2.84	3.27	3.10	16.47
Little Peconic Bay East	36	70036	0	0.00	0.00	0.00	0.01	3.33	3.74	4.08	8.04	11.32	5.20	3.02	4.19	4.76	4.96	3.63	3.75	4.29	3.60	3.30	3.56	3.04	2.85	3.29	2.97	13.05

Survey Area	ID	Code	-1	-0.5	0	0.5	1	1.5	2	2.5	3	3.5	4	4.5	5	5.5	6	6.5	7	7.5	8	8.5	9	9.5	10	10.5	11	>11
Little Peconic Bay East	41	70041	0	0.14	0.86	2.34	3.87	3.67	2.21	2.12	2.40	5.72	5.07	6.22	5.04	5.34	5.26	5.16	4.29	4.13	4.06	3.49	3.44	2.88	3.46	2.87	3.33	12.63
Little Peconic Bay East	42	70042	0	0.00	0.31	1.95	4.56	6.94	8.92	11.85	11.70	12.48	7.12	2.87	3.03	3.45	3.06	2.49	1.92	2.07	1.88	1.58	1.44	1.34	1.43	1.48	1.38	4.78
Little Peconic Bay East	43	70043	0	0.03	0.08	0.02	0.31	0.61	0.72	0.93	1.58	3.33	3.94	3.35	5.47	6.26	7.57	5.97	5.77	4.56	5.13	4.11	4.37	4.89	4.15	4.72	4.20	17.94
Little Peconic Bay East	44	70044	0	0.00	0.38	1.28	3.33	4.81	5.73	7.55	13.57	19.41	7.18	2.77	4.08	4.09	3.35	2.47	2.20	1.82	1.69	1.11	1.47	1.42	1.45	1.13	1.13	6.60
Little Peconic Bay East	45	70045	0	0.30	1.64	5.69	16.49	24.86	24.23	14.46	7.17	2.69	0.52	0.05	0.07	0.08	0.10	0.10	0.07	0.08	0.09	0.10	0.09	0.10	0.13	0.12	0.11	0.62
Little Peconic Bay East	46	70046	0	0.00	0.00	0.00	0.00	0.02	0.15	0.19	0.43	1.02	1.78	2.61	4.84	6.46	7.83	7.57	6.49	6.01	5.35	5.03	4.39	4.85	4.58	4.39	4.44	21.56
Little Peconic Bay East	47	70047	0	0.00	0.00	0.00	0.05	0.16	0.30	0.40	0.67	1.99	2.90	3.13	4.93	6.78	7.28	7.18	7.03	7.44	6.30	5.94	4.73	4.70	4.00	3.96	4.19	15.92
Little Peconic Bay East	48	70048	0	0.00	0.00	0.00	0.00	0.00	0.00	0.00	0.00	0.00	2.06	5.35	5.65	6.00	6.30	6.70	6.94	7.09	6.90	6.88	6.90	6.43	5.45	4.55	3.64	13.16
Little Peconic Bay East	49	70049	0	0.00	0.00	0.00	0.00	0.00	0.02	0.20	0.91	1.65	2.31	4.42	7.59	8.53	7.85	7.83	6.87	6.59	5.35	4.39	5.24	4.80	4.89	5.03	15.51	
Little Peconic Bay East	50	70050	0	0.13	0.59	2.85	6.57	9.96	8.81	8.88	10.32	13.53	5.90	1.49	2.39	3.22	3.30	2.89	2.38	1.88	1.70	1.87	1.80	1.96	1.72	1.28	1.02	3.54
Little Peconic Bay East	51	70051	0	0.23	0.39	0.80	1.65	2.20	2.79	3.36	9.89	16.51	7.07	4.57	4.51	5.17	4.93	3.93	3.53	3.57	3.24	2.64	2.11	2.30	2.21	2.30	1.88	8.22
Little Peconic Bay East	52 d1	70520																										
Little Peconic Bay East	52 d2	70521																										
Little Peconic Bay East	52A	70052	0	0.18	0.44	1.04	1.63	1.33	1.06	1.06	3.31	6.74	5.46	3.41	4.55	6.14	6.21	5.34	4.55	4.72	4.14	4.00	3.40	3.32	3.22	2.83	3.08	18.84
Little Peconic Bay East	53	70053	0	0.00	1.96	8.49	19.33	16.46	13.18	8.89	7.35	6.21	3.59	1.15	1.20	1.18	0.95	0.90	0.74	0.76	0.67	0.59	0.58	0.60	0.54	0.53	0.62	3.54
Little Peconic Bay East	54	70054	0	0.00	0.10	0.49	2.07	5.17	6.14	6.76	10.55	19.20	13.48	6.92	2.96	2.65	2.15	1.84	1.64	1.37	1.24	1.27	1.20	1.17	1.34	1.37	1.28	7.67
Little Peconic Bay East	55	70055	0	0.18	0.58	1.21	2.07	3.99	4.41	6.46	12.11	13.79	8.35	4.44	3.25	3.76	3.65	3.05	2.34	2.41	2.34	2.20	1.98	2.32	2.10	2.17	2.27	8.57
Little Peconic Bay East	56	70056	0	0.36	2.05	6.26	13.48	20.43	17.40	8.37	8.38	6.71	3.09	0.83	0.77	0.90	0.83	0.79	0.67	0.61	0.56	0.59	0.47	0.57	0.65	0.63	0.65	3.95
Little Peconic Bay East	57	70057	0	0.00	0.36	1.67	7.63	28.80	31.76	6.75	2.53	4.14	6.79	3.76	0.12	0.16	0.20	0.20	0.25	0.32	0.37	0.41	0.43	0.42	0.39	0.37	0.35	1.82
Little Peconic Bay East	58	70058	0	0.09	0.73	5.00	16.74	34.00	28.44	7.52	1.76	1.15	2.01	0.53	0.07	0.08	0.08	0.08	0.08	0.09	0.12	0.16	0.16	0.15	0.15	0.14	0.13	0.55
Little Peconic Bay East	59	70059	0	0.70	3.59	12.57	32.19	32.99	13.60	3.72	0.06	0.00	0.00	0.01	0.02	0.02	0.02	0.02	0.01	0.02	0.04	0.05	0.06	0.06	0.04	0.04	0.03	0.14
Little Peconic Bay East	60	70060	0	0.00	0.21	2.32	6.16	10.63	14.84	26.17	23.65	6.95	1.33	0.29	0.45	0.44	0.42	0.42	0.29	0.36	0.34	0.34	0.34	0.38	0.45	0.45	0.46	2.32
Little Peconic Bay East	61	70061	0	0.46	2.68	7.64	18.64	33.42	26.57	5.56	2.59	0.00	0.05	0.14	0.17	0.20	0.20	0.17	0.14	0.11	0.12	0.14	0.13	0.11	0.11	0.10	0.09	0.48
Little Peconic Bay East	62	70062	0	0.07	3.04	14.77	31.26	27.17	15.36	2.08	0.00	0.00	0.00	0.00	0.08	0.18	0.25	0.29	0.31	0.37	0.44	0.66	0.74	0.74	0.73	0.74	0.73	0.00
Little Peconic Bay East	63	70063	0	3.42	8.54	13.94	17.75	18.57	12.47	8.20	7.09	1.90	0.37	0.24	0.36	0.42	0.42	0.47	0.39	0.38	0.34	0.58	0.83	0.84	0.84	0.84	0.80	0.00
Little Peconic Bay East	64	70064	0	1.13	4.10	10.48	19.43	21.12	18.37	10.64	6.19	1.20	0.04	0.19	0.32	0.47	0.50	0.55	0.49	0.50	0.52	0.62	0.61	0.54	0.49	0.46	0.43	0.61
Little Peconic Bay East	65 d1	70650																										
Little Peconic Bay East	65 d2	70065	0	0.71	3.68	11.09	24.15	27.99	13.48	8.37	4.93	0.00	0.02	0.12	0.24	0.40	0.44	0.31	0.21	0.33	0.41	0.36	0.38	0.36	0.35	0.29	0.25	1.13
Little Peconic Bay East	66	70066	0	0.87	4.54	17.34	32.93	22.91	9.05	3.30	1.52	2.43	1.85	0.05	0.14	0.30	0.32	0.23	0.21	0.23	0.15	0.25	0.23	0.19	0.19	0.20	0.14	0.46
Little Peconic Bay East	67	70067	0	0.31	1.53	6.31	22.15	36.34	18.16	5.73	3.02	1.81	0.88	0.27	0.20	0.22	0.28	0.24	0.22	0.21	0.16	0.20	0.18	0.19	0.17	0.17	0.16	0.88
Little Peconic Bay East	68	70068	0	0.50	6.99	35.65	40.10	6.67	2.84	0.78	0.29	0.25	0.22	0.21	0.31	0.29	0.30	0.30	0.31	0.30	0.34	0.31	0.29	0.33	0.27	0.31	0.31	1.57
Great Peconic Bay West	1	100001	0	0.00	0.00	2.00	12.30	32.56	27.52	7.68	1.66	0.93	1.23	0.24	0.53	0.80	1.06	1.10	1.07	1.04	1.02	0.94	0.87	0.83	0.78	0.66	0.57	2.64
Great Peconic Bay West	2	100002	0	0.17	0.66	2.52	6.27	7.80	4.64	2.09	0.87	0.52	0.56	1.60	2.93	4.30	5.79	6.37	6.00	5.57	5.06	4.22	3.59	3.45	3.33	3.14	2.95	15.63
Great Peconic Bay West	3	100003	0	0.24	1.14	5.63	12.70	13.01	8.73	4.88	10.87	3.38	0.83	0.70	1.32	1.87	2.06	2.11	2.25	1.99	1.98	2.07	2.09	2.09	2.09	2.09	2.10	11.82
Great Peconic Bay West	4	100004	0	0.07	0.12	0.20	0.38	0.74	0.69	0.29	0.87	0.84	1.30	1.53	3.31	5.06	6.14	7.10	6.75	5.95	7.64	6.08	5.37	5.21	5.81	5.01	4.20	19.34

Survey Area	ID	Code	-1	-0.5	0	0.5	1	1.5	2	2.5	3	3.5	4	4.5	5	5.5	6	6.5	7	7.5	8	8.5	9	9.5	10	10.5	11	>11
Great Peconic Bay West	5	100005	0	0.02	0.00	0.06	0.18	0.48	0.66	0.96	2.06	2.07	1.78	1.48	2.26	3.65	5.13	5.96	6.01	6.03	5.87	5.61	5.46	5.16	4.73	4.66	4.49	25.24
Great Peconic Bay West	6	100006	0	0.04	0.27	1.12	4.43	14.15	27.63	9.32	1.82	1.46	0.94	1.30	1.81	2.42	3.06	3.38	3.24	3.32	3.09	2.45	2.01	1.93	1.72	1.53	1.32	6.24
Great Peconic Bay West	7	100007	0	0.21	0.51	1.45	3.05	5.33	3.11	1.18	0.42	1.39	1.65	2.02	3.95	5.74	6.39	7.37	6.55	5.46	5.05	4.43	3.14	3.44	3.43	3.26	3.18	18.29
Great Peconic Bay West	8	100008	0	0.22	1.49	6.82	21.92	31.74	18.06	6.92	2.69	1.04	0.22	0.10	0.25	0.50	0.67	0.60	0.57	0.63	0.74	0.60	0.59	0.56	0.42	0.35	0.34	1.92
Great Peconic Bay West	9	100009	0	0.97	1.62	3.01	7.22	11.83	10.19	9.35	12.63	6.64	3.27	2.81	1.11	1.79	2.22	2.09	1.98	2.18	2.31	2.35	2.18	2.06	1.94	1.79	1.69	4.76
Great Peconic Bay West	10	100010	0	1.16	4.81	13.43	25.66	22.80	17.18	11.44	1.94	0.00	0.00	0.01	0.05	0.09	0.11	0.10	0.11	0.09	0.11	0.08	0.09	0.07	0.07	0.08	0.08	0.44
Great Peconic Bay West	11	100011	0	0.41	0.67	3.35	12.59	31.79	23.85	4.15	2.12	1.58	3.77	6.53	0.31	0.59	0.81	0.79	0.67	0.65	0.57	0.47	0.42	0.38	0.37	0.38	0.39	2.38
Great Peconic Bay West	13	100013	0	0.00	0.55	3.33	14.19	39.12	14.74	4.60	1.60	2.31	2.54	3.00	0.45	0.83	0.99	0.91	0.94	0.87	0.92	0.77	0.73	0.66	0.67	0.71	0.70	3.90
Great Peconic Bay West	14	100014	0	0.06	0.22	0.51	0.92	0.83	0.64	0.40	0.23	0.28	1.14	3.15	5.02	7.39	8.98	9.41	8.16	8.52	8.51	6.04	4.80	5.48	5.54	5.79	5.97	2.01
Great Peconic Bay West	15	100015	0	0.33	0.66	1.49	4.11	6.79	3.79	2.13	2.97	2.59	2.10	1.76	2.42	4.52	6.29	6.10	5.21	5.08	4.45	3.61	3.27	2.98	2.86	2.97	3.07	18.44
Great Peconic Bay West	16	100016	0	0.02	0.21	0.87	2.44	3.12	1.74	1.12	0.91	0.76	1.04	1.67	3.12	5.46	6.46	6.50	6.56	6.12	5.29	4.19	4.07	5.20	4.58	4.11	3.82	20.62
Great Peconic Bay West	17	100017	0	0.08	0.23	0.64	1.24	0.98	0.62	0.50	1.27	0.90	1.42	2.84	4.07	5.62	7.18	7.53	7.47	7.45	5.84	4.42	4.39	5.01	4.54	4.14	3.71	17.90
Great Peconic Bay West	18	100018	0	0.26	0.89	4.21	10.36	12.25	7.00	5.29	4.84	2.39	1.56	1.42	1.35	2.67	3.72	3.84	3.31	3.70	3.03	2.94	2.97	2.57	2.59	2.58	2.55	11.75
Great Peconic Bay West	19	100019	0	0.11	0.28	0.40	0.69	1.05	1.55	1.12	1.25	0.98	0.85	0.64	1.14	3.94	6.54	6.85	6.74	8.47	8.65	8.16	8.09	7.97	7.50	5.23	3.72	8.08
Great Peconic Bay West	20	100020	0	0.00	0.08	0.26	0.44	0.93	1.06	0.76	0.86	1.75	2.28	1.42	2.60	5.53	7.01	7.19	6.86	5.87	5.70	6.05	4.94	5.06	5.11	4.22	3.89	20.18
Great Peconic Bay West	21	100021	0	0.00	0.38	1.49	3.01	4.11	5.47	5.30	3.93	2.95	2.31	1.67	2.35	3.44	4.64	5.30	5.06	4.46	4.26	3.82	3.18	3.20	3.49	3.44	3.41	19.31
Great Peconic Bay West	22	100022	0	0.01	0.04	0.09	0.23	0.73	2.02	1.36	0.64	1.55	1.51	1.56	2.54	3.79	5.17	6.03	5.88	5.47	4.79	4.12	3.70	3.20	3.64	4.28	4.84	32.81
Great Peconic Bay West	23	100023	0	0.83	1.78	3.80	11.83	26.78	18.28	4.36	4.13	7.41	12.59	1.51	0.24	0.43	0.51	0.51	0.51	0.48	0.42	0.32	0.31	0.41	0.35	0.31	0.30	1.60
Great Peconic Bay West	24	100024	0	0.00	2.11	10.53	22.74	27.67	10.74	3.75	1.08	3.35	4.23	1.16	0.17	0.31	0.50	0.64	0.72	0.82	0.95	1.04	1.07	1.07	1.00	0.90	0.83	2.65
Great Peconic Bay West	25	100025	0	0.35	1.91	8.32	27.99	42.54	14.76	3.12	0.90	0.00	0.00	0.00	0.01	0.01	0.00	0.01	0.01	0.01	0.01	0.00	0.01	0.00	0.01	0.00	0.01	0.02
Great Peconic Bay West	26	100026	0	0.00	0.23	3.77	24.81	56.59	11.90	1.39	0.00	0.00	0.24	0.17	0.03	0.03	0.02	0.02	0.03	0.08	0.11	0.10	0.07	0.06	0.05	0.05	0.04	0.22
Great Peconic Bay West	27	100027	0	0.01	0.04	0.12	0.20	1.08	0.91	0.34	0.43	1.92	2.17	1.75	3.29	5.12	6.52	7.22	8.20	8.12	7.05	5.80	4.68	5.54	5.28	4.38	3.67	16.17
Great Peconic Bay West	28	100028	0	0.11	0.83	5.27	21.17	41.51	18.95	3.59	0.93	1.35	0.49	0.06	0.12	0.20	0.30	0.34	0.36	0.39	0.40	0.38	0.36	0.35	0.33	0.31	0.30	1.62
Great Peconic Bay West	29	100029	0	0.15	1.84	5.80	21.53	42.45	20.38	4.84	1.97	0.10	0.00	0.01	0.03	0.05	0.06	0.08	0.06	0.07	0.05	0.06	0.05	0.05	0.05	0.04	0.05	0.22
Great Peconic Bay West	30	100030	0	1.95	3.00	6.44	20.40	47.15	17.00	2.67	0.00	0.00	0.00	0.06	0.07	0.10	0.11	0.11	0.08	0.08	0.07	0.06	0.07	0.07	0.06	0.06	0.07	0.31
Great Peconic Bay West	31	100031	0	0.67	2.12	9.08	30.61	36.30	9.65	4.33	3.55	1.59	0.44	0.00	0.02	0.08	0.12	0.13	0.13	0.14	0.16	0.14	0.14	0.14	0.13	0.10	0.07	0.14
Great Peconic Bay West	32	100032	0	1.90	7.10	22.02	41.21	22.40	4.24	0.79	0.00	0.00	0.00	0.01	0.02	0.03	0.03	0.03	0.02	0.02	0.03	0.02	0.02	0.02	0.02	0.01	0.02	0.08
Great Peconic Bay West	34	100034	0	0.36	2.05	9.78	27.80	36.26	14.41	2.65	0.00	0.00	0.00	0.10	0.35	0.48	0.58	0.52	0.42	0.41	0.34	0.32	0.34	0.34	0.31	0.33	0.33	1.56
Great Peconic Bay West	35	100035	0	0.11	0.86	4.97	18.46	26.48	16.57	11.34	12.17	1.51	0.00	0.07	0.28	0.40	0.44	0.42	0.46	0.46	0.49	0.45	0.43	0.40	0.35	0.37	0.38	2.18
Great Peconic Bay West	36	100036	0	0.05	1.79	10.64	30.10	36.38	12.98	4.96	2.62	0.00	0.00	0.01	0.01	0.03	0.03	0.04	0.03	0.03	0.03	0.03	0.02	0.02	0.02	0.03	0.02	0.13
Great Peconic Bay West	37	100037	0	0.82	5.17	21.08	42.92	21.80	4.10	2.39	1.21	0.04	0.00	0.00	0.01	0.02	0.03	0.03	0.03	0.03	0.03	0.02	0.02	0.01	0.02	0.02	0.03	0.17
Great Peconic Bay West	38	100038	0	0.00	0.00	0.01	0.03	0.06	0.03	0.01	0.00	0.00	0.00	0.92	2.74	5.86	7.24	6.48	7.56	7.06	6.58	6.35	6.32	6.32	6.32	6.32	6.32	17.43
Great Peconic Bay West	39	100039	0	0.01	0.05	0.20	0.46	0.68	0.62	0.24	0.60	1.34	2.37	2.44	3.48	5.88	8.50	9.37	8.07	5.99	6.99	5.88	4.08	4.81	4.72	3.86	3.36	16.00
Great Peconic Bay West	40	100040	0	0.12	0.34	0.62	0.74	1.15	1.00	0.75	0.56	0.90	1.21	1.97	4.03	6.00	7.28	7.89	6.87	6.90	4.98	5.33	3.89	3.76	3.95	4.07	3.91	21.78

Survey Area	ID	Code	-1	-0.5	0	0.5	1	1.5	2	2.5	3	3.5	4	4.5	5	5.5	6	6.5	7	7.5	8	8.5	9	9.5	10	10.5	11	>11
Great Peconic Bay West	41	100041	0	0.41	1.20	4.78	17.80	40.38	23.34	5.08	0.48	0.00	0.00	0.02	0.11	0.26	0.36	0.38	0.36	0.42	0.46	0.44	0.41	0.34	0.28	0.30	0.33	2.09
Great Peconic Bay West	42	100042	0	1.14	2.95	7.08	11.06	17.83	16.45	9.32	4.34	3.01	7.79	7.68	0.15	0.28	0.45	0.58	0.64	0.74	0.85	0.93	0.97	0.96	0.89	0.82	0.74	2.38
Great Peconic Bay West	43	100043	0	0.00	0.00	0.49	4.86	15.26	29.90	34.41	6.30	2.17	3.33	0.41	0.10	0.16	0.21	0.23	0.26	0.26	0.22	0.19	0.15	0.17	0.17	0.14	0.12	0.51
Great Peconic Bay West	44	100044	0	0.19	1.95	9.92	28.15	30.14	23.74	3.98	0.49	0.53	0.50	0.00	0.01	0.01	0.02	0.03	0.03	0.03	0.03	0.02	0.03	0.03	0.02	0.03	0.02	0.12
Great Peconic Bay West	45	100045	0	0.15	0.86	3.41	11.73	24.42	21.83	21.11	9.94	0.58	0.25	0.08	0.16	0.29	0.39	0.36	0.31	0.29	0.29	0.25	0.27	0.33	0.32	0.29	0.29	1.76
Great Peconic Bay West	46	100046	0	0.61	3.13	11.36	28.50	32.38	14.28	4.22	1.23	0.89	0.03	0.01	0.04	0.09	0.14	0.18	0.16	0.19	0.21	0.22	0.20	0.21	0.22	0.22	0.22	1.08
Great Peconic Bay West	47	100047	0	0.00	0.07	1.72	9.51	29.16	34.38	21.96	1.98	0.00	0.01	0.04	0.06	0.08	0.10	0.10	0.07	0.07	0.06	0.05	0.05	0.06	0.05	0.06	0.05	0.27
Great Peconic Bay West	48	100048	0	0.03	0.46	1.56	9.02	25.70	32.84	17.30	2.24	0.00	0.01	0.05	0.18	0.47	0.71	0.78	0.68	0.69	0.82	0.68	0.67	0.74	0.70	0.64	0.62	2.43
Great Peconic Bay West	49	100049	0	0.23	0.56	2.74	13.48	32.17	26.67	11.20	3.35	1.24	0.93	0.35	0.26	0.34	0.44	0.49	0.52	0.53	0.51	0.45	0.39	0.39	0.37	0.35	0.32	1.72
Great Peconic Bay West	50	100050	0	0.17	0.27	2.30	10.72	34.74	32.93	8.31	2.37	1.87	0.73	0.11	0.19	0.29	0.34	0.30	0.33	0.36	0.36	0.35	0.33	0.33	0.32	0.30	0.28	1.42
Great Peconic Bay West	51	100051	0	1.37	5.42	16.34	32.53	30.55	8.61	2.14	0.70	0.66	0.27	0.32	0.04	0.06	0.06	0.06	0.07	0.07	0.07	0.06	0.07	0.06	0.05	0.05	0.06	0.32
Great Peconic Bay West	52	100052	0	1.17	1.53	3.39	5.04	11.77	18.85	10.08	2.18	2.18	3.25	1.68	2.42	3.21	4.07	4.69	4.26	3.88	3.25	2.85	2.77	2.72	2.07	1.47	0.86	0.36
Great Peconic Bay West	53	100053	0	0.15	2.73	11.95	29.07	35.41	13.96	3.94	0.87	0.00	0.00	0.00	0.05	0.12	0.14	0.12	0.14	0.14	0.13	0.12	0.12	0.12	0.12	0.12	0.13	0.33
Great Peconic Bay West	54	100054	0	0.09	0.46	1.33	3.16	4.40	2.43	1.06	0.45	0.14	0.69	1.93	2.53	3.57	4.48	5.05	4.85	4.81	4.94	4.90	4.47	4.50	4.56	4.62	4.68	25.94
Great Peconic Bay West	55	100055	0	0.05	0.62	2.60	11.08	28.00	27.69	19.97	6.54	0.13	0.00	0.02	0.11	0.19	0.26	0.23	0.17	0.16	0.20	0.22	0.25	0.27	0.21	0.18	0.15	0.68
Great Peconic Bay West	56	100056	0	0.21	0.84	3.69	9.74	19.22	37.08	25.26	1.90	0.00	0.00	0.01	0.08	0.13	0.18	0.21	0.18	0.14	0.15	0.13	0.09	0.11	0.10	0.09	0.07	0.36
Great Peconic Bay West	57	100057	0	0.25	1.25	4.55	10.94	17.33	16.49	14.34	6.79	0.52	0.78	0.69	0.70	1.09	1.48	1.83	2.01	2.01	2.08	1.97	1.92	1.78	1.70	1.65	1.58	4.30
Great Peconic Bay West	58(0)	100580																										
Great Peconic Bay West	58(1)	100058	0	0.00	0.28	3.15	16.91	36.25	19.10	5.54	1.08	0.97	5.43	3.85	0.33	0.50	0.59	0.65	0.57	0.56	0.41	0.44	0.32	0.30	0.33	0.33	0.32	1.79
Great Peconic Bay West	59	100059	0	0.23	1.21	4.64	11.75	17.20	12.03	3.72	3.19	1.76	1.28	1.13	1.59	2.51	3.29	3.62	3.55	3.27	3.10	2.78	2.10	1.89	1.94	1.79	1.67	8.76
Great Peconic Bay West	60	100060	0	0.00	0.00	0.00	0.01	0.31	0.43	0.42	0.68	0.81	1.02	2.15	3.65	6.40	7.36	7.48	6.57	7.29	5.48	4.62	4.76	4.00	4.18	4.45	4.27	23.67
Great Peconic Bay West	61	100061	0	0.21	0.59	2.59	10.53	27.37	23.86	7.69	1.43	1.04	0.60	0.58	0.78	1.26	1.68	1.78	1.53	1.77	1.66	1.69	1.30	1.44	1.45	1.38	1.17	4.69
Orient Delta	60-OD	110060	0	0.43	2.73	9.31	22.17	22.22	10.78	8.12	2.71	2.23	4.90	3.80	0.54	0.70	0.86	0.85	0.71	0.77	0.68	0.69	0.68	0.73	0.63	0.57	0.49	1.70
Orient Delta	61-OD	110061	0	0.00	0.10	0.29	0.47	0.86	1.92	4.58	8.42	6.82	4.56	3.96	4.98	7.16	7.34	6.50	5.69	4.55	3.28	2.92	2.57	2.64	2.60	2.48	2.37	12.93
Orient Delta	62	110062	0	0.00	0.20	0.25	0.58	1.07	1.43	1.83	1.44	3.65	4.64	5.43	7.39	8.90	8.18	7.13	5.94	4.30	3.66	3.33	2.94	2.45	2.72	3.10	2.98	16.46
Orient Delta	64	110064	0	0.09	0.55	1.15	1.81	2.20	1.84	1.16	1.76	4.44	6.61	5.52	6.04	8.17	8.59	7.62	6.50	5.61	4.26	2.87	2.62	2.38	2.29	2.24	2.13	11.55
Orient Delta	65	110065	0	0.00	0.02	2.15	3.90	7.52	10.72	6.41	4.97	5.33	5.06	4.36	4.54	5.33	4.56	3.65	3.57	2.89	2.74	2.05	1.87	2.21	2.06	1.94	2.16	9.98
Orient Delta	66	110066	0	0.00	0.27	1.22	2.61	4.14	3.43	0.72	1.49	4.43	6.41	6.29	5.82	7.46	7.18	6.69	5.94	5.07	3.48	3.07	2.55	2.52	2.30	2.23	2.20	12.46
Orient Delta	67	110067	0	0.36	2.27	7.20	13.02	12.87	8.46	9.46	6.87	6.94	3.19	1.92	2.30	2.97	3.00	2.76	2.25	1.45	1.27	1.28	1.08	0.91	1.10	1.06	0.99	5.02
Orient Delta	68	110068	0	2.40	5.81	11.67	20.66	15.91	13.31	7.36	1.64	1.04	0.74	0.70	1.38	1.73	1.55	1.40	1.36	1.25	1.03	1.04	1.04	1.06	0.90	0.81	0.85	3.36
Orient Delta	69	110069	0	0.00	3.38	11.03	26.90	27.24	12.53	3.42	0.95	1.33	1.40	0.50	0.55	0.75	0.78	0.72	0.81	0.71	0.78	0.70	0.70	0.61	0.53	0.58	0.52	2.60
Orient Delta	70	110070	0	0.00	0.00	0.00	0.34	1.80	2.60	5.62	7.04	4.54	3.97	2.29	4.09	6.56	7.40	6.73	5.69	5.56	3.92	3.20	3.26	2.95	2.49	2.91	2.73	14.31
Orient Delta	73	110073	0	1.33	6.40	18.50	29.00	21.26	11.40	4.61	0.60	0.00	0.00	0.02	0.18	0.33	0.50	0.59	0.61	0.49	0.40	0.35	0.32	0.31	0.32	0.31	0.31	1.82
Orient Delta	74	110074	0	0.13	3.29	23.49	39.81	20.87	7.09	2.82	0.72	0.00	0.00	0.01	0.05	0.09	0.12	0.13	0.12	0.12	0.11	0.10	0.11	0.11	0.10	0.08	0.08	0.43
Orient Delta	75	110075	0	0.06	6.50	27.64	30.45	18.95	8.00	2.12	1.09	0.80	1.06	0.38	0.09	0.15	0.20	0.22	0.20	0.21	0.18	0.16	0.19	0.19	0.16	0.15	0.14	0.71

Survey Area	ID	Code	-1	-0.5	0	0.5	1	1.5	2	2.5	3	3.5	4	4.5	5	5.5	6	6.5	7	7.5	8	8.5	9	9.5	10	10.5	11	>11
Orient Delta	76	110076	0	0.01	1.41	6.71	6.69	7.11	3.59	3.06	2.43	1.96	1.52	1.59	2.20	3.62	3.63	3.36	3.71	3.96	4.50	4.65	4.57	3.97	4.32	3.95	3.69	13.82
Orient Delta	78	110078	0	0.00	5.21	19.90	26.97	16.77	9.82	3.32	0.67	0.98	1.81	0.59	0.66	0.95	1.00	0.97	0.82	0.97	0.94	1.01	0.94	0.96	0.87	0.83	0.76	2.26
Orient Delta	79	110079	0	1.72	8.79	17.83	27.87	23.24	8.03	2.47	0.57	0.58	0.66	0.27	0.29	0.50	0.62	0.66	0.60	0.58	0.55	0.46	0.43	0.45	0.44	0.38	0.38	1.61
Orient Delta	80	110080	0	0.20	0.45	1.34	4.13	10.10	8.95	3.90	1.28	0.49	1.11	1.04	2.07	3.61	4.24	4.45	4.63	3.92	3.84	3.87	3.50	3.42	3.48	3.60	3.45	18.93
Orient Delta	81(2)	110081	0	0.47	4.65	18.02	37.94	27.70	6.65	1.78	1.21	0.68	0.26	0.01	0.02	0.03	0.04	0.04	0.03	0.04	0.04	0.04	0.04	0.04	0.04	0.04	0.04	0.16
Orient Delta	82	110082	0	0.20	2.53	9.90	25.68	34.99	15.30	3.22	0.38	0.00	0.03	0.12	0.22	0.38	0.50	0.48	0.41	0.47	0.52	0.47	0.47	0.48	0.50	0.46	0.43	1.86
Orient Delta	86	110086	0	0.00	4.25	7.75	10.30	12.22	9.29	7.12	5.07	0.55	0.52	2.06	3.54	4.27	4.26	3.85	3.38	2.62	2.20	1.77	1.67	1.43	1.45	1.47	1.39	7.57
Orient Delta	90	110090	0	0.27	0.97	2.85	6.79	10.17	6.12	2.19	3.88	3.63	2.15	2.14	3.53	4.96	5.43	5.22	5.22	4.49	3.32	2.75	2.68	2.70	2.34	2.29	2.21	11.70
Orient Delta	92	110092	0	0.00	0.61	2.06	2.69	6.98	14.25	13.49	9.52	4.90	4.22	4.59	2.93	3.33	3.03	2.83	2.28	2.18	1.84	1.68	1.40	1.59	1.17	1.33	1.48	9.61
Orient Delta	93	110093	0	0.26	1.82	8.25	34.14	40.25	4.06	0.87	0.21	0.15	0.05	0.19	0.38	0.62	0.71	0.74	0.70	0.74	0.62	0.55	0.56	0.47	0.41	0.41	0.41	2.45
Orient Delta	98	110098	0	0.00	2.02	10.40	16.66	23.41	29.01	13.09	3.30	0.06	0.00	0.02	0.08	0.12	0.15	0.17	0.15	0.14	0.14	0.12	0.14	0.15	0.14	0.11	0.09	0.31
Orient Delta	100	110100	0	0.17	3.44	9.54	15.87	18.83	21.40	20.15	4.87	1.24	0.14	0.05	0.17	0.26	0.33	0.35	0.33	0.30	0.30	0.26	0.30	0.33	0.29	0.24	0.21	0.64
Orient Delta	101	110101	0	0.00	1.77	7.36	16.28	26.85	22.60	9.91	5.24	3.51	2.45	1.21	0.10	0.15	0.16	0.17	0.17	0.17	0.18	0.17	0.16	0.15	0.15	0.14	0.14	0.82
Orient Delta	104	110104	0	0.72	3.92	11.05	18.31	17.39	16.96	5.61	0.65	1.01	1.15	0.86	0.82	1.12	1.28	1.35	1.34	1.39	1.36	1.34	1.34	1.15	1.17	1.13	1.13	6.45
Orient Delta	106	110106	0	0.58	3.28	11.50	22.23	25.08	19.25	9.69	2.50	0.00	0.04	0.18	0.30	0.41	0.41	0.37	0.28	0.28	0.36	0.33	0.27	0.28	0.34	0.30	0.28	1.46
Orient Delta	108	110108	0	0.00	1.41	2.74	5.74	14.66	32.11	33.82	5.57	1.06	1.35	0.02	0.05	0.08	0.13	0.11	0.11	0.12	0.09	0.08	0.08	0.10	0.07	0.08	0.06	0.36
Orient Delta	109	110109	0	0.00	7.03	11.91	17.40	25.59	20.97	6.27	1.09	1.26	1.50	0.52	0.20	0.30	0.32	0.35	0.37	0.38	0.38	0.41	0.37	0.34	0.36	0.32	0.34	2.04
Orient Delta	111	110111	0	0.00	0.00	2.86	2.08	2.16	1.41	1.46	1.66	1.78	5.88	8.20	6.60	8.90	8.59	7.63	6.37	4.51	3.96	3.53	2.17	2.54	2.79	2.41	2.14	10.37
Orient Delta	112	110112	0	0.06	0.75	1.57	2.31	3.61	3.94	3.15	3.60	4.69	4.67	3.35	4.74	6.53	7.27	7.12	6.28	5.26	3.78	2.95	2.16	2.09	2.55	2.47	2.37	12.76
Orient Delta	116	110116	0	0.00	11.77	34.78	25.02	16.26	6.95	1.83	0.67	0.89	0.80	0.34	0.03	0.06	0.05	0.04	0.04	0.03	0.05	0.04	0.03	0.04	0.04	0.03	0.04	0.18
Orient Delta	117(0)	111170																										
Orient Delta	117(1)	110117	0	0.25	2.74	8.48	16.27	23.24	36.63	7.94	1.56	0.81	0.60	0.02	0.05	0.08	0.12	0.11	0.11	0.11	0.09	0.07	0.09	0.09	0.07	0.07	0.07	0.34
Orient Delta	118	110118	0	0.00	1.35	6.53	9.80	11.70	11.05	8.16	5.57	2.84	2.47	1.67	2.67	3.47	3.25	3.02	3.31	2.76	2.10	2.44	2.03	1.26	1.34	1.47	1.46	8.28
Orient Delta	119	110119	0	0.00	2.20	14.94	35.86	22.38	10.33	3.13	0.78	0.68	0.41	0.27	0.44	0.71	0.88	0.79	0.75	0.59	0.51	0.52	0.52	0.40	0.33	0.27	0.31	2.00
Orient Delta	120	110120	0	0.00	6.74	14.70	18.29	17.71	19.83	15.40	2.33	0.89	0.42	0.13	0.11	0.19	0.25	0.26	0.22	0.25	0.21	0.19	0.22	0.20	0.16	0.17	0.17	0.96
Orient Delta	121	110121	0	0.00	0.87	4.84	12.40	21.92	30.27	14.07	2.15	0.99	1.13	0.18	0.33	0.55	0.75	0.71	0.72	0.76	0.75	0.82	0.86	0.86	0.84	0.85	0.85	1.55
Orient Delta	122	110122	0	0.12	0.21	0.36	0.58	1.13	2.09	2.68	2.58	3.33	4.94	5.55	6.93	9.28	9.15	8.17	7.22	6.47	4.27	2.47	2.60	3.51	2.98	2.62	2.08	8.68
Orient Delta	123	110123	0	0.00	5.63	16.32	27.84	24.59	9.17	3.22	1.33	0.92	0.01	0.09	0.35	0.49	0.54	0.60	0.62	0.63	0.65	0.68	0.63	0.57	0.61	0.54	0.57	3.44
Orient Delta	124	110124	0	0.39	0.89	1.22	1.53	2.12	2.05	1.94	2.83	4.34	5.08	4.42	5.85	8.03	8.41	8.40	6.78	4.63	4.21	2.71	2.33	2.79	2.77	2.55	2.30	11.43
Orient Delta	125	110125	0	0.19	0.94	1.52	2.93	2.78	2.47	2.91	5.22	5.70	3.53	5.04	5.94	6.95	6.52	5.82	5.22	4.78	3.15	3.09	3.20	2.76	2.30	2.36	2.28	12.40
Orient Delta	126	110126	0	0.11	0.79	1.84	2.63	3.42	2.32	0.92	0.36	0.55	3.22	5.70	7.40	9.00	7.45	7.11	6.14	4.91	4.38	4.29	3.89	3.43	3.52	3.32	3.06	10.23
Orient Delta	127	110127	0	0.40	2.55	11.28	29.01	25.34	15.73	7.40	2.57	2.24	1.34	0.61	0.14	0.19	0.19	0.16	0.13	0.10	0.09	0.07	0.05	0.05	0.06	0.05	0.05	0.22
Orient Delta	128	110128	0	0.00	0.00	0.00	0.09	0.52	1.26	1.55	2.17	4.75	6.33	6.91	7.74	8.67	7.78	7.17	5.63	4.56	4.21	3.18	2.46	2.75	2.15	2.29	2.48	15.33
Orient Delta	129	110129	0	0.99	2.73	9.20	23.70	33.41	16.49	4.37	0.99	0.20	0.02	0.13	0.27	0.44	0.55	0.61	0.55	0.59	0.52	0.48	0.45	0.40	0.35	0.34	0.33	1.90

Survey Area	ID	Code	-1	-0.5	0	0.5	1	1.5	2	2.5	3	3.5	4	4.5	5	5.5	6	6.5	7	7.5	8	8.5	9	9.5	10	10.5	11	>11
Orient Delta	1300	111300	0	0.11	3.89	15.29	23.56	24.55	13.83	4.57	1.07	0.00	0.14	0.57	1.08	1.37	1.23	1.20	1.08	1.07	1.00	0.83	0.71	0.67	0.61	0.62	0.56	0.41
Orient Delta	1310	111310	0	0.32	3.78	11.44	25.94	32.75	18.18	3.52	0.75	1.04	0.92	0.09	0.09	0.12	0.14	0.13	0.12	0.10	0.07	0.05	0.04	0.04	0.05	0.05	0.04	0.24
Orient Delta	1320	111320	0	0.71	5.23	15.15	21.75	19.86	13.27	6.42	2.12	2.46	2.33	2.62	0.39	0.57	0.71	0.70	0.66	0.65	0.47	0.39	0.46	0.39	0.31	0.31	0.30	1.77
Orient Delta	1340	111340	0	0.91	2.89	5.15	5.00	6.65	7.27	4.08	3.78	4.91	6.21	2.74	4.03	5.11	5.41	5.02	4.32	3.18	3.07	2.17	2.00	1.83	1.61	1.87	1.75	9.04
Orient Delta	1350	111350	0	0.00	0.75	3.47	8.74	13.34	13.83	7.47	3.04	2.01	1.43	1.95	3.27	4.21	4.39	4.13	3.64	2.99	2.38	2.04	1.60	1.68	1.60	1.50	1.54	8.99
Orient Delta	1360	111360	0	0.62	3.58	12.28	24.14	25.46	12.39	6.56	1.83	1.69	1.19	1.29	0.26	0.48	0.61	0.64	0.72	0.65	0.53	0.60	0.46	0.50	0.42	0.42	0.40	2.27
Orient Delta	1370A	111371																										
Orient Delta	1370B	111370	0	0.35	1.57	7.14	18.55	22.87	19.82	9.58	4.01	1.29	1.74	0.58	0.43	0.79	1.34	1.67	1.41	0.92	0.64	0.60	0.66	0.67	0.64	0.61	0.58	1.57
Pipes Cove	131	110131	0	0.05	0.13	0.21	0.27	0.26	1.58	8.19	17.46	13.31	3.86	1.28	2.03	2.80	2.63	1.85	2.07	2.81	3.73	3.75	4.26	4.40	4.40	4.40	4.40	9.87
Pipes Cove	132	110132	0	0.05	0.84	2.67	5.84	8.97	12.15	28.71	23.14	6.29	1.52	0.34	0.56	0.69	0.69	0.57	0.60	0.53	0.55	0.52	0.51	0.59	0.47	0.49	0.45	2.21
Pipes Cove	134	110134	0	0.06	1.15	7.44	15.03	16.92	31.20	23.39	2.46	0.54	0.26	0.02	0.05	0.10	0.15	0.15	0.15	0.12	0.11	0.12	0.12	0.13	0.10	0.07	0.05	0.12
Pipes Cove	139	110139	0	0.08	0.71	2.55	7.88	13.03	10.80	8.91	11.75	9.35	6.00	2.55	2.64	2.63	2.16	1.83	1.46	1.62	1.36	1.38	1.20	1.23	1.10	1.13	1.06	5.60
Pipes Cove	140	110140	0	1.57	11.83	8.95	6.86	10.17	10.75	11.99	10.89	8.07	1.29	0.74	1.02	1.19	1.11	1.00	1.06	0.80	0.79	1.04	0.99	0.83	0.81	0.94	1.02	4.29
Pipes Cove	141	110141	0	0.00	0.10	1.15	2.37	3.27	3.61	7.51	19.58	22.22	8.01	2.96	1.66	2.09	2.17	2.09	2.02	1.90	1.71	1.66	1.63	1.54	1.52	1.45	1.38	6.39
Pipes Cove	142	110142	0	0.15	0.29	0.34	0.55	0.68	2.22	8.35	22.62	21.83	6.76	2.69	2.24	2.74	2.57	2.20	2.13	2.22	2.16	1.94	1.90	1.78	1.63	1.51	1.39	7.12
Pipes Cove	145	110145	0	0.00	0.57	1.91	4.70	5.06	4.89	6.63	16.74	10.13	5.84	2.03	1.82	2.83	3.01	2.97	2.70	2.55	2.65	2.42	2.28	2.13	2.03	1.88	1.95	10.27
Pipes Cove	146	110146	0	0.00	0.82	2.34	3.01	3.11	1.54	3.31	9.93	13.51	6.19	7.33	6.60	6.63	5.28	3.85	3.32	2.33	2.44	2.21	1.55	1.67	1.42	1.45	1.48	8.68
Pipes Cove	148	110148	0	0.02	0.86	4.59	9.86	12.28	9.81	6.93	7.08	7.94	4.73	1.25	1.64	2.35	2.44	2.42	2.18	2.43	2.25	2.29	2.09	1.94	1.81	1.55	1.65	7.61
Pipes Cove	150	110150	0	0.13	4.78	14.26	21.18	20.97	17.65	7.81	3.86	1.93	0.90	0.32	0.41	0.46	0.51	0.45	0.38	0.42	0.40	0.34	0.42	0.39	0.39	0.35	0.27	1.02
Pipes Cove	151	110151	0	0.00	0.48	5.25	12.41	13.85	12.45	20.22	11.43	2.73	2.28	1.40	1.28	1.53	1.36	1.21	0.99	1.14	1.04	0.96	0.98	0.98	1.08	0.91	0.89	3.16
Pipes Cove	152	110152	0	0.00	1.08	6.07	12.93	16.14	23.39	22.76	8.97	2.30	0.86	1.32	0.15	0.21	0.26	0.24	0.22	0.20	0.19	0.21	0.21	0.21	0.23	0.22	0.24	1.39
Pipes Cove	153	110153	0	0.00	0.94	5.69	12.28	12.40	12.45	21.73	20.69	3.49	1.45	0.69	0.49	0.62	0.65	0.56	0.48	0.50	0.43	0.44	0.42	0.36	0.39	0.39	0.37	2.09
Pipes Cove	154	110154	0	0.03	2.49	8.81	15.30	19.94	16.50	16.09	8.91	3.21	0.70	0.26	0.39	0.48	0.44	0.39	0.35	0.36	0.36	0.44	0.45	0.47	0.43	0.41	0.41	2.36
Pipes Cove	155	110155	0	0.00	0.00	4.84	7.84	9.34	6.82	7.21	9.81	8.47	5.62	2.05	2.63	3.34	3.15	2.71	2.59	2.72	2.68	2.29	2.19	1.96	1.73	1.79	1.64	6.58
Pipes Cove	156	110156	0	0.00	1.16	7.60	20.06	24.23	17.56	12.76	6.43	2.81	2.06	1.22	0.18	0.25	0.30	0.30	0.27	0.26	0.28	0.31	0.33	0.32	0.28	0.24	0.20	0.64
Pipes Cove	157	110157	0	0.34	2.22	6.41	10.54	12.14	31.39	21.67	5.17	2.13	2.16	0.86	0.22	0.30	0.33	0.33	0.33	0.31	0.34	0.30	0.33	0.29	0.27	0.26	0.22	1.14
Pipes Cove	160	110160	0	0.08	1.29	6.76	9.98	10.23	8.65	6.69	10.02	8.07	5.81	2.50	3.01	3.54	2.73	2.68	2.51	2.29	1.68	1.37	1.44	1.36	1.42	1.38	1.31	3.20
Pipes Cove	164	110164	0	0.17	2.25	9.99	23.69	23.78	11.95	7.11	5.86	2.28	2.08	0.33	0.53	0.69	0.71	0.63	0.67	0.60	0.54	0.63	0.67	0.62	0.56	0.55	0.53	2.57
Pipes Cove	168	110168	0	0.36	1.30	4.45	11.06	13.31	10.42	9.27	7.37	7.61	4.02	1.25	1.72	2.15	2.18	2.14	2.03	1.93	1.98	2.07	2.07	1.90	1.77	1.49	1.23	4.97
Pipes Cove	169	110169	0	0.00	0.72	12.78	20.91	24.26	16.55	7.46	4.97	7.07	2.30	0.06	0.09	0.15	0.20	0.25	0.24	0.22	0.19	0.19	0.20	0.20	0.18	0.15	0.13	0.52
Pipes Cove	174	110174	0	0.48	5.27	11.71	21.57	20.81	16.25	10.57	5.75	1.50	1.96	0.24	0.12	0.20	0.22	0.26	0.26	0.25	0.25	0.19	0.23	0.21	0.21	0.21	0.21	1.08
Pipes Cove	177	110177	0	0.00	0.92	3.73	9.61	10.29	12.61	21.20	22.37	4.89	2.60	0.84	0.76	0.87	0.83	0.79	0.68	0.68	0.66	0.68	0.57	0.56	0.53	0.53	0.48	2.38

Survey Area	Planned ID	Code	-1.0	-0.5	0.0	0.5	1.0	1.5	2.0	2.5	3.0	3.5	4.0	4.5	5.0	5.5	6.0	6.5	7.0	7.5	8.0	8.5	9.0	9.5	10.0	10.5	11.0	>11
West Shelter Island	40	120040	0.00	0.06	0.02	0.06	11.05	76.55	10.56	0.95	0.74	0.00	0.00	0.00	0.00	0.00	0.00	0.00	0.00	0.00	0.00	0.00	0.00	0.00	0.00	0.00	0.00	0.00
West Shelter Island	43	120043	0.00	0.23	3.55	14.96	31.56	32.59	13.27	2.82	0.97	0.06	0.00	0.00	0.00	0.00	0.00	0.00	0.00	0.00	0.00	0.00	0.00	0.00	0.00	0.00	0.00	0.00
West Shelter Island	33	120033	0.00	0.37	1.67	7.65	21.92	33.60	20.18	5.52	2.98	0.53	1.21	0.57	0.18	0.21	0.24	0.20	0.16	0.18	0.24	0.18	0.16	0.20	0.23	0.23	0.20	1.20
West Shelter Island	39	120039	0.00	0.03	1.46	7.33	19.24	32.22	27.30	8.96	2.27	1.13	0.06	0.00	0.00	0.00	0.00	0.00	0.00	0.00	0.00	0.00	0.00	0.00	0.00	0.00	0.00	0.00
West Shelter Island	31	120031	0.00	0.12	2.42	16.70	45.24	27.61	5.96	1.61	0.34	0.00	0.00	0.00	0.00	0.00	0.00	0.00	0.00	0.00	0.00	0.00	0.00	0.00	0.00	0.00	0.00	0.00
West Shelter Island	36	120036	0.00	0.00	0.08	1.59	5.12	10.16	15.63	35.79	27.13	4.02	0.49	0.00	0.00	0.00	0.00	0.00	0.00	0.00	0.00	0.00	0.00	0.00	0.00	0.00	0.00	0.00
West Shelter Island	42	120042	0.00	0.00	0.00	0.46	4.61	11.72	12.91	28.27	34.52	6.70	0.80	0.00	0.00	0.00	0.00	0.00	0.00	0.00	0.00	0.00	0.00	0.00	0.00	0.00	0.00	0.00
West Shelter Island	41	120041	0.00	0.00	0.00	0.27	1.87	3.28	5.25	18.28	41.59	15.69	3.27	1.56	0.33	0.48	0.60	0.66	0.63	0.56	0.58	0.54	0.41	0.52	0.56	0.50	0.45	2.18
West Shelter Island	44 a	120441																										
West Shelter Island	44 b	120442																										
West Shelter Island	44	120044	0.00	0.00	0.30	6.99	21.71	33.37	21.26	8.40	5.18	2.36	0.43	0.00	0.00	0.00	0.00	0.00	0.00	0.00	0.00	0.00	0.00	0.00	0.00	0.00	0.00	0.00
West Shelter Island	34a	120341																										
West Shelter Island	34	120034	0.00	0.17	2.72	16.71	29.43	31.34	14.02	3.93	1.59	0.09	0.00	0.00	0.00	0.00	0.00	0.00	0.00	0.00	0.00	0.00	0.00	0.00	0.00	0.00	0.00	0.00
West Shelter Island	32	120032	0.00	0.20	1.57	5.73	9.38	12.90	16.90	13.39	6.64	3.26	1.90	0.95	1.38	1.67	1.69	1.78	1.44	1.48	1.72	1.49	1.52	1.42	1.31	1.32	1.37	7.57
West Shelter Island	37	120037	0.00	0.24	2.75	14.03	28.01	26.57	12.60	4.47	1.33	0.71	0.68	0.37	0.30	0.39	0.45	0.45	0.50	0.39	0.56	0.68	0.57	0.84	0.63	0.50	0.50	1.48
West Shelter Island	38	120038	0.00	0.18	0.62	1.91	4.50	4.51	4.02	3.68	6.07	8.64	3.49	3.66	4.07	5.27	6.04	5.40	3.56	2.50	2.97	3.49	3.29	2.74	2.93	2.57	2.31	11.59
West Shelter Island	49	120049	0.00	0.08	1.20	4.23	7.13	8.68	7.68	5.83	9.88	10.57	4.97	3.12	3.23	4.01	4.18	3.51	2.36	1.86	2.22	2.05	1.63	1.20	1.15	1.15	1.15	6.91
West Shelter Island	35	120035	0.00	0.03	0.29	6.82	26.33	26.41	11.20	7.83	4.31	2.83	1.26	0.38	0.37	0.70	0.83	0.86	0.73	0.73	0.73	0.73	0.73	0.73	0.73	0.73	0.73	2.99
West Shelter Island	48a	120481																										
West Shelter Island	48	120048	0.00	0.01	0.54	7.78	23.32	26.09	10.95	4.95	3.25	3.16	1.96	1.56	1.27	1.67	1.92	1.76	1.41	0.88	0.85	0.84	0.67	0.59	0.67	0.59	0.55	2.75
West Shelter Island	30	120030	0.00	0.04	0.13	0.52	1.39	2.79	2.30	1.08	0.82	1.65	3.94	4.45	5.84	6.86	6.13	6.08	6.13	4.84	4.55	4.43	4.87	3.58	2.88	3.05	3.16	18.49
West Shelter Island	47	120047	0.00	0.00	0.00	0.00	0.00	0.00	0.00	0.00	0.00	0.00	0.00	0.00	7.83	10.82	11.23	8.46	7.25	7.54	6.50	5.74	4.33	3.51	4.20	4.14	3.45	15.03
West Shelter Island	21	120021	0.00	0.00	0.39	2.93	6.74	6.83	4.01	3.20	5.98	10.35	5.96	3.98	3.66	3.29	2.94	4.02	3.64	2.93	2.41	2.40	2.40	2.40	2.40	2.40	2.40	12.38
West Shelter Island	46	120046	0.00	0.14	1.05	3.45	7.37	9.28	7.95	3.67	2.25	2.04	2.51	3.78	4.72	6.55	7.05	6.67	5.88	3.88	2.96	2.60	2.10	2.25	2.40	1.94	1.56	5.90
Noyack Bay	18	120018	0.00	0.01	0.33	4.90	14.83	25.67	33.68	13.87	5.13	1.58	0.00	0.00	0.00	0.00	0.00	0.00	0.00	0.00	0.00	0.00	0.00	0.00	0.00	0.00	0.00	0.00
Noyack Bay	19a	120191	0.00	0.15	1.48	11.46	27.44	30.85	15.83	6.50	4.27	1.90	0.12	0.00	0.00	0.00	0.00	0.00	0.00	0.00	0.00	0.00	0.00	0.00	0.00	0.00	0.00	0.00
Noyack Bay	19	120019	0.00	0.05	2.40	14.38	30.04	29.50	13.72	6.66	2.61	0.64	0.00	0.00	0.00	0.00	0.00	0.00	0.00	0.00	0.00	0.00	0.00	0.00	0.00	0.00	0.00	0.00
Noyack Bay	20	120020	0.00	0.00	0.11	0.97	4.52	13.99	29.27	23.47	8.76	2.76	1.31	0.78	0.43	0.65	0.86	1.01	0.86	0.65	0.67	0.69	0.64	0.57	0.56	0.66	0.73	5.08
Noyack Bay	45	120045	0.00	0.00	1.15	6.19	15.93	14.83	14.16	13.80	17.34	8.73	2.97	0.76	0.14	0.21	0.25	0.28	0.25	0.19	0.24	0.22	0.19	0.21	0.22	0.22	0.22	1.31
Noyack Bay	17	120017	0.00	0.01	0.58	8.68	28.32	28.37	13.70	5.43	2.59	2.09	1.17	0.52	0.35	0.48	0.62	0.65	0.52	0.41	0.41	0.44	0.38	0.34	0.38	0.41	0.45	2.70
Noyack Bay	29	120029	0.00	0.14	0.61	6.52	17.77	31.48	27.18	8.01	2.56	1.01	0.69	0.40	0.15	0.24	0.30	0.30	0.22	0.19	0.19	0.21	0.25	0.23	0.15	0.15	0.15	0.93
Noyack Bay	28	120028	0.00	0.02	0.61	5.27	13.96	25.19	28.36	19.40	6.18	0.84	0.16	0.00	0.00	0.00	0.00	0.00	0.00	0.00	0.00	0.00	0.00	0.00	0.00	0.00	0.00	0.00
Noyack Bay	27	120027	0.00	0.01	1.22	7.09	16.63	26.94	23.89	14.14	7.79	2.27	0.00	0.00	0.00	0.00	0.00	0.00	0.00	0.00	0.00	0.00	0.00	0.00	0.00	0.00	0.00	0.00
Noyack Bay	10	120010	0.00	0.00	0.62	6.45	24.69	36.56	18.30	7.19	4.48	1.61	0.11	0.00	0.00	0.00	0.00	0.00	0.00	0.00	0.00	0.00	0.00	0.00	0.00	0.00	0.00	0.00

Survey Area	Planned ID	Code	-1.0	-0.5	0.0	0.5	1.0	1.5	2.0	2.5	3.0	3.5	4.0	4.5	5.0	5.5	6.0	6.5	7.0	7.5	8.0	8.5	9.0	9.5	10.0	10.5	11.0	>11
Noyack Bay	12	120012	0.00	0.13	1.44	8.88	28.42	44.30	15.48	1.35	0.00	0.00	0.00	0.00	0.00	0.00	0.00	0.00	0.00	0.00	0.00	0.00	0.00	0.00	0.00	0.00	0.00	0.00
Noyack Bay	9	120009	0.00	0.41	2.19	10.35	25.30	33.10	16.44	5.13	1.90	0.77	0.60	0.63	0.15	0.19	0.22	0.22	0.22	0.21	0.17	0.17	0.17	0.22	0.18	0.17	0.17	0.71
Noyack Bay	5	120005	0.00	0.10	1.49	8.38	19.28	22.08	13.34	8.61	4.60	2.67	1.23	0.93	1.04	1.31	1.55	1.73	1.54	1.16	1.00	1.08	1.24	1.17	0.97	0.80	0.62	2.06
Noyack Bay	4a	124001	0.00	0.02	0.07	0.31	0.62	0.95	1.27	0.85	0.54	0.79	1.01	3.12	4.89	7.17	8.04	7.89	7.06	5.88	5.39	4.84	4.21	4.18	3.39	4.08	4.02	19.44
Noyack Bay	6	120006	0.00	0.02	0.08	0.52	1.46	1.49	1.12	0.76	1.27	4.32	4.63	3.69	4.42	7.19	9.14	8.61	7.15	5.54	5.43	4.20	3.67	4.00	4.25	3.46	2.77	10.84
Noyack Bay	4b	124002	0.00	0.00	0.01	0.37	1.33	2.21	3.40	3.30	5.55	8.48	4.33	5.27	4.79	6.60	7.29	6.80	5.64	3.59	2.60	1.98	2.21	2.25	1.85	2.07	2.29	15.78
Noyack Bay	3	120003	0.00	0.00	0.91	6.60	12.58	10.84	6.52	3.02	2.19	3.52	2.55	1.53	2.10	3.60	4.30	3.96	4.28	3.03	2.73	1.61	2.09	2.20	2.20	2.20	2.20	13.21
Noyack Bay	1	120001	0.00	0.00	0.00	0.00	0.00	0.00	0.00	0.00	0.00	0.00	0.00	0.00	6.82	16.17	25.03	28.11	15.69	3.54	2.87	1.18	0.09	0.05	0.05	0.05	0.05	0.30
Noyack Bay	8	120008	0.00	0.00	0.18	2.30	12.60	27.06	30.26	12.89	4.65	1.22	0.39	1.32	0.32	0.47	0.54	0.52	0.40	0.37	0.30	0.35	0.38	0.40	0.38	0.37	0.35	1.98
Noyack Bay	2	120002	0.00	0.02	0.20	1.20	4.88	16.56	13.14	3.09	0.60	0.32	0.41	1.83	3.96	9.38	14.53	16.33	9.12	2.08	1.65	0.67	0.03	0.00	0.00	0.00	0.00	0.00
Noyack Bay	16	120016	0.00	0.01	0.00	0.02	0.11	0.26	0.42	0.48	0.56	1.24	2.44	4.85	5.82	7.05	7.52	6.39	5.52	5.45	4.96	4.69	4.18	3.89	4.31	4.13	3.93	21.75
Noyack Bay	7	120007	0.00	0.03	0.05	0.02	0.14	0.28	0.42	1.03	3.73	12.21	12.47	5.06	4.35	5.62	5.25	4.81	4.32	3.84	3.28	3.54	3.62	2.78	2.88	2.78	2.66	14.78
Noyack Bay	22	120022	0.00	0.07	0.26	0.68	1.20	1.83	2.90	4.23	11.61	21.81	9.56	4.86	3.40	3.95	4.50	4.57	3.89	3.14	2.68	2.50	2.29	2.13	1.74	1.40	1.07	3.73
Noyack Bay	23	120023	0.00	0.30	0.55	0.74	1.58	3.25	4.13	5.16	14.56	23.05	8.01	2.96	2.59	3.09	3.24	2.73	1.93	1.67	1.79	1.45	1.50	1.34	1.53	1.56	1.60	9.68
Noyack Bay	15	120015	0.00	0.09	0.19	0.29	1.08	1.93	2.70	5.24	15.33	19.73	7.91	2.97	2.31	3.16	4.06	4.16	3.52	2.89	2.51	1.97	1.99	2.25	1.89	1.53	1.53	8.77
Noyack Bay	900	120900	0.00	0.03	1.29	7.18	23.95	36.00	21.70	5.92	1.00	0.15	0.33	0.25	0.15	0.22	0.26	0.21	0.11	0.05	0.08	0.10	0.10	0.05	0.05	0.09	0.10	0.62
Noyack Bay	13a	120131	0.00	0.01	0.10	0.09	0.95	3.32	4.41	9.92	27.08	17.11	5.47	2.43	2.14	2.60	2.51	2.60	2.37	1.52	1.00	1.32	1.22	1.29	1.00	1.11	1.09	7.34
Noyack Bay	13b	120132	0.00	0.03	1.10	4.51	6.72	7.67	5.99	8.19	15.89	8.75	4.05	3.18	2.63	2.99	2.98	2.95	2.20	1.68	1.82	1.53	1.47	1.91	1.28	1.28	1.32	7.92
Noyack Bay	13c	120133	0.00	0.00	0.00	1.06	1.83	4.63	6.66	10.80	28.44	16.45	5.63	2.05	0.56	1.09	1.81	1.79	1.37	1.07	1.20	0.98	1.13	1.07	0.97	1.03	1.09	7.30
Noyack Bay	14	120014	0.00	0.02	0.11	1.10	4.42	8.66	10.22	16.25	19.94	7.39	2.98	2.08	1.36	1.93	2.18	1.67	1.59	1.38	0.94	1.23	1.01	0.81	1.25	1.18	1.34	8.95
Noyack Bay	25	120025	0.00	0.02	0.00	0.34	1.36	3.82	3.61	3.25	5.75	10.78	8.51	4.51	4.12	4.91	5.31	5.15	4.60	4.32	3.59	3.25	3.46	3.44	3.16	2.60	2.10	8.02
Noyack Bay	24	120024	0.00	0.00	0.01	0.59	2.70	5.88	7.79	11.93	21.82	19.64	5.19	1.73	0.90	1.09	0.82	0.81	0.84	0.73	1.34	1.93	2.03	2.03	2.03	2.03	2.03	4.09
Noyack Bay	26a	120261	0.00	0.10	0.05	2.24	7.09	6.62	6.86	9.69	24.71	13.97	3.88	0.98	0.70	1.24	1.86	2.14	1.71	0.77	0.53	0.76	0.61	0.92	1.17	1.41	1.43	8.56
Noyack Bay	26b	120262																										
Noyack Bay	26c	120263	0.00	0.00	0.00	0.46	4.07	8.76	10.94	15.72	29.19	10.85	3.26	0.97	0.25	0.67	0.90	1.15	1.09	0.86	0.69	0.87	1.03	0.79	0.86	1.09	1.02	4.49
Little Peconic Bay	62	120062	0.00	0.12	0.10	3.39	12.72	21.29	23.70	13.32	4.53	2.12	0.94	1.05	1.45	1.56	1.45	1.68	1.30	0.94	1.03	1.08	0.61	0.58	0.56	0.56	0.56	3.36
Little Peconic Bay	73a	120731	0.00	0.02	0.04	0.06	0.49	0.86	0.89	1.20	1.54	2.62	4.24	7.04	9.35	10.34	8.72	7.24	6.40	4.47	3.57	4.16	2.66	2.32	2.32	3.06	2.79	13.61
Little Peconic Bay	73b	120732	0.00	0.02	0.04	0.07	0.54	0.95	0.97	1.30	1.72	2.87	4.72	6.92	9.23	10.18	8.59	7.15	6.33	4.42	3.54	4.10	2.63	2.28	2.28	3.03	2.75	13.39
Little Peconic Bay	76	120076	0.00	0.00	0.15	0.70	0.93	1.26	1.05	1.25	1.54	2.22	2.17	3.98	5.72	7.57	7.98	7.54	5.65	4.49	4.73	4.02	2.73	2.46	3.13	3.40	3.61	21.74
Little Peconic Bay	65	120065	0.00	0.00	0.06	0.26	0.72	1.02	1.14	1.38	2.66	2.90	1.56	1.47	4.96	8.04	8.34	7.85	9.92	6.15	6.68	6.22	4.26	4.03	3.22	2.15	2.15	12.88
Little Peconic Bay	67	120067	0.00	0.00	0.40	3.27	14.66	29.70	30.09	6.65	2.24	0.24	0.68	0.24	0.69	0.94	1.05	1.14	1.03	1.00	0.98	0.81	0.63	0.50	0.55	0.43	0.47	1.61
Little Peconic Bay	66	120066	0.00	0.04	2.16	16.26	23.57	11.54	6.73	5.44	2.57	1.15	0.43	0.59	1.37	2.25	2.77	2.44	2.17	2.58	2.01	1.72	1.75	1.23	1.24	0.72	0.80	6.46
Little Peconic Bay	77	120077	0.00	0.01	0.05	0.23	0.64	0.74	0.39	0.22	0.56	0.72	1.34	2.56	4.76	7.40	8.46	7.35	6.81	5.58	6.18	4.58	5.02	3.85	3.45	3.60	3.62	21.88
Little Peconic Bay	63	120063	0.00	0.03	0.77	9.01	33.94	33.58	12.49	2.25	0.73	0.18	0.27	0.20	0.48	0.59	0.50	0.49	0.46	0.40	0.41	0.33	0.31	0.26	0.26	0.26	0.26	1.54
Little Peconic Bay	60	120060	0.00	0.01	0.04	0.12	0.29	0.70	0.55	0.83	0.87	1.10	2.65	3.40	6.31	7.61	6.25	4.25	6.12	5.33	7.19	6.85	6.92	4.65	3.52	3.05	3.05	18.31
Little Peconic Bay	0a	120000	0.00	0.00	0.05	0.48	1.11	1.88	1.67	2.04	2.71	5.27	6.14	4.28	6.53	7.69	7.05	6.56	5.99	4.77	4.79	4.06	3.33	3.16	2.53	2.20	2.34	13.42

Survey Area	Planned ID	Code	-1.0	-0.5	0.0	0.5	1.0	1.5	2.0	2.5	3.0	3.5	4.0	4.5	5.0	5.5	6.0	6.5	7.0	7.5	8.0	8.5	9.0	9.5	10.0	10.5	11.0	>11
Little Peconic Bay	0b	121002	0.00	0.15	0.53	1.29	6.14	7.38	4.38	7.34	9.63	18.06	14.35	3.25	2.84	2.87	2.23	2.00	1.81	1.36	1.41	1.09	0.91	1.00	0.69	0.87	0.72	7.71
Little Peconic Bay	68	120068	0.00	0.13	0.14	0.66	1.52	1.44	1.77	1.08	0.95	2.18	5.83	4.54	6.71	7.60	6.53	6.57	6.29	5.53	4.98	3.38	3.19	3.73	2.48	2.49	2.72	17.55
Little Peconic Bay	61	120061	0.00	0.05	0.03	0.04	0.48	2.36	4.14	4.10	5.69	15.22	12.41	5.18	5.78	5.02	4.45	3.59	3.53	2.87	2.40	2.26	2.13	2.06	1.93	1.74	2.10	10.44
Little Peconic Bay	70	120070	0.00	0.05	0.11	0.29	1.47	3.21	3.80	4.73	12.46	23.40	9.20	3.58	3.10	3.48	3.12	2.72	2.75	2.40	2.18	1.99	2.03	1.94	1.69	1.58	1.41	7.31
Little Peconic Bay	78	120078	0.00	0.00	0.03	0.07	0.26	0.40	0.44	0.42	0.89	4.97	8.10	4.58	6.24	7.06	5.31	6.90	8.07	4.90	5.04	4.23	3.41	2.67	3.00	2.66	2.74	17.61
Little Peconic Bay	74	120074	0.00	0.03	0.00	0.23	1.07	1.59	1.60	0.93	0.73	2.00	4.40	4.74	5.67	7.09	6.77	6.69	7.20	5.59	4.33	5.46	4.70	3.51	3.73	3.00	2.91	16.02
Little Peconic Bay	75	120075	0.00	0.00	0.51	3.71	7.72	12.34	9.30	5.93	3.85	8.74	6.78	3.52	3.25	3.66	3.39	3.07	2.76	2.05	2.59	2.20	1.52	1.39	1.31	1.30	1.30	7.82
Little Peconic Bay	64	120064	0.00	0.08	0.80	3.28	6.14	8.76	14.37	11.12	20.43	13.51	2.41	1.12	1.80	1.71	1.42	1.40	1.33	1.12	1.10	1.00	0.89	0.71	0.60	0.61	0.61	3.67
Little Peconic Bay	69	120069	0.00	0.00	0.69	2.50	4.43	20.46	32.49	14.77	15.84	2.75	0.89	0.46	0.24	0.30	0.31	0.35	0.33	0.28	0.24	0.13	0.15	0.20	0.20	0.20	0.24	1.51
Little Peconic Bay	72	120072	0.00	0.00	0.00	0.00	0.00	0.00	0.00	0.00	0.00	0.00	0.00	0.00	5.60	8.22	9.04	9.03	9.12	6.27	6.09	5.55	5.03	3.72	3.59	3.59	3.59	21.55
Little Peconic Bay	71	120071	0.00	0.02	0.10	0.43	1.11	1.67	1.39	1.40	3.86	7.15	3.89	3.71	6.41	7.07	6.82	6.77	6.72	5.71	5.71	4.34	4.80	3.88	4.03	4.32	4.02	4.68
Great Peconic Bay	108	120108	0.00	0.01	1.68	10.71	25.17	39.14	18.42	2.10	0.65	0.26	0.39	0.18	0.05	0.08	0.11	0.11	0.05	0.05	0.09	0.11	0.08	0.05	0.05	0.05	0.05	0.33
Great Peconic Bay	107	120107	0.00	0.00	0.85	12.24	19.97	36.29	26.53	1.50	1.38	0.24	0.01	0.05	0.05	0.05	0.05	0.05	0.02	0.05	0.03	0.05	0.05	0.05	0.05	0.05	0.05	0.32
Great Peconic Bay	106	120106	0.00	0.07	4.61	28.35	46.59	12.90	2.89	1.42	0.46	0.06	0.00	0.04	0.06	0.06	0.06	0.11	0.12	0.09	0.15	0.14	0.12	0.12	0.17	0.18	0.18	1.07
Great Peconic Bay	93	120093	0.00	0.00	0.12	1.20	5.90	20.77	50.86	13.37	0.54	0.00	0.04	0.26	0.30	0.30	0.35	0.40	0.34	0.23	0.03	0.19	0.29	0.43	0.55	0.55	0.55	2.41
Great Peconic Bay	105	120105	0.00	0.08	0.76	3.26	9.77	26.01	42.86	15.19	2.08	0.00	0.00	0.00	0.00	0.00	0.00	0.00	0.00	0.00	0.00	0.00	0.00	0.00	0.00	0.00	0.00	0.00
Great Peconic Bay	98	120098	0.00	0.00	0.17	0.99	8.27	29.56	37.81	12.71	3.21	1.31	0.97	0.32	0.26	0.35	0.31	0.40	0.35	0.25	0.24	0.19	0.09	0.16	0.24	0.17	0.20	1.48
Great Peconic Bay	97	120097	0.00	0.00	0.49	2.82	9.59	34.62	37.58	5.97	2.12	1.90	1.02	0.03	0.09	0.17	0.24	0.34	0.21	0.16	0.32	0.26	0.18	0.16	0.20	0.19	0.20	1.19
Great Peconic Bay	92	120092	0.00	0.00	0.00	0.54	4.02	20.28	31.06	19.94	9.15	5.70	1.95	0.52	0.54	0.51	0.39	0.34	0.36	0.25	0.27	0.31	0.28	0.28	0.34	0.45	0.63	1.85
Great Peconic Bay	91	120091	0.00	0.00	0.61	3.71	9.34	15.30	17.47	10.37	2.90	2.10	1.93	1.88	2.51	3.33	3.90	4.81	4.10	2.59	2.21	1.82	1.76	1.57	1.32	1.28	1.50	1.67
Great Peconic Bay	89	120089	0.00	0.03	0.30	1.68	8.44	28.68	31.39	12.91	2.23	0.91	0.78	0.61	0.56	0.85	0.90	0.86	0.81	0.81	0.75	0.75	0.70	0.51	0.62	0.62	0.55	2.77
Great Peconic Bay	99	120099	0.00	0.00	0.01	0.30	0.97	2.83	4.24	3.41	2.15	1.30	1.25	2.18	4.47	4.93	4.70	4.61	4.76	4.58	4.45	5.06	3.80	2.80	2.46	2.71	2.88	29.20
Great Peconic Bay	102	120102	0.00	0.02	0.02	0.11	0.41	0.43	0.51	0.50	1.02	3.08	3.22	3.09	4.92	6.24	7.64	7.86	6.52	5.50	4.16	4.70	4.14	2.65	3.36	3.74	3.74	22.41
Great Peconic Bay	84	120084	0.00	0.05	1.22	6.74	25.86	38.28	11.53	3.38	1.28	1.21	0.80	0.47	0.73	0.85	0.77	0.73	0.55	0.60	0.59	0.51	0.44	0.37	0.35	0.26	0.32	2.12
Great Peconic Bay	87	120087	0.00	0.07	6.26	29.01	28.34	23.12	5.86	0.00	0.11	0.00	0.01	0.13	0.24	0.30	0.38	0.38	0.30	0.30	0.44	0.53	0.61	0.74	0.74	0.67	0.56	0.90
Great Peconic Bay	85	120085	0.00	0.09	0.60	3.50	15.33	22.43	18.39	15.28	14.24	2.07	0.01	0.15	0.36	0.42	0.36	0.34	0.36	0.36	0.38	0.43	0.44	0.39	0.34	0.41	0.37	2.98
Great Peconic Bay	88	120088	0.00	0.01	0.60	3.40	12.73	34.79	36.46	8.58	0.87	0.15	0.25	0.10	0.05	0.06	0.10	0.10	0.10	0.10	0.10	0.10	0.16	0.16	0.16	0.13	0.10	0.63
Great Peconic Bay	81	120081	0.00	0.03	1.66	17.87	18.82	10.56	6.15	8.43	20.61	10.92	1.41	0.40	0.25	0.22	0.16	0.12	0.14	0.13	0.10	0.13	0.12	0.15	0.19	0.18	0.12	1.13
Great Peconic Bay	83	120083	0.00	0.00	0.03	0.14	0.25	0.59	0.97	1.62	11.69	26.59	8.49	2.29	2.57	3.24	3.13	3.26	2.77	3.05	2.74	2.80	2.10	1.79	2.53	2.57	2.32	12.48
Great Peconic Bay	86	120086	0.00	0.00	0.87	3.54	11.11	16.37	11.36	7.68	9.88	7.97	2.31	1.55	1.50	1.89	1.97	2.60	2.41	1.92	1.73	1.66	1.39	1.48	1.30	1.30	1.12	5.08
Great Peconic Bay	80	120080	0.00	0.14	0.20	0.48	1.79	2.96	3.63	3.86	11.44	17.58	6.22	2.03	4.02	4.77	4.79	5.09	4.49	4.54	3.96	3.27	3.30	3.01	2.59	2.15	1.94	1.77
Great Peconic Bay	82	120082	0.00	0.00	0.01	0.03	0.09	0.40	0.50	0.68	1.81	6.82	6.33	3.16	4.01	5.12	5.57	5.93	5.15	4.80	4.36	4.09	3.81	3.23	2.29	2.89	3.43	25.51

Survey Area	Planned ID	Code	-1.0	-0.5	0.0	0.5	1.0	1.5	2.0	2.5	3.0	3.5	4.0	4.5	5.0	5.5	6.0	6.5	7.0	7.5	8.0	8.5	9.0	9.5	10.0	10.5	11.0	>11
Great Peconic Bay	100	120100	0.00	0.00	0.00	0.15	0.64	1.08	1.36	0.84	0.61	2.57	4.32	3.49	5.55	7.42	7.26	8.68	8.66	5.96	5.48	3.58	4.26	3.43	2.38	2.64	2.80	16.81
Great Peconic Bay	101	120101	0.00	0.10	0.29	0.57	0.47	0.82	0.93	0.59	0.39	1.95	2.60	4.58	4.51	6.07	7.13	8.11	7.99	5.93	5.36	5.40	3.17	3.28	3.69	2.98	3.11	19.99
Great Peconic Bay	95	120095	0.00	0.01	2.12	10.49	20.16	13.98	5.11	2.82	13.47	7.18	1.16	0.65	0.90	1.40	1.84	2.06	1.88	1.46	1.57	1.45	1.05	1.07	1.19	1.05	0.96	4.95
Great Peconic Bay	111a	121111	0.00	0.00	0.00	0.00	0.57	31.04	61.53	5.87	0.91	0.09	0.00	0.00	0.00	0.00	0.00	0.00	0.00	0.00	0.00	0.00	0.00	0.00	0.00	0.00	0.00	0.00
Great Peconic Bay	111b	121112	0.00	0.00	0.00	0.02	1.45	35.51	58.63	4.04	0.34	0.00	0.00	0.00	0.00	0.00	0.00	0.00	0.00	0.00	0.00	0.00	0.00	0.00	0.00	0.00	0.00	0.00
Great Peconic Bay	90	120090	0.00	0.00	0.00	0.00	0.00	0.00	0.00	0.00	0.00	0.00	0.00	0.00	6.30	8.67	7.06	10.33	9.16	6.74	6.73	4.91	5.41	3.15	4.39	4.45	3.83	18.85
Great Peconic Bay	94	120094	0.00	0.00	0.01	0.10	0.21	0.42	0.31	0.16	0.08	0.13	0.94	2.88	5.87	8.71	7.96	8.93	7.98	6.35	7.35	5.12	5.27	3.06	3.93	3.36	3.15	17.70

Table B1.7: Grain size for particles smaller than 2 phi (gravel free) and percentage sand coarser than 2 phi (2006).

Survey Area	ID	Code	Median Size (phi)	Graphic Mean (phi)	Inclusive Graphic Standard Deviation (sorting)	Inclusive Graphic Skewness	Graphic Kurtosis	% Very Coarse, Coarse, and Medium Sand (-1 to 2 phi)	% Fine and Very Fine Sand (2 to 4 phi)	% Sand (gravel free)	% Mud (silt + clay) (gravel free)	% Silt (gravel free)	% Clay (gravel free)
Little Peconic Bay West	1	70001	7.1	7.1	3.8	-3.7	26.4	10.2	12.7	22.8	77.2	35.8	41.4
Little Peconic Bay West	2	70002	6.8	7.2	3.2	15.4	17.9	1.5	13.8	15.3	84.7	48.3	36.4
Little Peconic Bay West	3	70003	5.3	5.3	3.3	4.7	21.4	20.9	20.0	41.0	59.1	34.8	24.3
Little Peconic Bay West	4	70004	0.8	0.8	0.5	0.3	0.3	95.3	3.2	98.5	1.5	1.1	0.5
Little Peconic Bay West	5	70005	7.8	8.1	2.8	12.1	15.8	0.0	0.9	0.9	99.1	50.5	48.5
Little Peconic Bay West	6	70006	5.9	6.4	3.5	17.0	24.9	6.7	30.5	37.3	62.7	30.2	32.5
Little Peconic Bay West	7	70007	2.0	2.0	0.8	1.4	0.9	47.9	46.8	94.8	5.3	2.4	2.9
Little Peconic Bay West	8	70008	1.7	1.7	1.1	2.6	2.3	57.7	37.2	94.9	5.1	2.1	3.0
Little Peconic Bay West	9	70009	1.5	2.0	2.1	32.1	4.1	71.9	13.8	85.6	14.4	7.3	7.1
Little Peconic Bay West	10	70010	5.7	6.3	3.7	24.3	26.5	8.4	27.7	36.1	63.9	33.0	30.9
Little Peconic Bay West	11d1	70110											
Little Peconic Bay West	11d2	70011	2.8	3.6	3.1	44.2	10.1	31.5	43.7	75.2	24.8	11.7	13.1
Little Peconic Bay West	12	70012	7.2	7.6	3.1	13.6	17.6	0.9	10.3	11.2	88.8	46.9	41.9
Little Peconic Bay West	13	70013	4.3	5.4	3.9	42.2	27.9	17.6	31.1	48.7	51.3	24.1	27.2
Little Peconic Bay West	14	70014	7.3	7.5	3.8	4.1	27.5	6.4	13.5	19.9	80.1	35.6	44.5
Little Peconic Bay West	15	70015	1.0	1.0	0.5	0.1	0.4	95.6	2.0	97.6	2.4	0.9	1.6
Little Peconic Bay West	16	70016	1.4	3.1	3.6	70.9	21.1	63.3	8.4	71.7	28.3	13.5	14.8
Little Peconic Bay West	17	70017	1.5	1.8	1.6	21.7	3.1	69.5	19.8	89.3	10.7	5.6	5.2
Little Peconic Bay West	18	70018	1.8	1.9	0.7	0.9	0.8	59.8	36.7	96.5	3.5	1.8	1.7
Little Peconic Bay West	19	70019	2.1	2.1	0.8	1.1	0.9	36.0	58.6	94.6	5.4	2.5	3.0
Little Peconic Bay West	20	70020	3.0	4.3	3.6	52.8	23.8	32.1	28.8	60.9	39.1	20.1	19.0
Little Peconic Bay West	21	70021	2.6	3.4	2.5	35.6	5.2	17.6	62.0	79.7	20.3	9.8	10.6
Little Peconic Bay West	22	70022	6.5	7.0	3.6	20.3	24.2	1.5	23.4	24.9	75.1	37.8	37.3
Little Peconic Bay West	23	70023	4.5	5.6	3.6	39.3	24.4	12.0	33.8	45.8	54.2	28.1	26.1
Little Peconic Bay East	30	70030	6.3	7.0	3.4	25.6	21.3	1.6	18.5	20.1	79.9	44.9	35.0

Survey Area	ID	Code	Median Size (phi)	Graphic Mean (phi)	Inclusive Graphic Standard Deviation (sorting)	Inclusive Graphic Skewness	Graphic Kurtosis	% Very Coarse, Coarse, and Medium Sand (-1 to 2 phi)	% Fine and Very Fine Sand (2 to 4 phi)	% Sand (gravel free)	% Mud (silt + clay) (gravel free)	% Silt (gravel free)	% Clay (gravel free)
Little Peconic Bay East	30	70030	6.3	7.0	3.4	25.6	21.3	1.6	18.5	20.1	79.9	44.9	35.0
Little Peconic Bay East	31	70031	6.0	6.3	4.1	15.1	29.1	16.0	13.7	29.7	70.3	36.9	33.4
Little Peconic Bay East	32	70032	5.7	6.6	3.6	31.4	25.6	4.3	28.9	33.3	66.8	33.5	33.2
Little Peconic Bay East	33	70033	1.3	2.6	2.9	55.9	8.2	66.1	13.6	79.7	20.3	9.8	10.5
Little Peconic Bay East	34	70034	5.4	6.4	3.5	34.7	22.9	4.0	31.1	35.1	64.9	36.0	29.0
Little Peconic Bay East	35	70035	6.1	6.8	3.4	27.3	23.7	1.6	26.4	28.0	72.0	37.0	35.0
Little Peconic Bay East	36	70036	5.7	6.3	3.6	23.8	26.0	7.1	28.6	35.7	64.3	32.2	32.1
Little Peconic Bay East	37	70037	2.2	2.2	1.8	22.3	4.2	39.9	48.8	88.7	11.4	5.0	6.4
Little Peconic Bay East	38	70038	3.0	3.7	2.6	33.1	6.5	17.7	57.7	75.4	24.6	13.3	11.2
Little Peconic Bay East	39	70039	1.2	1.2	1.0	5.2	1.4	85.1	9.8	94.9	5.1	2.5	2.7
Little Peconic Bay East	40	70040	1.0	1.1	0.9	4.4	1.1	85.5	9.4	94.9	5.1	2.6	2.6
Little Peconic Bay East	41	70041	5.9	6.3	3.6	10.5	24.7	13.1	15.3	28.4	71.6	39.5	32.1
Little Peconic Bay East	42	70042	3.1	4.0	2.9	34.9	13.8	22.7	43.2	65.8	34.2	20.8	13.4
Little Peconic Bay East	43	70043	7.4	7.7	3.0	6.3	18.0	1.8	9.8	11.6	88.5	44.1	44.4
Little Peconic Bay East	44	70044	3.3	4.2	2.9	38.7	13.2	15.5	47.7	63.2	36.8	22.5	14.3
Little Peconic Bay East	45	70045	1.5	1.5	0.8	0.5	1.1	73.2	24.8	98.1	2.0	0.7	1.3
Little Peconic Bay East	46	70046	7.9	8.2	2.8	8.3	16.1	0.2	3.4	3.6	96.4	47.2	49.3
Little Peconic Bay East	47	70047	7.4	7.8	2.7	8.3	14.2	0.5	6.0	6.5	93.5	50.1	43.5
Little Peconic Bay East	48	70048	7.7	7.8	2.6	7.1	12.7	0.0	2.1	2.1	97.9	50.9	47.0
Little Peconic Bay East	49	70049	7.6	7.9	2.5	7.7	12.7	0.0	2.8	2.8	97.2	52.0	45.2
Little Peconic Bay East	50	70050	3.0	3.8	2.9	30.6	14.8	28.9	38.6	67.5	32.5	19.3	13.2
Little Peconic Bay East	51	70051	4.5	5.4	3.2	32.9	18.6	8.1	36.8	44.9	55.1	33.5	21.7
Little Peconic Bay East	52d1	70520											
Little Peconic Bay East	52d2	70521											
Little Peconic Bay East	52A	70052	6.7	7.1	3.7	13.5	26.1	5.7	16.6	22.3	77.8	39.1	38.7
Little Peconic Bay East	53	70053	1.6	2.0	2.2	32.3	8.1	59.4	26.0	85.5	14.5	7.6	7.0

Survey Area	ID	Code	Median Size (phi)	Graphic Mean (phi)	Inclusive Graphic Standard Deviation (sorting)	Inclusive Graphic Skewness	Graphic Kurtosis	% Very Coarse, Coarse, and Medium Sand (-1 to 2 phi)	% Fine and Very Fine Sand (2 to 4 phi)	% Sand (gravel free)	% Mud (silt + clay) (gravel free)	% Silt (gravel free)	% Clay (gravel free)
Little Peconic Bay East	54	70054	3.4	4.4	3.0	42.3	10.8	14.0	50.0	64.0	36.0	20.8	15.3
Little Peconic Bay East	55	70055	3.8	5.1	3.3	40.9	19.2	12.4	40.7	53.2	46.9	25.2	21.6
Little Peconic Bay East	56	70056	1.6	2.0	2.2	36.2	7.7	60.0	26.6	86.5	13.5	6.0	7.5
Little Peconic Bay East	57	70057	1.6	2.1	1.5	14.0	2.2	70.2	20.2	90.4	9.6	5.4	4.2
Little Peconic Bay East	58	70058	1.4	1.4	0.7	1.3	0.8	85.0	12.4	97.4	2.6	1.1	1.4
Little Peconic Bay East	59	70059	1.0	1.0	0.6	-0.2	0.6	95.6	3.8	99.4	0.6	0.2	0.4
Little Peconic Bay East	60	70060	2.3	2.2	1.5	12.3	3.1	34.2	58.1	92.3	7.8	3.0	4.7
Little Peconic Bay East	61	70061	1.3	1.2	0.7	-0.1	0.7	89.4	8.2	97.6	2.4	1.3	1.2
Little Peconic Bay East	62	70062	1.0	1.0	1.4	18.5	2.3	91.7	2.1	93.8	6.3	1.9	4.3
Little Peconic Bay East	63	70063	1.1	1.2	1.8	20.2	5.2	74.7	17.6	92.3	7.8	3.0	4.7
Little Peconic Bay East	64	70064	1.3	1.4	1.5	13.6	3.6	74.6	18.1	92.7	7.3	3.5	3.8
Little Peconic Bay East	65d1	70650											
Little Peconic Bay East	65d2	70065	1.1	1.2	1.2	7.9	2.1	81.1	13.3	94.4	5.6	2.5	3.1
Little Peconic Bay East	66	70066	0.9	1.0	0.9	3.0	1.2	87.6	9.1	96.7	3.3	1.6	1.7
Little Peconic Bay East	67	70067	1.2	1.3	0.8	1.9	0.9	84.8	11.4	96.2	3.8	1.8	1.9
Little Peconic Bay East	68	70068	0.5	0.5	1.0	11.2	1.1	92.8	1.6	94.3	5.7	2.3	3.4
Great Peconic Bay West	1	100001	1.5	1.9	1.8	30.0	2.8	74.4	11.5	85.9	14.1	6.9	7.3
Great Peconic Bay West	2	100002	6.7	6.3	4.2	-4.6	32.9	22.1	4.0	26.1	73.9	37.6	36.3
Great Peconic Bay West	3	100003	2.6	4.5	4.1	72.3	33.4	41.5	20.0	61.4	38.6	14.3	24.3
Great Peconic Bay West	4	100004	8.0	8.3	2.9	7.1	15.5	2.2	3.3	5.5	94.5	43.5	51.0
Great Peconic Bay West	5	100005	8.4	8.6	3.2	1.0	19.4	1.4	6.9	8.3	91.7	36.4	55.3
Great Peconic Bay West	6	100006	2.0	3.9	3.3	62.8	22.3	47.6	13.5	61.2	38.8	21.6	17.2
Great Peconic Bay West	7	100007	6.9	7.1	3.9	4.5	24.4	13.7	4.6	18.3	81.7	42.5	39.2
Great Peconic Bay West	8	100008	1.3	1.4	1.5	20.5	2.4	80.3	10.9	91.1	8.9	4.1	4.8
Great Peconic Bay West	9	100009	2.7	4.0	3.3	43.6	19.1	34.9	31.9	66.7	33.3	16.5	16.8
Great Peconic Bay West	10	100010	1.0	1.1	0.7	0.5	1.1	85.0	13.4	98.4	1.6	0.7	0.9

292

Survey Area	ID	Code	Median Size (phi)	Graphic Mean (phi)	Inclusive Graphic Standard Deviation (sorting)	Inclusive Graphic Skewness	Graphic Kurtosis	% Very Coarse, Coarse, and Medium Sand (-1 to 2 phi)	% Fine and Very Fine Sand (2 to 4 phi)	% Sand (gravel free)	% Mud (silt + clay) (gravel free)	% Silt (gravel free)	% Clay (gravel free)
Great Peconic Bay West	11	100011	1.5	2.1	1.9	21.7	3.3	72.7	11.6	84.3	15.7	10.9	4.8
Great Peconic Bay West	13	100013	1.3	2.1	2.2	42.4	4.4	71.9	11.1	83.0	17.0	8.9	8.1
Great Peconic Bay West	14	100014	7.1	7.3	2.2	3.2	8.9	3.2	2.1	5.2	94.8	59.2	35.6
Great Peconic Bay West	15	100015	6.6	6.5	4.2	3.9	31.9	17.2	9.8	27.0	73.0	35.8	37.2
Great Peconic Bay West	16	100016	7.6	8.0	3.5	-1.0	23.3	8.4	3.8	12.2	87.8	41.2	46.6
Great Peconic Bay West	17	100017	7.4	7.9	3.1	9.4	17.6	3.8	4.1	7.9	92.1	48.0	44.1
Great Peconic Bay West	18	100018	4.2	5.1	4.1	37.6	34.7	35.0	14.1	49.0	51.0	23.0	28.0
Great Peconic Bay West	19	100019	7.9	7.8	2.5	-8.1	11.8	4.1	4.2	8.3	91.7	43.0	48.8
Great Peconic Bay West	20	100020	7.9	8.2	3.0	5.8	17.4	2.8	5.7	8.4	91.6	42.2	49.4
Great Peconic Bay West	21	100021	6.8	6.7	4.1	3.1	33.8	14.5	14.5	29.0	71.0	31.2	39.9
Great Peconic Bay West	22	100022	8.8	8.8	3.3	-5.8	23.1	3.1	5.1	8.2	91.8	35.2	56.6
Great Peconic Bay West	23	100023	1.5	2.0	1.6	13.6	5.3	63.3	28.5	91.8	8.2	4.6	3.6
Great Peconic Bay West	24	100024	1.2	1.8	2.2	37.2	5.0	73.8	12.4	86.2	13.8	5.3	8.6
Great Peconic Bay West	25	100025	1.1	1.1	0.5	-0.1	0.4	95.9	4.0	99.9	0.1	0.1	0.1
Great Peconic Bay West	26	100026	1.1	1.1	0.3	0.0	0.2	97.3	1.6	98.9	1.1	0.5	0.6
Great Peconic Bay West	27	100027	7.6	7.9	2.9	8.6	15.1	2.4	4.9	7.2	92.8	47.3	45.5
Great Peconic Bay West	28	100028	1.2	1.2	1.1	11.5	1.4	87.8	6.4	94.2	5.8	2.2	3.6
Great Peconic Bay West	29	100029	1.2	1.2	0.5	0.1	0.5	92.2	6.9	99.1	0.9	0.4	0.5
Great Peconic Bay West	30	100030	1.2	1.1	0.5	-0.6	0.5	95.9	2.7	98.6	1.4	0.7	0.7
Great Peconic Bay West	31	100031	1.0	1.1	0.6	1.2	0.7	88.4	9.9	98.4	1.7	0.8	0.9
Great Peconic Bay West	32	100032	0.7	0.7	0.5	-0.2	0.4	98.9	0.8	99.7	0.4	0.2	0.2
Great Peconic Bay West	34	100034	1.1	1.1	1.1	11.9	1.7	90.7	2.7	93.3	6.7	3.2	3.5
Great Peconic Bay West	35	100035	1.4	1.6	1.5	18.3	3.8	67.4	25.0	92.5	7.5	3.0	4.5
Great Peconic Bay West	36	100036	1.0	1.0	0.6	0.5	0.6	91.9	7.6	99.5	0.5	0.2	0.3
Great Peconic Bay West	37	100037	0.7	0.7	0.5	0.3	0.5	95.9	3.6	99.5	0.5	0.2	0.3
Great Peconic Bay West	38	100038	8.4	8.4	2.3	1.2	10.6	0.1	0.0	0.1	99.9	44.5	55.4

Survey Area	ID	Code	Median Size (phi)	Graphic Mean (phi)	Inclusive Graphic Standard Deviation (sorting)	Inclusive Graphic Skewness	Graphic Kurtosis	% Very Coarse, Coarse, and Medium Sand (-1 to 2 phi)	% Fine and Very Fine Sand (2 to 4 phi)	% Sand (gravel free)	% Mud (silt + clay) (gravel free)	% Silt (gravel free)	% Clay (gravel free)
Great Peconic Bay West	39	100039	7.4	7.9	2.8	12.7	14.6	2.0	4.6	6.6	93.4	50.7	42.7
Great Peconic Bay West	40	100040	7.6	8.1	3.2	9.4	20.1	4.0	3.4	7.4	92.6	45.9	46.7
Great Peconic Bay West	41	100041	1.3	1.3	1.2	15.6	1.6	87.9	5.6	93.5	6.5	2.4	4.2
Great Peconic Bay West	42	100042	1.7	2.1	2.2	29.9	10.0	56.5	24.5	81.0	19.0	11.4	7.7
Great Peconic Bay West	43	100043	1.9	1.9	0.7	1.1	0.9	50.5	46.2	96.7	3.3	1.8	1.4
Great Peconic Bay West	44	100044	1.1	1.1	0.6	0.0	0.6	94.1	5.5	99.6	0.4	0.2	0.3
Great Peconic Bay West	45	100045	1.6	1.7	1.2	7.8	2.3	62.4	31.9	94.3	5.7	2.2	3.5
Great Peconic Bay West	46	100046	1.0	1.1	0.7	0.9	0.8	90.2	6.4	96.6	3.4	1.0	2.4
Great Peconic Bay West	47	100047	1.6	1.6	0.5	-0.1	0.6	74.9	24.0	98.8	1.2	0.6	0.6
Great Peconic Bay West	48	100048	1.6	1.7	1.6	26.7	2.7	69.6	19.6	89.2	10.8	4.4	6.5
Great Peconic Bay West	49	100049	1.5	1.6	1.3	14.6	2.1	75.9	16.7	92.6	7.4	3.4	4.0
Great Peconic Bay West	50	100050	1.5	1.5	1.0	7.4	1.2	81.1	13.3	94.4	5.6	2.3	3.3
Great Peconic Bay West	51	100051	0.9	0.9	0.6	-0.1	0.6	94.8	3.8	98.6	1.4	0.8	0.7
Great Peconic Bay West	52	100052	2.3	3.7	2.9	35.5	18.0	41.8	17.7	59.4	40.6	27.4	13.1
Great Peconic Bay West	53	100053	1.0	1.0	0.6	0.3	0.6	93.3	4.8	98.1	1.9	0.8	1.1
Great Peconic Bay West	54	100054	8.3	8.2	3.8	-15.7	26.6	11.9	2.3	14.2	85.8	32.1	53.7
Great Peconic Bay West	55	100055	1.6	1.6	0.6	0.2	0.8	70.0	26.6	96.7	3.3	1.4	2.0
Great Peconic Bay West	56	100056	1.7	1.6	0.6	-0.6	0.6	70.8	27.2	98.0	2.1	1.1	1.0
Great Peconic Bay West	57	100057	1.9	3.5	3.2	53.2	16.6	50.8	22.4	73.2	26.8	11.9	14.9
Great Peconic Bay West	58 (0)	100580											
Great Peconic Bay West	58 (1)	100058	1.4	2.0	1.6	16.2	2.3	75.7	13.0	88.7	11.3	7.5	3.8
Great Peconic Bay West	59	100059	2.3	4.1	3.8	67.8	29.1	47.1	10.0	57.0	43.0	22.1	20.9
Great Peconic Bay West	60	100060	7.9	8.4	2.9	12.8	17.1	0.8	2.9	3.7	96.3	46.4	50.0
Great Peconic Bay West	61	100061	1.6	3.2	3.1	56.0	8.7	65.1	10.8	75.9	24.1	11.0	13.1
Orient Delta	60-0D	110060	1.3	1.9	2.0	26.3	5.3	67.6	18.0	85.6	14.4	8.9	5.5
Orient Delta	61-0D	110061	5.8	6.3	3.4	23.2	21.4	3.7	24.4	28.0	72.0	43.5	28.5

294

Survey Area	ID	Code	Median Size (phi)	Graphic Mean (phi)	Inclusive Graphic Standard Deviation (sorting)	Inclusive Graphic Skewness	Graphic Kurtosis	% Very Coarse, Coarse, and Medium Sand (-1 to 2 phi)	% Fine and Very Fine Sand (2 to 4 phi)	% Sand (gravel free)	% Mud (silt + clay) (gravel free)	% Silt (gravel free)	% Clay (gravel free)
Orient Delta	62	110062	6.3	7.1	3.3	23.7	20.3	3.5	11.6	15.1	84.9	50.9	34.0
Orient Delta	64	110064	6.0	6.4	3.3	15.6	17.8	7.6	14.0	21.6	78.4	52.3	26.1
Orient Delta	65	110065	4.4	5.1	3.6	31.6	24.7	24.3	21.8	46.1	53.9	31.6	22.3
Orient Delta	66	110066	5.8	6.4	3.5	19.4	20.2	11.7	13.0	24.7	75.3	47.9	27.4
Orient Delta	67	110067	2.3	3.2	3.1	42.5	17.4	44.2	26.5	70.6	29.4	17.9	11.4
Orient Delta	68	110068	1.2	2.3	2.8	45.0	7.1	69.8	10.8	80.5	19.5	10.4	9.1
Orient Delta	69	110069	1.1	1.3	1.8	29.3	3.2	81.1	7.1	88.2	11.8	5.6	6.2
Orient Delta	70	110070	6.2	6.5	3.6	17.2	22.7	4.7	21.2	25.9	74.1	42.2	31.9
Orient Delta	73	110073	0.9	1.0	1.4	16.1	2.8	87.9	5.2	93.1	6.9	3.1	3.8
Orient Delta	74	110074	0.7	0.8	0.6	0.7	0.6	94.7	3.5	98.2	1.8	0.8	1.0
Orient Delta	75	110075	0.7	0.8	0.8	2.5	1.1	91.6	5.1	96.7	3.3	1.6	1.7
Orient Delta	76	110076	6.6	6.1	4.2	-11.5	37.0	25.5	9.0	34.5	65.5	26.6	39.0
Orient Delta	78	110078	0.9	1.6	2.2	37.8	5.0	78.7	6.8	85.5	14.6	6.9	7.6
Orient Delta	79	110079	0.8	0.9	1.5	19.7	2.8	87.5	4.3	91.8	8.2	4.1	4.2
Orient Delta	80	110080	6.7	6.5	4.3	1.2	40.6	25.2	6.8	32.0	68.1	27.8	40.3
Orient Delta	81(2)	110081	0.8	0.8	0.6	0.2	0.5	95.4	3.9	99.4	0.7	0.3	0.4
Orient Delta	82	110082	1.1	1.1	1.4	20.3	2.4	88.6	3.6	92.2	7.8	3.1	4.7
Orient Delta	86	110086	2.4	3.8	3.7	56.9	25.5	43.8	13.3	57.1	42.9	26.2	16.8
Orient Delta	90	110090	5.5	5.5	4.0	13.8	31.8	27.2	11.9	39.0	61.0	34.3	26.7
Orient Delta	92	110092	3.0	4.4	3.5	55.6	20.7	26.6	32.1	58.7	41.3	23.0	18.3
Orient Delta	93	110093	1.0	1.0	1.4	25.2	1.6	88.8	1.3	90.1	10.0	4.7	5.3
Orient Delta	98	110098	1.4	1.3	0.7	-0.4	0.9	81.5	16.4	97.9	2.1	1.0	1.1
Orient Delta	100	110100	1.5	1.5	0.9	0.2	1.7	69.3	26.4	95.7	4.4	2.1	2.3
Orient Delta	101	110101	1.4	1.5	0.9	2.0	1.5	74.9	21.1	96.0	4.0	2.3	1.7
Orient Delta	104	110104	1.4	3.0	3.4	66.1	11.4	68.4	8.4	76.8	23.2	9.5	13.7

295

Survey Area	ID	Code	Median Size (phi)	Graphic Mean (phi)	Inclusive Graphic Standard Deviation (sorting)	Inclusive Graphic Skewness	Graphic Kurtosis	% Very Coarse, Coarse, and Medium Sand (-1 to 2 phi)	% Fine and Very Fine Sand (2 to 4 phi)	% Sand (gravel free)	% Mud (silt + clay) (gravel free)	% Silt (gravel free)	% Clay (gravel free)
Orient Delta	106	110106	1.2	1.2	1.2	8.0	2.2	81.9	12.2	94.2	5.9	2.6	3.3
Orient Delta	108	110108	1.9	1.8	0.6	-0.6	0.6	56.7	41.8	98.5	1.5	0.7	0.8
Orient Delta	109	110109	1.2	1.2	1.5	14.9	3.2	82.9	10.1	93.0	7.0	2.8	4.2
Orient Delta	111	110111	5.9	6.4	3.2	14.5	18.0	8.5	10.8	19.3	80.7	54.8	26.0
Orient Delta	112	110112	5.9	6.2	3.7	15.4	22.2	12.2	16.1	28.3	71.7	44.3	27.4
Orient Delta	116	110116	0.5	0.6	0.7	1.1	0.8	94.8	4.2	99.0	1.0	0.6	0.4
Orient Delta	117 (0)	111170											
Orient Delta	117 (1)	110117	1.4	1.3	0.7	-0.5	0.8	87.6	10.9	98.5	1.5	0.7	0.8
Orient Delta	118	110118	2.6	4.0	3.6	57.1	25.8	40.4	19.0	59.5	40.5	22.3	18.3
Pipes Cove													

Table B1.8: Grain size for particles smaller than 2 phi (gravel free) and percentage sand coarser than 2 phi (2008).

Survey Area	Planned ID	Code	Median Size (phi)	Graphic Mean (phi)	Inclusive Graphic Standard Deviation (sorting)	Inclusive Graphic Skewness	Graphic Kurtosis	% Very Coarse, Coarse and Medium Sand (-1 to 2 phi)	% Fine and Very Fine Sand (2 to 4 phi)	% Sand (gravel free)	% Mud (silt + clay) (gravel free)	% Silt (gravel free)	% Clay (gravel free)
West Shelter Island	40	120040	1.20	1.20	0.22	0.00	0.07	98.31	1.69	100.00	0.00	0.00	0.00
West Shelter Island	43	120043	0.90	0.93	0.55	0.06	0.52	96.15	3.85	100.00	0.00	0.00	0.00
West Shelter Island	33	120033	1.20	1.23	0.84	2.45	1.11	85.39	10.24	95.63	4.37	1.98	2.40
West Shelter Island	39	120039	1.30	1.27	0.58	-0.06	0.66	87.57	12.43	100.00	0.00	0.00	0.00
West Shelter Island	31	120031	0.80	0.80	0.43	0.08	0.37	98.04	1.96	100.00	0.00	0.00	0.00
West Shelter Island	36	120036	2.20	2.07	0.62	-0.98	0.69	32.58	67.42	100.00	0.00	0.00	0.00
West Shelter Island	42	120042	2.40	2.20	0.68	-1.30	0.72	29.71	70.29	100.00	0.00	0.00	0.00
West Shelter Island	41	120041	2.70	2.73	1.28	13.52	1.64	10.66	78.82	89.48	10.52	5.38	5.14
West Shelter Island	44 a	120441											
West Shelter Island	44 b	120442											
West Shelter Island	44	120044	1.30	1.33	0.67	0.64	0.75	83.63	16.37	100.00	0.00	0.00	0.00
West Shelter Island	34a	120341											
West Shelter Island	34	120034	1.00	0.97	0.56	0.04	0.62	94.38	5.62	100.00	0.00	0.00	0.00
West Shelter Island	32	120032	2.00	3.62	3.53	65.15	18.38	46.68	25.20	71.87	28.13	12.12	16.01
West Shelter Island	37	120037	1.00	1.10	1.58	24.67	2.93	84.20	7.19	91.39	8.61	3.41	5.20
West Shelter Island	38	120038	5.35	5.77	3.78	20.08	26.95	15.73	21.87	37.61	62.39	33.46	28.93
West Shelter Island	49	120049	3.10	4.02	3.36	42.77	19.77	28.99	31.26	60.25	39.75	24.51	15.24
West Shelter Island	35	120035	1.20	1.67	1.99	36.22	5.25	71.07	16.23	87.30	12.70	5.33	7.37
West Shelter Island	48a	120481											
West Shelter Island	48	120048	1.30	2.15	2.31	34.57	6.45	68.69	13.32	82.00	18.00	11.33	6.67
West Shelter Island	30	120030	6.85	7.39	3.53	10.14	22.99	7.16	7.48	14.64	85.36	44.91	40.45
West Shelter Island	47	120047	7.25	7.75	2.60	16.68	13.28	0.00	0.00	0.00	100.00	59.61	40.39
West Shelter Island	21	120021	4.38	5.31	3.98	37.62	27.44	20.90	25.49	46.39	53.61	26.84	26.76
West Shelter Island	46	120046	5.05	4.90	3.44	7.24	23.57	29.25	10.48	39.72	60.28	41.51	18.76
Noyack Bay	18	120018	1.50	1.47	0.66	-0.06	0.63	79.42	20.58	100.00	0.00	0.00	0.00

Survey Area	Planned ID	Code	Median Size (phi)	Graphic Mean (phi)	Inclusive Graphic Standard Deviation (sorting)	Inclusive Graphic Skewness	Graphic Kurtosis	% Very Coarse, Coarse and Medium Sand (-1 to 2 phi)	% Fine and Very Fine Sand (2 to 4 phi)	% Sand (gravel free))	% Mud (silt + clay) (gravel free)	% Silt (gravel free)	% Clay (gravel free)
Noyack Bay	19	120019	1.00	1.03	0.66	0.51	0.72	90.09	9.91	100.00	0.00	0.00	0.00
Noyack Bay	20	120020	2.00	2.30	2.05	40.39	3.71	48.85	36.31	85.16	14.84	5.92	8.92
Noyack Bay	45	120045	1.80	1.83	1.12	1.20	2.51	52.27	42.84	95.11	4.89	2.32	2.57
Noyack Bay	17	120017	1.10	1.33	1.60	24.43	2.86	79.66	11.28	90.94	9.06	3.96	5.10
Noyack Bay	29	120029	1.40	1.37	0.78	1.14	0.98	83.69	12.26	95.96	4.04	1.98	2.07
Noyack Bay	28	120028	1.50	1.50	0.67	-0.11	0.77	73.41	26.59	100.00	0.00	0.00	0.00
Noyack Bay	27	120027	1.40	1.43	0.74	0.32	0.89	75.79	24.21	100.00	0.00	0.00	0.00
Noyack Bay	10	120010	1.20	1.23	0.61	0.72	0.72	86.62	13.38	100.00	0.00	0.00	0.00
Noyack Bay	12	120012	1.10	1.07	0.45	-0.27	0.31	98.65	1.35	100.00	0.00	0.00	0.00
Noyack Bay	9	120009	1.10	1.13	0.76	1.37	0.95	87.80	8.40	96.20	3.80	2.01	1.79
Noyack Bay	5	120005	1.40	2.35	2.47	35.65	6.24	64.67	17.11	81.78	18.22	10.27	7.95
Noyack Bay	4a	124001	7.35	7.92	3.02	11.32	18.00	3.24	3.19	6.43	93.57	49.44	44.14
Noyack Bay	6	120006	6.45	6.83	3.09	11.97	16.54	4.69	10.98	15.67	84.33	51.15	33.18
Noyack Bay	4b	124002	5.65	6.47	3.71	28.18	24.42	7.33	21.66	28.99	71.01	42.59	28.42
Noyack Bay	3	120003	4.28	5.11	4.25	39.72	35.46	37.44	11.29	48.73	51.27	25.55	25.72
Noyack Bay	1	120001	5.95	5.92	0.70	0.31	0.92	0.00	0.00	0.00	100.00	98.23	1.77
Noyack Bay	8	120008	1.60	1.67	1.28	12.90	2.02	72.40	19.15	91.55	8.45	4.23	4.22
Noyack Bay	2	120002	5.15	4.27	2.16	-14.28	11.10	36.00	4.42	40.42	59.58	58.88	0.70
Noyack Bay	16	120016	7.55	8.02	3.12	14.34	18.78	0.83	4.73	5.56	94.44	47.57	46.88
Noyack Bay	7	120007	5.85	6.63	3.32	28.67	22.22	0.94	29.45	30.39	69.61	36.55	33.06
Noyack Bay	22	120022	3.70	4.68	2.56	27.21	12.01	6.94	47.21	54.15	45.85	30.99	14.86
Noyack Bay	23	120023	3.40	4.88	3.24	51.75	15.62	10.55	50.78	61.33	38.67	20.01	18.67
Noyack Bay	15	120015	3.60	5.05	3.11	48.31	17.18	6.28	48.21	54.48	45.52	25.59	19.93
Noyack Bay	900	120900	1.20	1.20	0.55	0.20	0.66	90.14	7.40	97.54	2.46	1.33	1.13
Noyack Bay	13a	120131	3.00	4.18	2.76	46.47	11.24	8.87	59.58	68.45	31.55	17.18	14.37
Noyack Bay	13b	120132	2.90	4.05	3.48	50.55	19.81	26.00	36.88	62.89	37.11	20.41	16.70

Survey Area	Planned ID	Code	Median Size (phi)	Graphic Mean (phi)	Inclusive Graphic Standard Deviation (sorting)	Inclusive Graphic Skewness	Graphic Kurtosis	% Very Coarse, Coarse and Medium Sand (-1 to 2 phi)	% Fine and Very Fine Sand (2 to 4 phi)	% Sand (gravel free)	% Mud (silt + clay) (gravel free)	% Silt (gravel free)	% Clay (gravel free)
Noyack Bay	13c	120133	2.90	3.95	2.80	46.09	6.11	14.18	61.32	75.50	24.50	10.94	13.56
Noyack Bay	14	120014	2.60	3.95	3.28	57.77	14.19	24.53	46.56	71.10	28.90	13.14	15.77
Noyack Bay	25	120025	5.35	5.83	3.24	18.73	20.54	9.16	28.29	37.44	62.56	36.54	26.02
Noyack Bay	24	120024	2.90	4.25	2.96	40.66	6.26	16.97	58.58	75.55	24.45	8.27	16.18
Noyack Bay	26a	120261	2.80	3.72	3.12	49.14	8.45	22.95	52.25	75.20	24.80	9.94	14.86
Noyack Bay	26b	120262											
Noyack Bay	26c	120263	2.60	2.79	2.11	31.87	4.35	24.24	59.02	83.25	16.75	6.59	10.16
Little Peconic Bay	62	120062	1.70	2.42	2.29	33.34	4.77	61.33	20.91	82.23	17.77	10.45	7.31
Little Peconic Bay	73a	120731	6.05	6.89	3.06	25.42	16.15	2.36	9.60	11.96	88.04	57.13	30.92
Little Peconic Bay	73b	120732	6.05	6.89	3.08	25.10	16.31	2.59	10.61	13.20	86.80	56.35	30.45
Little Peconic Bay	76	120076	6.95	7.69	3.45	17.03	23.78	4.09	7.18	11.28	88.72	47.64	41.08
Little Peconic Bay	65	120065	6.75	7.22	2.89	13.17	14.56	3.19	8.49	11.68	88.32	53.40	34.91
Little Peconic Bay	67	120067	1.50	1.57	1.46	19.80	2.11	78.12	9.80	87.92	12.08	7.09	4.98
Little Peconic Bay	66	120066	1.20	2.98	3.49	72.59	23.43	60.29	9.60	69.89	30.11	16.18	13.94
Little Peconic Bay	77	120077	7.55	8.15	3.05	15.81	17.86	2.06	2.84	4.89	95.11	49.12	45.99
Little Peconic Bay	63	120063	1.00	1.07	1.09	11.62	1.59	89.83	3.44	93.26	6.74	3.54	3.20
Little Peconic Bay	60	120060	7.65	7.92	3.03	8.94	17.04	1.71	5.45	7.16	92.84	46.48	46.36
Little Peconic Bay	0a	120000	6.15	6.67	3.36	18.06	18.99	5.18	16.16	21.33	78.67	47.64	31.02
Little Peconic Bay	0b	121002	3.30	3.88	3.03	38.97	11.65	19.87	49.38	69.24	30.76	17.77	12.99
Little Peconic Bay	68	120068	6.55	7.23	3.51	16.64	21.86	5.67	10.04	15.71	84.29	48.75	35.54
Little Peconic Bay	61	120061	4.48	5.61	3.27	39.00	18.28	7.09	37.42	44.51	55.49	32.83	22.66
Little Peconic Bay	70	120070	3.50	4.82	3.02	44.01	15.20	8.92	49.79	58.72	41.28	23.34	17.95
Little Peconic Bay	78	120078	6.65	7.26	3.27	21.43	18.78	1.20	14.38	15.58	84.42	48.12	36.30
Little Peconic Bay	74	120074	6.85	7.36	3.30	12.90	19.39	4.52	8.06	12.58	87.42	48.09	39.33
Little Peconic Bay	75	120075	3.30	4.15	3.47	42.35	22.29	33.57	25.30	58.87	41.13	24.27	16.86
Little Peconic Bay	64	120064	2.60	2.95	2.33	25.99	5.75	33.43	47.47	80.90	19.10	11.00	8.10

Survey Area	Planned ID	Code	Median Size (phi)	Graphic Mean (phi)	Inclusive Graphic Standard Deviation (sorting)	Inclusive Graphic Skewness	Graphic Kurtosis	% Very Coarse, Coarse and Medium Sand (-1 to 2 phi)	% Fine and Very Fine Sand (2 to 4 phi)	% Sand (gravel free)	% Mud (silt + clay) (gravel free)	% Silt (gravel free)	% Clay (gravel free)
Little Peconic Bay	64	120064	2.60	2.95	2.33	25.99	5.75	33.43	47.47	80.90	19.10	11.00	8.10
Little Peconic Bay	69	120069	1.70	1.87	0.89	2.71	1.39	60.57	34.25	94.82	5.18	2.53	2.64
Little Peconic Bay	72	120072	7.65	8.28	2.80	17.56	15.15	0.00	0.00	0.00	100.00	53.37	46.63
Little Peconic Bay	71	120071	6.25	6.40	2.86	3.35	14.24	4.72	16.30	21.02	78.98	48.91	30.07
Great Peconic Bay	108	120108	1.10	1.07	0.53	-0.14	0.49	95.14	3.40	98.54	1.46	0.72	0.73
Great Peconic Bay	107	120107	1.20	1.10	0.53	-0.42	0.49	95.87	3.12	98.99	1.01	0.37	0.64
Great Peconic Bay	106	120106	0.60	0.60	0.47	0.54	0.37	95.41	1.94	97.35	2.65	0.69	1.97
Great Peconic Bay	93	120093	1.70	1.63	1.27	18.43	1.44	78.86	13.95	92.81	7.19	2.21	4.98
Great Peconic Bay	105	120105	1.60	1.53	0.52	-0.46	0.44	82.73	17.27	100.00	0.00	0.00	0.00
Great Peconic Bay	98	120098	1.60	1.60	0.72	2.33	0.76	76.80	18.20	95.01	4.99	2.47	2.53
Great Peconic Bay	97	120097	1.50	1.47	0.65	1.36	0.57	85.09	11.00	96.10	3.90	1.54	2.36
Great Peconic Bay	92	120092	1.80	2.00	1.23	10.97	2.01	55.90	36.74	92.65	7.35	3.21	4.15
Great Peconic Bay	91	120091	2.10	3.32	2.85	37.90	17.06	46.43	17.29	63.72	36.28	25.34	10.94
Great Peconic Bay	89	120089	1.60	1.73	1.60	26.89	3.04	70.52	16.83	87.35	12.65	6.14	6.51
Great Peconic Bay	99	120099	7.75	7.93	3.89	-0.91	30.34	8.34	8.10	16.45	83.55	34.66	48.90
Great Peconic Bay	102	120102	7.25	7.92	3.26	17.20	20.39	1.50	7.83	9.33	90.67	45.94	44.74
Great Peconic Bay	84	120084	1.10	1.27	1.39	19.54	2.02	83.67	6.67	90.34	9.66	5.28	4.39
Great Peconic Bay	87	120087	0.70	0.77	1.47	23.95	2.86	92.66	0.12	92.77	7.23	2.48	4.75
Great Peconic Bay	85	120085	1.60	1.73	1.64	22.54	4.18	60.32	31.60	91.92	8.08	2.71	5.36
Great Peconic Bay	88	120088	1.40	1.37	0.50	-0.04	0.44	87.98	9.85	97.83	2.17	0.74	1.43
Great Peconic Bay	81	120081	1.50	1.60	1.13	1.20	2.98	55.08	41.37	96.46	3.54	1.53	2.02
Great Peconic Bay	83	120083	3.90	5.68	3.31	56.56	20.80	1.98	48.38	50.36	49.64	23.05	26.59
Great Peconic Bay	86	120086	2.40	3.52	3.12	45.05	16.92	43.26	27.83	71.09	28.91	15.57	13.33
Great Peconic Bay	80	120080	4.38	5.08	2.67	17.33	14.36	9.19	39.10	48.29	51.71	33.67	18.03
Great Peconic Bay	82	120082	7.35	7.77	3.59	14.06	24.78	1.03	15.64	16.67	83.33	38.09	45.25

Survey Area	Planned ID	Code	Median Size (phi)	Graphic Mean (phi)	Inclusive Graphic Standard Deviation (sorting)	Inclusive Graphic Skewness	Graphic Kurtosis	% Very Coarse, Coarse and Medium Sand (-1 to 2 phi)	% Fine and Very Fine Sand (2 to 4 phi)	% Sand (gravel free)	% Mud (silt + clay) (gravel free)	% Silt (gravel free)	% Clay (gravel free)
Great Peconic Bay	82	120082	7.35	7.77	3.59	14.06	24.78	1.03	15.64	16.67	83.33	38.09	45.25
Great Peconic Bay	100	120100	6.75	7.45	3.13	20.01	17.13	3.23	8.35	11.58	88.42	52.51	35.91
Great Peconic Bay	101	120101	7.15	7.82	3.19	17.39	18.57	3.18	5.52	8.70	91.30	49.69	41.61
Great Peconic Bay	95	120095	1.70	2.92	3.13	51.78	11.35	51.87	24.63	76.50	23.50	11.76	11.73
Great Peconic Bay	111a	121111	1.60	1.57	0.25	-0.03	0.10	93.14	6.86	100.00	0.00	0.00	0.00
Great Peconic Bay	111b	121112	1.50	1.50	0.22	0.00	0.10	95.61	4.39	100.00	0.00	0.00	0.00
Great Peconic Bay	90	120090	7.55	8.12	2.72	16.50	13.78	0.00	0.00	0.00	100.00	54.99	45.01
Great Peconic Bay	94	120094	7.35	7.88	2.81	16.63	14.57	1.05	1.31	2.36	97.64	56.04	41.60

Table B1.9: Shell presence in 2006 samples.

#ID	ID	AREA	OYSTERS	OYSTER	JINGLE	SLIPPER	CLAM	GASTROPODS	BIVALVE
1	1	LPecBavW							
2	2	LPecBavW							
3	3	LPecBavW	Y	Y		y			
4	4	LPecBavW							
5	5	LPecBavW							other bivalve
6	6	LPecBavW							
7	7	LPecBavW	Y						
8	8	LPecBavW	Y						
9	9	LPecBavW			y	y			
10	10	LPecBavW		?					
111	11 d1	LPecBavW	Y	Y		y			
112	11 d2	LPecBavW							
12	12	LPecBavW							
13	13	LPecBavW	Y	Y				sllipper	
14	14	LPecBavW		?					
15	15	LPecBavW							
16	16	LPecBavW							
17	17	LPecBavW							
18	18	LPecBavW				y			other bivalve
19	19	LPecBavW							
20	20	LPecBavW	Y	Y					
21	21	LPecBavW		Y	y	y (2 kinds)	clam	gastropods	other bivalve
22	22	LPecBavW							
23	23	LPecBavW		Y					
30	30	LPecBavE							
31	31	LPecBavE	Y	Y					
32	32	LPecBavE		Y					
33	33	LPecBavE	y						
34	34	LPecBavE	Y	Y					
35	35	LPecBavE							
36	36	LPecBavE							
37	37	LPecBavE	Y	Y	y	y			
38	38	LPecBavE	Y	Y					

#ID	ID	AREA	OYSTERS	OYSTER	JINGLE	SLIPPER	CLAM	GASTROPODS	BIVALVE
39	39	LPecBavE							
40	40	LPecBavE		_	y	y			
41	41	LPecBavE							
42	42	LPecBavE	Y	Y					
43	43	LPecBavE							
44	44	LPecBavE	Y	Y		y			
45	45	LPecBavE							
46	46	LPecBavE							
47	47	LPecBavE							
48	48	LPecBavE							
49	49	LPecBavE							
50	50	LPecBavE	Y	Y					
51	51	LPecBavE							
521	52 d1	LPecBavE	Y						
522	52 d2	LPecBavE	Y						
523	52A	LPecBavE							
53	53	LPecBavE		Y		y			
54	54	LPecBavE	Y	Y					
55	55	LPecBavE							
56	56	LPecBavE							
57	57	LPecBavE				y			
58	58	LPecBavE							
59	59	LPecBavE		?		y			
60	60	LPecBavE							
61	61	LPecBavE			y	y			
62	62	LPecBavE							
63	63	LPecBavE							
64	64	LPecBavE							
651	65 d1	LPecBavE				y			
652	65 d2	LPecBavE							
66	66	LPecBavE							
67	67	LPecBavE							
68	68	LPecBavE							

Table B1.10: Shell presence in 2008 samples.

Survey Area	ID	Year	Shell present?	Oyster Shell Present?	Slipper Shell Present?
West Shelter Island	38	2008	y	y	n
West Shelter Island	42	2008	y	y	n
West Shelter Island	49	2008	y	y	n
Noyack Bay	14	2008	y	y	n
Noyack Bay	17	2008	y	y	n
Noyack Bay	24	2008	y	y	n
Noyack Bay	132 (13b)	2008	y	y	n
Noyack Bay	133 (13c)	2008	y	y	n
Noyack Bay	261 (26a)	2008	y	y	n
Noyack Bay	262 (26b)	2008	y	y	n
Noyack Bay	263 (26c)	2008	y	y	n
Noyack Bay	4002 (4b)	2008	y	y	n
Little Peconic Bay	0 (0a)	2008	y	y	y
Little Peconic Bay	1002 (0b)	2008	y	y	y
Little Peconic Bay	61	2008	y	y	y
Little Peconic Bay	70	2008	y	y	n
Little Peconic Bay	71	2008	y	y	y
Little Peconic Bay	75	2008	y	y	y
Little Peconic Bay	731 (73a)	2008	y	y	y
Little Peconic Bay	732 (73b)	2008	y	y	y
Great Peconic Bay	80	2008	y	y	n
Great Peconic Bay	86	2008	y	y	n

Survey Area	ID	Year	Shell present?	Oyster Shell Present?	Slipper Shell Present?
West Shelter Island	21	2008	n	n	n
West Shelter Island	33	2008	y	n	n
West Shelter Island	34	2008	y	n	n
West Shelter Island	35	2008	n	n	n
West Shelter Island	37	2008	n	n	n
West Shelter Island	40	2008	n	n	n
West Shelter Island	41	2008	n	n	n
West Shelter Island	43	2008	y	n	n
West Shelter Island	46	2008	n	n	n
West Shelter Island	47	2008	y	n	n
West Shelter Island	481 (48a)	2008	n	n	n
Noyack Bay	1	2008	n	n	n
Noyack Bay	2	2008	n	n	n
Noyack Bay	3	2008	n	n	n
Noyack Bay	5	2008	n	n	n
Noyack Bay	6	2008	n	n	n
Noyack Bay	7	2008	n	n	n
Noyack Bay	8	2008	n	n	n
Noyack Bay	9	2008	y	n	n
Noyack Bay	10	2008	n	n	n
Noyack Bay	12	2008	y	n	n
Noyack Bay	15	2008	y	n	n
Noyack Bay	16	2008	n	n	n
Noyack Bay	18	2008	y	n	n
Noyack Bay	19	2008	n	n	n
Noyack Bay	20	2008	y	n	n
Noyack Bay	22	2008	y	n	n
Noyack Bay	23	2008	y	n	n
Noyack Bay	25	2008	n	n	n
Noyack Bay	27	2008	n	n	n
Noyack Bay	28	2008	n	n	n
Noyack Bay	29	2008	n	n	n
Noyack Bay	45	2008	y	n	n
Noyack Bay	131 (13a)	2008	y	n	n
Noyack Bay	191 (19a)	2008	y	n	n

Survey Area	ID	Year	Shell present?	Oyster Shell Present?	Slipper Shell Present?
Noyack Bay	900 (9a)	2008	y	n	n
Noyack Bay	4001 (4a)	2008	n	n	n
Little Peconic Bay	60	2008	n	n	n
Little Peconic Bay	62	2008	y	n	n
Little Peconic Bay	63	2008	y	n	n
Little Peconic Bay	64	2008	y	n	n
Little Peconic Bay	65	2008	n	n	n
Little Peconic Bay	66	2008	n	n	n
Little Peconic Bay	67	2008	y	n	n
Little Peconic Bay	68	2008	n	n	n
Little Peconic Bay	69	2008	y	n	n
Little Peconic Bay	72	2008	n	n	n
Little Peconic Bay	74	2008	n	n	n
Little Peconic Bay	76	2008	n	n	n
Little Peconic Bay	77	2008	n	n	n
Little Peconic Bay	78	2008	n	n	n
Great Peconic Bay	81	2008	n	n	n
Great Peconic Bay	82	2008	n	n	n
Great Peconic Bay	83	2008	y	n	n
Great Peconic Bay	84	2008	y	n	n
Great Peconic Bay	85	2008	y	n	n
Great Peconic Bay	87	2008	y	n	y
Great Peconic Bay	88	2008	y	n	n
Great Peconic Bay	89	2008	y	n	n
Great Peconic Bay	90	2008	n	n	n
Great Peconic Bay	91	2008	n	n	n
Great Peconic Bay	92	2008	y	n	y
Great Peconic Bay	93	2008	y	n	y
Great Peconic Bay	94	2008	n	n	n
Great Peconic Bay	95	2008	n	n	n
Great Peconic Bay	97	2008	y	n	y
Great Peconic Bay	98	2008	y	n	n
Great Peconic Bay	99	2008	n	n	n
Great Peconic Bay	100	2008	n	n	n
Great Peconic Bay	101	2008	n	n	n
Great Peconic Bay	102	2008	n	n	n

Survey Area	ID	Year	Shell present?	Oyster Shell Present?	Slipper Shell Present?
Great Peconic Bay	105	2008	y	n	y
Great Peconic Bay	106	2008	n	n	n
Great Peconic Bay	107	2008	y	n	n
Great Peconic Bay	108	2008	y	n	n
Great Peconic Bay	1111 (111a)	2008	n	n	n
Great Peconic Bay	1112 (111b)	2008	n	n	n

Table B1.11: Description of foraminifera and 1 mm to 63 μm sand in select 2008 samples.

ID (2008) Samples	Any Foraminifera?	Coiled Foraminifera?	Shell hash in sand	Description of 1 mm to 63 μm fraction of sand	Notes on Foraminifera
26 c	y	y	y	Mostly oyster shell hash at coarse end, very fine end mostly quartz / rock sand. Intermediate sizes significant portion biogenic: foraminifera and shell fragments, as well as nonbiogenic sand (quartz and rock)	At least 3 different shapes including rose, and third round one and including a wide range of sizes from slightly bigger than 63 μm (~100) to almost 5 times that.
20	y	y	y	Foraminifera only occasionally seen, mostly quart an rock with lots of shell hash fragments	1 rose shaped, sample also included 3 gastropods at almost 1mm: snail shaped, 2 mud dog snail like
42	y	y	y	A few foraminifera mixed in with mostly quart and shell fragments and maybe mica	At least 3 different shapes including rose, and third round one and including a wide range of sizes from slightly bigger than 63 μm (~100) to almost 5 times that.
23	y	y	few	Quite a few foraminifera (Small sample) with mostly quartz sand and mica, a few shell fragments	(Entire subsample measured)
12	y	n	few	Homogenous fairly coarse beige sand. Almost entirely quartz other mineral rock grains rare, few shell fragments. No coiled foraminifera	Elongate foraminifera only, and there were only a few in over 32 g of sand.
13c	y	y	y	Quite a few foraminifera, fairly coarse ample to very fine (overall fine). Lots of rock/quartz grains, large shell fragments	At least 3 different shapes including rose, and third round one and including a wide range of sizes from slightly bigger than 63μm (~100) to almost 5 times that.
13b	y	y	m	A few foraminifera mixed in, lots of shell fragments and quartz/ rock fragment grains. Much finer sample with large fragments and sand grains.	At least 3 different shapes including rose, and third round one, at least one black one, includes wide range of sizes from slightly bigger than 63 μm (~100) to almost 5 times that.
45	y	y	y	Fairly coarse sample to very fine, lots of quartz / rock fragments. A significant fraction small shell fragments. A few foraminifera are mixed in.	Only most common shape

Table B1.12: Core locations, WISE trip Great Peconic Bay.

Core ID	Grab ID	Date	Sample	Note	Latitude	Longitude	Sediment
1		3/28/09	core1	At anchor	40.93653	-72.48083	Mud
2		3/28/09	core 2	At anchor	40.93627	-72.48112	Mud
3		3/28/09	core 3		40.93523	-72.47675	Mud
	0	3/28/09	grab 0		40.93275	-72.48235	mud
4		3/28/09	core 4		40.93608	-72.47755	mud
5		3/28/09	core 5		40.93297	-72.47750	Mud with oysters at base
6		3/28/09	core 6		40.93510	-72.47662	Mud
7		3/28/09	core 7		40.94260	-72.46037	Gravel

Table B1.13: Inventories measured in 2009 Cores 1 and 4 from Great Peconic Bay. Italics=value small enough to be in error range.

Core	Core Interval (depth cm)	Average depth	Excess Pb-210 dpm/g	Cs-137 dpm/g	Excess Th-234 dpm/g	Ln Pb-210	Ln Th-234	% Water	Change in Depth (cm)	Bulk Density g/cm3	Average Inventory per cm	Inventory Pb-210 per interval	Total Inventory Pb-210
Core 1	0-4	2	18.2 ± 2.0	0.1 ± 0.0	-	2.9	-	57.3	-4	0.59	0.6	42.7 ± 2.7	
	4-7	5.5	16.5 ± 1.7	-0.5 ±-0.1	-	2.8	-	52.6	-3	0.68	0.7	33.7 ± 3.7	
	7-10	8.5	7.1 ± 1.2	-1.1 ±-0.5	-	2.0	-	47.5	-3	0.79	0.8	16.8 ± 1.9	
	10-12	11	3.8 ± 0.9	0.9 ± 0.1	-	1.3	-	44.1	-2	0.87	0.9	6.5 ± 1.6	
	12-14	13	*-2.7 ± 0.4*	*-0.9 ±-0.8*	-		-	46.2	-2	0.82	0.8	*-4.5 ±-1.1*	
	14-16	15	*0.1 ± 0.7*	*-0.4 ±-0.1*	-	*-2.1*	-	48.8	-2	0.76	0.8	*0.2 ± 0.0*	
	16-18	17	*-1.5 ± 0.7*	*-1.1 ±-0.6*	-		-	45.2	-2	0.84	0.8	*-2.6 ±-0.6*	
	18-22	20	*-1.3 ± 0.7*	*-0.6 ±-0.2*	-		-	46.9	-4	0.80	0.8	*-4.2 ±-0.3*	
	22-24	23	*-5.2 ± 0.6*	*-0.7 ±-0.3*	-		-	50.5	-2	0.73	0.7	*-7.5 ±-1.9*	
	24-26	25	*-3.6 ± 0.6*	*-0.6 ±-0.2*	-		-	48.4	-2	0.77	0.8	*-5.5 ±-1.4*	
	26+	26	*-4.3 ± 1.5*	*-1.3 ±-0.7*	-		-	46.5	-1	0.81	0.8	*-3.5 ±-3.5*	
	Total												85.9 ± 1.2
Core 4	0-2	1.0	2.8 ± 0.3	-0.1 ±-0.1	0.2 ± 0.1	1.0	*-1.5*	57.3	-2	0.59	0.59	3.3 ± 0.8	
	2-4	3.0	*0.3 ± 0.3*	*-0.1 ±-0.0*	0.9 ± 0.5	*-1.1*	*-0.1*	56.3	-2	0.61	0.61	*0.4 ± 0.1*	
	4-6	5.0	*0.1 ± 0.2*	*-0.1 ±-0.0*	*-0.5 ± 0.2*	*-2.1*	*0.0*	51.2	-2	0.71	0.71	*0.2 ± 0.0*	
	6-8	7.0	*-0.1 ± 0.2*	*-0.0 ±-0.0*	0.5 ± 0.4	*0.0*	*-1.3*	50.5	-2	0.73	0.72	*-0.1 ±-0.0*	
	10-12	11.0	*-0.2 ± 0.1*	*-0.0 ±-0.0*	*-0.9 ±-0.1*	*0.0*	*0.0*	34.8	-2	1.11	1.10	*-0.3 ±-0.1*	
	14-16	15.0	*0.2 ± 0.1*	*-0.1 ±-0.1*	*0.0 ± 0.5*	*-1.5*	*-1.3*	47.4	-2	0.79	0.79	*0.4 ± 0.1*	
	18-20	19.0	*-0.7 ± 0.1*	*-0.1 ± 0.0*	*-1.1 ±-0.1*	*0.0*	*0.0*	48.9	-2	0.76	0.76	*-1.1 ±-0.3*	
	Total												3.6 ±0.9

Table B1.14: Percentage water content (WC) and loss on ignition (LOI) in Cores 1, 3, and 4.

Core	ID Core Sample Interval	Percent Water Content	Percent LOI
Core 1	core 1 0-4 cm	57	4
	core 1 4-7 cm	53	4
	core 1 7-10 cm	48	4
	core 1 10-12 cm	44	3
	core 1 12-14 cm	46	3
	core 1 14-16 cm	49	3
	core 1 16-18 cm	45	4
	core 1 18-20 cm	47	3
	core 1 22-24 cm	51	3
	core 1 24-26 cm	48	3
	core 1 26+ cm	47	4
Core 3	core 3 0-2 cm	47	0
	core 3 2-4 cm	47	3
	core 3 4-6 cm	49	3
Core 4	core 4 0-2 cm	57	3
	core 4 2-4 cm	56	3
	core 4 4-6 cm	51	3
	core 4 6-8 cm	51	3
	core 4 8-10 cm	49	3
	core 4 10-12 cm	35	25
	core 4 12-14 cm	52	3
	core 4 14-16 cm	47	2
	core 4 16-18 cm	48	3
	core 4 18-20 cm	49	3
	core 4 20+ cm	49	3

Fig. B1.1: Photograph of shells before selection of shell to date from a grab, and prior to cutting of shell subsample to be dated. Grab #70 shells are depicted after being rinsed. Wet (TR, BL) and dry (TL, BR) shells are shown, as well as the final shell selected (BR).

Fig. B1.2: Photograph of shells from grab #61 before selection of shell to date from a grab, and prior to cutting of shell subsample to be dated. Shells have been rinsed and dried, but have not been vigorously cleaned yet. Shell on the left hand side was selected and cleaned prior to cutting.

Fig. B1.3: Photograph of shells from grab #38-2006 and selected shell before cutting it for dating. View of hinge area is focused on.

Fig. B1.4: Examples of shells selected for dating prior to cutting shells to be dated. Views of the hinge and another side of shells 0b (left hand side) and 26C (right hand side) are shown.
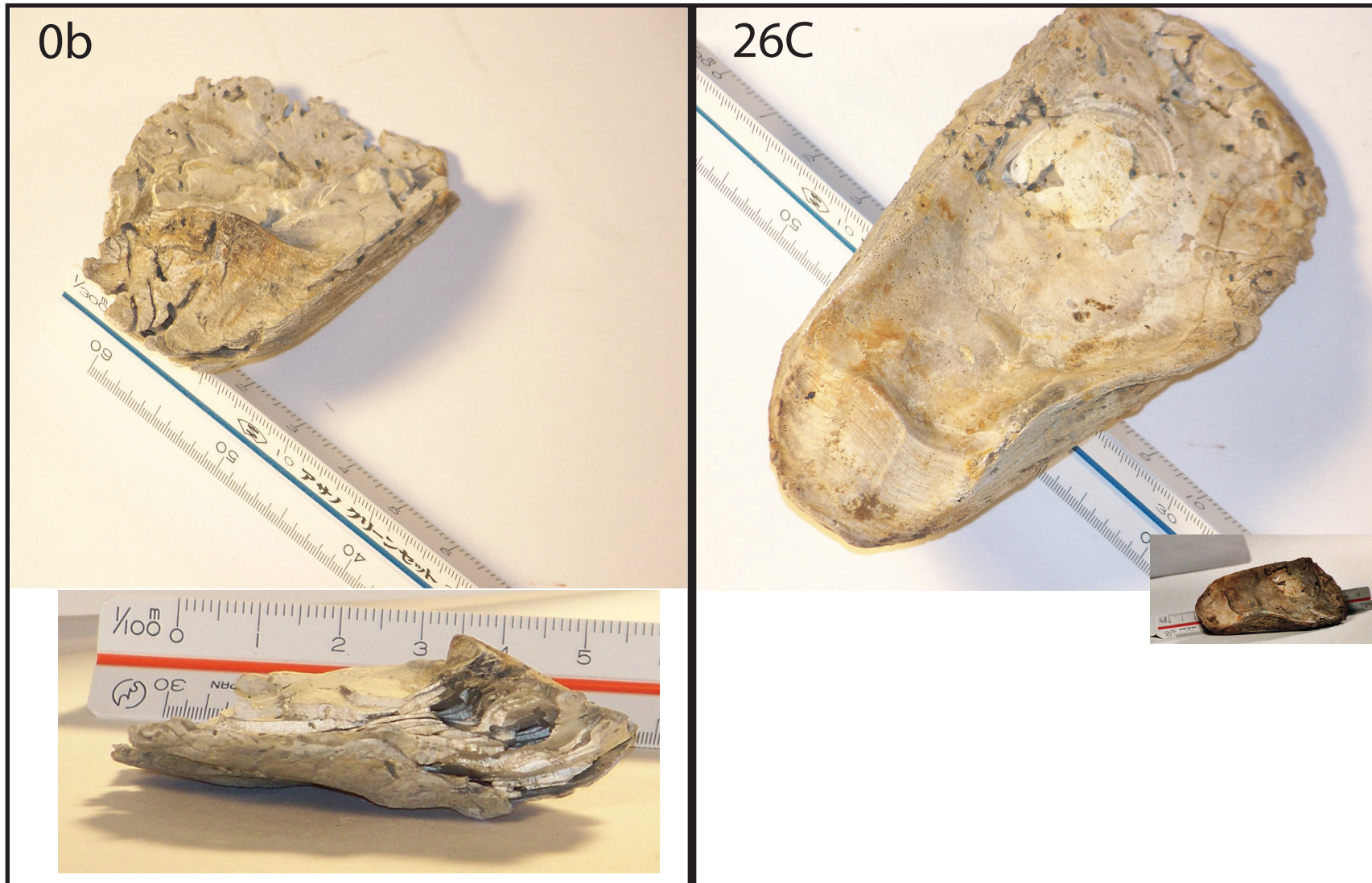
Fig. B1.5: Examples of modern shells both Aquaculture from the Peconic Estuary (unwashed), and shells from a local beach in Stony Brook, NY.

316
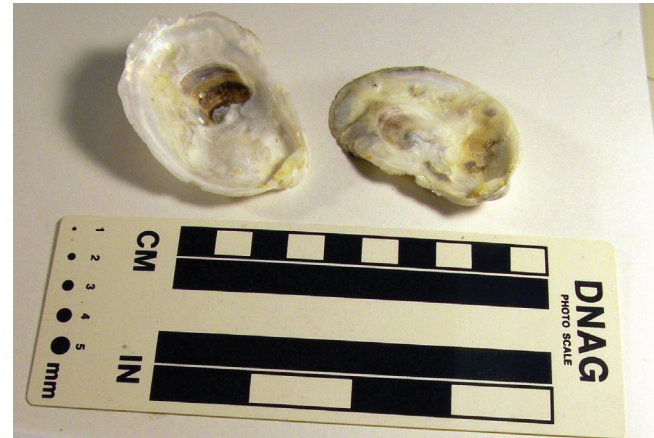
Fig. B1.6: µCT scan of shells. Left = includes 0b top, Right= 26C midsection view along length of shell. View made with Amira

317
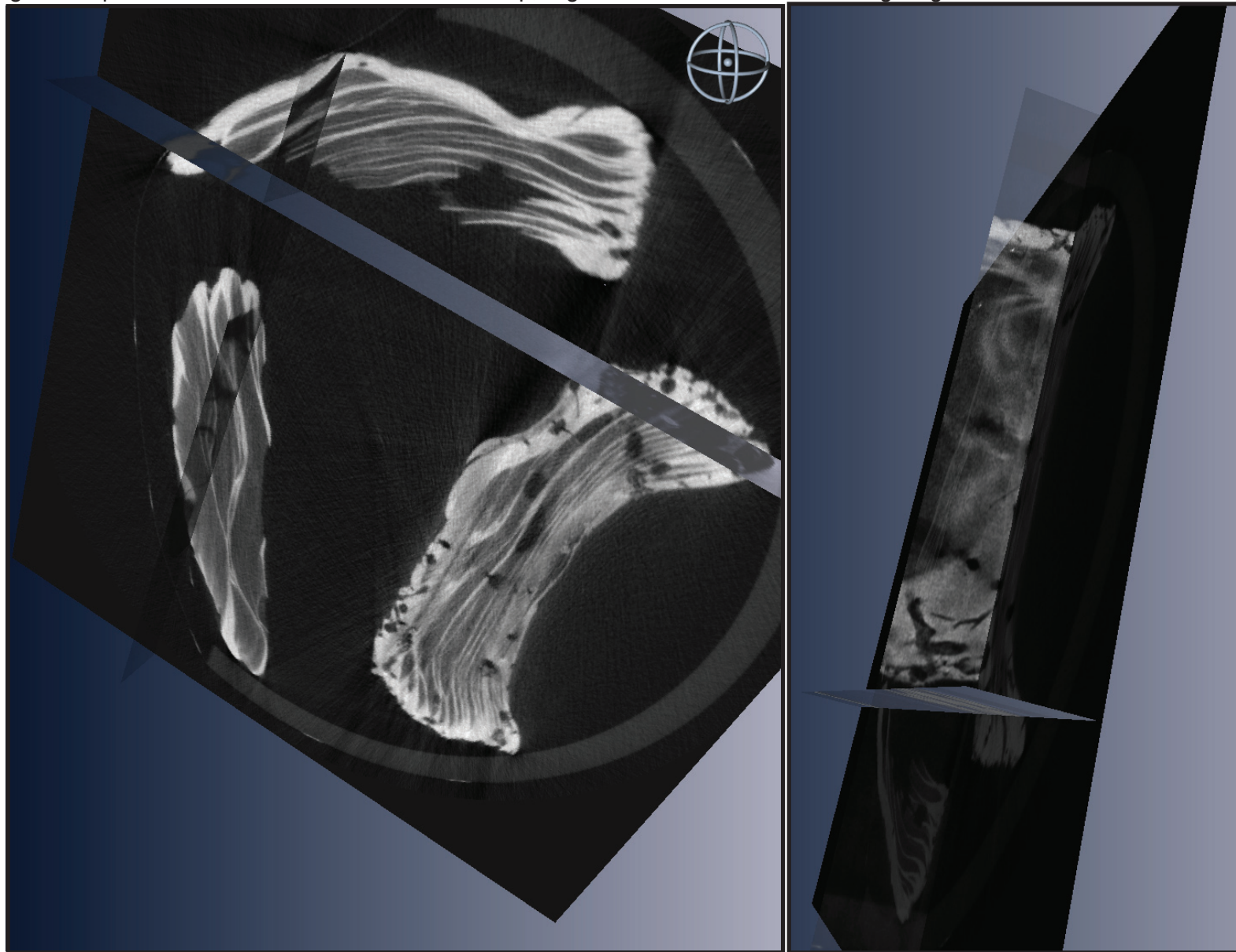
Fig. B1.7: 0b (top) & 70 (bottom) post cutting before sending off for ^{14}C.
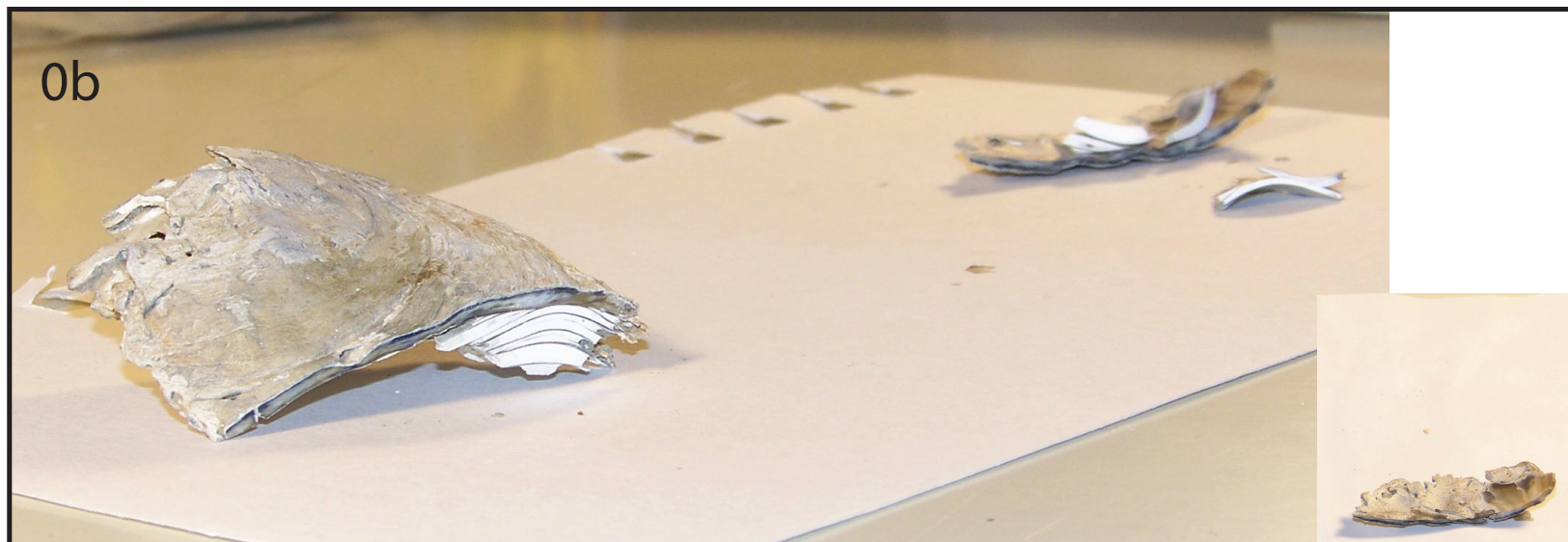
Fig. B1.8: Portion of shells cut to be sent for dating. For 26C both halves of the shell are shown, as well as the zoomed in view of the portion to be sent for dating. Portion of shells 61 & 38 are shown.
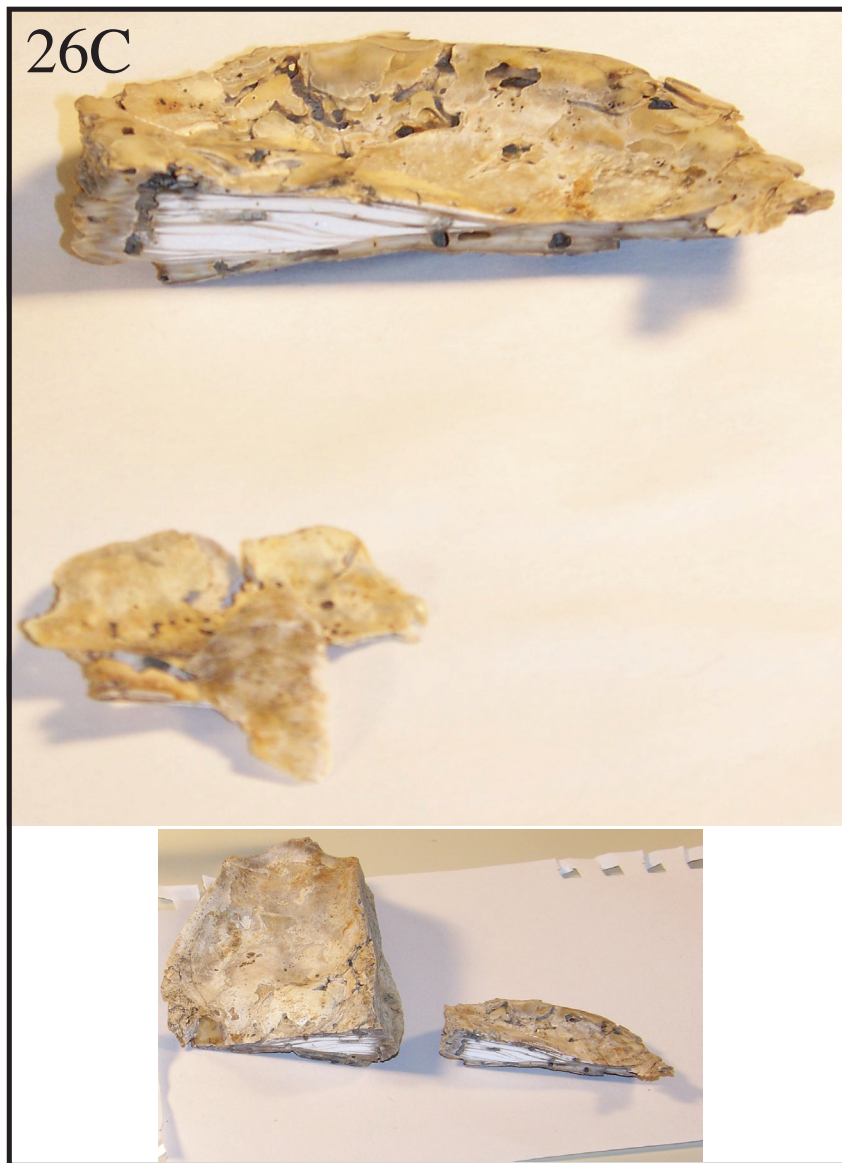
Fig. B1.9: Portion of shells 61, 70, 38, 0b and 26C that were sent to be ^{14}C dated.
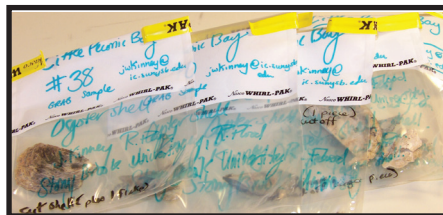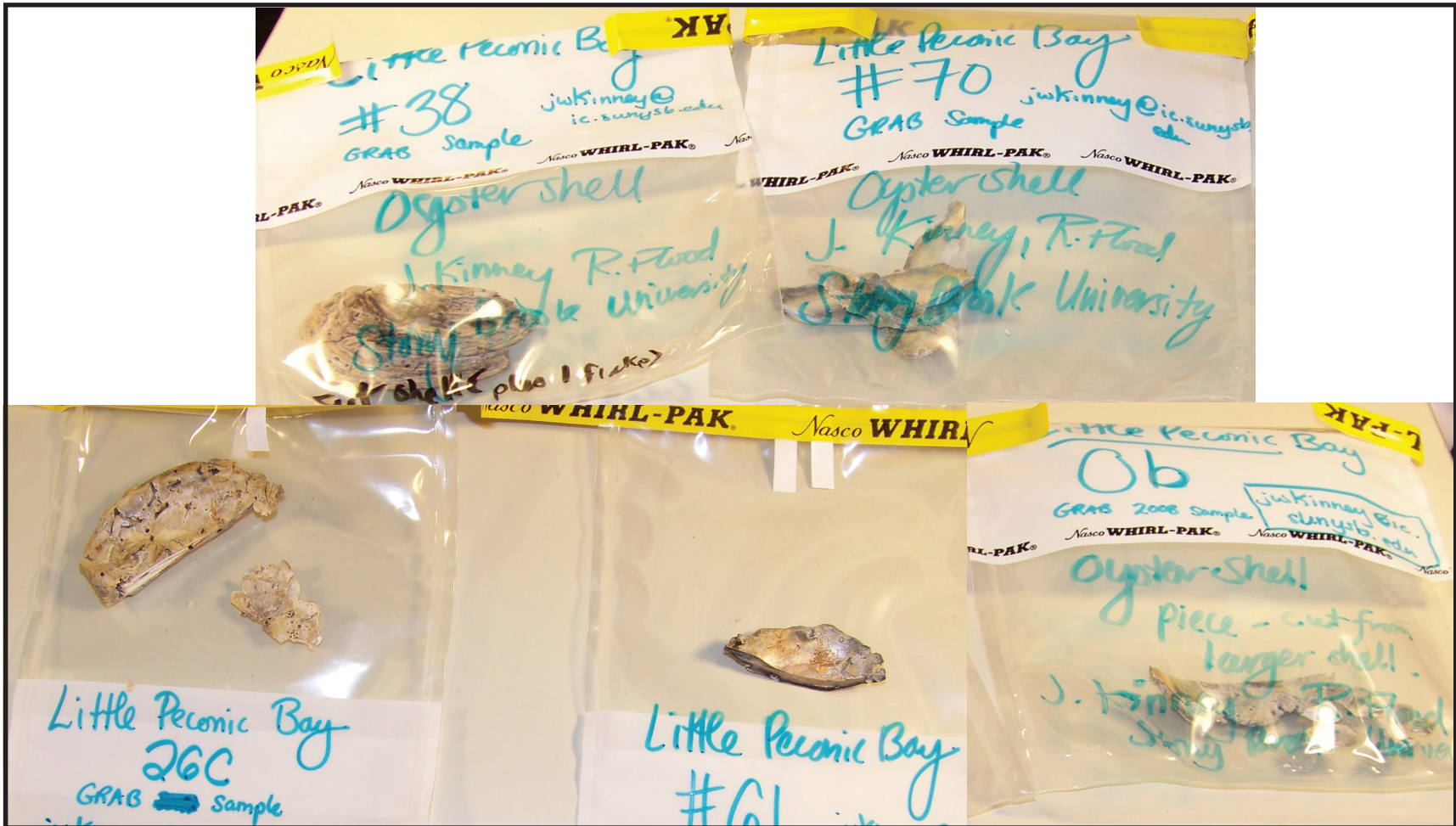
Fig. B2.1: Examples of grab samples in lab with oysters and sediment. 70 -2008 (Little Peconic Bay) Lots of fine sand; 61-2008 (Little Peconic Bay) Mud with Oystesrs. 38 -2006 (Little Peconic Bay) Lots of sand. Note that 2006 samples were allowed to sit a few weeks and much of the excess moisture dried before photographs were taken, whereas 2008 samples were photographed within a few days after sampling.

321
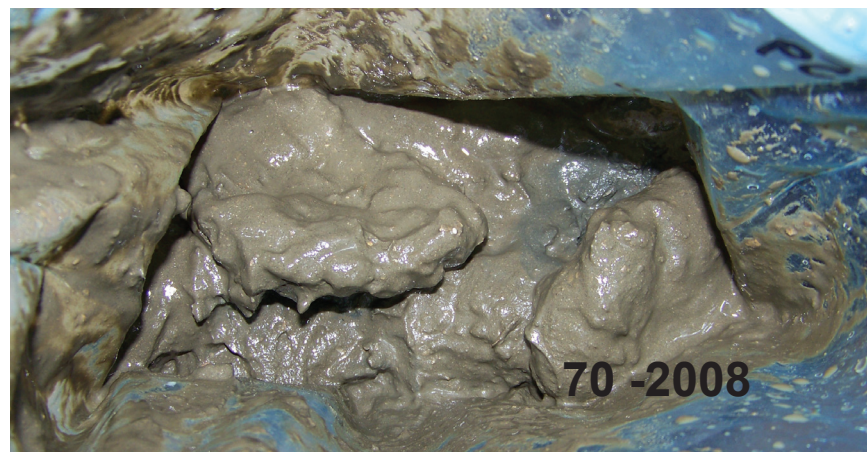
Fig. B2.2: Examples of shells covered with different grain size matrixes. Photos of samples from grabs in sample bags. From the top left hand corner clockwise: 4b-2008 (Noyack) = some very fine sand with mud, 26C-2008, = sandy, 0a-2008= muddy, 73-2008= mud sand mixture, 4b-2008 (Noyack), 26C-2008 (Noyack),73 -2008 (Little Peconic Bay), 0a -2008 (Little Peconic Bay)

4b -2008

26C -2008

73 -2008

0a -2008
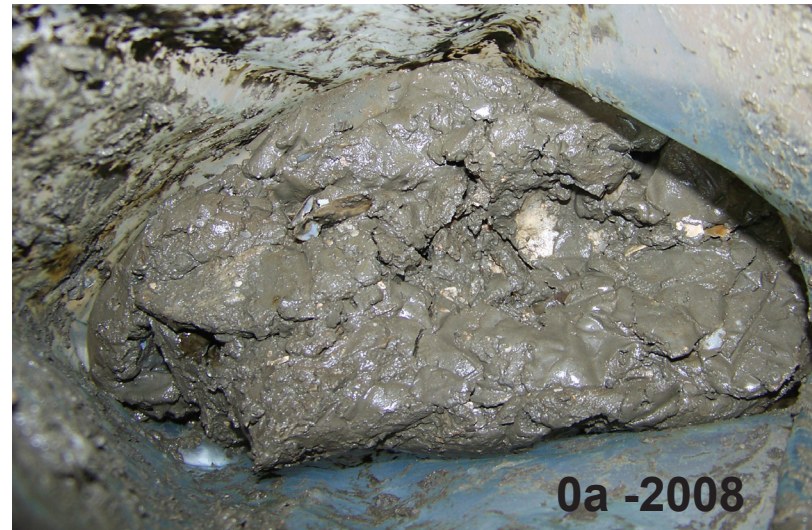
Fig. B2.3: Photograph of core #5 pulled and split to shows consistency. The core was pulled into two sections. Top of photograph shows the mud in the top of the core, especially inside the cores (split length wise). Bottom photograph shows the oysters found in the bottom section of the core at ~ 5 cm. View looking down at ~5 cm horizon.

core 5 (top of core)

core 5 oyster shells at base of core
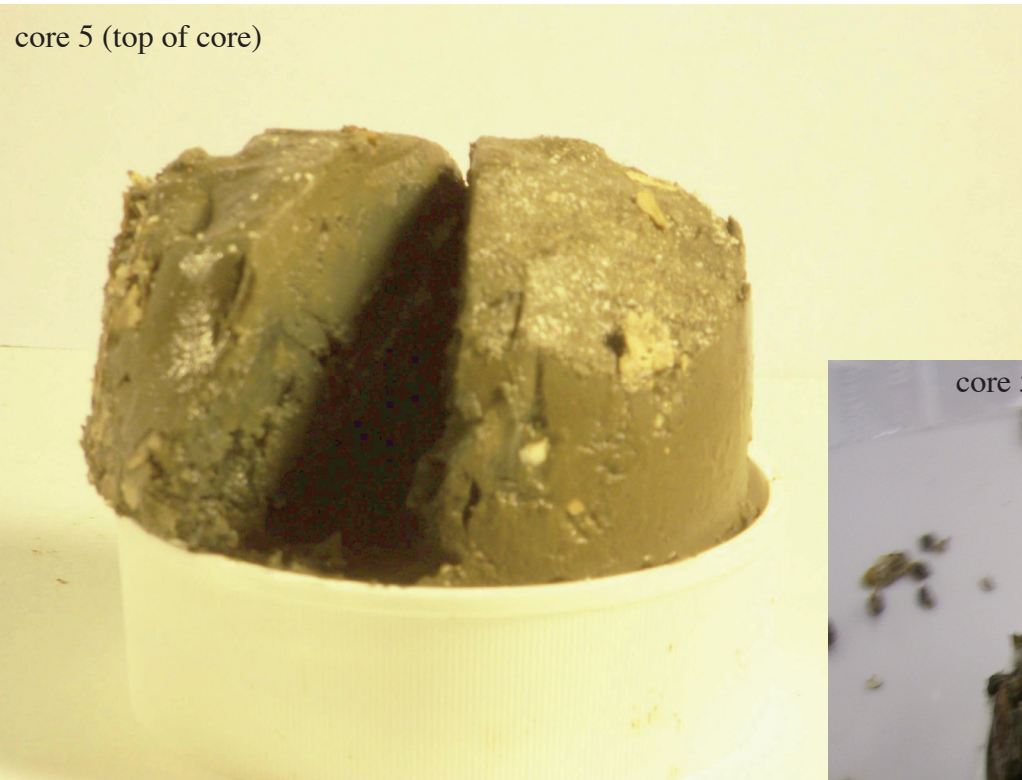
APPENDIX C: GEOCHEMICAL ANALYSIS

Appendix C1: Detailed procedures from Chapter 5

Preparation protocols:

Protocols for preparing samples were made to maximize use of samples (and subsamples) for both strontium and possible later oxygen analysis. Subsamples were prepared by removing an appropriate volume of ground sample from the shell followed by dissolution for strontium analysis. More details on subsampling choices are found in the Chapter 5. Oxygen analysis was done later.   Approximately 20 –200 µg carbonate is used for $\partial^{18}O$ analysis on an isotope mass spectrometer (Schöne et al., 2003; Schöne et al., 2006; Schöne & Fiebig, 2009; Surge, 2001; Takesue & Van Geen, 2003; Dettman, Reische & Lohmann, 1999; Jones, Quitmyer & Andrus, 2005; Kirby, 2000), thus we tried to create enough subsample from the original samples to keep at least this much material after Sr analysis.

We did not remove organic matter within shell subsamples as it is generally advised to not remove organic matter before analysis unless strictly necessary when preparing carbonate shells for $\partial^{18}O$ and $\partial^{13}C$ analysis (Weirzbowski, 2007; Serrano et al., 2008). The increased noise created by removing organic matter is larger than any variation created by organic matter released from the carbonate shell matrix upon acidification (Wierzbowski, 2007). Further, extremely fine grinding of carbonate species is required to remove organic matter bound in the shell matrix (Weirzbowski, 2007). Most studies are focused on removing any surface organic matter rather than removing a tiny component that may be present in the shell that may be released during the dissolution of the carbonate by phosphoric acid.

^{87}Sr /^{86}Sr Preparation Methods:

Analysis methods for ^{87}Sr /^{86}Sr followed the same procedures outlined in Kallenberg (2005) and Cochran et al. (2003) with some modification. The biggest change was that we were able to use a pneumatic pump to run multiple samples at once with a controlled flow, rather than just letting gravity control the flow through columns. Thus, our samples were drilled out or crushed, and the material was transferred into vials. The ground carbonate shell was dissolved in three drops of 7N HNO_3. Samples were then heated in the plastic vials to dry overnight on a mini plate. The samples were then dissolved in 3N HNO_3 (two to three drops) and centrifuged at 4000 rpm for 10 minutes. Samples were then pipetted into the prepped columns of Sr Resin (three drops of 3N HNO_3). Additional drops of 3N HNO_3 were slowly added with the pneumatic pump set at 0.5 rpm while the first few drops flowed through the resin. Sr-spec Resin by Eichrom is designed to allow for the Sr to bind to the resin in the concentrated HNO_3 solution allowing the rest of the elements to flow through the column. After the 3N HNO_3 drops dripped through the column, the pump was stopped briefly. Quartz distilled H_2O was then dropped into the columns and allowed to elute the Sr from the Resin (~20 drops). This elute was then captured in new, clean labeled, vials that held 2 drops of Phosphoric Acid in their bases. The eluted Sr was then dried in the tubes overnight. Multiple articles explain Sr column procedure in detail and an overview can be found on the Eichrom web site: http://www.eichrom.com/products/info/sr_resin.cfm.

Sr samples were then loaded for the TIMS mass spectrometer. The dried sample of Sr was dissolved in 2N HNO_3. Then a pipette was used to remove the Sr, and load the solution onto a baked-out tungsten (W) filament. Subsequent samples were loaded and run on baked-out rhenium (Re) filaments, rather than on the W filament. These samples followed a similar procedure with about 1/5 of the sample volume loaded onto a filament via pipette. For runs of Sr standard, SRM (standard reference material) 987, a similar volume to aliquots of Sr from shell samples was

loaded onto a filament. Sr loader is also added in preparation of the filament prior to adding the Sr.

For strontium analyses multiple aliquots of the same subsample of shell were run on the TIMS. More than one subsample of the same part of a shell was run through the Sr wet chemistry preparation and then run in the TIMS to obtain the reproducibility.

Calculating $^{87}Sr/^{86}Sr$ values

A standard of SRM 987 was run on both Re and W filaments to determine the offset from the known standard value. This offset was then later added to the measured values of our samples.

We calculated a weighted mean and standard deviation of samples in order to combine data from both Re and W filaments. In order to properly take into account the number of runs of each sample when calculating the mean, a weighted mean was used. The basic formula is

$$\text{weighted mean} = \frac{\sum_{i=1}^{n}(x_i * wt_i)}{\sum_{i=1}^{n}(wt_i)}$$

where wt is the weight value, or in this case the number of runs in a set, and x is the value of a set of runs.

The formula used in order to calculate the standard deviation, takes the basic standard deviation formula and includes weights. We must keep track of two sets of weighted values, as we have a weighted mean for samples run on Re filaments, and a separate weighted mean for the samples run on a W filament. Thus, we must introduce x_1 and x_2 and wt_1 and wt_2 to keep track of the data from Re filaments vs. from the W filaments, respectively. The standard offset for Re and W filaments, o_1 and o_2, was also added to the mean. An offset of 0.0000124 was applied for W filaments, while the offset

327

for Re filaments applied was 0.0000081. We use the weighted mean in place of the regular mean.

Weighted Mean using Re + W filaments $= \dfrac{\left(\left(\sum\limits_{i=1}^{n}\left(x_{1_i} * wt_{1_i}\right)\right) + o_1\right) + \left(\left(\sum\limits_{i=1}^{n}\left(x_{2_i} * wt_{2_i}\right)\right) + o_2\right)}{\sum\limits_{i=1}^{n}\left(wt_{1_i}\right) + \sum\limits_{i=1}^{n}\left(wt_{2_i}\right)}$

In order to figure out the standard deviation the

$$\text{standard formula} = \left(\frac{1}{n-1}\sum_{i=1}^{n}\left(x_i - \bar{x}\right)^2\right)^{\frac{1}{2}}$$

Now add a weight to the standard deviation value

$$\text{Standard deviation with one weight } = \frac{1}{\sum wt_1 - 1}\sum\left(\left(x_i - \bar{x}\right)^2 * wt\right)^{\frac{1}{2}}$$

However, to find the equation we used, we also had to include the weighted mean, and the weighted values for each of the two different filaments.

Standard deviation using weight for Re and W

$$= \left(\frac{1}{\left(\sum\limits_{i=1}^{n}\left(wt_1 + wt_2\right) - 1\right)} * \left(\sum_{i=1}^{n}\left(\left(x_1 - \bar{x}_1\right)^2 * wt_1\right) + \left(\left(x_2 + \bar{x}_2\right)^2 * wt_2\right)\right)\right)^{\frac{1}{2}}$$

So we replace the single $\bar{x}$ or mean of x with the two separate means, and write out the actual equation for these weighted means.

Standard deviation using weight and the weighted mean for Re and W

$$= \left(\frac{1}{\sum\limits_{i=1}^{n}(wt_i - 1)} * \sum_{i=1}^{n}\left(x_i - \left(\frac{\sum\limits_{i=1}^{n}\left(x_i * wt_i\right)}{\sum\limits_{i=1}^{n}\left(wt_i\right)}\right)\right)^2\right)^{\frac{1}{2}}$$

or

$$= \left(\left(\frac{1}{\sum\left(wt_1 + wt_2\right) - 1}\right) * \left(\sum\left(x_1 - \frac{\sum\left(x_1 - wt_1\right)}{\sum\left(wt_1\right)}\right)^2 + \sum\left(x_2 - \frac{\sum\left(x_2 - wt_2\right)}{\sum\left(wt_2\right)}\right)^2\right)\right)^{\frac{1}{2}}$$

Standard Decay equations:

The standard equations for radioactive decay show the relationship of amount of isotope with time using half-life $N(t) = N_o e^{(-t/t_0)} = N_o 2^{\left(-t/t_{1/2}\right)}$, the relationship of decay constant to half-life $t\frac{1}{2} = \ln(2/\lambda)$, and change in amount isotope for a decay constant $\lambda = dt\big/_{(-dN/N)}$. Where N= number of atoms (amount of isotope), N_0 is the initial amount of isotope at time 0. t = time, t_0= time 0, $t_{1/2}$ it the half-life of a given isotope, λ=decay constant of a given isotope. The half-life of Radon ^{222} is 3.8235 days, which gives λ^{222}Rn =0.18145214 days. The half-life of ^{226}Ra is 1620 years. Expressed in days half-life ($t_{1/2}$) for ^{226}Ra is 584,730 days. Radium decay using days has a decay constant of

$$N = N_t \Big/ 2^{\left(-t/(584730 days)\right)} = 0.00000117 \cdot$$

Ra^{226} via Radon Emanation:

^{226}Ra was measured for the first set of samples by gamma spectroscopy using the Ge 3 Kev and well gamma detectors, and subsequently all of the samples were measured using its daughter ^{222}Rn via radon emanation on a scintillation counter at SoMAS Stony Brook University. Measurement of ^{226}Ra by the decay of ^{222}Rn was used to calculate the dpm/g of ^{226} Ra in a sample. Counting efficiency for ^{222}Rn via this method, radon emanation, is much higher than that of gamma spectroscopy counting for the decay of ^{226}Ra. The short half-life of ^{222}Rn of a few days makes is suitable for counting its parent ^{226}Ra, with ^{222}Rn t 1/2 = 3.825d. The error percentage drops considerably when one increases the number of counts obtained over time. The branching coefficient is much higher for the amount of energy released by ^{222}Rn decay (alpha decay) measured by the scintillation counter than by the gamma energy released by ^{226}Ra. Only about 3% of the energy of a ^{226}Ra decay is in the gamma spectrum. For gamma spectroscopy counting of ^{226}Ra we used the 352 Kev peak. Well counter vials, and jars used in the 3 Kev detectors were compared to sediment standards run on the same geometry.

Most of the energy for ^{226}Ra decay is actually in the alpha decay. While the ^{222}Rn gives off 3 flashes per decay recorded on the scintillation counter. This gives us three times as many counts per minute per decay. We can readily isolate the radon through radon emanation to have it counted on the scintillation counter, but isolating ^{226}Ra to measure its alpha decay is more difficult. The increased efficiency and lower errors of the radon emanation technique seemed needed considering the very low levels of Ra^{226} in the shells to begin with in modern oyster shell. Too much shell material would be need to be ground up to get an equivalent measurement via gamma spectrometry. Shells run on the gamma detector initially were also ground up via mortar and pestle in the same way as those prepared for radon emanation, and a subsample of material was later taken from the large sample for the radon emanation for the bulk sample run on the gamma detector first. Measurement of ^{226}Ra requires truly clean and sediment free crushed shell, which is difficult given the condition of sponge eaten oyster shells.

The next step was to dissolve the carbonate (crushed shell) in HCl. Dissolution was done by adding HCl a few mL at a time. An estimate of how much HCl would be needed to dissolve the shell was based on the amount needed to dissolve the subsample of shell #70. Gradually some HCl was added as a 1:1 (DI with 36% HCl) solution to the mass of ground shell. After dissolution of the shell a more dilute 1N HCl solution was added. The goal is to have enough DI/HCl solution to make sure that at least 1% HCl or pH greater than 0.1 was present in all of the beakers after dissolution of the shell. In this case we chose to get close to a 1N concentration. A total volume of solution of 115 mL was used for all of the samples in gas bottle bubblers of the same volume/size. This was slightly more than 1/3 of the volume of the container.

Several steps were performed to make sure residual sediment was removed. Initially, the dissolved sample was centrifuged to remove any residue sediment. Considering how much sediment could be trapped in a given shell this seemed prudent. Samples were also put through filter paper to try to remove any floating particles/ larger

330

organics that might have sediment attached.   If any particulate sediment residue remained in the sample, it may have been small buoyant fluffy organic particles.

The solution is placed in the glass wash bottle bubbler container with connected rubber outlet and inlet tubes that are sealed (clamped) to allow for ingrowth of ^{222}Rn from the decay of ^{226}Rn for a few weeks. The samples are allowed to sit in order for the ^{222}Rn to reach secular equilibrium, with a minimum of two weeks to ensure that this happened.

After ingrowth, the samples were measured via Rn extraction. Wash bottles with samples were hooked up to the extraction board to flush the Rn into the dry ice cooled charcoal column by pumping it through with helium. Before flowing into the charcoal column, the gases from the bubbler flowed through Drierite ($CaSO_4$) to adsorb water vapor and Ascerite (a form of sodium hydroxide ($NaOH$) coated vermiculite (non-fibrous silicate)) to adsorb CO_2 and acid gases. Next the Rn is flushed into a counting cell from the charcoal column by heating the column in the furnace while flushing with helium. Three hours after filling of the cell, enough time for the daughters of ^{222}Rn to reach equilibrium, counting on the scintillation counter was performed. The scintillation counter (a photo multiplier) was used to count the photo emission events (alpha decays) in the samples overnight.

Background values for the cells are subtracted from the total counts per minute. A single extraction board, and charcoal column were used to reduce sources of error. Efficiencies on the two detectors are calculated by counting standards, blank empty bottles, DI blank bottles, and some of the regular samples on both detectors and on both cells. A radium standard of 8.645 dpm was used in the same wash bottle bubblers. The empty bottle blank, and DI bottle blank were in the same wash bottle bubblers as well.

The counter measures the number of minutes and the photo emission counts. This is used to calculated cpm (counts per minute). The blank value, water bottle, was

subtracted as well (Table C1.5-C1.7). Counter efficiency for each detector, and cell efficiencies are important to calculate. Cell efficiencies were calculated for each detector. A single charcoal column was used for all samples so no correction for differences in columns was required. Cell background values before each fill were recorded and subtracted from the cpm value. Then this new net cpm value is divided by 3 flashes per alpha particle decay, and then by the counter and cell efficiency. This is then used to calculate the decay rate. This new decay per minute (dpm) number is plugged into the equation showing activity

$$A_0 = \frac{NetCPM}{\left(e^{\left(-t*\lambda_{Rn^{222}}\right)}\right)}$$

to give us the original activity in the sample or A_0. A blank in these units was then subtracted.

Standard calculations were then used to calculate the A_0, our report ^{226}Ra value, where $A=A_0e^{\lambda t}$, λ =0.000001172 days A_0 = Amount (# of decays) at time 0, A= Amount (# of decays) at time t, t=time, and λ = decay constant. Time for decay of Radon was calculated as the time between the midpoint of filling and the midpoint of counting on a detector. The error can be described with the following equations where Counts = number of counts and t= number of hours till counted:

Percentage error for ^{226}Ra A_0= $\left(\left(\sqrt{Counts} + \sqrt{(t \times 0.13)}\right) \Big/ \left(Counts - (t \times 0.13)\right)\right) \times 100$

Error +/- for ^{226}Ra age corrected A_0

$$= \left(\left(\sqrt{Counts} + \sqrt{(t \times 0.13)}\right) \Big/ \left(Counts - (t \times 0.13)\right)\right) \times AgeCorrectedA_0$$

Percent error for counts = $\left(\sqrt{Counts} \Big/ (Counts)\right) \times 100$

Table C1.1: Strontium raw data table: $^{87}Sr/^{86}Sr$ TIMS results W filament.

Sample ID	Date	Mean of $^{87/86}Sr$	SD	SD%	SE(M)	SE (M)%	Number of Values kept	Number of Runs
987	1/1/10	0.710205	0.000102	0.0144	0.000015	0.0021	194	200
987	1/5/10	0.710198	0.000093	0.0131	0.000014	0.0019	191	200
987	3/4/10	0.710444	0.000194	0.0273	0.000051	0.0072	58	60
987	3/5/10	0.710229	0.000112	0.0158	0.000016	0.0023	196	200
987	3/5/10	0.710227	0.000074	0.0104	0.000015	0.0021	96	100
987	3/5/10	0.710264	0.000124	0.0174	0.000018	0.0025	195	200
987	3/9/10	0.710269	0.000075	0.0105	0.000011	0.0015	194	200
987	3/9/10	0.710204	0.000076	0.0107	0.000011	0.0016	188	200
987	3/11/10	0.710244	0.000088	0.0123	0.000016	0.0023	116	120
987	3/11/10	0.710302	0.000106	0.0149	0.000049	0.0068	19	20
987	3/12/10	0.710243	0.000089	0.0126	0.000013	0.0018	195	200
987	3/12/10	0.710246	0.000102	0.0143	0.000023	0.0033	76	80
987	3/12/10	0.710439	0.000188	0.0264	0.000059	0.0084	40	40
987	3/12/10	0.710228	0.000097	0.0137	0.000014	0.0020	191	200
987	3/20/10	0.710247	0.000118	0.0165	0.000017	0.0024	190	200
987	3/20/10	0.710209	0.000100	0.0141	0.000014	0.0020	192	200
987	3/20/10	0.710197	0.000091	0.0128	0.000013	0.0018	194	200
987	3/20/10	0.710174	0.000087	0.0123	0.000013	0.0018	191	200
38L_2006	3/18/10	0.709180	0.000076	0.0107	0.000011	0.0016	192	200
38L_shell	3/15/08	0.709127	0.000896	0.1263	0.000401	0.0565	20	20
61_L	3/16/10	0.709141	0.000076	0.0107	0.000015	0.0022	97	100
61_L	3/16/10	0.709170	0.000077	0.0109	0.000016	0.0022	98	100
61_L	10-Mar	0.709125	0.000061	0.0086	0.000011	0.0016	115	120
70_L	3/15/08	0.709192	0.000074	0.0105	0.000020	0.0028	55	60
70_L	3/15/08	0.709143	0.000176	0.0249	0.000081	0.0114	19	20
Ob_L	3/20/10	0.709164	0.002156	0.3041	0.000964	0.1360	20	20
Aq_Std_3	3/17/10	0.709192	0.000083	0.0118	0.000012	0.0017	194	200
Aq_Std_3	3/18/10	0.709225	0.000096	0.0135	0.000018	0.0025	116	120
C1_1st	3/20/10	0.709352	0.000149	0.0210	0.000031	0.0043	94	100
C1_Shell	1/1/10	0.709161	0.000079	0.0111	0.000015	0.0021	115	120
C1_Shell	1/5/10	0.709174	0.000096	0.0135	0.000019	0.0027	97	100

Table C1.2: Strontium raw data table: $^{87}Sr/^{86}Sr$ TIMS results W filament excluded values.

Sample ID	Date	Mean of $^{87/86}Sr$	SD	SD%	SE(M)	SE (M)%	Number of Values kept	Number of Runs
Ob_L	3/20/10	0.708059	0.002188	0.3091	0.001004	0.1418	19	20
26C_L_ chalky	3/20/10	0.709286	0.000158	0.0223	0.000030	0.0042	112	120
26C_L_ chalky	3/20/10	0.709321	0.000149	0.0210	0.000039	0.0055	58	60
61_L	3/10/10	0.709408	0.000119	0.0167	0.000056	0.0079	18	20

Mean Root Squared, SD=Standard Deviation, SE=Standard Error

Table C1.3: Strontium raw data table: $^{87}Sr/^{86}Sr$ TIMS results Re filament.

ID	Date	Mean of $^{87/86}Sr$	SD	SD %	SE (M)	SE (M) %	Number of Values kept	Number of Runs
987	4/19/10	0.710226	0.000064	0.009	0.000009	0.0013	190	200
987	4/19/10	0.710235	0.000052	0.007	0.000008	0.0011	186	200
987	4/20/10	0.710222	0.000089	0.013	0.000015	0.0022	133	140
987	4/20/10	0.710218	0.000063	0.009	0.000009	0.0013	190	200
987	4/20/10	0.710229	0.000067	0.009	0.000010	0.0014	191	200
987	4/21/10	0.710539	0.000375	0.053	0.000120	0.0169	39	40
987	4/21/10	0.710295	0.000073	0.010	0.000020	0.0028	56	60
987	4/21/10	0.710300	0.000092	0.013	0.000024	0.0034	57	60
987	4/21/10	0.710318	0.000079	0.011	0.000026	0.0037	37	40
987	4/21/10	0.710242	0.000089	0.013	0.000017	0.0023	116	120
987	4/21/10	0.710235	0.000090	0.013	0.000013	0.0018	193	200
987	4/22/10	0.710238	0.000081	0.012	0.000012	0.0017	191	200
987	4/23/10	0.710207	0.000082	0.012	0.000012	0.0017	194	200
987	4/24/10	0.710200	0.000069	0.010	0.000023	0.0032	37	40
987	4/24/10	0.710198	0.000068	0.010	0.000010	0.0014	190	200
987	4/25/10	0.710286	0.000089	0.013	0.000013	0.0018	192	200
987	4/26/10	0.710281	0.000093	0.013	0.000019	0.0027	95	100
987	4/27/10	0.710260	0.000078	0.011	0.000011	0.0016	196	200
987	4/27/10	0.710189	0.000084	0.012	0.000037	0.0053	20	20
987	4/27/10	0.710175	0.000110	0.015	0.000049	0.0069	20	20
987	4/27/10	0.710239	0.000069	0.010	0.000031	0.0044	20	20

SD=Standard Deviation, SE=Standard Error

ID	Date	Mean of $^{87/86}$Sr	SD	SD %	SE (M)	SE (M) %	Number of Values kept	Number of Runs
987	4/28/10	0.710241	0.000069	0.010	0.000016	0.0022	75	80
987	4/28/10	0.710227	0.000071	0.010	0.000010	0.0014	194	200
987	4/28/10	0.710231	0.000075	0.011	0.000034	0.0048	19	20
987	4/28/10	0.710206	0.000055	0.008	0.000008	0.0011	191	200
987	4/29/10	0.710362	0.000099	0.014	0.000032	0.0044	39	40
987	4/29/10	0.710221	0.000061	0.009	0.000014	0.0019	78	80
987	4/29/10	0.710229	0.000075	0.011	0.000011	0.0015	190	200
987	4/30/10	0.710225	0.000082	0.012	0.000022	0.0030	58	60
987	4/30/10	0.710218	0.000122	0.017	0.000039	0.0055	39	40
987	4/30/10	0.710201	0.000064	0.009	0.000009	0.0013	188	200
987	5/2/10	0.710249	0.000098	0.014	0.000014	0.0020	190	200
987	5/2/10	0.710254	0.000085	0.012	0.000012	0.0017	190	200
987	5/5/10	0.710355	0.000104	0.015	0.000033	0.0047	39	40
987	5/6/10	0.710211	0.000084	0.012	0.000027	0.0038	38	40
987	5/6/10	0.710244	0.000062	0.009	0.000016	0.0023	56	60
987	5/6/10	0.710234	0.000083	0.012	0.000012	0.0017	191	200
987	5/7/10	0.710193	0.000087	0.012	0.000028	0.0040	38	40
987	5/7/10	0.710224	0.000089	0.013	0.000013	0.0018	190	200
987	5/9/10	0.710333	0.000089	0.013	0.000029	0.0041	37	40
987	5/13/10	0.710229	0.000087	0.012	0.000013	0.0018	190	200
987	5/14/10	0.710202	0.000081	0.011	0.000012	0.0016	189	200
987	5/14/10	0.710225	0.000094	0.013	0.000013	0.0019	195	200
987	5/15/10	0.710246	0.000108	0.015	0.000016	0.0022	193	200

SD=Standard Deviation, SE=Standard Error

ID	Date	Mean of $^{87/86}$Sr	SD	SD %	SE (M)	SE (M) %	Number of Values kept	Number of Runs
26_C	4/21/10	0.709131	0.000071	0.010	0.000010	0.0015	192	200
26C_Avg	4/28/10	0.709154	0.000105	0.015	0.000015	0.0021	193	200
26C_Avg	4/28/10	0.709152	0.000065	0.009	0.000010	0.0014	172	180
26C_L_chalky_layer	5/6/10	0.709154	0.000058	0.008	0.000027	0.0038	19	20
26C_L_chalky_layer	5/6/10	0.709167	0.000087	0.012	0.000013	0.0019	171	180
38_Avg	4/26/10	0.709167	0.000065	0.009	0.000021	0.0030	38	40
38_Avg	4/26/10	0.709181	0.000074	0.010	0.000011	0.0016	175	180
38_Avg	4/27/10	0.709181	0.000074	0.010	0.000011	0.0016	175	180
38_Avg	5/1/10	0.709148	0.000071	0.010	0.000010	0.0014	192	200
61_Avg	4/30/10	0.709139	0.000073	0.010	0.000017	0.0023	76	80
61_Avg	4/30/10	0.709168	0.000051	0.007	0.000014	0.0019	57	60
61_Avg	4/30/10	0.709199	0.000087	0.012	0.000028	0.0039	39	40
61_Avg	5/8/10	0.709175	0.000083	0.012	0.000012	0.0017	191	200
70_Avg	4/22/10	0.709184	0.000129	0.018	0.000041	0.0058	39	40
70_Avg	4/22/10	0.709171	0.000065	0.009	0.000021	0.0030	39	40
70_Avg	4/22/10	0.709196	0.000079	0.011	0.000012	0.0017	172	180
70_Avg	5/7/10	0.709208	0.000113	0.016	0.000021	0.0030	113	120
70_avg	5/7/10	0.709202	0.000193	0.027	0.000089	0.0125	19	20

SD=Standard Deviation, SE=Standard Error

ID	Date	Mean of $^{87/86}$Sr	SD	SD %	SE (M)	SE (M) %	Number of Values kept	Number of Runs
Aq_std	4/26/10	0.709158	0.000076	0.011	0.000034	0.0048	20	20
Aq_std	4/26/10	0.709255	0.000106	0.015	0.000024	0.0034	76	80
Aq_std	4/26/10	0.709217	0.000106	0.015	0.000016	0.0023	171	180
Aq_Std	5/9/10	0.709210	0.000081	0.011	0.000015	0.0021	113	120
Aq_Std	5/9/10	0.709289	0.000109	0.015	0.000050	0.0070	19	20
Aq_Std	5/9/10	0.709221	0.000111	0.016	0.000017	0.0024	169	180
Aq_Std_2	4/28/10	0.709126	0.000105	0.015	0.000048	0.0068	19	20
Aq_Std_4	4/22/10	0.709146	0.000080	0.011	0.000012	0.0016	188	200
Aq_Std-2	4/28/10	0.709155	0.000064	0.009	0.000010	0.0015	152	160
C1_1st	4/30/10	0.709258	0.000102	0.014	0.000046	0.0064	20	20
C1_1st	4/30/10	0.709388	0.000161	0.023	0.000072	0.0102	20	1
C1_1st	4/30/10	0.709384	0.000131	0.019	0.000043	0.0060	38	40
C1_1st	4/30/10	0.709287	0.000073	0.010	0.000024	0.0033	38	40
C1_1st	4/30/10	0.709205	0.000200	0.028	0.000092	0.0129	19	20
C1_1st	5/2/10	0.709281	0.000131	0.019	0.000060	0.0085	19	20
C1_1st	5/2/10	0.709295	0.000093	0.013	0.000042	0.0059	20	20
C1_1st	5/2/10	0.709235	0.000077	0.011	0.000035	0.0050	19	20
C1_Avg	5/1/10	0.709224	0.000076	0.011	0.000013	0.0018	134	140
C1_Hinge	5/1/10	0.709181	0.000068	0.010	0.000012	0.0017	134	140
C1 Hinge	5/14/10	0.709224	0.000092	0.013	0.000014	0.0020	172	180
C1 Hinge	5/15/10	0.709216	0.000256	0.036	0.000118	0.0166	19	20

SD=Standard Deviation, SE=Standard Error

ID	Date	Mean of $^{87/86}$Sr	SD	SD %	SE (M)	SE (M) %	Number of Values kept	Number of Runs
S1_Chalky	4/26/10	0.709201	0.000100	0.014	0.000046	0.0064	19	20
S1_Chalky	4/26/10	0.709241	0.000070	0.010	0.000019	0.0026	56	60
S1_Chalky	4/26/10	0.709282	0.000075	0.011	0.000034	0.0048	19	20
S1_Chalky	4/27/10	0.709167	0.000056	0.008	0.000011	0.0016	95	100
S1_Chalky	4/27/10	0.709206	0.000057	0.008	0.000008	0.0012	194	200
S1_Chalky_redo	5/2/10	0.709253	0.000099	0.014	0.000046	0.0064	19	20
S1_Chalky_redo	5/2/10	0.709193	0.000083	0.012	0.000012	0.0017	190	200
S1_hinge	5/1/10	0.709332	0.000109	0.015	0.000036	0.0050	37	40
S1_hinge	5/1/10	0.709360	0.000157	0.022	0.000051	0.0072	38	40
S1 Hinge	5/14/10	0.709182	0.000100	0.014	0.000014	0.0020	190	200
0b_Avg	5/7/10	0.709213	0.000091	0.013	0.000014	0.0020	171	180
Ob_Avg	4/21/10	0.709160	0.000102	0.014	0.000015	0.0021	190	200
Ob_Avg	10-Apr	0.709160	0.000102	0.014	0.000015	0.0021	190	200
S1 1st	5/13/10	0.709250	0.000087	0.012	0.000016	0.0023	117	120
S1 1st	5/13/10	0.709259	0.000090	0.013	0.000021	0.0029	75	80

SD=Standard Deviation, SE=Standard Error

Table C1.4: Strontium raw data table: ^{87}Sr/^{86}Sr TIMS results Re filament, excluded sets.

	ID	Date	Mean of $^{87/86}$Sr	SD	SD %	SE (M)	SE (M) %	Number of Values kept	Number of Runs
Excluded 1st set	70_Avg	5/7/10	0.709381	0.000125	0.018	0.000056	0.0079	20	20
	C1_1st	5/2/10	0.709145	0.000102	0.014	0.000047	0.0066	19	20
	C1_1st	4/30/10	0.710220	0.000065	0.009	0.000015	0.0021	76	80
Excluded 2nd set	S1_1st_part	4/30/10	0.709159	0.000070	0.010	0.000012	0.0017	135	140

SD=Standard Deviation, SE=Standard Error

Table C1.5 : Standards run for ^{226}Ra.

Standard Samples	^{226}Ra dpm Blank Corrected A0 from midpoint	% Err
^{226}Ra Std 13 8.645dpm	8.406	0.85
^{226}Ra Std 13 8.645dpm	8.960	0.75
^{226}Ra Std 13 8.645dpm	10.638	0.97

Table C1.6: Bottles blanks for [226]Ra that were basis of a value of 0.13 used as blank correction

Sample run (Blanks)	A0 dpm from midpoint dpm	% error
Bottle Air	0.174	5.1
Bottle Air	0.118	6.1

Table C1.7: ^{226}Ra blanks.

Blanks run (Bottle of air, or Dionized water and air)	Ao from midpoint dpm	% Error	counted decays per minute	net cpm
Bottle Air	0.17	5.1	0.33	0.16
Bottle Air	0.12	6.1	0.11	0.19
Bottle Air	0.23	4.6	0.21	0.38
Bottle Air	0.03	7.1	0.02	0.05
DW blank for washbottle	0.29	15.3	0.26	0.47
DW blank for washbottle	0.29	3.9	0.27	0.58
DW blank for washbottle	0.40	3.1	0.37	0.66

Table C1.8: ^{87}Sr/^{86}Sr **Values: Comparison of S1 15 psu sample excluding and including the 1st run.**

ID	^{87}Sr/^{86}Sr Average
S1 15 psu *(S1 1st part)* value excluded	0.709262 ±0.0000046
S1 15 psu (S1 1st part) *include excluded value	*0.709223 ±0.000062*

*For S1 1st part, one run seemed too low so we excluded it. However, as this only leaves only 2 out of 3 runs, and the difference was not large, we choose to report the mean with and without the rejected value. All other samples for which a run was rejected, had a mean of at least 3 accepted runs to compare it to.

Fig. C.1: Example of the portion of aquaculture shells cut for radium analysis. The rear portion of four shells were used for Southold Bay and Goose Creek samples.

Rear portion of shell cut off, after a large growth ridge

Fig. C.2: Subsampling of aquaculture shells S1 (Southold 1) and C1 (Goose Creek 1). Aquaculture Shells grown out in the Peconic Estuary had subsampled drilled out in order to have material for $^{87}Sr/^{86}Sr$ isotope analysis. Both aquaculture shells are from the same year known and known to be about 1.5 years old. The subsampled areas are outlined to show the ares that was drilled. The first part of the shell, representing the earlier stages of grow out in the more brackish controlled seed growth environment at 10 -15 psu. (C1 1st part and S1 1st part.) C1 first part was grown at the Cornell Cooperative Extension in Southold. S1 1st part was grown by Aeros. A second subsample was taken from both shells within the outer portion of shell that represents when the shells were actually growing in the Peconic Estuary (C1 2nd part and S1 2nd part). The growth bands of the shell can be clearly seen in the cut shell. These growth bands typically represent annual bands of growth in wild oysters as the rate of shell growth changes when environmental conditions such as temperature change. In the aquaculture shells an abrupt growth line occurs when the shells were transferred, which gives them an artificial equivalent to a change in season growth break. The mirror cut of the shells (undrilled) shows,the growth bands more clearly.
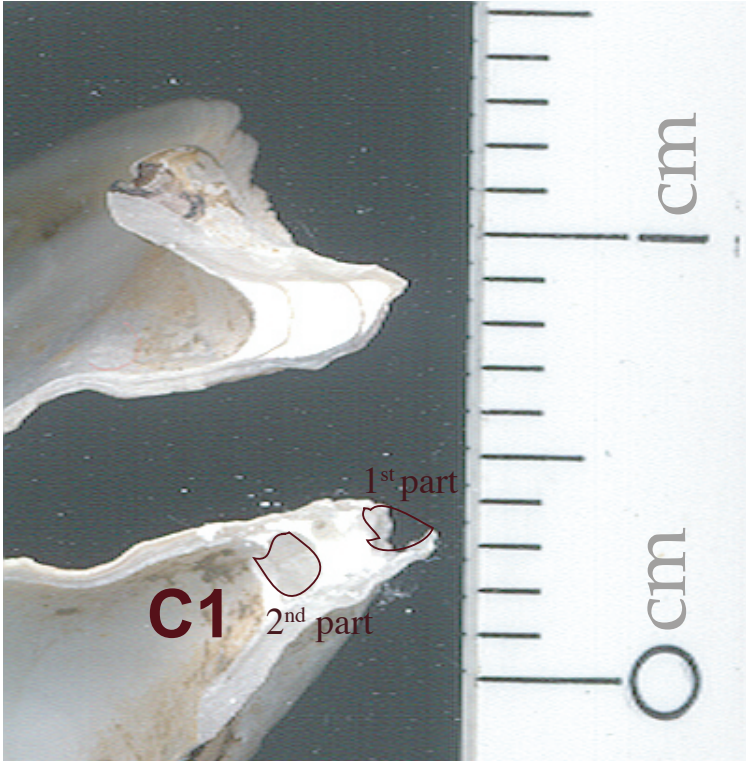
C1

1st part

2nd part

S1

1st part

2nd part

Fig. C.3: Subsampling of relict shell 26C. Relict shell #26C subsampling for $^{87}Sr/^{86}Sr$ analysis by drilling, Inset A depicts the average sample taken along the fresh face of the cut hinge. Inset B depicts the chalky layer of shell subsampled from the fresh cut of outer shell material.
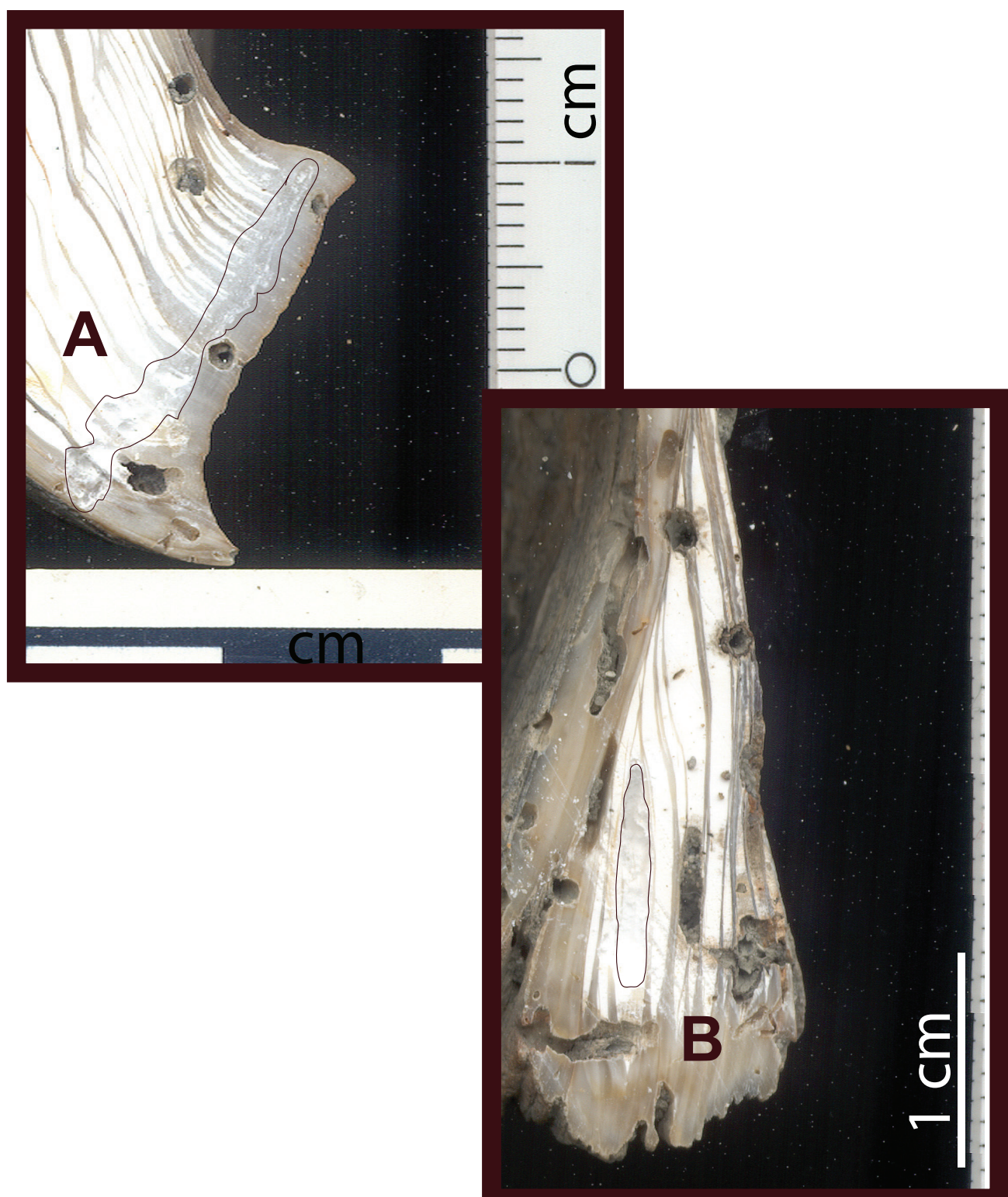
348

Fig. C.4: Sampling of shells #70, #0b, and #38 by drilling. #38 A shows average subsampling by drilling across growth bands at hinge. #38 B shows chalky layer subsampled (the same area before subsampling is also depicted adjacent to A). #0b, A shows average subsampling by drilling across growth bands at hinge. #0b, B shows the sampling of the chalky layer.   #70 A shows how the average sample was created by sampling across all of the growth bands. The chalky layer subsampled can also be seen in this view. #70 B shows the subsampling of a chalky layer.
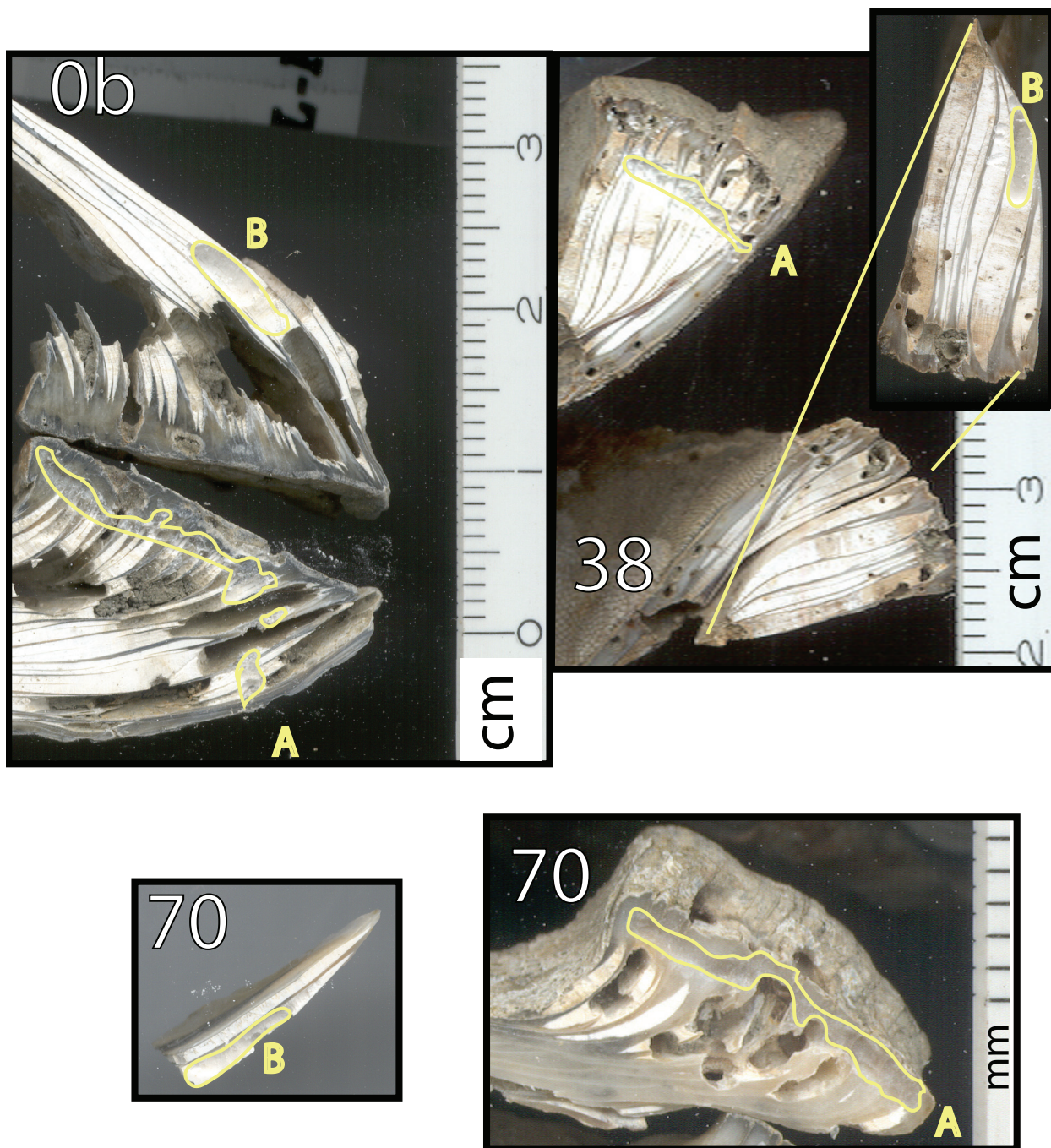
Fig. C.5: Additional view of shell #70, showing the cut through the hinge and the mirror view of the shell.

Fig. C.6: Subsampling of #61. Shell #61 subsampling for $^{87}Sr/^{86}Sr$ analysis by drilling, inset View A depicts the average sample taken along the fresh face of the cut hinge, inset B depicts the chalky layer of shell subsampled from the fresh cut of outer shell material.